AMC Consultants Pty Ltd
ABN 58 008 129 164

Level 12, 477 Collins Street
Melbourne Vic 3000
Australia

T +61 3 8601 3300
E melbourne@amcconsultants.com

amcconsultants.com

Report

Technical Report Summary-Initial Assessment of TOML and NORI Properties, Clarion-Clipperton Zone

TMC the metals company Inc.

AMC Project 0225054
Effective date: 4 August 2025

Qualified Persons:
AMC Consultants Pty Ltd
MARGIN - Marine Geoscience Innovation
APYS Subsea Ltd
Canadian Engineering Associates Ltd
Lanasera Pty Ltd
Anthony O'Sullivan, Chief Development Officer, TMC the metals company Inc.
Dr. Michael Clarke, Environmental Manager, TMC the metals company Inc.
Rutger Bosland, Chief Innovation and Offshore Technology Officer, TMC the metals company Inc.
Adam Price, Project Controls Manager, TMC the metals company Inc.

1 Executive summary

1.1 Introduction

A very large nickel, manganese, cobalt, and copper resource occurring as polymetallic nodules is located on the seafloor in the Clarion-Clipperton Zone (CCZ) of the north-east Pacific Ocean. TMC the metals company Inc. (TMC), through their wholly owned subsidiaries, are undertaking assessment on the technical and economic viability of recovering metals from polymetallic nodules to support increasing demand from electrification, electric vehicle (EV) battery and stainless-steel demand. Working with offshore and onshore partners, TMC has designed and demonstrated nodule collection and processing systems that can generate nickel, copper, cobalt and manganese products with little to no solid waste (AMC Consultants, 2025).

Four consortia of offshore development companies demonstrated the technical feasibility of collecting, lifting, and converting nodules into metals in the 1970s, but development of the industry was frustrated by the absence of regulation and a governing body. In 1994, the United Nations (UN) established the International Seabed Authority (ISA) pursuant to the UN Convention on the Law of the Sea (UNCLOS). The ISA governs the development of seabed resources for UNCLOS member states in the territories beyond the exclusive economic zones governed by coastal states. This international territory is known as the Area.

TMC through its subsidiaries, Nauru Ocean Resources Inc. (NORI) and Tong Offshore Mining Limited (TOML), holds exploration contracts for a total of ten areas in the CCZ regulated by the ISA. NORI holds exploration rights to four areas (NORI A, B, C, and D) totaling 74,830 km^2 that were granted in July 2011. TOML holds exploration rights to six areas (TOML A, B, C, D, E and F) covering 74,713 km^2 under an exploration contract approved in July 2011 and then formalized on 11 January 2012.

These exploration contracts were granted and formalize an exploration area, for a term of 15 years with a program of activities approved for the first five-year period. NORI and TOML have a priority right to apply for an exploitation contract to exploit polymetallic nodules in the respective Contract Areas (ISA Regulation 24(2)). Both the NORI and TOML exploration contracts may be extended for periods of five years at a time beyond the initial 15-year period, provided NORI and TOML have made efforts in good faith to comply with the requirements of the plan of work. These exploration contracts do not confer any commercial production rights. A separate Plan of Work for exploitation must be submitted and approved by the ISA Council before any commercial recovery may occur.

At the time of this report, the ISA is yet to finalize the Mining Code, including Regulations on the Exploitation of Mineral Resources in the Area as required under UNCLOS.

In 1980, the Unites States of America (U.S) enacted the Deep Seabed Hard Mineral Resources Act (DSHMRA) 30 U.S.C. §1401 et seq.) authorizing the National Oceanic and Atmospheric Administration (NOAA) to issue licenses for exploration and permits for commercial recovery from the deep seabed. These activities are limited to areas beyond national jurisdiction and are intended to ensure that U.S. entities can participate in seabed mining despite the US not being a party to the UNCLOS or the 1994 Implementation Agreement.

TMC, through its wholly owned subsidiary The Metals Company USA LLC (TMC USA) has submitted requests directly under the U.S. regulatory regime governed by DSHMRA. These applications are summarized below:

- Exploration License for the USA-A Area which covers 65,186 km^2 in the CCZ.
- Exploration License for USA-B Area which covers 121,789 km^2 in the CCZ.

USA-A includes the existing ISA approved exploration Area identified as NORI Area D and TOML area F. USA-B includes the existing ISA approved exploration Areas identified as NORI Areas A, B, C and TOML Areas A, B, C, D, and E.

These applications are still under review and commencement of Commercial Recovery by TMC USA is subject to approval of these licenses under DSHMRA. At the time of writing this report, TMC USA does not hold any exploration licenses or commercial recovery permits under the DSHMRA framework.

TMC USA has submitted applications for such rights, and subject to regulatory review and approval, anticipates that any future commercial recovery activities would be conducted pursuant to a permit issued by National Oceanic and Atmospheric Administration (NOAA) under the U.S. legal regime.

Any reference in this Initial Assessment (IA) to activities proposed to be conducted by TMC USA is inherently uncertain and should be considered forward-looking in nature. No assurance can be given that any permit under DSHMRA will be issued, or that if issued, such permit will contain terms and conditions commercially or operationally viable for the project considered in this IA.

This IA considers only the Areas for which TMC have mineral rights, specifically, the NORI and TOML Areas subject to existing ISA approved exploration licenses (collectively known as the Property). This IA specifically excludes NORI Area D as this is the subject of a separate Pre-Feasibility Study (PFS) (AMC Consultants, 2025).

A phased development is outlined for the NORI and TOML areas that make up the TMC Property. Each offshore collection system comprises collectors on the seafloor, Vertical Transport System (VTS), and Production Vessels (PV) that are expected to collect polymetallic nodules. The nodules are expected to be transferred from the PV to a Transport Vessel (TV). The polymetallic nodules are expected to be shipped to onshore processing facilities, where established processing technology are expected to be used to produce manganese silicate, a feedstock for silico-manganese alloy production used in steel making, and nickel-cobalt-copper matte which is expected to be refined into products in the US that can be used in energy, defense, manufacturing, and infrastructure.

A converted drillship, the Hidden Gem, reclassed as the world's first deepwater mining ship, was used by NORI to support successful test mining in 2022 (Test Mining), where 3,000 wet metric tonnes (wmt) of nodules were lifted to the surface. Learnings from the Test Mining and further testing and modelling completed by Allseas has informed engineering of the First-Generation Mining System (1st Gen), the commercial-scale system as described in the NORI Area D Technical Summary Report (AMC Consultants, 2025). The engineering of the Second-Generation Mining System (2nd Gen) is expected to be informed by the operational and environmental performance of the 1st Gen.

TMC has commissioned AMC Consultants Pty Ltd (AMC) to conduct an IA of developing the full ground position held by TMC through its subsidiaries NORI and TOML. An IA is a conceptual study of the potential viability of Mineral Resources. This Initial Assessment is preliminary in nature, includes Inferred Mineral Resources and describes the economic viability of mining and processing systems that are at conceptual stage of development. However, many of the concepts in the IA are based on systems studied and designed at a prefeasibility level for NORI Area D (AMC Consultants, 2025).

This IA indicates that development of the Mineral Resources within the NORI and TOML Areas, is potentially technically and economically viable and indicates a positive economic outcome is possible. Headline results of the IA financial evaluation are provided in Table 1.1. However, due to the low level of confidence in much of the Mineral Resource base, the need for more exploration, and the need for more detailed evaluation of aspects of the Project, such as seafloor bathymetry, engineering design,

environmental characterization, and mine planning, the technical and economic viability has not yet been demonstrated.

Table 1.1 Project headline financials

Item	UOM	Amount
Total Revenue	US$M	$298,923
Post-Tax NPV8	US$M	$18,081
Post-Tax NPV0	US$M	$122,364
Project IRR (Real Terms)	%	35.6%
Project Payback – after pre-production period	Years	2
EBITDA	US$M	$171,852
EBITDA per tonne (dry nodules)	US$/t	$349
Total Project Capital	US$M	8,852

Note: The economic projections presented in this table are based on Measured, Indicated, and Inferred Mineral Resources and do not support a determination of Mineral Reserves or demonstrate economic viability

1.2 Location

The Property is located within the CCZ of the northeast Pacific Ocean (Figure 3.1) between Hawaii and Mexico. The western end of the CCZ is approximately 1,000 km south of the Hawaiian island group. From here, the CCZ extends over 4,500 km east-northeast, in an approximately 750 km wide trend, with the eastern limits approximately 2,000 km west of southern Mexico. The region is well-located to ship nodules to the American continent or across the Pacific to Asian markets.

The Property comprises of nine separate areas (NORI A, B, C, TOML A, B, C, D, E and F) with a combined area of 124,381 $km^{2.}$

1.3 Regulatory environmental and the tenements

The principal regulatory environments governing the international seabed area include:

- The UN Convention on the Law of the Sea, of 10 December 1982 (The Convention).
- The 1994 Agreement relating to the Implementation of Part XI of the UN Convention on the Law of the Sea of 10 December 1982 (the 1994 implementation Agreement).
- The Deep Seabed Hard Mineral Resources Act (DSHMRA) (30 U.S.C. §1401 et seq.)

Part XI of the Convention and the 1994 Implementation Agreement deals with mineral exploration and exploitation in the Area, providing a framework for entities to obtain legal title to areas of the seafloor from the ISA for the purpose of exploration and eventually exploitation of resources.

The Convention entered into force on 16 November 1994. As of October 2024, the Convention had been signed by 169 States Parties[1] and the European Union. The US is currently not a party to the Convention.

The Deep Seabed Hard Mineral Resources Act, enacted in 1980 by the U.S., authorizes the issuance of Exploration Licenses and Commercial Recovery Permits over the deep seabed. These activities are limited to areas beyond national jurisdiction and are intended to ensure U.S. entities can participate in seabed mining despite not being party to UNCLOS.

[1] https://itlos.org/en/main/the-tribunal/states-parties/

To date, the ISA has issued regulations on prospecting and exploration for polymetallic nodules in the Area.

At the time of this report, the ISA is yet to finalize the Mining Code, including Regulations on the Exploitation of Mineral Resources in the Area as required under UNCLOS.

Consequently, TMC, through its wholly owned subsidiary TMC USA on April 28 2025, submitted applications for two exploration licenses and a commercial recovery permit under the U.S. regulatory regime governed by DSHMRA.

These applications are still under review and TMC's claim to these areas under DSHMRA are subject to approval of these licenses and permits by NOAA. NOAA has advised TMC USA that the exploration license applications are substantially complete, which provides TMC USA with the priority right to areas subject to application, which includes the Property, for the duration of the application process.

1.4 Geology and Mineral Resources

Seafloor polymetallic nodules occur in all oceans, but the CCZ hosts a relatively high abundance of particularly nickel and copper-rich nodules. The CCZ seafloor forms part of the Abyssal Plains, which are the largest physiographic province on Earth.

The average depth of the seafloor in the Project area ranges from 3,800 m to over 6,000 m. The Abyssal Plains are traversed by ridges and are punctuated by inactive volcanoes rising 500 up to 2,000 m above the seafloor.

The formation and distribution of polymetallic nodules in the CCZ are primarily controlled by water depth, latitude, and seafloor sediment type. Geological domains identified include volcanic outcrops, volcanic highs, sediment drifts, and high-slope (>6°) areas, which were excluded from resource estimates.

Exploration data underpinning the Mineral Resource estimates comprise historical sampling by Pioneer Contractors using free-fall grab samplers (FFG) and box core (BC) samplers, supplemented by recent campaigns conducted by NORI and TOML involving box coring, dredging, multibeam echosounder MBES surveys, side scan sonar, sub-bottom profiling, autonomous underwater vehicle (AUV) deployments, and photographic seabed imaging.

Nodule abundance is reported on a wet basis with an assumed moisture content of 28% for TOML areas, and 24% for NORI-A, B, and C. No significant correlations were found between moisture content and nodule size, grade, or geological domain. Nodule size measurements and long-axis estimation methods were applied to improve abundance estimates from photographic data.

Mineral Resource estimation employed geostatistical techniques including declustering to correct for sample spacing bias, variogram modeling to characterize spatial continuity, and Ordinary Kriging for grade interpolation. The Mineral Resource classification follows SEC Regulation S-K (subpart 1300), with Measured, Indicated, and Inferred categories assigned based on data density and quality (Table 1.2). Areas with sparse data or high uncertainty, such as volcanic highs and steep slopes, were excluded.

Table 1.2 NORI and TOML Mineral Resource estimates, in situ, at 4 kg/m^2 abundance cut-off

Area	Classification	Tonnes (Mwmt)	Abundance (wet kg/m^2)	Ni (%)	Cu (%)	Co (%)	Mn (%)
NORI-A	Inferred	72	9.3	1.35	1.06	0.22	28.0
NORI-B	Inferred	36	11.0	1.43	1.13	0.25	28.9
NORI-C	Inferred	402	11.0	1.26	1.03	0.21	28.3
TOML-A	Inferred	114	11.1	1.11	0.96	0.23	25.0
TOML-B	Measured	3	11.8	1.3	1.0	0.2	27.6
TOML-B	Indicated	14	11.1	1.3	1.1	0.2	28.6
TOML-B	Inferred	63	9.1	1.2	1.0	0.3	25.9
TOML-C	Indicated	15	8.6	1.3	1.2	0.2	30.5
TOML-C	Inferred	115	9.0	1.3	1.1	0.2	28.2
TOML-D	Indicated	29	12.2	1.3	1.2	0.2	30.1
TOML-D	Inferred	102	9.0	1.3	1.2	0.2	28.8
TOML-E	Inferred	58	10.6	1.3	1.1	0.2	28.7
TOML-F	Indicated	12	21.6	1.5	1.2	0.1	32.5
TOML-F	Inferred	244	16.6	1.4	1.2	0.1	32.2

Note: Tonnes are quoted on a wet basis; grades are reported on a dry basis consistent with industry practice. Moisture content was estimated to be 28% w/w for TOML and 24% for NORI-A, -B, and -C. These estimates are presented on an undiluted basis without adjustment for resource recovery. The estimates in this table include Inferred, Measured and Indicate Mineral Resources. These are not Mineral Reserves and do not have demonstrated economic viability.

1.5 Development plan and mining methods

The development plan for the Property envisions a phased, 23-year mining operation leveraging advanced offshore technologies including remotely operated Collector Vehicles (CV), VTS, and PVs. Mining is expected to target polymetallic nodules on seafloor slopes up to 6°, with recovered nodules transported to onshore facilities for processing into manganese silicate and nickel-cobalt-copper products essential for steelmaking and battery materials.

The life of mine schedule prioritizes higher grade areas, commencing with TOML-F before progressing through the other areas in a systematic sequence designed to optimize resource extraction and maintain steady production aligned with processing capacity. Environmental safeguards such as buffer zones are integrated throughout the plan. This approach, informed by exploration in the NORI and TOML areas and Test Mining and environmental studies conducted in NORI Area D provides a framework for developing the Mineral Resource in the wider Property. The development of these NORI and TOML areas are expected to benefit from the offshore and onshore experience gained through operating in NORI Area D.

The mining method for the NORI and TOML areas employs bespoke deep-sea technology featuring remotely operated, self-propelled, tracked CVs equipped with Coandă nozzles to efficiently recover polymetallic nodules from the seafloor. These CVs are expected to operate on slopes up to 6°, removing nodules while minimizing sediment disturbance. Nodules are expected to be transported via a VTS using airlift or hydraulic pumps to PVs on the surface, where dewatering and offloading is expected to occur before shipment to processing facilities.

These 2nd Generation Production Systems are expected to build on successful Test Mining conducted in 2022 in NORI Area D and a decade of experience that is expected to be gained from operating a 1st Generation Production System in the NORI Area D.

A total of eight PVs are expected to operate within the Property across the 23 year mine life. Each PV is fitted with three 20 m wide CVs and is capable of producing 7 million wet metric tonnes per annum (Mwmtpa) of nodules in the high abundance areas within TOML-F and 5 Mwmtpa in the other areas that make up the Property.

The fleet of production, transport, and supply vessels are expected to be coordinated through centralized offshore control centers, enabling safe, efficient, and adaptive operations with reduced offshore personnel exposure. This innovative mining approach is designed to maximize resource recovery while maintaining environmental stewardship and operational reliability in the challenging deep-sea environment.

1.6 Mineral processing and metallurgical testing

The mineral processing strategy is supported by extensive bench-scale and pilot-scale metallurgical testwork that has demonstrated the technical feasibility of converting polymetallic nodules into marketable products. Bulk sampling and Test Mining successfully recovered nodule material from NORI Area D that was used for large scale processing trials.

The processing flowsheet involves drying and calcining the nodules in a rotary kiln(s) followed by electric furnace (RKEF) smelting to produce two immiscible phases: a nickel-cobalt-copper-rich alloy and a manganese silicate oxide slag. A pilot plant campaign produced 35 t of calcine that was then smelted at eXpert Process Solutions (XPS, a division of Glencore) and tested in industrial scale trials by Pacific Metals company Ltd (PAMCO), producing demonstration quantities of these target products with stable operation and emissions compliant with relevant regulations. High recoveries were achieved, including approximately 97% for nickel, 93% for cobalt, 94% for copper, and 99% for manganese. The alloy is expected to be further processed in Peirce-Smith converters to generate a matte product containing 5% iron. This was also piloted at XPS with suitable quantities of matte generated to feed downstream refinery bench-scale testing.

Matte is expected to be refined hydrometallurgically using a two-stage leach process, followed by copper electrowinning, cobalt and nickel solvent extractions (SX), impurity removal steps and crystallization of the nickel and cobalt phases to generate sulfate products. The copper phase that are expected to be generated following the electrowinning is copper cathode. Bench-scale testing at Lakefield, Ontario (SGS) was able to generate about 1 kg of nickel and cobalt sulfates suitable for use in batteries.

The process design leverages existing ferronickel production assets in Indonesia with minor modifications to accommodate nodule feedstock, supporting cost-effective commercial-scale operations. New build refineries in the USA are expected to then complete the conversion of the matte produced in Indonesia to saleable materials.

1.7 Market studies

Benchmark Mineral Intelligence (BMI) was contracted by TMC to provide market overviews for three commodities: nickel, cobalt, and copper and to provide forecasts for the premia/discounts for nickel and cobalt sulfate over nickel metal price forecasts.

CRU Group (CRU) was commissioned by NORI to examine the marketability and pricing for the three intermediate products that are expected to be produced (CRU, 2024):

- Nickel-cobalt-copper alloy.
- Nickel-cobalt-copper matte.
- Manganese silicate.

Additionally, CRU was retained to provide manganese ore market forecasts.

The global market for critical metals like nickel, cobalt, and copper is expected to grow significantly, driven by demand from sectors such as the transportation, electrical infrastructure and consumer goods sectors. BMI and CRU forecast the following metal supply, demand and price scenarios:

- Nickel production, led by Indonesia, is expected to rise from 3.6 Mt in 2025 to 4.9 Mt by 2035, fuelled by about equal its demand in stainless steel and EV batteries.
- Cobalt demand is expected to grow at a 5.8% compound annual growth rate through 2030, dominated by battery production, with supply heavily reliant on the Democratic Republic of Congo (DRC) and China. But as mines begin to deplete reserves and the visibility for new assets into the 2030s is limited, BMI's expectation for mine supply is a slight decline into the 2030s.
- Manganese remains essential for steelmaking, although projected demand is forecast to remain flat. However, this is expected to be tempered by rapid demand growth in battery-grade products.
- Copper, a critical for green energy infrastructure, faces an 8 Mt shortfall by 2035, despite production increases in Africa.
- Prices for these metals are forecast to rise steadily due to tightening supply-demand dynamics.

TMC manganese silicate and TMC matte are expected by CRU to gain market traction given their high quality. CRU notes:

- TMC manganese silicate offers advantages in silico-manganese alloy production and battery applications, with demand projected to grow alongside manganese markets.

1.8 Environmental studies, permitting, community, or social impact

Extensive environmental baseline studies and impact assessments have been conducted in NORI Area D and are planned to be expanded across the other NORI and TOML areas to support responsible deep-sea mining development in the CCZ. These studies are expected to encompass geological, oceanographic, biogeochemical, benthic ecological, and trace metal analyses, building from the current knowledge base generated through extensive offshore efforts in NORI Area D and the growing dataset in published literature.

The ISA provides an exploration regulatory framework, requiring comprehensive Environmental and Social Impact Assessments (ESIA) and Environmental Impact Statements (EIS) as prerequisites for moving to exploitation licensing. Both NORI and TOML are compliant with current ISA exploration contract obligations.

Environmental management plans are expected to incorporate mitigation strategies informed by the 2022 Test Mining, which demonstrated limited and manageable environmental impacts.

Key social benefits include community development and training programs, particularly supporting the Republic of Nauru and Tonga. The absence of competing economic uses and landowner displacement further supports the project's social license. A key environmental benefit compared to terrestrial mines is that the project is expected to essentially produce zero waste from the mining and processing of the nodules.

Overall, the environmental and social programs establish a strong foundation for sustainable seabed mineral development while ensuring adherence to evolving international and national regulatory requirements.

1.9 Capital and operating cost estimates

The proposed strategy for the project includes engaging contract miners to conduct polymetallic nodule collection and transport to existing RKEF facilities in Indonesia with Contractor capital investment recovered in the first 10 years of operation. Sustaining capital during PV class surveys is included for the collection equipment. RKEF processing in Indonesia is expected to be by tolling arrangement. Matte from RKEF facilities in Indonesia is expected to be shipped to the USA for refinement through TMC built / owned / operated infrastructure with associated capital expenditure (CAPEX) and operating expenditure (OPEX) included.

The CAPEX for the NORI and TOML projects is estimated at approximately US$15,000 million, encompassing Project capital of $8,850 million, sustaining capital over the life of mine (LOM) of US$5,300 million, with closure costs estimated at US$805 million.

OPEX is forecasted at approximately US$126,000 million over the LOM, averaging US$188.3 per wet metric tonne of nodules processed. Key OPEX components include collection, transport, processing, refining, consumables, and corporate costs, with processing and refining representing the largest shares.

These cost estimates, prepared to an IA -level confidence standard, incorporate contingencies and reflect current engineering designs and operational plans.

1.10 Economic evaluation

The economic evaluation of the NORI and TOML projects demonstrates potential for strong financial viability based on a real, ungeared, post-tax discounted cash flow model using an 8% discount rate over a 23-year life of mine starting in 2037. The analysis incorporates metal price forecasts, metallurgical recoveries, payabilities, and detailed cost structures without inflation or escalation.

In the model, the proposed project delivers a post-tax net present value (NPV8) of approximately US$18,100 million and an EBITDA of US$172,000 million over the LOM. Sensitivity analyses highlight the project's resilience to fluctuations in metal prices, operating costs, and capital expenditures. Cash cost analysis positions the operation competitively within the global nickel market, supported by significant by-product credits from cobalt, copper, and manganese.

Overall, the economic evaluation confirms the robust commercial potential of the project under current assumptions. However, due to the low level of confidence in much of the Mineral Resource base, the need for more exploration, and the need for more detailed evaluation of aspects of the Project, such as seafloor bathymetry, engineering design, environmental characterization, and mine planning, the technical and economic viability has not yet been demonstrated.

1.11 Qualified Person's conclusions and recommendations

The Qualified Persons (QPs) recommend advancing the NORI and TOML projects through continued engineering development, environmental management, and operational planning to support a prefeasibility study.

Key priorities include more detailed bathymetric surveys, detailed definition and increase in confidence in the Mineral Resources, developing mine plans aligned with finalized Commercial Recovery Permit conditions, design and testing of 2nd Gen CVs, VTSs, PVs, and associated infrastructure, refinement of CAPEX and OPEX estimates. The buildup of experience expected through development and operation of the 1st Gen in NORI Area D are expected to be important for derisking the Project.

Expanding engineering studies and design efforts for the hydrometallurgical plant capabilities is required to meet required plant availability to manage proposed production volumes. Engagement and commercial arrangements with existing or emerging industry partners is key to TMC operating strategy and therefore recommended.

Environmental monitoring and adaptive management frameworks should be refined and aligned with finalized Commercial Recovery Permit conditions.

These recommendations collectively aim to mitigate risks, improve technical and economic outcomes, and support responsible advancement of the TMC Property.

Contents

1 Executive summary i
1.1 Introduction i
1.2 Location iii
1.3 Regulatory environmental and the tenements iii
1.4 Geology and Mineral Resources iv
1.5 Development plan and mining methods v
1.6 Mineral processing and metallurgical testing vi
1.7 Market studies vi
1.8 Environmental studies, permitting, community, or social impact vii
1.9 Capital and operating cost estimates viii
1.10 Economic evaluation viii
1.11 Qualified Person's conclusions and recommendations viii

2 Introduction 4
2.1 Registrant, terms of reference and purpose of report 4
2.2 Sources of information and data 5
2.3 Qualified personnel 5
2.4 Update to a previously filed Technical Report 7

3 Property description and location 8
3.1 Tenements and permits 8
3.1.1 United Nations Convention on the Law of the Sea 11
3.1.1.1 International Seabed Authority 13
3.1.2 Deep Seabed Hard Mineral Resources Act (DSHMRA) 13
3.1.2.1 National Oceanic and Atmospheric Administration (NOAA) 13
3.2 Exploration contract obligations and sponsorship 14
3.2.1 Work program 15
3.2.2 Royalties and taxes 16

4 Accessibility, climate, local resources, infrastructure and physiography 17
4.1 Accessibility and infrastructure 17
4.2 Climate 17

5 History 18
5.1 Overview 18
5.2 Pioneer Contractors 18
5.3 NORI 22
5.4 TOML 23

6 Geological setting and mineralization 24
6.1 Global distribution of nodules 24
6.2 Regional tectonic setting and topographic features 24
6.3 Regional geological domains 26
6.4 Regional trends in polymetallic mineralization 27
6.5 Nodule formation and sedimentation 33
6.6 Nodule facies 36
6.7 Diagenetic crusts 1
6.8 Moisture content of nodules 1
6.9 Density of nodules 2
6.10 Abundance of nodules in NORI and TOML 3
6.11 Nodule size distribution 4

6.11.1 NORI Area D - Physical measurement of size and estimation of abundance 4
6.11.2 NORI Area D - Measurement of nodule dimensions using image processing 6
6.11.3 TOML Areas – Measurement of nodule sizes 10

7 Exploration 11
7.1 Free fall grab sampling method 11
7.2 Box core sampling method 12
7.3 Comparison of FFG and BC samples 15
7.4 Multibeam Bathymetry methods 16
7.5 Historical exploration data 16
7.5.1 Pioneer Contractor sample data supplied to NORI 17
7.5.2 Pioneer Contractor sample data supplied to TOML 19
7.6 NORI exploration data 21
7.6.1 Dredging and nodule sampling 21
7.6.2 Box-coring and nodule sampling 23
7.6.3 MBES surveys 23
7.6.4 AUV surveys 24
7.6.5 Long axis estimation 25
7.6.6 Geotechnical data collection 27
7.7 TOML exploration data 27
7.7.1 Dredging and nodule sampling 28
7.7.2 Box-coring and nodule sampling 29
7.7.3 MBES surveys 33
7.7.4 Deep-tow surveys 33
7.7.5 Long axis estimation 34
7.7.6 Geotechnical data collection 38

8 Sample preparation, analysis, and security 44
8.1 Pioneer Contractor data 44
8.2 TOML data 44
8.2.1 Box core samples 44
8.2.2 Abundance estimates by LAE method 46
8.3 NORI-A, B, C data 46

9 Data verification 48
9.1 TOML data 48
9.2 NORI-A, B, C data 49

10 Mineral processing and metallurgical testing 50
10.1 Metallurgical testwork 50
10.2 Bulk sample collection testwork 51
10.3 Bulk sampling testing laboratories 52
10.4 Summary of test work results 52
10.4.1 Round robin assaying program 52
10.4.2 Key findings of calcination at FLS 55
10.4.3 Piloting – Electric Furnace Smelting at XPS – Metallurgical Summary 56
10.4.4 Smelting: metallurgical results 58
10.4.4.1 Partition coefficients (PC) in smelting 58
10.4.4.2 Slag chemistry 62
10.4.4.3 Elemental distribution – partition coefficients in converting 63
10.4.5 Demonstration scale trials at PAMCO 67

10.4.6 Hydrometallurgical refinery bench scale testing 68
10.4.6.1 Two-stage leaching 68
10.4.6.2 Cobalt refining 69
10.4.6.3 Nickel refining 69
10.5 Iron in final matte 70
10.6 Manganese silicate 70
10.7 Summary and QP's opinion 71

11 Mineral Resource estimates 72
11.1 Cautionary note regarding Mineral Resource estimates 72
11.2 Estimation process for NORI-A, B and C 72
11.2.1 Geological domains 72
11.2.2 Nodule sample data 72
11.2.3 Declustering 74
11.2.4 Top-cuts 74
11.2.5 Spatial continuity 75
11.2.6 Geological block model 77
11.2.7 Mineral Resource estimation 77
11.2.8 Mineral Resource classification 78
11.3 Estimation process for TOML-A, B, C, D, E and F 78
11.3.1 Geological domains 79
11.3.2 Nodule sample data 83
11.3.3 Sample statistics 84
11.3.4 Representativeness of sampling 91
11.3.5 Spatial continuity 95
11.3.6 Variography of nodule coverage estimated from photo profiles 99
11.3.7 Variography of nodule abundance estimated from photo profiles 100
11.3.8 Variography of the backscatter data 100
11.3.9 Geological block model 101
11.3.10 Mineral Resource estimation 102
11.3.11 Mineral Resource classification 102
11.4 Cut-off grade 102
11.5 Estimation results 103
11.5.1 NORI-A, B and C 103
11.5.1 TOML-A, B, C, D, E and F 106

12 Mineral Reserve estimates 113

13 Mining methods 114
13.1 Overview 114
13.2 Development plan 114
13.3 Offshore mining system 114
13.3.1 Test Mining in NORI Area D in 2022 114
13.3.2 First generation production system to operate in NORI Area D (1st Gen) 116
13.3.3 Second generation production system (2nd Gen) 117
13.3.3.1 Mining concept 117
13.3.3.2 PV 118
13.3.3.3 Collector Vehicle (CV) 119
13.3.3.4 Vertical Transport System (VTS) 122
13.3.3.5 Dewatering 124
13.3.3.6 Nodule handling, storage and offload 124
13.3.3.7 TV 124
13.3.3.8 Operating conditions and downtime 125

13.4 Offshore support and logistics 126
13.5 Mining philosophy 127
13.6 Offshore operations 127
13.6.1 PVs 127
13.6.2 TVs 127
13.6.3 SVs 128
13.6.4 Onshore control centre and Offshore maintenance 128
13.6.5 Marine infrastructure 128
13.7 Update of potential mining domains 129
13.8 LOM basis of design 135
13.8.1 Mine planning factors overview 135
13.8.2 Quantity of nodules recovered by the collector vehicle 136
13.8.2.1 Potential mining domains 136
13.8.2.2 Buffer Zones 137
13.8.2.3 Geo-obstacles 137
13.8.2.4 Gap between collector paths 138
13.8.2.5 Nodule collection recovery 138
13.8.2.6 Overall recoverable inventory 139
13.8.3 Quantity of nodules recovered to market 140
13.8.3.1 Physical capacity of the CVs 140
13.8.3.2 Weather 140
13.8.3.3 Planned maintenance and unplanned repairs 141
13.8.3.4 Field efficiency 142
13.8.3.5 Production rate summary 142
13.9 LOM plan 143
13.9.1 LOM plan assumptions 143
13.9.2 LOM plan result 144

14 Processing and recovery methods 151
14.1 Overview 151
14.2 Flowsheet options screening and selection 152
14.2.1 Manganese product and associated market 152
14.2.2 Near zero solid waste generation 154
14.3 Process description 154
14.3.1 Alloy production 155
14.3.2 Matte production 155
14.3.3 Matte refining 155
14.4 Flowsheet development 156
14.4.1 Literature review 156
14.4.2 Bench-scale test work 157
14.4.3 Concept engineering 158
14.4.4 Piloting 158
14.4.4.1 Piloting overview 158
14.4.4.2 Calcining at FLSmidth 159
14.4.4.3 Smelting, sulfidation and converting at XPS 161
14.4.5 Demonstration scale calcining and smelting trials 163
14.4.6 Manganese silicate slag quality 164

15 Project infrastructure 165
15.1 Onshore engineering 165
15.1.1 Overview 165
15.1.2 Front-end nodule processing to matte in Indonesia 165

15.1.2.1 Recent build-out of RKEF processing capacity in Indonesia 166
15.1.2.2 Increasing difficulty sourcing high-grade saprolite ores 166
15.1.2.3 Economic performance: Increasing losses 167
15.1.2.4 Prospects for polymetallic nodule processing 167
15.1.2.5 Indonesian processing cost benchmarking 168
15.1.2.6 Product quality specifications 169
15.1.3 Matte refining in the US 170
15.1.3.1 Further processing of nodules in the US 170
15.1.4 Production plan 170
15.2 Offshore infrastructure 172

16 Market studies 173
16.1 TMC offtake agreement 173
16.2 Marketing analysis 173
16.3 Market outlook 174
16.3.1 Nickel 174
16.3.1.1 Nickel market overview 174
16.3.1.2 Nickel supply 174
16.3.1.3 Nickel demand 174
16.3.1.4 Nickel supply gap and prices 175
16.3.2 Cobalt 175
16.3.2.1 Cobalt market overview 175
16.3.2.2 Cobalt supply 175
16.3.2.3 Cobalt demand 175
16.3.2.4 Cobalt supply gap and prices 175
16.3.3 Manganese 176
16.3.3.1 Manganese market overview 176
16.3.3.2 Manganese supply 176
16.3.3.3 Manganese demand 176
16.3.3.4 Manganese supply gap and prices 176
16.3.3.5 EMM and MnSO4 177
16.3.4 Copper 177
16.3.4.1 Copper market overview 177
16.3.4.2 Copper supply 177
16.3.4.3 Copper demand 177
16.3.4.4 Copper supply gap and prices 177
16.4 TMC manganese silicate 177
16.5 TMC matte 178
16.6 Refinery products 179
16.7 Revenue forecasts 179

17 Environmental studies, permitting and social or community impact 182
17.1 Permitting process 182
17.1.1 ISA 182
17.1.1.1 NORI 183
17.1.1.2 TOML 183
17.1.1.3 Compliance status 183
17.1.2 Deep Seabed Hard Mineral Resources Act 184
17.1.2.1 Compliance status 184
17.1.2.2 Alternate permitting pathways 184
17.2 Transferable information from NORI Area D and TOML-F 185
17.2.1 Baseline studies 185

17.2.1.1 Regional geological setting 185
17.2.1.2 Substrate composition and geotechnical characteristics 185
17.2.1.3 Polymetallic nodules: Abundance, chemistry, and variability 185
17.2.1.4 Water mass distribution and circulation dynamics 186
17.2.1.5 Biogeochemical baselines: Nutrients, organic carbon, and carbonate chemistry 186
17.2.1.6 Benthic biological communities: Diversity, connectivity, and temporal variability 187
17.2.1.7 Trace metals in sediments and porewaters 188
17.2.2 Test mining 188
17.2.3 Summary and implications for the wider CCZ 189
17.3 Scope of baseline studies 189
17.4 Post mining land uses 191
17.5 Remediation 191
17.6 Tailings 191
17.7 Mitigation plans 192

18 Capital and operating costs 193
18.1 Introduction 193
18.2 Operating strategy 193
18.2.1 Baseline operating assumptions 194
18.3 CAPEX 195
18.3.1 Production vessel #5-12 195
18.3.2 Refining facility 195
18.3.3 Sustaining CAPEX 196
18.3.4 Closure CAPEX 196
18.4 OPEX 197
18.4.1 Collection costs 198
18.4.2 Shipping costs 198
18.4.3 Contractor (offshore) costs 199
18.4.4 Consumables (offshore fuel) costs 199
18.4.5 Processing cost 200
18.4.6 Refining cost 201
18.4.7 Corporate cost 201

19 Economic analysis 203
19.1 Cautionary statement regarding forward-looking information 203
19.2 Methodology used 204
19.3 Economic model parameters 204
19.4 Total development costs 204
19.5 Total sustaining costs 204
19.6 Total closure costs 204
19.7 Total operating costs 204
19.8 Commodity prices 205
19.9 Recovery rates 205
19.10 Payable terms 205
19.11 Royalty / Payments 206
19.11.1 Nauru continuity benefits 206
19.11.2 Tonga continuity benefits 206
19.11.3 Low Carbon Royalty (LCR) 207
19.12 Taxes 207
19.13 Economic analysis 207

19.14 Sensitivity analysis 226
19.15 Cash cost analysis 227
19.16 Conclusion economic analysis 228
20 Adjacent properties 229
20.1 TOML-F 229
20.2 NORI-C 230
20.3 TOML-D and TOML-E 230
20.4 TOML-C 230
20.5 TOML-B and NORI-B 231
20.6 NORI-A 231
20.7 TOML-A 231
21 Other relevant data and information 232
22 Interpretation and conclusions 233
22.1 Mineral tenure 233
22.2 Exploration and data verification 233
22.3 Mineral processing testwork 234
22.4 Mineral Resource 234
22.5 Mining methods 235
22.6 LOM planning 235
22.7 Processing 236
22.8 Infrastructure 236
22.9 Market studies 236
22.10 Environmental studies 237
22.11 Capital and operating costs 238
22.12 Economic evaluation 238
23 Recommendations 239
24 References 240
25 Reliance on information provided by the registrant 246

Tables

Table 1.1 Project headline financials iii
Table 1.2 NORI and TOML Mineral Resource estimates, in situ, at 4 kg/m^2 abundance cut-off v
Table 2.1 List of Qualified Persons responsible for each Section 5
Table 2.2 TMC Qualified Persons responsible for each section 6
Table 3.1 NORI Area details 9
Table 3.2 NORI Area extents 9
Table 3.3 TOML exploration area in the CCZ 9
Table 3.4 TOML area extents 9
Table 5.1 NORI and TOML ISA exploration Contract Areas and Pioneer Contractors 18
Table 6.1 Polymetallic Nodule Facies in NORI Area D 36
Table 7.1 Summary of Pioneer Contractor sample assay data from the NORI Areas 18
Table 7.2 Summary of Pioneer Contractor sample assay data in TOML areas 20
Table 7.3 Summary of Historical Samples from the Reserved Areas outside the TOML Contract Area 20
Table 7.4 NORI-A, B, C datasets 21

Table 7.5 Assay Results for NORI-B Nodule Samples 23
Table 7.6 TOML datasets by area and by campaign 28
Table 10.1 Comparison of bulk sample analyses with NORI Area D measured resource for the test mining area. 51
Table 10.2 Location and testing methods of laboratories used 52
Table 10.3 Analytical methods undertaken by each laboratory 53
Table 10.4 Nickel laboratory results 54
Table 10.5 Copper laboratory results 54
Table 10.6 Cobalt laboratory results 54
Table 10.7 Manganese laboratory results 55
Table 10.8 CRM results for each laboratory 55
Table 10.9 Updates to Process Design Criteria from pilot kiln test work 56
Table 10.10 Pilot calcine blend assay vs. process model update mass balance 56
Table 10.11 Pilot metal assays vs. process model mass balance 57
Table 10.12 Pilot smelting slag assays vs. process model mass balance 57
Table 10.13 Pilot matte assays vs. process model mass balance 58
Table 10.14 Optimum leach parameters and extractions 68
Table 10.15 Optimum leach assays 69
Table 10.16 Assays of input and output streams from the CoSX 69
Table 10.17 Comparison between TMC's lab-generated cobalt sulfate crystals with an external third-party specification 69
Table 10.18 Comparison between TMC's lab-generated nickel sulfate crystals with two external third-party specifications 70
Table 10.19 Target specifications for manganese silicate 70
Table 11.1 Summary statistics of samples within the NORI Area used for the 2012 Mineral Resource estimate. 72
Table 11.2 Minimum and maximum UTM coordinates for NORI Areas 74
Table 11.3 NORI-A, B, C and D declustered statistics (historic data only) 74
Table 11.4 NORI-A, B, C and D top cuts used for NORI 2012 Mineral Resource estimate 75
Table 11.5 Variogram models for NORI-A, B and C 75
Table 11.6 NORI-A, B and C block model framework (UTM coordinates) 77
Table 11.7 NORI-A, B and C model variables 77
Table 11.8 Minimum and maximum UTM coordinates for each TOML Area 84
Table 11.9 Statistics of all samples within the TOML Areas 85
Table 11.10 Declustered statistics of all nodule samples within TOML Area 85
Table 11.11 Statistics of Pioneer Contractor samples within the TOML Areas 85
Table 11.12 Statistics of TOML samples within the TOML Areas 85
Table 11.13 Statistics of TOML LAE samples within the TOML Areas 85
Table 11.14 Variogram models 97
Table 11.15 Comparison of model areas and actual license areas 101
Table 11.16 NORI-TOML breakeven cut-off abundance estimate 103
Table 11.17 NORI-A, B and C Mineral Resource estimate, in situ, at 4 kg/m^2 abundance cut-off .. 104

Table 11.18 TOML Area Mineral Resource estimate, in situ, at a 4 kg/m^2 nodule abundance cut-off 107
Table13.1 2nd Gen PV key specifications 119
Table 13.2 2nd Gen TV Key Specifications 124
Table 13.3 PV key operating parameters 127
Table 13.4 TV average cycle time estimate 128
Table 13.5 Slope and seamount adjustments 136
Table 13.6 Geo-obstacle assumptions 137
Table 13.7 Geo-obstacle mine planning factors 138
Table 13.8 Nodule recovery components 139
Table 13.9 Overall nodule inventory by area, outside of areas >6º and seamount and lease buffers with <4 kg/m^2 abundance cut off. 139
Table 13.10 Additional losses and recoverable inventory summary 140
Table 13.11 Metocean statistics for the Property 141
Table 13.12 Production rate summary 143
Table 13.13 LOM plan production summary 145
Table 14.1 Simple Screening Process for Various Nodule Processing Flowsheet Options 152
Table 14.2 Summary of Bench-scale Test Work 158
Table 14.3 Summary of pilot scale test work 159
Table 15.1 Summary of the benchmarked costs derived from SMM source data 168
Table 15.2 Sample grades of key pay metals for the matte being generated in Indonesia 169
Table 15.3 Sample specification for the manganese silicate product generated in Indonesia 169
Table 15.4 TMC USA IA production plan 171
Table 16.1 Metal and metal sulfate price forecasts (real US$ 2025) 179
Table 16.2 Metallurgical recoveries 179
Table 16.3 Ni-Co-Cu matte payable terms percentage of LME benchmark prices 179
Table 16.4 Forecast payable metal production - metal in matte 180
Table 16.5 Forecast payable refined metal production - metal in sulfate and cathode 180
Table 16.6 Forecast production – manganese in manganese silicate 180
Table 16.7 Revenue Forecast US$ 2025 Real 181
Table 18.1 Total CAPEX summary 195
Table 18.2 PV recovered CAPEX summary 195
Table 18.3 Refining facility recovered CAPEX summary 196
Table 18.4 Sustaining CAPEX 196
Table 18.5 Closure CAPEX 197
Table 18.6 OPEX summary 197
Table 18.7 OPEX unit cost US$/wmt summary 198
Table 18.8 Collection costs summary 198
Table 18.9 Shipping Costs Summary 199
Table 18.10 Offshore contractor costs summary 199
Table 18.11 Offshore fuel costs summary 200
Table 18.12 Processing costs summary 200

Table 18.13 Refining summary 201
Table 18.14 Corporate costs summary 201
Table 19.1 Total operating costs 205
Table 19.2 Average LOM commodity prices 205
Table 19.3 Recovery rates 205
Table 19.4 LOM average payable terms 206
Table 19.5 Nauru continuity benefits payment schedule 206
Table 19.6 Tonga continuity benefits payment schedule 206
Table 19.7 Summary of forecast project economics 208
Table 19.8 Project cash flow on an annualized basis 210
Table 19.9 C1 Nickel cash cost 227
Table 19.10 All-in Sustaining Cost 228
Table 20.1 Mineral Resource for NORI Area D, at 30 June 2025, at 4 wet kg/m^2 abundance cut-off 229
Table 20.2 Summary of Mineral Resource reported for BGR exploration Contract Area 230

Figures

Figure 3.1 Location of NORI and TOML Project and other ISA exploration areas within the CCZ. ... 8
Figure 3.2 NORI and TOML Areas 10
Figure 3.3 Map of seafloor jurisdictions 12
Figure 3.4 Maritime space under the 1982 UNCLOS 12
Figure 4.1 Global cargo shipping network 17
Figure 5.1 Schematic of Lockheed Group's 1970s trial mining system 20
Figure 5.2 Remote operated collector used by the Lockheed Group in 1970s trial mining 20
Figure 6.1 Schematic diagram of average abundance of polymetallic nodules in four major locations 24
Figure 6.2 Bathymetric map of the Clarion-Clipperton Fracture Zone 25
Figure 6.3 Formation of abyssal hills at mid-oceanic ridges 25
Figure 6.4 Map of nickel grade distribution in the CCZ 28
Figure 6.5 Map of cobalt grade distribution in the CCZ 29
Figure 6.6 Map of copper grade distribution in the CCZ 30
Figure 6.7 Map of manganese grade distribution in the CCZ 31
Figure 6.8 Map of abundance distribution in the CCZ 32
Figure 6.9 Polymetallic Nodule Types 34
Figure 6.10 Sections through a S-type Nodule (left) and a R-type Nodule with a S-type core (right) 34
Figure 6.11 Example nodules found in the TOML area 35
Figure 6.12 Examples of nodules recovered during the 2018 NORI Area D campaign 35
Figure 6.13 Camera Imagery Showing Change from Type 3 Nodules (right) to Type 2 (left) 37
Figure 6.14 Map of nodule classification compared to backscatter intensity 38
Figure 6.15 Density data from TOML Areas B, C, D and F and Hessler and Jumars (1974) 3
Figure 6.16 Schematic representation of average proportion of nodules by depth in the box cores in NORI Area D campaign C3 4

Figure 6.17 Scatter plot comparing axis lengths of 500 manually measured nodules 5
Figure 6.18 Scatter plot comparing actual versus predicted nodule abundance in C7A box cores .. 6
Figure 6.19 Scatter plot of nodule major axis dimension versus nodule intermediate axis dimension for all nodules 7
Figure 6.20 Box plots of nodule major axis dimension for all box cores 8
Figure 6.21 Log probability plot of nodule major axis dimensions by interpreted nodule facies 9
Figure 6.22 Plans showing nodule sizes and types from TOML F and sub-areas B1, C1, D1, D2, and F1 10
Figure 7.1 Cartoon showing the recovery of nodules using a free fall grab sampler 12
Figure 7.2 Cartoon showing the recovery of nodules using a BC sampler 12
Figure 7.3 KC Denmark 0.75 m^2 box corer 14
Figure 7.4 Comparison of returned abundances from BC and FFG at test stations within the KORDI exploration area 15
Figure 7.5 MBES operations schematic 16
Figure 7.6 Box plots of sample grades within the NORI areas compared with all other data from the Reserved Blocks 19
Figure 7.7 Box Plots of Pioneer Contractor sample assay data within the TOML Contract Areas . 21
Figure 7.8 Examples of Nodule Samples Recovered during NORI's 2012 Exploration Campaign . 22
Figure 7.9 Photos of Nodules Collected from NORI-A during the 2013 NORI campaign 23
Figure 7.10 Example of AUV camera photo mosaic from NORI Area D, showing nodules 25
Figure 7.11 Comparison of nodule long axis measurements, taken using digital calipers, and individual nodule wet weight for BC001, BC002, BC003, and BC005 26
Figure 7.12 Dredge sample locations in TOML areas from CCZ13 and CCZ15 campaigns 29
Figure 7.13 Nodule abundance and BC locations, TOML-B sub-area B1 30
Figure 7.14 Nodule abundance and BC locations, TOML-C sub-area C1 30
Figure 7.15 Nodule abundance and BC locations, TOML-D sub-area D2 31
Figure 7.16 Nodule abundance and BC locations, TOML-D sub-area D1 31
Figure 7.17 Nodule abundance and BC locations, TOML-F and sub-TOML-F1 32
Figure 7.18 CCZ13 MBES bathymetry coverage 33
Figure 7.19 Photo-profile logging of nodule coverage (%) and outcrop types in TOML Areas 34
Figure 7.20 Example of LAE measurement using bottom shot, top shot and grid photographs 36
Figure 7.21 TOML-B correlations with best fit factors (L) and Felix 1980 factors (R) 37
Figure 7.22 TOML-C correlations with best fit factors (L) and Felix 1980 factors (R) 37
Figure 7.23 Comparison of physical samples and LAE in TOML-B and C 38
Figure 7.24 High degree of sediment "powder" and cover in TOML-D 38
Figure 7.25 Shear Strength Class and BC locations, Area B1 40
Figure 7.26 Shear Strength Class and BC locations, Area C1 40
Figure 7.27 Vane Shear Strength Class and BC locations, Area D2 41
Figure 7.28 Vane Shear Strength Class and BC locations, Area D1 41
Figure 7.29 Vane Shear Strength Class and BC locations, Areas F and F1 42
Figure 7.30 Summary vane shear results from TOML areas 43
Figure 9.1 Comparison between TOML BC and dredge samples and historical samples 49
Figure 10.1 Bulk sampling dredge used to collect the bulk sample for metallurgical pilot tests 52

Figure 10.2 Copper partition coefficients during smelting 59
Figure 10.3 Nickel and cobalt partition coefficients during smelting 60
Figure 10.4 Manganese in metal vs. iron in slag 61
Figure 10.5 Phosphorus partition coefficients 62
Figure 10.6 Manganese and phosphorus in slag versus iron in slag 63
Figure 10.7 Nickel partition coefficients in converting 64
Figure 10.8 Copper partition coefficients in converting 65
Figure 10.9 Cobalt partition coefficients in converting 66
Figure 10.10 Manganese partition coefficients in converting 67
Figure 11.1 NORI-A, B, C and D, showing location of historic data 73
Figure 11.2 Variogram map of nickel for NORI-A, B and C 76
Figure 11.3 Major and semi-major variograms for nickel 77
Figure 11.4 TOML-A interpreted geological domains 80
Figure 11.5 TOML-B interpreted geological domains 81
Figure 11.6 TOML-C interpreted geological domains 82
Figure 11.7 TOML-D and E interpreted geological domains 82
Figure 11.8 TOML-F interpreted geological domains 83
Figure 11.9 Location of the historical sample data provided by the ISA and IOM and the TOML data 84
Figure 11.10 Histogram and log-probability plot of abundance for all samples within TOML Areas . 86
Figure 11.11 Histogram and log-probability plot of Mn for all samples within TOML Areas 86
Figure 11.12 Histogram and log-probability plot of Ni for all samples within TOML Areas 87
Figure 11.13 Histogram and log-probability plot of Cu for all samples within TOML Areas 87
Figure 11.14 Histogram and log-probability plot of Co for all samples within TOML Areas 88
Figure 11.15 Log-probability plots for abundance, Mn, Ni, Cu and Co by TOML Areas 89
Figure 11.16 Box plots for abundance, Mn, Ni, Cu and Co by TOML Areas 90
Figure 11.17 Photo-profile line CCZ15-F01 that crosses TOML-B1 91
Figure 11.18 Comparison of nodule coverage against nodule abundance 92
Figure 11.19 Comparison of nodule abundance estimated from photos against nodule abundance estimated manually using the LAE method 93
Figure 11.20 Nodule abundance photo-profile line CCZ15-F01 that crosses sub-area B1 Measured Mineral Resource 94
Figure 11.21 Nodule abundance photo-profile line CCZ15-F02 that crosses sub-area B1 Measured Mineral Resource 94
Figure 11.22 Nodule abundance photo-profile line CCZ15-F04 that crosses sub-area B1 Measured Mineral Resource 95
Figure 11.23 Semi-variogram maps for abundance, Mn, Ni, Cu and Co 96
Figure 11.24 Abundance omni-directional, 060° and 150° directional variograms 97
Figure 11.25 Mn omni-directional, 060° and 150° directional variograms 98
Figure 11.26 Ni omni-directional, 060° and 150° directional variograms 98
Figure 11.27 Cu omni-directional, 060° and 150° directional variograms 98
Figure 11.28 Co omni-directional, 060° and 150° directional variograms 99

Figure 11.29 Omni-directional and 060° directional variograms for nodule coverage estimated from sea floor photos 99
Figure 11.30 Omni-directional and 060° directional variograms for nodule abundance estimated using the LAE method from sea floor photos 100
Figure 11.31 Omni-directional variograms for backscatter values 101
Figure 11.32 Combined NORI-A, B and C abundance tonnage curves 104
Figure 11.33 Map of sample distribution and block model estimates of nickel, NORI 2012 estimates 105
Figure 11.34 Map of sample distribution and block model estimates of abundance, NORI 2012 estimates 106
Figure 11.35 Combined TOML-A, B, C, D, E and F abundance tonnage curves 107
Figure 11.36 Map showing block model and sample distribution for Abundance Mn, Ni, Cu and Co in TOML Area A 108
Figure 11.37 Map showing block model and sample distribution for Abundance Mn, Ni, Cu and Co in TOML Area B 109
Figure 11.38 Map showing block model and sample distribution for Abundance Mn, Ni, Cu and Co in TOML Area C 110
Figure 11.39 Map showing block model and sample distribution for Abundance Mn, Ni, Cu and Co in TOML Area D and Area E 111
Figure 11.40 Map showing block model and sample distribution for Abundance Mn, Ni, Cu and Co in TOML Area F 112
Figure 13.1 The Hidden Gem post completion of Test Mining 115
Figure 13.2 Photographs of the Test Mining Collector 115
Figure 13.3 Illustration of the First-Generation Production System during nodule offloading operations. 116
Figure 13.4 Artist impression of a second-generation PV with three seafloor CVs and TV alongside 117
Figure 13.5 Artist impression of the PV showing key components 119
Figure 13.6 Artist impression of a single seafloor collector. Note: Umbilical not shown 120
Figure 13.7 Schematic representation of the collector head. 121
Figure 13.8 Artist impression of the VTS connecting the PV on the surface to the CV on the seafloor 122
Figure 13.9 Basic airlift configuration 123
Figure 13.10 Artist impression of TV in port with hatches open during nodule offloading operations 125
Figure 13.11 MV Island Commander, example of offshore supply vessel used in the oil and gas industry 126
Figure 13.12 Comparison of slopes >6° in original and denoised bathymetry, NORI-A 130
Figure 13.13 Comparison of slopes >6° in original and denoised bathymetry, NORI-B 130
Figure 13.14 Comparison of slopes >6° in original and denoised bathymetry, NORI-C 131
Figure 13.15 Comparison of slopes >6° in original and denoised bathymetry, TOML-B 131
Figure 13.16 Comparison of slopes >6° in original and denoised bathymetry, TOML-C 132
Figure 13.17 Comparison of slopes >6° in original and denoised bathymetry, TOML-DE 132
Figure 13.18 Comparison of slopes >6° in original and denoised bathymetry, TOML-F 133

Figure 13.19 Bathymetric maps of NORI-A, B, C and D 134
Figure 13.20 Bathymetric maps of TOML-B, C, D, E and F 135
Figure 13.21 Artistic impression of CV operations showing a gap between collection paths 138
Figure 13.22 NORI-TOML mining progression by lease 144
Figure 13.23 LOM plan annual production by lease 145
Figure 13.24 LOM plan annual nodule abundance and grades 146
Figure 13.25 TOML-F collection sequence by year 146
Figure 13.26 TOML-D/TOML-E collection sequence by year 147
Figure 13.27 NORI-C collection sequence by year 147
Figure 13.28 TOML-B collection sequence by year 148
Figure 13.29 TOML-C collection sequence by year 148
Figure 13.30 NORI-B collection sequence by year 149
Figure 13.31 NORI-A collection sequence by year 149
Figure 13.32 TOML-A collection sequence by year 150
Figure 14.1 2018 production of manganese ore (blue) compared to 60 ktpa nickel equivalent project (green) 153
Figure 14.2 2017 Manganese ore consumption by end-use project 153
Figure 14.3 Major Equipment and Associated Streams from Pyrometallurgical Process 154
Figure 14.4 Major Equipment and Associated Stream from the Hydrometallurgical Refinery 156
Figure 14.5 Schematic of kiln and ancillary equipment as originally configured 160
Figure 14.6 Pilot Plant Rotary Kiln, Feed-End to Right. 161
Figure 14.7 Pilot Plant DC Furnace and Ancillary Equipment 162
Figure 14.8 DC Furnace Dimensions 163
Figure 15.1 Total 2023 production capacity for ferronickel and nickel pig iron smelting, and number of existing smelting facilities by country 166
Figure 15.2 Rapid increase in Indonesian ore demand, decreasing saprolite ore grades and increase ore imports from the Philippines 167
Figure 19.1 Forecast project post-tax free cash flow (US$ M) 208
Figure 19.2 Tornado Graph 226

List of Acronyms

AAS	Atomic absorption spectroscopy
AC	Alternating current
ALS	ALS Laboratory Group
AMC	AMC Consultants Pty Ltd
AMR	Arbeitsgemeinschaft Meerestechnisch Rohstoffe
APEI	Area of Particular Environmental Interest
AUV	Autonomous underwater vehicle
BC	Box core
BGR	German Federal Institute for Geosciences and Natural Resources
BMI	Benchmark Mineral Intelligence
BV	Bureau Veritas laboratory
CAGR	Compound annual growth rate
CCZ	Clarion-Clipperton Zone
CIF	Cost, insurance and freight
CIM	Canadian Institute of Mining, Metallurgy and Petroleum
CoV	Coefficient of variation
CRU	CRU Group
CV	Collector vehicle
The Convention	United Nations Convention on the Law of the Sea 1982
DC	Direct current
DeepGreen	DeepGreen Metals Inc.
DGE	DeepGreen Engineering Pte. Ltd.
DHI	DHI Water and Environment
DISCOL	Disturbance and Recolonisation Experiment
DOMES	Deep Ocean Mining Environmental Study
DP	Dynamic positioning
DRC	Democratic Republic of Congo
DSHMRA	Deep Sea Hard Mineral Resources Act
EF	Electric furnace
EIA	Environmental Impact Assessment
EIS	Environmental Impact Statement
EMM	Electrolytic manganese metal
EMMP	Environmental Management and Monitoring Plan
EMS	Environmental Management System
ESIA	Environmental and Social Impact Assessment
ESG	Environment, social and governance
EW	Electro-winning
EV	Electric vehicle
FFG	Free-fall grab samplers
FLS	FLSmidth
FOB	Free on board
FV	Finishing vessel
Glencore	Glencore International Ag

Golder	Golder Associates Pty Ltd.
HPAL	High-pressure acid leaching
HPMSM	High-purity $MnSO_4$ monohydrate
Hs	Significant wave height
IA	Initial Assessment
ICP-MS	Inductively coupled plasma mass spectrometry
ID	Inside diameter
IDW	Inverse Distance Weighting – an estimation method utilising distance-weighted local averages
IFREMER/Ifremer	Institut Français de Recherche pour l'Exploitation de la Mer (French Research Institute for Exploitation of the Sea)
Inco	International Nickel Corporation
IMDG	**The International Maritime Dangerous Goods Code**
IMSBC	International Maritime Solid Bulk Cargoes Code
IOM	**Interoceanmetal Joint Organisation**
IRR	Internal rate of return
ISA	International Seabed Authority
IX	Ion exchange
KPM	Kingston Process Metallurgy
LARS	Launch and recovery system
LED	Light-emitting diode
LME	London Metal Exchange
LRMC	Long Run Marginal Cost
MBES	Multi-beam echo sounder
MHP	mixed hydroxide precipitate
MSP	mixed sulfide precipitate
MOU	Memorandum of understanding
NI 43-101	Canadian National Instrument 43-101
NOAA	National Oceanic and Atmospheric Administration
NORI	Nauru Ocean Resources Inc.
NN	Nearest neighbour estimation method
NOAA	National Oceanic and Atmospheric Administration
NPI	Nickel pig iron
NPV	Net present value
OK	Ordinary kriging – an estimation method utilising distance-weighted local averages
OMI	Ocean Mining Inc.
OMCO	Ocean Minerals Company
PAMCO	Pacific Metals Company
PFS	Pre-feasibility study
PLS	Pregnant liquor/leach solution
POX	Pressure oxidative leaching
PRZ	Preservation reference zone
PSD	Particle size distribution
PV	Production vessel
QA/QC	Quality assurance and quality control
QP	Qualified Person, as defined by Canadian National Instrument 43-101

R-type	Rough type nodules
Regulations	Regulations on Prospecting and Exploration for Polymetallic Nodules in the Area
ROV	Remotely operated vehicle
RKEF	Rotary kiln and electric furnace
SBP	Sub-bottom profiler
SGS	SGS Lakefield, Ontario
SLN	Société le Niquel
SMM	Shanghai Metal Markets
S-R-type	Smooth-rough type nodules
SSS	Sidescan sonar
S-K 1300	Subpart 1300 of Regulation S-K promulgated by the US Securities and Exchange Commission
S-type	Smooth type nodules
SV	Support vessel
SX	Solvent extraction
TOC	Total organic carbon
TOML	Tonga Off-shore Mining Limited
TMC	TMC the metals company Inc.
TMC USA	The Metals Company USA LLC
TV	Transport vessel
UN	United Nations
US	Unites States of America
UNCLOS	United Nations Convention on the Law of the Sea
USBL	Ultra-short baseline
UTM	Universal Transverse Mercator Cartesian coordinate system
UTP	Underwater transponder array
Var	Variance
VTS	Vertical transport system
XPS	eXpert Process Solutions, a division of Glencore
XRF	X-ray fluorescence analysis
Yuzhmorgeologiya	State Enterprise Yuzhmorgeologiya (Russian Federation)

List of elements

Al	Aluminum
As	arsenic
Ba	barium
Ca	calcium
Cd	cadmium
Ce	cerium
Cl	chlorine
Co	cobalt
Cu	copper
Fe	iron
H_2O	hydrogen dioxide
H_2S	hydrogen sulfide
K	potassium
La	lanthanum
Mg	magnesium
Mn	manganese
MnO	manganese oxide
MnO_2	manganese dioxide
Mo	molybdenum
Na	sodium
NaHS	sodium hydro sulfide
Na_2S	sodium sulfide
Nd	neodymium
Ni	nickel
P	phosphorus
Pb	lead
REE	rare earth elements
S	sulfur
SiO_2	silicon dioxide
Sr	strontium
Ti	titanium
V	vanadium
Y	yttrium
Zn	zinc
Zr	zirconium

List of units

°	degree
°C	degrees Celsius
%	percent
% w/w	% mass/mass or weight
µm	microns
cm	centimeter
cm/s	centimeter per second
dmtu	dry metric tonne unit
G	gram
GWh	gigawatt-hours
ka	Thousand years
kg	kilogram
kg/m^2	kilograms per square meter (surface abundance)
km	kilometer
km^2	square kilometer
kn	knots
kPa	kilopascal
kt	kilotonne (metric)
kt/a	kilotonnes (metric) per annum
kWh/h	kilowatt hours per hour
kWh/t	kilowatt hours per tonne
Kt	Knots (nautical miles per hour)
Lb	pound
m	meter
m/h	meters per hours
m/s	meters per second
m^2	square meter
m^3	cubic meter
m^3/y	cubic meters per year
mbsl	meters below sea level
mg/L	milligrams per liter
mm	millimeter
MPa	megapascal
mt	metric tonnes
Mmt	million tonnes
Mmtpa	million tonnes per annum
Mwmt	million wet metric tonnes
Mwmtpa	million wet metric tonnes per annum
mV	millivolt
MW	megawatt
nm	nautical mile
ppm	parts per million
ppmw	parts per million weight

s	second
t	tonne (metric)
t/d	tonnes (metric) per day
t/h	tonnes (metric) per hour
US$	US dollar
wmt	Wet metric tonnes
y	year

2 Introduction

A very large nickel, manganese, cobalt, and copper resource occurring as polymetallic nodules is located in the Clarion-Clipperton Zone (CCZ) of the northeast Pacific Ocean between Hawaii and Mexico. The nodules are located at depths of between 4,000 to 6,000 m and have been explored with considerable success between the mid-1960s and the present day using a variety of deep-sea technologies. Successful trial extraction in the CCZ has also been carried out to demonstrate that the nodules can be collected and pumped to a surface platform and processed for recovery of metals.

Interest in seafloor mineral deposits grew through the 1960s. Several commercial and government funded organizations and consortia started exploring the oceans as part of a cooperative program known as the International Decade of Ocean Exploration. These organizations became known as Pioneer Contractors.

Exploration of the seafloor in international waters is administered by two governing bodies; the International Seabed Authority (ISA) the regulator of the United Nations Convention on the Law of the Sea (UNCLOS) and the National Oceanic and Atmospheric Administration (NOAA), the regulator of the U.S. Deep Seabed Hard Mineral Resources Act (DSHMRA). These regulatory frameworks operate independently of one another.

TMC the metals company Inc. (TMC), through its wholly owned subsidiaries. NORI and Tonga Ocean Minerals Limited (TOML), hold exploration contracts with the ISA.

NORI holds exploration rights to four areas (NORI Area A, B, C, and D) in the CCZ that were granted by the ISA in July 2011. TOML holds exploration rights to six areas (TOML-A, B, C, D, E, and F) in the CCZ, under an exploration contract approved in July 2011, and then formalized on 11 January 2012 by the ISA.

TMC, through its wholly owned subsidiary TMC USA has submitted requests directly under the U.S. regulatory regime governed by DSHMRA. These applications are summarized below:

- Exploration License for the USA-A Area which covers 65,186 km^2 in the CCZ
- Exploration License for USA-B Area which covers 121,789 km^2 in the CCZ

USA-A includes the existing ISA approved exploration Area identified as NORI Area D and TOML area F. USA-B includes the existing ISA approved exploration Areas identified as NORI Areas A, B, C and TOML Areas A, B, C, D, and E.

As of the effective date of this report, these applications remain under review by NOAA. Any future rights to these U.S. areas remain contingent upon approval of the submitted applications. Accordingly, this report only assesses Mineral Resources located within areas covered by the ISA exploration contracts held by NORI and TOML.

2.1 Registrant, terms of reference and purpose of report

The registrant is TMC the metals company Inc. (TMC). TMC commissioned AMC Consultants Pty Ltd (AMC) to undertake an Initial Assessment (IA) of the Mineral Resources contained in NORI Area A, B, and C, and TOML-A, B, C, D, E, and F (combined as the Property) and compile a Technical Report Summary compliant with SEC Regulation S-K (subpart 1300). This IA is preliminary in nature, includes Inferred Mineral Resources, and is not supported by a pre-feasibility or feasibility study. Mineral Resources are not Mineral Reserves and do not have demonstrated economic viability.

This IA contains forward-looking statements within the meaning of the U.S. securities laws. These statements include projections, expectations, and assumptions regarding future technical, regulatory,

financial, and operational outcomes for areas of the NORI and TOML Contract Areas not currently covered by a pre-feasibility or feasibility study. These statements are based entirely on Measured, Indicated, and Inferred Mineral Resources and do not reflect demonstrated economic viability. The projected development scenarios, cost estimates, timelines, and financial metrics such as IRR and NPV are preliminary in nature and may differ materially from actual results due to changes in technical data, market conditions, permitting outcomes, regulatory frameworks, or other factors.

For a discussion of material risks and uncertainties that could affect these forward-looking statements, see “Item 1A. Risk Factors” and “Cautionary Note Regarding Forward-Looking Statements” in TMC’s most recent Annual Report on Form 10-K, as supplemented in subsequent SEC filings. Readers are also referred to the full cautionary statement regarding forward-looking information included in Chapter 19 of this report.

2.2 Sources of information and data

This Technical Report Summary is based on information and reports supplied by TMC, NORI, TOML, and TMC USA or in the public domain.

2.3 Qualified personnel

This Technical Report is authored by several experts or “Qualified Persons” (QPs), as defined in Subpart 1300 of Regulation S-K promulgated by the US Securities and Exchange Commission (S-K 1300). The QPs are listed in Table 2.1 and Table 2.2. The QPs have not visited the site, as the nodules, which are the subject of the Technical Report, are located in the north-east Pacific Ocean and lie at a depth of approximately 4,500 m below sea level. As permitted by Item 1302(b)(2)(iii), personal inspection has been substituted with inspection of sample material and survey data collected using remotely operated vehicles (ROV), which the QPs consider reasonable given the depth and location of the deposit. Nodules are only accessible to autonomous or remotely operated specialist underwater vehicles.

Table 2.1 List of Qualified Persons responsible for each Section

Qualified Person	Responsible for the following report Sections:
AMC Consultants Pty Ltd	Sections 1.1, 1.4, 1.11, 2.1 - 2.4, 4, 5.1, 5.3, 6.8 - 6.10, 6.11.2, 7.1 - 7.4, 8.1, 8.2.1, 8.2.2, 8.3, 9.2, 11, 12, 13.7, 13.8.1, 13.8.2, 13.9, 20, 21, 22.2, 22.4, 22.6, 23 - 25
MARGIN - Marine Geoscience Innovation	Sections 6.1 - 6.6, 6.11.1, 7.6.2 - 7.6.5
APYS Subsea Ltd	Sections 7.6.6, 7.7.6
Canadian Engineering Associates Ltd	Sections 1.6, 10, 14, 15, 22.3, 22.7, 22.8
Lanasera	Sections 1.10, 19, 22.12
TMC the metals company Inc.	1.2, 1.3, 1.5, 1.7 - 1.9, 3.1, 3.1.1, 3.1.1.1, 3.1.2, 3.1.2.1, 3.2, 3.2.1, 3.2.2, 5.2, 5.4, 6.7, 6.11.3, 7.5.1, 7.5.2, 7.6.1, 7.7.1 - 7.7.5, 8.2, 9.1, 13.1 - 13.6, 13.8.3, 16 - 18, 22.1, 22.5, 22.9 - 22.11 Refer to Table 2.2

Further details on the QP’s employed by the Registrant are provided in Table 2.2.

Table 2.2 TMC Qualified Persons responsible for each section

Qualified Person	Responsible for the following report sections:
Anthony O'Sullivan, Chief Development Officer Anthony is a mining executive with over 30 years of experience in mineral exploration and project development. As Chief Development Officer at TMC, he oversees technical and strategic development of deep-sea polymetallic nodule projects. He has over 20 years' experience in subsea resource development with 10 of these years' experience in polymetallic nodule development involving exploration, development of environmental impact statements and permitting, project development, offshore equipment design, onshore processing and product marketing. He has held senior roles at Nautilus Minerals and BHP Billiton and is a co-inventor on multiple subsea mining patents. He is a current fellow of the AusIMM.	Sections 1.2, 1.3, 1.7, 3.1, 3.1.1, 3.1.1.1, 3.1.2, 3.1.2.1, 3.2, 3.2.1, 3.2.2, 5.2, 5.4, 6.7, 6.11.3, 7.5.1, 7.5.2, 7.6.1, 7.7.1, 7.7.2, 7.7.3, 7.7.4, 7.7.5, 8.2, 9.1, 16, 22.1, 22.9
Rutger Bosland, Chief Innovation and Offshore Technology Officer Rutger is an offshore engineer and project leader with a track record of delivering pioneering technologies in deep-sea mining and heavy-lift engineering. He led the technical development of Pioneering Spirit, the world's largest offshore construction vessel, and oversaw the successful design, build, and testing of Allseas' integrated nodule collection system aboard Hidden Gem. Under his direction, Allseas executed the first integrated nodule collection trials in the Pacific Ocean since the 1970s. At TMC, he now leads the development and commercial scaling of the polymetallic nodule collection system. He is a current member of AusIMM.	Sections 1.5, 13.1, 13.2, 13.3, 13.4, 13.5, 13.6, 13.8.3, 22.5
Dr. Michael Clarke, Environmental Program Director Michael is an environmental scientist with extensive experience in marine biology, mining, environmental impact assessments, and regulatory compliance. At TMC, he leads the Environmental Program for the project, overseeing baseline studies, monitoring, and stakeholder engagement. He has contributed to the development of novel adaptive management systems and environmental monitoring protocols tailored to deep-sea mining. Michael is certified as an Environmental Practitioner and Impact Assessment Specialist by the Environmental Institute of Australia and New Zealand (EIANZ) and has participated in the planning and offshore execution of multiple research campaigns to the NORI Area D site.	Sections 1.8, 17, 22.10
Adam Price, Project Control Manager Adam is a seasoned project controls and analysis professional with over 15 years of experience managing estimate, cost, schedule, financial economics/planning /reporting and risk performance across large-scale, complex construction and infrastructure projects. In his current role at TMC, Adam leads the strategic planning, capital and operating estimating, economic analysis, modelling, implementation, and oversight of integrated project controls systems across all phases of project delivery—from Pre-Feasibility (PFS) and Feasibility Studies (FS) through to execution. Adam has worked across a wide range of estimating and contracting models and has a deep understanding of commercial structures and their implications on project performance and risk. His expertise spans the full project lifecycle, with a strong focus on establishing robust estimates, baselines, developing earned value management systems, and driving data-informed decision-making to optimize outcomes. Adam is a member of AACE International and AusIMM.	Sections 1.9, 18, 22.11

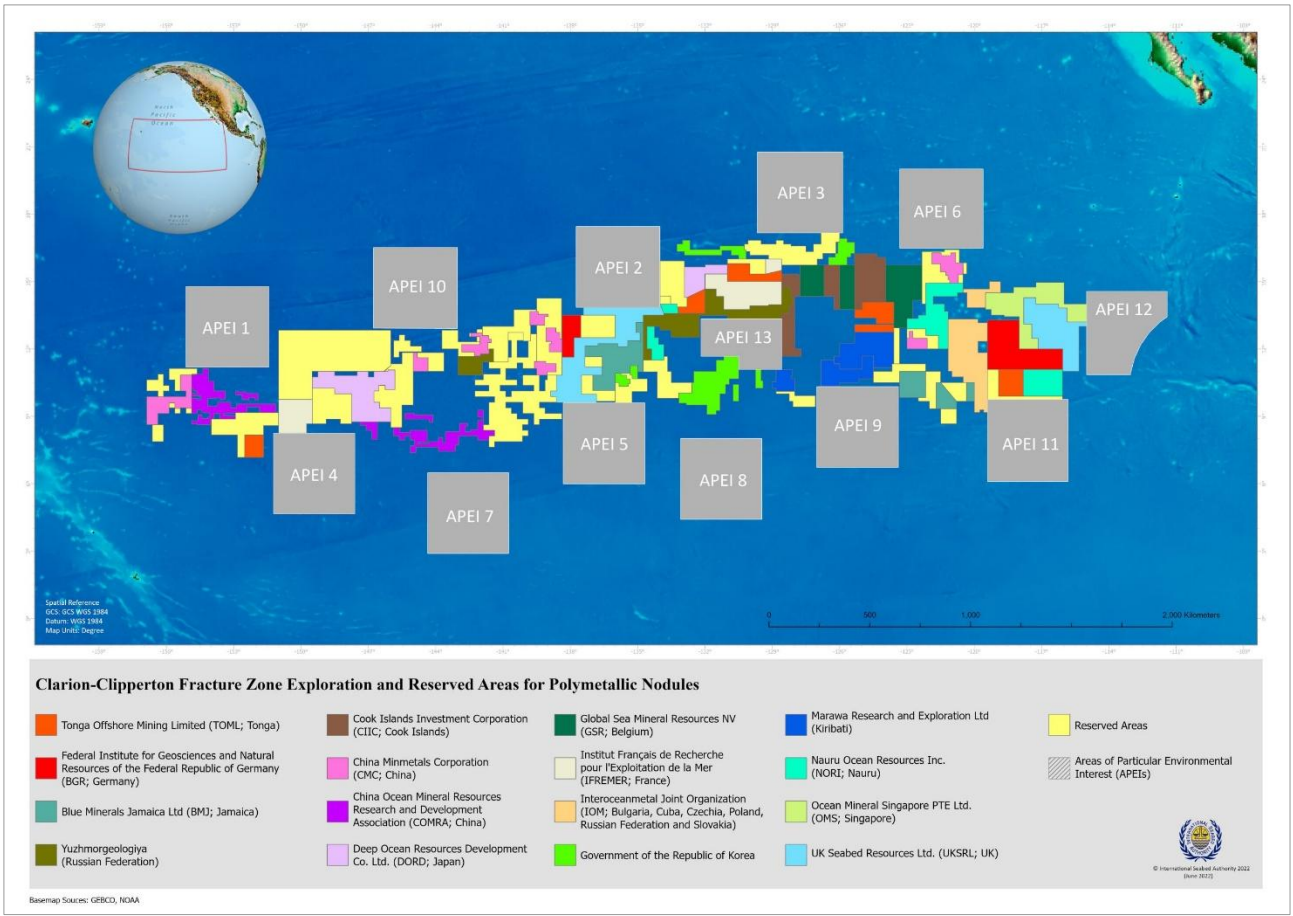
2.4 Update to a previously filed Technical Report

This IA refers to Mineral Resources previously reported for the NORI (AMC Consultants, 2021a) and TOML areas (AMC Consultants, 2021b). There has been no change to the Mineral Resources previously reported in these reports. This IA considers the combined Mineral Resources contained in NORI Area A, B, and C, and TOML-A, B, C, D, E and F.

3 Property description and location

The NORI and TOML properties are located within the CCZ of the northeast Pacific Ocean Figure 3.1. The CCZ is located in international waters between Hawaii and Mexico. The western end of the CCZ is approximately 1,000 km south of the Hawaiian island group. From here, the CCZ extends over 4,500 km east-northeast, in an approximately 750 km wide trend, with the eastern limits approximately 2,000 km west of southern Mexico. The region is well-located to ship nodules to the US or across the Pacific to Asian markets.

Figure 3.1 Location of NORI and TOML Project and other ISA exploration areas within the CCZ.



Source: https://www.isa.org.jm/map/clarion-clipperton-fracture-zone, downloaded 22 July 2025.

3.1 Tenements and permits

NORI holds exploration contracts covering four areas with a combined area of 74,830 km^2 (NORI Area A, B, C, and D) in the CCZ that was granted by the ISA in July 2011. Table 3.1 and Table 3.2 provide details regarding the location of the NORI areas. This IA considers only the NORI – A, B and C areas. NORI Area D is subject to a separate Technical Report Summary that is supported by a PFS (see AMC Consultants, 2025).

Table 3.1 NORI Area details

Area	Size (km²)	ISA number	Pioneer Contractors
A	8,924	13	Yuzmorgeologiya
B	3,519	15	Yuzmorgeologiya
C	37,227	22	Interoceanmetal Joint Organisation (IOM)
D	25,160	25	Arbeitsgemeinschaft Meerestechnisch Rohstoffe (AMR)

Table 3.2 NORI Area extents

Area	Minimum Latitude (DD)	Maximum Latitude (DD)	Minimum Longitude (DD)	Maximum Longitude (DD)	Minimum UTM X (m)	Maximum UTM X (m)	Minimum UTM Y (m)	Maximum UTM Y (m)	UTM Zone
A	11.5000	13.00000	-134.5830	-133.8330	545220.4	627276.0	1271339	1437255	8
B	13.5801	14.00000	-134.0000	-133.2000	607995.7	694759.8	1501590	1548425	8
C	12.0000	14.93500	-123.0000	-120.5000	500000.0	769458.3	1326941	1652649	10
D	9.8950	11.08333	-117.8167	-116.0667	410465.2	602326.1	1093913	1225353	11

DD – Decimal degrees, UTM - Universal Transverse Mercator map projection

TOML holds exploration rights to six areas (TOML A, B, C, D, E and F) with a combined area of 74,713 km² (Table 3.3 and Table 3.4) in the CCZ under an exploration contract approved in July 2011, and then formalized on 11 January 2012 by the ISA.

Table 3.3 TOML exploration area in the CCZ

Exploration Area	Reserved areas	Area (km²)
Area A	2	10,281
Area B	15	9,966
Area C	16	15,763
Area D	20	15,881
Area E	21	7,002
Area F	25	15,820
Total		**74,713**

Table 3.4 TOML area extents

Area	Minimum Latitude (DD)	Maximum Latitude (DD)	Minimum Longitude (DD)	Maximum Longitude (DD)	Minimum UTM X (m)	Maximum UTM X (m)	Minimum UTM Y (m)	Maximum UTM Y (m)	UTM Zone
A	7.167 N	8.167 N	151.667 W	152.510 W	553972	647187	792205	902968	05N
B	13.580 N	14.667 N	132.000 W	133.200 W	694518	824685	1502009	1623605	08P
C	15.000 N	15.800 N	128.583 W	131.000 W	284947	544791	1658371	1747847	09P
D	13.125 N	14.083 N	123.583 W	125.333 W	247293	437022	1451031	1557860	10P
E	12.750 N	13.083 N	123.583 W	125.333 W	246693	436796	1409563	1447513	10P
F	9.895 N	11.083 N	117.817 W	118.917 W	289835	410804	1093917	1225828	11P

DD – Decimal degrees, UTM - Universal Transverse Mercator map projection

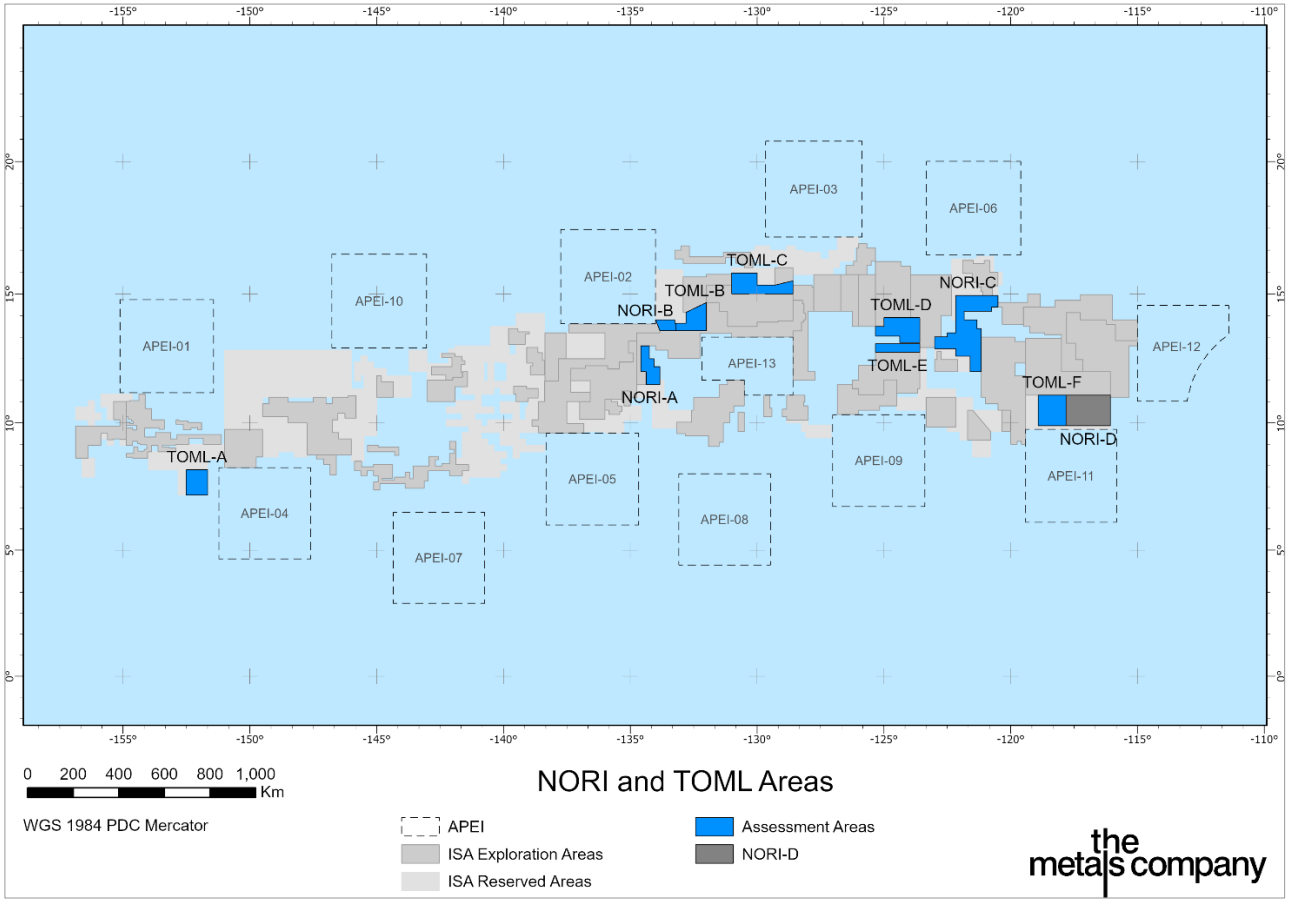
Figure 3.2 shows the location of the NORI and TOML Contract Areas. These contracts were granted for a term of 15 years and cover a program of activities for the first five-year period. These contracts also formalize the rights of NORI and TOML around tenure. Pursuant to the Regulations, NORI and TOML

have priority right to apply for an exploitation contract to exploit nodules over the exploration Contract Area (ISA Regulation 24 (2)).

In April 2025, TMC USA submitted two applications (USA-A and USA-B) for polymetallic nodule exploration licenses and one application for a commercial recovery permit to NOAA under the U.S. DSHMRA framework. These exploration applications cover the NORI and TOML areas (Figure 3.2) currently held by TMC under the NORI and TOML ISA exploration contracts.

At the time of writing this report, TMC USA does not hold any exploration licenses or commercial recovery permits under the DSHMRA framework. However, TMC USA has submitted applications for such rights, and subject to regulatory review and approval, anticipates that any future commercial recovery activities would be conducted pursuant to a permit issued by NOAA under the U.S. legal regime. No assurance can be given that such rights will be granted or that regulatory approvals will be obtained on the anticipated timeline or terms.

Figure 3.2 NORI and TOML Areas



Source: TMC USA

To date, no commercial recovery permits for extracting minerals from the seafloor within the Property have been granted under ISA or DSHMRA.

3.1.1 United Nations Convention on the Law of the Sea

The Area is defined as the seabed and subsoil beyond the limits of national jurisdiction (UNCLOS Article 1). Figure 3.3 shows a map of the Area (blue zone) as well as 200 nautical mile exclusive economic zones (grey zone) and extended continental shelf zones (orange zone). Figure 3.4 shows the relationship between depth, distance and jurisdiction.

The principal UNCLOS policy documents governing the Area include:

- The UNCLOS, of 10 December 1982 (The Convention).
- The 1994 Agreement relating to the Implementation of Part XI of the United Nations Convention on the Law of the Sea of 10 December 1982 (the 1994 implementation Agreement).

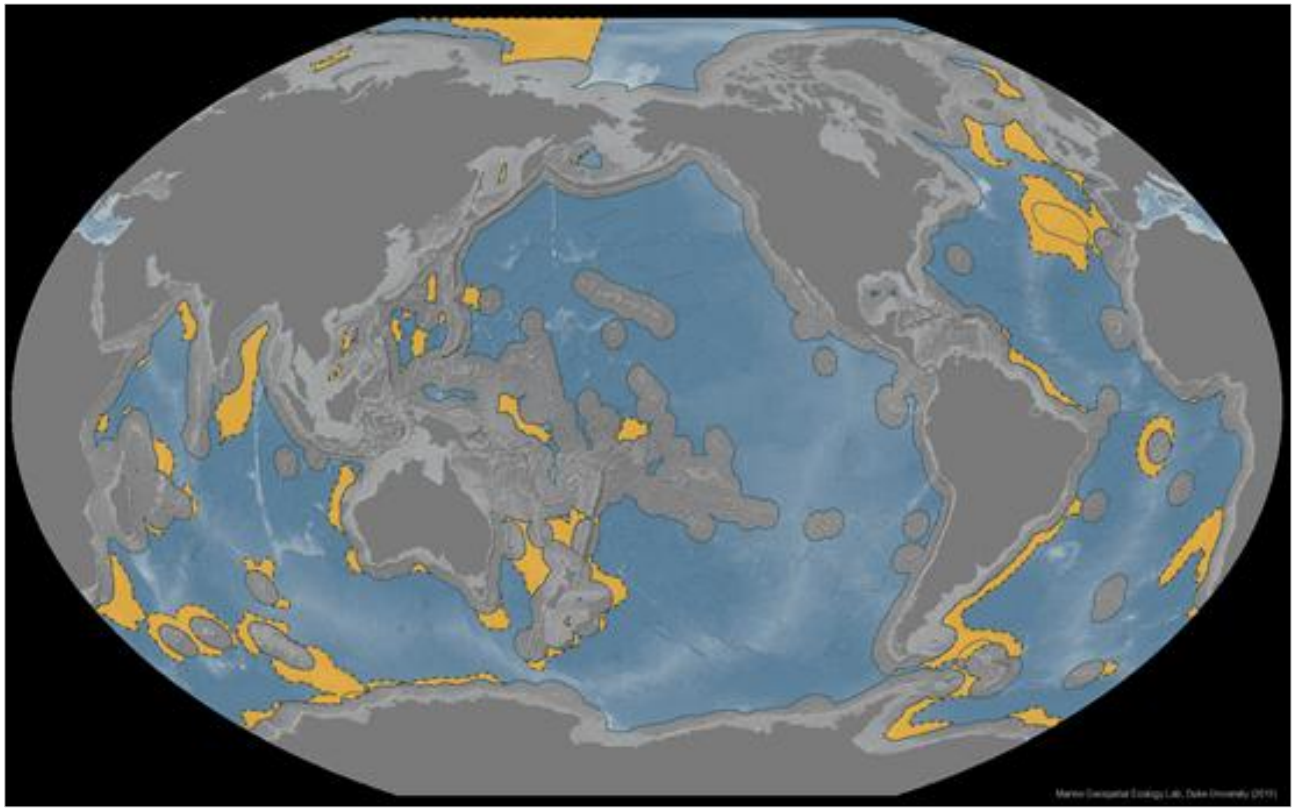
The Convention deals with, among other things, navigational rights, territorial sea limits, exclusive economic zone jurisdiction, the continental shelf, freedom of the high seas, legal status of resources on the seabed beyond the limits of national jurisdiction, passage of ships through narrow straits, conservation and management of living marine resources in the high seas, protection of the marine environment, marine scientific research, and settlement of disputes.

Part XI of the Convention and the 1994 Implementation Agreement deals with mineral exploration and exploitation in the Area, providing a framework for entities to obtain legal title to areas of the seafloor from the ISA for the purpose of exploration and eventually exploitation of resources.

The Convention entered into force on 16 November 1994. A subsequent agreement relating to the implementation of Part XI of the Convention was adopted on 28 July 1994 and entered into force on 28 July 1996. The 1994 Implementation Agreement and Part XI of the Convention are to be interpreted and applied together as a single instrument.

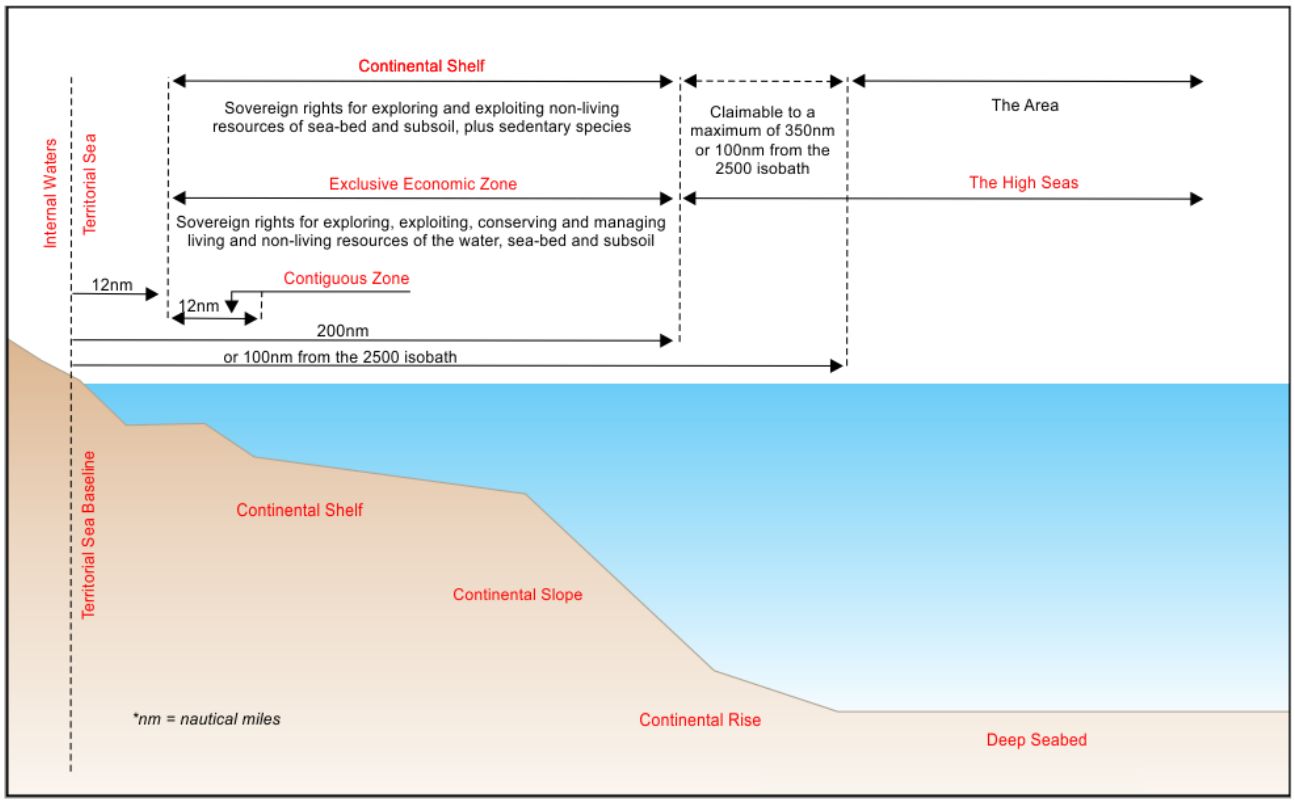
As of 20 July 2025, the Convention had been signed by 169 States (countries) and the European Union. The US is currently not a party to the Convention.

Figure 3.3 Map of seafloor jurisdictions



Note: International seabed area map (blue zone) as well as 200 nautical mile exclusive economic zones (grey zone) and extended continental shelf zones (orange zone). Source: Marine Geospatial Ecology Lab, Duke University (2011).

Figure 3.4 Maritime space under the 1982 UNCLOS



Source: TMC - adapted from UNCLOS, 1982

3.1.1.1 International Seabed Authority

The ISA is an autonomous international organization established under the Convention and the 1994 Implementation Agreement to organize and control activities in the Area, particularly with a view to administering and regulating the development of the resources of the Area in accordance with the legal regime established in the Convention and the 1994 Implementation Agreement.

All rules, regulations, and procedures issued by the ISA to regulate prospecting, exploration, and exploitation of marine minerals in the Area are issued within a general legal framework established by the Convention and the 1994 Implementation Agreement.

To date, the ISA has issued (https://www.isa.org.jm/mining-code/ Regulations):

- The Regulations (adopted 13 July 2000 and updated in 2013; the Regulations).
- The Regulations on Prospecting and Exploration for Polymetallic Sulfides (adopted 7 May 2010).
- The Regulations on Prospecting and Exploration for Cobalt-Rich Ferromanganese Crusts in the Area (July 2012).

The ISA is currently working on the development of a legal framework to regulate the exploitation of polymetallic nodules in the international seabed area.

3.1.2 Deep Seabed Hard Mineral Resources Act (DSHMRA)

While the ISA regulates seabed mining for UNCLOS member states, the U.S. maintains its own regulatory regime. The U.S. legal framework for seabed mineral activities in areas beyond national jurisdiction is governed by the Deep Seabed Hard Mineral Resources Act (DSHMRA), enacted in 1980 (30 U.S.C. §1401 et seq.). This Act authorizes the National Oceanic and Atmospheric Administration (NOAA) to issue licenses to US citizens for exploration and permits for commercial recovery of polymetallic nodules containing manganese, nickel, cobalt, and copper from the deep seabed.

These activities are limited to areas beyond national jurisdiction and are intended to ensure that U.S. entities can participate in seabed mining despite the US not being a party to UNCLOS or the 1994 Implementation Agreement.

3.1.2.1 National Oceanic and Atmospheric Administration (NOAA)

NOAA is the U.S. federal agency responsible for administering the Deep Seabed Hard Mineral Resources Act (DSHMRA), which establishes a legal regime for the exploration and commercial recovery of hard Mineral Resources from the deep seabed in areas beyond national jurisdiction. All rules, regulations, and procedures issued by NOAA to regulate prospecting, exploration, and recovery of marine minerals under DSHMRA are issued within the legal framework established by the Act and its implementing regulations under 15 CFR, Subchapter D. To date, NOAA has issued:

- The regulations governing the issuance of exploration licenses for polymetallic nodules in areas beyond national jurisdiction (15 CFR Part 970).
- The regulations governing the issuance of commercial recovery permits for polymetallic nodules (15 CFR Part 971).

NOAA is currently responsible for reviewing and processing applications for both exploration licenses and commercial recovery permits submitted by U.S. entities. In April 2025, the President of the US signed an Executive Order establishing a national policy to advance U.S. leadership in seabed mineral exploration and responsible commercial recovery, emphasizing environmental stewardship, supply chain resilience, and interagency coordination.

In May 2025, NOAA released a draft update to its DSHMRA regulatory framework, including proposed revisions to streamline the application process for commercial recovery permits and enhance environmental safeguards. The draft incorporated feedback from interagency consultations, industry stakeholders, and environmental groups, and was published for public comment via the Federal Register. NOAA has stated its intent to finalize the revised regulations by early 2026, in alignment with the Executive Order's directive to modernize the permitting process and ensure timely access to critical minerals.

Pursuant to DSHMRA and 15 CFR § 970.209, a licensee who submits a timely and substantially complete application for a commercial recovery permit for the same area covered by their exploration license is granted a priority of right over other applicants, provided regulatory requirements are met.

Further permitting detail is outlined in Section17.

3.2 Exploration contract obligations and sponsorship

NORI and TOML, under their ISA exploration contracts, are required to, among other things:

- Submit an annual report to the ISA.
- Meet certain performance and expenditure commitments.
- Pay an annual overhead charge (currently US$60,000) to cover the costs incurred by the ISA in administering and supervising the contract.
- Implement training programs for personnel of the ISA and developing countries in accordance with a training program proposed by NORI and TOML in its application and five-year work plans.
- Take measures to prevent, reduce, and control pollution and other hazards to the marine environment arising from its activities in the Area.
- Maintain appropriate insurance policies.
- Establish environmental baselines against which to assess the likely effects of its program of activities on the marine environment.
- Establish and implement a program to monitor and report on such effects.

NORI is sponsored to carry out its mineral exploration activities in the Area by the Republic of Nauru, pursuant to a certificate of sponsorship signed by the Government of Nauru on 11 April 2011.

TOML is sponsored to carry out its mineral exploration activities in the Area by The Kingdom of Tonga, pursuant to a certificate of sponsorship signed by The Kingdom of Tonga on the 23 September 2021.

Sponsorship of an entity requires the sponsoring State to certify that it assumes responsibility for the entity's activities in the Area in accordance with the Convention. NORI and TOML as incorporated entities in their respective countries (Nauru and Tonga) are subject to applicable regulations and legislation applicable to their respective national regulatory frameworks.

As sponsoring nations, both the Republic of Nauru and The Kingdom of Tonga have enacted Seabed Mineral Acts (Nauru International Seabed Minerals Act 2015 and Tongan Seabed Minerals Act 2014) to regulate and manage their respective countries' involvement in deep sea mineral activities.

In June 2017 and September 2021, NORI and TOML, entered into Sponsorship Agreements with the Republic of Nauru and The Kingdom of Tonga, respectively formalizing certain obligations of the parties in relation to exploration and potential exploitation of the Contract Area of the CCZ. The NORI sponsoring agreement was revised on June 4, 2025.

Under the Sponsorship Agreements, NORI and TOML have the exclusive right to explore for nodules in the Area pursuant to the contracts for exploration dated between the ISA and NORI and TOML (the "exploration contracts").

The terms of the NORI and TOML Sponsorship Agreements are aligned with the duration of each exploration contract (15 years) and contain provisions for automatic extension for a further 20 years upon reaching the Minimum Recovery Level (as such term is defined in the Sponsorship Agreement) under an ISA exploitation contract.

3.2.1 Work program

As of the date of this Technical Report, both NORI and TOML are in the fourteenth year of their exploration contracts.

Under the NORI and TOML exploration contracts, 23 offshore campaigns were completed over 997 days focused on resource assessment, seabed mapping, and environmental baseline studies in the Clarion Clipperton Zone.

Key offshore work included deploying and testing a full-scale prototype CV that recovered 3,000 mt of nodules from NORI Area D, extensive bathymetric and geotechnical surveys, metocean mooring deployments for oceanographic data, and comprehensive benthic and water column biological monitoring using remotely operated vehicles (ROVs), (AUVs), and other instruments.

These efforts established a detailed understanding of seafloor conditions, mining system performance, and environmental impacts to support commercial recovery planning.

Both NORI and TOML have submitted detailed annual reports to the ISA which include financial statements on levels of expenditure on the Contract Area.

As of the date of this report, TMC USA has submitted two applications for exploration licenses, USA-A and USA-B. These are currently being reviewed by NOAA in accordance with 15 CFR Part 970.

The activities included in the proposed exploration plan for USA-A include:

- Completing resource definition and environmental baseline data collection outside the NORI Area D initial development area.
- Pursuing the commercial recovery permit application for the NORI Area D, where sufficient work has already been completed.
- Advancing mine planning and feasibility studies for offshore nodule collection systems and onshore processing facilities in the USA.

The activities included in the proposed exploration plan for USA-B include:

- Selecting an Initial Development Area by mapping the entire Contract Area using hull-based multibeam surveying (where it has not been done already) and assessing Mineral Resource distribution to Inferred status.
- Conducting reconnaissance environmental baseline sampling and habitat mapping to support selection of the Initial Development Area, followed by completing an environmental scoping study and obtaining approval for the environmental baseline program.
- Upgrading Mineral Resource definition to Indicated status through closer-spaced sampling, completing habitat mapping to define a two-year mining area and Preservation Reference Zones (PRZ), and identifying a preliminary development sequence.

- Completing comprehensive environmental baseline studies to meet NOAA regulations, concurrently upgrading the Initial Development Area to Measured Mineral Resource status with detailed bathymetric, photographic, and geotechnical surveys for collector path planning.
- Undertaking mine planning and pre-feasibility studies for offshore nodule-collection systems in partnership with Allseas and onshore processing facilities in the USA, culminating in preparation of a Commercial Recovery Permit application supported by pre-feasibility, environmental impact assessment (EIA), and management plans.

3.2.2 Royalties and taxes

Under DSHMRA, royalties and taxes payable on any future commercial recovery of polymetallic nodules by U.S. entities in areas beyond national jurisdiction are governed by domestic U.S. law rather than international frameworks such as the ISA, to which the U.S. is not a party.

DSHMRA does not prescribe specific royalty rates, it authorizes NOAA to issue exploration licenses and commercial recovery permits, with terms and conditions that may include financial obligations. These obligations are determined on a case-by-case basis during the permitting process and are designed to ensure that U.S. seabed mining activities are conducted responsibly and in alignment with national interests.

NOAA's regulatory framework under DSHMRA includes provisions for public comment and environmental review but does not currently mandate a fixed royalty or taxation regime akin to the ISA's proposed ad valorem models. As such, financial terms are negotiated individually and may evolve with future legislative or executive directives, such as the April 2025 Executive Order promoting U.S. leadership in seabed mineral recovery.

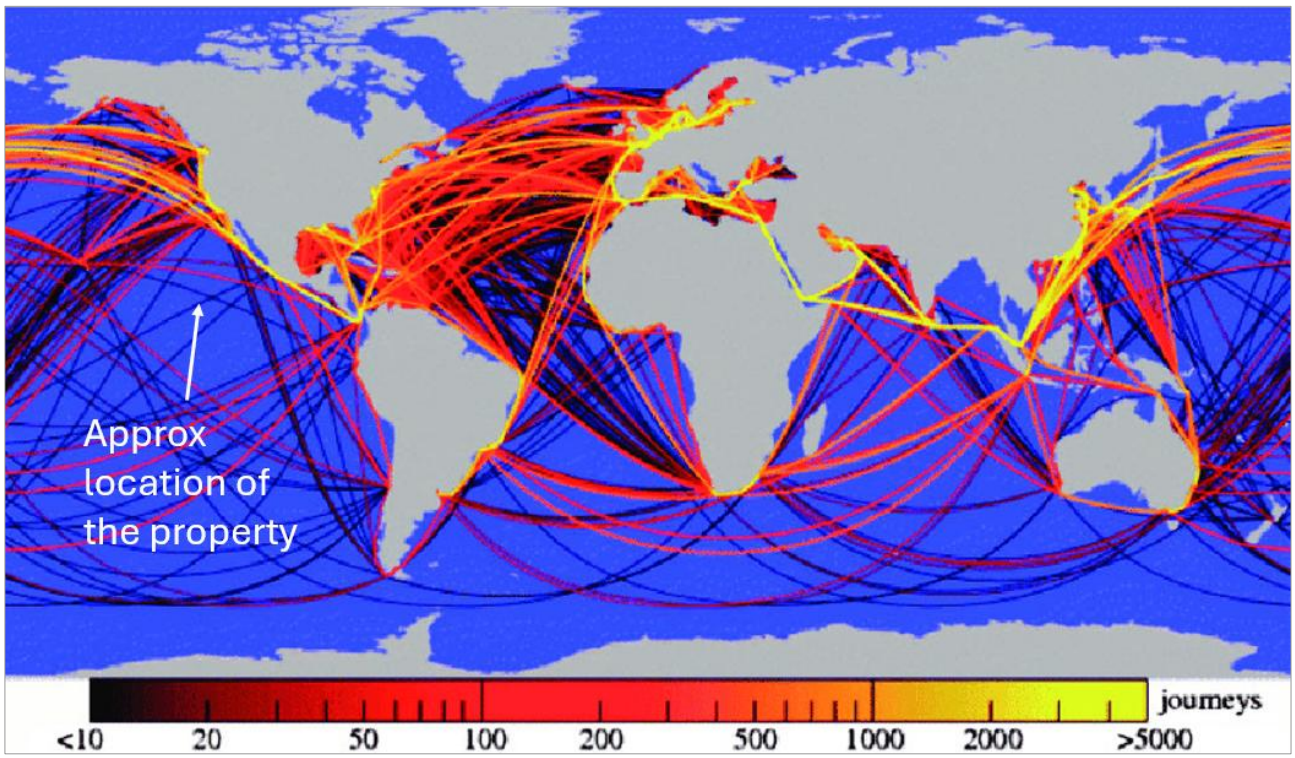
A revised sponsorship agreement with NORI has been signed. The updated agreement with NORI, announced in June 2025, ensures that the Republic of Nauru continue to receive financial benefits, training, and community development support. Importantly, it introduces "continuity benefits" that are expected to be activated once commercial production begins, either by NORI or another TMC subsidiary. A similar revised agreement is currently being finalized with The Kingdom of Tonga.

4 Accessibility, climate, local resources, infrastructure and physiography

4.1 Accessibility and infrastructure

The CCZ lies between Hawaii and Mexico and is accessible by ship from various ports in the US and South America. As the CCZ deposit does not include any habitable land and is not near coastal waters. All personnel and material is expected to be transported to the project area by ship. The region is well located to ship nodules to the American continent or across the Pacific Ocean to Asian markets. The CCZ is generally outside major shipping lanes as indicated in Figure 4.1 which shows the global cargo shipping network, illustrating the trajectories of all cargo ships bigger than 10,000 gross tonnage during 2007.

Figure 4.1 Global cargo shipping network



Note: The color scale indicates the number of journeys along each route.
Source: Adapted from Kaluza et al. 2010.

4.2 Climate

The CCZ has a tropical oceanic climate, with average temperatures of from 20°C to 32°C. Minimum and maximum temperatures generally occur in March and September, respectively (ISA, 2001), and the average sea surface temperature is 25°C. The CCZ is located in open ocean and is subject to tropical weather patterns.

Off-shore operations are planned to run throughout the year, with the exception of hurricane events, which are expected to occur once every three years. Tropical hurricanes are difficult to predict due to their erratic frequency but have high intensity over short periods and occur mostly during the period from May to October (Tilot, 2006, GSR 2018).

5 History

5.1 Overview

Submarine ferromanganese concretions were first discovered in the Kara Sea off Siberia in 1868 (ISA 2010a, citing Earney 1990). HMS Challenger, during its round the world expedition from 1873 to 1876, collected many small dark brown balls, rich in manganese and iron, which were named manganese nodules (ISA 2010a, citing Murray and Reynard [1891], Manheim [1978], and Earney [1990]).

Since the 1960s, polymetallic nodules have been recognized as a potential source of nickel, copper, cobalt, and manganese, and have been comparatively well studied because of their potential economic importance (Mero 1965). Scientific expeditions demonstrated that polymetallic nodules have a widespread occurrence in the world's oceans although their metal content and concentration vary from region to region.

During the International Decade of Ocean Exploration (1971 – 1980) and prior to the implementation of UNCLOS, many offshore exploration campaigns were completed in the CCZ by international organizations and consortia (the Pioneer Contractors). Several at-sea trial mining operations were also successfully carried out in the CCZ in the 1970s to test potential mining concepts. These system tests evaluated the performance of a self-propelled and several towed collection and mining devices, along with submersible pumps and airlift technology for lifting the nodules from the deep ocean floor to (SV).

NOAA monitored some of these tests as part of the Deep Ocean Mining Effects Study (DOMES II) program. The information collected during these activities provided key inputs to the impact analysis presented by NOAA in its Final Programmatic Deep-Sea Mining Environmental Impact Statement in 1981.

5.2 Pioneer Contractors

For the purpose of this report, the Pioneer Contractors include those entities that carried out substantial exploration in the Area prior to the entry into force of UNCLOS, as well as those entities that inherited such exploration data. This Section describes some of the more important activities of the Pioneer Contractors. Table 5.1 lists the Pioneer Contractors that operated in the areas that form the NORI and TOML areas.

Table 5.1 NORI and TOML ISA exploration Contract Areas and Pioneer Contractors

Area	Size (km^2)	Pioneer Contractor
NORI A	8,824	Yuzhmorgeologiya
NORI B	3,519	Yuzhmorgeologiya
NORI C	37,227	Interoceanmetal Joint Organisation
TOML A	10,281	DORD[1]
TOML B	9,966	Yuzhmorgeologiya
TOML C	15,763	Ifremer
TOML D	15,881	DORD
TOML E	7,002	KORDI, Interoceanmetal Joint Organisation
TOML-F	15,820	Arbeitsgemeinschaft Meerestechnisch Rohstoffe (AMR) and Ocean Management Inc. (OMI)

Notes: [1] Deep Ocean Resources Development Co. Ltd

NORI Area D and TOML-F were originally explored AMR. AMR subsequently joined Ocean Management Inc. (OMI). The OMI consortium comprised Inco Ltd (Canada), AMR (Federal Republic of Germany),

SEDCO Inc. (US), and Deep Ocean Mining Co. Ltd (Japan). OMI completed a successful trial mining operation in 1978. Hydraulic pumps, an air lift system, and towed collectors were tested in approximately 4,500 m of water. Approximately 800 t of nodules were recovered.

Kennecott consortium (now a division of Rio Tinto) first became seriously interested in seafloor polymetallic nodules in 1962 (Agarwal et al. 1979). In the 1970s, Kennecott developed and tested components and subsystems of a seafloor mining system and also carried out significant polymetallic nodule metallurgical processing test work.

Ocean Mining Associates (OMA) was formed in the mid-1970s, and comprised Essex Minerals (US), Union Seas (Belgium), Sun Ocean Ventures (US), with Deepsea Ventures as contractor. OMA conducted trial mining in the CCZ in 1977-78, recovering about 550 tonnes of nodules via suction dredge and airlift systems.

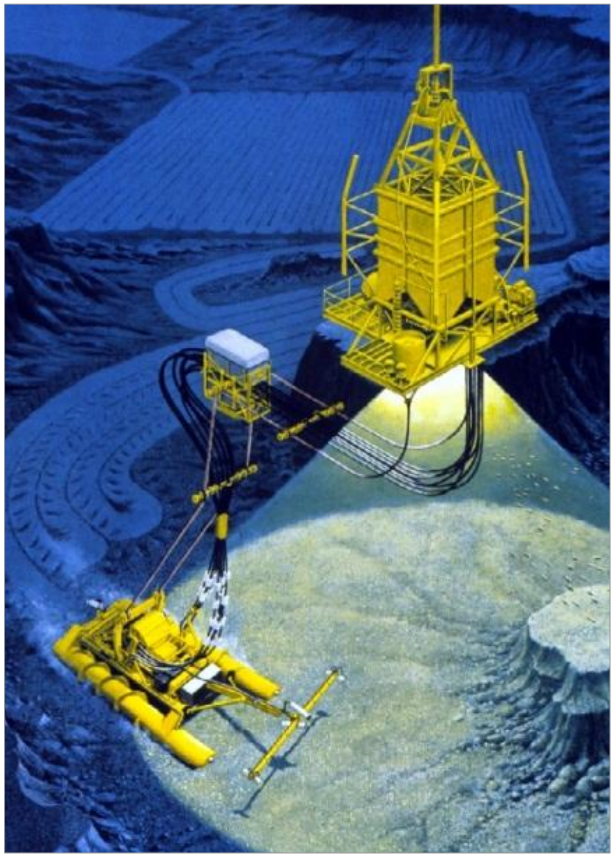
Between 1969 and 1974, Deepsea Ventures Inc. carried out 16 survey cruises of three to four weeks' duration each, to define the extent of the polymetallic nodule deposit discovered by them in 1969 in the CCZ. As reported by Deepsea Ventures Inc:

"These activities included the taking of some 294 discrete samples, including the bulk dredging of some 164 tonnes of manganese nodules from some 263 dredge stations, 28 core stations and three grab sample stations, cutting of some 28 cores, approximately 1000 lineal miles of survey of seafloor recorded by television and still photography, etc. As a result, the deposit of nodules identified with the discovery has been proved to extend generally throughout the entire area (American Society of International Law, 1975)."

Also active in the CCZ was the Ocean Minerals Company (OMCO), comprising Amoco Minerals Co. (US), Lockheed Missiles and Space Company Inc. (US), Billiton International Metals BV, and dredging company Bos Kalis Westminster (Netherlands). In a program lasting 16 years, OMCO collected thousands of free-fall grab and BC samples of nodules from its claim area and carried out trial mining. Lockheed's design efforts resulted in over 80 patents, a seafloor production system that consisted of a remote-controlled collector and crusher, a seafloor to surface slurry riser system, the first industrial scale DP system for a vessel, and a metallurgical processing plant (Spickermann, 2012).

In 1978, OMCO used a remote controlled fully maneuverable self-propelled miner with conveyor and crusher Figure 5.1 and Figure 5.2 to trial mine polymetallic nodules in the CCZ at approximately 4,500 m below sea level. The miner used an Archimedes screw drive system to provide traction and accurate maneuverability on the seafloor. Nodules were picked up by the miner and transferred to the buffer, where they were to be pumped to the surface by an airlift system.

Figure 5.1 Schematic of Lockheed Group's 1970s trial mining system



Source: DeepGreen. Used with permission of Prof. Jin Chung.

Figure 5.2 Remote operated collector used by the Lockheed Group in 1970s trial mining



Source: Spickerman 2012.

Yuzhmorgeologiya (Russian Federation) conducted extensive sampling in NORI Areas A and B using enclosed FFG combined with photographic units. Their sample preparation and chemical analysis methods closely resembled those of OMCO.

Six Pioneer Contractors are known to have surveyed areas within the TOML areas and collected samples of polymetallic nodules. Much of this work overlapped as it predated the signing of the Law of the Sea. These Pioneer Contractors include the Japanese group, Deep Ocean Resources Development Co. Ltd. (DORD), the South Korean group (KORDI), Yuzhmorgeologiya, the French group (Ifremer), the German group (FIGNR or BGR), and OMCO. The timing and location (ISA, 2003) of the OMCO sampling is known but the results are not available outside of ISA published contour maps. The samples within the TOML Area used for the Mineral Resource estimate were collected by Yuzhmorgeologiya, DORD, KORDI, IOM, and Ifremer.

Interoceanmetal Joint Organization (IOM), a consortium of Bulgaria, Cuba, Czech Republic, Poland, Russia, and Slovakia, registered as a Pioneer Contractor in 1992. IOM focused on geological and geophysical surveys covering large parts of the eastern CCZ, followed by research into mining system design and metallurgical processing.

Preussag (Germany) explored the CCZ in the 1970s using FFG and box corers. Their detailed laboratory procedures included cleaning, drying, photographing, measuring, crushing, pulverizing, and assaying nodules for key metals using atomic absorption spectrophotometry (AAS) and X-ray fluorescence (XRF).

AFERNOD (Association française pour l'étude et la recherche des nodules) / GEMONOD (France) completed programs backed by the French government, starting in the 1970s. The programs were focused on exploration near Marquesas Islands and the CCZ. Innovative mining concepts were developed, including free-shuttle autonomous vehicles and hydraulic lift systems. Detailed biological studies and metallurgical test work were conducted.

Deepsea Ventures Inc (DVI) was active from the mid-1960s, supported by US academic research. DVI conducted collector and airlift trials in the Blake Plateau and later formed part of the OMA consortium focusing on higher-grade nodules in the central CCZ.

DORD (Japan) began manganese nodule exploration activities in 1983 and was formally accepted as a Pioneer Contractor in late 1987. Between 1981 and 1989 it spent some JPY20 B (~US$80 M at the time; Kajitani, 1990). Much of the research and development expenditure was on a mining system concept, models and simulations and pilot development.

KORDI (now KIOST: Korea) began studying CCZ nodules in the 1980s, with collaboration and data collection through the 1990s. From 1995–2002, they defined Mineral Resources and established environmental baselines. Since 2002, research prioritized environmental impacts and benthic experiments, with detailed surveys and sampling. Their mining concept has undergone successful pool, shallow, and deep sea testing, with pilot-scale subsea components built and tested in 2015.

COMRA (China) conducted multiple oceanographic expeditions from 1978 onwards, with pilot-scale vehicle tests and lifting experiments conducted in the early 2000s.

Further details of these programs are presented in:

- The technical report summary titled “Technical Report Summary--Initial Assessment of the NORI Property, Clarion-Clipperton Zone, for Deep Green Metals Inc.” (the “NORI Technical Report”), with an effective date of March 17, 2021 (AMC Consultants, 2021a).
- The technical report summary titled “Technical Report Summary--TOML Mineral Resource, Clarion-Clipperton Zone, Pacific Ocean, for Deep Green Metals Inc.” (the “TOML Technical Report”), with an effective date of March 26, 2021 (AMC Consultants, 2021b).

5.3 NORI

NORI completed several offshore campaigns that included collection of geological data between 2012 and 2023. The offshore campaigns were named as follows:

Campaign 1. In 2012, NORI completed an offshore exploration campaign in NORI-C and Area D aboard the RV Mt. Mitchell, which sailed from the port of Seattle. NORI conducted extensive hull-based multibeam geophysical surveying of the seafloor and bulk sampling.

Campaign 2. In 2013, NORI carried out a second exploration campaign within NORI-A and B. This cruise was carried out in collaboration with TOML, using the RV Mt. Mitchell, and focused on hull-based multibeam bathymetry in NORI-A and B, identifying nodule fields based on acoustic data (including interpretation of backscatter data), and recovering bulk polymetallic nodule samples.

Campaign 3. In 2018, NORI conducted a successful survey and seafloor sampling program in NORI Area D. The work completed included detailed survey work using an multi-beam echo sounder (MBES) deployed on an AUV, side scan sonar (SSS), sub-bottom profiler (SBP), and camera payload; collection of 45 box cores from which nodule samples, biological samples and geotechnical samples were collected.

Campaign 6A and 6B. In 2019, NORI conducted two campaigns (6A and 6B) in NORI Area D. Campaign 6A was undertaken from 19/08/2019 to 03/10/2019 and Campaign 6B was undertaken from 10/11/2019 to 21/12/2019. The work completed included collection of 207 box cores from which nodule samples, biological samples, and geotechnical samples were collected.

Further details of Campaigns 1 to 6B are presented in:

- The technical report summary titled “Technical Report Summary--Initial Assessment of the NORI Property, Clarion-Clipperton Zone, for Deep Green Metals Inc.” (the “NORI Technical Report”), with an effective date of March 17, 2021 (AMC Consultants, 2021a).

Campaign 7A and 7B. In 2022 NORI completed an integrated collection system test, supported by the *Hidden Gem* collector vessel in NORI Area D. Campaigns 7A and 7B in NORI Area D were primarily concerned with collecting environmental data. Campaign 7A was conducted prior to the collector system test and Campaign 7B was collected after the collector system test. Box cores were collected and environmental sampling and geotechnical testing, including in situ cone penetration tests (CPT) conducted from a ROV, were carried out. High resolution AUV MBES bathymetric, side scan and SBP and camera imagery surveying within the collector system test area were completed.

Campaign 8

Campaign 8A was conducted in late 2023 and early 2024, 12 months after completion of Test Mining, and was focused on collecting benthic biological data and conducting high resolution mapping work in the proposed initial production area within the NORI Area D. During this campaign six (6) box cores were collected to provide additional resource information in areas which had not been directly impacted by collection.

Additionally, 196 line km of AUV deployed MBES, SSS, SBP, and 245 line km of camera data were collected over an area of 245.712 km^2 in areas delineated as runs 19 and 20 in the NORI Area D PFS (AMC, 2025).

5.4 TOML

TOML completed offshore campaigns in 2013 and 2015 to collect data define Mineral Resources. The offshore campaigns were named as follows:

CCZ13. In 2013, the MBES system of the chartered vessel RV Mt Mitchell was used to map the seafloor in TOML Areas B through F. Dredge samples were collected from TOML B and TOML D to confirm the nodule grades indicated by Pioneer Contractor samples and support metallurgical test work.

CCZ15. In 2015, TOML used the experienced team and equipment spread on the RV Yuzhmorgeologiya to sample and image map priority areas so that a higher confidence and expanded Mineral Resource could be estimated, and to collect environmental baseline and geotechnical data. A total of 113 box cores were collected from TOML-B, TOML-C, TOML-D, TOML-E and TOML-F for resource definition purposes. Biological samples and geotechnical samples were also collected. Deep-tow sonar, including SSS, SBP and high-resolution bathymetry were completed.

Further details of these programs are presented in:

- The technical report summary titled “Technical Report Summary-TOML Mineral Resource, Clarion-Clipperton Zone, Pacific Ocean, for Deep Green Metals Inc.” (the “TOML Technical Report”), with an effective date of March 26, 2021 (AMC Consultants, 2021b).

6 Geological setting and mineralization

6.1 Global distribution of nodules

Seafloor polymetallic nodules occur in all oceans, and the CCZ hosts a relatively high abundance of nodules. Other relatively dense zones are found in the Peru Basin in the southeast Pacific, the centre of the north Indian Ocean, and the Cook Islands Figure 6.1.

Figure 6.1 Schematic diagram of average abundance of polymetallic nodules in four major locations



Source: GRID-Arendal 2014b.

6.2 Regional tectonic setting and topographic features

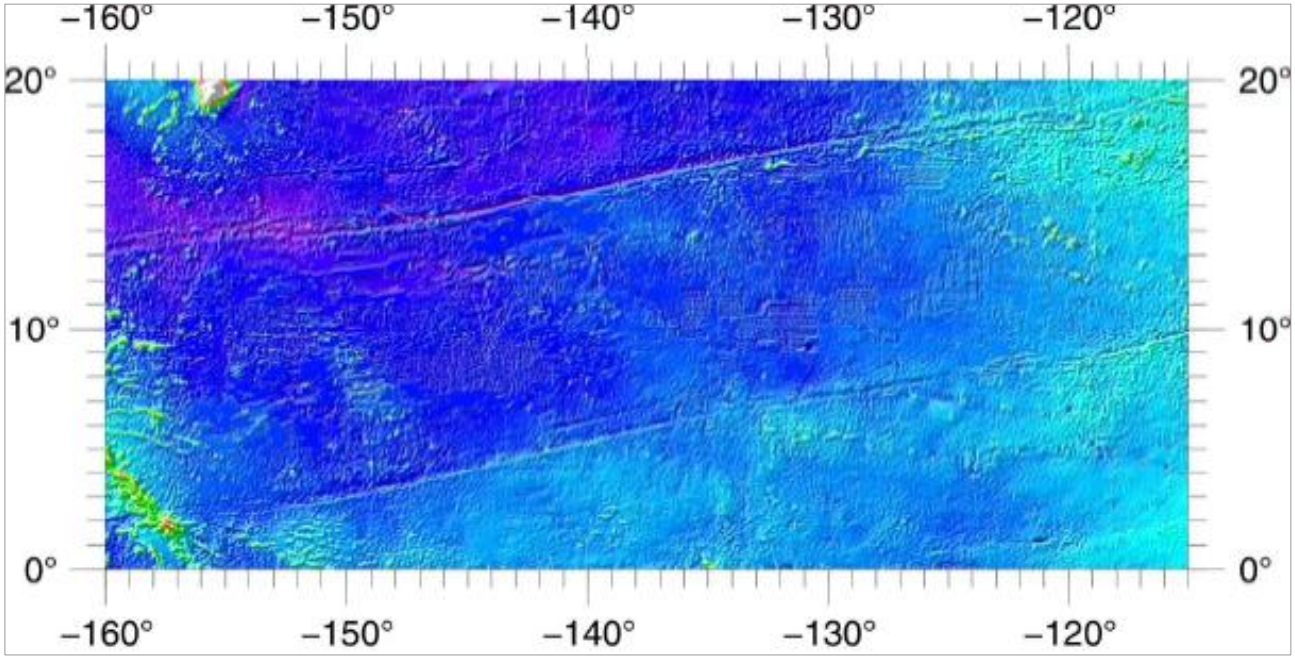
The CCZ is defined by two major west-south-west and east-north-east trending fracture zones running through the seafloor; the Clipperton Fracture Zone to the south and the Clarion Fracture Zone to the north. These fractures zones can be seen clearly on the bathymetric map Figure 6.2. The eastern and western limits can be defined by the Mathematicians Seamounts or Ridge in the east, and the Republic of Kiribati or Line Islands in the west.

The CCZ seafloor forms part of the Abyssal Plains, which are the largest physiographic province on Earth, covering some 70% of the area of ocean basins and 30% of the Earth's surface (ISA 2004). The Abyssal Plains are traversed by ridges, believed to have formed from the process of seafloor spreading. Orientation is north-north-west to south-south-east (locally ±20°), with amplitude of 50 m to 300 m (maximum 1,000 m; Hoffert 2008) and wavelength of 1 km to 10 km. The Abyssal Plains are punctuated by extinct volcanoes rising 500 m to 2,000 m above the seafloor.

Depth increases from 3,800 m to 4,200 m at 115° west to 4,800 m to 5,200 m at 130° west, and 5,400 m to 5,600 m at 145° west.

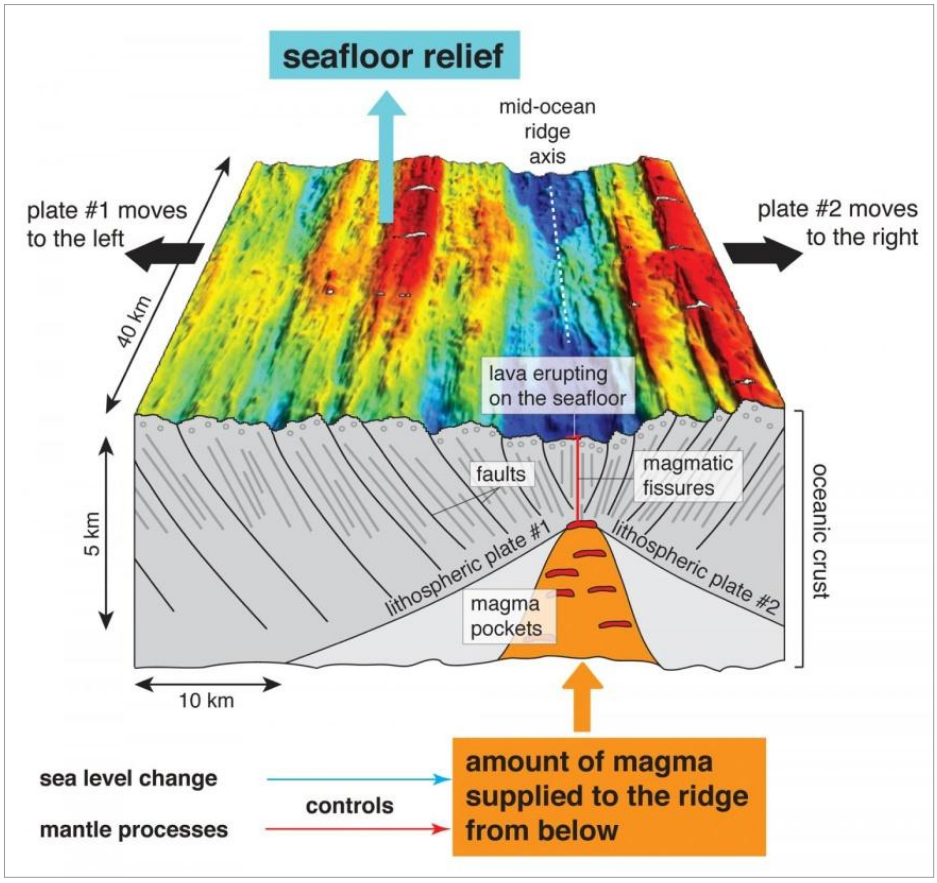
The seafloor sediments exhibit trends perpendicular to the fracture zones, from predominant carbonate sediments in the south-eastern extreme to predominant siliceous red clay in the west north-west.

Figure 6.2 Bathymetric map of the Clarion-Clipperton Fracture Zone



Source: ISA 2010.

Figure 6.3 Formation of abyssal hills at mid-oceanic ridges



Source: modified from Olive et al. (2015)

6.3 Regional geological domains

Classification of the seafloor into geological domains allows the important geological, topographic, and tectonic features which characterize nodule prospectivity to be captured for Mineral Resource estimation and mine planning purposes. Based on analysis of bathymetric data together with BC data, TMC recognized and mapped eight geological domains within NORI Area D:

1) **Abyssal plains:** these constitute the majority of the CCZ and are characterized by gentle slopes of 0° to 6°, and nodules lying on soft sediment. Nodules were observed to be ubiquitous in this domain wherever it was surveyed and sampled. It is considered a highly- prospective domain for nodules.
   The abyssal plains can be further divided into three subdomains based on backscatter response and ground-truthing (box core samples and land-out video footage):
   - Areas considered indicative of Type 2 and 3 nodule facies (see Table 6.1), as determined from high amplitude backscatter response.
   - Areas considered indicative of Type 1 nodule facies (see Table 6.1), as determined from moderate amplitude backscatter response.
   - Sediment drift domains—characterized by a soft sediment ooze with low amplitude backscatter response, and extremely low to no nodule abundance.
   - Volcanic cones (see below).
2) **Abyssal hills:** these are topographically higher features, oriented NNW-SSE, and are parallel to one another. Slopes of the hills are mostly gentle on the western side, while they are very steep at the eastern side, likely representing horsts (fault blocks) bounded by inward-dipping normal faults and outward-dipping volcanic growth faults respectively.
3) **Abyssal hills (hard)**: abyssal hills where the hill crests are associated with the occurrence of hardgrounds, caused by proximity of underlying (harder) Neogene-age footwall sediment succession at the seafloor, typically covered by a veneer of unconsolidated sediment.
4) **Slopes ≥ 6°**: these are associated with the flanks of abyssal hills, where the slope is 6° or greater, and are likely associated with hardgrounds and/or volcanic debris and volcanic outcrop development typically associated with NNW trending faults. These steep slopes are considered to have low nodule prospectivity but have not been fully tested with sampling or photography.
5) **Slopes ≥ 6° (hard)**: these are associated with the flanks of abyssal hills where the slope is 6° or greater, and are associated with hardground development, typified by outcropping (harder) Neogene-age sedimentary rocks. These steep slopes are considered to have low nodule prospectivity, based on limited box core sampling, AUV SBP data and photography.
6) **Volcanic outcrops:** these are associated with volcanic growth-faults along the abyssal hill flanks, which trend NNW-SSE, and are elongated, narrow bodies mapped through integration of AUV SBP and camera data with EM 122 MBES data backscatter data.
7) **Volcanic cones**: these are typically grouped in chains and follow the east-southeast “Hawaiian trend”. These are isolated features and were not sampled, however, due to their volcanic origin, steep slopes (>6°) and dominant high-intensity backscatter (typically associated with volcanic outcrop), they are also considered to have low nodule prospectivity.
8) **Volcanic high:** this is a macro-scale topographic feature situated in the SE corner of NORI Area D. It is interpreted as a relic volcanic intersection high, which also includes a relic transform parallel trough. Both are volcanic related features associated with the Clipperton transform zone, situated to the south of NORI Area D.

Geological investigations and the mapping of geological domains are less advanced in the other NORI and TOML areas, compared to NORI Area D. Features such as abyssal plains, abyssal hills, volcanic cones, and slopes ≥ 6° have nonetheless been identified in these areas using MBES surveys. In addition, sediment drifts ponded in depressions, covering approximately 7 % of TOML Areas B to F, have been

interpreted from MBES data. There is also evidence for sediment accumulation near the base of some seamounts.

6.4 Regional trends in polymetallic mineralization

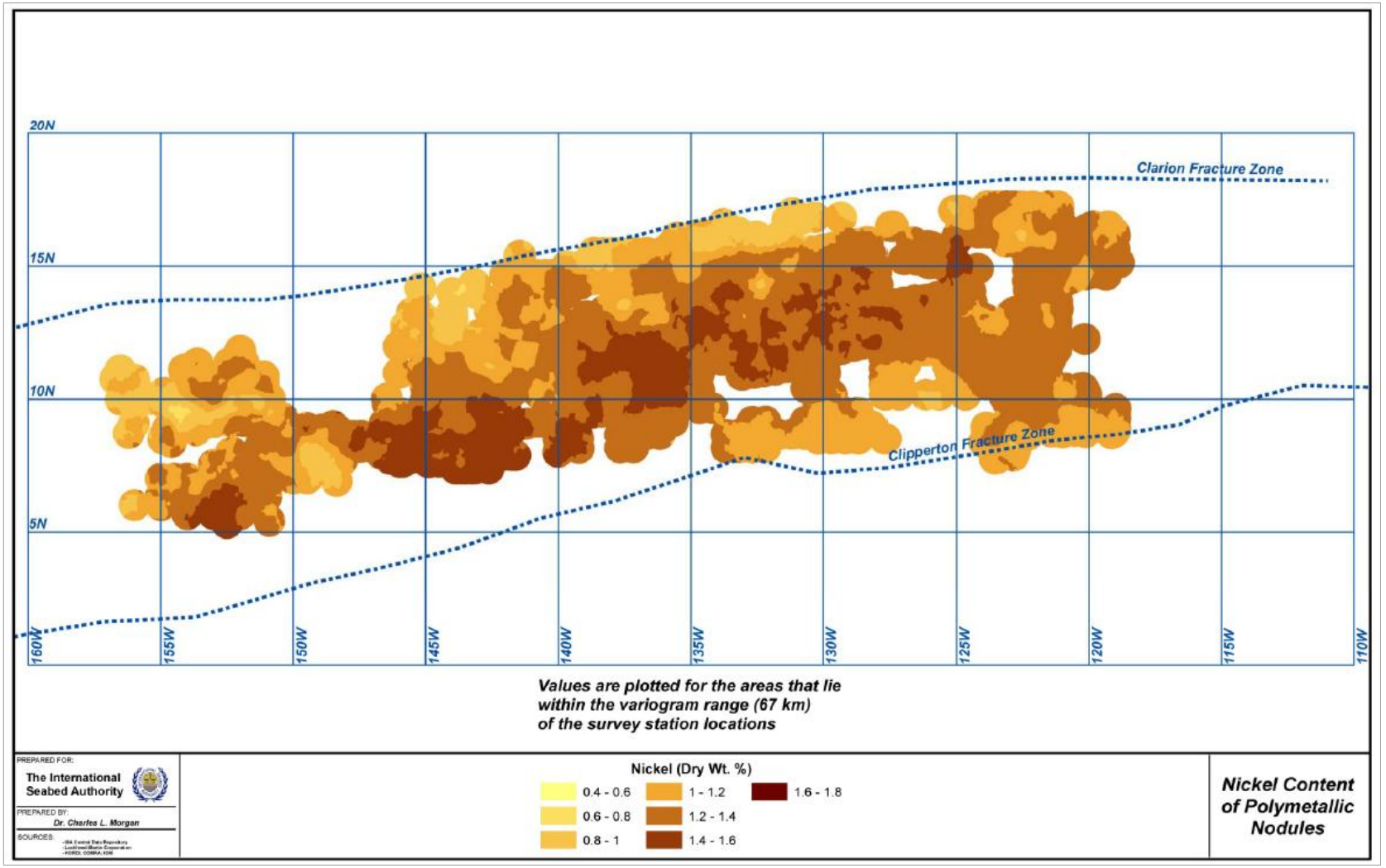
The ISA completed a geological modelling project in 2009, based on data collected by Pioneer Contractors over the preceding 30 years (ISA, 2010a).

Nodule chemistry varies only slightly within the CCZ. Figure 6.4 to Figure 6.7 show the distribution of nickel, cobalt, copper, and manganese grades across the CCZ, as estimated by the ISA. The high continuity and low variability of grades across vast distances is remarkable. Copper and manganese generally increase towards the southeast, cobalt is generally higher towards the north, and nickel is generally higher towards the centre and southwest of the CCZ. The reason for these very large-scale trends is not clear. The German data for NORI Area D were not included in the ISA geological model.

The nodules vary in abundance, in some cases touching one another and covering more than 70% of the seafloor. The highest concentrations of nodules have been found on abyssal plains between 4,000 m and 6,000 m below sea level.

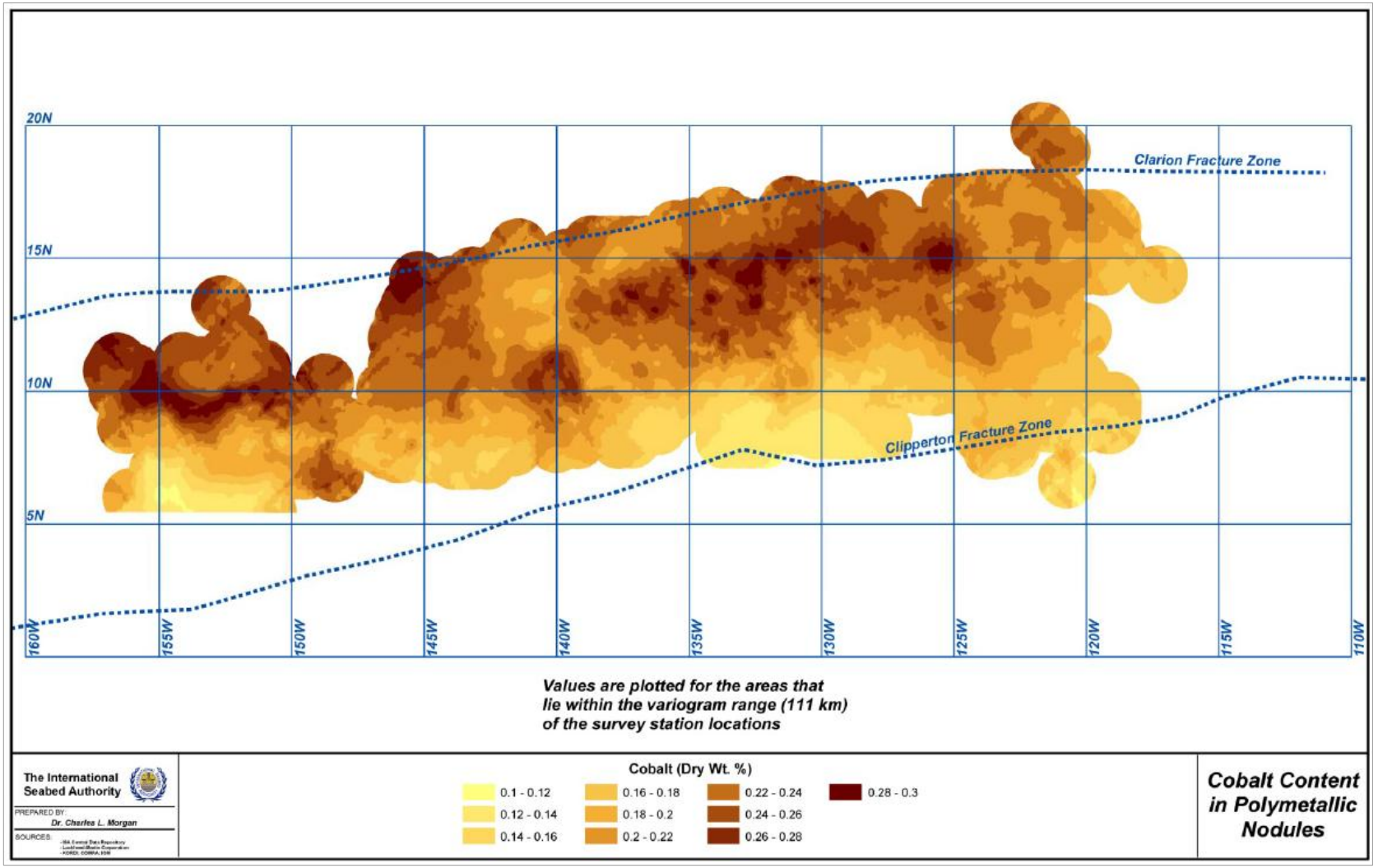
Figure 6.8 shows estimated nodule abundance data from the ISA geological model project. Data analysis shows that variability of nodule abundance is significantly higher than variability of metal grades.

Figure 6.4 Map of nickel grade distribution in the CCZ



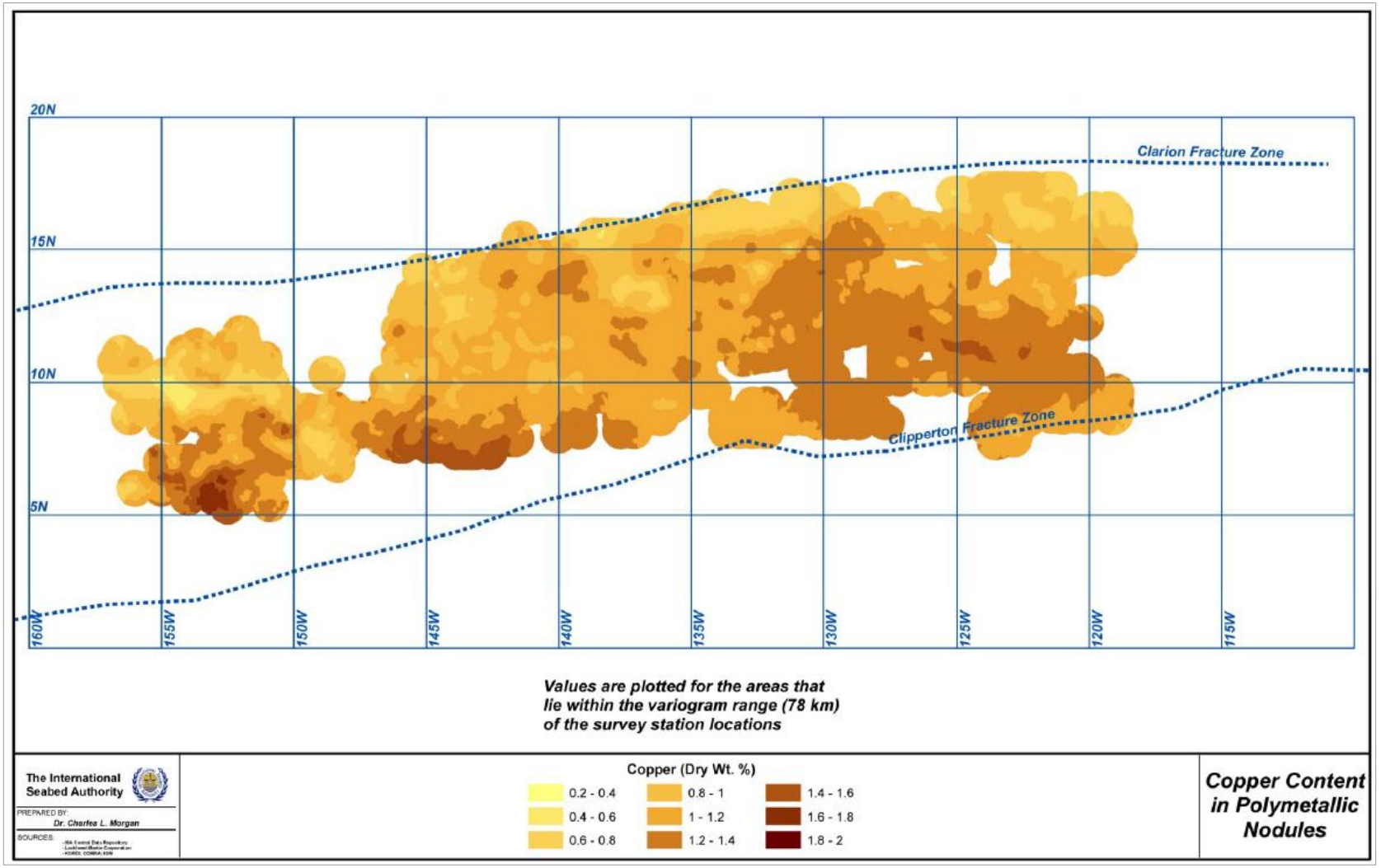
Source: ISA (2009)

Figure 6.5 Map of cobalt grade distribution in the CCZ



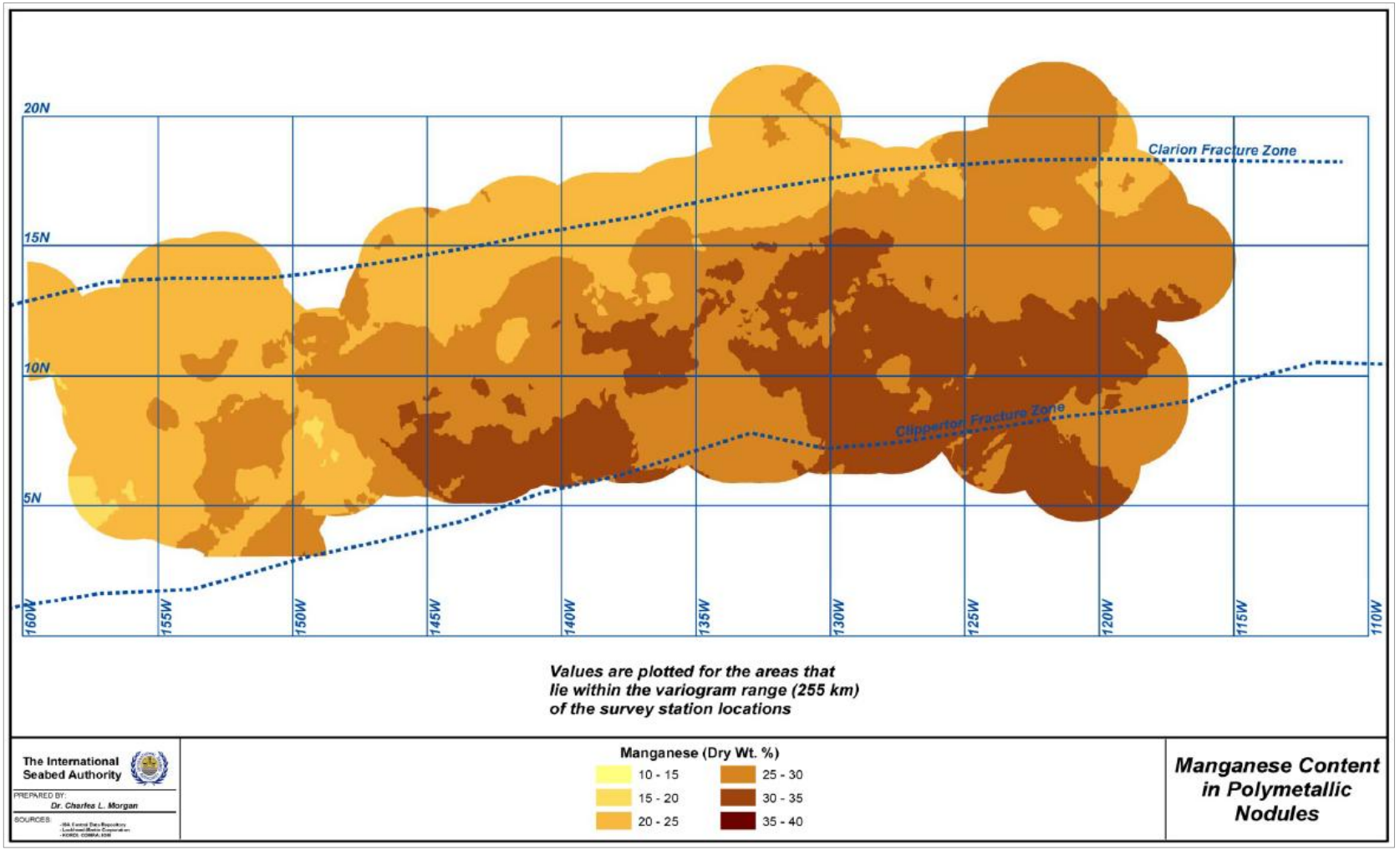
Source: ISA

Figure 6.6 Map of copper grade distribution in the CCZ



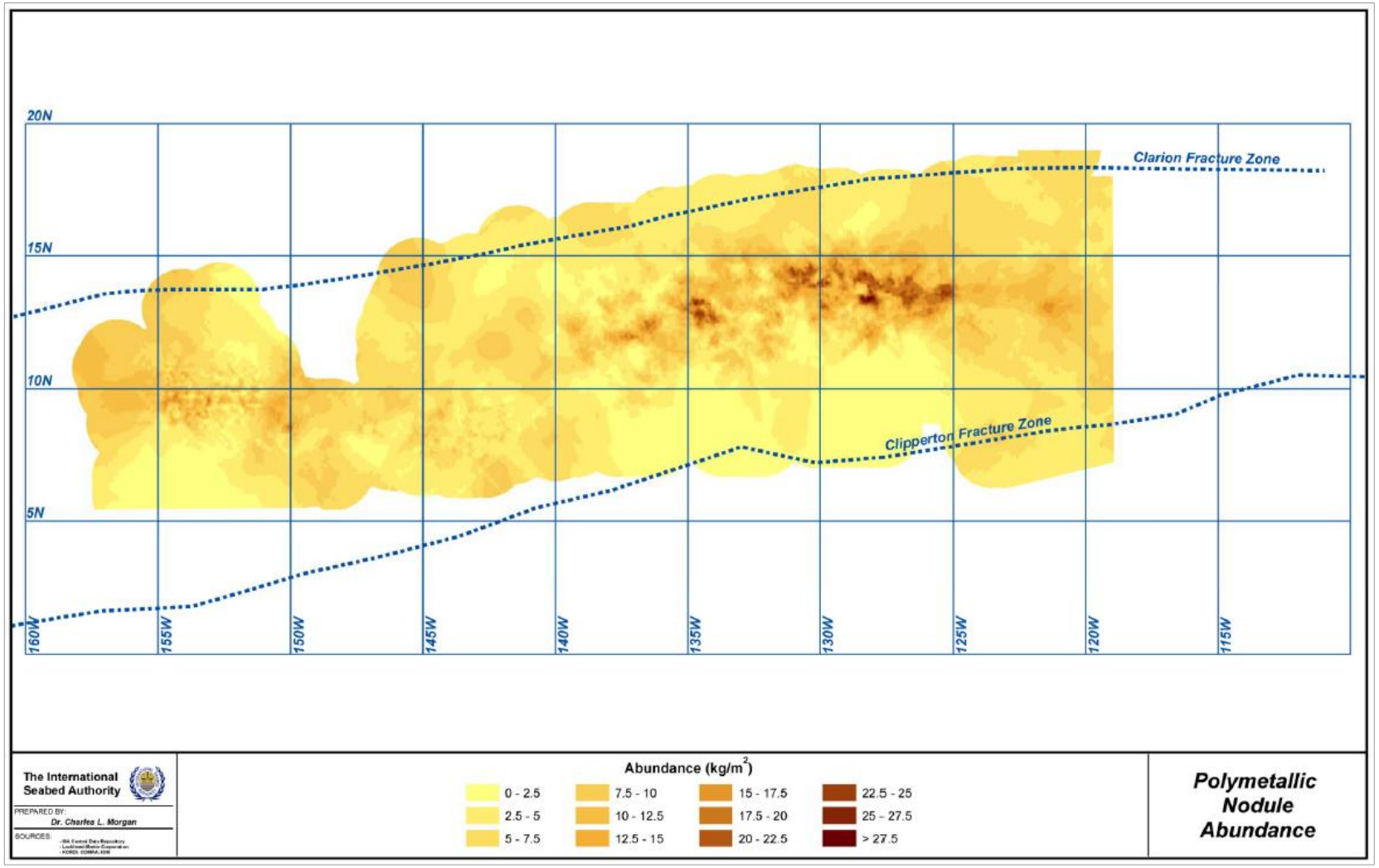
Source: ISA

Figure 6.7 Map of manganese grade distribution in the CCZ



Source: ISA

Figure 6.8 Map of abundance distribution in the CCZ



Source: ISA

6.5 Nodule formation and sedimentation

Seafloor polymetallic nodules are composed of nuclei and concentric layers of iron and manganese hydroxides and formed by precipitation of metals from seawater. The metal accumulation rates are slow, and it takes a few million years to form a nodule (Skowronek et al, 2021).

Nodules are abundant in abyssal areas with oxygenated bottom waters, low sedimentation rates (less than 10 cm per thousand years), and where sources of abundant nuclei occur (Hein et al. 2013). Nodules grow on 0.1 cm to 1 cm nuclei (e.g., pieces of pumice and older broken nodules) and generally range from about 1 cm to 12 cm in their longest dimension, with the low to middle-range typically the most common (1 to 5 cm).

The specific conditions of the CCZ (water depth, latitude, and seafloor sediment type) are considered to be the key controls for its formation, along with the following factors:

- Supply of metals to the growing surface.
- Presence of a nucleus.
- The erosive forces caused by benthic currents.
- Occurrence of semi-liquid surface layer on the seafloor (sediment water interface).
- Bioturbation.

The highest values of metals in nodules are thought to be developed on the seabed in the equatorial regions away from land sources of sediments. In these regions surface waters have high primary productivity. Tiny plants and animals concentrate the metals from seawater and when they die, they sink to the seafloor, dissolve, and release the metals into the pore water of seafloor sediments. Sediments from the CCZ consist mostly of clays and siliceous biological casts. Sands and larger sediments are not generally found so far from land, and the commonly formed carbonate biological casts dissolve on the seabed in these deep-water regions faster than they accumulate.

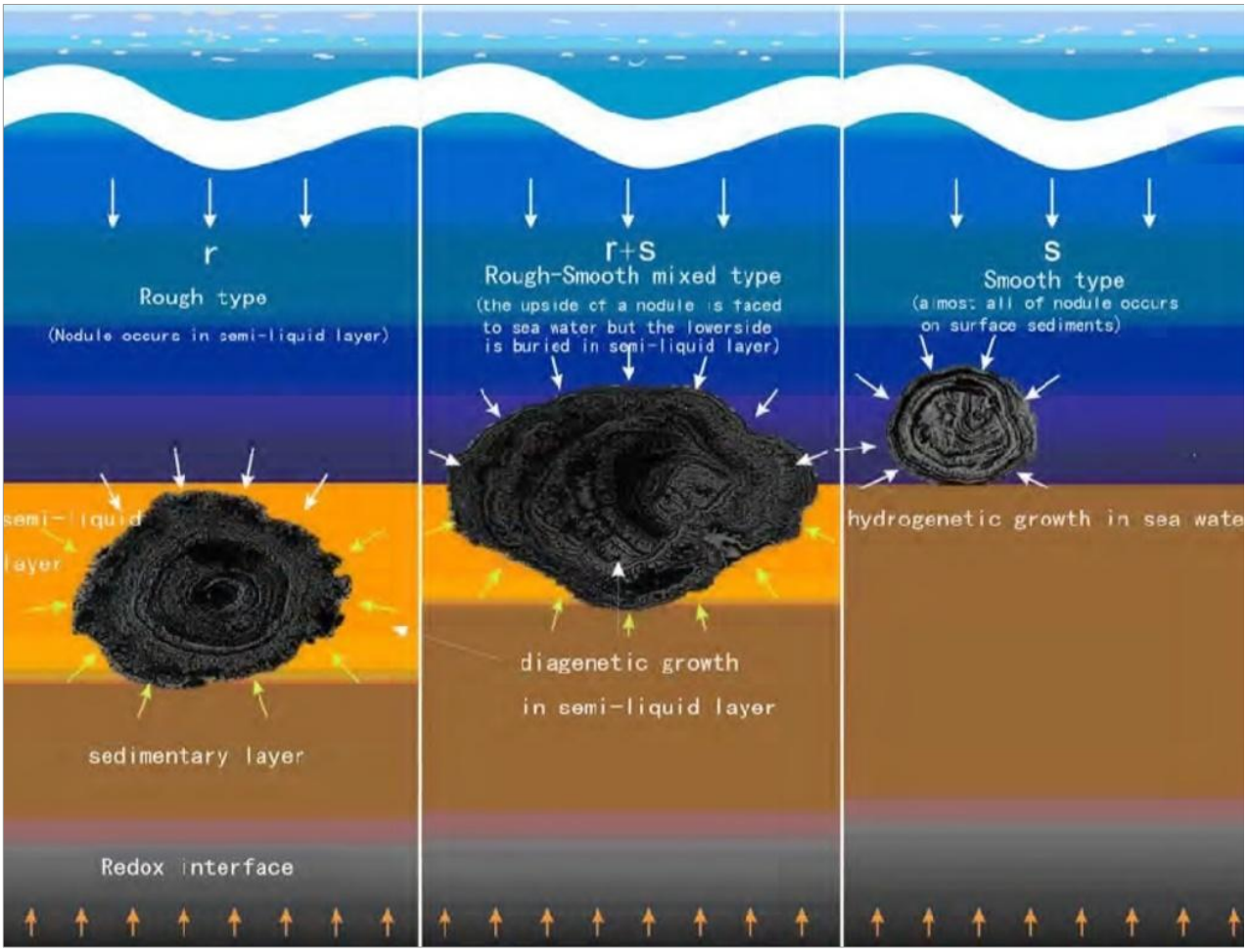
Nodules are classified according to their morphology or texture, as:

- S-type (smooth type).
- R-type (rough type).
- S-R-type (smooth-rough mixed type).

It is postulated that the different textures are related to the position of the growing nodule, relative to the seafloor, as shown in Figure 6.9. The S-type nodules are interpreted to have grown by absorption of metals directly from seawater (hydrogenetic processes), the Rough type nodules (R-type) are interpreted to have absorbed metals from the water within the seafloor sediment (diagenetic processes), and the Smooth-rough type nodules (S-R-type) are interpreted to have grown as a result of both hydrogenetic and diagenetic processes.

In the NORI and TOML areas, most of the polymetallic nodules lie on the seafloor, often partly covered with soft sediment. In other locations, some nodules have been recorded as completely buried but the frequencies of such subsurface occurrences are very poorly defined (e.g., Kotlinski and Stoyanova (2006).

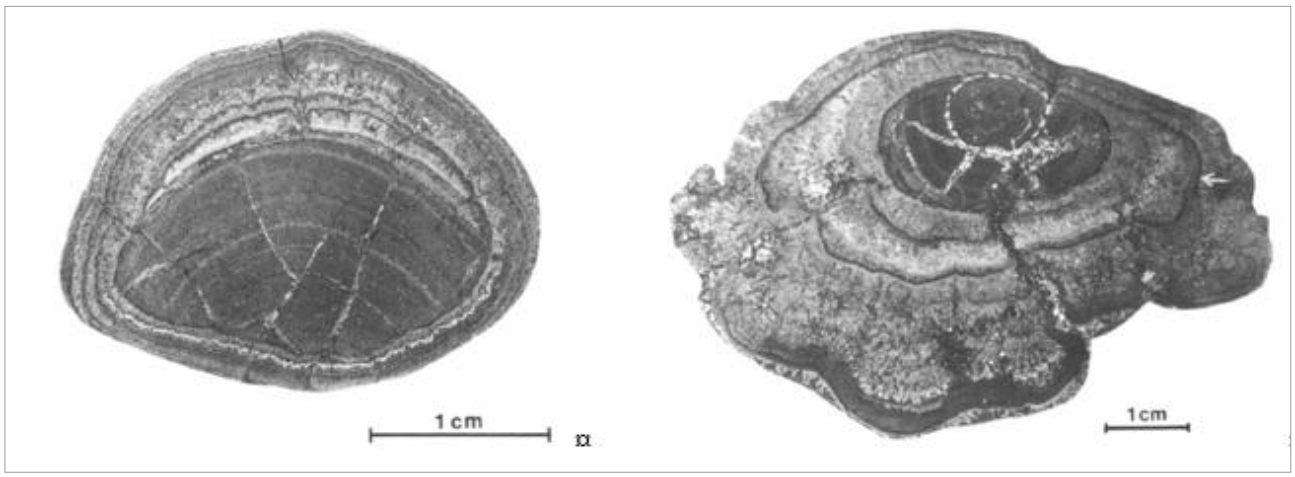
Figure 6.9 Polymetallic Nodule Types



Source: ISA (2010)

NORI and TOML developed classification systems for nodules similar to the ISA system, using descriptors of nodule form, such as size, shape, texture, and fragmentation. These were recorded and the logs were captured in digital databases. Examples of nodule type are shown in Figure 6.10, Figure 6.11 and Figure 6.12.

Figure 6.10 Sections through a S-type Nodule (left) and a R-type Nodule with a S-type core (right)



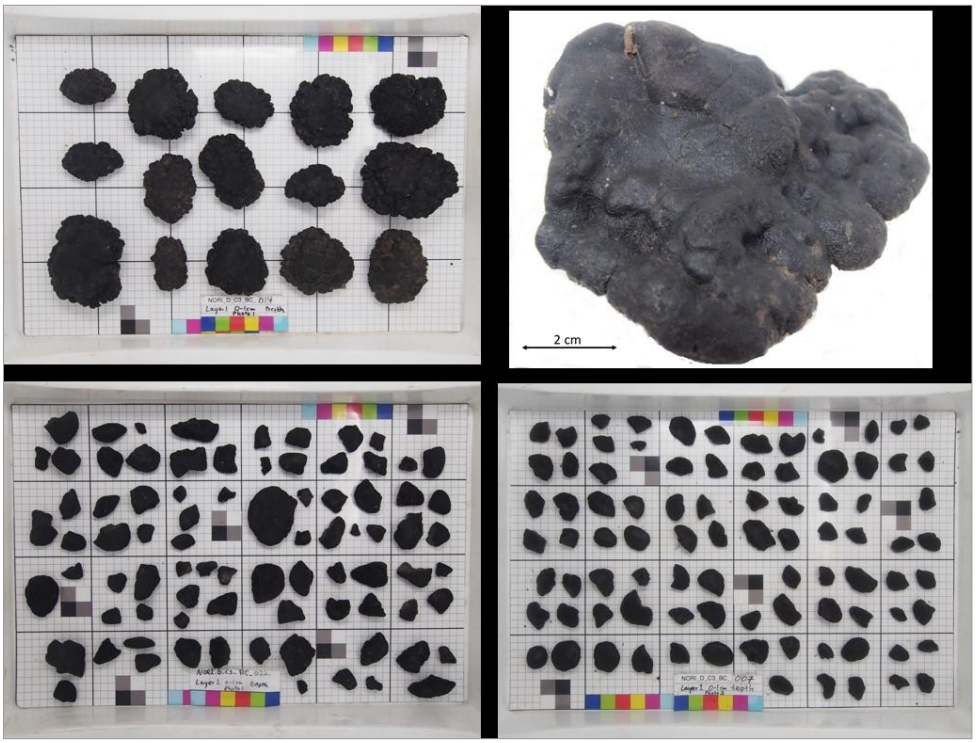
Source: von Stackelberg and Beiersdorf (1991).

Figure 6.11 Example nodules found in the TOML area



Source: TMC. Smooth (top left), rough-smooth (top right), rough (bottom left) and overturned rough-smooth (bottom right) types.

Figure 6.12 Examples of nodules recovered during the 2018 NORI Area D campaign

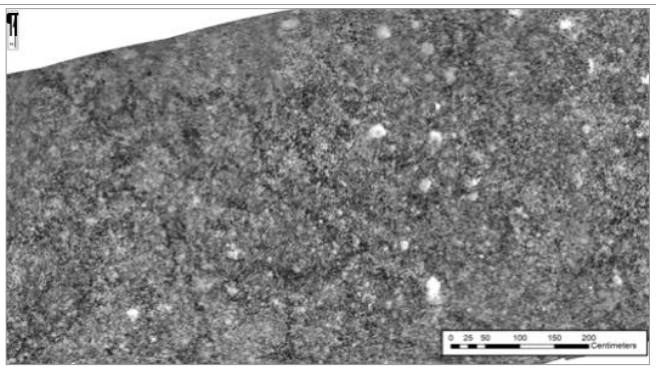
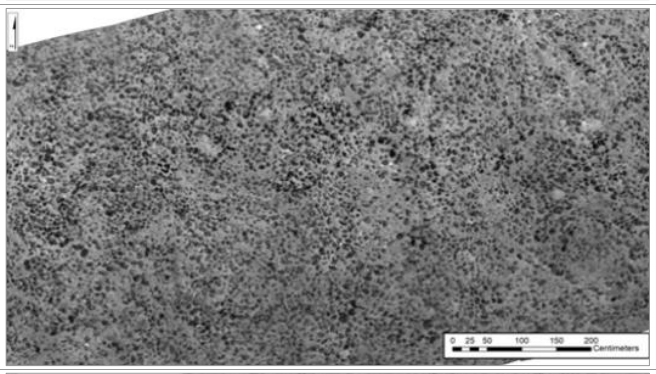
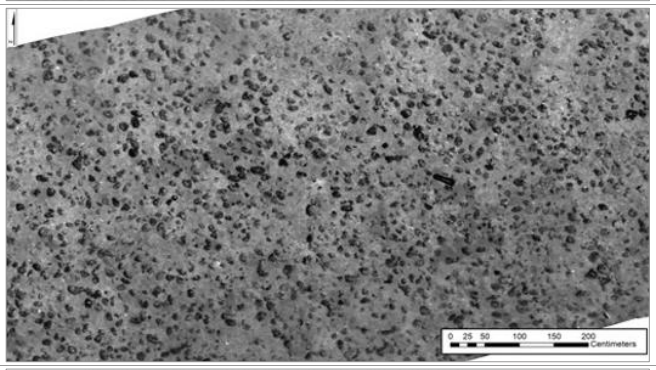
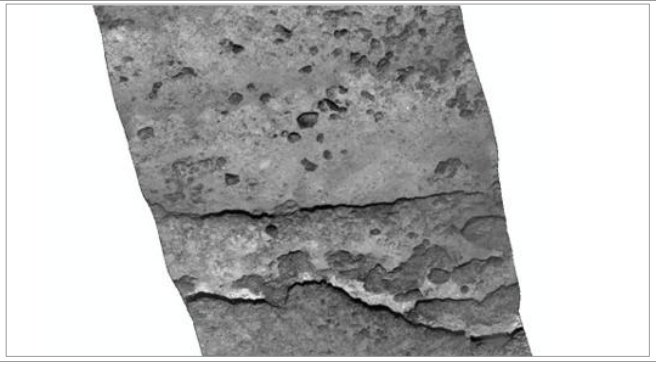


Upper left – example of large nodules with rough texture. Top right – close-up of large nodule. These nodules were the least-dominant size class. More common were nodules in the 2-5 cm range, as shown by examples in lower left and right. Source: TMC

6.6 Nodule facies

Nodule size, shape and texture can be quite variable within a single sample. As a consequence, it is difficult to apply practical classification schemes based on these characteristics to broad areas of the seafloor. In order to characterize nodule occurrences on the seafloor at a larger, more practical scale, NORI identified three broad *facies* of nodule distribution. These are based on nodule coverage and the range of nodule sizes, as interpreted from camera imagery. They are summarized in Table 6.1.

Table 6.1 Polymetallic Nodule Facies in NORI Area D

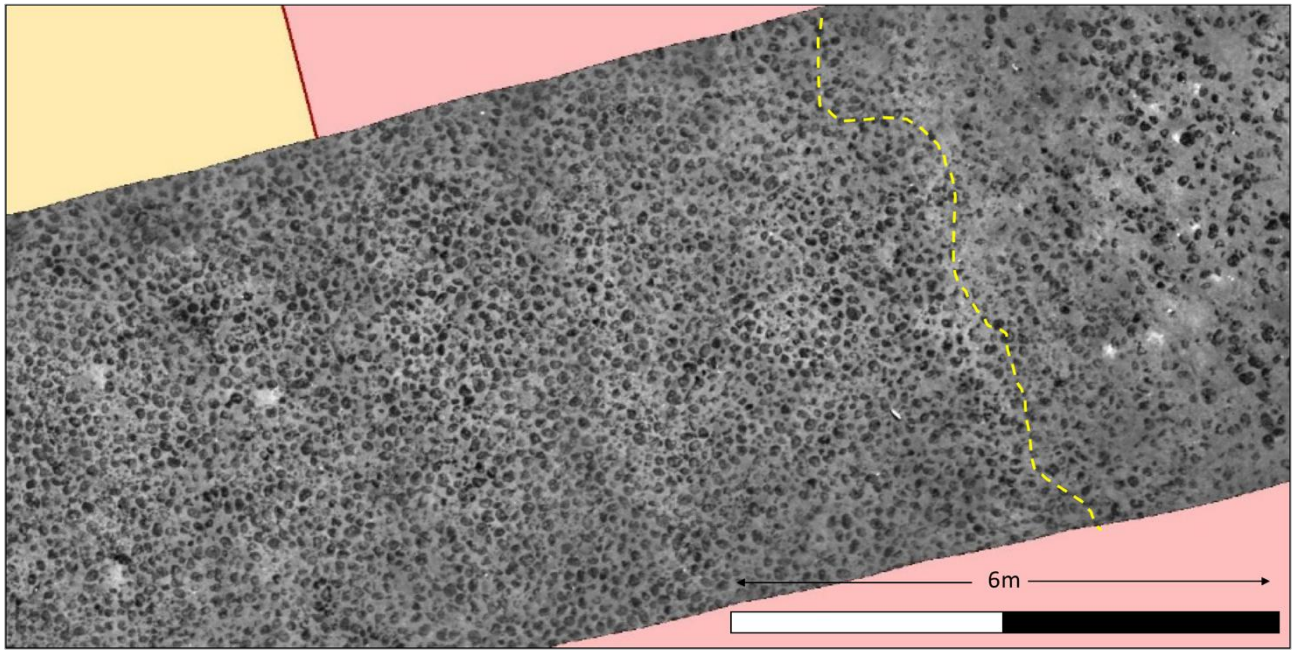
Nodule camera facies type	Description	Example
Type 1 - densely packed / interconnected	>50% of seafloor covered by nodules ~1 – 10 cm length	
Type 2 - mostly individual / locally interconnected	~20 – 40% of seafloor covered by nodules Mostly 5–20 cm length	
Type 3 – mostly individual / sparse	10 – 20% of seafloor covered by nodules Mostly 5 – 20 cm length	
Other	Volcanic outcrop - associated with NW-SE ridges	

Type 1 nodule facies is typically characterized by >50% nodules (by area of coverage). The majority of these nodules are typically medium-sized and are closely packed, with many nodules in contact with their neighbors.

Types 2 and 3 are characterized by larger nodules, and the nodules are typically separated (i.e., there are noticeable sediment gaps between individual nodules).

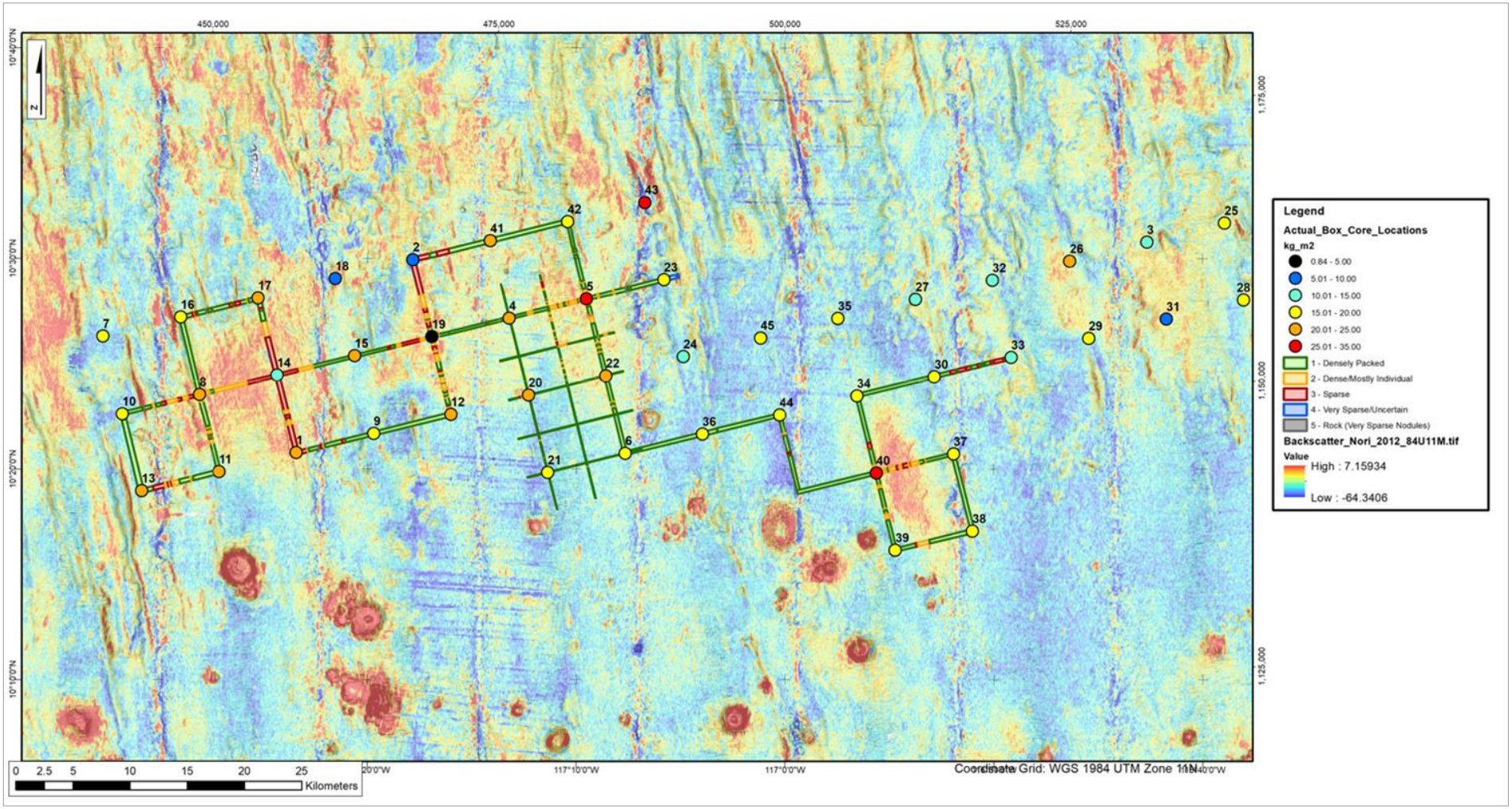
In high-resolution camera imagery, facies boundaries may be quite sharp (i.e., not gradational) and variable over short distances (<100 m), as illustrated in Figure 6.13.

Figure 6.13 Camera Imagery Showing Change from Type 3 Nodules (right) to Type 2 (left)



Nodule distributions can be mapped by measuring the backscatter (return signal) response from multi-beam echo sounding (MBES) from vessels on the ocean surface. Type 1 nodule facies correlates with moderate-amplitude backscatter areas and is the most common facies. Type 2 and 3 nodule facies typically correlate with higher-amplitude backscatter areas. These correlations are shown in Figure 6.14, which shows the density of nodule coverage according to photographic traversing by AUV. In this figure, the ribbon-tracks are colored as Type 1 (green), Type 2 (yellow), Type 3 (red) against a background of backscatter data. The backscatter data are colored by amplitude; high-amplitude areas associated with Type 2 and 3 nodule facies shown in warmer colors, with Type 1 represented by colder colors. The highest amplitude signals indicate volcanic outcrops associated with seamounts and ridge-tops.

Figure 6.14 Map of nodule classification compared to backscatter intensity



Source: MARGIN. Note: box core locations are labelled with box core number and coloured by abundance. Ribbon-track coloured by facies Type: Type 1 (green), Type 2 (yellow), Type 3 (red)) against a background of backscatter data. The backscatter responses are coloured by amplitude; high-amplitude areas associated with Type 2 and 3 nodule facies shown in warmer colours, with Type 1 represented by colder colours.

6.7 Diagenetic crusts

Minor amounts of ferro-manganese crust were observed in photo-profiles collected from TOML areas. Two types of crusts were logged in a few locations by TOML and have been recognized by other workers (e.g., Menot et al., 2010):

- Massive crust is five to ten centimeters thick and is typically found in blocks tens of centimeters wide but occasionally as pavement; and
- Crustal-nodules are small to medium sized (<20 cm) discrete fragments of ferro-manganese that can grade into nodules.

In total, crusts were logged in ~0.6% of the photo-profiles, with crustal nodules more common (~0.5%) and massive crusts being present in only ~0.1% of the photographs Neither type was collected in box cores during the TOML CCZ15 campaign, and their extent is deemed insignificant in terms of the Mineral Resource estimate.

6.8 Moisture content of nodules

The moisture content of polymetallic nodules determined by laboratory analysis is the free (chemically unbound) water occurring within the pore spaces of the individual nodules which is released by drying of the samples prior to chemical analysis. The drying temperature for this is typically 105°C. Moisture contents of the nodules in the NORI and TOML areas are reported on a wet basis (wet weight-dry weight)/wet weight.

The nodules also contain chemically-bound water and hydroxide ions, mainly within manganese and iron minerals. Manganese minerals with various types of crystalline lattice have different levels of thermal stability. Layered manganese minerals (buserite I, asbolane-buserite, and birnessite) are stable up to 120°C –150°C; asbolane up to 180°C, vernadite, up to ~500°C; todorokite up to 600°C, and pyrolusite up to 670°C (Novikov and Bogdanova, 2007). The chemically-bound water and any other volatiles, such as carbon dioxide, are measured by measuring the loss of mass on ignition (LOI) that occurs when the samples are heated from 105°C to 1000°C.

The moisture content of the nodules in the NORI and TOML areas has been measured at various stages throughout the exploration and related scientific programs. The conditions under which the samples were collected, stored and dried varied and, consequently, some systematic differences between data sets were observed. In order to understand these differences, AMC reviewed the moisture content data from NORI Area D, TOML, the Federal Institute for Geosciences and Natural Resources (BGR) Contract Areas, and Interoceanmetal Joint Organization (IOM) Contract Area.

Studies of the impact of drying nodules for different lengths of time by TOML and NORI indicate that nodules should be dried for at least 24 hours. In the studies reviewed, moisture contents of about 28% were reported for the nodules dried at 105°C or 110°C for 24 hours and moisture contents of 32% were reported for those dried for 48 – 72 hours. This suggests gradual breakdown of very loosely-bound water of crystallization during extended drying periods.

Differences between the nodule moisture contents measured in the off-shore campaigns at NORI Area D are probably due primarily to differences in the time of exposure of the nodules to air prior to sealing in plastic sample bags. It is likely that in a production environment there will be some fluctuation in moisture content of shiploads of nodules due to variations in ambient conditions during handling and transport.

No correlations were identified between the moisture contents of the NORI Area D nodules and assays, nodule size fraction, nodule type, abundance, bathymetry, or geological domain.

So far as estimation of metal production units is concerned, the wet abundances must be converted to dry abundances. This should be done using the measured moisture contents, on a sample by sample basis. In this way any biases arising from different handling of the samples prior to sealing them, will not compromise the estimation of dry abundance and metal content. The corollary of this is that dry abundance should be estimated in the Mineral Resource block model.

The current estimate of moisture content of in situ nodules in NORI Area D is 28%, based on data from Campaign 6, 7 and 8 box cores and sampling of 3000 t of nodules recovered during the collector system test in 2022.

The current estimate of the moisture content of nodules in NORI-A, NORI-B and NORI-C is 24% and in the TOML areas is 28%.

For production planning and accounting, it is necessary to use the wet abundance of nodules calculated by adding the moisture content to the estimate of dry abundance.

6.9 Density of nodules

In 2018, during campaign C3, NORI measured the density of 45 samples of individual nodules or batches of nodules. Non-breakable beakers ranging from 200 ml to 2L were used for taking nodule weights and for volume displacements. These measurements were used to calculate wet density values. The average of the results was 2.0 t/m^3 (wet).

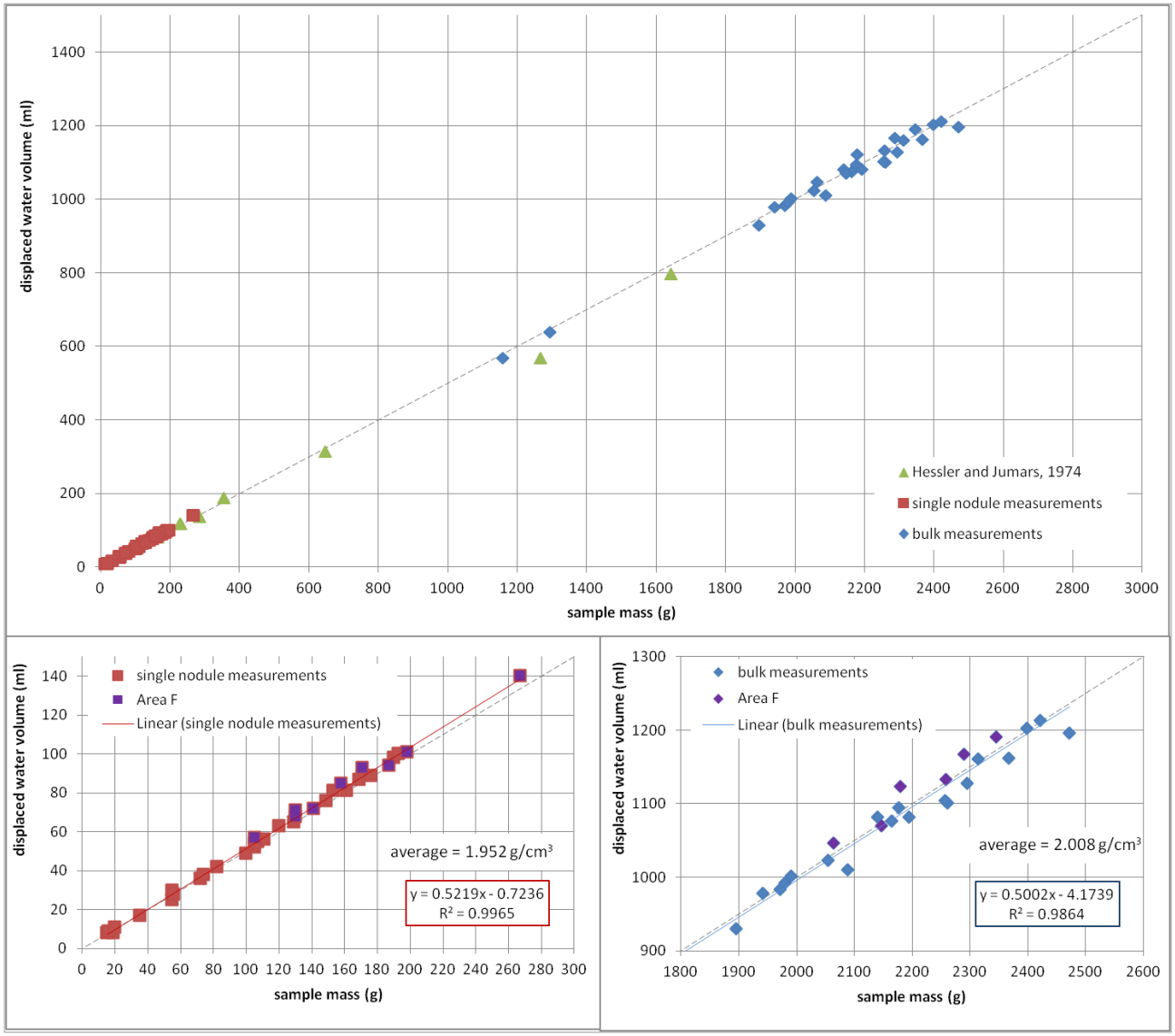
TOML measured the density of 76 individual nodules or batches of nodules from TOML Area B, C, D and F (AMC Consultants, 2016). The batches of nodules included fragments and sand resulting from attrition during transport and handing. The mean density of 34 individual nodules was 1.95 t/m^3 (wet) and that of 27 batches of nodules was 2.0 t/m^3 (wet).

TOML confirmed historical results from the north Pacific by Hessler and Jumars (1974). Figure 6.15 shows the data from TOML and Hessler and Jumars. The data points are consistent with a mean density of 2.0 t/m^3 (wet).

Baláž (2022) reported the results of investigation of nodules in the IOM contract TOML-From 2016 to 2021. The IOM Contract Area is in the eastern part of the CCZ but not immediately adjacent to NORI Area D. A total of 1,005 individual and batch sample measurements were reported, with a mean of 1.96 t/m^3 (wet) (Figure 6.15).

AMC considers that a wet density of 2.0 t/m^3 is supported by the data and is appropriate for use on the NORI and TOML areas.

Figure 6.15 Density data from TOML Areas B, C, D and F and Hessler and Jumars (1974)

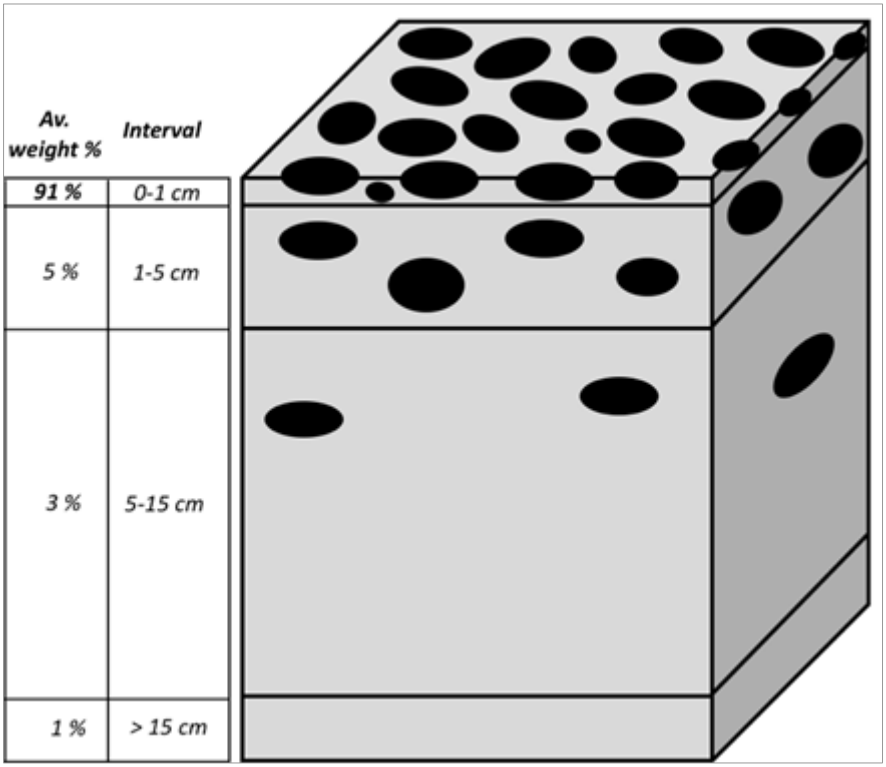


Source: TOML

6.10 Abundance of nodules in NORI and TOML

In detailed sampling of nodules by depth in the box cores from NORI Area D, on average, 96% of the nodules were recovered between the surface and a depth of 5 cm. Figure 6.16 presents a schematic representation of the average proportion of nodules by depth in the box cores in campaign C3 from NORI Area D. The nodules recovered below 5 cm depth from NORI Area D were generally interpreted to have been pushed into the soft clay by the BC frame. There were only two box cores where nodules deeper than 15 cm were confidently observed *in situ*, but these nodules were so friable that they crumbled when attempts were made to remove the surrounding clay and were not recoverable.

Figure 6.16 Schematic representation of average proportion of nodules by depth in the box cores in NORI Area D campaign C3



Source: TMC

The abundance of buried nodules in NORI-A, B, and C is poorly known at this time. Buried nodules were not included in Mineral Resource estimates.

In the TOML areas, nodules buried more than 10 cm beneath the surface were observed but are not very common. A total of 16 out of the 113 box cores taken during CCZ15 had buried nodules, however all of these were located in Area D and F. If just Areas D and F are considered then buried nodules were found in about 23.8% of samples which is a similar ratio to that described by Kotlinski and Stoyanova (2006). Buried nodules tend to be of much lower abundance and larger than the average nodules found at the surface. They were collected from the box-cores in CCZ15 purely for reference purposes and their weights and chemical analyses were not included in the dataset supporting the Mineral Resource statement.

6.11 Nodule size distribution

Understanding of the particle size distributions (PSD) of the nodules is important for the engineering design of the collector and for estimating nodule recovery during mining operations. The collector is expected to pick up nodules up to a certain maximum size and nodules greater than this size may be left on the seafloor. Therefore, measurements of nodule dimensions and understanding of how nodule dimensions vary across the NORI and TOML areas is expected to enhance the accuracy of mine plans and recovery predictions.

6.11.1 NORI Area D - Physical measurement of size and estimation of abundance

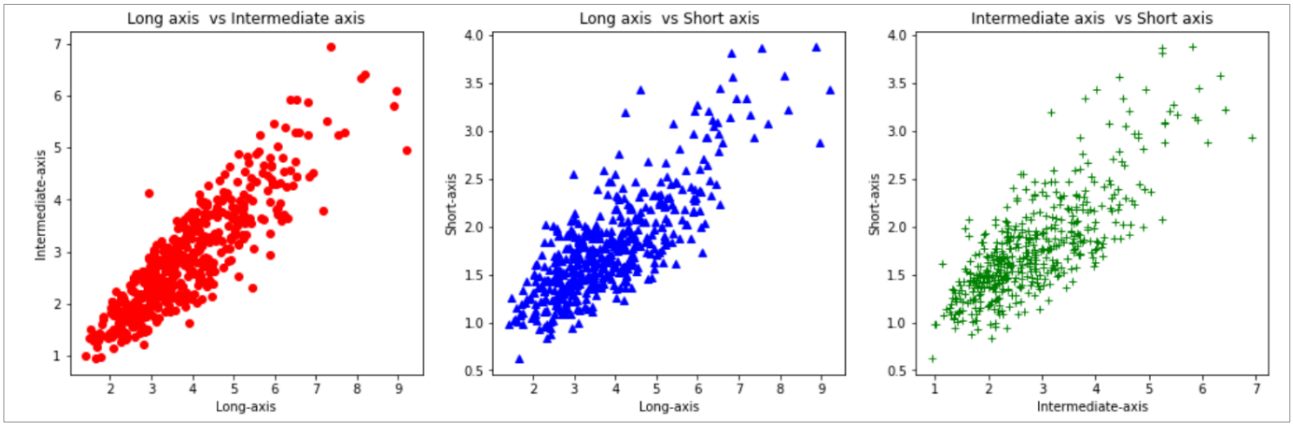
Subsea imagery, BC top shots, and laboratory photographs of trays of nodules, only provide measurements of the major and intermediate axes of the nodules. During Campaign 7A at NORI Area D, the axial lengths of selected nodules were manually measured during offshore nodule processing.

The objective was to assess whether addition of the short (vertical) axis measurement can be used to significantly improve the estimation of nodule abundance from subsea imagery.

For each tray of nodules presented for photography in the offshore laboratory, the major, intermediate, and minor axes of the four nodules in the corners of each tray were measured. This resulted in 500 individual measurements acquired over the campaign, from 22 box cores.

The first step in the analysis of the data was to assess whether there was a relationship between major (X), intermediate (Y) and short (Z) axes data. Figure 6.17 shows scatter plots comparing the axial lengths of the 500 nodules. It is clear that the axial lengths are positively, linearly correlated. Variability in these relationships increase as the size of the nodule increases (seen as a comet-tail distribution, widening with increase in axes length).

Figure 6.17 Scatter plot comparing axis lengths of 500 manually measured nodules



Source: MARGIN

A regression model was established to predict short axis lengths Z_i as a function of major axis X_i and intermediate axis Y_i,. The data was split into test (70%) and training (30%) subsets. An initial regression model with an R^2 of 0.66 was achieved:

$$Z_i = 0.2323X_i + 0.1396Y_i + 0.5081$$

The model has a training set accuracy of 0.687 and test set accuracy of 0.601, so the model is not significantly over-fitting the data.

ImageJ image-processing software was used to measure the major and intermediate axes of all the nodules in the laboratory photographs of the trays of nodules collected from the 22 BC's in Campaign 7A. All the nodules were weighed as part of the normal BC processing, so each BC had a measured nodule abundance.

The new regression model was then applied to all the ImageJ data to derive an estimate of minor axis length for each nodule. The volume of each nodule was then estimated, assuming that each nodule is a perfect ellipsoid, using the following equation:

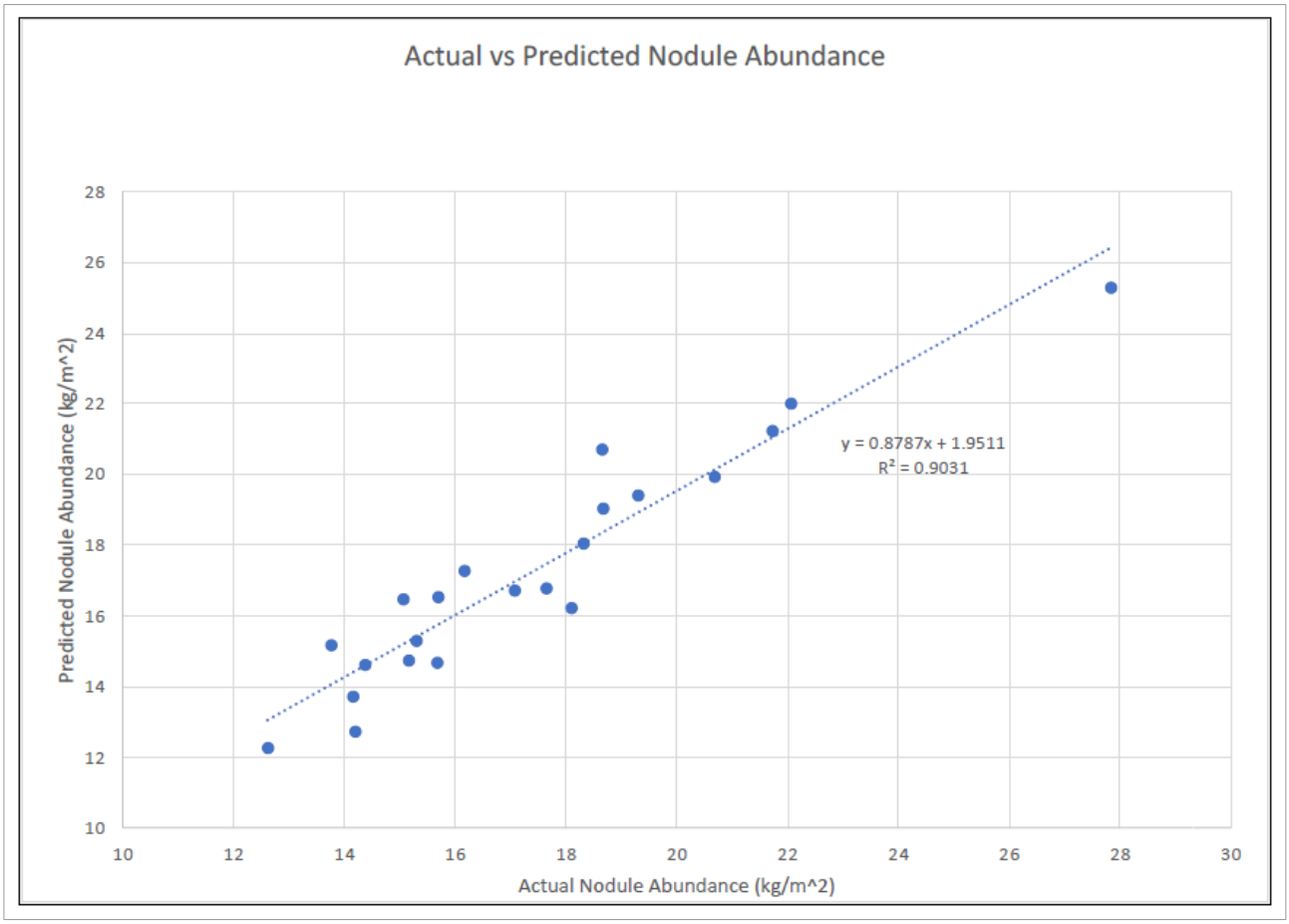
$$V = (4/3) * \pi * X_i/2 * Y_i/2 * Z_i/2,$$

The estimated nodule volumes were then converted to nodule weights using an assumed nodule wet density of 2 g/cm^3. This density value is supported by 45 measurements by NORI, 76 by TOML (AMC Consultants, 2016) and 1005 by IOM (Baláž, P. 2022).

Figure 6.18 shows a scatter plot comparing the nodule abundance measured by weighing the nodules in each of the 22 box cores versus the nodule abundance estimated from the axes lengths. There is a very strong linear correlation and a linear regression model shows an R^2 value of 0.90.

The study shows that it may be possible to apply this method to high resolution AUV images to generate estimates of nodule abundance that are sufficiently accurate to inform production planning. The tray images show numerous broken nodules and are likely to be more fragmented compared to in-situ seafloor imagery and are thus not perfect ellipsoids. Nonetheless, the method performed remarkably well.

Figure 6.18 Scatter plot comparing actual versus predicted nodule abundance in C7A box cores



Source: MARGIN

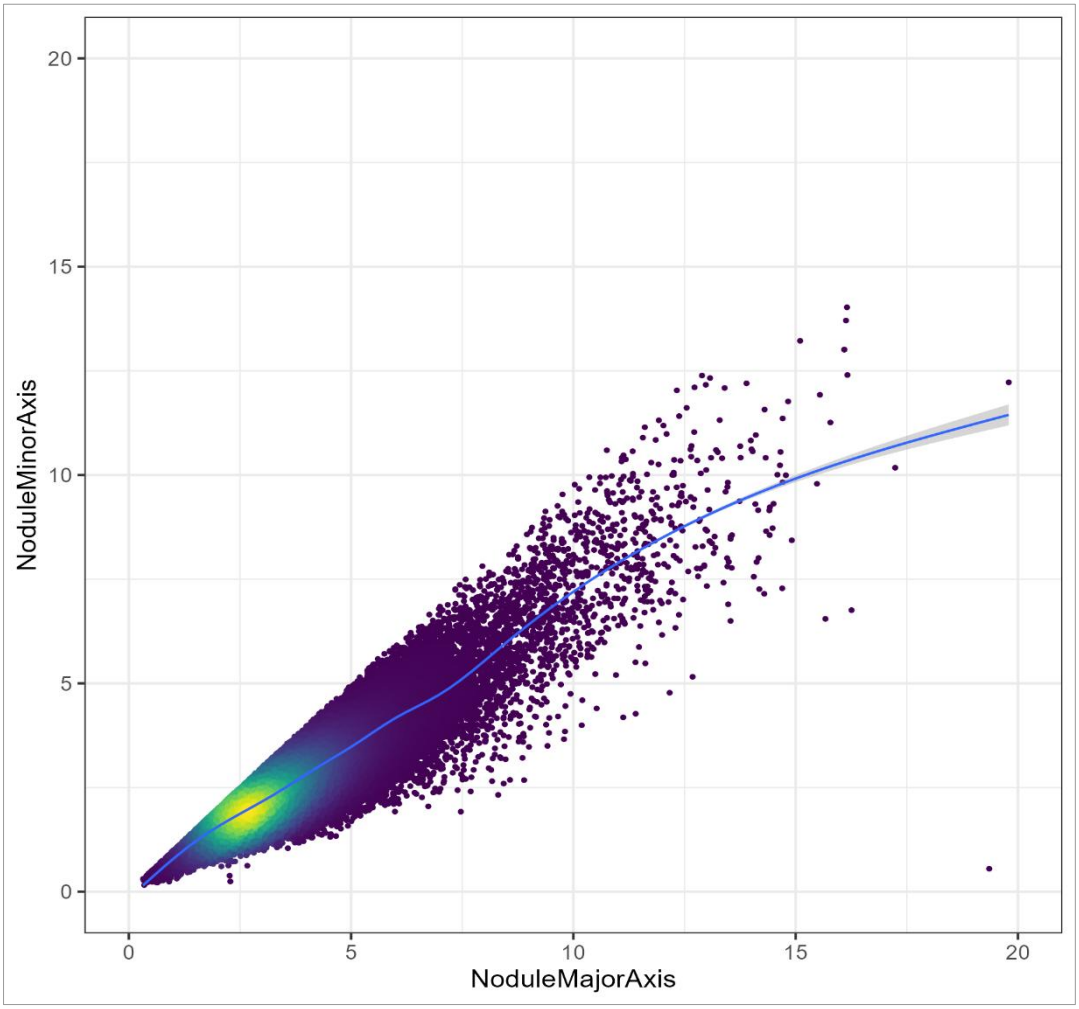
6.11.2 NORI Area D - Measurement of nodule dimensions using image processing

During Campaign 3 at NORI Area D, an image classification approach was tested for measuring the long and intermediate axes of individual nodules taken from BC samples. NORI collected nodule size measurements from the BC samples by photographing all the nodules nominally greater than 1 cm in length and then using ImageJ to automate the measurement of the orthogonal major and intermediate axes of the nodules. The minor axis of the nodules is the vertical axis of the nodules which cannot be seen in the photographs. Nodules < 1 cm diameter were bagged and sealed into small clear sample packets and included in the photographs but not measured by the image processing software. They were included in the weighing process and are included in the abundance measurements. The image

classification method showed a very good correlation against hand-held calliper measurement (see Section 6.11.1) and was adopted for subsequent offshore campaigns at NORI Area D.

The NORI Area D data consists of 232,068 individual nodule measurements from 287 box cores. Figure 6.19 shows a scatter plot of the major axis length versus the intermediate axis length for all the nodules in this data set. The points are colored according to the local density of points, where the light green cloud highlights the region with the most points. A curve is fitted to the data using a non-linear smoothing algorithm. The plot demonstrates that most nodules manifest some ellipticity, confirmed by the cloud of points lying below the 1:1 line, along which any circular nodules would lie. The mean ratio nod_intermediate : nod_major is 0.75 and the ratio nod_intermediate : nod_minor is similar. Note that the data does not discriminate between whole nodules and broken fragments.

Figure 6.19 Scatter plot of nodule major axis dimension versus nodule intermediate axis dimension for all nodules

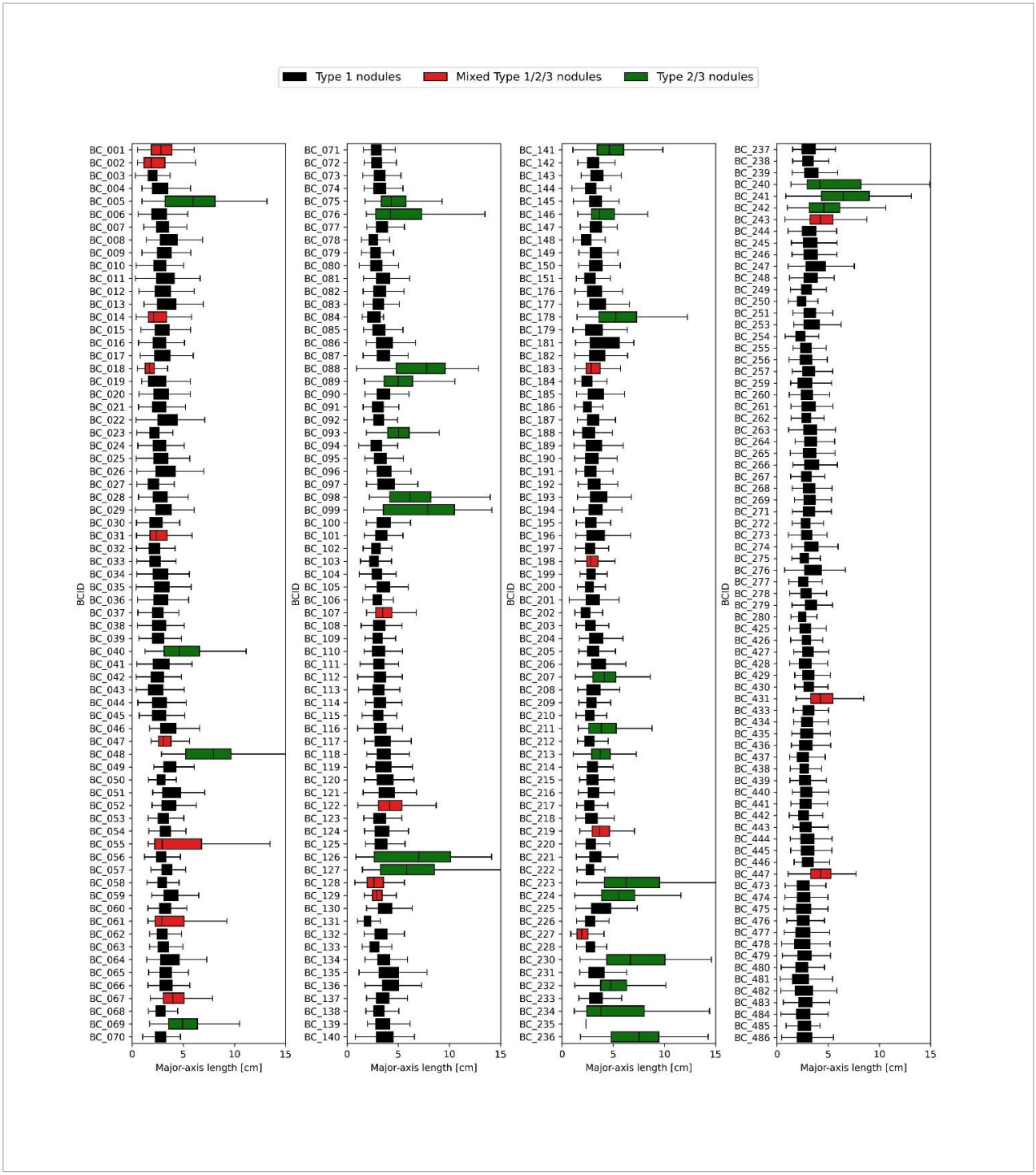


Source: AMC

Figure 6.20 shows boxplots of the major axis lengths of all 287 box cores. It shows that most of the box cores exhibit a median length in the range 2 cm - 3 cm, and in most cases at least 75% of the nodules (as indicated by the righthand limit of the boxes) are less than 5 cm. This is typical of Type 1 nodule facies (colored black in Figure 6.20). The nodule size distributions are in all cases positively skewed. That is, the distributions show a tail of longer nodule lengths extending to the right of the plots.

In most cases, the skewness is weak and the tail is short. However, the box plots and histograms show that 48 box cores are dominated by larger nodules or have more strongly skewed distributions or even bimodal distributions, with a large population of small values and a small population of higher values. These anomalous box cores correlate with the extent of Type 2/3 nodule facies interpreted from backscatter data. Kuhn and Rühlemann, (2021b) made similar statistical observations in the BGR Contract Area, to the north of NORI Area D.

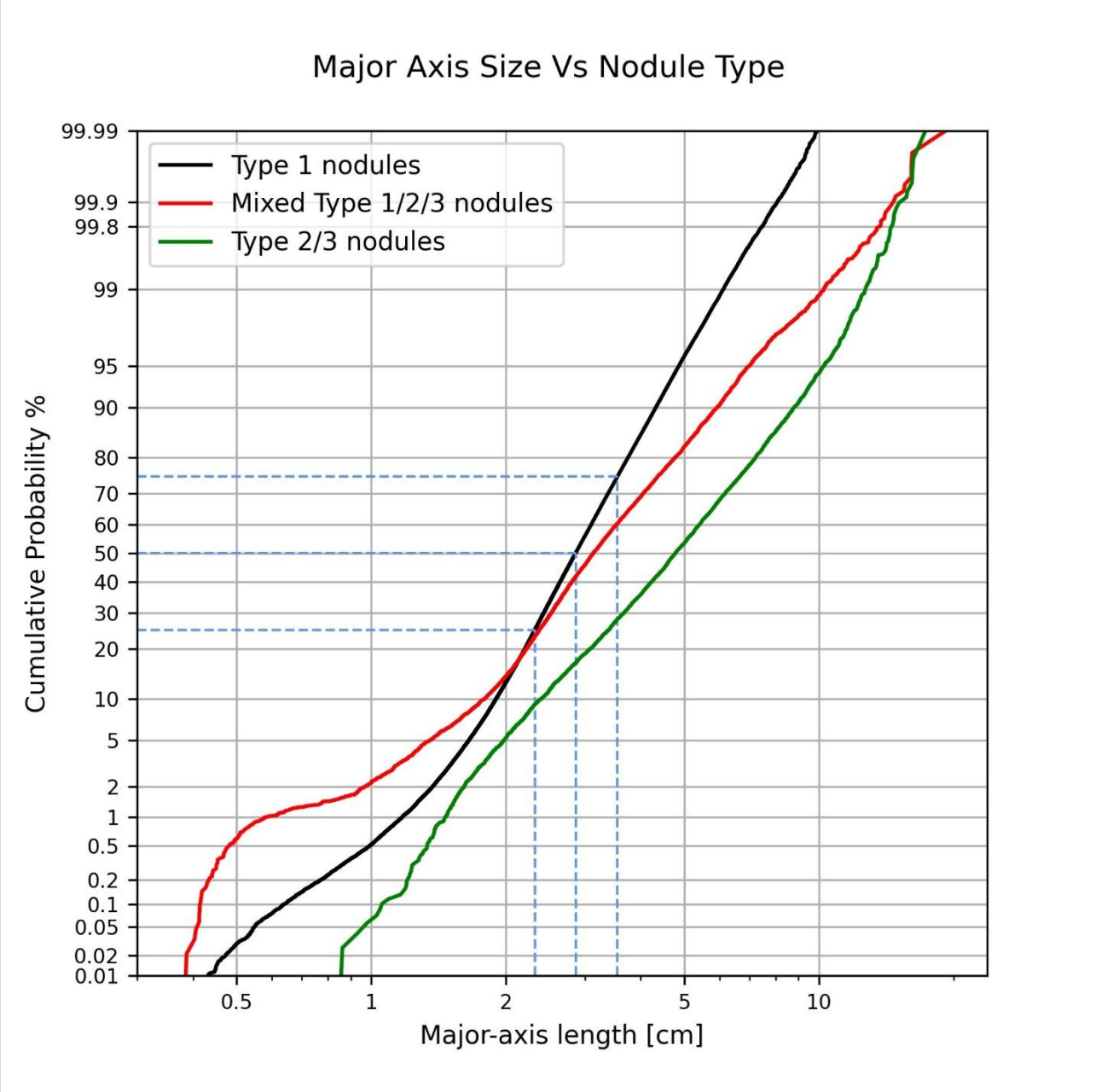
Figure 6.20 Box plots of nodule major axis dimension for all box cores



Source: AMC

Figure 6.21 shows a plot of the cumulative distributions of nodule major axis lengths for all the 287 box cores from NORI Area D for which the ImageJ major axis length data were available. The data was divided into Type 1, Type 2/3, and mixed Type 1 and Type 2/3 groups. The plot shows that there are significant differences between the statistical distributions of major axis length in the three nodule types. The Type 1 box cores have the smallest median major axis length. The Type 2/3 box cores have the largest median major axis length. The mixed facies box cores have an intermediate size distribution. These statistical features illustrate the complexity of nodule size distributions at the local scale and the need for further work to improve the spatial definition of Type 2/3 nodule facies.

Figure 6.21 Log probability plot of nodule major axis dimensions by interpreted nodule facies



Source: AMC

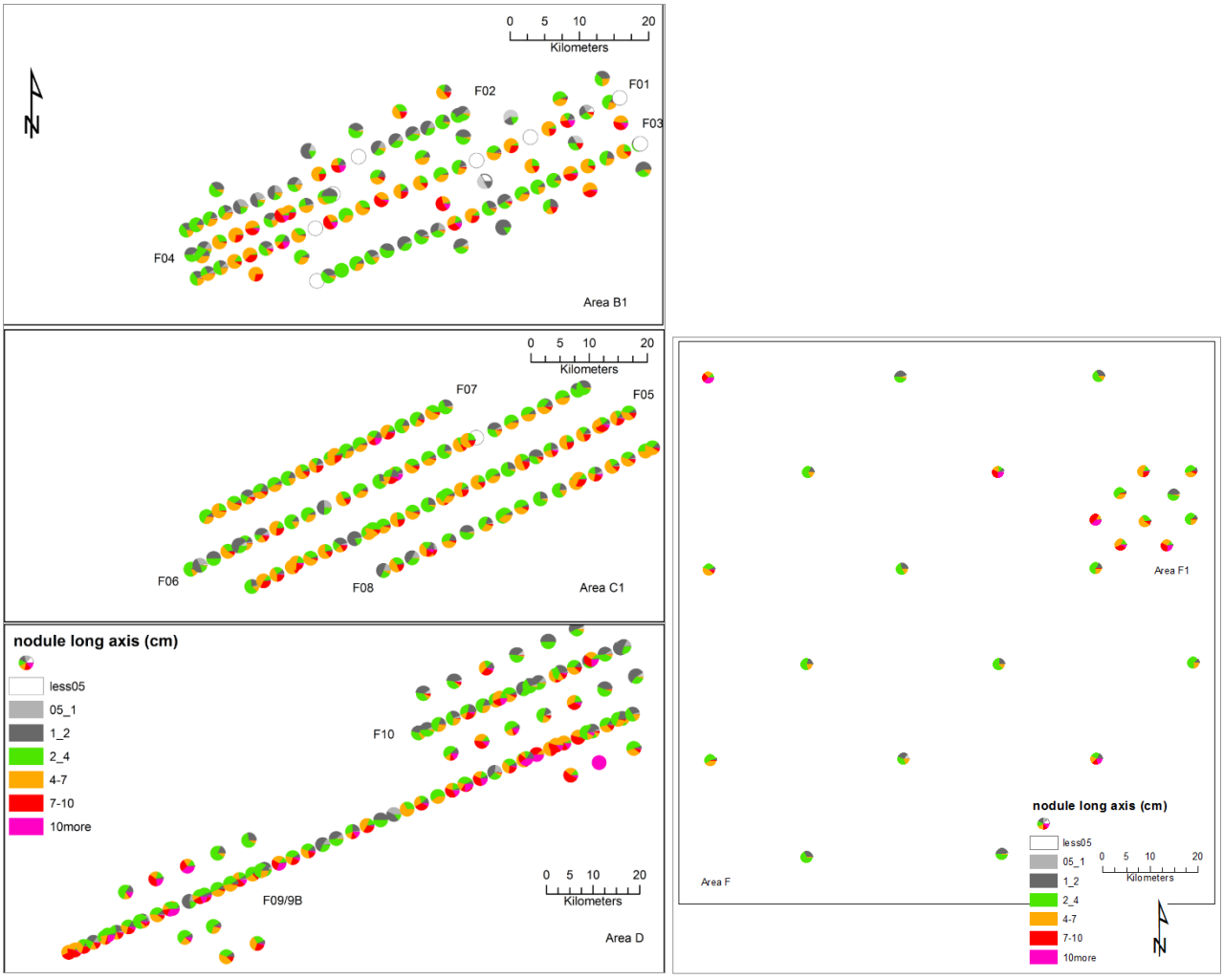
6.11.3 TOML Areas – Measurement of nodule sizes

TOML made physical measurements of nodule dimensions in box cores and measurements using the long axis estimation method applied to photo-profile images. Roughly every 100th image was measured for the purpose of estimating abundance. The results of these measurements are shown in Figure 6.22. The distribution of nodule long axis length at each BC and photograph location is represented by pie-charts.

The surveyed TOML areas host a range of nodule sizes at each location and there is variation on a scale of several kilometers across the surveyed areas. Within TOML-D, there is a mixture of sizes with some very large nodules found in the BC samples. Bigger nodules were recovered from the BC than were measured on the photo-profiling lines because partial cover by sediments resulted in an underestimation of nodule length.

The characteristics of nodule size and nodule size variation appear similar in NORI Area D and TOML-B, C, D, E and F. For the IA, it is reasonable to assume that mining systems designed for NORI Area D would be appropriate for the TOML areas.

Figure 6.22 Plans showing nodule sizes and types from TOML F and sub-areas B1, C1, D1, D2, and F1



Source: TMC. Top: B1, Middle-left: C1, Bottom-left: D1-D2, Bottom right: F and F1

7 Exploration

Exploration in the NORI and TOML areas can be considered in terms of three broad phases:

- Historical work and data collected by the Pioneer Contractors who returned Reserved Areas to the ISA. This work underpins much of the Inferred Mineral Resource estimate for NORI A, B and C, and TOML A- F.
- Offshore exploration campaigns completed by NORI in 2012, 2013, 2018, and 2019. This work underpins the Mineral Resource estimate for NORI Area D.
- Offshore campaigns completed by TOML in 2013 and 2015. This work underpins part of the Inferred Mineral Resource estimates as well as all of the Indicated and Measured Mineral Resource estimates for TOML A- F.

This report presents information summarized from these exploration programs. Further details of these programs are presented in:

- The technical report summary titled “Technical Report Summary--Initial Assessment of the NORI Property, Clarion-Clipperton Zone, for Deep Green Metals Inc.” (the “NORI Technical Report”), with an effective date of March 17, 2021 (AMC Consultants, 2021a).
- The technical report summary titled “Technical Report Summary--TOML Mineral Resource, Clarion-Clipperton Zone, Pacific Ocean, for Deep Green Metals Inc.” (the “TOML Technical Report”), with an effective date of March 26, 2021 (AMC Consultants, 2021b).

Additional information is provided in the Technical Report on NORI Area D, Clarion Clipperton Zone Mineral Resource Estimate, April 2019 (AMC Consultants, 2019).

Nodule abundance (wet kg/m^2) is derived by dividing the weight of nodules recovered by a sampling device by the surface area covered by the sampler.

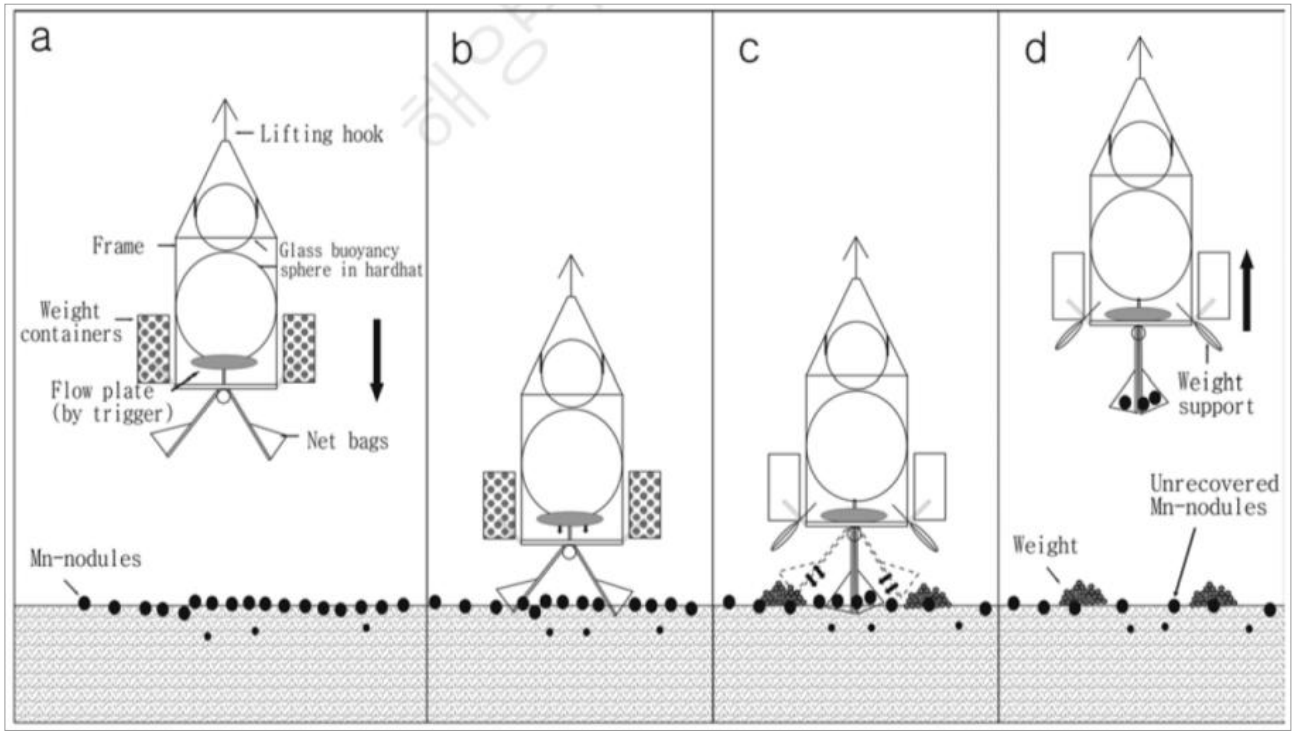
7.1 Free fall grab sampling method

Free fall grab (FFG) samplers have been widely used in the CCZ for collection of samples of nodules. The principal components of FFG samplers are a pair of spring-loaded clamshell net bags for collecting the sample, an air-filled sphere to create buoyancy and containers filled with ballast.

The operation of a FFG sampler is shown schematically in Figure 7.1. The FFG sampler is released, untethered, over the side of the exploration ship and sinks to the seafloor under the weight of the ballast. When the FFG sampler makes contact with the seafloor ejection of the ballast is triggered which makes the sampler buoyant. As the sampler begins to rise, the clamshell net bags close, capturing the nodules at the land-out point. After it reaches the sea-surface, the FFG sampler is recovered by the boat.

FFG samplers are quicker, easier and cheaper to operate than box corers and so were preferred by the Pioneer Contractors for much of the early exploration. However, research shows that they produce less accurate, conservative, measures of nodule abundance.

Figure 7.1 Cartoon showing the recovery of nodules using a free fall grab sampler

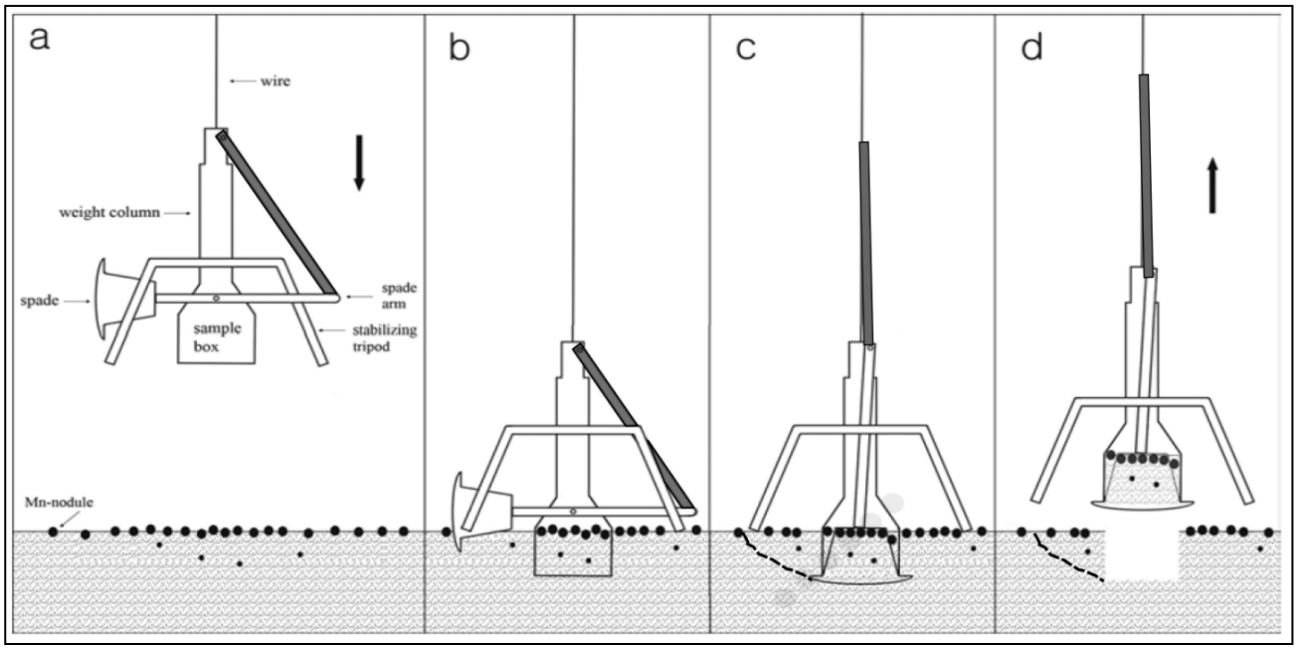


Source: Lee et al., (2008).

7.2 Box core sampling method

The BC is the preferred sampling method for retrieving polymetallic samples for resource evaluation and environmental studies. The BC consists of a steel box (without a base), a trigger, a plunger, and a rotating spade-like bottom plate. Upon land out on the seafloor, the trigger is released which allows the plunger to push the open sample box into the substrate. Upon retraction, the cutting shovel rotates under the box while cutting into the seafloor and sealing the sample box from below (Figure 7.2).

Figure 7.2 Cartoon showing the recovery of nodules using a BC sampler



Modified after: Lee et al., (2008).

Box corers have been used in the CCZ since the 1970s. As they collect a relatively undisturbed sample of the seabed, they are seen by most explorers as the best possible sampling device to measure the nodule abundance in any given location. Box cores come in different sizes ranging from typically 0.1 m^2 or 0.25 m^2 to 1 m^2. Larger box cores provide more accurate measurements of the nodule abundance, especially if the nodules are large or sparsely distributed. Figure 7.3 shows photographs of a KC Denmark 0.75 m^2 box corer used for sampling at NORI Area D.

Both TOML and NORI carried out BC sampling. Handling of nodules and chain of custody were supervised by the Lead Scientists. Nodule sampling for geological purposes was carefully integrated with collection of biological data. The differences between the sampling procedures in the various campaigns were minor. In summary, the procedure was as follows:

- When the box cores arrive on deck, photograph the nodules in situ.
- Remove the nodules from the box and weigh in the laboratory.
- Photograph the nodules on a white background with a graticular scale.
- Split some samples to create duplicates for assaying.
- Pack the nodule samples in specially marked paint pails and seal with tamper-proof tape.
- Store the pails in a refrigerated container (reefer) on deck prior to transport to assay laboratories.

In most samples, there were no buried nodules, although some were occasionally entrained by the sides of the box or the shovel. If present, buried nodules were separated at the point of collection from the box and were washed, weighed, and packed separately. Entrained nodules were sampled for reference purposes only and were not weighed.

Figure 7.3 KC Denmark 0.75 m^2 box corer



Note: Insert top right shows USBL beacon (circled top) and GoPro camera and lighting system (circled bottom)

7.3 Comparison of FFG and BC samples

Comparison of nodule abundance measurements by FFG and box cores suggests that FFG commonly underestimate the actual abundance (e.g., Hennigar, Dick and Foell, 1986). This is due to smaller nodules escaping the sampler during ascent and larger nodules around the edge of the sampler being knocked out during the sampling process. Additionally, FFG occasionally fail to return any nodules where nodule abundance is known to be very high because the sampler fails to penetrate the layer of nodules.

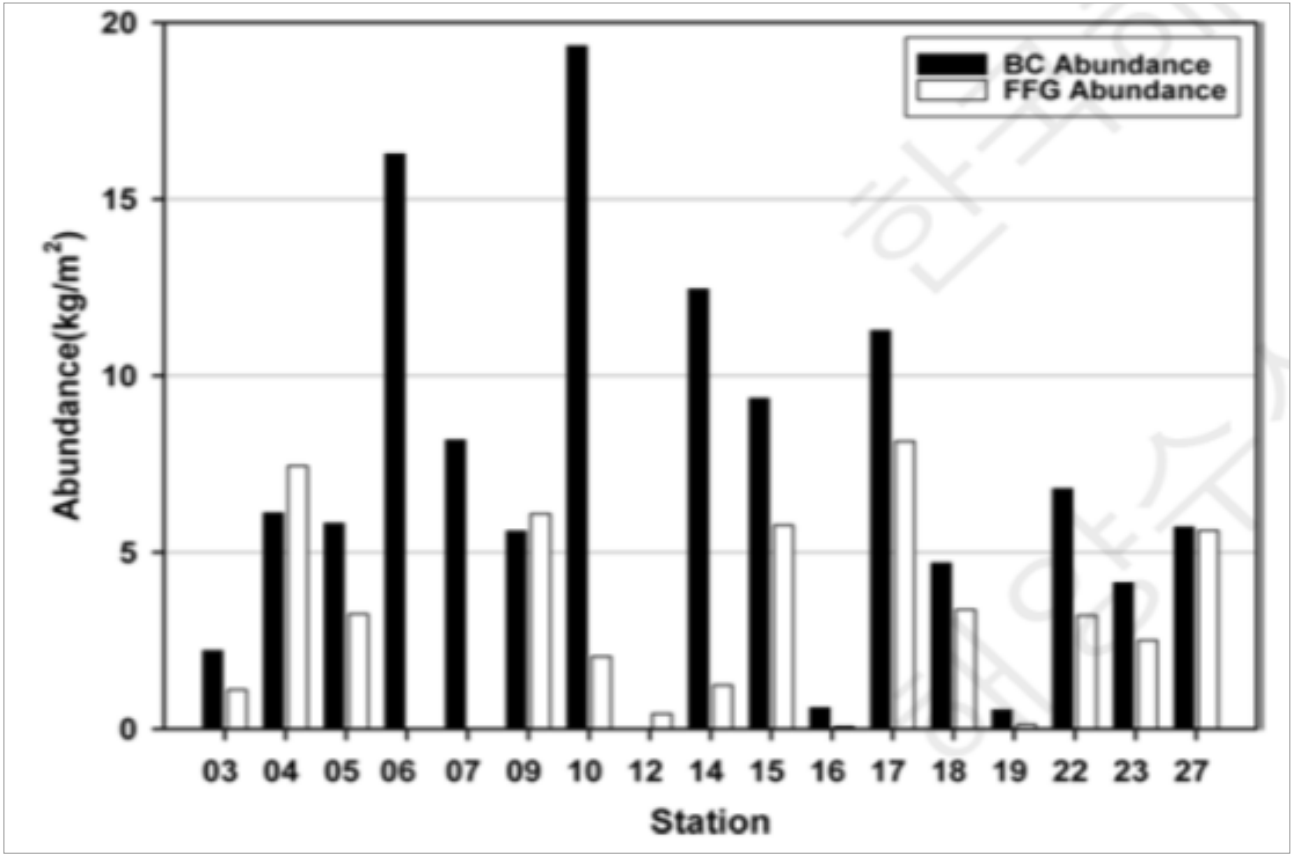
Lee et al. (2008) compared FFG BC data in some detail. They found a wide range but consistent differences with FFG under-reporting compared to BC (Figure 7.4). They recommended an overall correction factor of 1.4 to convert FFG abundance to BC abundance. However, they acknowledged that any simple factor lacks precision.

No corrections were applied to the nodule abundance data in the TOML and NORI areas because:

- Sample collection type is not specified in the historical data (i.e. proportion and identity of BC versus FFG samples is unknown (although most are likely to be FFG).
- The size of collector and nodule sizes is not specified in the historical data.

Therefore, estimates of nodule abundance estimates based on historical samples are likely to be conservative.

Figure 7.4 Comparison of returned abundances from BC and FFG at test stations within the KORDI exploration area

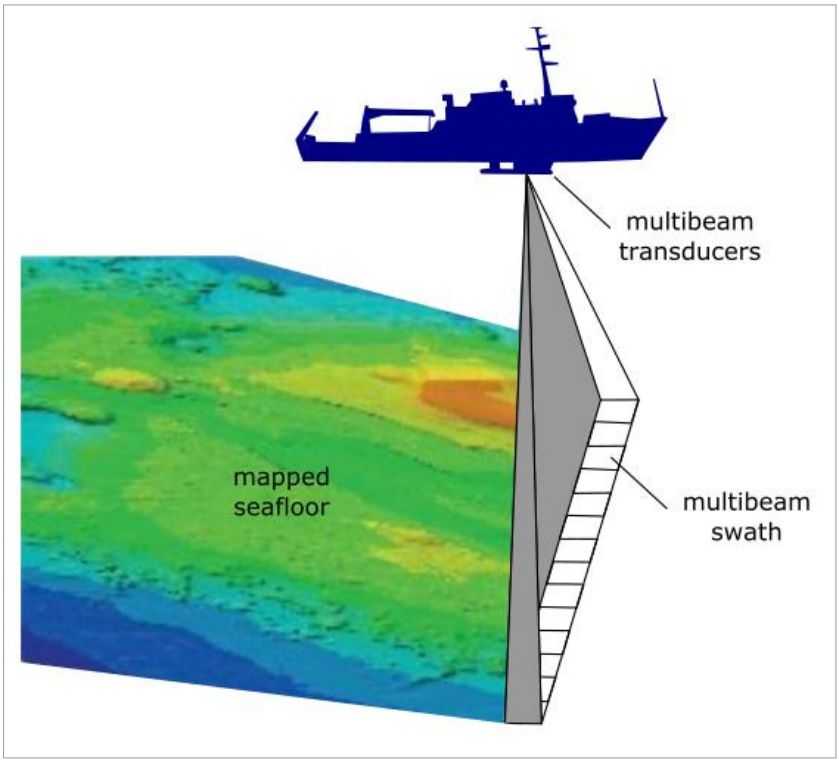


Source: Lee et al., (2008).

7.4 Multibeam Bathymetry methods

MBES is used to determine the depth of water (bathymetry) and the acoustic reflectance (backscatter) of the seabed. It operates by transmitting a focused acoustic pulse (Figure 7.5) from a specially designed transducer across a swath across the vessel track. These pulses return as a set of receive beams that are weaker and narrower and whose arrival time at the detector varies depending on speed through the water column and distance. Thus, position and depth can be measured and seafloor hardness can be qualitatively assessed from the attenuation of the backscattered acoustic pulse.

Figure 7.5 MBES operations schematic



Source: TOML

7.5 Historical exploration data

Six exploration groups are known to have surveyed areas within the TOML Contract Areas and collected samples of polymetallic nodules. Much of this work overlapped as it predated the signing of the Law of the Sea. These include the Japanese group (DORD), the South Korean group (KORDI), the Russian Federation group (Yuzhmorgeologiya), the French group (Ifremer), the German group (FIGNR or BGR), and the consortium, OMCO. The timing and location (ISA, 2003) of the OMCO sampling is known but the results are not available outside of ISA published contour maps.

Sampling of seafloor nodules within the NORI areas was conducted by three Pioneer Contractors; AMR, State Enterprise Yuzhmorgeologiya of the Russian Federation and IOM, a consortium formed by Bulgaria, Cuba, the Czech Republic, Poland, the Russian Federation, and Slovakia.

Virtually all the samples in the TOML areas and NORI A, B and C were obtained by free fall grab (FFG) samplers, although a few results from box corers (BC) were also included.

Each of the Pioneer Contractors used their own procedures for sampling and assaying. The differences in methods were relatively minor. The general approach was as follows:

- The nodule samples cleaned of any adhering sediment, weighed and photographed.
- The nodules were air-dried in order to make it practical to crush and sub-sample them.
- The crushed samples were dried at 105°C or 110°C for various lengths of time in order to drive off all free moisture.
- The dried samples were pulverized and sub-sampled for assaying.
- The grades of manganese, nickel, cobalt, copper, iron and in some cases zinc, silica, calcium, and magnesium were analyzed by mixed acid digest followed by atomic absorption spectrophotometry (AAS) or pressed-powder X-ray fluorescence. Yuzhmorgeologiya used a photometric (electrometric) titration method for determination of manganese.
- Some Contractors reportedly used polymetallic nodule Certified Reference Materials (CRMs) (e.g., NOD-P-1; Flanagan and Gottfried, 1980) and duplicate samples for quality assurance and quality control (QA/QC), however details of the CRMs and QA/QC results were not included in the datasets supplied by the ISA.

Upon making an application for an exploration contract under ISA regulations, the Pioneer Contractors were required to submit sufficient data and information to enable designation of a reserved area based on the estimated commercial value. This sample data provided the basis of the database held by the ISA.

Systematic QA/QC information was not provided to TOML or NORI by the ISA. Nonetheless, the acceptance of the data by the ISA suggests the ISA was satisfied with the quality of the data.

The quality of the Pioneer Contractor data was assessed Golder Associates Pty Ltd r 2015 (Golder) using comparative measures between the different datasets. The correlation of data from different sources, including Pioneer Contractors and government scientific institutes, provides a satisfactory level of quality assurance to support Mineral Resource estimates at an Inferred level of confidence.

7.5.1 Pioneer Contractor sample data supplied to NORI

Statistics for the samples that contain both abundance and grade data inside the NORI Areas are tabulated in Table 7.1 and illustrated as boxplots in Figure 7.6. The box plots show the range of grades; the box represents the range of grades in the middle 50% of the samples, centered on the median (middle value) and box width reflects number of samples. The dashed lines represent the range of the lowest 25% and highest 25% of the data.

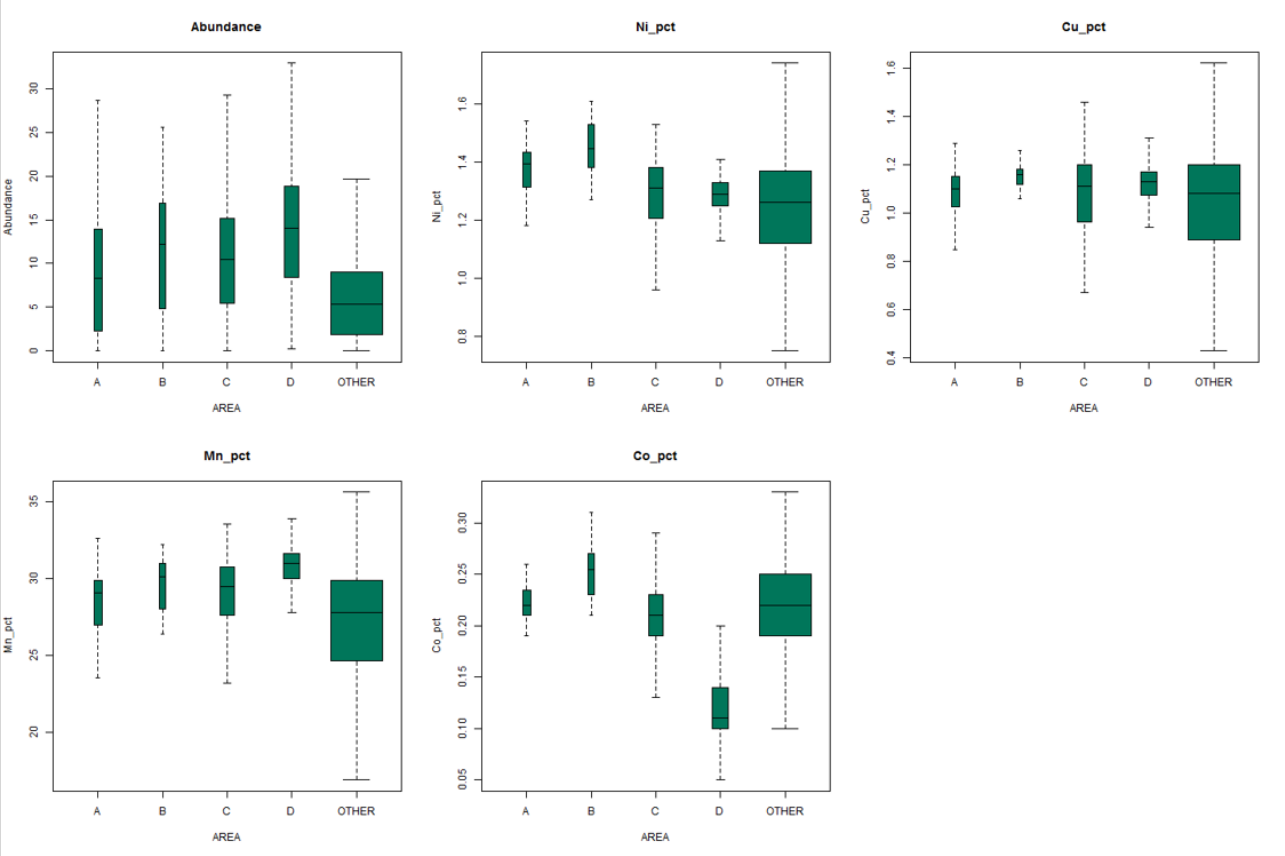
The range of the assays (as summarized by the coefficient of variation(CoV) is remarkably low compared to most terrestrial Mineral Resources. Abundance values vary more widely, making abundance the key variable of uncertainty in Mineral Resource estimation.

Table 7.1 Summary of Pioneer Contractor sample assay data from the NORI Areas

NORI Area	Grade	Number	Min	Max	Mean	Median	Var	CoV
A	Abundance (wet kg/m^2)	50	0	28.7	9.3	8.2	57.37	0.81
	Ni (%)	40	1.04	1.75	1.37	1.39	0.02	0.09
	Cu (%)	40	0.66	1.29	1.07	1.1	0.02	0.12
	Mn (%)	40	19.77	32.6	28.06	28.98	8.58	0.1
	Co (%)	40	0.16	0.28	0.22	0.22	0.00	0.11
B	Abundance (wet kg/m^2)	31	0	25.55	11.24	12	50.54	0.63
	Ni (%)	26	1.01	1.61	1.42	1.44	0.02	0.1
	Cu (%)	26	0.72	1.26	1.12	1.16	0.02	0.11
	Mn (%)	26	20.8	32.2	28.88	29.8	9.94	0.11
	Co (%)	26	0.21	0.31	0.25	0.25	0.00	0.09
C	Abundance (wet kg/m^2)	152	0	44.1	10.55	10.33	52.90	0.69
	Ni (%)	135	0.68	1.53	1.27	1.31	0.03	0.12
	Cu (%)	135	0.4	1.46	1.05	1.11	0.05	0.21
	Mn (%)	135	12.84	33.54	28.63	29.42	11.65	0.12
	Co (%)	135	0.12	0.33	0.21	0.21	0.00	0.17
D	Abundance (wet kg/m^2)	159	0.2	52.2	14.12	13.9	72.24	0.6
	Ni (%)	159	1.09	1.41	1.28	1.29	0.00	0.05
	Cu (%)	159	0.88	1.5	1.14	1.13	0.01	0.1
	Mn (%)	159	23.8	33.9	30.58	31	3.12	0.06
	Co (%)	159	0.05	0.2	0.12	0.11	0.00	0.26

Notes: Var = variance; CoV = coefficient of variation.

Figure 7.6 Box plots of sample grades within the NORI areas compared with all other data from the Reserved Blocks



Source: AMC. Note: Box size represents 1st and 3rd quartiles centered on the median and box width reflects number of samples.

7.5.2 Pioneer Contractor sample data supplied to TOML

The statistics for the samples that contain both abundance and grade data inside the TOML Contract Areas are tabulated in Table 7.2. Samples in the CCZ but outside the TOML Contract Area are presented in Table 7.3. Figure 7.7 shows box plots of Pioneer Contractor sample assay data within the TOML Contract Areas. The data shows that the TOML Contract Areas have similar ranges of grade and abundance to the rest of the CCZ deposit.

The CoV of grades are low compared to most terrestrial Mineral Resources. Abundance values vary more widely, making abundance the key variable of uncertainty in Mineral Resource estimation.

Table 7.2 Summary of Pioneer Contractor sample assay data in TOML areas

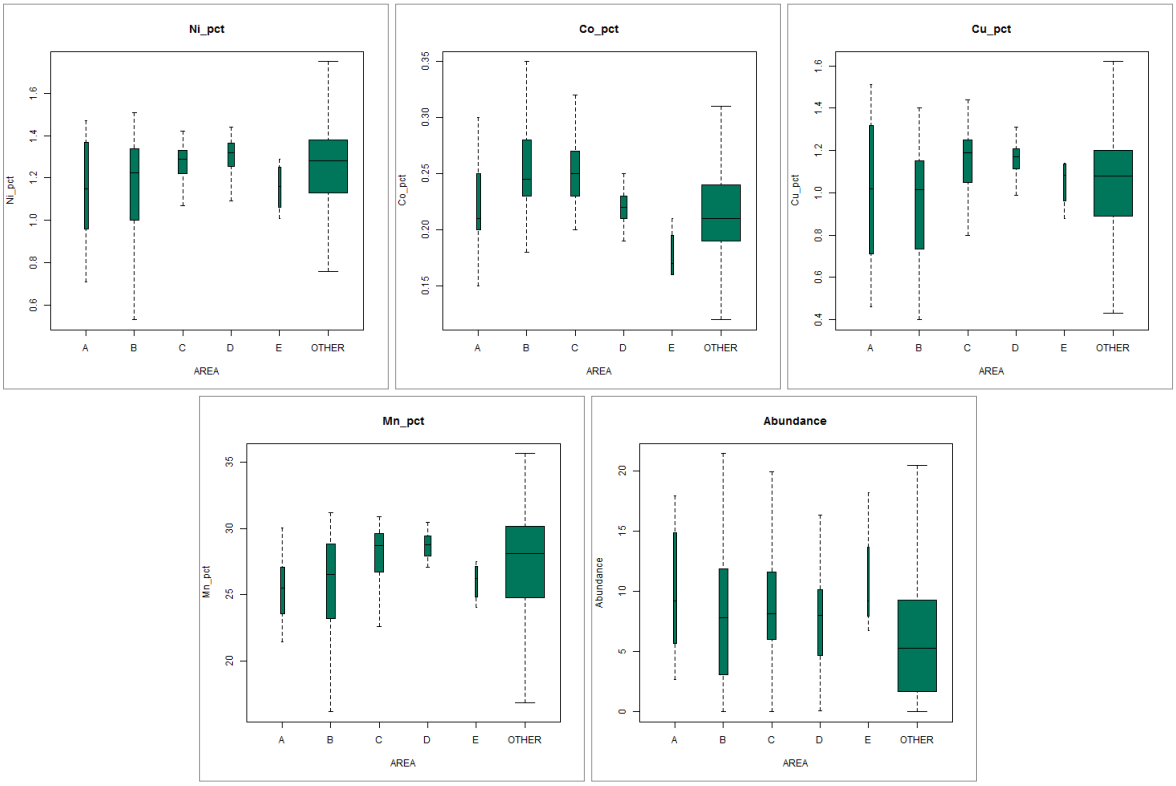
TOML Area and source	Grade	Number	Min	Max	Mean	Median	Var	CoV
A (data from DORD)	Abundance (wet kg/m²)	18	2.68	17.93	10.12	9.19	25.81	0.50
	Ni (%)	18	0.71	1.47	1.14	1.15	0.06	0.21
	Cu (%)	18	0.46	1.51	1.00	1.02	0.12	0.35
	Mn (%)	18	21.46	30.05	25.40	25.50	5.95	0.10
	Co (%)	18	0.15	0.30	0.22	0.21	0.00	0.18
B (from Yuzhmor-geologiya)	Abundance (wet kg/m²)	88	0.03	26.00	8.82	8.09	34.46	0.67
	Ni (%)	88	0.53	1.51	1.16	1.23	0.05	0.20
	Cu (%)	88	0.40	1.40	0.94	1.02	0.07	0.28
	Mn (%)	88	10.30	31.20	25.40	26.55	17.56	0.16
	Co (%)	88	0.02	0.35	0.25	0.25	0.00	0.24
C (from Ifremer)	Abundance (wet kg/m²)	78	1.35	21.25	9.98	9.17	17.64	0.42
	Ni (%)	78	0.93	1.42	1.27	1.29	0.01	0.08
	Cu (%)	78	0.71	1.44	1.15	1.19	0.02	0.13
	Mn (%)	78	22.01	30.90	27.91	28.55	4.54	0.08
	Co (%)	78	0.14	0.32	0.25	0.25	0.00	0.12
D (from DORD)	Abundance (wet kg/m²)	36	0.12	16.37	7.68	7.78	16.73	0.53
	Ni (%)	36	1.09	1.44	1.31	1.32	0.01	0.06
	Cu (%)	36	0.79	1.36	1.16	1.17	0.01	0.09
	Mn (%)	36	22.79	30.45	28.52	28.76	2.16	0.05
	Co (%)	36	0.19	0.30	0.22	0.22	0.00	0.09
E (from KORDI, IOM)	Abundance (wet kg/m²)	10	1.48	22.90	11.34	9.22	46.51	0.60
	Ni (%)	10	0.96	1.43	1.21	1.21	0.03	0.15
	Cu (%)	10	0.69	1.27	1.07	1.11	0.03	0.16
	Mn (%)	10	24.04	31.34	27.54	27.17	6.66	0.09
	Co (%)	10	0.16	0.27	0.21	0.22	0.00	0.19
F	Only two samples - statistics not calculated							

Notes: Var = variance; CoV = coefficient of variation.

Table 7.3 Summary of Historical Samples from the Reserved Areas outside the TOML Contract Area

	Mn (%)	Co (%)	Ni (%)	Cu (%)	Abundance (wet kg/m²)
Count	2188	2188	2188	2188	2188
Minimum	4.14	0.05	0.15	0.12	0.01
Maximum	35.62	3.23	1.75	1.62	52.20
Mean	27.47	0.21	1.25	1.04	8.21
Median	28.47	0.21	1.30	1.09	7.10
Standard Deviation	4.06	0.08	0.20	0.24	6.06
Coefficient of Variation	0.15	0.40	0.16	0.24	0.74

Figure 7.7 Box Plots of Pioneer Contractor sample assay data within the TOML Contract Areas



Source: AMC. Note: Box size represents 1st and 3rd quartiles centered on the median and box width reflects number of samples

7.6 NORI exploration data

Offshore campaigns were completed by NORI in NORI -C and Area D in 2012, and NORI-A and NORI-B in 2013. Detailed exploration data was gathered in NORI Area D in 2018, 2019, and as part of a collector system test in 2022. Table 7.4 summarizes data collected from each NORI area.

Table 7.4 NORI-A, B, C datasets

	MBES (km^2)	Photo-profile (line km)	Dredge (kg)	Box core (#)	Deep Tow Sonar (line km)
NORI-A	8,924	–	190	–	–
NORI-B	2,911	–	85	–	–
NORI-C	25,720	–	28	–	–

Note: MBES excludes AUV data.

7.6.1 Dredging and nodule sampling

In 2012, bulk samples were collected by five dredge deployments in NORI-C and 28 dredge deployments in NORI Area D. Approximately 280 kg of nodules were recovered from NORI-C and approximately 4,500 kg from NORI Area D. Video footage was also obtained during dredge deployments and, together with the samples recovered, provided physical verification of nodules within NORI-C and NORI-D. Figure 7.8 shows examples of the nodules recovered.

Twenty (20) nodule samples (two (2) from NORI-C and 18 from NORI Area D) were assayed. Each sample for assaying, was a subsample of a free fall grab sample and weighed approximately 1 kg. Results of assaying indicated a mean grade of 1.20% nickel, 1.03% copper, 27.9% manganese, and 0.13% cobalt.

These mean values are consistent with the mean grades derived from the historical grab samples in NORI-C and NORI Area D (see Table 7.1). The cobalt value of 0.13% confirmed the cobalt grades recorded from samples in the German data in NORI Area D. A drying test undertaken on a nodule sample collected during the NORI 2012 campaign indicated moisture loss of 24% at 120 °C.

Figure 7.8 Examples of Nodule Samples Recovered during NORI's 2012 Exploration Campaign



Source: TMC

In 2013, dredging was carried out using an epibenthic sled that was designed by KC Denmark Research Equipment specifically for polymetallic nodules sampling. Approximately 190 kg of nodules were recovered from NORI-A and approximately 85 kg of nodules were recovered from NORI-B.

Figure 7.9 Photos of Nodules Collected from NORI-A during the 2013 NORI campaign



Source: TMC

Four subsamples from NORI-A and B were sent to ALS Laboratories in Brisbane for preparation and analysis. The samples were dried at 120 C for 12 hours then assayed using a four-acid digest specifically designed for high-manganese samples, followed by AAS (method Mn-AA62) and four-acid digest followed by Inductively coupled plasma mass spectrometry (ICP-MS) for concentrates (ME-MS61c). The Mn-AA62 method has a claimed precision of ±5%. Table 7.5 shows the results for cobalt, copper, iron, manganese, molybdenum, and nickel. The average moisture content after drying at 120 C for 12 hours was 28.7%.

Table 7.5 Assay Results for NORI-B Nodule Samples

Sample ID	Co (%)	Cu (%)	Fe (%)	Mn (%)	Mo (ppm)	Ni (%)
NA1	0.23	1.08	5.27	29.0	589	1.36
NA2	0.22	1.12	5.06	28.9	545	1.34
NB1	0.25	1.16	5.62	29.2	601	1.38
NB2	0.25	1.11	5.60	28.2	590	1.38

Note: Co = cobalt, Cu = copper, Fe = iron, Mn = manganese, Mo = molybdenum, Ni = nickel, ppm = parts per million

7.6.2 Box-coring and nodule sampling

Due to the prioritization of work on NORI Area D, no box-coring has yet been undertaken by NORI in NORI-A, B, or C.

In NORI Area D, a total of 252 box cores were acquired during the 2018 and 2019 offshore campaigns. The sample spacing was generally 10 km by 10 km or 7 km by 7 km. Spatial analysis showed that this spacing was sufficient to classify the Mineral Resources in these areas as Indicated Mineral Resources. For the IA of NORI A, B and C it is reasonable to assume that BC sampling programs on similar spacings to those used in NORI Area D could potentially provide data suitable for upgrading Mineral Resource estimates in NORI A, B and C to a level of confidence sufficient for mine planning and a PFS.

7.6.3 MBES surveys

In 2012, NORI completed an offshore exploration campaign in NORI-C and NORI Area D aboard the RV Mt. Mitchell using a hull-mounted Kongsberg Simrad EM120 12 kHz, full-ocean depth multibeam system. Due to swath width and vessel orientation relative to course-made-good, some data were

recorded beyond the bounds of those areas. Approximately 69.1% of NORI-C (25,720 km^2) was surveyed. NORI Area D was surveyed in its entirety (25,439 km^2).

In 2013, NORI carried out an offshore exploration campaign within NORI-A and B using RV Mt. Mitchell. This campaign was focused mapping bathymetry, identifying nodule fields based on acoustic data (including interpretation of backscatter data), and recovering bulk polymetallic nodule samples. A hull-mounted Kongsberg Simrad EM120 12 kHz, full-ocean depth multibeam system was used to survey approximately 8,924 km^2 in NORI-A and approximately 2,911 km^2 in NORI-B. The Applanix Pos MV 320 V4 system was used to measure vessel position and attitude, and a dual Trimble Zephyr unit was used as the Global Positioning System (GPS) system.

First pass processing of the data was carried out with the intent identifying areas of nodule abundance to be further surveyed with higher resolution AUV-based sonar and to selecting priority areas for nodule sampling. More sophisticated processing to clean the MBES data and achieve the highest possible resolution maps of the bathymetry was not carried out for NORI A, B and C at that time and NORI's attention shifted almost exclusively to NORI Area D.

7.6.4 AUV surveys

Due to the prioritization of work on NORI Area D, no AUV surveys were undertaken by NORI in NORI-A, B or C.

MBES surveys show that the topography of the seafloor in NORI-A to C and TOML-A to F shows many of the geological features mapped in NORI Area D, such as abyssal plains, abyssal hills, volcanic cones, and slopes ≥ 6°. The nodules recovered from NORI-A to C and TOML-A to F are also similar in size and shape to those from NORI Area D, although nodule facies mapping and analysis of genetic types (hydrogenetic or diagenetic) has not yet been undertaken. Consequently, the information gathered by AUV surveys in NORI Area D is considered to provide insight to the possible distribution patterns of nodules on the seafloor in NORI-A to C and TOML-A to F and supports the assumptions of the IA.

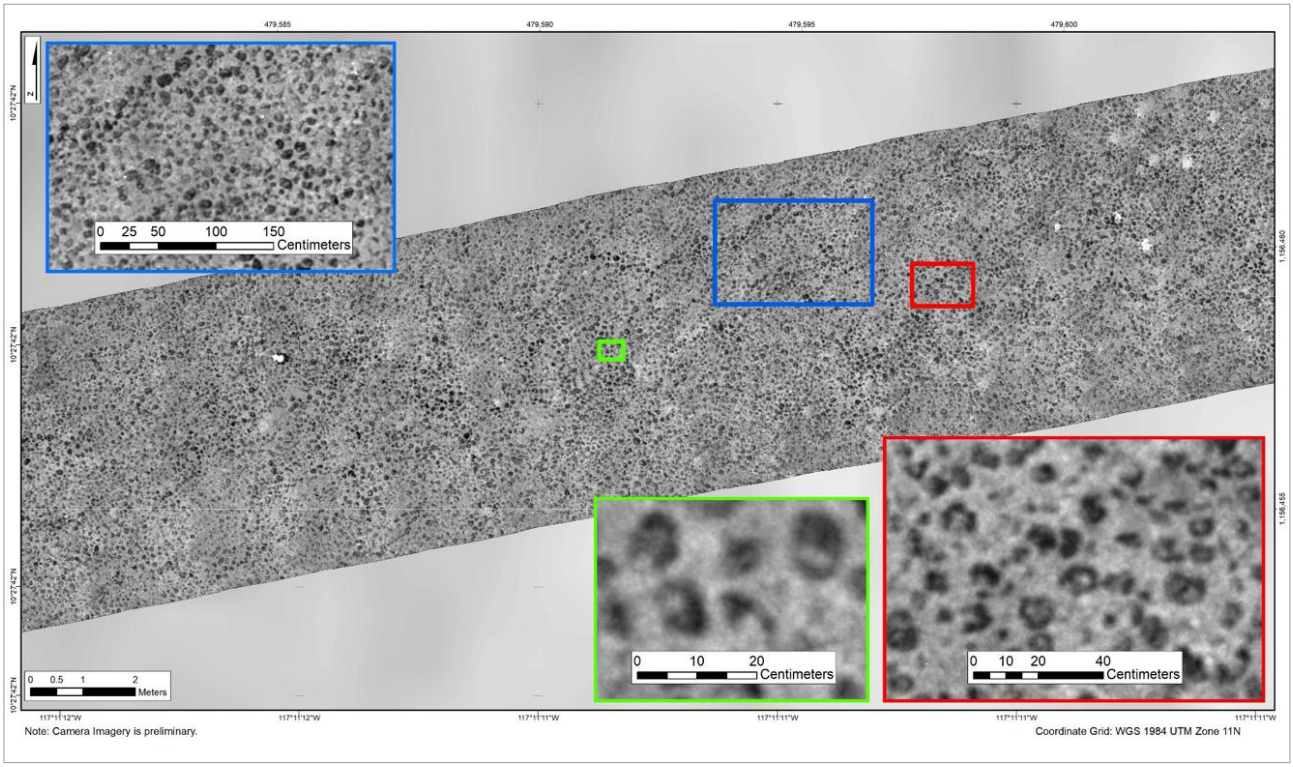
Successful AUV surveys were conducted by NORI in 2018 over selected sub-areas within NORI Area D. An ESVII 4500 m-rated Kongsberg Hugin AUV was used to conduct the detailed survey work, utilizing an MBES, SSS, SBP and camera payload. The surveys included:

- Reconnaissance lines collected at 35 m AUV altitude in order to assess geological and near-surface conditions prior to acquiring low-altitude camera data.
- Camera lines collected at 6 m AUV altitude in order to map the distribution and abundance of the nodules.
- MBES, SSS and SBP data lines collected at 22 m altitude in a 10 km x 15 km area, in order to evaluate geologic and near-surface conditions for future Test Mining activities.

There was an excellent correlation between the AUV bathymetric data and that collected by hull-based multibeam methods in 2012, providing confidence in both sets of results. Low-altitude surveys using the AUV's camera payload provided visual continuity of nodule distribution between the majority of the BC sample sites along the surveyed lines.

A 3.5 km × 3.5 km grid of camera data was acquired over the Test Mining Site provided near-continuous photomosaic coverage. Each camera frame was 6 m across-track and 4 m along-track. Figure 7.10 provides an example.

Figure 7.10 Example of AUV camera photo mosaic from NORI Area D, showing nodules



Source: MARGIN

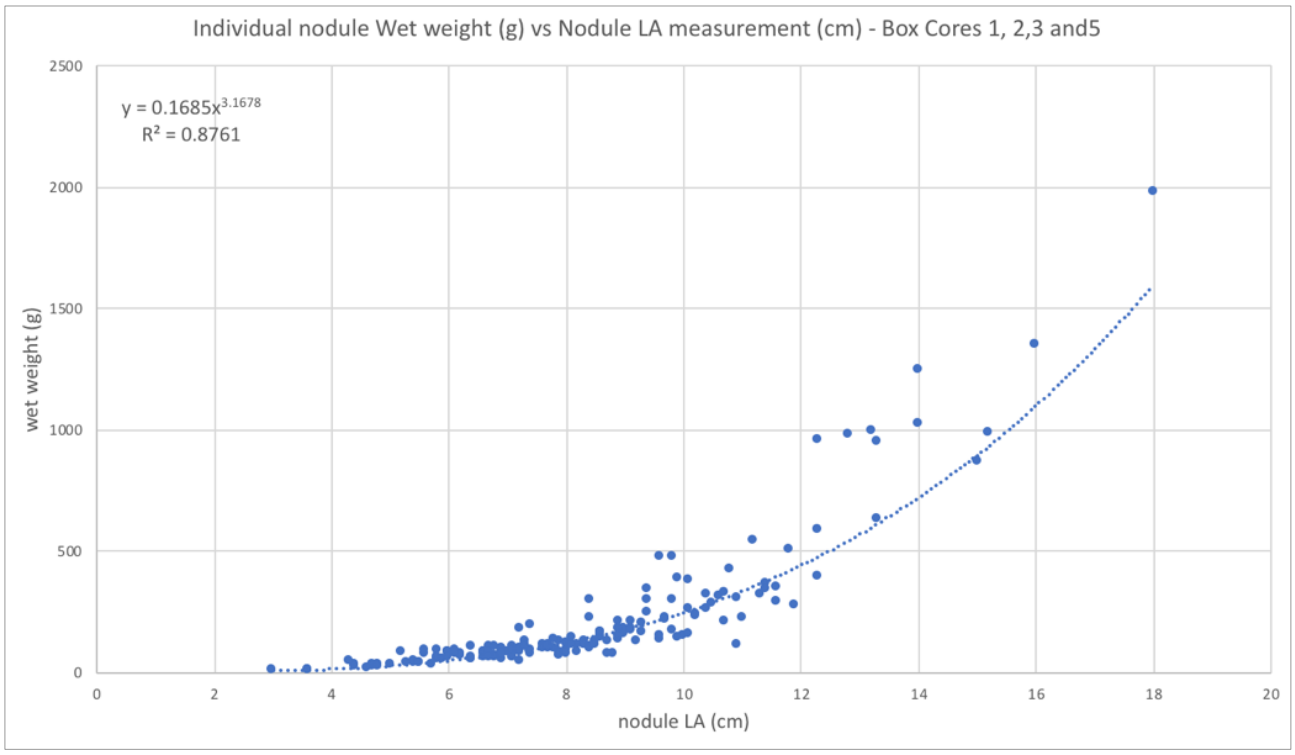
7.6.5 Long axis estimation

Although box coring is an effective method for measuring nodule abundance, it is slow and expensive. Therefore, it is advantageous if BC estimates can be supplemented by an alternative method. There is a well-documented relationship between nodule length and nodule wet weight (e.g., Felix, 1980):

$$Log_{10}(nodule\ wet\ weight) = (2.71)(log_{10}(long\ axis\ length)–0.18$$

The process of estimating the weight of nodules using the nodule length is called Long Axis Estimation (LAE). NORI confirmed this relationship by taking measurements of the long-axis length of individual nodules, using digital calipers, and wet weight, for nodules from NORI Area D BC samples BC001, BC002, BC003, and BC005 (Figure 7.11).

Figure 7.11 Comparison of nodule long axis measurements, taken using digital calipers, and individual nodule wet weight for BC001, BC002, BC003, and BC005



Source: MARGIN

In areas where nodules are not closely packed, image processing techniques can be used to identify each nodule in a photograph unambiguously and measure its long axis length. In this case, it is possible to estimate nodule abundance from photographs. However, if nodules are closely packed and touch each other, image processing techniques are currently unable to reliably discriminate each individual nodule.

NORI developed an alternative methodology for NORI Area D using a combination of long-axis measurement and percentage nodule coverage which was applied to the data. A multiple linear regression relationship between percentage nodule coverage estimated from the photographs and mean nodule long-axis measurement from six BC samples within the Test Mining Site was found to provide a good correlation with nodule abundance.

Subsets (1 m × 1 m) of AUV camera data acquired on a 3.5 km × 3.5 km grid pattern over the NORI Area D Test Mining site were extracted for each intersection point of the survey lines. The percentage nodule coverage was measured by applying a color threshold to the image to distinguish nodules from sediment. This allowed the percentage area covered by nodules in the image to be calculated. Mean nodule long axis measurements were manually extracted from these images. Nodule abundance estimates were then derived for each of these intersection points, resulting in a 3.5 km × 3.5 km grid of nodule estimation points over the Test Mining site which were used to supplement the Mineral Resource estimate for NORI Area D.

7.6.6 Geotechnical data collection

No geotechnical data is currently available from NORI-A, B or C.

Geotechnical data collected from BC tests and samples, and *in situ* testing in NORI Area D is considered to provide insight to the likely geotechnical conditions on the seafloor in NORI-A, B or C, and is sufficient to support this IA.

Geotechnical soils data was systematically collected across the NORI Area D site during Campaign 3, Campaign 6 and Campaign 7. BC samples were geotechnically investigated to a maximum depth of 0.50 m below sea floor. BC samples were sub-sampled, geotechnically described and tested onboard the recovery vessel. Box cores from Campaign 6 and Campaign 7 were additionally subject to cone penetrometer testing and a subset were subject to a series of tests, including shear vane profiles and plate load tests. Sub-samples from the Campaign 6 BC were transported ashore and a comprehensive campaign of laboratory testing was undertaken. During Campaign 7 seabed in-situ testing was conducted down to 2.2 m below seabed by an ROV deployed Cone Penetration Test system.

An assessment of the soils across the NORI Area D area was made based on observations from the fieldwork and onshore laboratory testing reports. In general terms the seafloor across the abyssal plains can be classified as a very soft (extremely low strength) silty clay, that in parts is very silty and sometimes silt like. There are exceptions to this classification associated with depressions or high areas of seafloor such as ridge lines, abyssal hills and volcanic features.

7.7 TOML exploration data

TOML completed offshore campaigns in 2013 and 2015 to collect data define Mineral Resources. Much of the exploration was focused on smaller sub-areas within TOML-B, C, D, and F areas in order to increase understanding of local variations in seafloor conditions and nodule mineralization. TOML-A was only explored by dredging and TOML-E was only explored with an MBES survey and a single water column survey.

Table 7.6 summarizes data collected from each TOML area. MBES (12 kHz MBES echo-sounding) includes bathymetric and backscatter products and geological geomorphological interpretation. Photo-profile includes still and video products and logging. Dredge sample data includes grade characterization and some size distribution data. Water column includes temperature, pressure, turbidity and in some cases physical samples and current. BC data includes nodule grade and abundance, fauna, and in some cases vane shear and/or sediment characterization. Deep-tow sonar includes SSS, sub-bottom profiler and micro survey and altimetry. Further details of these programs are presented in:

- The technical report summary titled “Technical Report Summary--Initial Assessment of the NORI Property, Clarion-Clipperton Zone, for Deep Green Metals Inc.” (the “NORI Technical Report”), with an effective date of March 17, 2021 (AMC Consultants, 2021a).
- The technical report summary titled “Technical Report Summary--TOML Mineral Resource, Clarion-Clipperton Zone, Pacific Ocean, for Deep Green Metals Inc.” (the “TOML Technical Report”), with an effective date of March 26, 2021 (AMC Consultants, 2021b).

Table 7.6 TOML datasets by area and by campaign

	MBES (km^2)	Photo-profile (line km)	Dredge (#)	Water column (#)	Box core (#)	Deep Tow Sonar (line km)
TOML-A	–	–	2 CCZ15	–	–	–
TOML-B	9,966 CCZ13	–	–	–	–	–
Sub-area B1	Included in B	178 CCZ15	1 CCZ13	14 CCZ15	30 CCZ15	88 CCZ15
TOML-C	15,763 CCZ13	–	–	–	–	–
Sub-area C1	Included in C	231 CCZ15	1 CCZ15	14 CCZ15	16 CCZ15	32 CCZ15
TOML-D	15,881 CCZ13	92 CCZ15	6 CCZ13	–	–	–
Sub-area D2	Included in D	47 CCZ15	2 CCZ13	26 CCZ15	26 CCZ15	120 CCZ15
TOML-E	7,002 CCZ13			1 CCZ13		
TOML-F	15,820 CCZ13		4 CCZ13	15 CCZ15	15 CCZ15	
Sub-TOML-F1	Included in F			9 CCZ15	10 CCZ15	
Total	64,432	587	17	259	113	280

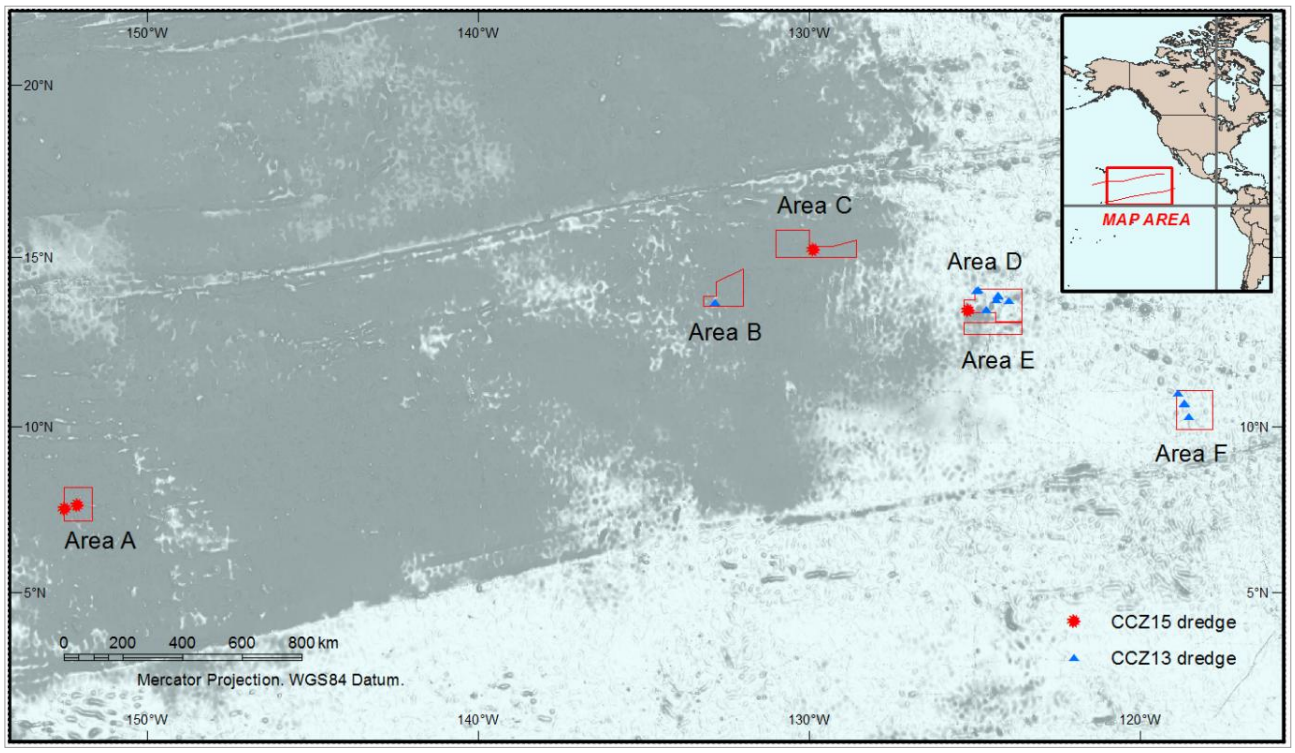
Note: CCZ13 = TOML 2013 offshore campaign, CCZ15 = TOML 2015 offshore campaign

7.7.1 Dredging and nodule sampling

Dredging was carried out during both the CCZ13 and CCZ15 campaigns. The intent was to collect samples for whole rock chemical analysis and metallurgical test work. Seventeen sites were sampled (Figure 7.12).

The samples were logged and sub-sampled extensively (up to 30 fragments per dredge sample). The sub-samples were assayed to confirm historical grades and to study variability in grade, used in drying test work and used for metallurgical test work.

Figure 7.12 Dredge sample locations in TOML areas from CCZ13 and CCZ15 campaigns



Source: TMC

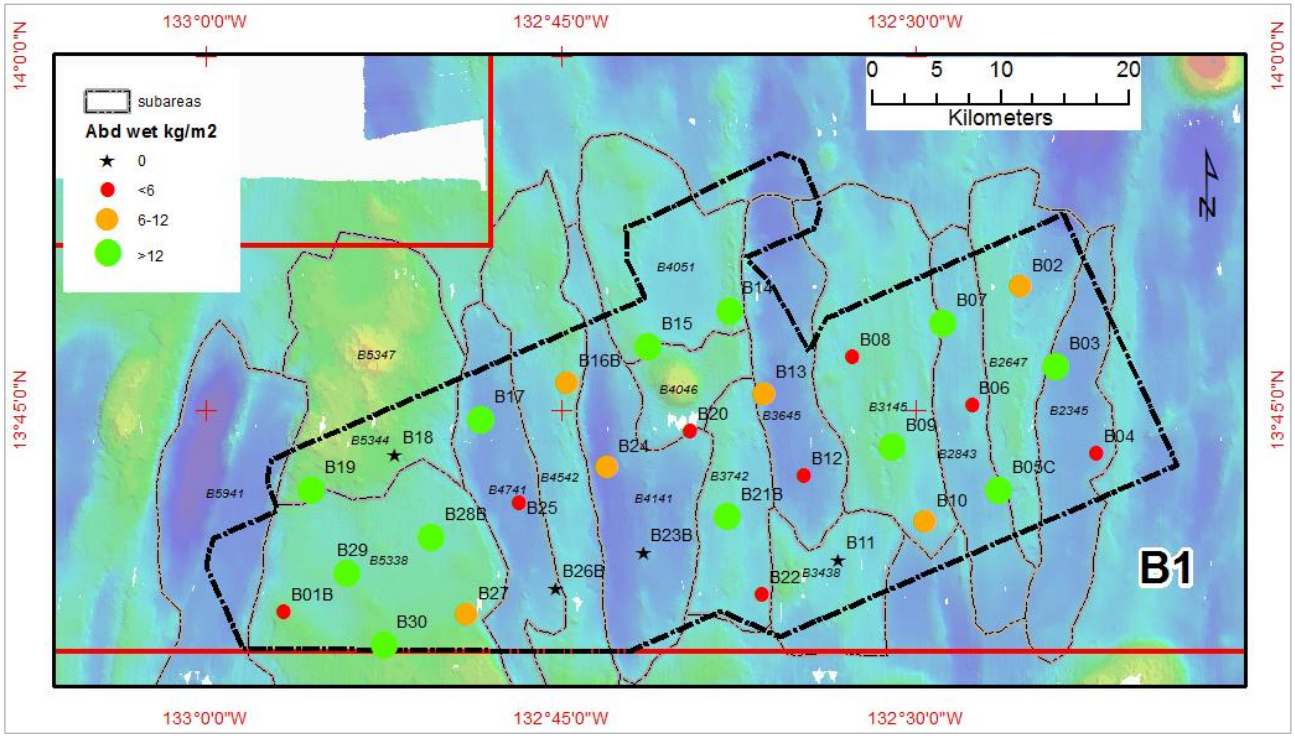
7.7.2 Box-coring and nodule sampling

Box-coring was undertaken to collect samples for Mineral Resource estimation, to collect biological samples for environmental base-line measurement and to collect geotechnical data. Landing points were chosen to avoid steeper areas (>10° slope) based on pre-existing multi-beam data. Two types of box corers were used:

- 0.75 m^2 box corer manufactured by KC Denmark, similar to the ones used by NORI.
- 0.25 m^2 box corer manufactured by YMG based on a design from the 1970s.

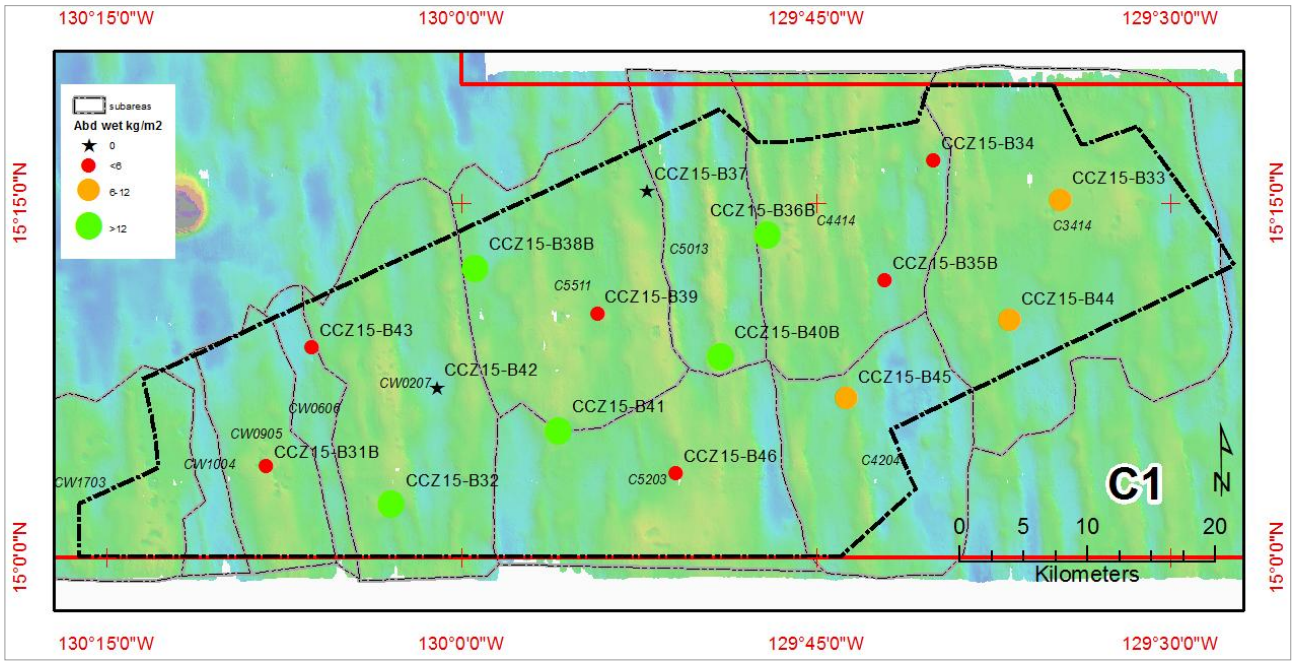
Figure 7.13 to Figure 7.17 show nodule abundances at the BC locations and the MBES bathymetry. Nodule abundances are reported in wet kg/m^2.

Figure 7.13 Nodule abundance and BC locations, TOML-B sub-area B1



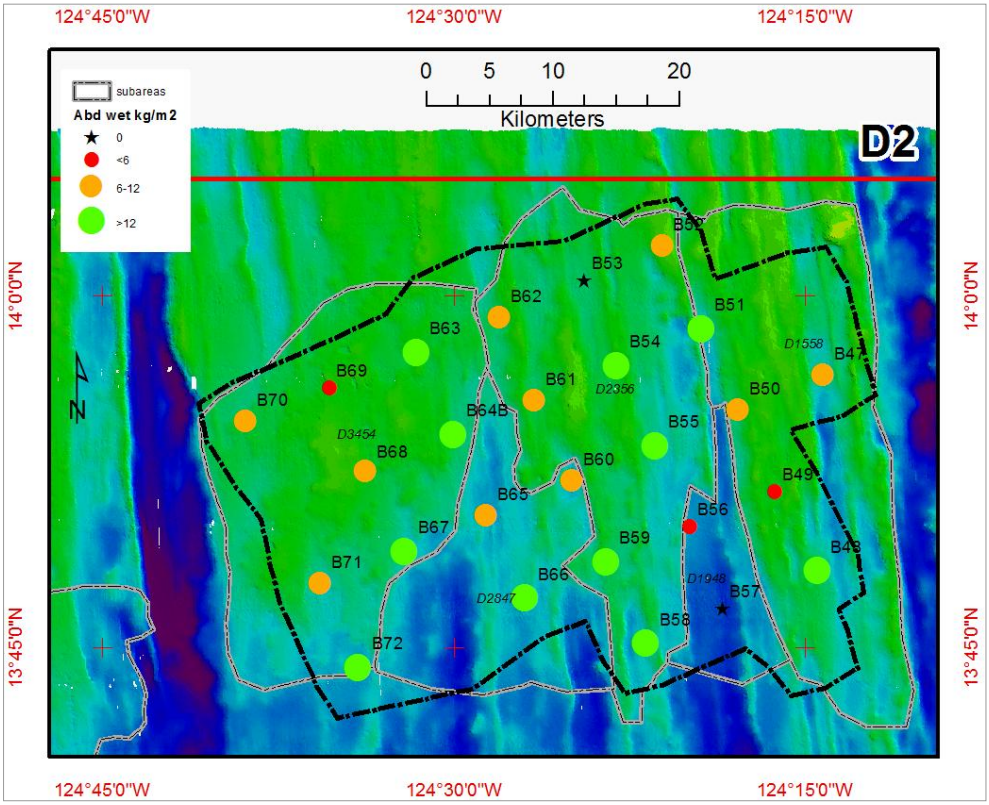
Source: TMC

Figure 7.14 Nodule abundance and BC locations, TOML-C sub-area C1



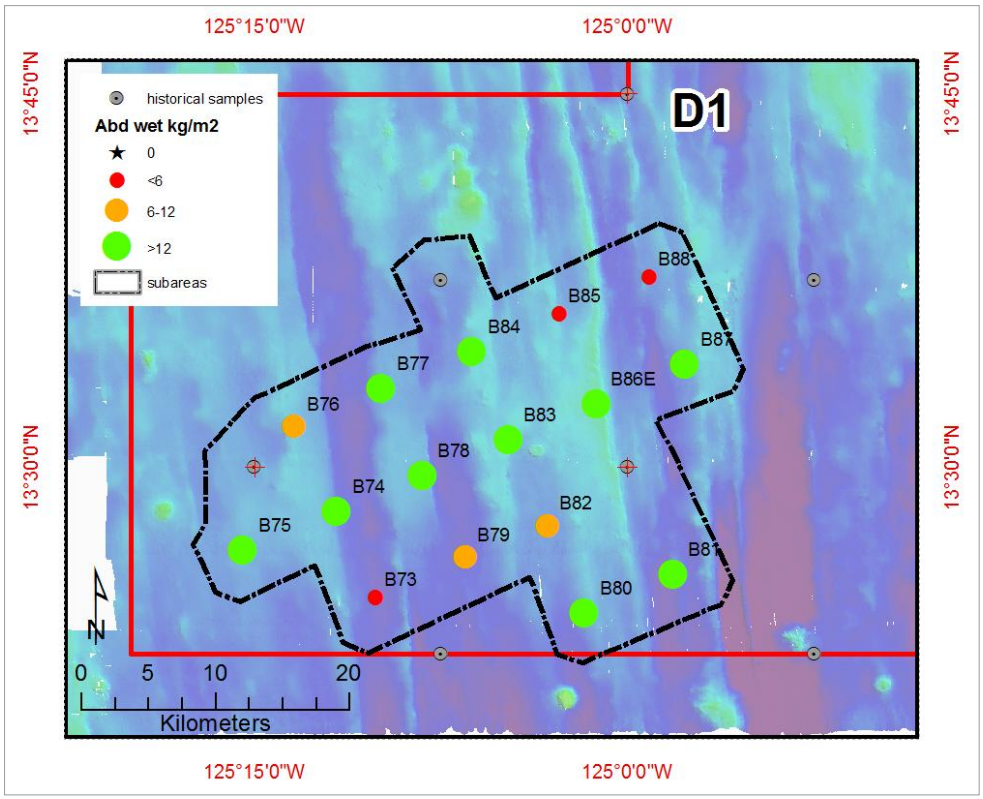
Source: TMC

Figure 7.15 Nodule abundance and BC locations, TOML-D sub-area D2



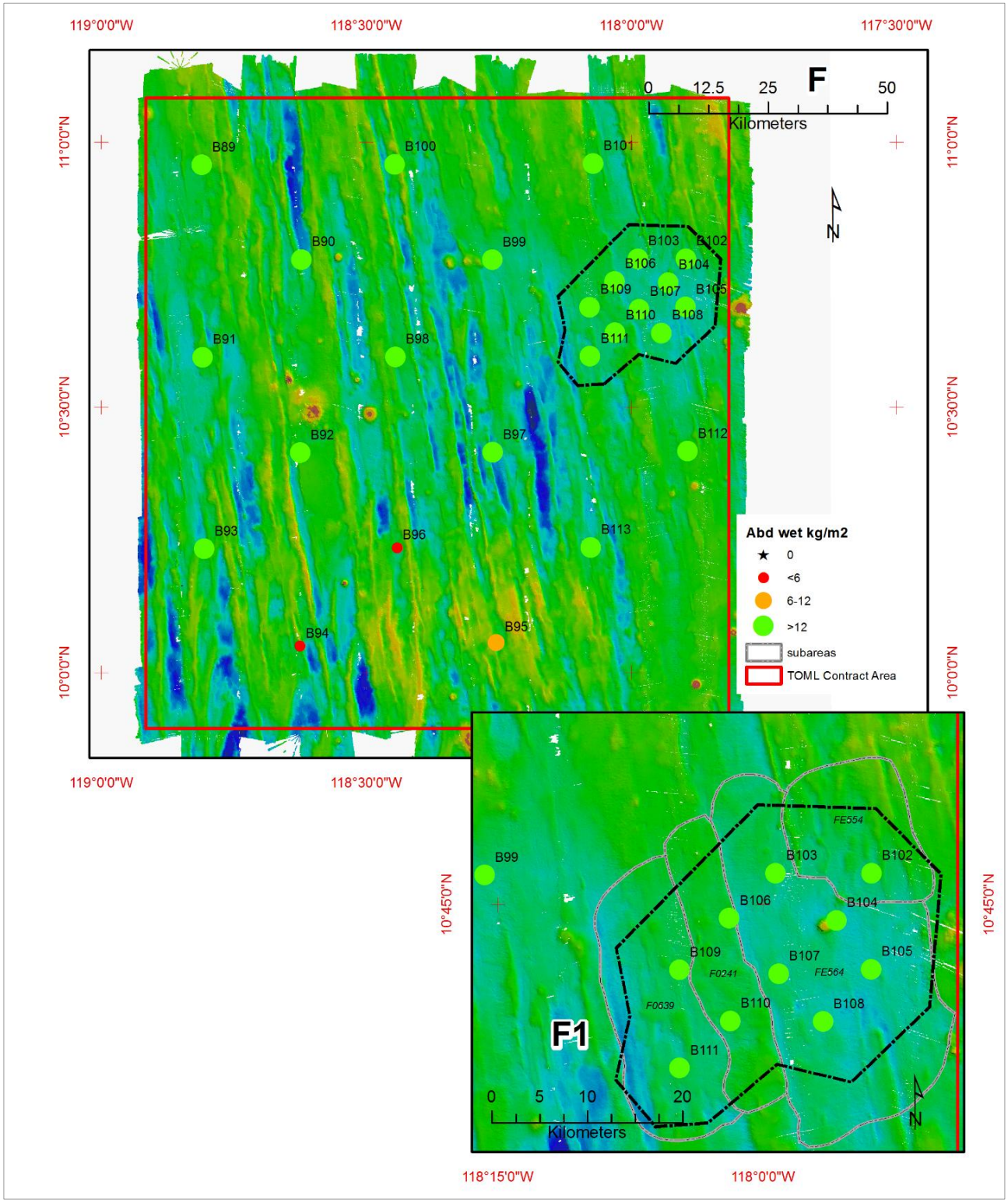
Source: TMC

Figure 7.16 Nodule abundance and BC locations, TOML-D sub-area D1



Source: TMC

Figure 7.17 Nodule abundance and BC locations, TOML-F and sub-TOML-F1



Source: TMC

7.7.3 MBES surveys

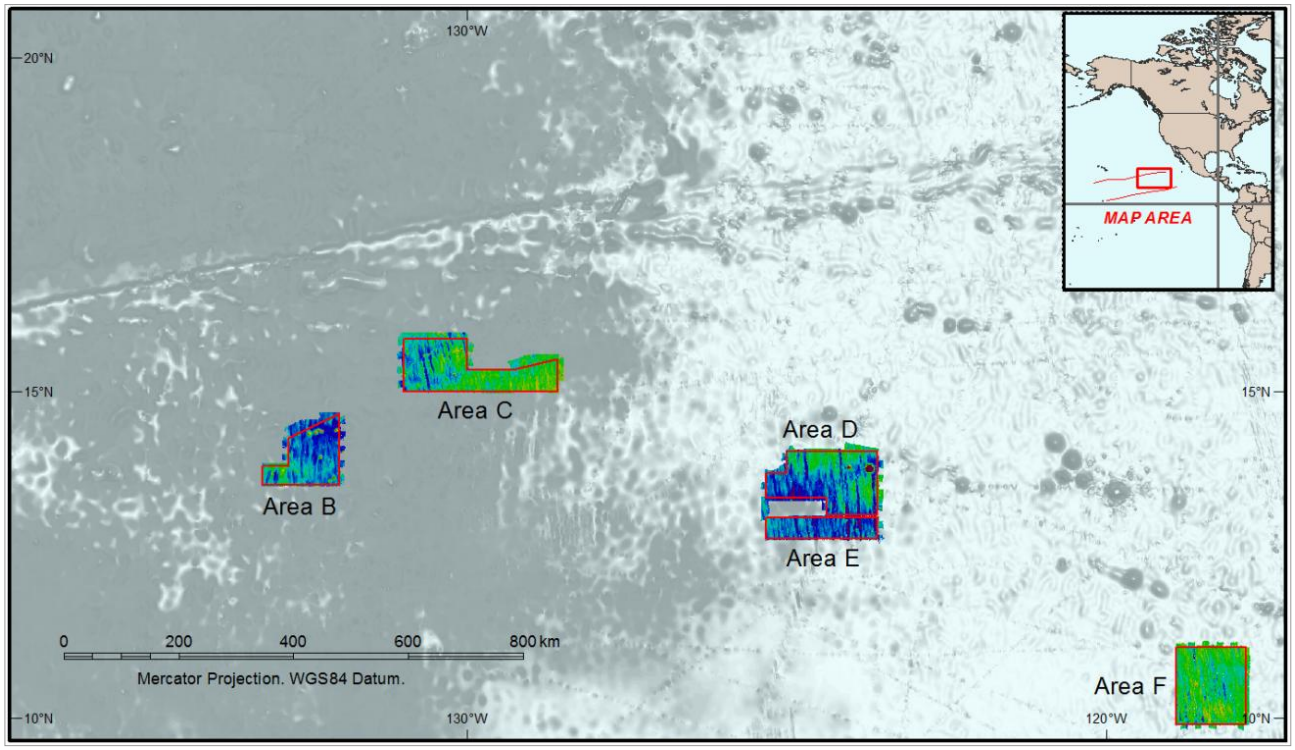
During the CCZ13 campaign the RV Mt Mitchell operated a hull-mounted Kongsberg EM120 MBES over TOML- B through - F. This equipment operates at 12 kHz and is capable of operation in up to 11,000 m water depth. It has better than 5 m vertical resolution and ~60 m horizontal resolution for bathymetry and ~30 m for backscatter at water depths between 4,500–6,000 m. It has a maximum swath width of 6 times the water depth but the effective swath width varies from 2 to 6 times the water depth depending on the depth, sea state and heading.

Conductivity-temperature-depth (CTD) soundings were performed at each of the survey areas in 2013. The primary reason for this is that the MBES system requires an accurate full water column sound velocity profile with which to perform real time beam steering and location calculations.

TOML-A was not surveyed.

The MBES results are shown at a small scale in Figure 7.18. The bathymetry shows that almost the entire area is composed of abyssal plains and abyssal hills. The bathymetry and backscatter together show that most of the area is covered by nodule bearing sediment. Larger scale maps of the bathymetry are presented in Section 13.7.

Figure 7.18 CCZ13 MBES bathymetry coverage



Source TMC. Relief range blue to yellow is about 400 m scaled by each area. Background is the GEBCO bathymetric product

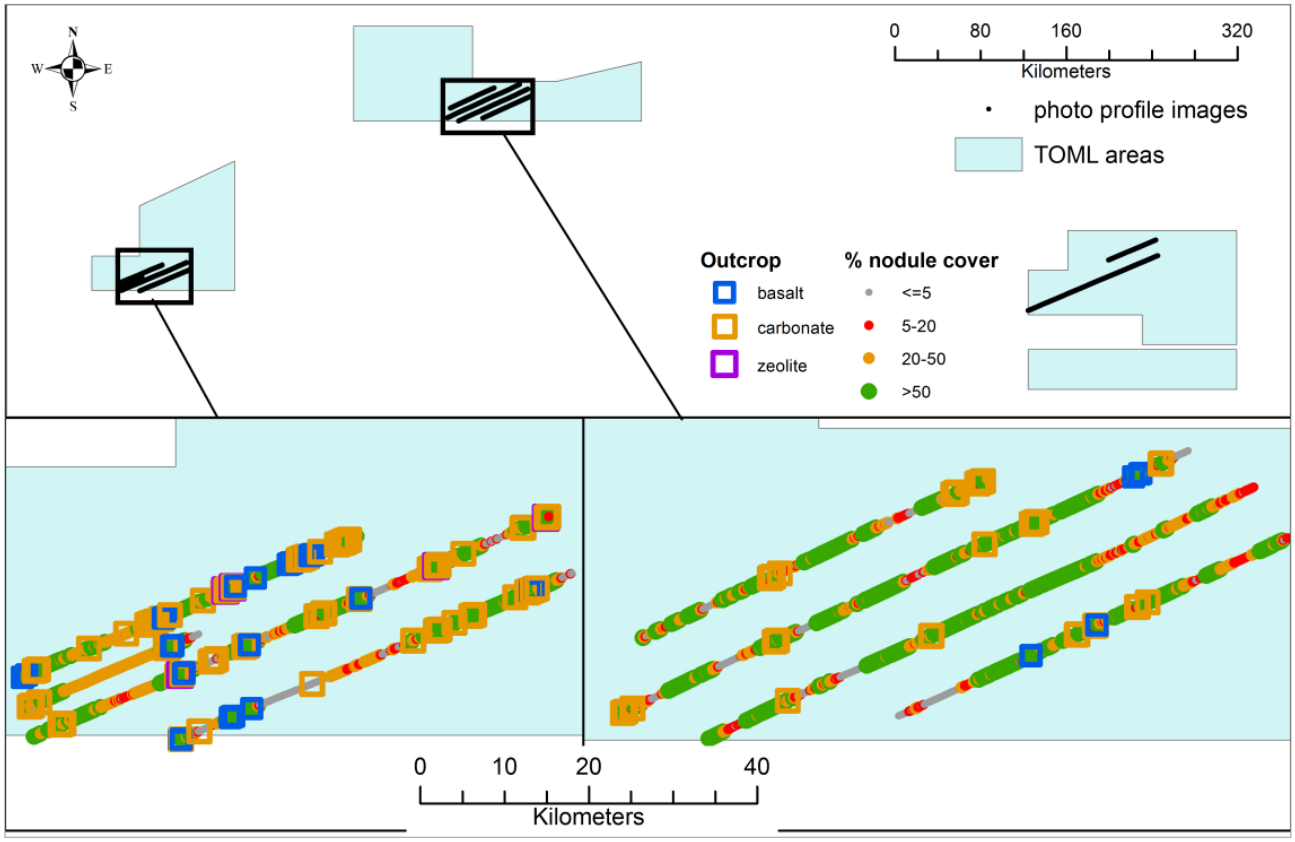
7.7.4 Deep-tow surveys

A photo-profiling survey was undertaken in 2015 using a towed camera system along ten lines in parts of TOML-B, C and D, by contractor Yuzhmorgeologiya. Photographs were taken automatically at an altitude of 3.5 m above the seafloor, a minimum of 30 seconds apart and continually uploaded to the vessel where scientists collected them from the central server and logged them for geology and biology.

The photographs provided data on short-range continuity of nodules and photogrammetric estimates of nodule abundance for Mineral Resource estimation. The photographs also provided a census of mega-fauna and macro-fauna for environmental base line measurement and habitat mapping. Finally, photo-profiling helped calibrate the MBES and deep-towed sonar results.

The percentage nodule coverage was measured by applying a color threshold to the image to distinguish nodules from sediment, allowing the percentage area covered by nodules in the image to be calculated. This was useful for visual assessment of nodule continuity. When combined with observations of outcrop, the nodule coverage plots give a good indication of the high levels of continuity for the nodules (Figure 7.19). The process was not successful in TOML-D where sediment obscures the nodules.

Figure 7.19 Photo-profile logging of nodule coverage (%) and outcrop types in TOML Areas



Source: TMC. Note: Insets only shown for Area B (left) and C (right)

7.7.5 Long axis estimation

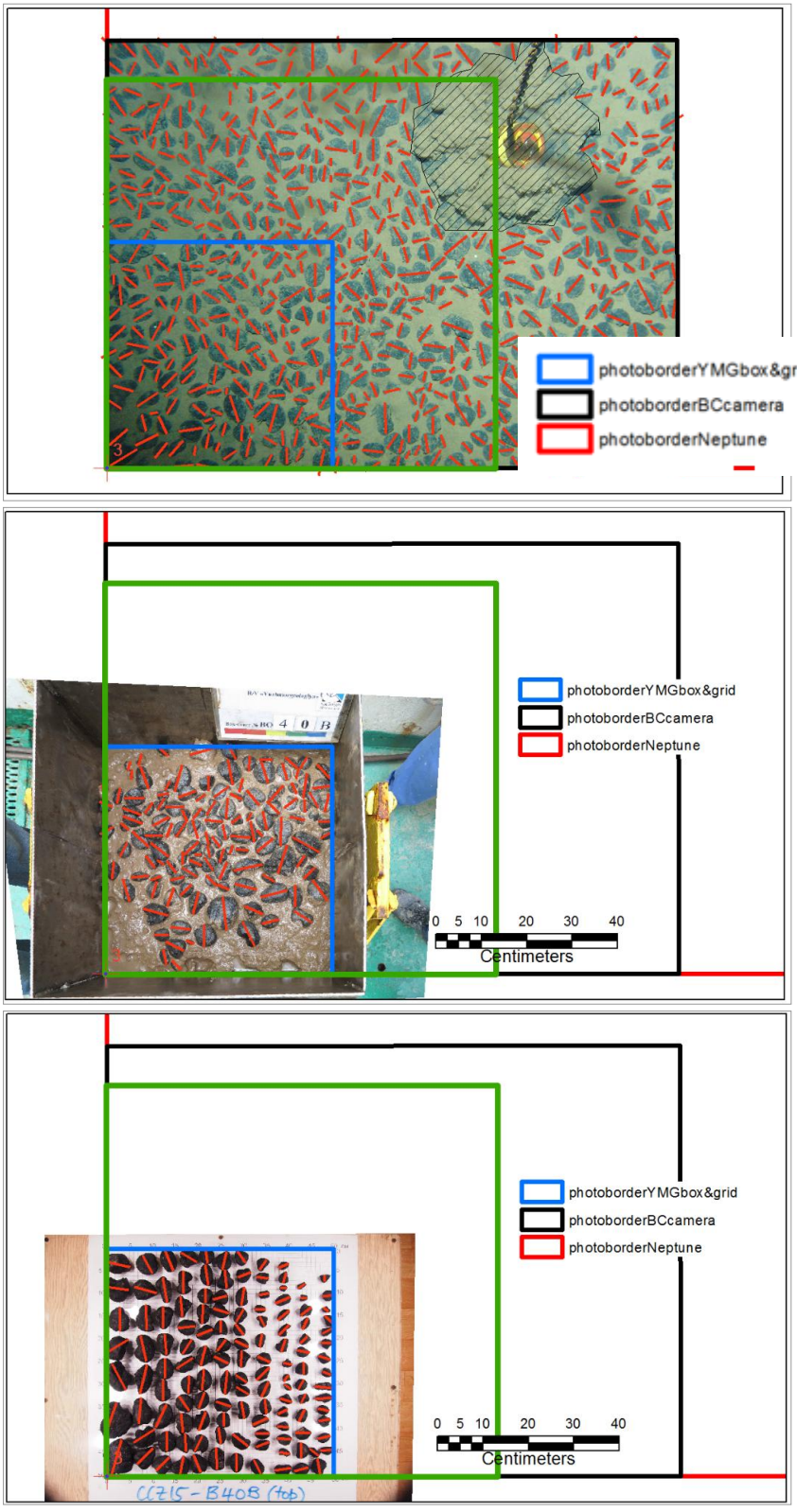
TOML used a BC mounted camera system to collect seabed photos from TOML-B, C, D and F (bottom shots). Photographs taken on the vessel included top shots of the sample in the BC as it landed on deck and photographs of the nodules from the BC on a gridded background, after washing off mud. Figure 7.20 shows examples of the three types of photographs.

In TOML- B and C, it proved possible to use the bottom shots and the top shots to estimate the weighed abundance of each box core. The process involved referencing the photos to scale in a GIS package. A line was digitized along the long axis of each nodule before recording the length of each line into a database. The line measurements were then analyzed in MS Excel, comparing the total calculated weight with the total actual sample weight. Accurate weighing of individual nodules was not possible

due to the heave of the vessel, but a motion compensated scale was used to accurately weigh entire BC samples (±50 g).

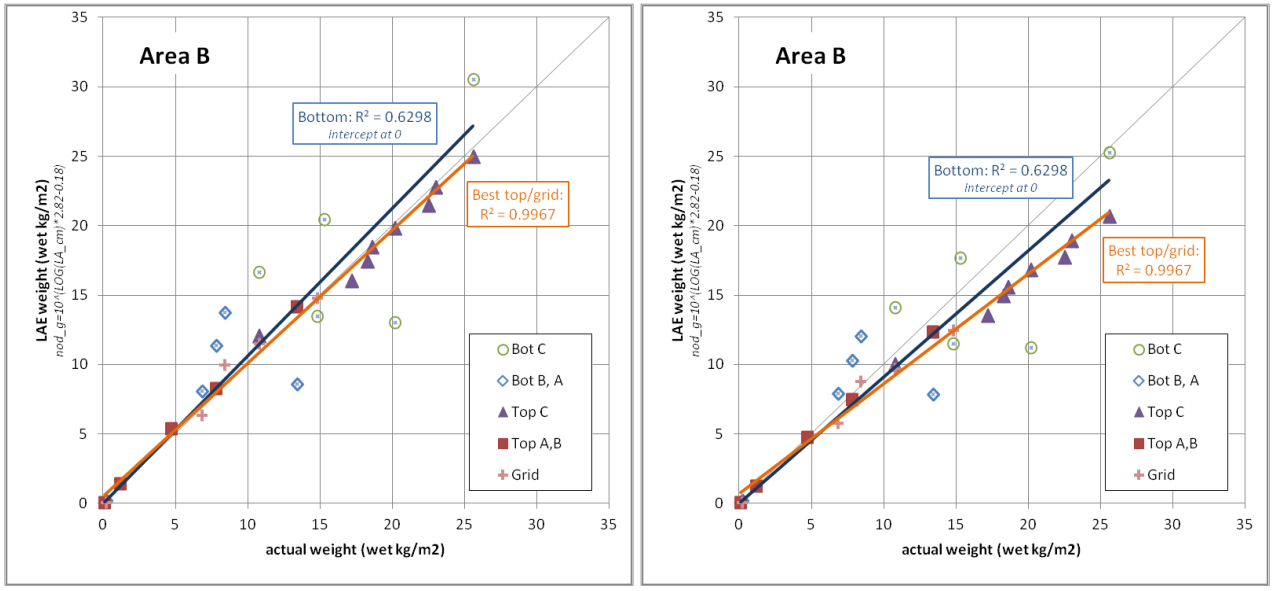
In TOML-B, long-axis estimates were made using bottom shots, top shots and, where needed, sample grid photos. Initially the formula of Felix (1980) (see Section 7.6.5) was used to estimate the nodule weights but a much better fit was achieved if the factors were modified (Figure 7.21). The need to modify the factors probably relates to differences in nodule shape between areas.

Figure 7.20 Example of LAE measurement using bottom shot, top shot and grid photographs



Source: TMC. Note: Green frame is area sampled by the box core. Top: “bottom shot”, middle, “top shot”, bottom “grid photograph”

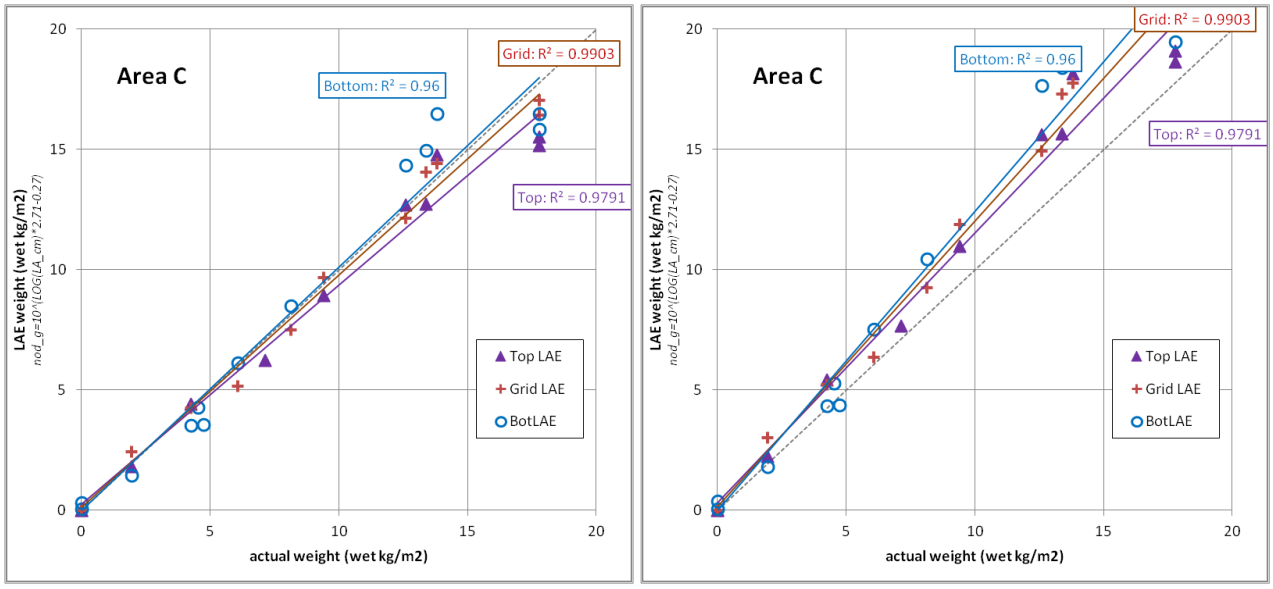
Figure 7.21 TOML-B correlations with best fit factors (L) and Felix 1980 factors (R)



Source: TMC

The process was then extended to TOML-C. Again, the factors in the Felix (1980) formula were adjusted to improve accuracy (Figure 7.22). In TOML-C the correlations between bottom photograph-based estimates and actual weights show less scatter; this might be due to a slightly different camera with a wider field of view being used.

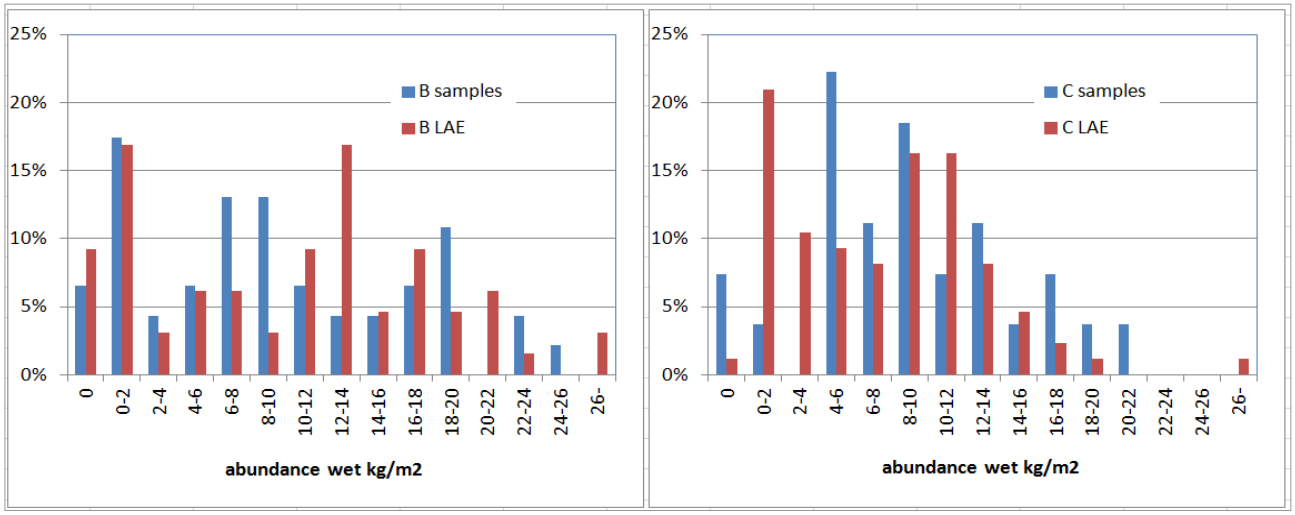
Figure 7.22 TOML-C correlations with best fit factors (L) and Felix 1980 factors (R)



Source: TMC

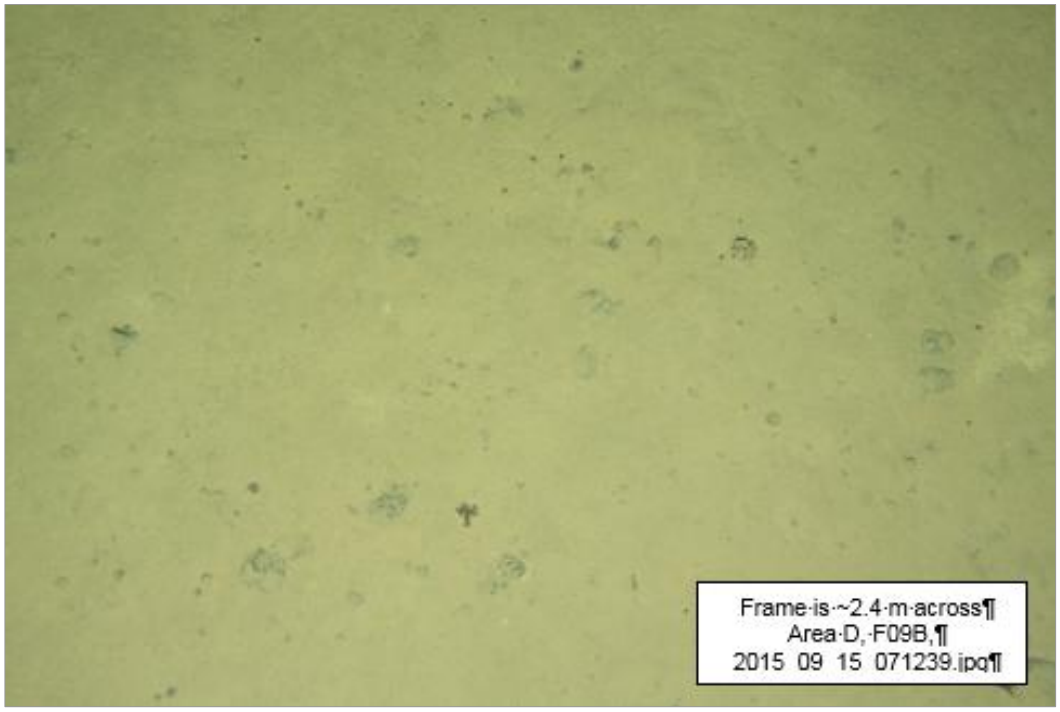
The modified formula was also applied to the towed camera system photographs (approximately every 100th image) with results broadly agreeing with the BC samples. Figure 7.23 compares the distribution of nodule sizes in the box cores in TOML-B and C with the distributions estimated by LAE. In TOML-D however, the partial cover of the nodules by unconsolidated sediment (Figure 7.24) confounded the process. In TOML-F, no towed camera survey was done, but a visual comparison between bottom shots, top shots and grid photos revealed good exposure of nodules.

Figure 7.23 Comparison of physical samples and LAE in TOML-B and C



Source: TMC

Figure 7.24 High degree of sediment “powder” and cover in TOML-D



Source: TMC

7.7.6 Geotechnical data collection

Vane shear test measurements were collected in all box cores from TOML areas that were recovered in an undisturbed state. A calibrated hand-held shear vane device with a 33 mm vane was used. Vane shear strength was classified into one of four classes:

- W is mostly weak from top to base.
- A is all stiff from top to base.
- G is soft at the top with gradual stiffening with depth.
- S is soft at the top with more sudden stiffening with depth.

Data was also reviewed by box and the most coherent reading selected. Averaging of readings was not undertaken as some measurements were taken in disturbed sediment, especially near the base. The most coherent readings were generally taken in the center of the box.

Figure 7.25 to Figure 7.29 show the vane shear strength classifications at the BC locations and the MBES bathymetry. Figure 7.30 shows the vane shear strength profiles by area.

The data shows clear differences in the uppermost part of the sediment between areas, with:

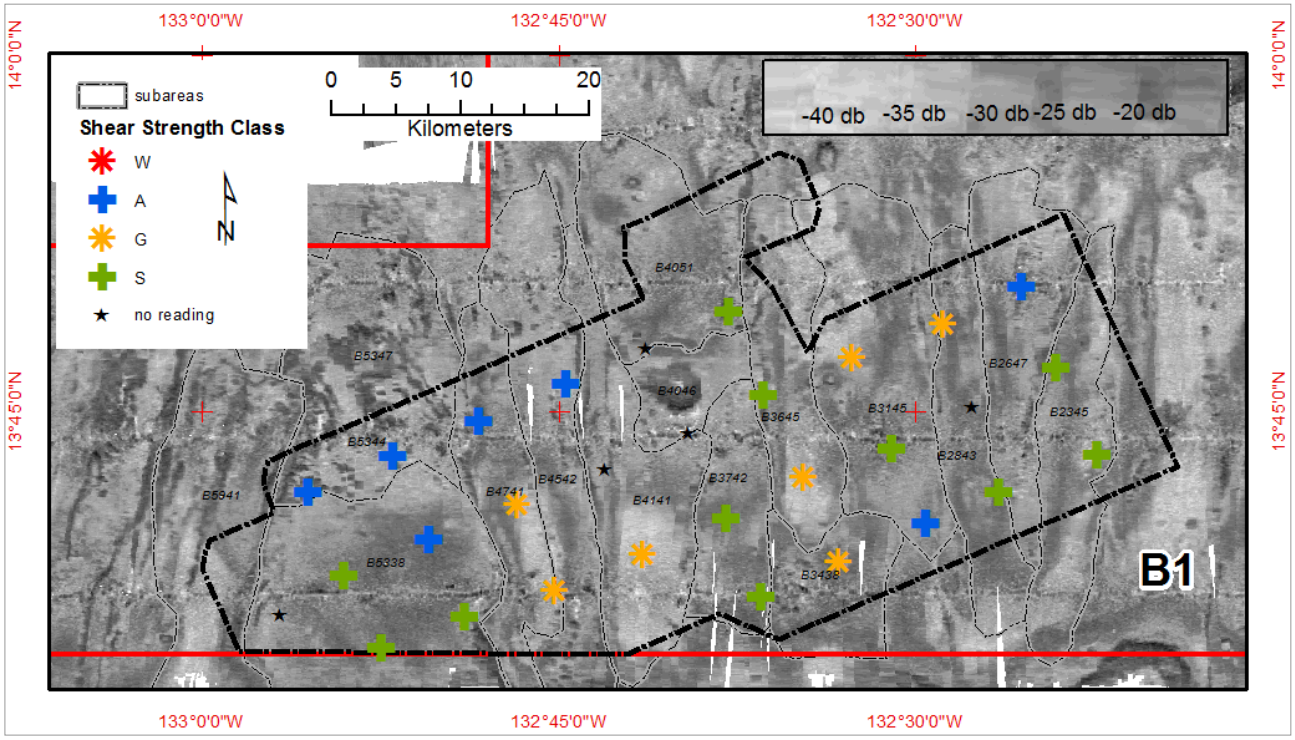
- TOML-C1 showing consistently suddenly stiffening ground conditions (mostly class S).
- TOML-D1 showing a slightly wider range to TOML-C1 including some more rapidly stiffening situations (mostly class S).
- TOML-B1 and TOML-D2 have a wider range of conditions and both areas have occurrences of sediment drift.
- TOML-F (and F1) has a universally weak upper layer then generally and gradually stiffens (mostly class G).

The soil strength properties of the TOML sediments appear to be similar to those investigated at NORI Area D. At TOML the soil strengths are broadly similar to NORI Area D at depths down to 0.3 m below seabed. The TOML sediments are indicated as ~2 kPa stiffer than the general trend observed at the NORI Area D Initial Mining area.

The TOML Class W, G and S are all comparable in strength to NORI Area D where the increase in shear strength from seabed to a range of 4-6 kPa at 20 cm to 30 cm below seabed is observed. TOML Class A has a similar profile to the higher ground/ridges investigated at NORI Area D where shear strength up to 14 kPa was observed.

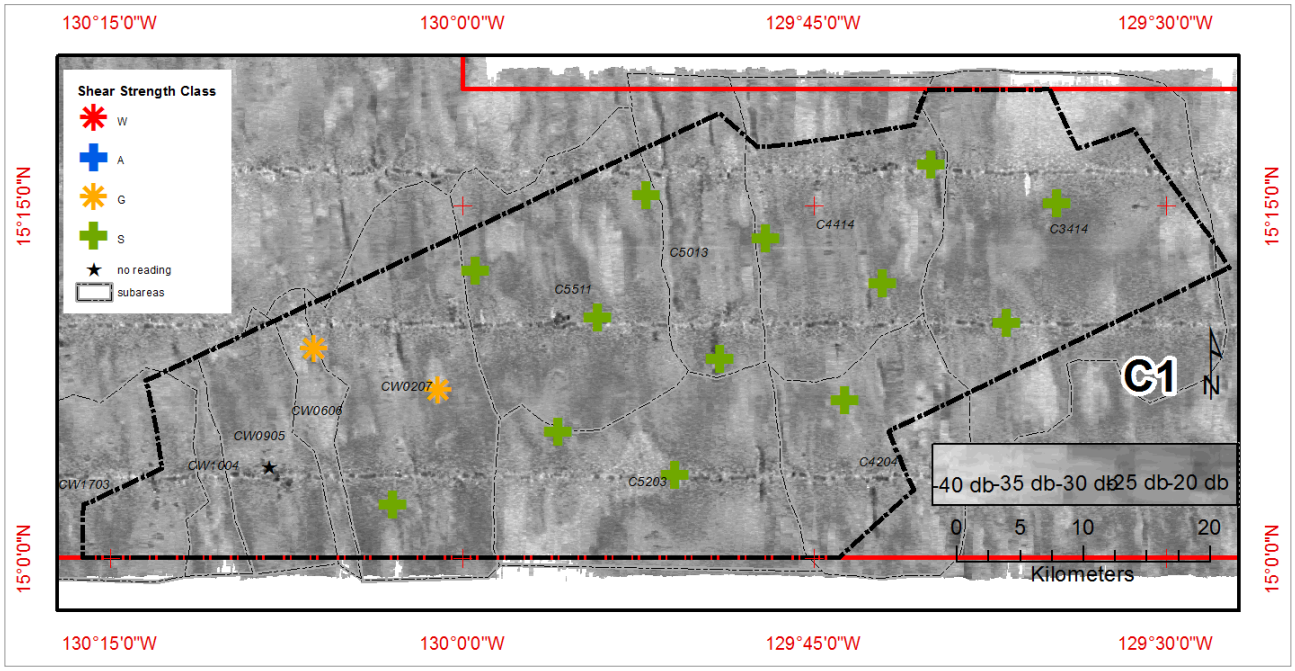
The available data indicates that it is reasonable to assume in this IA that mining systems designed for NORI Area D would be appropriate, from a geotechnical perspective, for the TOML areas. More detailed investigation is required in future to confirm these observations.

Figure 7.25 Shear Strength Class and BC locations, Area B1



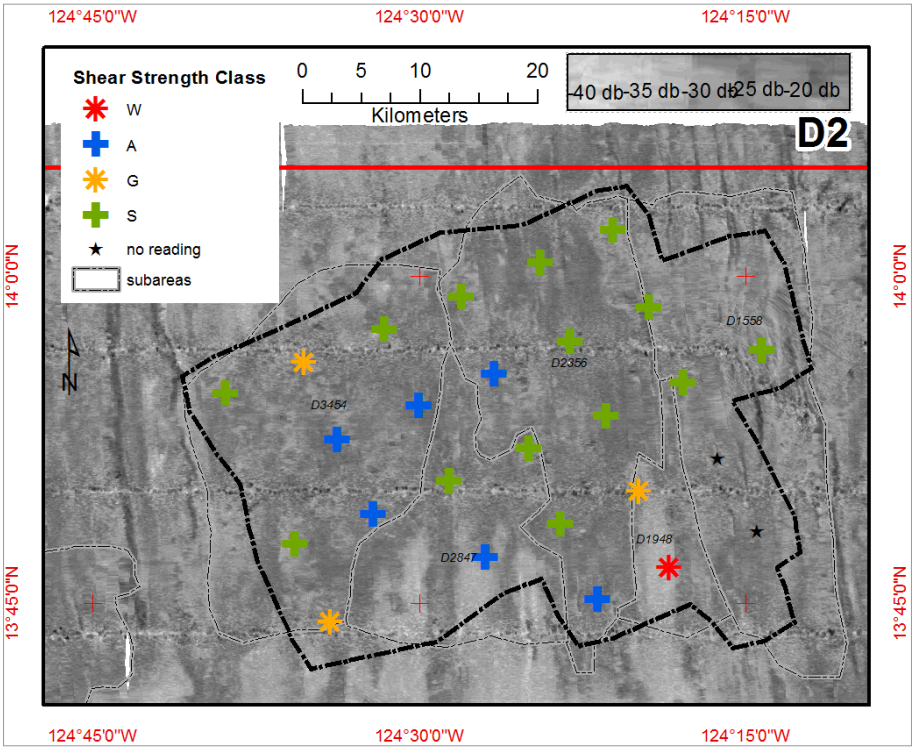
Source: TMC

Figure 7.26 Shear Strength Class and BC locations, Area C1



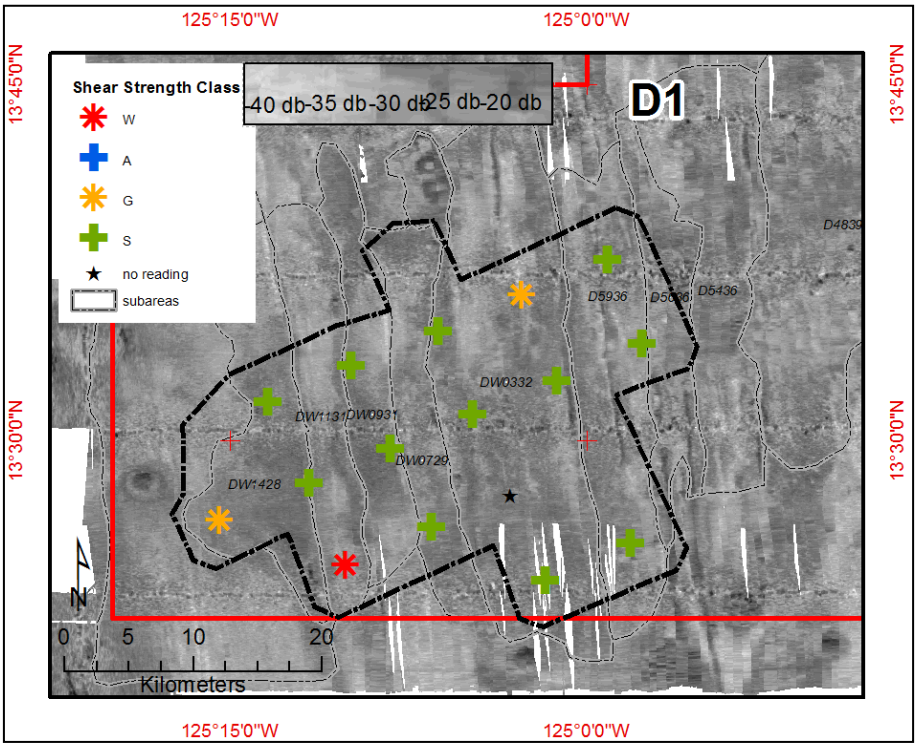
Source: TMC

Figure 7.27 Vane Shear Strength Class and BC locations, Area D2



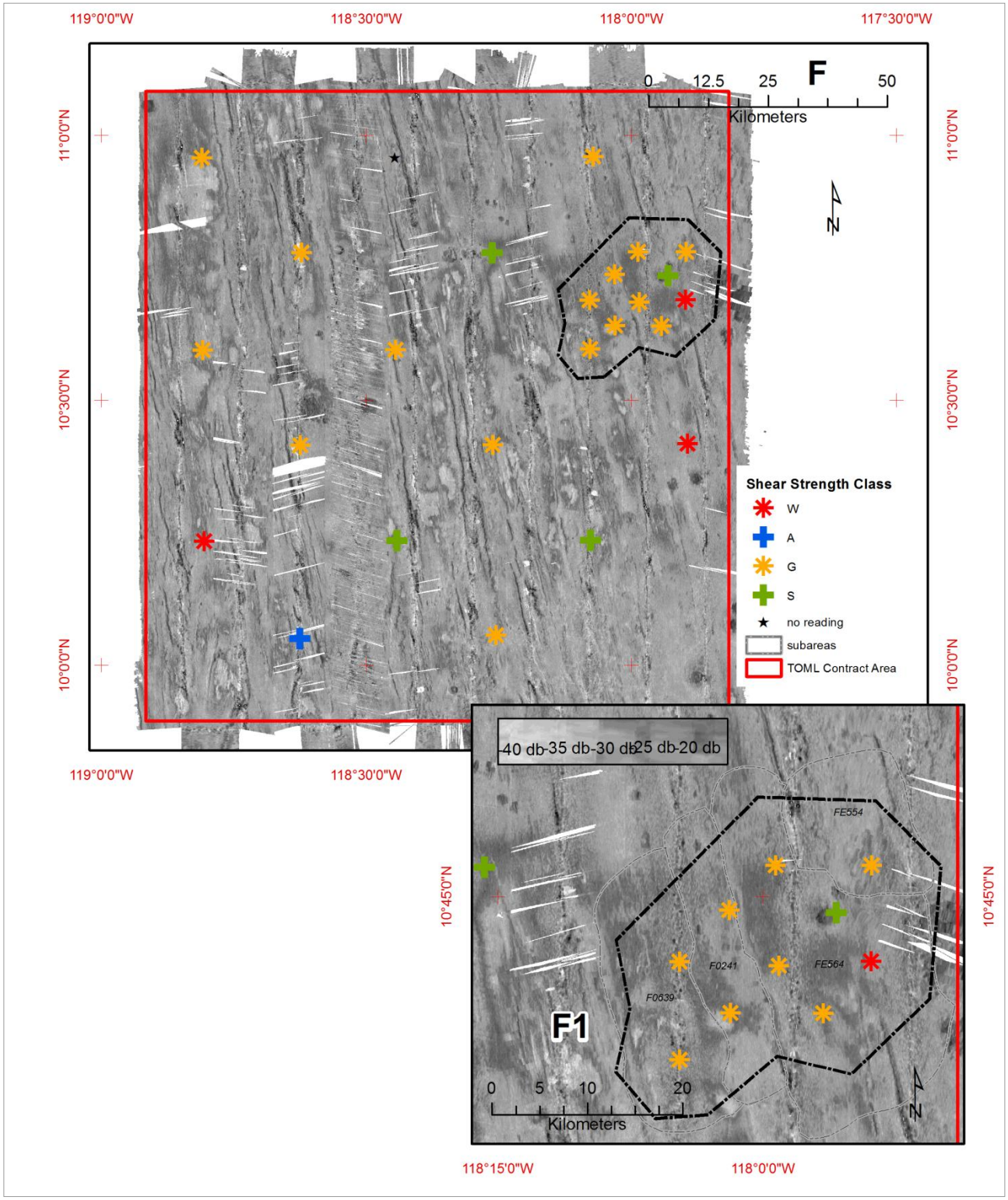
Source: TMC

Figure 7.28 Vane Shear Strength Class and BC locations, Area D1



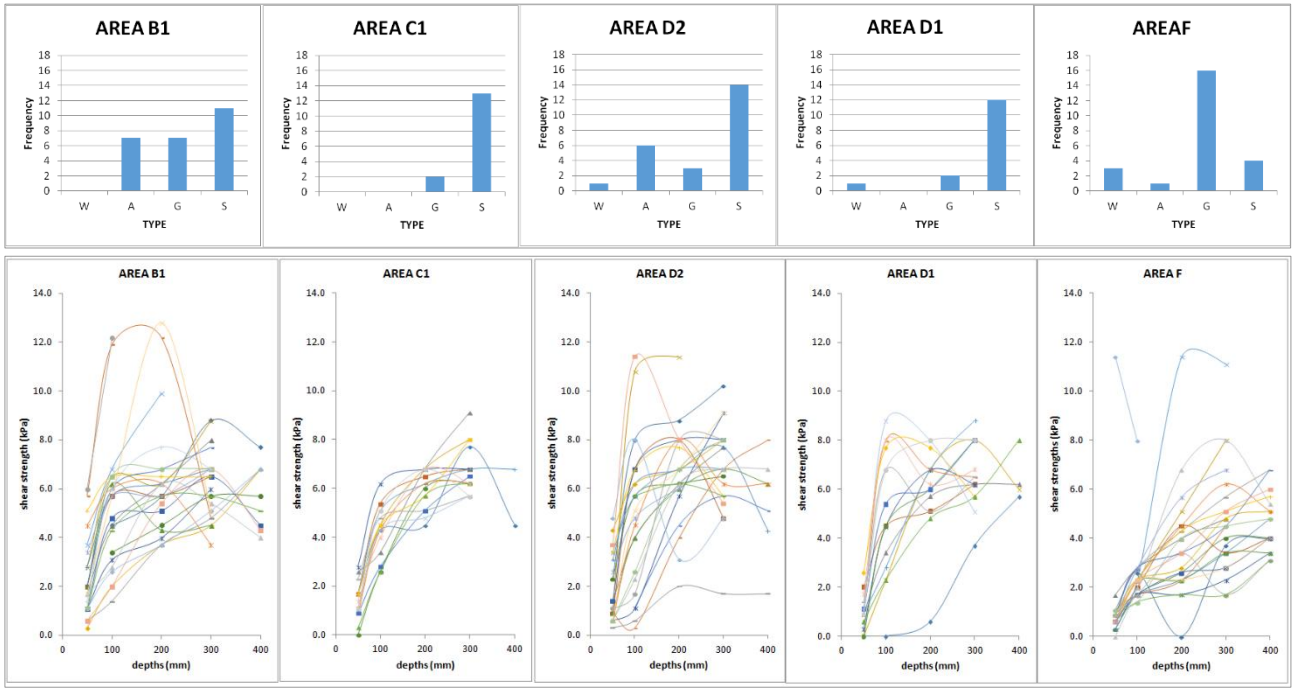
Source: TMC

Figure 7.29 Vane Shear Strength Class and BC locations, Areas F and F1



Source: TMC

Figure 7.30 Summary vane shear results from TOML areas



Source: TMC

8 Sample preparation, analysis, and security

8.1 Pioneer Contractor data

Consultants Golder Associates (Golder, 2015) sent requests to the Pioneer Contractors and received partial responses from Yuzhmorgeologiya (TOML-B) and DORD (TOML-A and D) which are included below. Golder Associates also compiled information from Dr Charles Morgan who had been previously directly involved with one of the US exploration programs (OMCO) that was carried out during the same period as these other programs. Morgan conferred with representatives of other Pioneer Contractors at several formal professional meetings and informal settings, comparing methods and procedures used for sample collection, analysis, and quality control. Many aspects of the OMCO procedures were used by the other explorers. The description of sample preparation and analysis methods provided below is based on these enquiries.

Free fall grab samplers were generally used. Each of the DORD sample stations was a combination of three sub-sampling points which effectively form an isosceles triangle with lengths of sides 1.4 nm, 1.4 nm and 2.0 nm.

The differences between the sampling procedures used by the Pioneer Contractors were minor. In summary, the procedures included:

- Removal of the nodules from the sampler and weighing in a laboratory. In many cases, it is unknown exactly when the nodule weights were taken by the Pioneer Contractors. However, OMCO air-dried the nodules prior to weighing, so it is possible that the wet abundance measurements may be slightly conservative.
- Photographing of nodules on a white background with a graticular scale.
- Splitting of some samples to create duplicates.
- Preparation of sub-samples for assaying by drying, crushing and pulverizing to a fine pulp (e.g., **100 mesh** particle **size (0.074 mm**).
- Final drying of the pulps before assay at 105°C to 110°C to constant weight.
- Multi-acid digest of the pulps and analysis by Atomic Absorption Spectrophotometry (AAS). OMCO's standard analysis included determination of Mn, Fe, Co, Ni, Cu, Zn, Si, Ca and Mg. Yuzhmorgeologiya determined Ni, Cu, Co and Fe by AAS and Mn by photometric (electrometric) titration.
- The inclusion of standard reference samples and/or CRMs formulated by the U.S. Geological Survey (NOD A-1 and NOD P-1; see Flanagan and Gottfried, 1980) for quality control. Unfortunately, no systematic QAQC information is available as this information was not provided by the Pioneer Contractors to the ISA.

Overall, the comparison of the sampling and assaying between the Pioneer Contractors (Section 9) shows that the data are adequate for geological modelling and are reliable for Mineral Resource estimation at an Inferred level of confidence. This is supported by the very similar grades obtained in the TOML and NORI sampling.

8.2 TOML data

8.2.1 Box core samples

Box core sampling and assaying by TOML are described in detail in the technical report summary titled "Technical Report Summary--TOML Mineral Resource, Clarion-Clipperton Zone, Pacific Ocean, for Deep Green Metals Inc." (the "TOML Technical Report"), with an effective date of March 26, 2021 (AMC Consultants, 2021b). The key points are as follows.

BC sampling was managed only by the TOML ship-based science team under the supervision of one Chief Scientist and two Lead Scientists.

After air-drying to remove surface water, the primary samples were weighed (air-dried weight; used for abundance estimation for the Mineral Resource estimate) and then some samples were split for field duplicates by cone and quarter.

Sample security was managed during the chain of custody by transport of samples in drums that were sealed with tamperproof tape.

The submitted primary and field duplicate samples were prepared and analyzed by ALS Global in Brisbane using XRF. This laboratory has extensive experience in the analysis of high manganese materials by the XRF method. ALS operates quality systems based on international standards ISO/IEC17025:1999 "General requirements for competence of calibration and testing laboratories" and ISO9001:2000 "Quality Management Systems - Requirements".

- Samples were dried at 90° – 105° C, before preparation for assaying.
- After drying, samples were jaw crushed in a Jacques jaw crusher to bring particle size to less than 10 mm. The crushed samples were then pulverized in an LM5 mill to a pulp with typical particle size >85% passing 75 um.
- Pulps were dried at 105°C for a minimum of 1 hour immediately before assaying.
- ALS method XRF26s, which is specifically designed for difficult to fuse chromite and manganese ores, was used. The dried pulp was fused in a platinum crucible and analyzed with X-ray fluorescence for:
  - LOI, Al_2O_3, BaO, CaO, Cr_2O_3, CoO, Fe_2O_3, K_2O, CuO, MgO, MnO, Na_2O, P_2O_5, SO_3, SiO_2, NiO, TiO_2, PbO, ZnO.
- The dried pulp was also dissolved by four-acid digest and analyzed by inductively-coupled atomic emission spectrophotometry (ICP-AES method ME-ICP61a) for:
  - Ag, Al, As, Ba, Be, Bi, Ca, Cd, Co, Cr, Cu, Fe, Ga, K, La, Mg, Mn, Mo, Na, Ni, P, Pb, S, Sb, Sc, Sr, Th, Ti, Tl, U, V, W, Zn. Many of these elements were at levels below the detection limit of ME-ICP61a.

Jacobs is the Laboratory operated by the Integrated Environmental Studies Program Group, Earth and Space Sciences Program, at Jacobs University in Bremen, Germany. This group had been involved in nodule analysis and study for over 10 years. Duplicate samples and pulps were analyzed at Jacobs as part of the TOML quality control program.

Jacobs supplied data by single acid (0.5M HNO_3) digest, inductively-coupled optical emission spectrophotometry (ICP-OES) for:

Al, Ca, Co, Cu, Fe, K, Mg, Mn, Na, Ni, Sr, V, Zn

They also supplied data by 0.5M HNO_3, inductively-coupled mass spectrophotometry (ICP-MS) for selected samples:

Li, Be, Sc, Ti, Rb, Y, Zr, Nb, Mo, Te, Cs, Ba, La, Ce, Pr, Nd, Sm, Eu, Gd, Tb, Dy, Ho, Er, Tm, Yb, Lu, Hf, Ta, W, Pb, Th, U

For the 104 BC samples submitted to ALS, 34 were duplicated (32.6%) with:

- 25 submitted duplicates to ALS (24.0%); and
- 15 field duplicates to Jacobs (14.4%).

Six submitted primary samples were duplicated both as ALS and Jacobs field duplicates (5.7%). Comparisons of duplicate results for Ni, Cu, Co and Mn indicated that the assay results showed close agreement, generally without bias. The most notable discrepancy was for copper, where there appears to be a bias of the order of 0.05% Cu to 0.1% Cu with Jacobs reading higher than ALS.

Blank samples (i.e., material known to have very low grades of the elements of economic interest) were included in the samples sent to ALS. All blanks assayed below detection limit for Ni, Mn, Cu, Co, indicating that no contamination had occurred from nodule samples to blank samples during the sample preparation.

TOML also submitted samples of the NOD P-1 CRM formulated by the U.S. Geological Survey amongst the submitted primary samples and duplicates. The ALS assays for the CRMs were satisfactory.

TOML had clear and secure chain of custody for the nodule samples collected during their exploration campaigns. Sufficient duplicates have been submitted to demonstrate the lack of significant error in the chemical analyses. Data storage was secure and there is no evidence of any tampering of grade and abundance measurements. Overall, the data are considered to be reliable for Mineral Resource estimation. This is supported by the very similar grades and abundances obtained in the historical sampling.

8.2.2 Abundance estimates by LAE method

High resolution photographs of the seafloor were taken during the CCZ15 campaign. The photos were transmitted from the towed camera sled in real time to a camera operator and were automatically named with the date and time (in UTC) of the survey. File posting location was on a secure server (airwalled) with access by camera operator, surveyor and geoscientists.

Location of the camera sled at the time of photography was recorded separately by the Yuzhmorgeologiya hydrographic surveyor on watch using a combination of vessel GPS and either Ultra-short baseline (USBL) signal or estimate of position from length of line out. Survey periods are recorded in the bridge log, vessel log and daily progress reports. Photos were logged in near real time for geology and biology, with periodic updates of photo files to the filing on the TOML master computer.

Abundance estimates were made only for select photos due to the intense nature of the work and issues with sediment cover in some areas. Normally in TOML-B1 and C1 every 100th photo was selected. The selected photos were georeferenced to a template in a GIS program by a geoscientist and the long axis of each nodule within selected swaths was digitized. Each photo was checked by the Lead Geoscientist on watch and by the Lead Geoscientist designated accountable for data quality. The Chief Scientist ran a routine to measure the digitized lengths and also compiled the data into a MS Access database. Copies of the processed data were passed, via email, to the Mineral Resource Qualified Person midway through the photo-profiling program and after the campaign.

8.3 NORI-A, B, C data

The Mineral Resource estimates for NORI-A, B and C are based on data collected by the Pioneer Contractors AMR, Yuzmorgeologiya, and IOM.

Virtually all the samples in the TOML areas and NORI A, B and C were obtained by free fall grab (FFG) samplers, although a few results from box corers (BC) were also included.

Upon making an application for an exploration contract under ISA regulations, the Pioneer Contractors were required to submit sufficient data and information to enable designation of a reserved area based

on the estimated commercial value. This sample data provided the basis of the database held by the ISA. The acceptance of the data by the ISA suggests the ISA was satisfied with the quality of the data.

The quality of the Pioneer Contractor data was assessed using comparative measures between the different datasets (Golder, 2015). The correlation of data from different sources, including Pioneer Contractors and government scientific institutes, provides a satisfactory level of quality assurance to support Mineral Resource estimates at an Inferred level of confidence.

9 Data verification

The original assay sheets for the individual samples collected by the Pioneer Contractors from within the TOML and NORI Areas are not available for auditing against the values in the database. Neither AMC, NORI nor TOML have had access to the original assay sheets for the individual samples that are within the Contract Areas, nor the quality control procedures used by the laboratories and the ISA. However, the consistency between the abundance and grade data collected by the Pioneer Contractors, as presented in Section 9.1, supports the contention that the quality of the Pioneer Contractor data is satisfactory.

It is also reasonable to infer that the Pioneer Contractor data are of sufficient quality for Mineral Resource estimation because the ISA is an independent agency with significant accountability under the Law of the Sea. Part of its mandate is the receipt and storage of seafloor sampling data suitable for the estimation of nodule resources and the legally binding award of licenses. It is reasonable to assume that a reasonable level of care was applied by the ISA.

Data collected by NORI and TOML is well-documented and was subject to satisfactory QA/QC processes. Documentation verified by the Qualified Person includes photographs, daily exploration reports, digital logging sheets and original assay reports.

Assaying of nodules collected by NORI in 2012, 2013, 2018, and 2019 confirmed the mean grades of the historical grab samples and support the contention that the quality of the Pioneer Contractor data is satisfactory for inclusion in Mineral Resource estimation. The main limitation with the Pioneer Contractor data is the likelihood that some of the abundance values were too low, due to loss of nodules from the FFG. Estimates of abundance that include Pioneer Contractor data are therefore likely to be conservative.

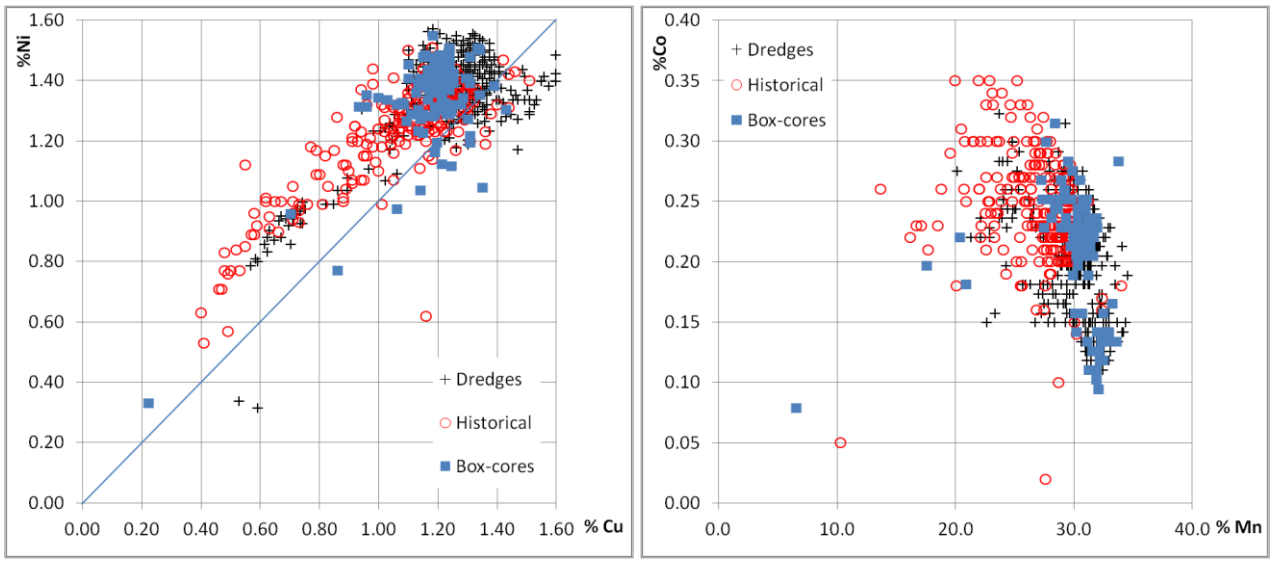
In the opinion of the Qualified Person the sample preparation, security, and analytical procedures were adequate for estimation of Mineral Resources.

9.1 TOML data

The CCZ13 and CCZ15 BC sample results for TOML were compared with the samples from the Pioneer Contractors within the TOML areas (Figure 9.1). The TOML and Pioneer Contractor samples are not from the same individual locations, therefore a perfect correlation is not expected. Nevertheless, there is good correspondence. High Cu and Mn grades are less common in the historical samples but the ranges are the same. This comparison provides additional support for the reliability of the Pioneer Contractor data for use in the estimation of Inferred Mineral Resources.

The The Qualified Person, as defined by Canadian National Instrument 43-101 (QP) considers that the combination of the TOML and historical nodule sample data (physical samples and photo based long axis estimates) combined with detailed backscatter, photo profiling and geological interpretation is sufficient to estimate polymetallic nodule Indicated Mineral Resources in parts of TOML-B, C, D and F and Measured Mineral Resources in one small especially data rich area of TOML-B.

Figure 9.1 Comparison between TOML BC and dredge samples and historical samples



Source: TMC

9.2 NORI-A, B, C data

The Mineral Resource estimates for NORI-A, B and C are based on data collected by the Pioneer Contractors AMR, Yuzhmorgeologiya, and IOM.

Box core sampling completed by NORI in NORI Area D and TOML has supported the abundances reported by the Pioneer Contractors as well as grades of Ni, Co, Cu, and Mn. It is reasonable to assume that a similar correlation is likely in the NORI-A, B and C Contract Areas and that the abundances reported by the Pioneer Contractors can be relied upon for estimation of Inferred Mineral Resources. It is likely that any errors in the Pioneer Contractor data are on the conservative side, due to the use of FFG samplers.

10 Mineral processing and metallurgical testing

10.1 Metallurgical testwork

Work commenced with review of the extensive literature regarding nodule mineralogy and historical metallurgical processing outlining:

- Nodules are fine-grained intergrowths of a complex suite of ferromanganese oxide and hydroxide minerals with nickel-copper-cobalt ingrained into the structure of the ferromanganese minerals.
- As a result, mineral dressing methods are not possible to upgrade to mineral concentrates, and flow sheet development focused on whole nodule treatment, initially by pyrometallurgical methods followed by hydrometallurgical refining.

TMC has completed an extensive metallurgical flowsheet selection, development and proof of concept program over the last fourteen years. The selected flowsheet involves a front-end pyrometallurgical process, where the nodules are first put through a rotary kiln and then further processed in an electric arc furnace. The furnace generates two materials – a manganese silicate slag representing TMC USA's final manganese product, and a nickel-copper-cobalt alloy that is rich in iron. The alloy is further processed pyrometallurgically in Peirce-Smith Converters, where sulfur is added and iron removed to generate a higher-valued matte product. The matte product can then be fed into a downstream hydrometallurgical refinery which separates the nickel, copper and cobalt into their individual components to generate final products.

Testwork has been conducted on the entire flowsheet to date, with larger-scale demonstrations completed for the RKEF aspects of the flowsheet, consistent with TMC's strategy to begin operations through using existing RKEF facilities. Product development testing has also been conducted along with the flowsheet development and testing program.

Preliminary bench-scale testing was completed by Kingston Process Metallurgy (KPM), a specialized research and development metallurgical facility based in Kingston, Ontario, Canada. TMC selected the FLSmidth Inc. (FLS) facility in Whitehall, Pennsylvania, USA for pilot-scale rotary kiln calcining trials. Prior to the trials, some bench scale testing was completed at FLS in parallel with KPM testwork. The rotary kiln calcining piloting was executed successfully in November of 2020, generating approximately 35 t of calcined material from 75 t of nodules collected from NORI Area D.

The EF smelting, sulfidation and converting pilot scale trials were conducted by the XPS (A Glencore subsidiary) testing facility in Sudbury, Ontario, Canada. Bench-scale testing was conducted at XPS prior to the piloting on both synthetic and pilot generated materials. The smelting trials were also successful, generating approximately 1,700 kg of alloy and 25 t of manganese silicate. The furnace was then used for the sulfidation and converting piloting, as pilot-scale Peirce-Smith converters do not exist. Approximately 332 kg of final nickel-copper-cobalt matte was generated.

Two programs were conducted for product development. The first, a full bench-scale testing program which generated nickel and cobalt sulfates suitable for use in batteries from the matte generated at XPS was commissioned at SGS Lakefield, Ontario (SGS) Canada in Lakefield, Ontario using a combined atmospheric and pressure sulfuric acid leach flowsheet. The second program, on the manganese silicate product, was conducted at Norwegian laboratory SINTEF Industri, who specialize in the processing of manganese ores. The SINTEF program was also successful in generating silico-manganese alloy using TMC's manganese silicate as the sole manganese source, first at bench scale and later at the kilogram scale. Silico-manganese alloy is a key additive in steel manufacturing, and the success of this program represents the demonstrated value in use to potential customers in using silico-manganese alloy derived from TMC's manganese silicate product compared with their existing

feedstocks. The success of this program also confirms that the company's near zero solid waste processing objective was met, as a usable material has been generated from a TMC final product.

10.2 Bulk sample collection testwork

Key findings of the exploration work documented in Section 7 of this report are that:

- The chemical composition and mineralogy of nodules in the Property is remarkably consistent.
- Nodules can be classified into three different categories (types 1 to 3), based primarily on size and morphology. The majority of the Mineral Resource is comprised of type 1 nodules.

Utilising this work, an area to the north and west of the identified Test Mining Trial area was selected to collect a nodule bulk sample to undertake metallurgical pilot testing. This bulk sample was collected from 6 separate areas using a bespoke designed 6 m-wide ploughing system (Figure 10.1), which was deployed to the seafloor using the main anchor winches of the *MV Maersk Launcher*, an anchor handler tug supply vessel that was used to deploy the system.

The system was designed to recover nodules from the top 5 cm of the seafloor and reject the surface sediment through a metal mesh which retained the nodules. The system successfully collected 77.3 t of nodules from 62 runs along a total run length of 5.8 km. A scallop-dredge mesh was used with mesh size varied from 10 mm to 19 mm. The fines rejection was not fully successful, with the nodules needing to be washed ahead of being processed. This is not expected to be an issue for the commercial-scale collection system as demonstrated by the Test Mining completed in 2022 outlined in section 13, where little seafloor sediment was lifted to the surface.

A total of 62 samples were taken of the bulk sample and assayed to confirm sample grade and moisture. Grab samples were taken primarily from the middle (number 4 of 6) chain bags during unloading. Samples were shipped to ALS in Brisbane and analysed using the same analysis method for samples used for resource evaluation; moisture by OA-GRA05 and analysis by X-ray fluorescence using ALS code ME-XRF26s. Table 10.1 shows a comparison of the nodule analysis for the bulk sample compared to the measured resource for the test mining area. The nodule grades compare well with slightly elevated moisture for the bulk sample which can be attributed to high moisture in the entrained sediment.

Table 10.1 Comparison of bulk sample analyses with NORI Area D measured resource for the test mining area.

Category	Moisture	Ni	Cu	Co	Mn
	%	%	%	%	%
Bulk Sample					
Mean	29.7	1.40	1.18	0.12	32.9
Max	30.9	1.45	1.29	0.14	34.5
Min	28.2	1.35	1.12	0.09	31.4
Standard Deviation	0.60	0.0002	0.0005	0.0001	0.0053
Measured Resource (Test Mining Area)	28	1.41	1.15	0.13	31.9
Difference in mean	1.7	-0.01	0.03	-0.01	1.05

Runs were planned to collect type 1, 2 and 3 nodules, nominally in the proportions of the NORI Area D Mineral Resource.

Samples were bagged into one tonne bulka bags and were brought by the *MV Maersk Launcher* to San Diego and then trucked directly to FLS's facility in Pennsylvania where calcining was undertaken. A 5 t reference sample has been retained in storage in San Diego.

Figure 10.1 Bulk sampling dredge used to collect the bulk sample for metallurgical pilot tests



Source: TMC

It is the QP's opinion that the bulk nodule sample collected for pilot testing is representative of the NORI Area D field, particularly for the Initial Mining Area from which some of the sample was extracted.

10.3 Bulk sampling testing laboratories

Feed samples, products and intermediate control samples were analyzed by the various testing laboratories using the methods outlined in Table 10.2.

Table 10.2 Location and testing methods of laboratories used

Name	Location	Testing/Assaying Methods
KPM	Kingston, Ontario, Canada	ICP-OES, ICP-MS, various microscopy methods
FL Smidth	Whitehall, PA, USA	XRF, XRD
eXpert Process Solutions (XPS)	Sudbury, Ontario, Canada	XRF, ICP-OES
SGS Canada Inc.	Lakefield, Ontario, Canada	ICP-OES, ICP-MS
SINTEF Industri	Trondheim, Norway	ICP

10.4 Summary of test work results

10.4.1 Round robin assaying program

TMC conducted a round robin assaying program with Japanese operator PAMCO, using 22 t of nodules collected during NORI's Test Mining in Q4 of 2022. The nodule sample was delivered to PAMCO in March

of 2023. The program involved 10 standard samples that were created by PAMCO and sent for assay by several participating labs (including PAMCO internally).

The following procedure was undertaken at PAMCO to generate each of the 10 standard samples for assay:

1 Take 60 kg of nodules from flexible container bag.
2 Dry using a dryer at 105℃ until weight is constant. Dry weight of the nodules was 45 kg.
3 Pulverize the entire mass to -150 µm using a disc mill.
4 Divide the mass into 3 bags containing 15 kg per bag (Bags A, B and C).
5 Using a rifle divider, separate each of the 3 bags into 2 separate subsamples, each containing 7.5 kg (A1, A2, B1, B2, C1, C2).
6 Create 2 composites using one subsample from each bag (A1+B1+C1, A2+B2+C2).
7 Mix the new composites in a plastic bag.
8 Divide the composites into 2 samples (Composite 1a, 1b, 2a, 2b).
9 Mix to make 2 new composites (1a+2a, 1b+2b).
10 Repeat Steps 8 and 9 three times. This still results in 2 composites (X and Y).
11 Divide the 2 composites into 10 samples per composite (X1-X10, Y1-Y10).
12 Mix subsamples based on their corresponding numbers (X1+Y1 = standard sample 1).
13 Place each of the samples into individual bottles.

The following laboratories were contracted to conduct analysis as part of this program:

- PAMCO, Hachinohe, Aomori, Japan.
- ALS, Brisbane, QLD, Australia.
- SGS Canada, Lakefield, ON, Canada.
- Kingston Process Metallurgy, Kingston, ON, Canada.

The program required each laboratory to conduct analysis on nickel, copper, cobalt and manganese only. Table 10.3 summarizes the analytical methods undertaken by each of the laboratories to complete this task.

Table 10.3 Analytical methods undertaken by each laboratory

Element	PAMCO Method	KPM Method	ALS Method	SGS Method
Nickel (Ni)	JIS M 8126: Dimethylglyoxime Precipitation Separation EDTA Titration Method	ICP-OES	XRF – Chromite / Manganese Ore – Disc / XRF	XRF
Copper (Cu)	JIS M 8242: Inductively Coupled Plasma Emission Spectrometry (ICP-OES)			
Cobalt (Co)	JIS M 8129: Inductively Coupled Plasma Emission Spectrometry (ICP-OES)			
Manganese (Mn)	JIS M 8232: Potassium Permanganate Titration			

Table 10.4 to Table 10.7 shows the outcomes from each of the laboratories for each of the elements specified. All values are in weight %. Average, standard deviation (SD) and CV are shown.

Table 10.4 Nickel laboratory results

Bottle No	PAMCO	ALS	KPM	SGS
1	1.4317	1.460	1.410	1.390
2	1.4362	1.462	1.470	1.410
3	1.4381	1.438	1.370	1.390
4	1.4330	1.457	1.410	1.390
5	1.4334	1.445	1.460	1.400
6	1.4304	1.424	1.400	1.390
7	1.4351	1.456	1.440	1.390
8	1.4347	1.435	1.400	1.380
9	1.4343	1.427	1.350	1.380
10	1.4364	1.434	1.440	1.380
Average	1.4343	1.4438	1.4150	1.3900
SD	0.0023	0.0141	0.0381	0.0094
CoV(%)	0.16	0.98	2.69	0.68

Table 10.5 Copper laboratory results

Bottle No	PAMCO	ALS	KPM	SGS
1	1.1382	1.162	1.170	1.130
2	1.1528	1.162	1.220	1.140
3	1.1462	1.157	1.150	1.150
4	1.1433	1.160	1.170	1.130
5	1.1334	1.132	1.190	1.150
6	1.1396	1.146	1.160	1.140
7	1.1272	1.150	1.160	1.130
8	1.1231	1.144	1.150	1.160
9	1.1342	1.146	1.130	1.160
10	1.1339	1.158	1.180	1.140
Average	1.1372	1.1517	1.1680	1.1430
SD	0.0088	0.0098	0.0249	0.0116
CoV(%)	0.78	0.85	2.13	1.01

Table 10.6 Cobalt laboratory results

Bottle No	PAMCO	ALS	KPM	SGS
1	0.1430	0.1440	0.1400	0.1400
2	0.1462	0.1450	0.1400	0.1400
3	0.1436	0.1410	0.1400	0.1300
4	0.1438	0.1430	0.1400	0.1400
5	0.1415	0.1400	0.1400	0.1400
6	0.1414	0.1400	0.1300	0.1400
7	0.1431	0.1430	0.1400	0.1400
8	0.1444	0.1400	0.1400	0.1400
9	0.1445	0.1400	0.1300	0.1400
10	0.1423	0.1410	0.1400	0.1400
Average	0.1434	0.1417	0.1380	0.1390
SD	0.0015	0.0019	0.0042	0.0032
CoV(%)	1.02	1.33	3.06	2.28

Table 10.7 Manganese laboratory results

Bottle No	PAMCO	ALS	KPM	SGS
1	31.600	32.063	31.5000	31.700
2	31.770	31.978	31.3000	31.800
3	31.620	31.823	32.6000	31.700
4	31.665	32.039	31.5000	31.700
5	31.680	31.714	31.5000	31.700
6	31.785	31.404	31.9000	31.600
7	31.745	31.962	32.6000	31.600
8	31.665	31.474	32.7000	31.700
9	31.815	31.428	32.0000	31.700
10	31.785	31.575	31.5000	31.600
Average	31.713	31.746	31.910	31.6800
SD	0.076	0.261	0.540	0.0632
CoV(%)	0.24	0.82	1.69	0.20

QA/QC was completed with a sample of CRM manufactured by the USGS, known as NOD-P-1, at all laboratories except for ALS, who used alternative CRMs. Previous analysis of the USGS-NOD-P-1 was completed at ALS for a separate analytical program, and these results are included in Table 10.8 showing CRM results for each of the laboratories. All values are in weight%.

Table 10.8 CRM results for each laboratory

Lab	Nickel (Ni%)	Copper (Cu%)	Cobalt (Co%)	Manganese (Mn%)
PAMCO	1.372	1.171	0.233	29.92
ALS	1.34	1.15	0.22	29.12
KPM	1.28	1.14	0.21	28.3
SGS	1.31	1.15	0.22	29.4

The results showed good alignment between the laboratories using varying analytical methodologies providing confidence in the results. It is the QP's opinion that analytical methods used for the metallurgical samples were suitable and provided reliable results.

10.4.2 Key findings of calcination at FLS

The nodules were successfully calcined by FLS in a 15 m long, 0.9 m diameter kiln under conditions consistent with the intended commercial operation. Table 10.9 summarizes the updates to the project process design criteria (PDC) arising from the calcining test work at FLS.

Table 10.9 Updates to Process Design Criteria from pilot kiln test work

Parameter	Units	Original PDC	FLS Pilot Kiln/Update	Comment
Nodule Angle of Repose	Deg.	N/A	42.5	Email from R. Penso, 24-Feb-21 10:24 AM
Degree of Nickel Reduction	%	20	20	FLS did not detect any Ni reduction, but given the degree of Fe reduction, it is expected. Therefore, keep PDC value
Degree of Cobalt Reduction	%	30	30	Not measured, keep PDC value
Degree of Copper Reduction	%	50	50	Not measured, leave at PDC value
Degree of Iron Reduction to Wüstite	%	85	100	None to metallic
Degree of Iron Reduction to Magnetite	%	15	N/A	
Degree of MnO2 to MnO by Thermal Decomposition	%		80	Based on MnO2 from 48.74% to avg 9.7% during oxidizing run
Degree of MnO2 to MnO by Reduction	%		20	By difference. No detectable MnO2 after reduction runs
LOI in Calcine	%	0.5	0.4	Average during oxidizing at 950°C
Dusting Rate of Nodules	%	5	5	Pilot was 2.1% dry basis, but this may be optimistic given the scale vs. commercial. FLS tumble test gave similar results to laterites, but fines screened out in both cases. FLS conclusion: “Given the lack of fines present in the nodule sample the overall dusting potential is lower than typical nickel laterite kiln operations”. So leave at 5%
Dust Nickel Enrichment Factor (Dust/Feed)	wt/wt	1.3x	1.0x	If anything, Ni in dust is depleted
Dust Iron Enrichment (Dust/Feed)	wt/wt	1.3x	1.0x	Fe in feed, sediment and baghouse dust all about the same Also, Co, Cu about the same as in feed
Dust Potassium Enrichment (Dust/Feed)	wt/wt		5x	Na also said to be higher*
LOI in Dust	dry wt%	5	16	Same as feed**
Moisture in Dust	**wt%**	**5**	**3**	**2.91% measured**

Notes: *Na in feed = 1.77%, Na in dust = 2.6, i.e., possibly within assaying error.
**Unexpected since TGA tests show low temperature weight loss.

10.4.3 Piloting – Electric Furnace Smelting at XPS – Metallurgical Summary

Table 10.10, Table 10.11, Table 10.12 and Table 10.13 compare the principal elements for the main stages of pyrometallurgical processing (calcination, smelting, sulfidation, and converting) between the piloting campaigns and the latest version of a process model developed for the project. The process model was originally derived from a nickel laterite model, which was modified as understanding of the differences for the nodule system has developed over the course of the project. The results obtained in the piloting campaigns allowed for further refinement of process modelling for nodule processing.

Table 10.10 Pilot calcine blend assay vs. process model update mass balance

Smelting	%Ni	%Co	%Cu	%Mn	%Fe	%S
Mass Balance Calcine	1.58	0.16	1.29	35.2	7.55	0.12
Pilot Calcine Blend	**1.66**	**0.15**	**1.32**	**37.2**	**7.76**	**0.27**

Table 10.11 compares smelting campaign metal tap major element assays to the values in the project process model. There is significant assay variation. On average, nickel and cobalt grades are high compared to the mass balance values—nickel, was high in calcine. Manganese was lower in the alloy than expected given the relatively high iron, which may provide some insight into the relationship between degree of reduction and the relative concentration of these elements reporting to the alloy. Sulfur is a deleterious element for ferronickel producers and has received considerable attention in process modelling. Clearly, the nodule process, with its different slag chemistry, does not appear to have this issue. By inspection of the %S columns in Table 10.11 and Table 10.12, it can be seen that sulfur deports much more to slag and much less to metal than is normally assumed for nickel laterite slags.

Table 10.11 Pilot metal assays vs. process model mass balance

Smelting	**%Ni**	**%Co**	**%Cu**	**%Mn**	**%Fe**	**%S**
Mass Balance Furnace Alloy	15.8	1.5	12.5	3.6	61.9	0.54
Pilot Average*	18.1	1.9	11.9	1.1	65.0	0.03
Campaign 1 (Tap 11)	15.6	1.5	10.3	1.4	67.5	0.03
Campaign 2 (Tap 8)	17.7	1.5	10.1	1.2	65.1	0.00
Campaign 2 (Tap 15)	18.6	2.4	12.3	0.8	63.3	0.05
Campaign 2 (left in furnace)	**20.4**	**2.1**	**14.8**	**1.0**	**64.1**	**0.03**

Note: *Simple average, not weighted

Table 10.12 compares the ranges for slag chemistry from the main slag taps for the two campaigns to the mass balance values. The mass balance values lie within the range achieved. Phosphorus can be controlled to the levels in the mass balance.

Table 10.12 Pilot smelting slag assays vs. process model mass balance

Smelting	**%Mn**	**%Fe**	**%Si**	**%P**	**%S**
Mass Balance Furnace Slag	40.7	1.8	10.9	0.06	0.05
Campaign 1	39.1 – 43.0	1.0 – 7.9	10.2 – 11.3	0.01 – 0.17	0.41 – 1.07
Campaign 2	**40.1 – 44.1**	**0.8 – 4.8**	**9.9 – 11.2**	**0.02 – 0.23**	**0.34 – 0.49**

In Table 10.13, the matte sample that was closest to the target intermediate matte (i.e. the nearly steady-state operating point of the sulfidation vessel in the commercial process) is compared to the mass balance composition. The target sulfidation operating point is 30% Fe and the closest sample to that was at 35.6% Fe. The table also compares the final matte obtained in the pilot campaign to the mass balance final matte. Pilot nickel levels seem significantly higher than projected whereas cobalt is lower. It should be borne in mind that the mass balance is based on the recycle of slag from the finishing vessel (FV) back to the sulfidation vessel to improve pay-metal recoveries, which was not possible for the pilot work. This explains the low value for cobalt, which has a much lower partition coefficient than nickel and copper at low levels of iron in matte. This highlights why it is important not to rely on the recoveries achieved in the once-thru test work, but instead to apply measured partition coefficients to the process model to estimate recoveries in the commercial plant. The recirculating loads will have little impact on these coefficients.

Table 10.13 Pilot matte assays vs. process model mass balance

Sulfidation, Converting	%Ni	%Co	%Cu	%Mn	%Fe	%S
Mass Balance Intermediate Matte	27.3	3.0	20.6	0.01	30.0	13.0
Pilot Closest (Matte 4)	28.5	2.4	18.4	0.04	35.6	13.6
Mass Balance Final Matte	40.9	3.4	30.5	0.01	5.0	20.0
Pilot Final Matte	**45.8**	**2.8**	**30.5**	**0.00**	**9.9**	**16.4**

Overall, it can be concluded that the pilot campaigns to process the calcine to matte for subsequent hydrometallurgical treatment largely achieved the expected metal and matte targets, albeit falling somewhat short on iron concentration target, while providing additional insights into the metallurgy of nodule processing.

10.4.4 Smelting: metallurgical results

Metallurgical control was generally good and covered a range of compositions and degrees of reduction. This is best illustrated by the amount of residual iron in slag, which ranged from just under 1% Fe to nearly 5% Fe, whereas the current mass balance is 1.8% Fe. While the proposed operating point is within the band of the test work, the range experienced provides an opportunity to understand metallurgical trends as a function of iron grade in the slag.

10.4.4.1 Partition coefficients (PC) in smelting

Overall recoveries of elements to alloy as reported in the mass balances for the pilot work are not useful for predicting commercial recoveries due to:

- Poor accountability in some cases.
- Pilot results encompass a range of conditions with respect to degree of reduction, and not just the target conditions for the commercial operation.
- Pilot trials did not include recycle streams which are used commercially to maximize pay metal recovery.

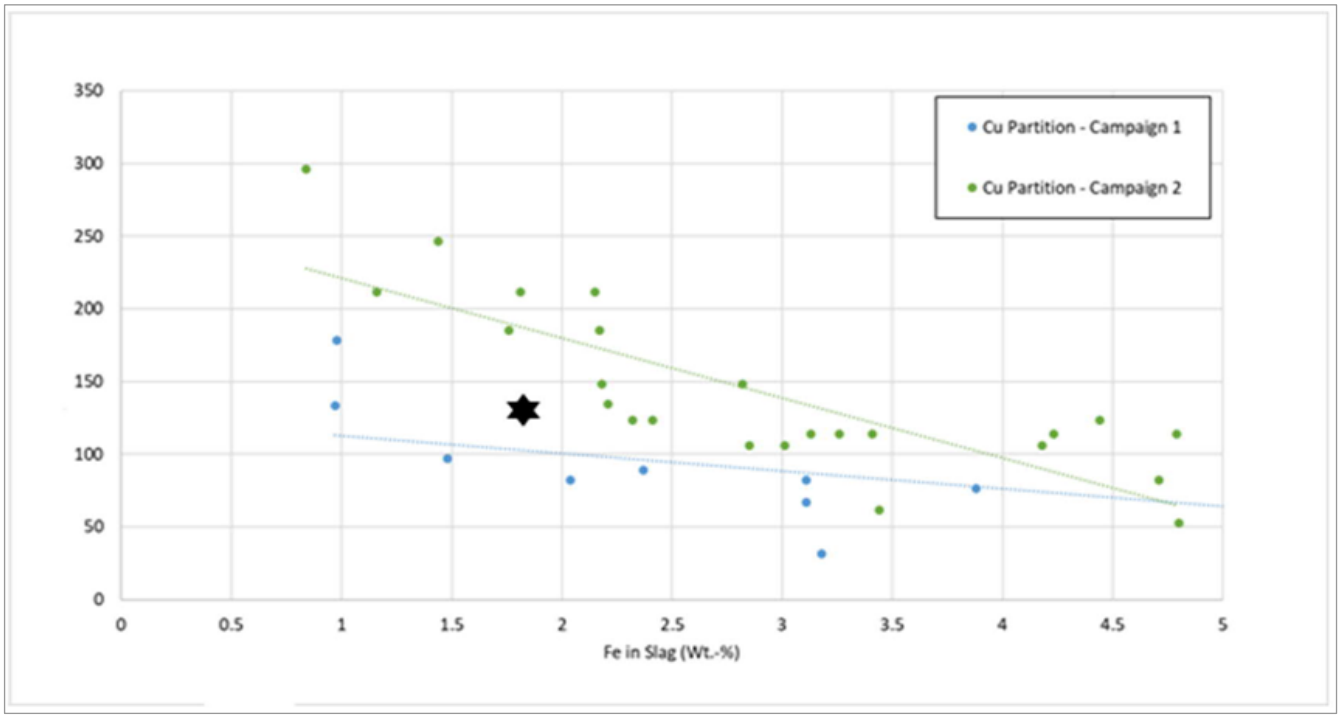
Instead, predictions of recovery can be made using partition coefficient information from the test work at the target degree of reduction. This is represented by the amount of iron reduced to the alloy or the iron content of the resultant slag, which is currently 1.8% Fe in the process model, but may be adjusted to 1.5% (see Section 10.4.4.2).

$$Partition\ Coefficient = \frac{wt\%\ X\ in\ Metal}{wt\%\ X\ in\ Slag}$$

Copper partition coefficients

Figure 10.2 shows the Cu partition coefficients (PCCu) reported for the two smelting campaigns as a function of iron grade in the slag. There are reasonably clear trends, particularly for Campaign 2, showing higher coefficients at lower iron, i.e., more reducing conditions. Also shown is the target point in the process model (PCCu = 130 at 1.8% Fe displayed as a ★). It lies near the middle of the pilot data at that given amount of iron in slag. There is a case to be made for the Campaign 2 data being better than for Campaign 1 due to better temperature control, which would yield PCCu = ~190 at 1.5% Fe, however it is recommended that it is left at the current more-conservative value.

Figure 10.2 Copper partition coefficients during smelting



Source: TMC

Nickel and cobalt partition coefficients

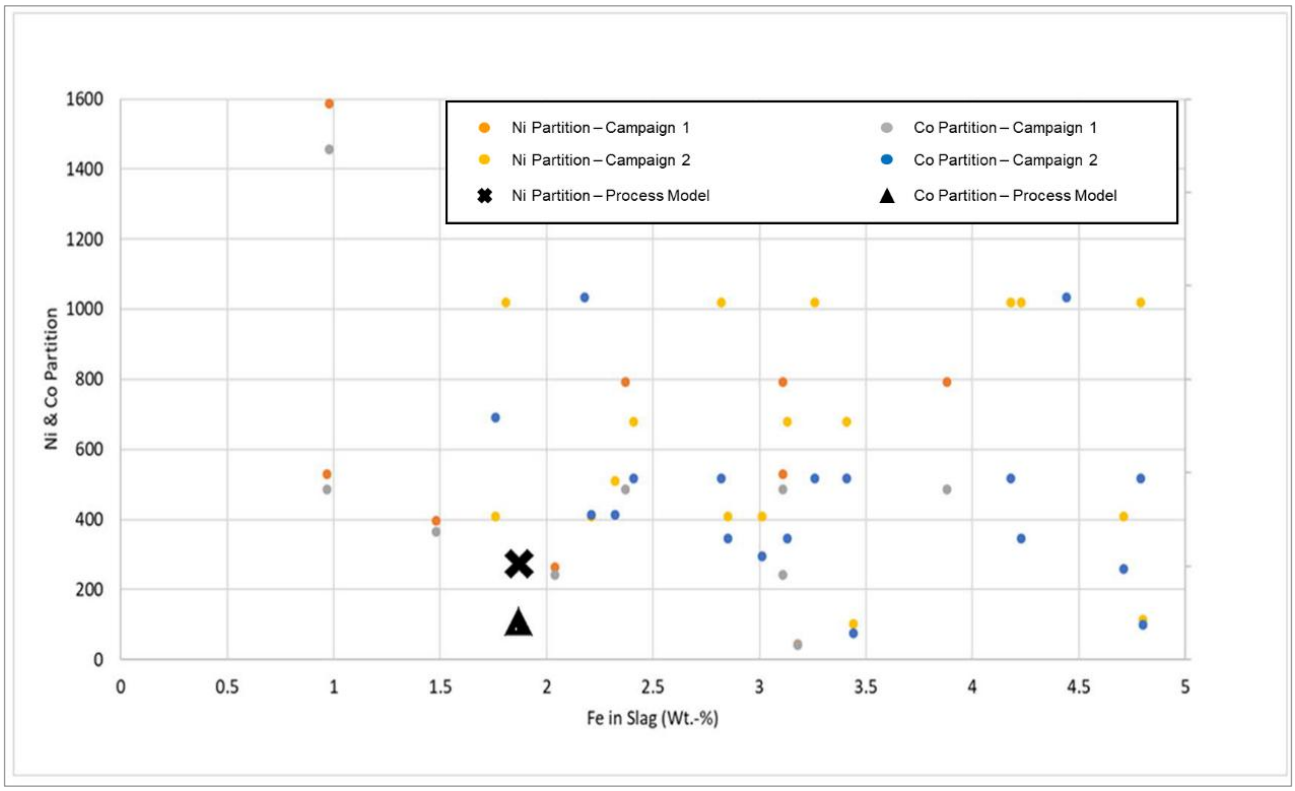
Figure 10.3 shows the partition coefficients for nickel and cobalt obtained during the smelting campaigns. There is a great deal of scatter and no clear trend with iron (degree of reduction). One major reason for the scatter is that the concentrations reported in slag are very low. As reported in the pilot mass balances (excluding outliers):

- Nickel ranges between 0.010 to 0.060, and
- Cobalt between 0.001 to 0.007.

Thus, the PCs are highly sensitive to slight variations due to assay uncertainties.

Current process model (1.8% Fe) values for nickel and cobalt partition coefficients during smelting are 285 and 120 respectively and these are shown as X (nickel partition coefficient = 285) and Δ (cobalt partition coefficient = 120) in Figure 10.3. They are clearly at the lower end of the range calculated for the pilot plant operation. However, given the wide scatter and assay uncertainty of the pilot data, it is not proposed to change the process model values. It can be said, however, that the pilot values certainly don't indicate that the commercial values will be any lower than the current model values.

Figure 10.3 Nickel and cobalt partition coefficients during smelting

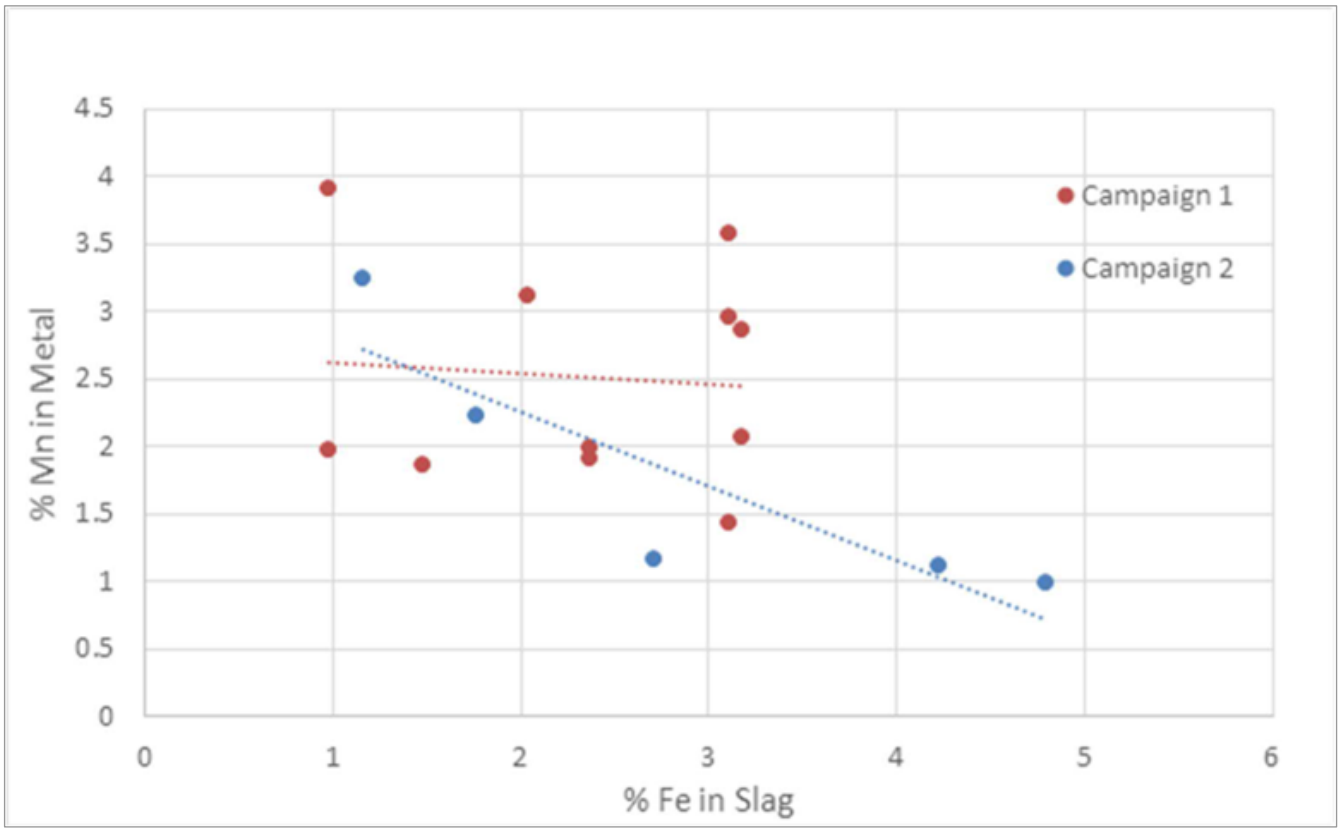


Source: TMC

Manganese deportment

Figure 10.4 shows manganese in metal versus iron in slag. There is considerable scatter but there are no high levels of manganese in metal. The values are generally lower than what was achieved during Smelt Test 8 at KPM during the bench-scale testing (considered to be a benchmark), which is favorable considering any of the over-reduced smelt tests at KPM yielded manganese in metal levels of up to 50%. While Campaign 2 appears to show a trend to lower manganese at higher iron in slag, which would be expected, the same cannot be said of Campaign 1. The data support that, for an operating range of 1-2% Fe in slag, a value for manganese in metal of 2.5% manganese can be adopted in process modelling.

Figure 10.4 Manganese in metal vs. iron in slag

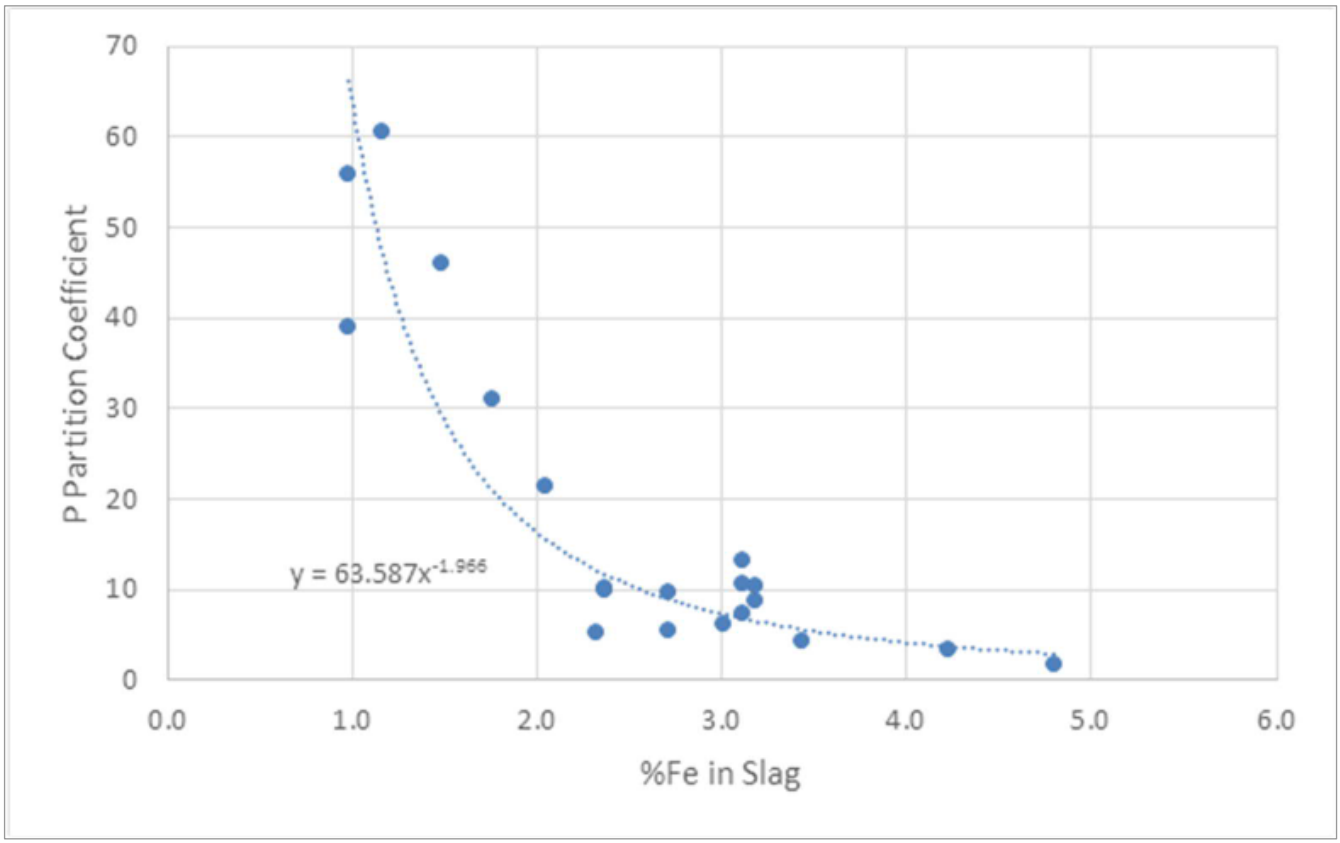


Source: TMC

Phosphorus Partition Coefficient

Figure 10.5 shows phosphorus partition coefficients for both campaigns combined. The process model used a value of 25, with iron at 1.8% Fe, which is broadly in keeping with the data from the pilot operation. Using the regression curve will give a phosphorus partition coefficient of approximately 30 at 1.5% Fe in slag.

Figure 10.5 Phosphorus partition coefficients



Source: TMC

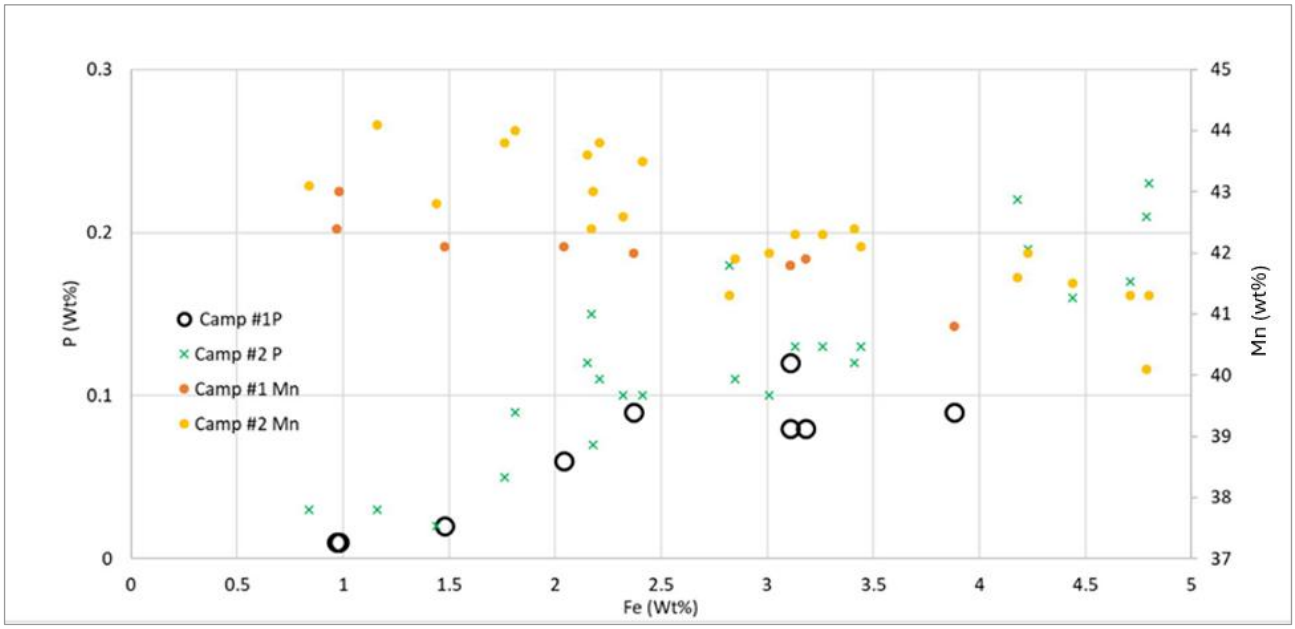
10.4.4.2 Slag chemistry

The slag produced during smelting is proposed to be sold as a feed to the silico-manganese industry. Desirable feeds are high in manganese and low in iron and phosphorus. A simplified guidance is:

- Mn >40% or MnO >50%,
- Mn/Fe ~25 or FeO ~2%, and
- Mn/P >670.

In Figure 10.6, it can be seen that for iron at or below 2% Fe, manganese in slag is about 43% (59% MnO). At 1.5% Fe, both the Mn/Fe ratio and %FeO requirements are met. There is a clear trend for low phosphorus at low iron, and at 1.5% Fe, phosphorus in slag appears likely to be below 0.05% P, yielding Mn/P > 860. Iron at 1.5% Fe is quite close to the current process model value of 1.8% Fe, which was based on reducing 80% of the iron from the slag.

Figure 10.6 Manganese and phosphorus in slag versus iron in slag



Source: TMC

10.4.4.3 Elemental distribution – partition coefficients in converting

In the commercial operation, the sulfidation vessel operates within a narrow range of chemistry near the target intermediate matte composition (currently 30% Fe). This matte composition is selected so as to produce a slag that has acceptable pay-metal losses and can be sold as aggregate or similar useful product. The matte is then taken to a FV where the iron is blown down to the target grade (currently 5% Fe). This produces a slag that has higher levels of pay-metals and needs to be recycled back to the sulfidation vessel to achieve acceptable overall recoveries. It was not possible to perform slag recycle in the piloting process and thus the overall recoveries achieved in pilot sulfidation and converting are not representative of the proposed commercial operation. Instead, the partition coefficients obtained during piloting can be considered for use in the process model, which does include slag recycle, to calculate commercial recoveries.

$$Partition\ Coefficient = \frac{wt\%\ X\ in\ Matte}{wt\%\ X\ in\ Converter\ Slag}$$

The following sub-sections show the partition coefficients reported for the pilot work together with small scale work performed with artificial mattes at XPS in 2020 (XPS, 2020). Also shown, where available, are partition coefficients from two commercial smelters (Benchmark A and B) processing Ni-Cu-Co sulfide concentrates. (Benchmark A' information is the same operation as Benchmark A, but is from a different source.)

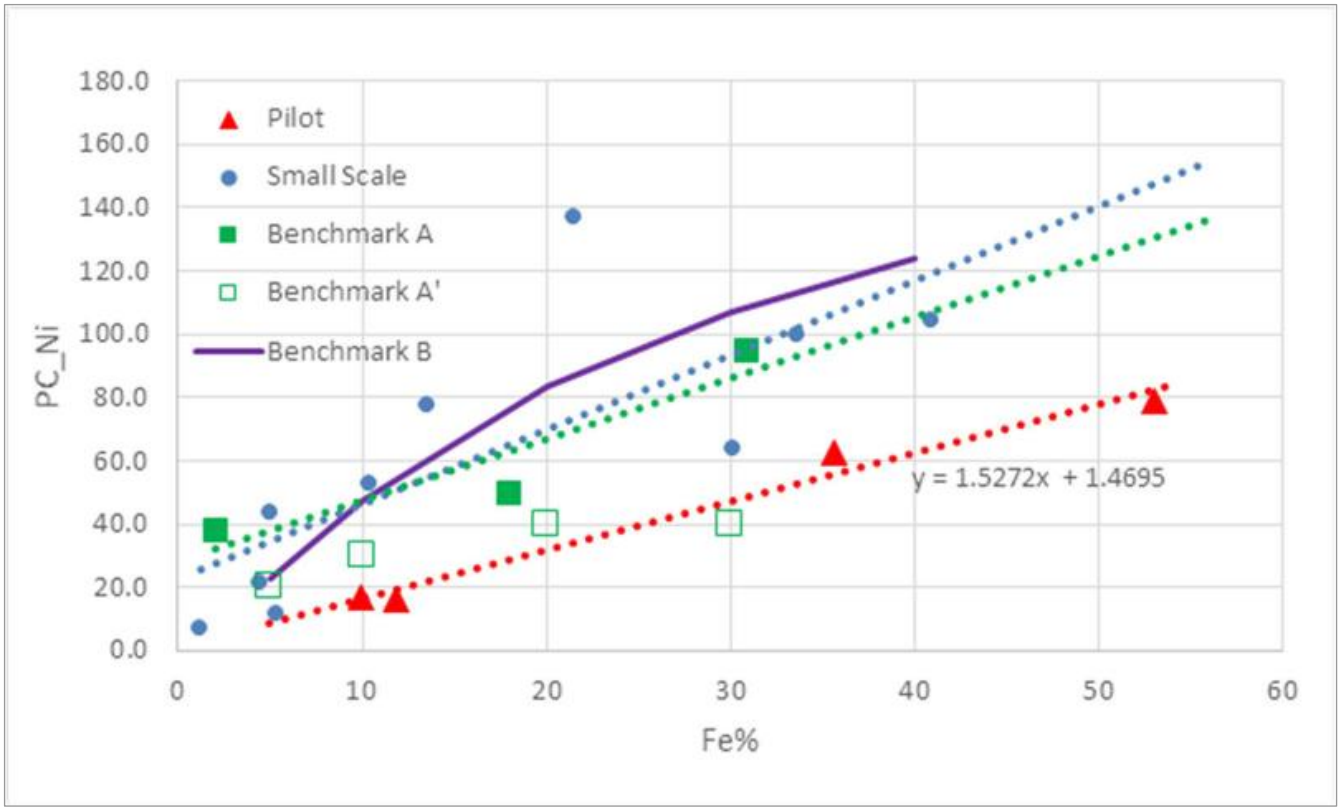
The availability of benchmark information for commercial converting operations means that there needs to be less reliance placed on the pilot results for nickel, copper and cobalt (unlike smelting, where there are no commercial benchmarks for this system). The pilot converting was perhaps the most challenging part of the piloting. Nevertheless, the partition coefficients obtained were reasonably in line with the benchmark values (perhaps to the low side). In general, it can be said that the proposed commercial converting operation should be able to obtain partition coefficients within the range of pilot, small-scale and benchmark values.

Given the importance of these coefficients to overall recoveries, the relevant samples were sent to another laboratory for re-assay. There were no significant differences.

Nickel Partition Coefficients

Figure 10.7 shows nickel partitions from test work and benchmark. The results from piloting are disappointingly low compared to the small-scale (artificial matte) results and two sets of benchmark numbers. They are, however, in agreement with the 'Benchmark A' information (no trendline was plotted for those data).

Figure 10.7 Nickel partition coefficients in converting

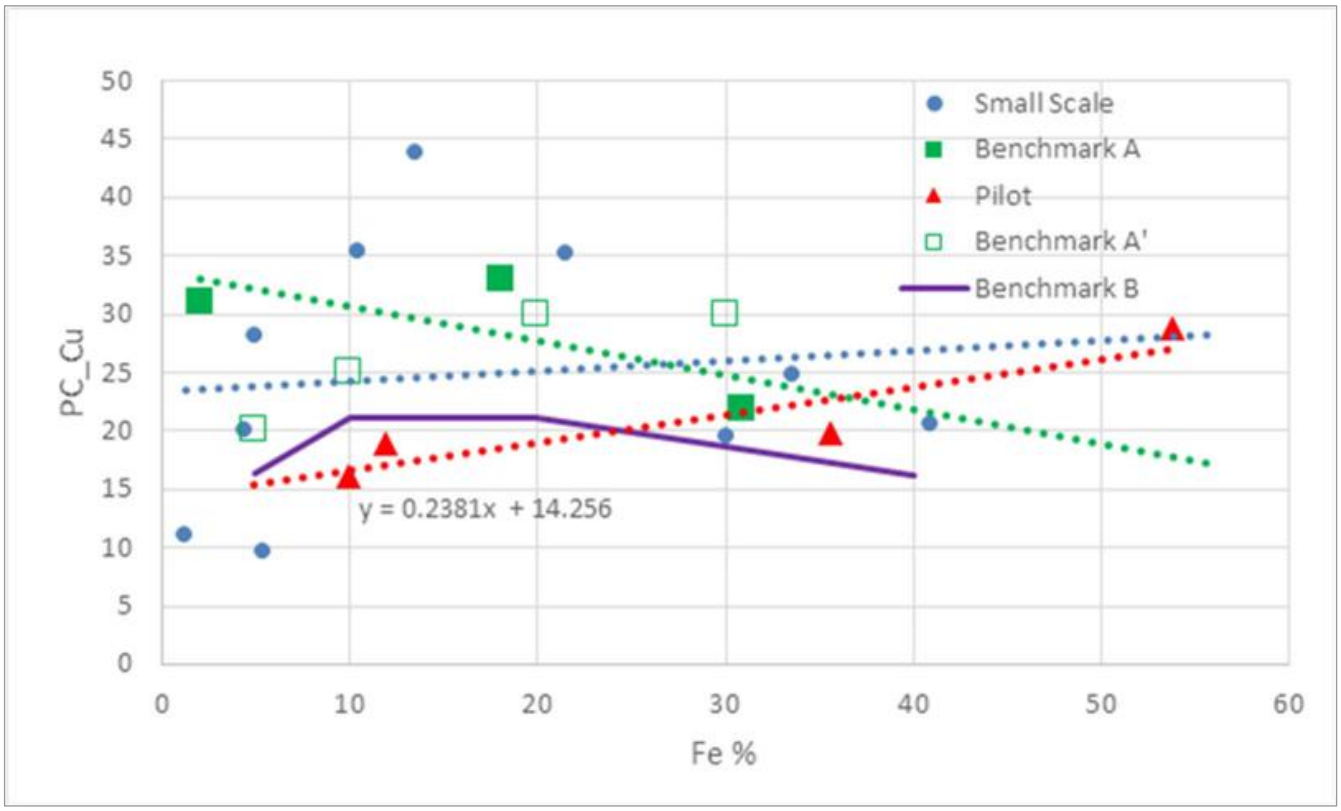


Source: TMC

Copper Partition Coefficients

Results and benchmarks for copper are shown in Figure 10.8. In the range of interest, there are no obvious trends with %iron in matte. There is little to differentiate the different sets of data.

Figure 10.8 Copper partition coefficients in converting

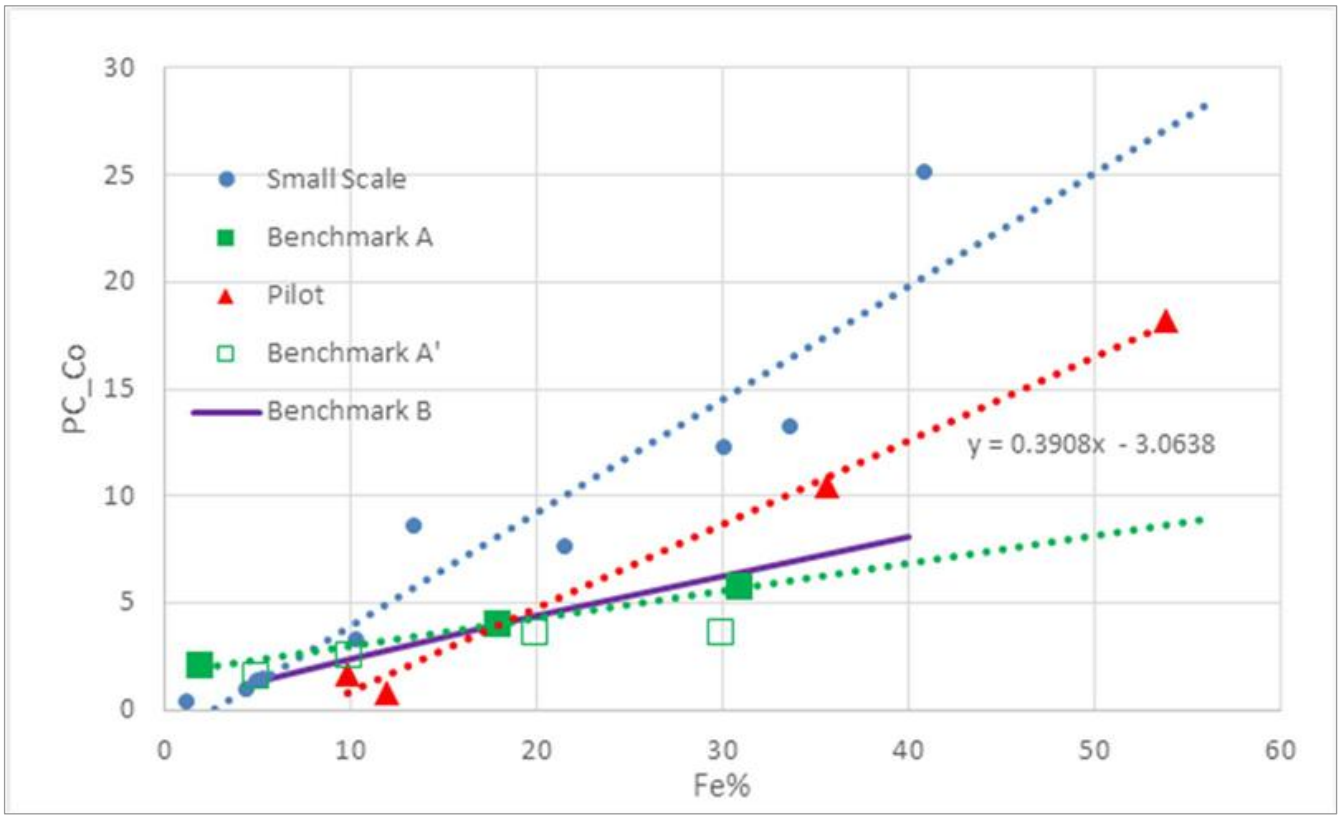


Source: TMC

Cobalt Partition Coefficients

Figure 10.9 shows partition information for cobalt. The pilot trend at the slag discard point (30% Fe) is within the range of benchmark and small-scale test work results.

Figure 10.9 Cobalt partition coefficients in converting

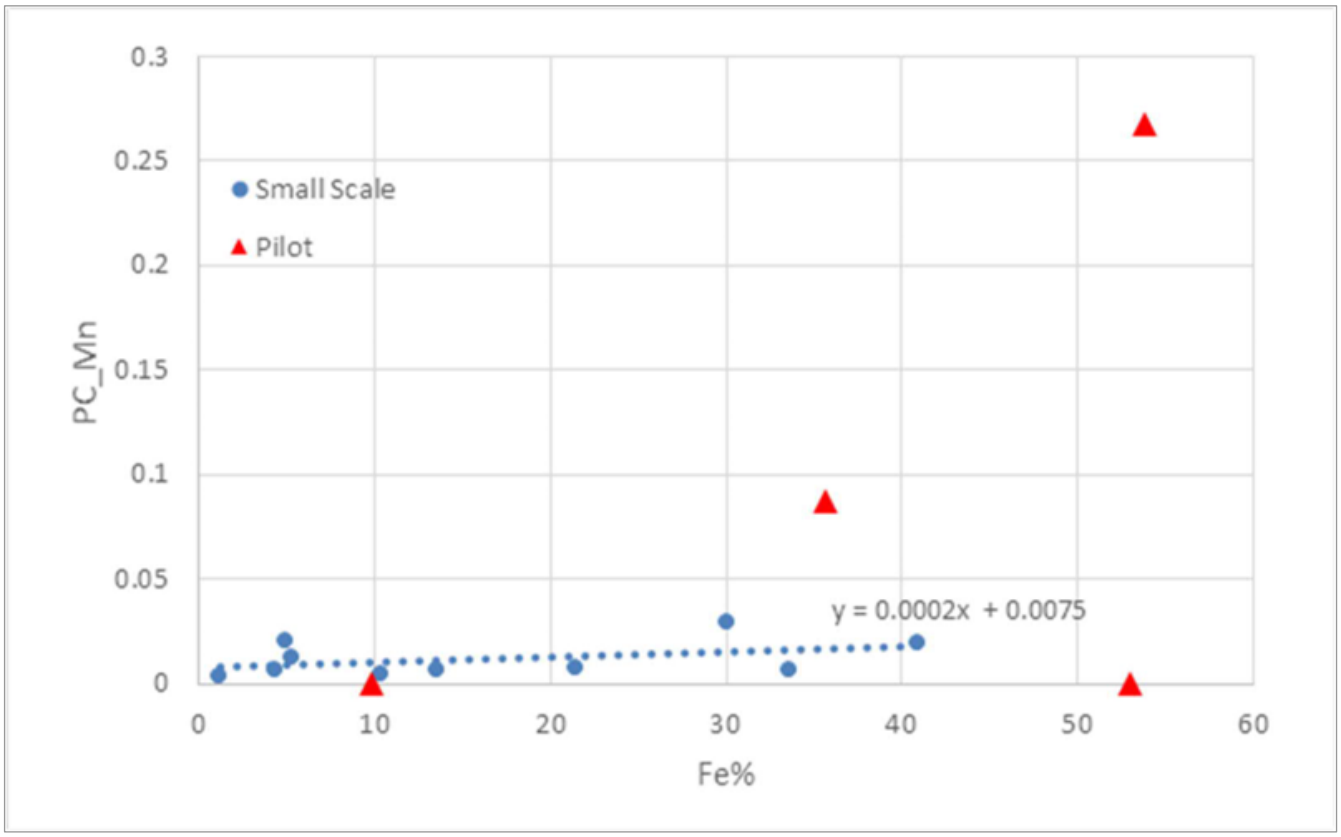


Source: TMC

Manganese Partition Coefficients

Manganese partition coefficients are shown in Figure 10.10. The pilot data are few and widely scattered. They do not provide any conclusive information. The current process model has simply adopted a fixed value for manganese in product matte, namely 0.01wt%. It is proposed that manganese deportment be changed to a partition coefficient basis using the small-scale correlation shown in Figure 10.10.

Figure 10.10 Manganese partition coefficients in converting



Source: TMC

10.4.5 Demonstration scale trials at PAMCO

TMC and PAMCO recently completed a demonstration scale trial at an existing RKEF facility in Hachinohe, Japan, using the 2000 t of nodules collected from NORI Area D. The nodules were calcined over six campaigns using a commercial scale rotary kiln. The calcine was collected in storage bins and smelted over four campaigns in a 4,000 kVA furnace. The furnace is located in the plant's recycling operation and has previously been used to process fly ash, though at the time of the trials it was not in operation.

Several calcining campaigns were required as the calcine had to be cooled prior to transfer to the smelting facility and the hot calcine storage capacity was limited. The time between campaigns was four to six weeks which allowed for the cooling and transfer of the calcine.

During the smelting campaigns, it was determined that better manganese silicate properties could be obtained by changing the iron in slag target down from 1.8 to 1.1. The reduction in iron drives the manganese to phosphorus ratio to be greater than 1000, which is very desirable for the market. The resultant manganese silicate that was produced under these conditions represents an even more attractive product composition relative to the original target. The improvement to the target manganese silicate specification is expected to feed into a revision of TMC's marketing material and conversations with external parties around the sale of the product.

The smelting campaign also assessed refractory wear, and the results show that greater lining erosion was experienced in comparison to baseline laterite operations. Furnace upgrade modifications may be required for long term vessel integrity, workplace safety and equipment reliability. These furnace upgrades and associated capital costs required to prepared furnaces for processing nodules are

expected to be considered in the commercial arrangement with Indonesian RKEF facilities that TMC plans to toll the nodules through. These and any other relatively minor modifications will be assessed on a plant-by-plant basis depending on the equipment available on each site.

The campaigns were able to produce demonstration quantities of on target alloy and manganese silicate. These materials are planned for use in potential downstream product development, as well as for product samples for marketing and demonstration purposes.

The campaigns also proved that the off gas cleaning equipment works for nodule feed as is, and all emissions were compliant with relevant regulations. It is expected that this will translate to any potential Indonesian operation. Overall, it was demonstrated that all major process parameters were all in line with expectations and confirmed that stable operations producing target products is achievable commercially.

10.4.6 Hydrometallurgical refinery bench scale testing

Following the generation of matte at XPS, a bench-scale hydrometallurgical refining program was conducted by TMC at the SGS Canada testing facility in Lakefield, Ontario. The program culminated in generation of nickel and cobalt sulfate crystals, which represent final products that TMC USA intends to produce out of the US-based refinery.

10.4.6.1 Two-stage leaching

Bench-scale leach tests demonstrated that high levels of nickel and cobalt leaching (75% Ni, 63% Co) from the matte were possible in the atmospheric leach stage provided the matte was exposed to sufficient oxidizing conditions. While initial testing achieved desired nickel and cobalt performance, the resulting leach liquors contained excessively high amounts of copper for the two-stage leach approach. Through a process development program, various test parameters were evaluated to assess their impact on reducing copper levels in the leach liquors. Variations in oxidization time, overall reaction time, and acid addition were all considered, and it was determined that an atmospheric leach with an acid addition of 498 kg/t and 48-h overall retention time was able to achieve 75% nickel extraction while limiting copper levels in the Pregnant liquor/leach solution(PLS) to just 0.6 g/L. The optimized atmospheric leach was operated under oxidizing conditions for the initial 6 h with the reactor operated under slight pressure to improve the oxygen contact time in the lab scale reactor and then without atmosphere control for the remainder of the test.

The second stage of leaching is a pressure oxidation (POX) performed on the atmospheric leach (AL) residue, and the results from this program indicated that at 180 °C and 600 kPa oxygen overpressure, 98% of the nickel was leached from the AL residue. This resulted in overall nickel leaching of 99.5% while also leaching 97% of the copper. Key parameters and results of the optimized AL and POX conditions are listed in Table 10.14. Assays of notable components for both liquors and residues from the atmospheric leach and POX are shown in Table 10.15.

Table 10.14 Optimum leach parameters and extractions

Leach	Temp	Time	Oxygen over-pressureO2	Stage Extractions (%)			
	°C	h	kPa	Ni	Cu	Co	Fe
AL	95	48	70	75	-15	56	-17
POX	180	2	600	98	97	98	-1

Table 10.15 Optimum leach assays

Leach	Liquor Assays (g/L)					Residue (%)			
	Ni	Cu	Co	Fe	H_2SO_4	Ni	Cu	Co	Fe
AL	84.1	0.59	4.72	0.003	0	15.5	52.7	1.64	3.60
POX	16.6	50.3	1.62	0.19	14	0.51	5.28	0.11	37.9

10.4.6.2 Cobalt refining

The first stage of the processing for the PLS was a pH adjustment stage, where the pH of the PLS was increased to 4.9 to remove additional copper and any trace iron remaining. Lab-scale cobalt SX (CoSX) testing was conducted using a solvent mixture of 10% Cyanex 272 in Exxsol D80 at an organic to aqueous phase ratio (O/A) of 1/1, a contact temperature of 40 °C, and an equilibrium contact pH of 5.0 via the addition of ammonium hydroxide solution. Process development resulted in selection of a 10 g/L cobalt as cobalt sulfate solution as the aqueous feed to the CoSX scrubbing tests in which magnesium and trace levels of co-loaded nickel were fully removed from the loaded organic phase. Sulfuric acid was used to strip the organic phase. Assays for the feed (pH adjusted AL PLS) and the resultant strip liquor are summarized in Table 10.16.

Table 10.16 Assays of input and output streams from the CoSX

Stream	Ni (g/L)	Cu (g/L)	Co (g/L)	Mn (g/L)	Mg (g/L)
CoSX Feed Liquor	84.3	0.55	5.10	0.10	0.605
CoSX Strip Liquor	< 0.1	4.80	79.4	2.00	0.044

Process development testing has demonstrated that copper IX (CuIX) using Lewatit® MDS TP 208 is able to fully extract the copper from the CoSX strip liquor. Multiple resins were tested for the removal of manganese from the cobalt strip liquor without success, but oxidation of manganese from the soluble Mn^{2+} state to the nonsoluble Mn^{4+} has been demonstrated to be successful. In initial laboratory tests, this is achieved using Caro's acid (H_2SO_5, made by combining sulfuric acid and hydrogen peroxide). The cobalt refining work culminated in the generation of cobalt sulfate crystals. TMC sourced an external third-party specification for cobalt sulfate and compared them with analysis of the lab-generated cobalt sulfate crystals produced as SGS, presented in Table 10.17.

Table 10.17 Comparison between TMC's lab-generated cobalt sulfate crystals with an external third-party specification

	TMC Result	Comparative Specification
Co (wt%)	22.1	> 20.5
Cu (ppm)	< 5	< 5
Ca (ppm)	< 100	< 50
Fe (ppm)	< 100	< 10
Mg (ppm)	82	< 100
Na (ppm)	< 100	< 300

10.4.6.3 Nickel refining

Nickel SX (NiSX) testing was conducted on samples of CoSX raffinate produced during CoSX testing, identifying 40% Versatic 10 in Exxsol D80 as the desired solvent mixture for the loading of nickel. Optimum contact pH was 6.35, and contact temperature was 50°C. Trace levels of cobalt, magnesium, and manganese were scrubbed using a 15 g/L nickel as nickel sulfate solution. The scrubbed organic was stripped with sulfuric acid to produce a strip liquor that assayed at 117 g/L nickel. The strip liquor

was further concentrated via evaporation to directly produce nickel sulfate crystals with a calculated purity of 99.996% (total impurity content of 40 g/t). As with cobalt sulfate, TMC sourced some external third-party specifications and compared them with the analyses of the crystals generated at SGS, presented in Table 10.18.

Table 10.18 Comparison between TMC's lab-generated nickel sulfate crystals with two external third-party specifications

	TMC Result	Comparative Specification 1	Comparative Specification 2
Ni (wt%)	>= 22.0	>= 22.0	>= 22.0
Cu (ppm)	< 1	<= 5	<= 5
Ca (ppm)	< 20	<= 20	<= 50
Fe (ppm)	< 5	<= 10	<= 10
Mg (ppm)	2.3	<= 20	<= 50
Na (ppm)	< 20	<= 500	<= 200

10.5 Iron in final matte

The current process model has a final matte iron composition of 5% iron. The target iron in matte is based on limiting the amount of iron going into the downstream hydrometallurgical refinery (the lower the iron the better) while maintaining reasonable recoveries of pay metals.

Potential economic exploitation of the matte could be affected if the iron content is too high. The eventual customer looking to further refine the matte into individual pay metals components is expected to have issues processing with high iron contents.

10.6 Manganese silicate

The manganese silicate product is a key contributor to the overall economic case for the project. With nodules containing around 30% manganese, the manganese silicate is expected to represent approximately 90% of the product generated from the flowsheet by mass. The intended market for the manganese silicate is as a feed for silico-manganese production, which is a key additive in steel manufacturing. Market analyses have shown that key indicators for a high value product in this area are based on achieving the following targets for manganese silicate as identified in Table 10.19.

Table 10.19 Target specifications for manganese silicate

Component	Target Specification (wt%)
Mn	> 40
Fe	1 – 2
Mn / P	> 670

These targets are based on a combination of high grades of manganese relative to other sources, as well as limiting impurities like iron and phosphorus. The impurity profile of target and pilot generated products are consistent with presently understood market requirements.

During the piloting of TMC’s flowsheet, 25 t of manganese silicate was generated, most of which met the target parameters. The material from the most representative tap (Campaign 2, Tap 4) was then used to perform silico-manganese generation testing at a laboratory in Trondheim, Norway. Results from this program identified at both lab and kilogram scale that silico-manganese alloy can be generated using TMC’s manganese silicate as the sole source of manganese. Producing manganese silicate that meets the targets as outlined in the table above and the success of the program in Norway

provided confidence in TMC's strategy to sell the manganese silicate for use in silico-manganese alloy production.

10.7 Summary and QP's opinion

TMC has undertaken a metallurgical development process that has included extensive review of relevant technical information in the literature, appropriately scoped and detailed bench-scale and pilot-scale testwork that demonstrated the fundamentals of the process, and executed appropriate process engineering to support the project economic analysis. In addition, the scope of the project is to employ existing assets presently operated to produce ferronickel from nickel laterite ore. The nodule feed process is analogous to nickel laterite operations in terms of equipment, consumables, estimated flowrates, temperatures, and other conditions. The estimated data employed compare reasonably with commercial benchmarks.

It is the QP's opinion that the experimental and benchmark data are adequate to demonstrate that existing RKEF assets are suitable for smelting polymetallic nodules into saleable products with proven markets that meet potential customer quality requirements. The QP also endorses the fact that preliminary bench scale testing has shown that generation of final nickel and cobalt products suitable for use in battery applications is possible using intermediates derived exclusively from pyrometallurgical processing of nodules.

11 Mineral Resource estimates

11.1 Cautionary note regarding Mineral Resource estimates

The estimates of Measured, Indicated, and Inferred Mineral Resources presented in this section are not Mineral Reserves and do not demonstrate economic viability. No pre-feasibility or feasibility study has been completed for the Property. Inferred Mineral Resources are considered too speculative geologically to have the economic considerations applied to them that would enable classification as Mineral Reserves, and there is no certainty that any portion of the Mineral Resources will be converted to Mineral Reserves or result in future development or production.

11.2 Estimation process for NORI-A, B and C

Mineral Resources were first estimated for NORI-A, B, C and D by Golder Associates in late 2012 (Golder, 2015), primarily using data collected by the Pioneer Contractors. Data collected by NORI in 2018 and 2019 was used by AMC to update the Mineral Resource estimate for NORI Area D in 2020.

The Mineral Resource estimates for NORI-A, B and C have not been updated. The existing Mineral Resource estimate generated by Golder in 2012 remains the current estimate. There has been no new exploratory work conducted in the areas to warrant an update to the estimates.

All information for this section has been summarized from Golder 2015 technical report. The information presented for NORI Area D in this section is provided only for comparison.

11.2.1 Geological domains

Based on the geophysical interpretation of the NORI multibeam data there are areas identified as low nodule density and possible lava flows and outcrops in NORI-C. These areas cover a lower percentage of NORI-C than the areas identified as high, medium, or indeterminate nodule density. The areas identified as low nodule density and possible lava flows and outcrops are numerous, discontinuous, and are generally smaller than the average sample spacing. Since the NORI Area falls within a single bathymetric domain (abyssal hill province) and entirely within the CCZ deposit boundary, it was not considered necessary to domain the data for an Inferred Mineral Resource.

11.2.2 Nodule sample data

The data was checked for anomalous or erroneous data and cross-checked with data supplied directly by the ISA. Resetting zero assay values to missing and zero abundance values to 0.01 where there are assay values. Summary statistics for the data are listed in Table 11.1. Note that this summary includes Pioneer Contractor data for NORI Area D.

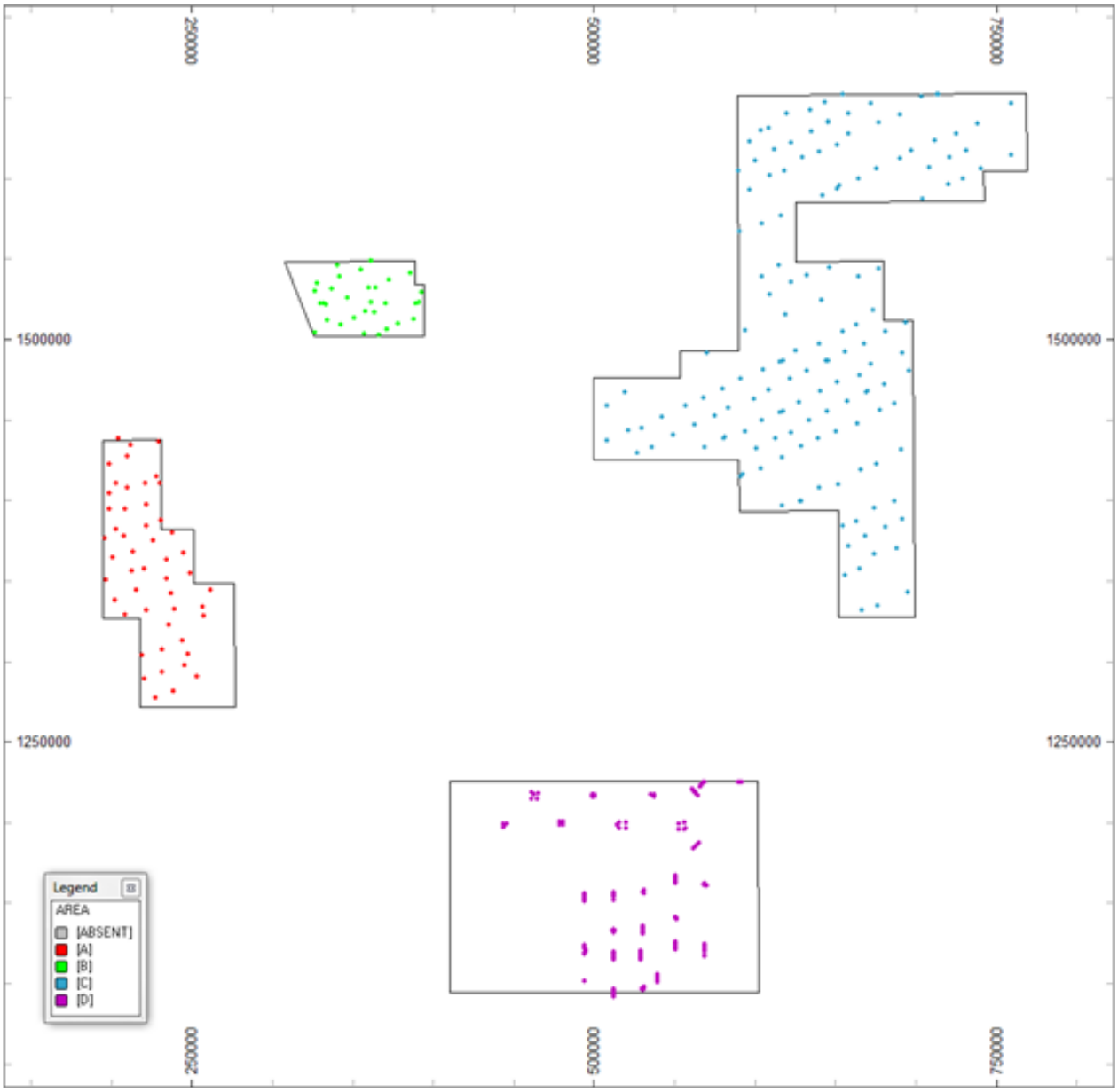
Table 11.1 Summary statistics of samples within the NORI Area used for the 2012 Mineral Resource estimate.

Variable	Samples	Missing	Min	Max	Mean	Var	CV	Median
Ni (%)	360	32	0.68	1.75	1.30	0.016	0.10	1.31
Co (%)	360	32	0.05	0.33	0.17	0.004	0.35	0.19
Cu (%)	360	32	0.40	1.50	1.10	0.028	0.15	1.13
Mn (%)	360	32	12.84	33.90	29.45	8.406	0.10	30.20
Abundance (wet kg/m^2)	**392**	**0**	**0**	**52.2**	**11.9**	**64.303**	**0.67**	**12.00**

Source: Golder 2015. Var = variance; CV = coefficient of variation; Ni = nickel; Co = cobalt; Cu = copper; Mn = manganese

Latitude/longitude coordinates were converted to Universal Transverse Mercator Cartesian coordinate system (UTM) coordinates using WGS 84 datum. The minimum and maximum UTM coordinates for each of the NORI areas are listed in Table 11.2. To streamline the estimation process, the coordinates of the data in each area were modified to bring the data for the four areas closer together, so the Mineral Resources could be estimated in a single block model. A plan of the Area locations in transformed space is presented in Figure 11.1. The apparent distances between the Areas in this figure are not real distances.

Figure 11.1 NORI-A, B, C and D, showing location of historic data



Source: AMC
NB: NORI-A, B, C and D cover several UTM zones but were overlaid to facilitate modelling of all areas in one model. The apparent distances between the Areas in this figure are not real distances.

Table 11.2 Minimum and maximum UTM coordinates for NORI Areas

Area	Pioneer Contractor		UTM Easting	UTM Northing	UTM Zone
NORI-A	Yuzhmorgeologiya	Minimum	546318.6	1276704.2	8
		Maximum	612250.2	1438373.8	
NORI-B	Yuzhmorgeologiya	Minimum	627009.7	1502544.4	8
		Maximum	693143.2	1548239.6	
NORI-C	IOM	Minimum	508307.5	1651913.6	10
		Maximum	759829.0	1331443.7	
NORI Area D	AMR	Minimum	444252.3	1091225.8	11
		Maximum	**592471.8**	**1224898.2**	

Source: Golder 2015.Yuzhmorgeologiya = State Enterprise Yuzhmorgeologiya (Russian Federation). IOM = Inter Ocean Metal Joint Organisation; AMR = Arbeitsgemeinschaft Meerestechnisch Rohstoffe.

11.2.3 Declustering

Declustering was used to remove potential biases in statistics that can arise from variable sample spacing, which can arise from the multiple sampling at close locations as the ship undertakes its voyage.

Normal cell declustering without any boundaries can present issues where the edge cells become overweighted as the cell size is increased. A modified cell declustering algorithm was used that weights the cells to the block model volume within each cell. The process provides a declustering weight which is used to weight the univariate statistics (Table 11.3). For this method, the cell size was optimized for a square window size of 30 km and the origin offset 10 times.

Table 11.3 NORI-A, B, C and D declustered statistics (historic data only)

Variable	Samples	Min	Max	Mean	Var	CoV	Median
Ni (%)	360	0.68	1.75	1.29	0.021	0.11	1.32
Co (%)	360	0.05	0.33	0.19	0.003	0.27	0.20
Cu (%)	360	0.40	1.50	1.08	0.035	0.17	1.12
Mn (%)	360	12.84	33.90	28.91	10.524	0.11	29.81
Abundance (wet kg/m^2)	**392**	**0**	**52.20**	**11.57**	**66.736**	**0.71**	**11.00**

Source: Golder 2015 Var = variance; CoV = coefficient of variation

11.2.4 Top-cuts

The Cov is very small for nodule abundance, nickel, copper, manganese, and cobalt, suggesting that the application of top-cuts is not necessary. However, due to the wide spacing of samples, a top-cut was applied to trim the high (99.5th percentile) values to reduce the likely impact of the high-grade outliers.

The presence of outliers (extreme values) and the need to apply “top-cut” values or “capping” (where samples above a certain threshold are assigned the top-cut value) to sample populations was assessed using a number of techniques:

- Examination of grade distributions using cumulative probability plots.
- Statistical assessment of the grade distributions.
- Examination of the spatial locations of identified outlier samples.

Top cuts defined in Table 11.4 are roughly equivalent to the 99.5th percentile of the mineralized samples and do not have a significant impact on the average grade. Application of top cuts reduced the mean only for manganese, which was reduced by a very low 0.2% of the uncut mean. This is simply because the grades within the CCZ are very consistent due to the deposit's hydrogenetic and diagenetic origin.

Table 11.4 NORI-A, B, C and D top cuts used for NORI 2012 Mineral Resource estimate

Variable	Top-Cut Value (%)
Ni	1.56
Co	0.31
Cu	1.46
Mn	33
Abundance	32

Source: Golder 2015

11.2.5 Spatial continuity

The samples with top-cuts applied were used for variogram analysis. Search parameters were generally as follows:

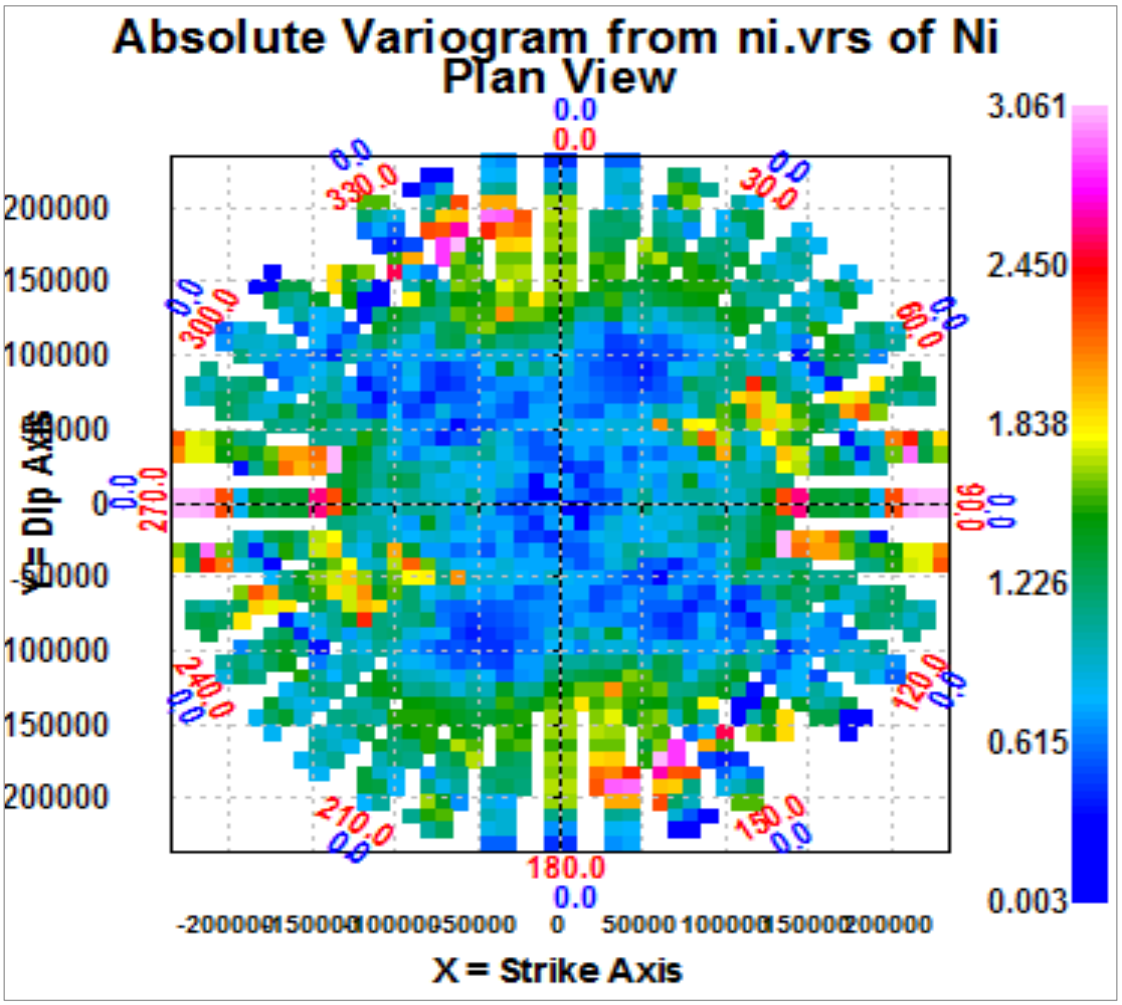
- Lag distance of 5 km.
- Horizontal search angle of 15°.
- Vertical search angle of 15°.
- Horizontal distance of 30 km.

Single structure Gaussian models with common nugget and incremental sill levels showed good structure and were used for all variogram modelling. The variograms were scaled to the population Var. Variogram maps were calculated for the purpose of determining direction of greatest continuity. The variogram map for nickel is shown as an example in Figure 11.2. Variogram models are presented in Table 11.5.

Table 11.5 Variogram models for NORI-A, B and C

Variable	Nugget	Sill	Range Along Strike(km)	Range Cross Strike(km)
Ni	0.2	0.8	20	20
Co	0.2	0.8	30	30
Cu	0.2	0.8	30	30
Mn	0.2	0.8	50	50
Abundance	0.2	0.8	30	30

Figure 11.2 Variogram map of nickel for NORI-A, B and C



Source: Golder 2015

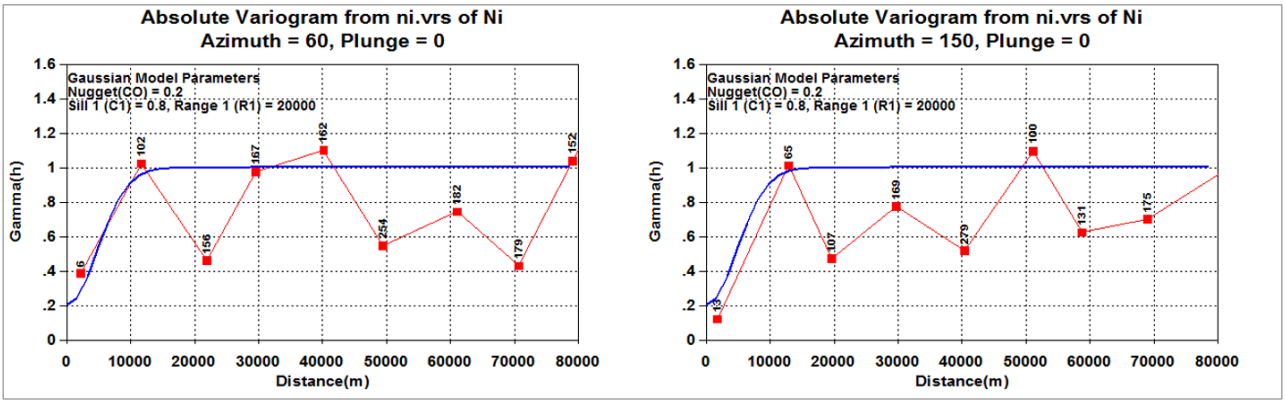
Where possible, similar values for the variogram model parameters for nickel, cobalt, copper, manganese, and abundance were chosen, to ensure relationships between the elements were respected implicitly during estimation and reflected in the resource estimate. Also, the same type of variogram model was fitted to the experimental variograms.

Gaussian variogram models were fitted to the experimental variograms. Typically, spherical models are sufficient for modelling the spatial continuity, but in this case the Gaussian model better fits the data. Gaussian models give greater weight to the very close samples (in the range of 0 to 5 km) and then rapidly decay to the sill compared with the spherical model. This fits in with the likely short-range variability possibly being controlled by the ridges, which are of the frequency of 3 to 5 km and oriented approximately north-northwest.

The directions of greatest continuity from the variogram maps are 060° and 150°, which are roughly parallel and orthogonal to the broad regional trend of the CCZ. Smaller scale local trends oriented parallel with ridges are not visible in the wide-spaced data. The long-range experimental variograms for abundance are erratic with an almost nugget model.

Major and semi-major variograms for nickel are shown in Figure 11.3.

Figure 11.3 Major and semi-major variograms for nickel



Source: Golder 2015. Red line is actual data and blue line is modelled curve

11.2.6 Geological block model

The block model was built using the framework defined in Table 11.6 and with additional block attributes listed in Table 11.7. A vertical block size of 1 m was used, essentially creating a two-dimensional model. The 1 m thickness is simply to give the blocks a default value. The tonnage of nodules in each block was estimated from the surface area of the block multiplied by the abundance (kg/m^2) estimate. Parent blocks were split into sub-blocks at the Contract Area boundaries to improve resolution.

The total area of the block model, including NORI Area D is 74,840 km^2 which is 100.01% of the actual total area of the NORI Area of 74,830 km^2. This indicates that the sub-blocks provided satisfactory resolution for estimating the Contract Area boundaries.

Table 11.6 NORI-A, B and C block model framework (UTM coordinates)

	Easting	Northing	Elevation
Model origin (m)	195000	1093000	–0.5
Model limit (m)	775000	1653000	0.5
Model extent (m)	580000	560000	1
Parent block dimensions (m)	10000	10000	1
Number of parent blocks	58	56	1
Minimum sub-block size	500	500	1

Table 11.7 NORI-A, B and C model variables

Variable	Type	Description
Area	alphanumeric	Contract Area (A to D)
Ni	numeric	Estimated Ni weight % value
Co	numeric	Estimated Co weight % value
Cu	numeric	Estimated Cu weight % value
Mn	numeric	Estimated Mn weight % value
Abundance	numeric	Estimated nodule abundance wet kg/m^2

11.2.7 Mineral Resource estimation

Ordinary kriging (OK) was used to estimate nickel, cobalt, copper, manganese, and abundance in the block model. Grades were estimated on a parent block basis using block discretization of 3 by 3 by 1.

Grades were also estimated using inverse distance weighting (IDW) to the power of 2 and nearest neighbor estimation (NN) for validation of the Ordinary kriging – an estimation method utilizing distance-weighted local averages (OK) estimates.

To ensure that all blocks in the model had values for nickel, cobalt, copper, manganese, and abundance, a three-pass elliptical search strategy was used for selecting the neighboring samples for estimation. Dimensions of the search ellipse radii were based on the ranges of the variogram models and average sample spacing. The search pass ellipse radii that were used are:

- PASS 1: 30 km by 30 km.
- PASS 2: 60 km by 60 km (pass 1 expanded by a factor of 2).
- PASS 3: 90 km by 90 km (pass 1 expanded by a factor of 3).

A minimum of 1 and a maximum of 8 samples were allowed per octant for each search pass, with a minimum of 4 and maximum of 32 samples per estimate. The required minimum number of samples per estimate was relaxed to 1 sample for the third search pass. The relatively large number of samples used in the estimate will ensure the estimates are smoothed for this early stage of evaluation.

To complete the block estimates and avoid potential issues for missing grades the third and final search passes used large search radius to ensure most relevant blocks were assigned estimated grades. This ensured that nearly all mineralized blocks were assigned estimates. Any remaining unassigned grades were set to 0.01% for nickel, cobalt, and copper, and to 26.86% for manganese.

The Mineral Resource model was validated by comparing the global mean and Vr of the model against alternative nearest neighbor and inverse distance weighting estimates and the declustered samples. The mean grades compare favorably and the expected Vr reduction is observed, indicating that the estimate is satisfactory.

11.2.8 Mineral Resource classification

Mineral Resource classification was done on the basis of the quality and uncertainty with the sample data. Accordingly, NORI-A, B and C are considered to have sufficient data and continuity to warrant Inferred Mineral Resource classification in accordance with SEC Regulation S-K (subpart 1300).

In the Qualified Person's opinion, the Mineral Resources have reasonable prospects of economic extraction. No fatal flaws have been identified. It is reasonable to expect that, with further engineering design and testwork, the technical and economic factors relevant to the collection of nodules and the extraction of nickel, cobalt, copper and manganese products from the nodules can be resolved. Accordingly, it is the Qualified Person's opinion that all issues relating to all relevant technical and economic factors likely to influence the prospect of economic extraction can be resolved with further work.

11.3 Estimation process for TOML-A, B, C, D, E and F

Estimation of tonnage and grade for TOML-A, B, C, D, E, and F was undertaken in 2016. The estimates are based on the historical BC and free fall-grab nodule sampling (262 samples) supplemented with TOML box cores (113 samples) and photo-profile data (20,857 frames over 587 line km). Only sample data within the TOML Area was used to inform the estimates. Further details are presented in the technical report summary titled "Technical Report Summary--TOML Mineral Resource, Clarion-Clipperton Zone, Pacific Ocean, for Deep Green Metals Inc." (the "TOML Technical Report"), with an effective date of March 26, 2021 (AMC Consultants, 2021b).

The modelling methodology used for estimating the Mineral Resource was determined through careful consideration of the scale of deposit, geological mechanism and controls behind nodule formation and nature of the sampling method. The approach involved estimating nodule abundance and grades into a two-dimensional block model. abundance, in wet kg/m^2, was used for calculating tonnage. abundance and grades were estimated using OK. The OK estimates were validated using IDW and Nearest neighbour estimation method (NN) estimates.

11.3.1 Geological domains

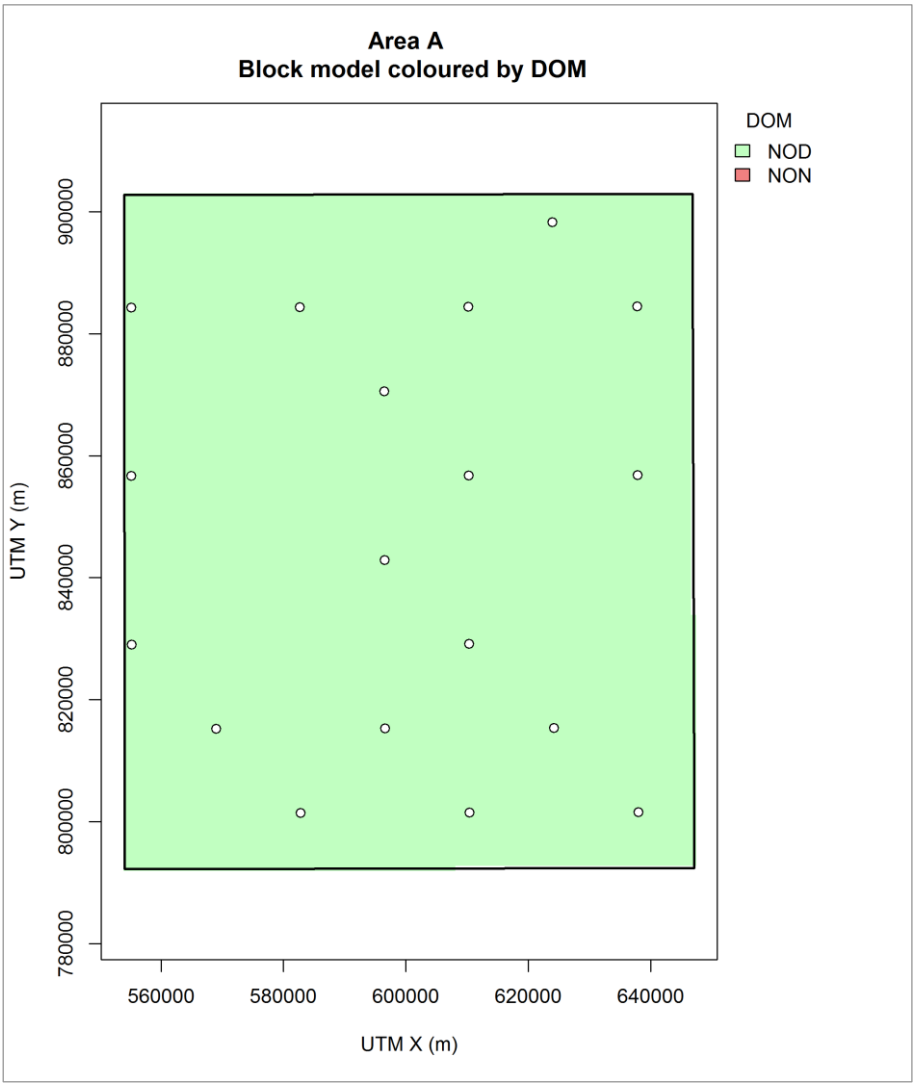
The entire TOML Area falls within the regional abyssal hill domain. Based on interpretation of the GEBCO bathymetry data from the ISA, and TOML's own bathymetry, less than 2% of the TOML Area is covered by isolated sea mounts. Within the TOML Area there are small, disconnected zones where there are no polymetallic nodules present or the polymetallic nodule abundance is very low. These zones are controlled by local geology (presence of basalt or carbonate ooze) and bathymetry.

The TOML Area was split into two domains. Areas with polymetallic nodules and areas predominately without polymetallic nodules. The MBES bathymetry and the backscatter data was used to interpret the parts of TOML-B through F with no polymetallic nodules. For the Mineral Resource estimate two broad domains were interpreted from the data. These are:

1. NOD – polymetallic nodule domain. This domain exists almost everywhere and extends beyond the boundaries of the TOML Areas.
2. NON – areas with no or low nodule abundance of polymetallic nodules. This domain includes areas covered with soft sediment, seamounts and areas with basalt. Nodule abundance in the NON areas was set to zero in the block model. It was not defined in TOML-A as that area has not been surveyed by MBES.

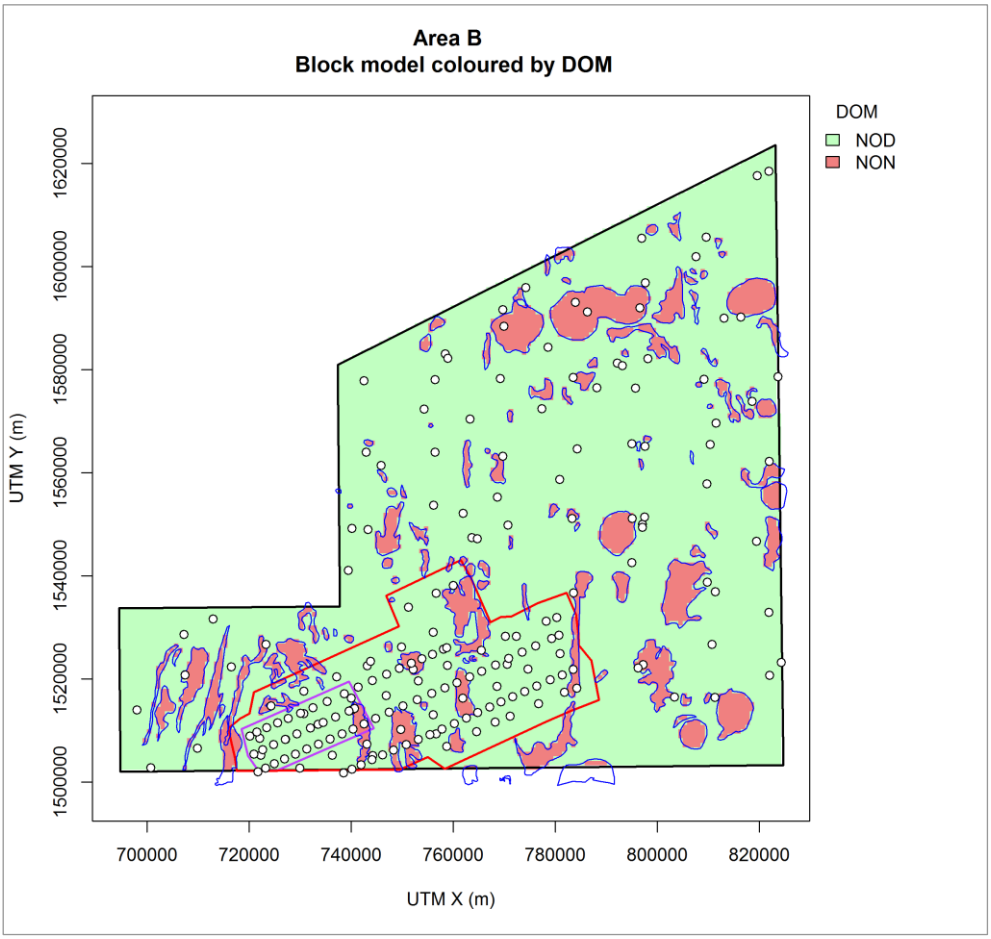
Figure 11.4 through to Figure 11.8 show the geological domains in the TOML Contract Areas used for the Mineral Resource estimate. Sample locations are indicated by white circles.

Figure 11.4 TOML-A interpreted geological domains



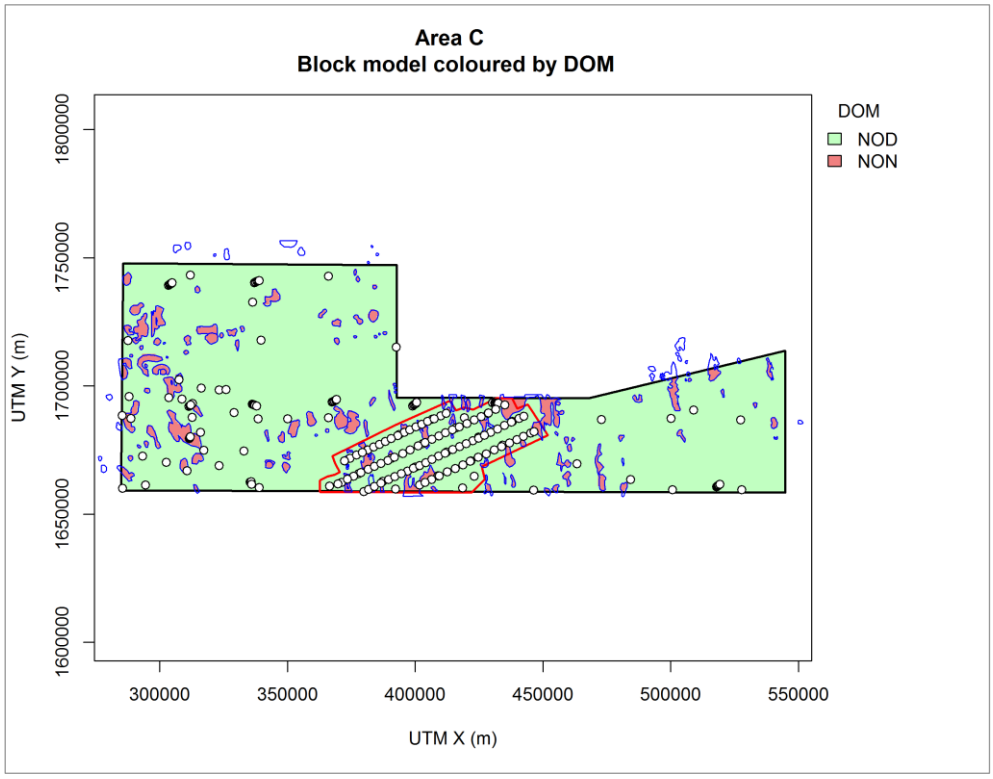
Source: TMC

Figure 11.5 TOML-B interpreted geological domains



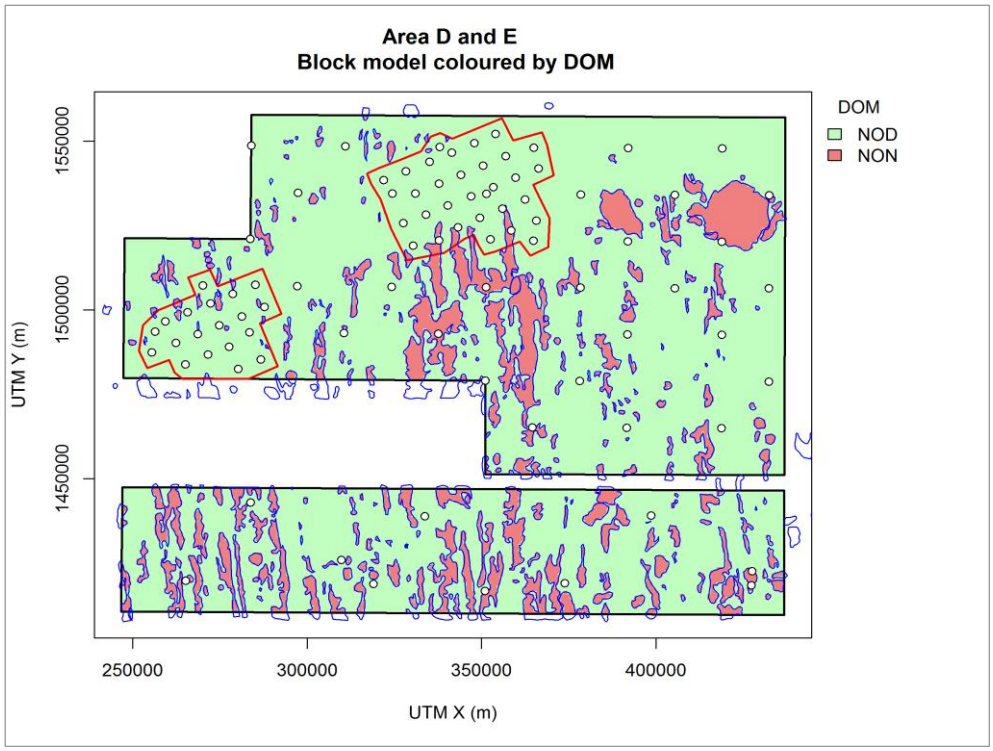
Source: TMC

Figure 11.6 TOML-C interpreted geological domains



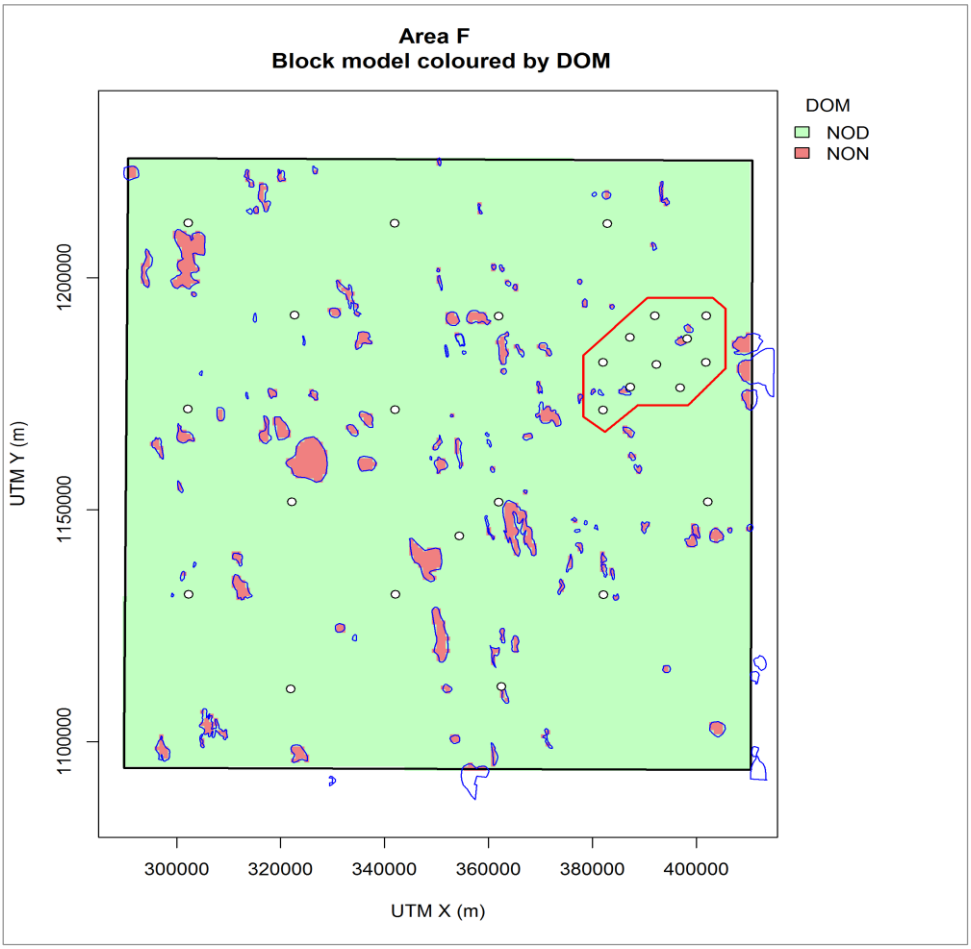
Source: TMC

Figure 11.7 TOML-D and E interpreted geological domains



Source: TMC

Figure 11.8 TOML-F interpreted geological domains



Source: TMC

11.3.2 Nodule sample data

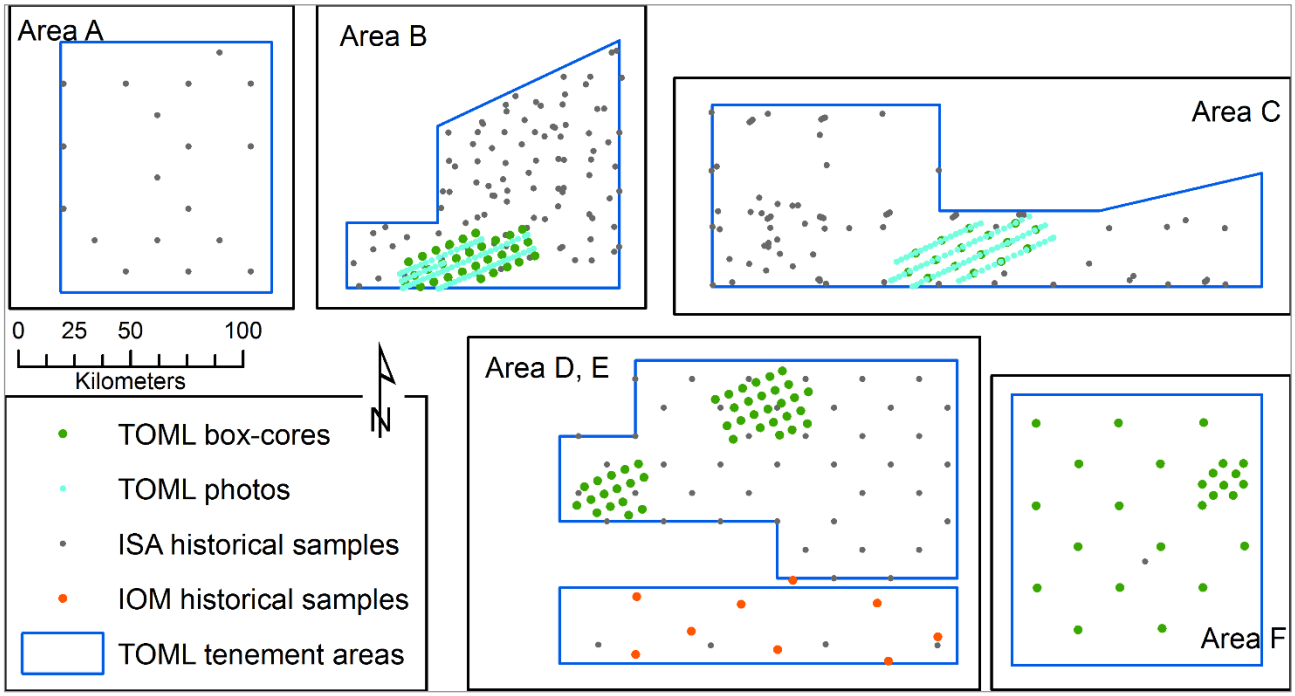
Box core and free fall grab sampling data from the Pioneer Contractors was initially provided to TOML by the ISA. This data included samples for TOML-A, B, C, D, E and F (Figure 11.9). An additional eight samples within TOML-E were provided by IOM. The data were provided in comma delimited format. The historical polymetallic nodule sample data consists of 2,211 records of which only 268 of the nodule samples fall within the TOML Area.

Polymetallic nodule samples were collected during the TOML 2015 campaign within the TOML-B, C, D, and F. A total of 104 BC samples were collected, sampled and assayed.

A separate data set containing the nodule abundance for 113 TOML BC samples and calculated abundance for 536 sea floor photos was provided by TOML. The calculated abundance was derived from every 100th photo of the TOML 2015 sea floor photo-profiling, providing an average spacing of 2.7 km between photo observation points. The photos were processed manually by measuring the long axis of every nodule within the photo or within a subset of the photo. This enabled an accurate estimate of the nodule abundance in each photo.

The spatial coordinates of the data were in digital latitude and longitude. For spatial modelling and Mineral Resource estimation the coordinates were transformed into (UTM) using the World Geodetic System (WGS 84) spatial reference system. Table 11.8 lists the minimum and maximum UTM coordinates for each TOML Area.

Figure 11.9 Location of the historical sample data provided by the ISA and IOM and the TOML data



Source: TMC

Table 11.8 Minimum and maximum UTM coordinates for each TOML Area

TOML Area	Easting		Northing		UTM Zone
	Min (m)	Max (m)	Min (m)	Max (m)	
A	553 976.1	647 191.3	792 205.9	902 969.6	5
B	694 523.4	824 684.8	1 502 007	1 623 606	8
C	284 947.0	544 795.5	1 658 368	1 747 831	9
D	247 296.3	437 027.2	1 451 032	1 557 860	10
E	246 691.9	436 798.9	1 409 560	1 447 514	10
F	289 837.4	410 806.1	1 093 913	1 225 830	11

The Pioneer Contractor and TOML data were combined into a single data set and checked for anomalous or erroneous values. The zero assay values in the historical data represent absent data and were reset to absent value where abundance was recorded as zero, and to 0.01 where abundance was greater than zero.

11.3.3 Sample statistics

The descriptive statistics of the nodule sample data are listed in Table 11.9 to Table 11.13. Comparison of the Pioneer Contractor samples within the TOML Area (Table 11.11) and the TOML BC samples (Table 11.12) indicate slightly higher mean grades for abundance, Mn, Ni and Cu, and slightly lower Co for the TOML samples.

Table 11.9 Statistics of all samples within the TOML Areas

Variable	Samples	Missing	Min (%)	Max (%)	Mean (%)	Var	CoV	Median
Abundance	527	9	0	30.77	9.50	43.088	0.69	8.79
Mn	338	198	6.54	33.79	27.91	13.426	0.13	28.9
Ni	338	198	0.33	1.55	1.26	0.034	0.15	1.31
Cu	338	198	0.22	1.51	1.09	0.046	0.2	1.16
Co	338	198	0.02	0.35	0.23	0.002	0.21	0.23

Var = variance; CoV = coefficient of variation

Declustering weights were calculated and applied to the nodule sample data to assess the potential bias in the descriptive statistics that can arise from clustering of sample data. Table 11.10 lists the declustered nodule descriptive statistics for all samples within the TOML Contract Area. Declustering the data resulted in a slight increase in the mean of abundance, but no significant change for Mn, Cu and Co indicating that the statistics are not significantly affected by clustering.

Table 11.10 Declustered statistics of all nodule samples within TOML Area

Variable	Samples	Missing	Min (%)	Max (%)	Mean (%)	Var	CoV	Median
Abundance	527	9	0	30.77	10.20	39.35	0.61	9.16
Mn	338	198	6.54	33.79	28.09	10.414	0.11	28.71
Ni	338	198	0.33	1.55	1.26	0.03	0.14	1.31
Cu	338	198	0.22	1.51	1.11	0.045	0.19	1.16
Co	338	198	0.02	0.35	0.22	0.003	0.24	0.22

Var = variance; CoV = coefficient of variation

Table 11.11 Statistics of Pioneer Contractor samples within the TOML Areas

Variable	Samples	Missing	Min (%)	Max (%)	Mean (%)	Var	CoV	Median
Abundance	253	9	0.03	26.0	8.82	27.134	0.59	8.09
Mn	234	28	10.3	32.4	26.88	11.097	0.12	27.67
Ni	234	28	0.53	1.51	1.22	0.034	0.15	1.27
Cu	234	28	0.4	1.51	1.06	0.053	0.22	1.13
Co	234	28	0.02	0.35	0.24	0.002	0.18	0.24

Var = variance; CoV = coefficient of variation

Table 11.12 Statistics of TOML samples within the TOML Areas

Variable	Samples	Missing	Min (%)	Max (%)	Mean (%)	Var	CoV	Median
Abundance	113	0	0.0	29.13	12.23	66.384	0.67	12.6
Mn	104	9	6.54	33.79	30.23	11.006	0.11	30.84
Ni	104	9	0.33	1.55	1.34	0.025	0.12	1.37
Cu	104	9	0.22	1.43	1.18	0.019	0.12	1.2
Co	104	9	0.08	0.31	0.21	0.003	0.24	0.22

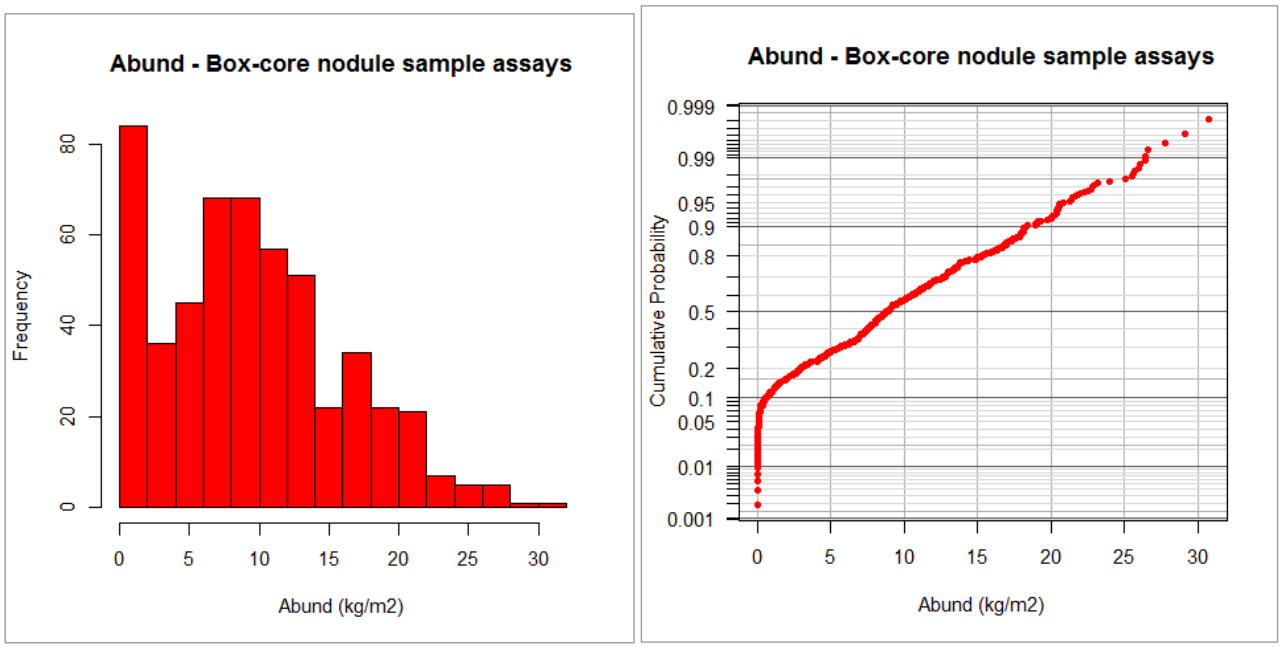
Var = variance; CoV = coefficient of variation

Table 11.13 Statistics of TOML LAE samples within the TOML Areas

Variable	Samples	Missing	Min (%)	Max (%)	Mean (%)	Var	CoV	Median
Abundance	161	0	0	30.77	8.65	45.745	0.78	8.78

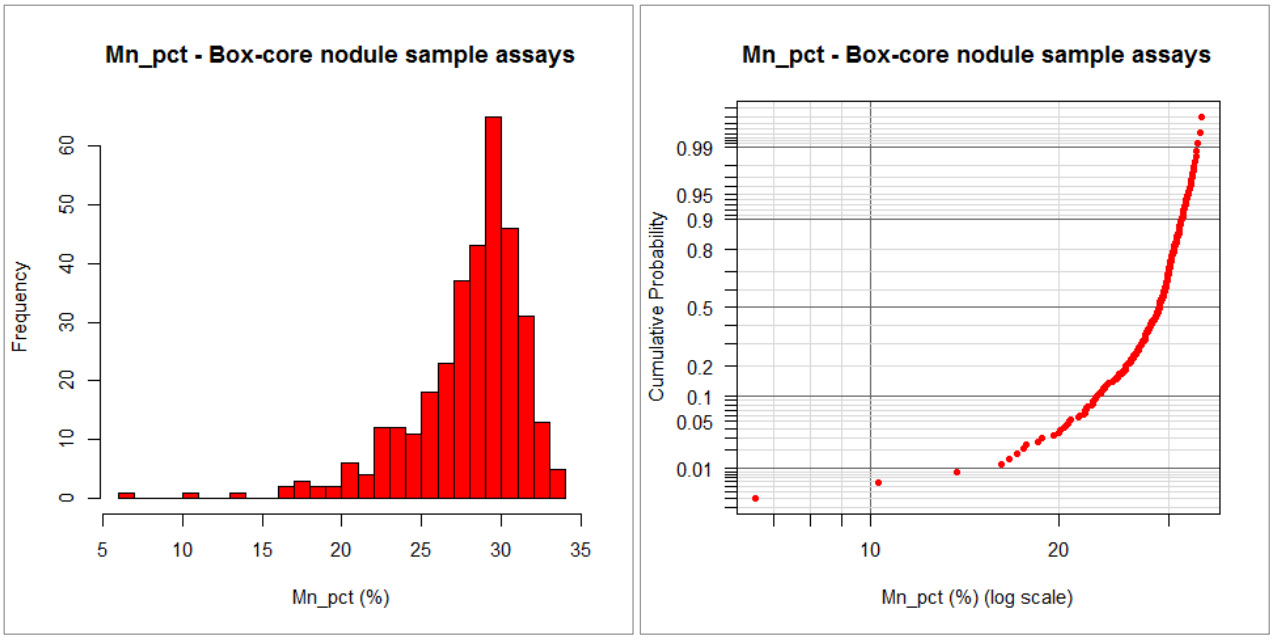
Var = variance; CoV = coefficient of variation

Figure 11.10 Histogram and log-probability plot of abundance for all samples within TOML Areas



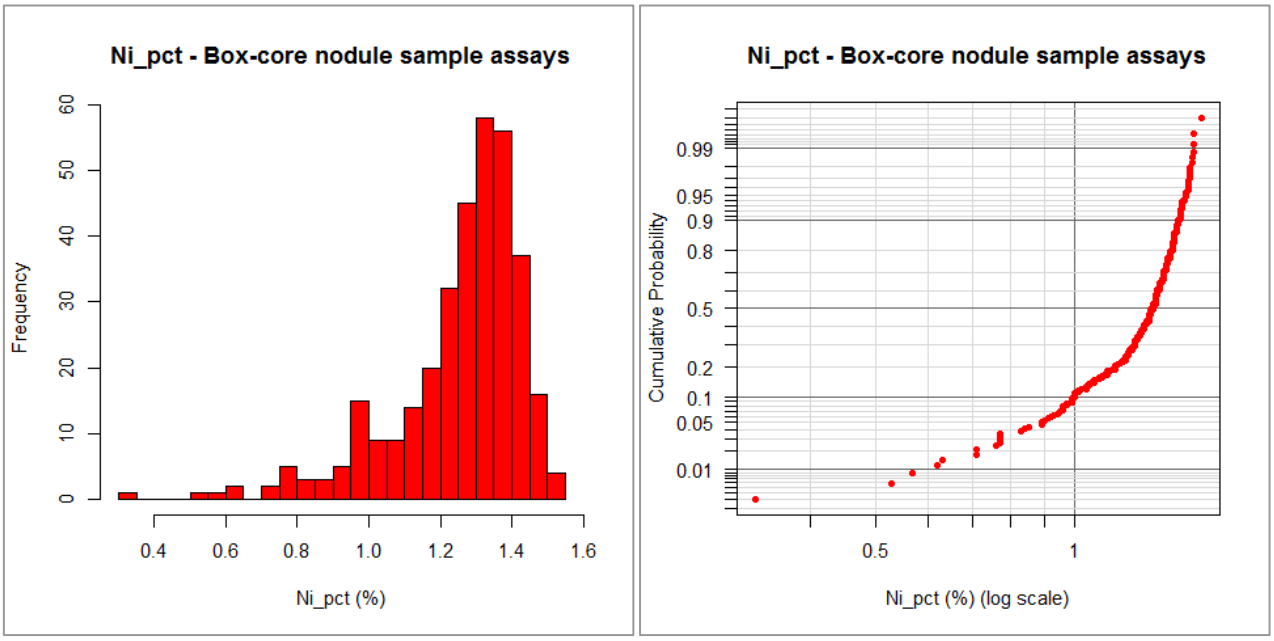
Source: TMC

Figure 11.11 Histogram and log-probability plot of Mn for all samples within TOML Areas



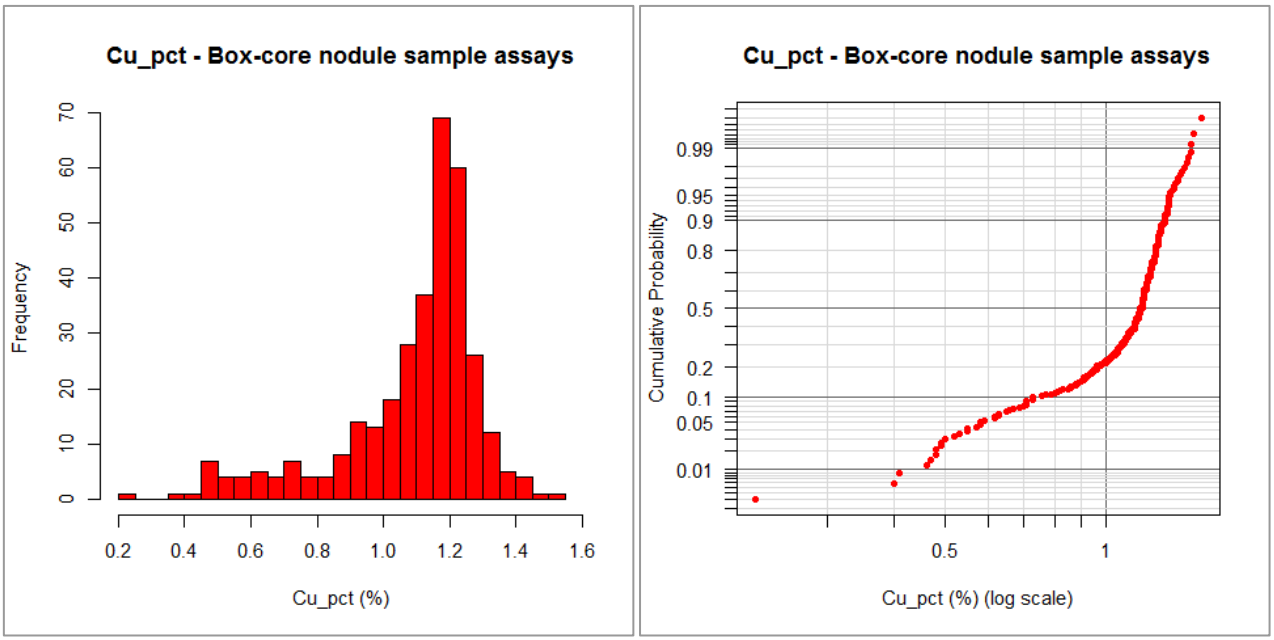
Source: TMC

Figure 11.12 Histogram and log-probability plot of Ni for all samples within TOML Areas



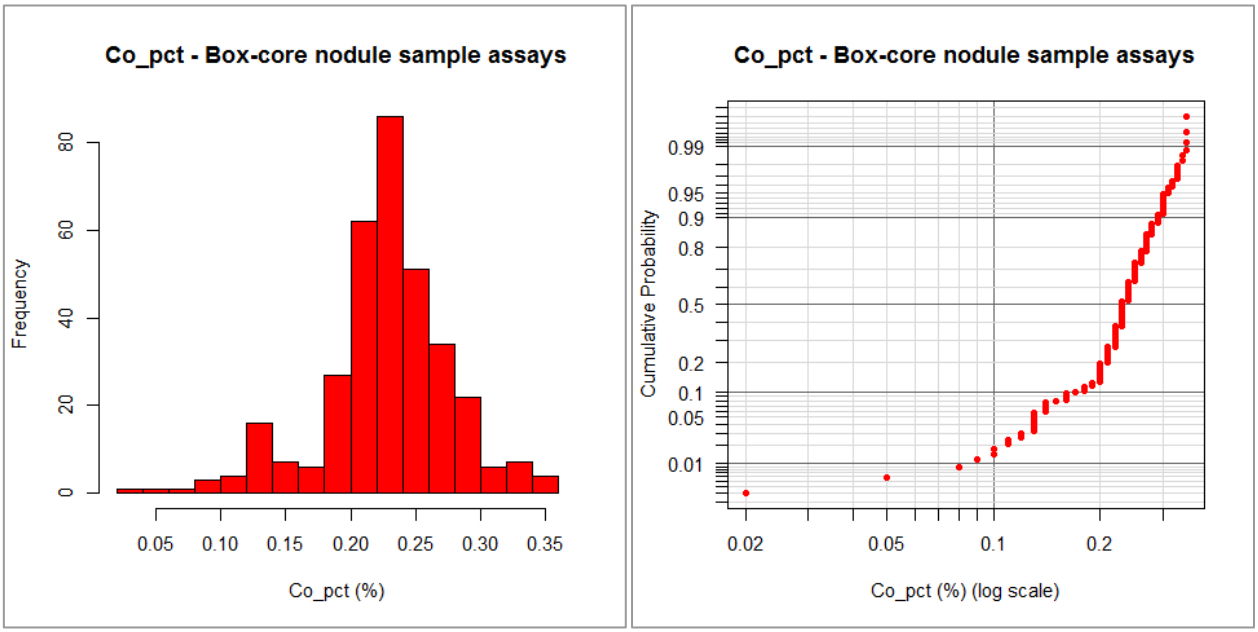
Source: TMC

Figure 11.13 Histogram and log-probability plot of Cu for all samples within TOML Areas



Source: TMC

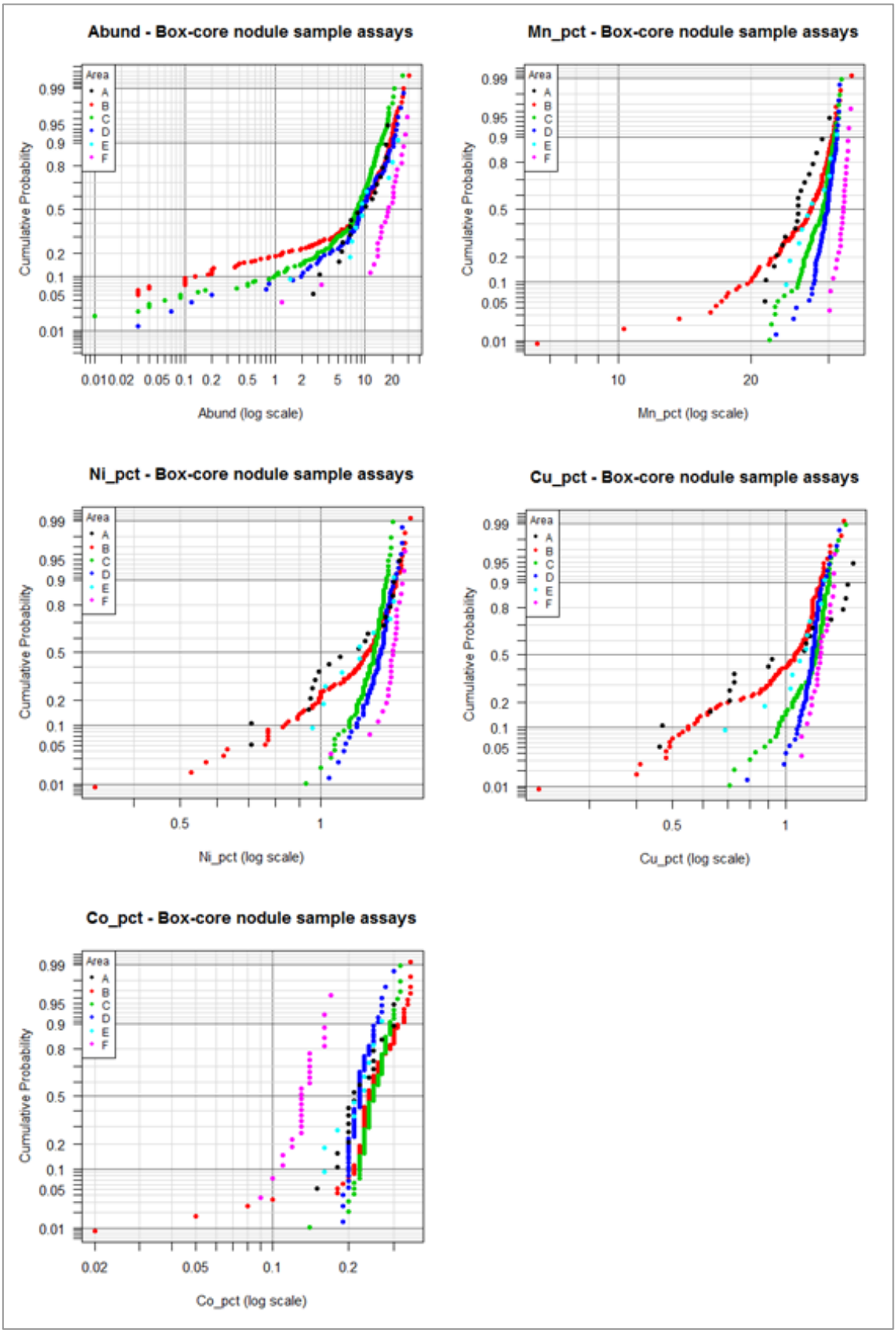
Figure 11.14 Histogram and log-probability plot of Co for all samples within TOML Areas



Source: TMC

The log-probability plots (Figure 11.15) for abundance, Mn, Ni, Cu and Co by TOML Area indicate variations in the grade distributions between the areas, as is expected from the ISA maps shown in Section 6.4. The distributions for Ni and Cu for samples in TOML-A, B and E are different than the samples in TOML-C, D and F. This feature is also present in the full CCZ data set and is interpreted to be due to regional-scale geological differences. Nodule samples from TOML-F show significantly lower Co than samples from all the other areas while Mn shows a gradual increase from TOML-A and B through to TOML-F.

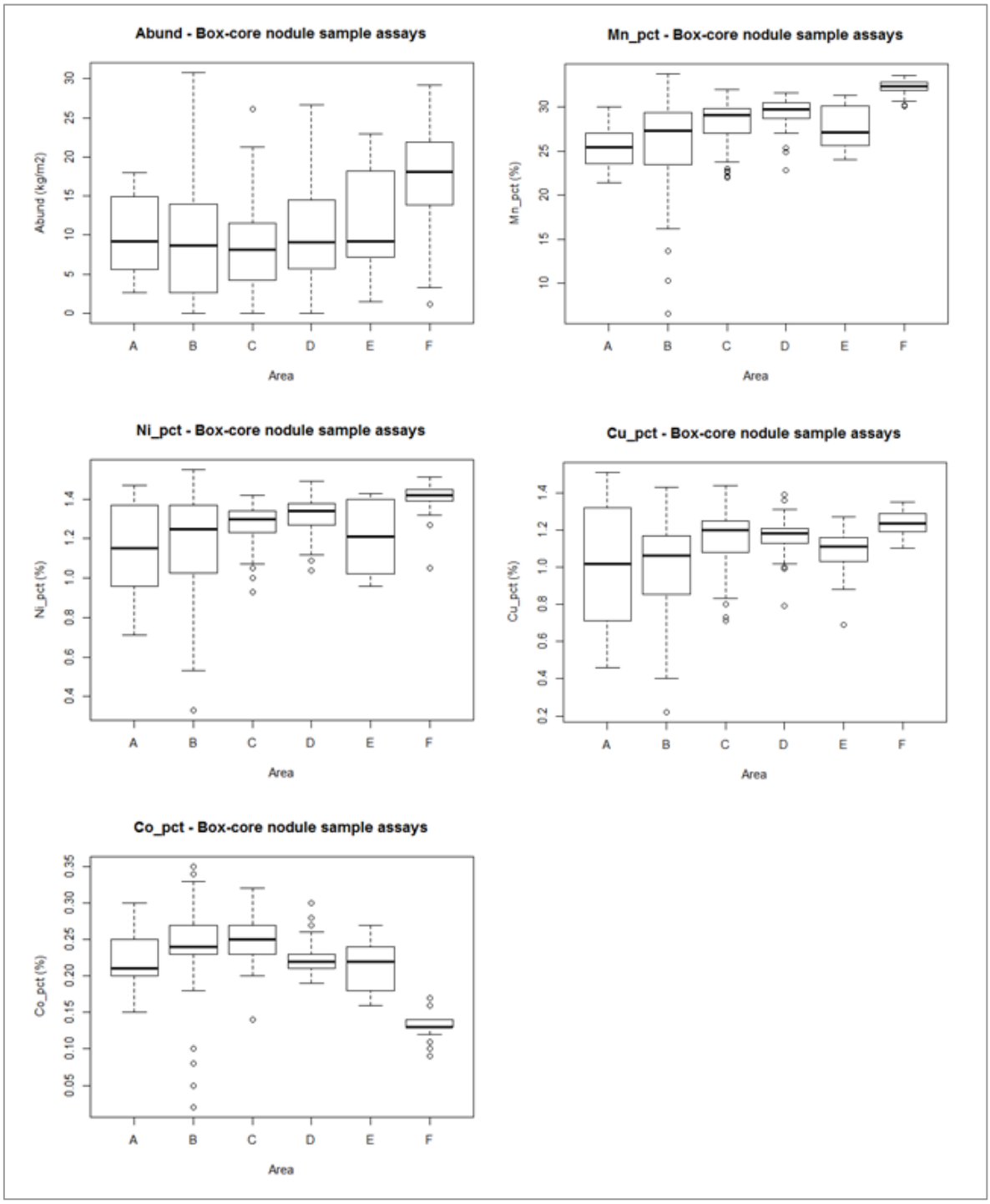
Figure 11.15 Log-probability plots for abundance, Mn, Ni, Cu and Co by TOML Areas



Source: TMC

Box plots provided in Figure 11.16 clarify the differences in assays between TOML Contract Areas. These plots also reveal that the Var in Ni and Cu is higher for TOML-A and B than the other areas. Also, TOML-E shows higher Ni Var similar to TOML-A and B. TOML-F appears to have anomalously high Mn with a much lower Var than all other areas. TOML-F appears to also have higher median Ni and Cu and significantly lower Co values.

Figure 11.16 Box plots for abundance, Mn, Ni, Cu and Co by TOML Areas



Source: TMC

The coefficients of variation for nodule abundance, Mn, Ni, Cu and Co are very small, suggesting that the application of top-cuts is not necessary. Also, the approximate natural limits for absorption of the Ni (~6.02%), Cu (~8.03) and Co (~6.60%) metals, suggested in the study by Novikov and Bogdanova (2007), are significantly higher than the maximum values (Ni=1.55%, Cu=1.51%, Co=0.35%) in the data. This suggests that all the Ni, Cu and Co values are within natural limits. The presence of outliers (or 'extreme' values) was assessed by examining the summary statistics and probability plots. No outliers were detected. Top cuts were not applied to the data prior to grade estimation.

11.3.4 Representativeness of sampling

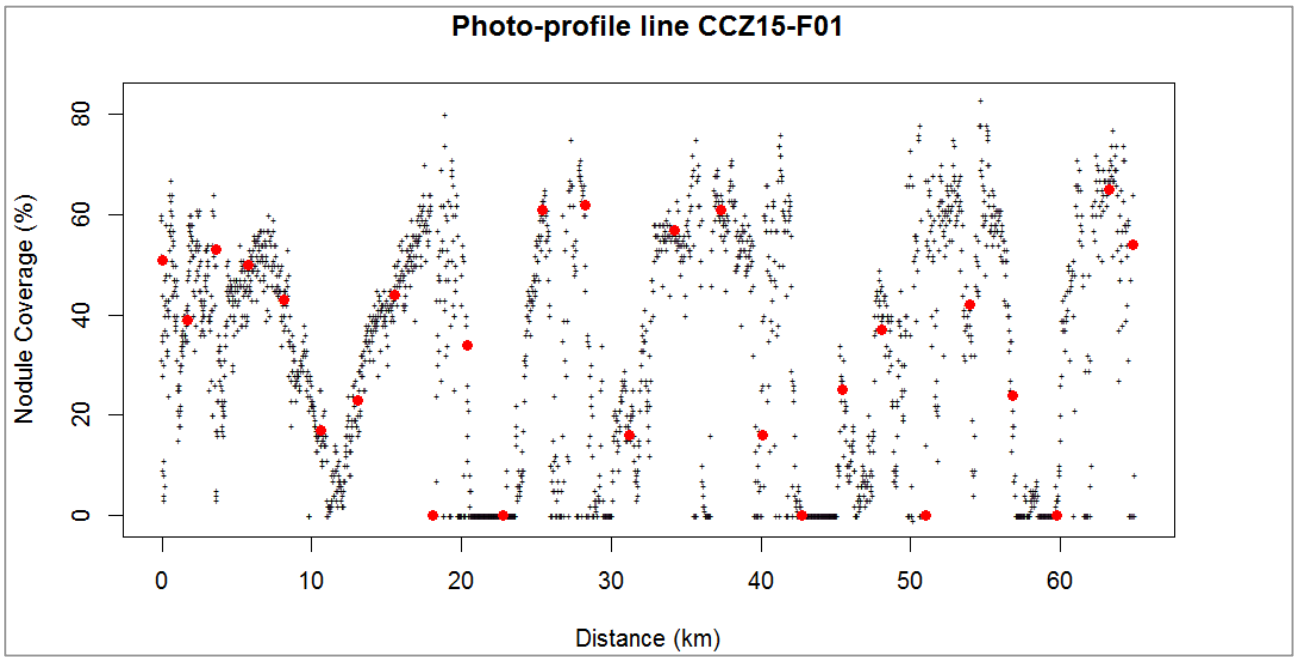
Box core sampling by TOML in 2015 confirmed the presence of nodules at similar grade and abundance to the wider spaced sampling by Pioneer Contractors.

The representativeness of the sampling with respect to the abundance of nodules and continuity across the seafloor was examined using sea floor photographs. TOML collected continuous sea floor photo profiles along three (3) lines in TOML-B1 and four (4) lines in TOML-C. From these photos it is possible to derive the nodule coverage (%) using automated image processing techniques.

The percent nodule coverage is the amount of image pixels identified as nodules divided by the total number of pixels in the photo. It is also possible to use the LAE method for determining nodule abundance. Figure 11.17 shows the nodule coverage for one of the lines that cross the TOML sub-area B1. These plots show the presence of nodules between BC locations. The average distance between each photo is approximately 25 m and ranges from 5 m to 79 m.

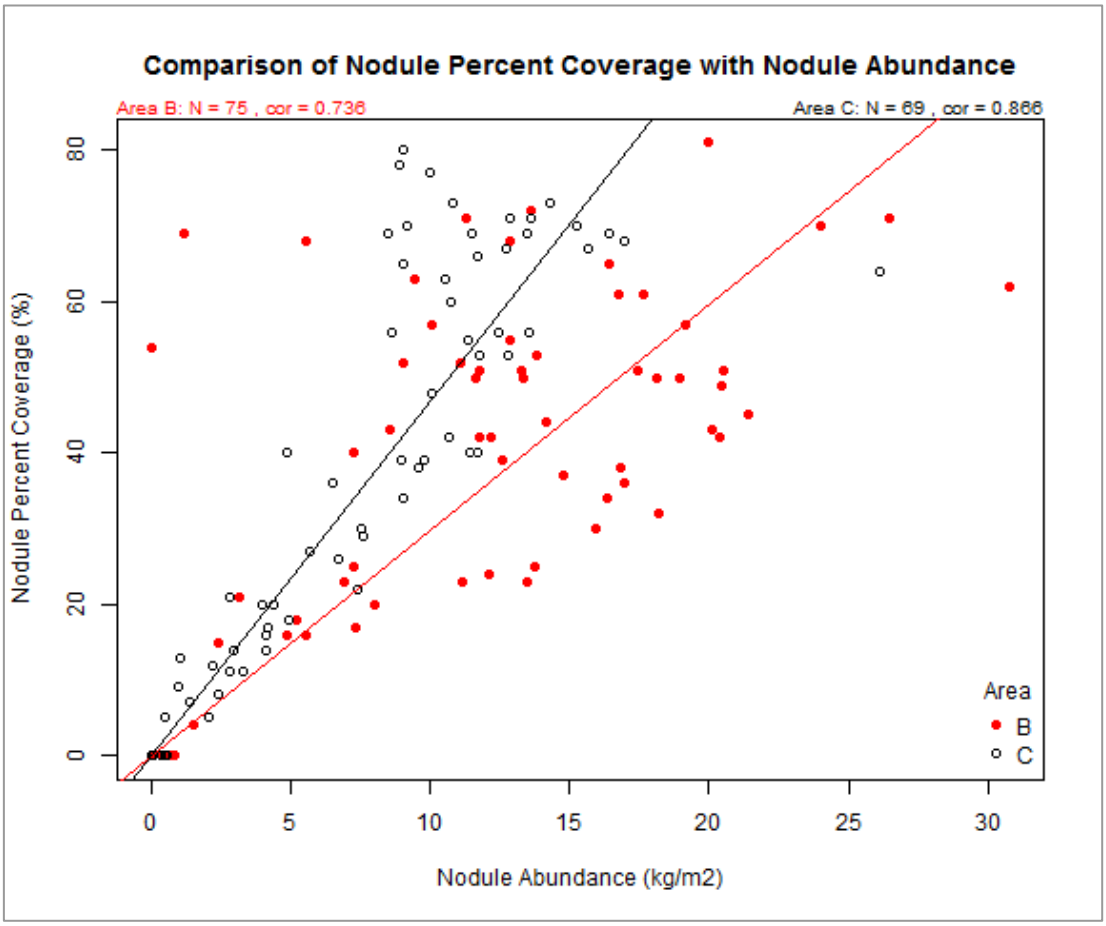
Figure 11.17 also shows the location of the images from which abundance was estimated using the LAE method. Nodule coverage estimated from the sea floor photos shows a positive correlation with nodule abundance from LAE (Figure 11.18).

Figure 11.17 Photo-profile line CCZ15-F01 that crosses TOML-B1



Source: TMC
Red dots – nodule coverage for seafloor photos which were used in the manual estimate of abundance using the long-axis estimation method and used in the Mineral Resource estimate. Black dots – nodule abundance for all other seafloor photos.

Figure 11.18 Comparison of nodule coverage against nodule abundance



Source: TMC

There is also very good agreement between the nodule abundance estimated from automated analysis of the seafloor photos and the nodule abundance estimated from manual measurement of the nodule long-axis (Figure 11.19).

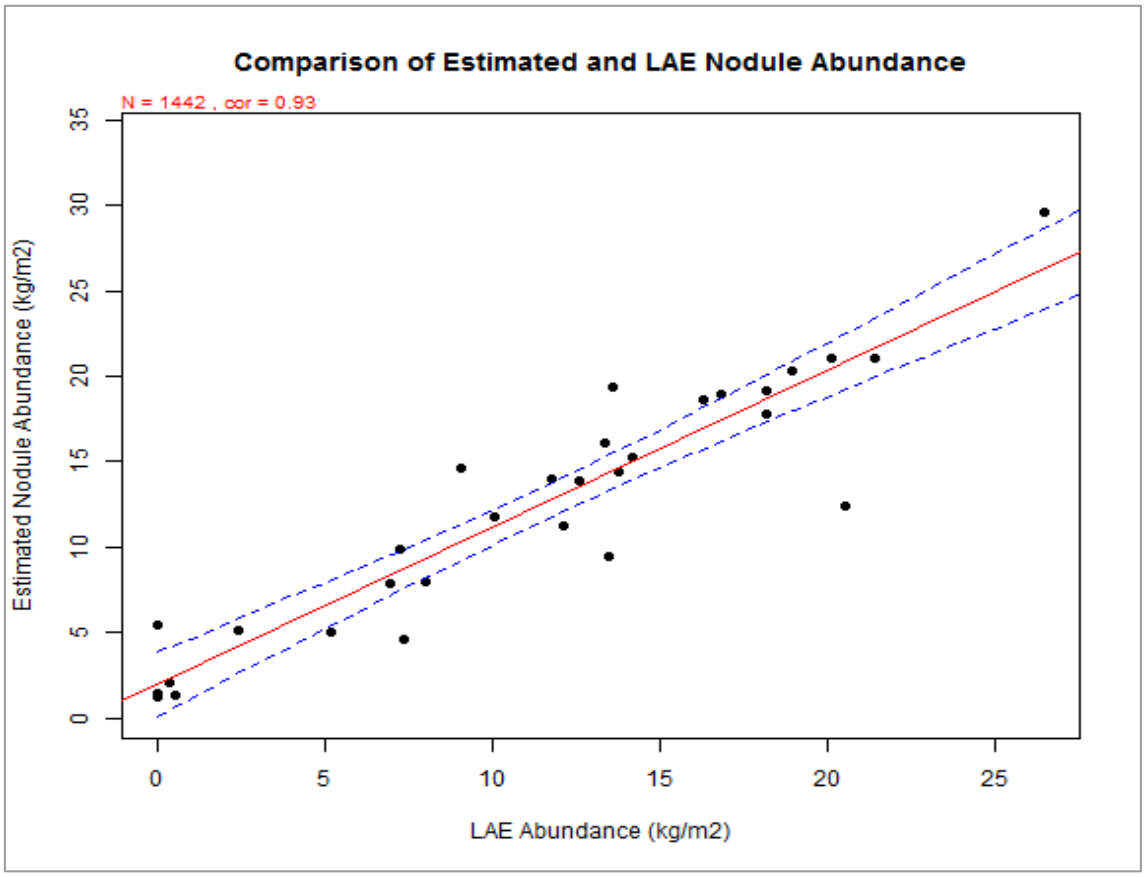
Figure 11.20 to Figure 11.22 show plots of the nodule abundance estimated from the seafloor photos. Note that the distance between each photo is approximately 30 m. The plots show that, notwithstanding short scale fluctuations, abundance varies gradually in a structured manner over many kilometers.

Polymetallic nodule grades (Table 11.9) within the CCZ have very low coefficients of variation which indicate a low risk in estimating grades and that ordinary kriging is an appropriate technique to use for estimation. The dredge sampling program conducted by TOML on polymetallic nodules during their 2013 campaign, included analysis of multiple individual nodules taken from each dredge sample. It confirmed the very low Var in the nodule grades at the local scale.

Variograms of the polymetallic nodule grades of Mn, Ni, Cu and Co within the TOML Area show reasonable spatial continuity with ranges greater than the average sample spacing. The long variogram ranges for the nodule grades reflect the very large-scale diffuse distribution of metals within the ocean water column and that the manganese acts like a sponge absorbing the metals. The variogram for abundance, on the other hand, has significantly shorter ranges. This reflects the mechanism of nodule formation and the less continuous distribution of nodules.

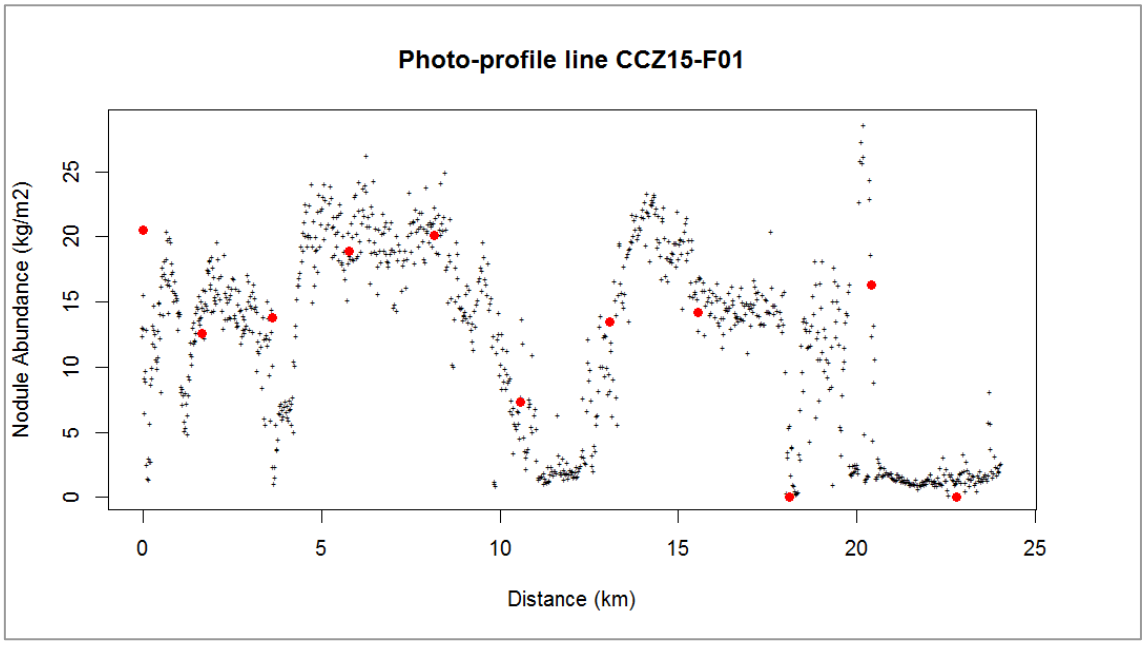
The Qualified Person considers that the BC and free fall grab sample spacing within the TOML-A to F are sufficient to demonstrate continuity of Mn, Ni, Cu and Co. The addition of photo profiling enables confidence in the continuity of nodule abundance.

Figure 11.19 Comparison of nodule abundance estimated from photos against nodule abundance estimated manually using the LAE method



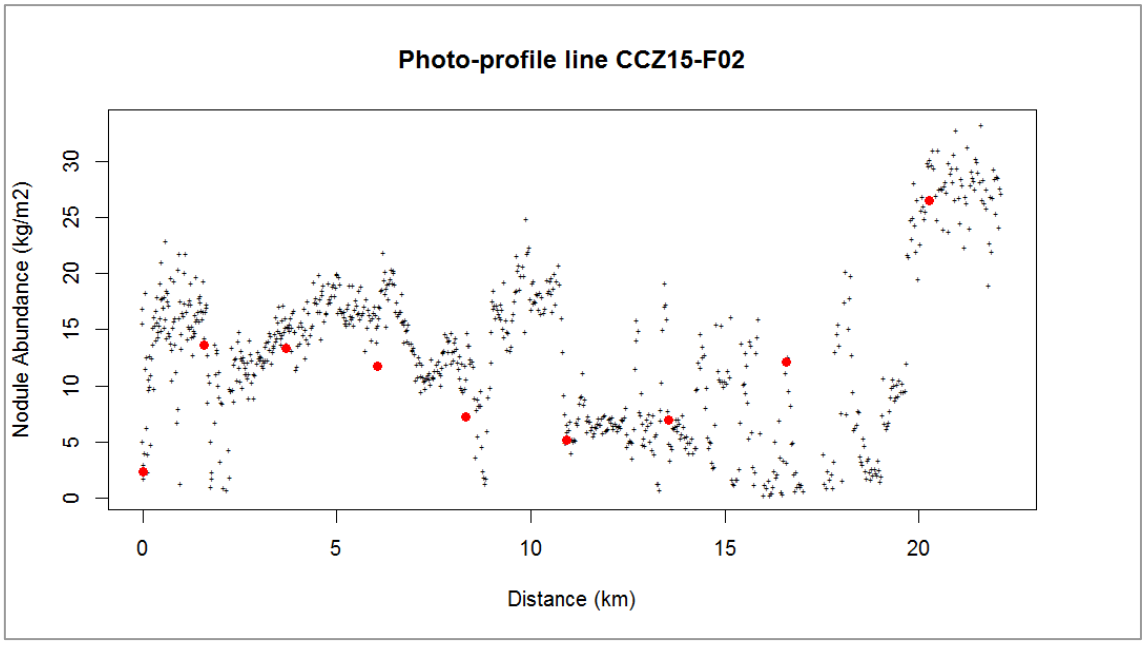
Source: TMC. Note: The red line is the fitted linear regression. The blue dashed lines are the 95% confidence intervals for the linear regression model.

Figure 11.20 Nodule abundance photo-profile line CCZ15-F01 that crosses sub-area B1 Measured Mineral Resource



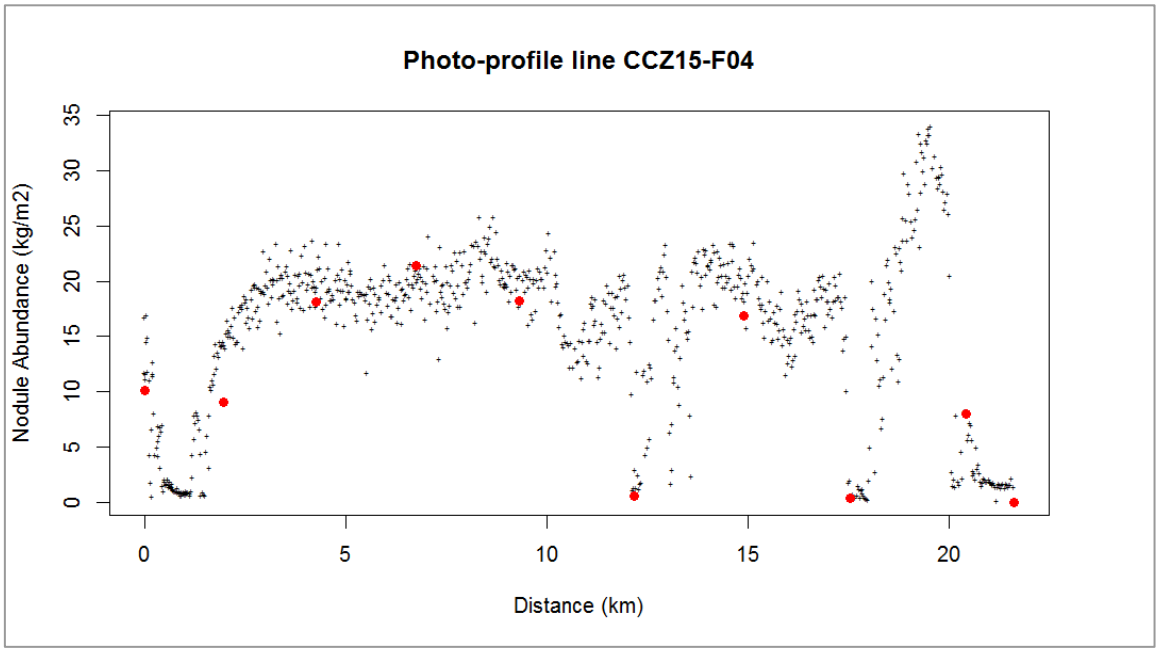
Source: TMC. Note: Red dots – nodule coverage for seafloor photos which were used in the manual estimate of abundance using the long-axis estimation method and used in the Mineral Resource estimate. Black dots – nodule abundance for all other seafloor photos.

Figure 11.21 Nodule abundance photo-profile line CCZ15-F02 that crosses sub-area B1 Measured Mineral Resource



Source: TMC. Note: Red dots – nodule coverage for seafloor photos which were used in the manual estimate of abundance using the long-axis estimation method and used in the Mineral Resource estimate. Black dots – nodule abundance for all other seafloor photos.

Figure 11.22 Nodule abundance photo-profile line CCZ15-F04 that crosses sub-area B1 Measured Mineral Resource

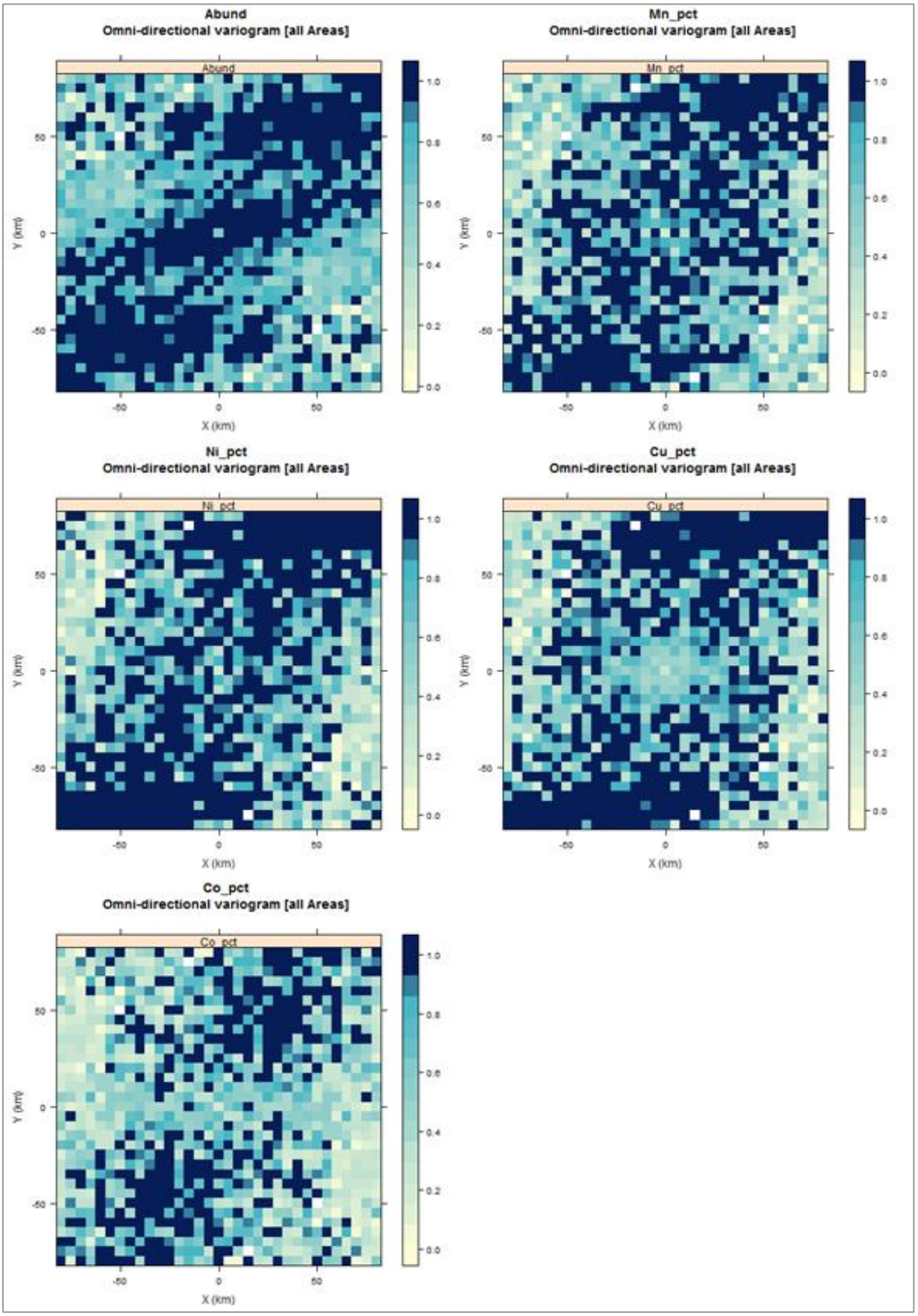


Source: TMC. Note: Red dots – nodule coverage for seafloor photos which were used in the manual estimate of abundance using the long-axis estimation method and used in the Mineral Resource estimate.
Black dots – nodule abundance for all other seafloor photos.

11.3.5 Spatial continuity

All nodule samples (historical BC and free fall-grabs, TOML BC and photos) within the TOML Contract Area were combined and used for analysis of spatial continuity. The experimental semi-variograms were scaled to the population Var. Variogram maps (Figure 11.23) were calculated for the purpose of determining the direction of greatest continuity.

Figure 11.23 Semi-variogram maps for abundance, Mn, Ni, Cu and Co



Source: TMC

Spherical semi-variogram models were fitted to the experimental variograms using two structures (Figure 11.24 to Source: TMC

Figure 11.28, Table 11.14). Where possible, consistent parameters were used between the fitted variogram models for each direction and each of the variables. This was done to ensure element relationships or correlations evident between samples are respected implicitly during estimation and reflected in the resource estimate. Also, the same type of variogram model was fitted to the experimental semi-variograms.

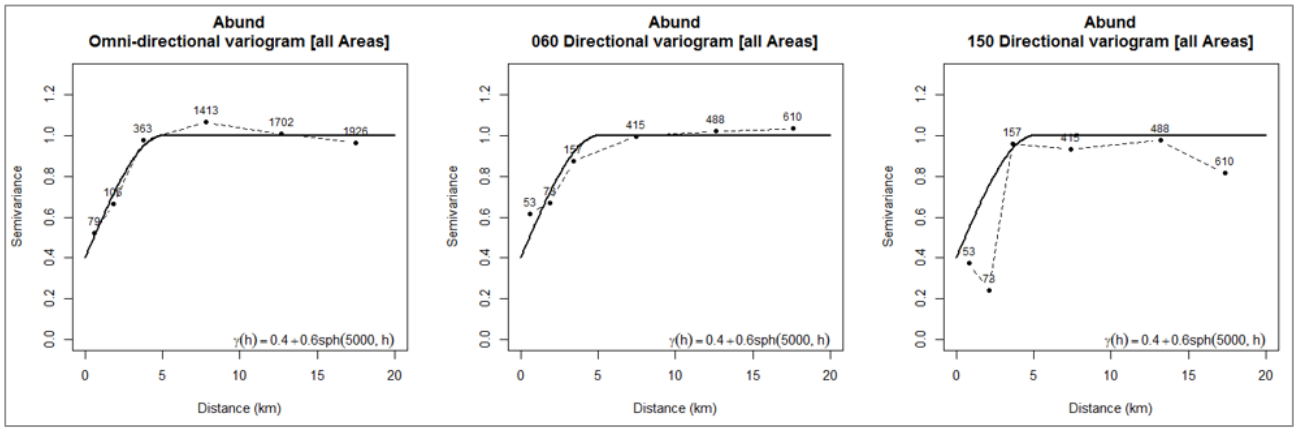
The directions of greatest continuity deduced from the variogram maps appear to be approximately 150° and 060°. Abundance and Cu show no anisotropy in the variogram ranges while Mn and Ni appear to show greater continuity in the 150° direction and Co shows greater continuity in the 060° direction. The 060° direction is roughly parallel to the broad regional trend of the CCZ and the 150° direction is parallel to the abyssal hills. Smaller scale local trends oriented parallel with bathymetry ridges are not visible in the wide spaced data.

The variogram models listed in Table 11.14 were used in estimating the values for nodule abundance, Mn, Ni, Cu and Co.

Table 11.14 Variogram models

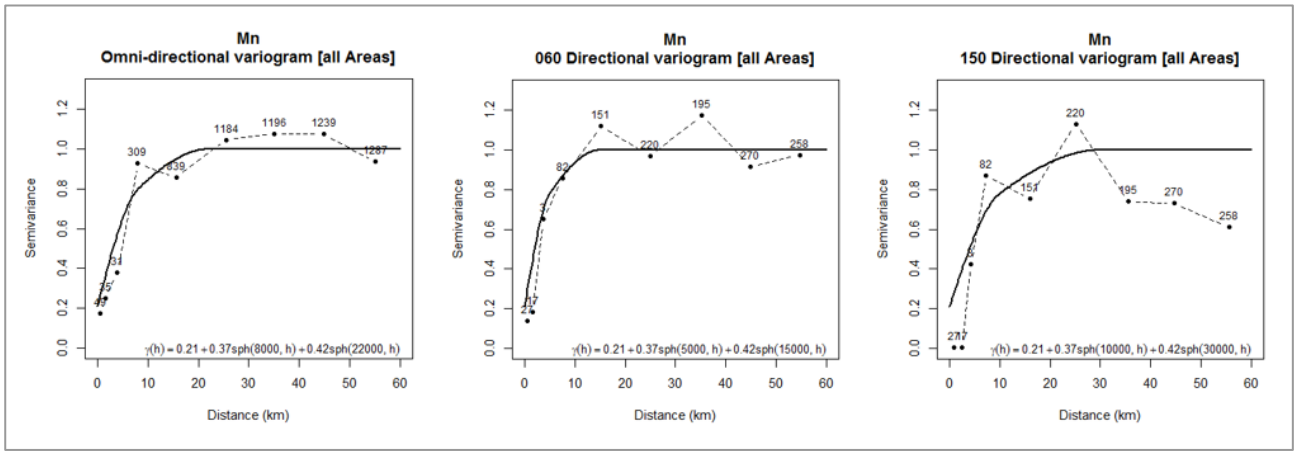
Variable	Nugget	Spherical Structure 1			Spherical Structure 2			Anisotropy Ratio
	C0	C1	Range H1		C2	Range H2		
			060° (km)	150° (km)		060° (km)	150° (km)	
Abundance	0.40	0.60	5	5	–	–	–	1.0
Mn	0.21	0.37	5	10	0.42	15	30	0.5
Ni	0.21	0.37	5	10	0.42	15	30	0.5
Cu	0.21	0.37	22	22	0.42	70	70	1.0
Co	0.21	0.37	22	16	0.42	70	50	0.714

Figure 11.24 Abundance omni-directional, 060° and 150° directional variograms



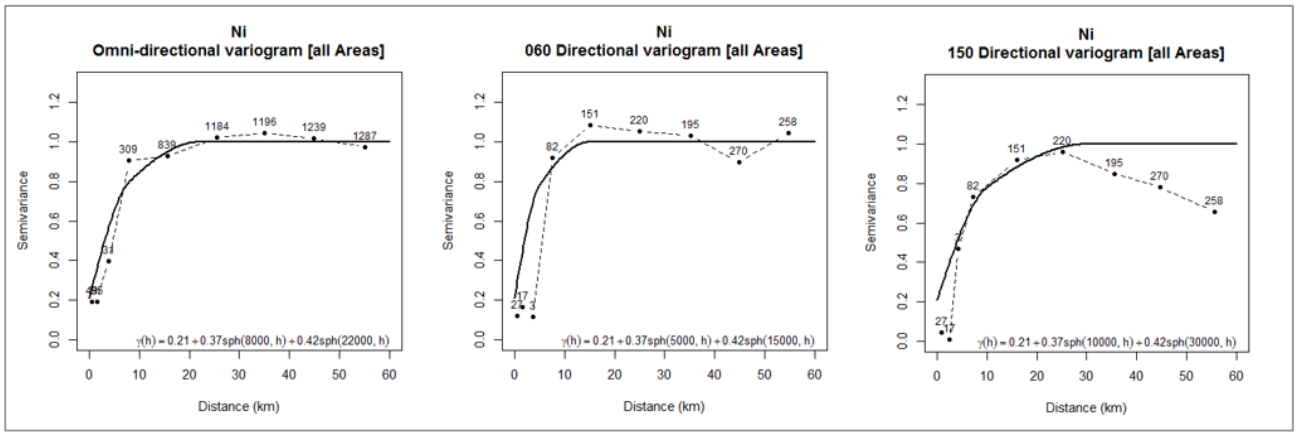
Source: TMC

Figure 11.25 Mn omni-directional, 060° and 150° directional variograms



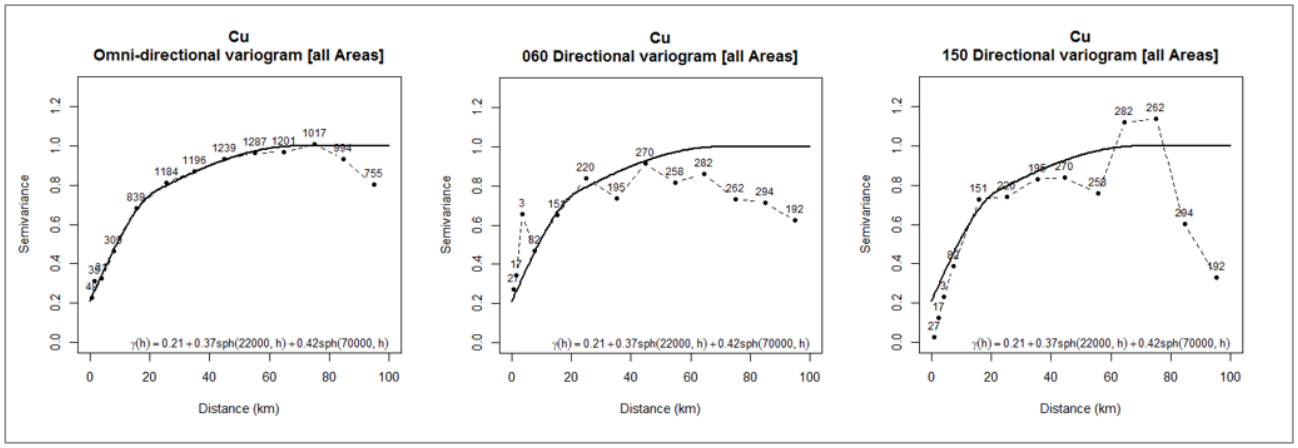
Source: TMC

Figure 11.26 Ni omni-directional, 060° and 150° directional variograms



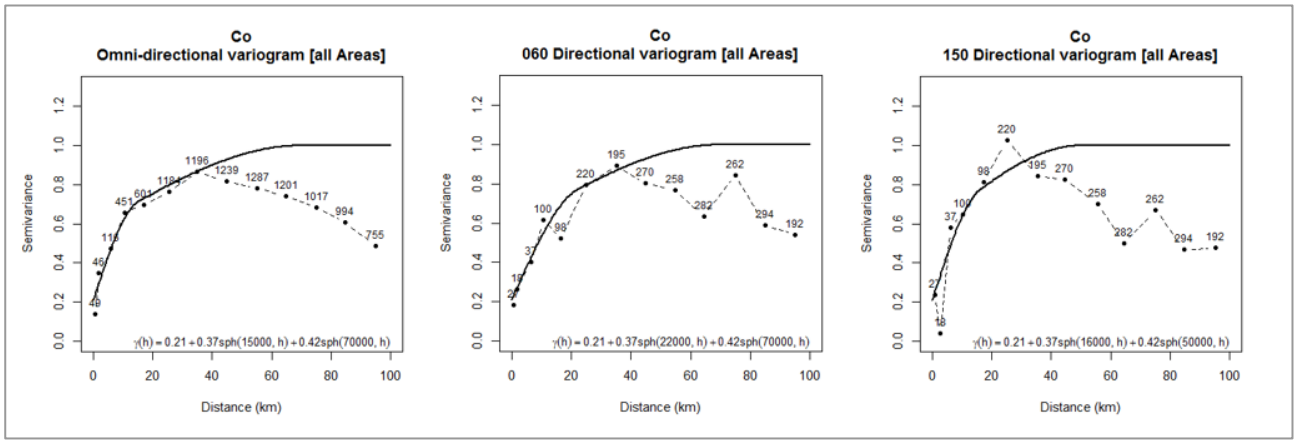
Source: TMC

Figure 11.27 Cu omni-directional, 060° and 150° directional variograms



Source: TMC

Figure 11.28 Co omni-directional, 060° and 150° directional variograms



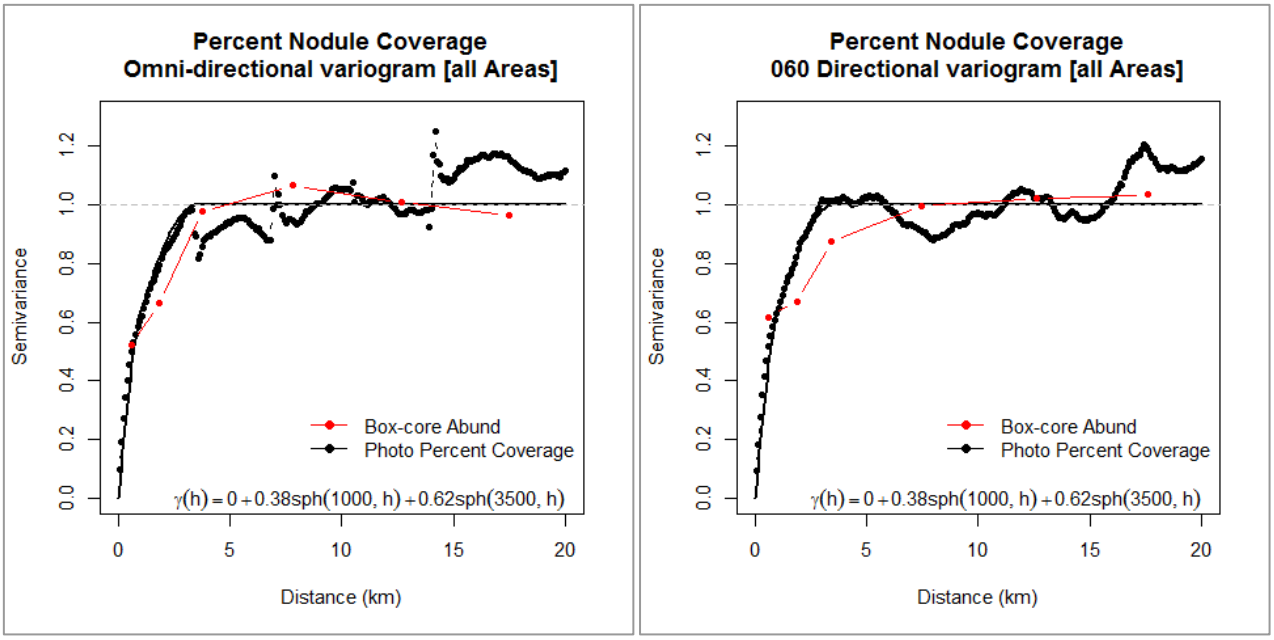
Source: TMC

11.3.6 Variography of nodule coverage estimated from photo profiles

The continuity of nodule abundance as measured by the abundance variograms was checked by using the photo profile data.

The omni-directional and 060° directional variograms (Figure 11.29) for the nodule coverage (%) estimated from the sea floor photos are similar to the variograms of abundance calculated from the physical samples. The range of nodule coverage is slightly shorter than the range of the abundance calculated from the physical samples. The large number of close spaced photos allows for a better estimate of the very short-range spatial variability and nugget. The periodic fluctuations evident in the sill at ranges of approximately 7.5 km and 15 km could be related to the spacing between the abyssal hills.

Figure 11.29 Omni-directional and 060° directional variograms for nodule coverage estimated from sea floor photos



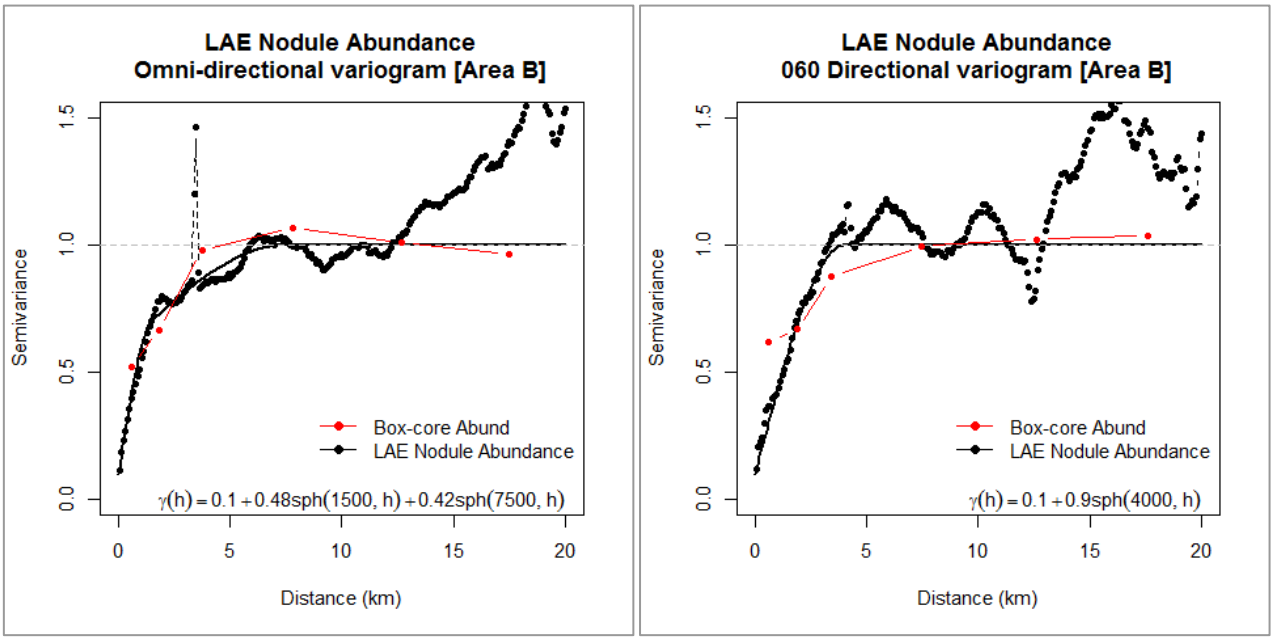
Source: TMC

11.3.7 Variography of nodule abundance estimated from photo profiles

The nodule abundance estimates derived from the seafloor photos using the LAE method were used to check the continuity of nodule abundance and compared with the variograms from the physical sample data.

Compared with the nodule coverage variograms (Figure 11.29), the LAE nodule abundance omni-directional variograms (Figure 11.30) show a slightly longer range of 7,500 m. The same periodic fluctuations evident in the nodule coverage variograms are also present in the 060° directional variogram while the omni-directional variogram hints at the presence of a long-range trend in the data. The omni-directional variogram is very similar to the nodule sample variogram but again shows a very low nugget Var.

Figure 11.30 Omni-directional and 060° directional variograms for nodule abundance estimated using the LAE method from sea floor photos

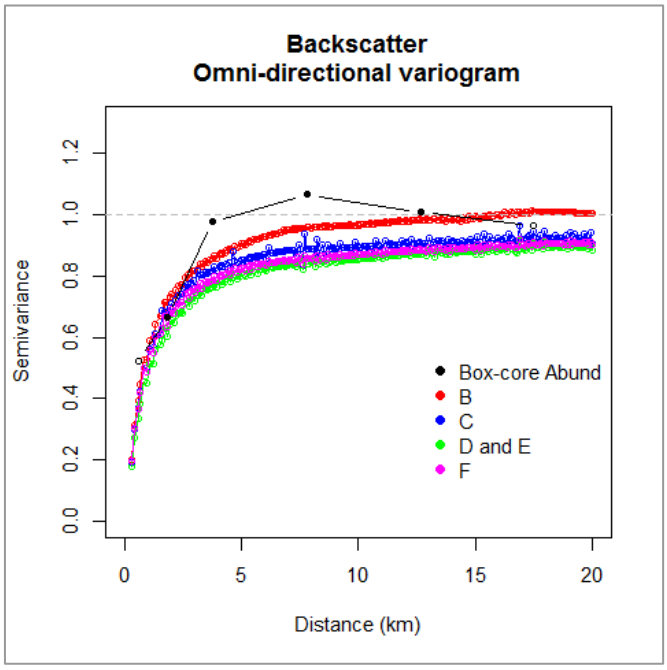


Source: TMC

11.3.8 Variography of the backscatter data

The backscatter data shows limited correlation with abundance but, in a broad sense, can be used to delineate zones of nodules from zones with very low to no nodules (the no nodule (NON) domain). Omni-directional variograms (Figure 11.31) of the backscatter values indicate spatial continuity that is consistent with the nodule sample data. The omni-directional variogram of the nodule sample data has a shorter range than the backscatter variograms but with similar very short range spatial variability. TOML-B has the shortest range of the backscatter variograms and TOML-D and E have the longest.

Figure 11.31 Omni-directional variograms for backscatter values



Source: TMC

11.3.9 Geological block model

Six block models were constructed, one for each TOML Contract Area (A through to F). Each model was blocked according to the data spacing. Blocks of 1.75 km by 1.75 km were used to fill the areas tested by BC and photo profiles on a 3.5 km by 3.0 km grid (Measured Mineral Resource). Blocks of 3.5 km by 3.5 km were used to fill areas tested by BC sampling on a nominal spacing of approximately 7 km by 7 km (Indicated Mineral Resources), while the remainder were filled with blocks of 7.0 km by 7.0 km (Inferred Mineral Resources). Sub-cells with dimensions of 0.875 km by 0.875 km were used to accurately represent the boundaries of the TOML Areas, the areas interpreted to contain no nodules and the boundaries between Measured and Indicated.

The total area of the block model is 74,683 km^2 which is 99.96% of the actual total area of the TOML Areas of 74,713 km^2 (Table 11.15). This indicates that the sub-blocks provided satisfactory resolution for estimating the Area boundaries.

Table 11.15 Comparison of model areas and actual license areas

Area	Actual Area (m^2)	Model Area (m^2)	Percent Difference
TOML-A	10 280.560	10 309.141	0.278
TOML-B	9 966.266	9 950.062	–0.163
TOML-C	15 763.385	15 785.656	0.141
TOML-D and E	22 882.804	22 843.953	–0.170
TOML-F	15 819.900	15 794.078	–0.163
All	74 712.915	74 682.891	–0.04

11.3.10 Mineral Resource estimation

Ordinary Kriging (OK) was used to estimate abundance, Mn, Ni, Cu and Co into the block model. Grades were estimated on a parent block basis using block discretization of 5 by 5 by 1. Grades were also estimated using NN and IDW to the power of 2 for validation of the OK estimates. Blocks and sub-blocks within the NON domain were set to zero.

Three separate estimation passes were run, one for each parent cell size. The estimates for Measured and Indicated Mineral Resource used a search range of 30 km while for Indicated and Inferred a search range of 70 km was used. A minimum of 1 and a maximum of 3 samples were allowed per octant search with a maximum of 8 samples per estimate.

The Mineral Resource model was validated by comparing the global mean and Var of the model against alternative NN and IDW estimates and the declustered samples. The mean grades compare favorably and the expected Var reduction is observed, indicating that the estimate is satisfactory.

11.3.11 Mineral Resource classification

Classification of the Mineral Resource into Measured, Indicated and Inferred categories, in accordance with SEC Regulation S-K (subpart 1300), considered: the nodule sample quality, uncertainty in the nodule sample abundance and grades, continuity of nodule abundance and grade and scale of the deposit.

- Inferred Mineral Resource classification was based on sampling by Pioneer Contractors on a nominal spacing of 20 km, the variation and uncertainty in the sample quality, and the likely presence of short-range variation to nodule abundance.
- Indicated Mineral Resource classification was based on BC sampling by TOML on a nominal spacing of approximately 7 km by 7 km (including photo profiling in some cases at 7 km by 3 km), supplemented by sampling by Pioneer Contractors.
- Measured Mineral Resource was based on BC sampling by TOML on a nominal spacing of approximately 7 km by 7 km plus photo-profiling on a nominal spacing of 3.5 km by 3.0 km, supplemented by sampling by Pioneer Contractors.

11.4 Cut-off grade

Mining operations typically use an economic value to differentiate between material that is mined to generate revenue (ore) and material that is either left behind or considered as waste. The cut-off value is derived from an economic assessment to determine the minimum grade of material that generates an acceptable profit or the minimum grade of material that allows a marketable product to be produced.

Nodules are remarkably consistent in grade and the characteristic that will contribute most to determine profitability is abundance, which is more variable. Furthermore, assessment by Allseas identified that a minimum abundance value is required to achieve the production rate required to meet annual production targets for a given collector speed. Therefore, the variable chosen to define the cut-off for definition of Mineral Resources was abundance.

The method of calculation of the cut-off determines the minimum average nodule abundance needed during steady state operations such that the revenue minus costs (excluding capital) is greater than zero. Revenue includes metal pricing and metallurgical processing recoveries, and the costs include the collection, transport, processing, corporate costs, and royalties.

Although the breakeven cut-off abundance varies slightly by area because grades vary slightly by area, a cut-off of 4 kg/m^2 abundance was chosen as a reasonable average for the NORI and TOML Areas, based on the estimates of costs and revenues presented in this report.

Assumptions used for the estimation are as described throughout this 2025 IA, the key parameters are as follows:

- Mine planning assumptions as described in Section 0, LOM basis of design (1.8 Mwmt annual tonnage mined per CV).
- Metal prices, metallurgical recoveries, and metal payabilities as described in Section 19, economic evaluation.
- Operating cost assumption as described in Section 18.
- Nodule grades as described in Section 11.5.

The abundance cut-off estimation for the areas that make up the Property are shown in Table 11.16.

Table 11.16 NORI-TOML breakeven cut-off abundance estimate

Area	Opex ($/wmt)	Production (m^2/hr)	Nodule Revenue ($/wmt)	Opex per hour ($/hr)	Breakeven Abundance (kg/m^2)	Revenue per hour ($/hr)
NORI A	188	33,660	484	61,339	3.8	61,339
NORI B	188	33,660	517	61,339	3.5	61,339
NORI C	188	33,660	465	61,339	3.9	61,339
TOML A	188	33,660	430	61,339	4.2	61,339
TOML B	188	33,660	458	61,339	4.0	61,339
TOML C	188	33,660	491	61,339	3.7	61,339
TOML D	188	33,660	492	61,339	3.7	61,339
TOML E	188	33,660	478	61,339	3.8	61,339
TOML F	188	33,660	488	61,339	3.7	61,339

The calculations indicate that a cut-off of 4 kg/m^2 abundance, as has been used for Mineral Resource estimates in NORI Area D, is appropriate for definition of the Mineral Resources in NORI -A, B, and C and TOML -A, B, C, D, E and F.

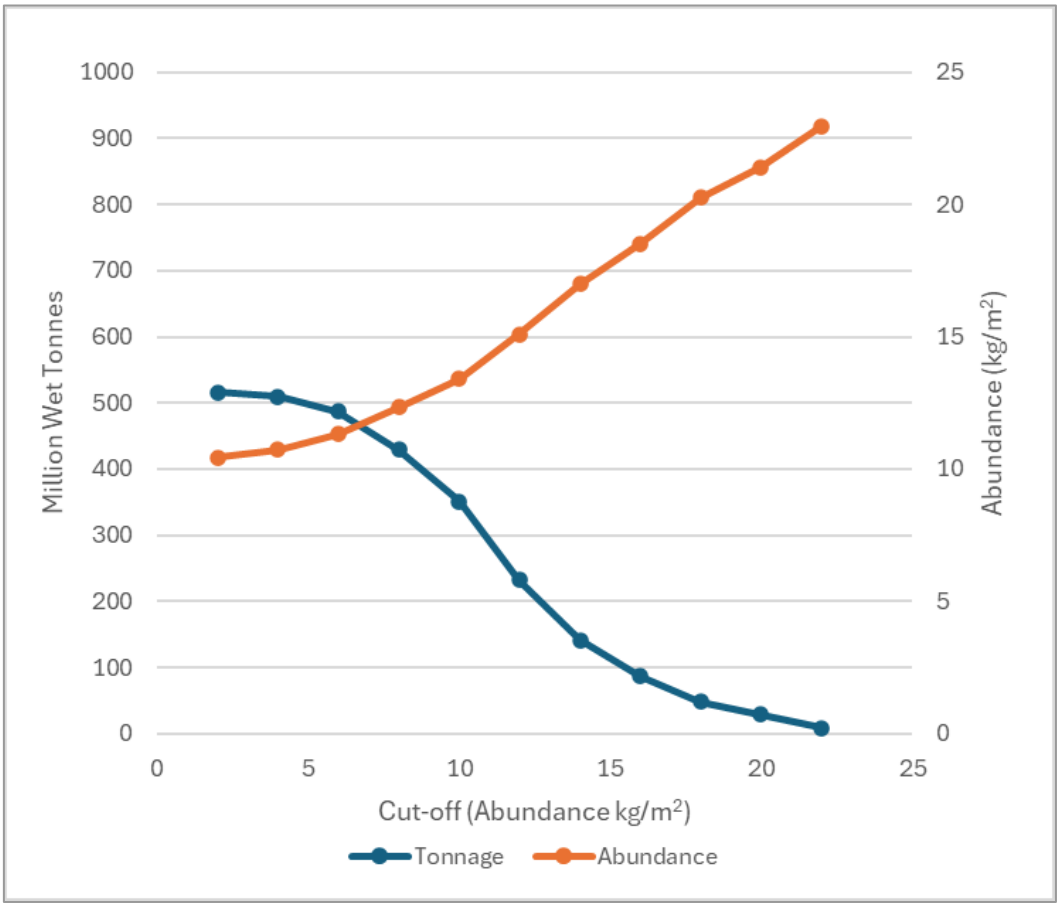
11.5 Estimation results

11.5.1 NORI-A, B and C

The nodule abundance and tonnage curves for various nodule abundance cut-offs (kg/m^2) are presented in Figure 11.32. The curves indicate rapid reduction in global tonnage between abundance cut-offs of approximately 6 to 20 kg/m^2, which brackets the mean abundance for the NORI Area.

The Mineral Resources, with an effective date of 31 December 2020, are reported in Table 11.17 at an abundance cut-off value of 4 kg/m^2. This cut-off is justified by the estimates of costs and revenues presented in Section 11.4.

Figure 11.32 Combined NORI-A, B and C abundance tonnage curves



Source: AMC

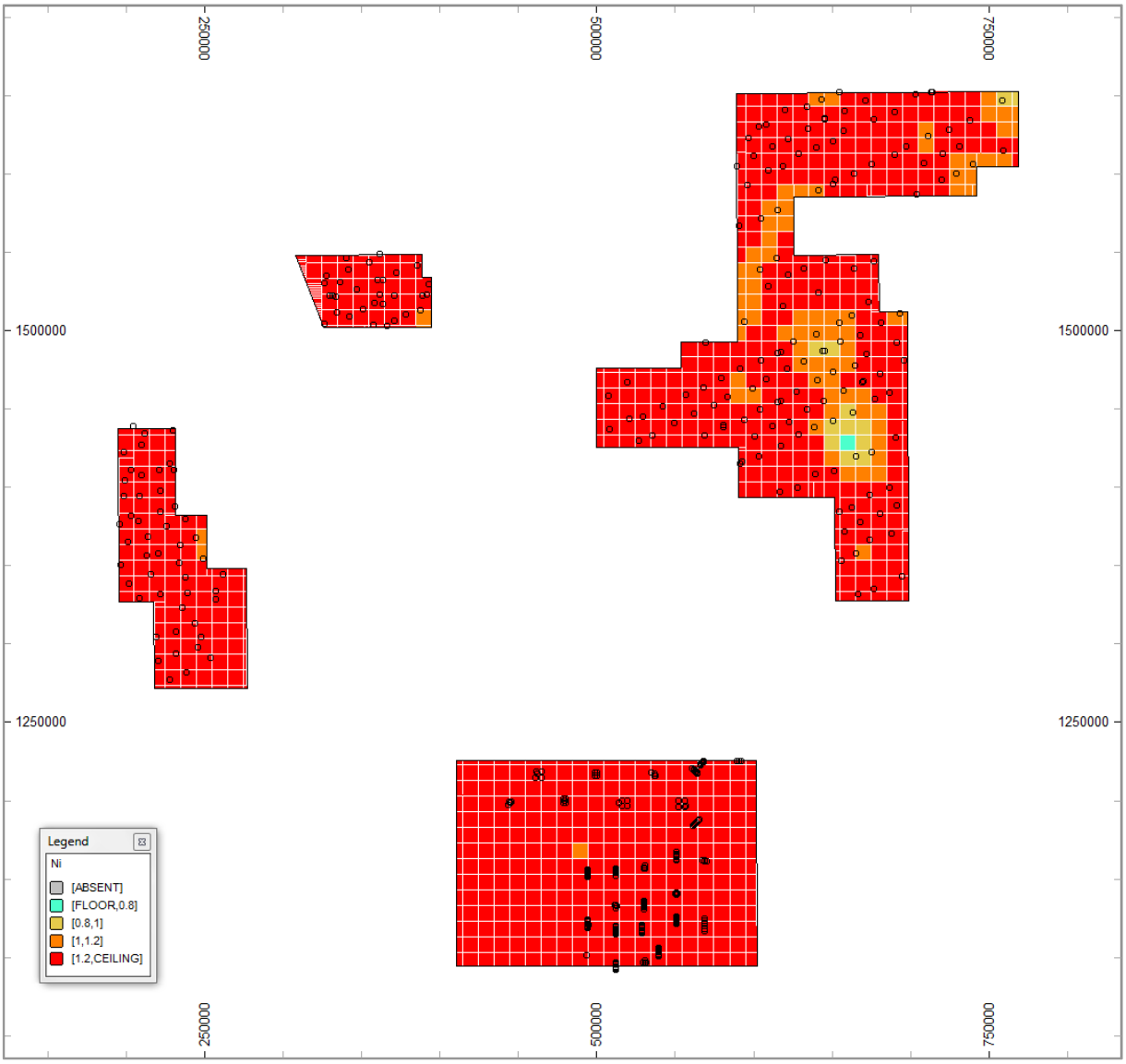
Table 11.17 NORI-A, B and C Mineral Resource estimate, in situ, at 4 kg/m² abundance cut-off

NORI Area	Category	Nodule tonnage (Mt (wet))	Abundance (wet kg/m²)	Ni (%)	Cu (%)	Co (%)	Mn (%)
NORI-A	Inferred	72	9.4	1.35	1.06	0.22	28.0
NORI-B	Inferred	36	11	1.43	1.13	0.25	28.9
NORI-C	Inferred	402	11	1.26	1.03	0.21	28.3

Source: Golder 2015. Note: Tonnes are quoted on a wet basis and grades are quoted on a dry basis, which is common practice for bulk commodities. Moisture content was estimated to be 24% w/w. These estimates are presented on an undiluted basis without adjustment for resource recovery.

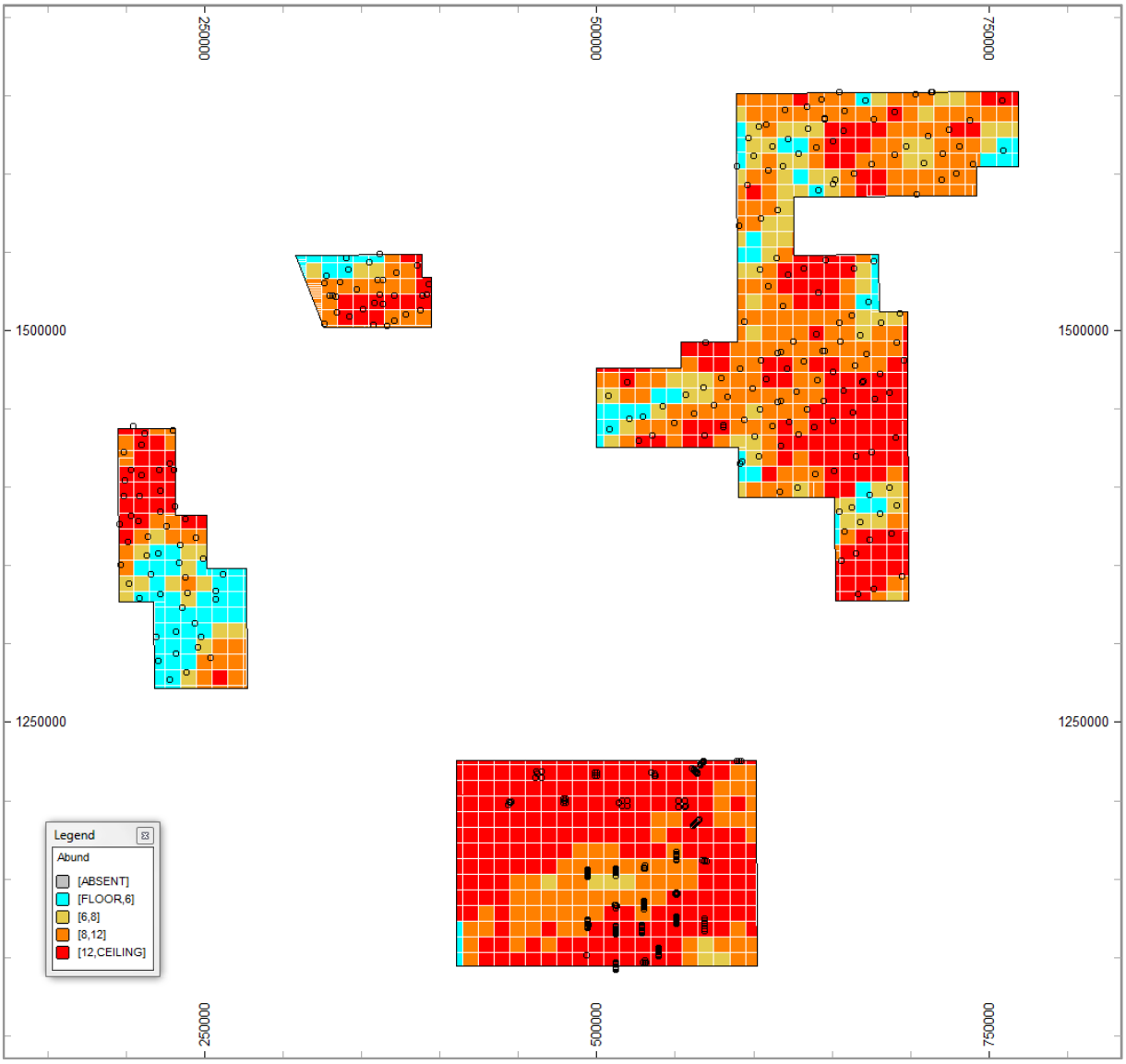
Figure 11.33 shows sample locations and estimated block grades for nickel and Figure 11.34 shows sample locations and estimated abundance. The low variability of the estimates is consistent with the homogenous nature of the nodule chemistry across the NORI Area.

Figure 11.33 Map of sample distribution and block model estimates of nickel, NORI 2012 estimates



Source: TMC. Note: NB: Areas A, B, C and D cover several UTM zones but were overlaid to facilitate modelling of all areas in one model. The apparent distances between the Areas in this figure are not real distances. The estimates for NORI Area D were superseded in 2021 (AMC Consultants, 2021a)

Figure 11.34 Map of sample distribution and block model estimates of abundance, NORI 2012 estimates



Source: TMC. Note: NB: Areas A, B, C and D cover several UTM zones but were overlaid to facilitate modelling of all areas in one model. The apparent distances between the Areas in this figure are not real distances. The estimates for NORI Area D were superseded in 2021 (AMC Consultants, 2021a)

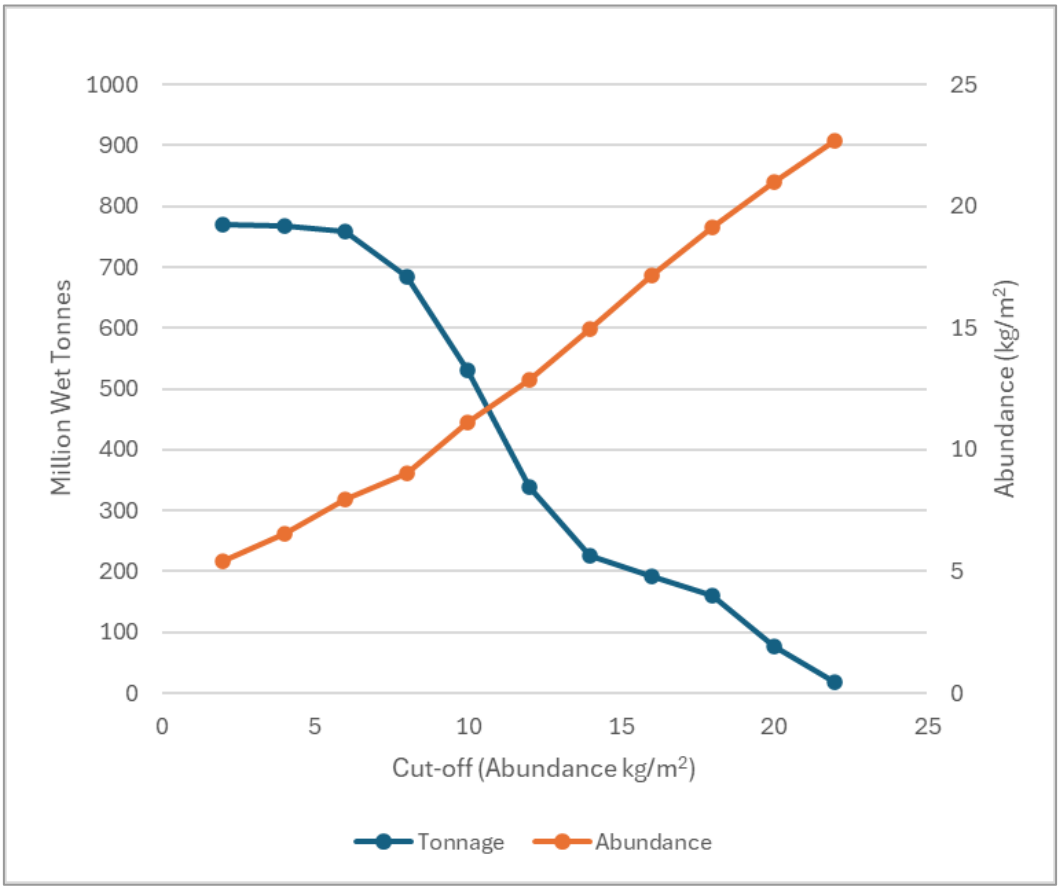
11.5.1 TOML-A, B, C, D, E and F

The nodule abundance and tonnage curves for various nodule abundance cut-offs (kg/m^2) are presented in Figure 11.35. At abundance cut-offs of 7 kg/m^2 or less the tonnage and grade are relatively insensitive. Above 7 kg/m^2, global tonnage declines rapidly.

The Mineral Resources, with an effective date of 31 December 2020, are reported in Table 11.18 at an abundance cut-off value of 4 kg/m^2. This cut-off is justified by the estimates of costs and revenues presented in this IA.

Figure 11.36 to Figure 11.40 show plans of the estimated block grades for abundance, Ni, Co, Cu, and Mn, resource class, and the sample locations. The low variability of the estimates is consistent with the homogenous nature of the nodule chemistry across the TOML Area.

Figure 11.35 Combined TOML-A, B, C, D, E and F abundance tonnage curves



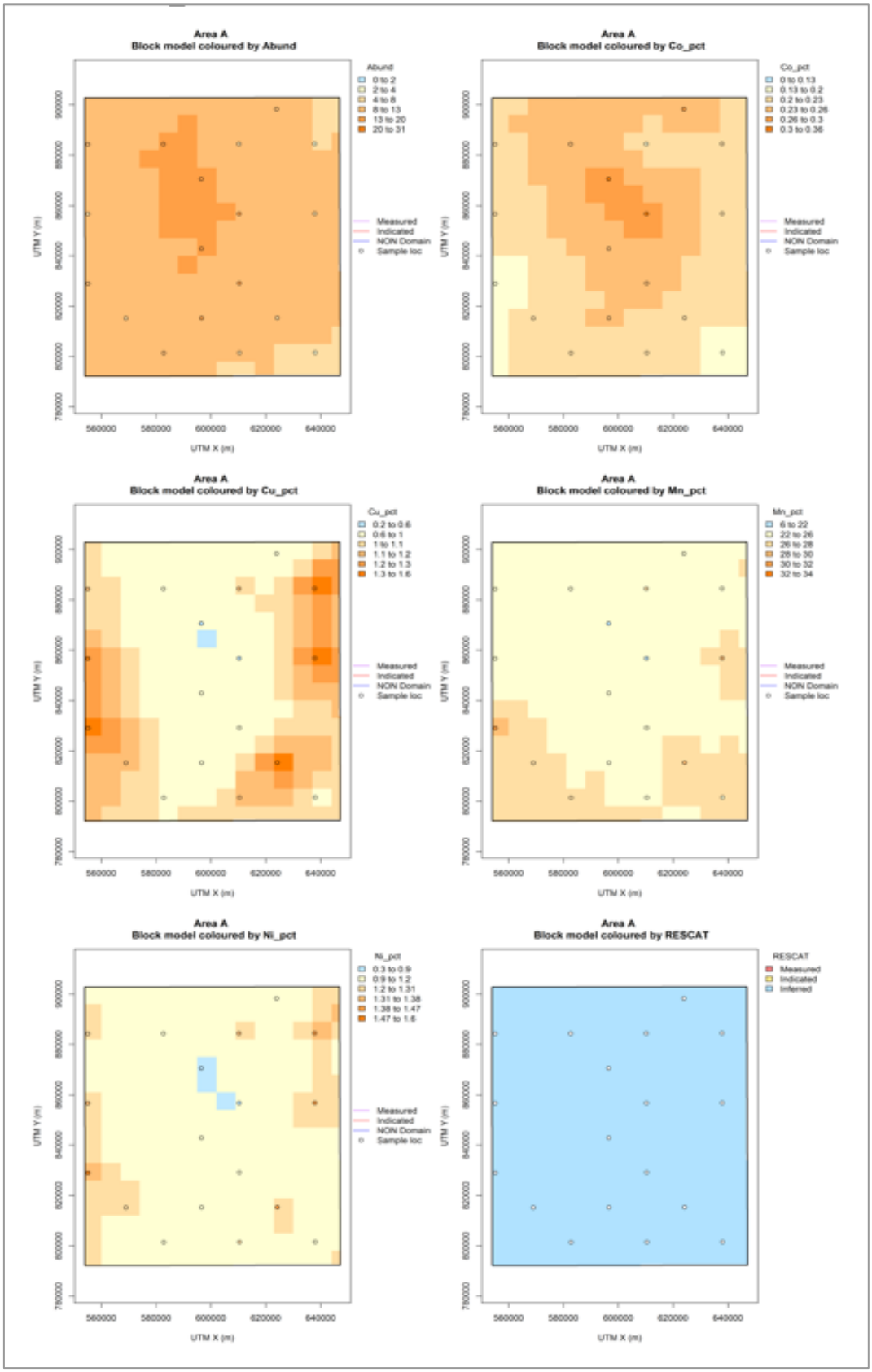
Source: AMC

Table 11.18 TOML Area Mineral Resource estimate, in situ, at a 4 kg/m² nodule abundance cut-off

TOML Area	Classification	Tonnes (x10⁶ wet t)	Abundance (wet kg/m²)	Ni (%)	Cu (%)	Co (%)	Mn (%)
A	Inferred	114	11.0	1.1	1.0	0.2	25.0
B	Measured	3	11.8	1.3	1.0	0.2	27.6
B	Indicated	14	11.1	1.3	1.1	0.2	28.6
B	Inferred	63	9.1	1.2	1.0	0.3	25.9
C	Indicated	15	8.6	1.3	1.2	0.2	30.5
C	Inferred	115	9.0	1.3	1.1	0.2	28.2
D	Indicated	29	12.2	1.3	1.2	0.2	30.1
D	Inferred	102	9.0	1.3	1.2	0.2	28.8
E	Inferred	58	10.6	1.3	1.1	0.2	28.7
F	Indicated	12	21.6	1.5	1.2	0.1	32.5
F	Inferred	244	16.6	1.4	1.2	0.1	32.2
Total	**Measured**	**2.6**	**11.8**	**1.3**	**1.0**	**0.2**	**27.6**
Total	**Indicated**	**69.6**	**11.8**	**1.3**	**1.2**	**0.2**	**30.3**
Total	**Inferred**	**696**	**11.3**	**1.3**	**1.1**	**0.2**	**29.0**

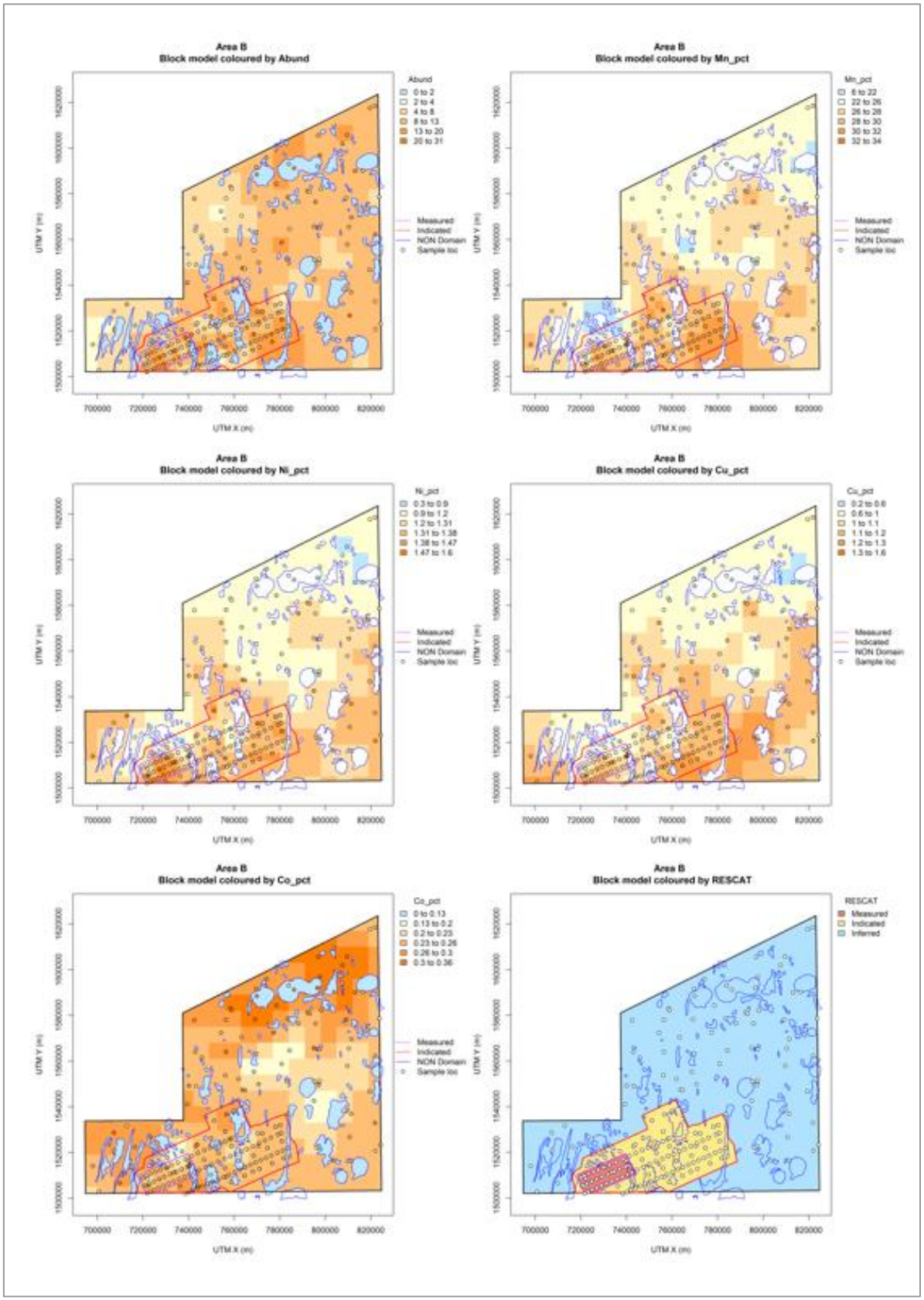
Note: Tonnes are quoted on a wet basis and grades are quoted on a dry basis, which is common practice for bulk commodities. Moisture content was estimated to be 28% w/w. These estimates are presented on an undiluted basis without adjustment for resource recovery.

Figure 11.36 Map showing block model and sample distribution for Abundance Mn, Ni, Cu and Co in TOML Area A



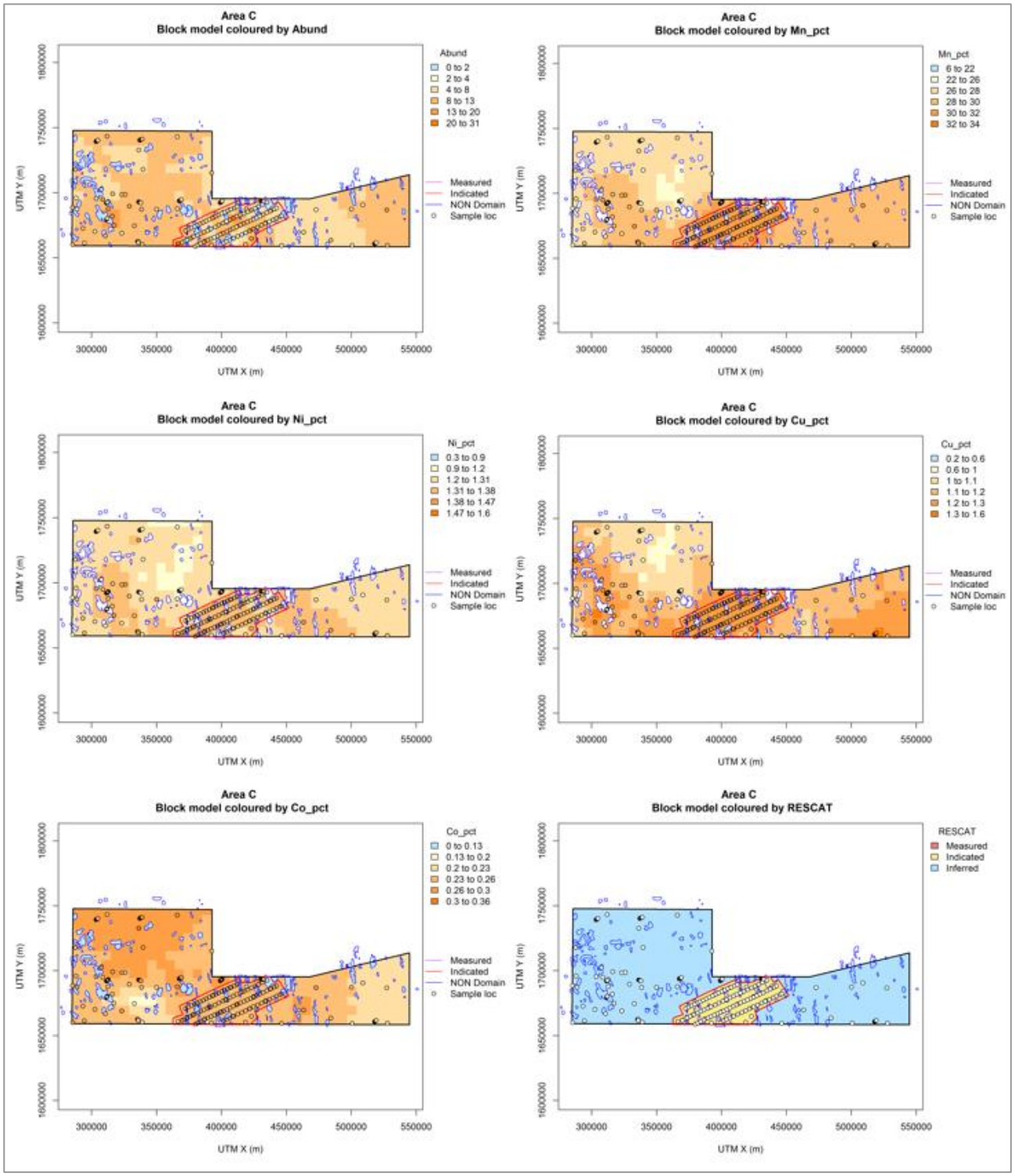
Source: TMC

Figure 11.37 Map showing block model and sample distribution for Abundance Mn, Ni, Cu and Co in TOML Area B



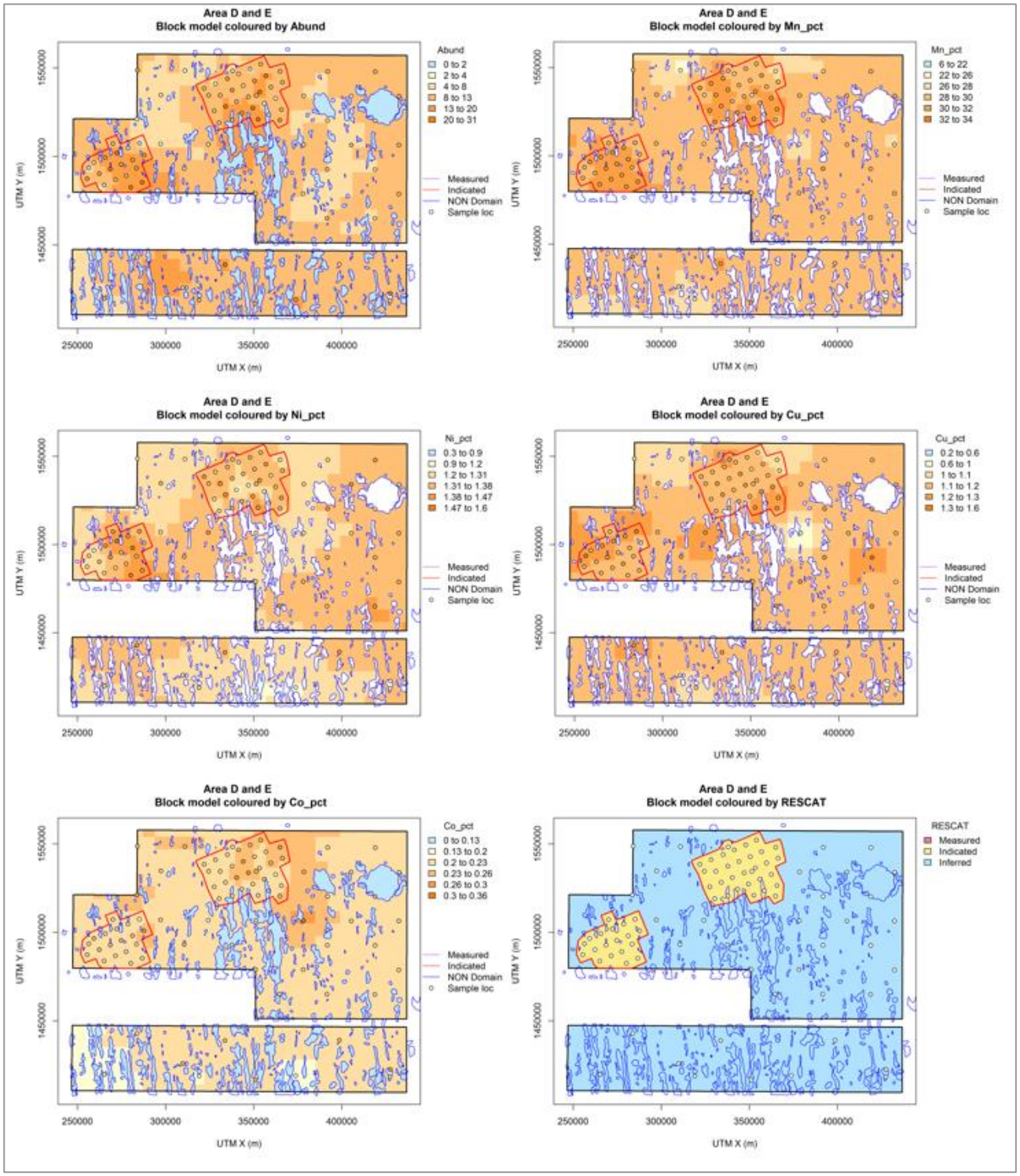
Source: TMC

Figure 11.38 Map showing block model and sample distribution for Abundance Mn, Ni, Cu and Co in TOML Area C



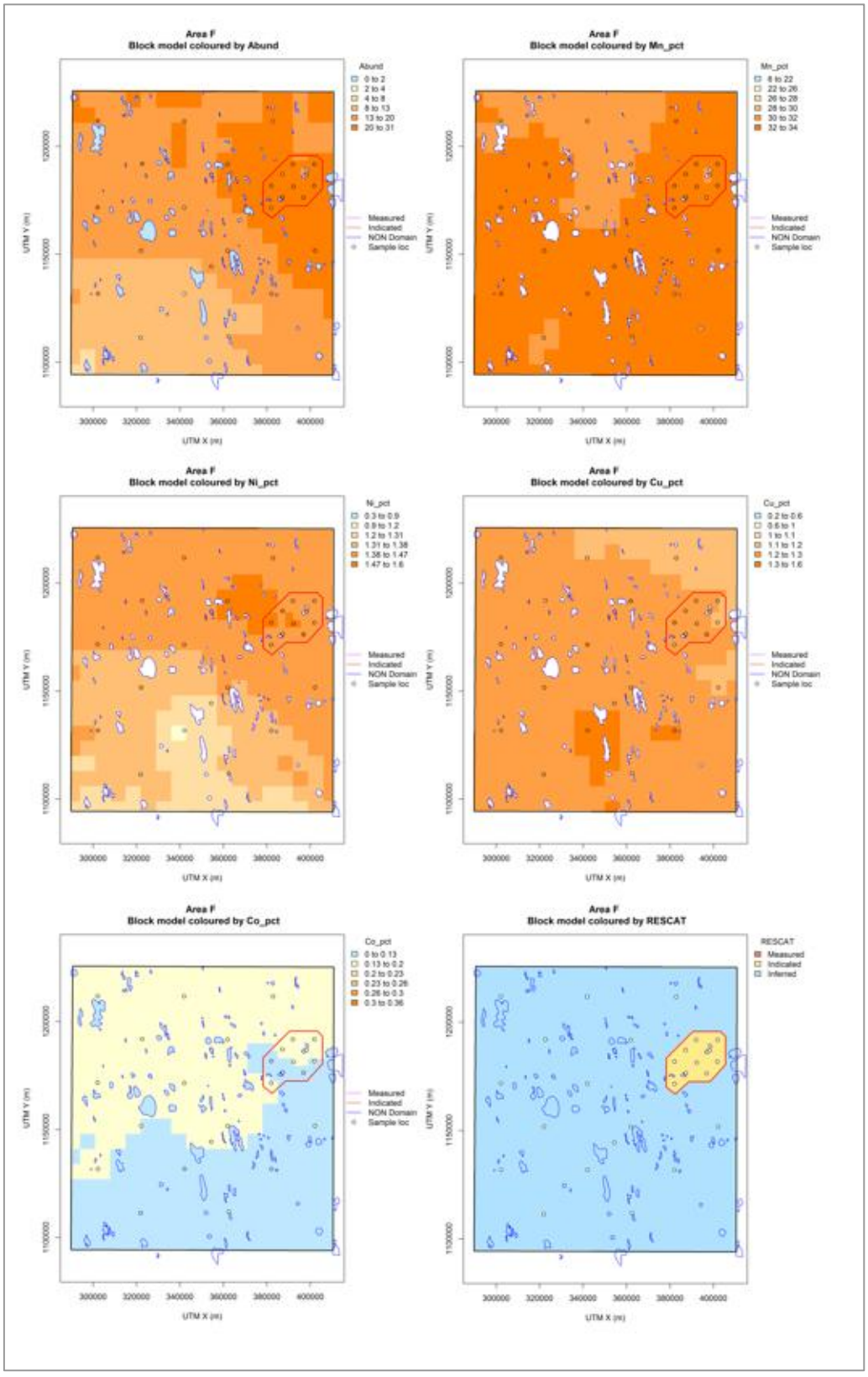
Source: TMC

Figure 11.39 Map showing block model and sample distribution for Abundance Mn, Ni, Cu and Co in TOML Area D and Area E



Source: TMC

Figure 11.40 Map showing block model and sample distribution for Abundance Mn, Ni, Cu and Co in TOML Area F



Source: TMC

12 Mineral Reserve estimates

There are no Mineral Reserve estimates for the TMC Property outside of the NORI Area D, and the potential viability of the Mineral Resources has not yet been supported by detailed mine design or optimization processes nor a PFS or a feasibility study.

13 Mining methods

13.1 Overview

The nodule mining equipment and mining methods proposed in this IA build on the Test Mining and extensive engineering programs completed by TMC and its partners as part of the NORI Area D prefeasibility study. Given the nascent nature of the industry, commercially available deep-sea nodule collection systems are non-existent, necessitating the development of custom-engineered mining solutions tailored to the specific environmental and operational conditions within the TMC Property.

13.2 Development plan

TMC propose to begin mining in the NORI and TOML areas of higher nodule abundance. A total of eight separate 2nd Generation Production Systems (2nd Gen) are expected to be employed, moving to new areas once higher abundance areas are mined out in a manner that sustains consistent production rates across the life of mine.

Each of the eight 2nd Gen systems consists of a PV that powers seafloor CVs in addition to a VTS, dewatering plant, and nodule handling and offloading infrastructure. The PV is expected to be supported by TVs that receive dewatered nodules from the PV and transport the nodules to port for processing. Supply vessels provide resupply of fuel, personnel and logistics and operate out of the mainland USA. Each of the eight systems is assumed to be identical and capable of meeting a nameplate capacity of 7 Mwmtpa in the TOML-F area and 5 Mwmtpa in the other areas of lower abundance.

The first three PVs are brought online over a three-year period in the TOML-F area, with the five additional systems coming online over a period of 5 years.

All nodules are assumed to be shipped to a receiving deepwater port in Indonesia for unload and processing to matte before shipping to the USA for further refinement.

13.3 Offshore mining system

The 2nd Gen systems are expected to build on operational experience gained through NORI Area D Test Mining and the operation of a 1st Gen system in NORI Area D, if TMC's Commercial Recovery Permit is granted. The following sections provide an overview of the Test Mining and 1st Gen system, followed by a description of the 2nd Gen system that are expected to be used to recover and transport nodules from the TMC Property to shore for processing.

13.3.1 Test Mining in NORI Area D in 2022

TMC conducted Test Mining on the seafloor in September to November 2022 from the *Hidden Gem*. During the test led by Allseas, the test CV drove across over 80 km of seafloor, collecting approximately 4,500 wmt of nodules and lifted over 3,000 wmt up a 4,300 m riser system to the *Hidden Gem*. The Allseas-designed test mining system achieved all test production milestones and reached a sustained production rate of approximately 85 wmt per hour.

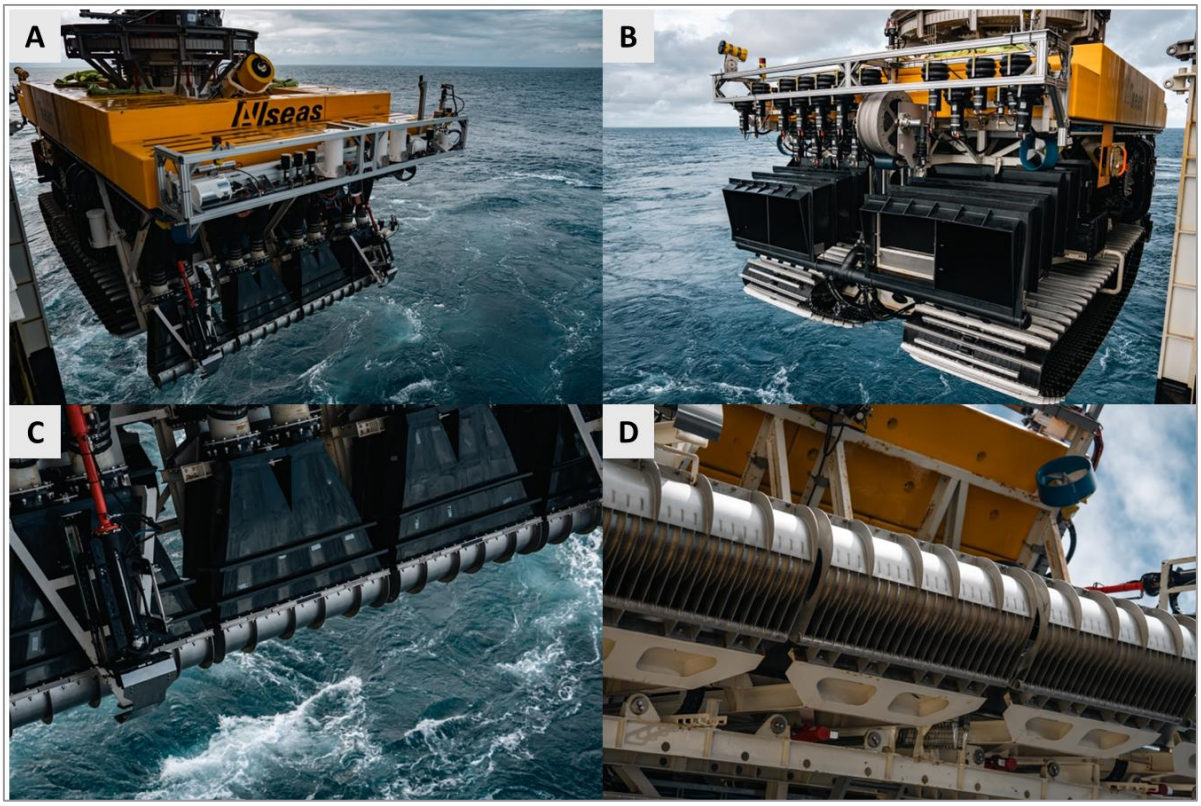
The Test Mining was conducted within a small area in NORI Area D, selected after completion of detailed bathymetric and photographic surveys in 2018. The Test Mining System consisted of a tracked collector that removed nodules from the seafloor using a Coandă nozzle, an air lift VTS and mechanical shaker screen for the dewatering process. The working principles of this test system are carried through to the 1st Gen proposed for development of NORI Area D.

Figure 13.1 The Hidden Gem post completion of Test Mining



Source: TMC

Figure 13.2 Photographs of the Test Mining Collector



Source: TMC
Note: A) Forward View, B) Aft View, C) Top View of Coandă Nozzles, D) Close-up of Coandă nozzles (collector heads)

13.3.2 First generation production system to operate in NORI Area D (1st Gen)

The Hidden Gem is expected to serve as the PV and operational base for the initial commercial operations in the NORI Area D. The Hidden Gem is expected to undergo modifications to upgrade mining and nodule handling equipment from the Test Mining configuration to meet increased production rates required for commercial scale operations. This upgraded vessel along with supporting transfer and supply vessels are termed the First-Generation Production System (1st Gen) and is capable of achieving a nominal production rate of 3 Mwmtpa.

Design of the 1st Gen and associated equipment is expected to draw on experience gained during Test Mining and includes similar mining system configurations and working principles. The 1st Gen PV houses the following:

- 2 x 15.5 m wide Collectors (effective collection width of 15 m).
- 2 x LARS.
- Air lift VTS.
- Dewatering plant to separate the nodules from seawater.
- Nodule storage holds and offloading conveyor booms for the nodules to be loaded onto the nodule transfer vessel.

The TV receives nodules from the PV during mining operations. The TV then performs an in-field transfer to load Cape-size bulk carriers with nodules for shipping to port.

Figure 13.3 Illustration of the First-Generation Production System during nodule offloading operations.



Source: TMC

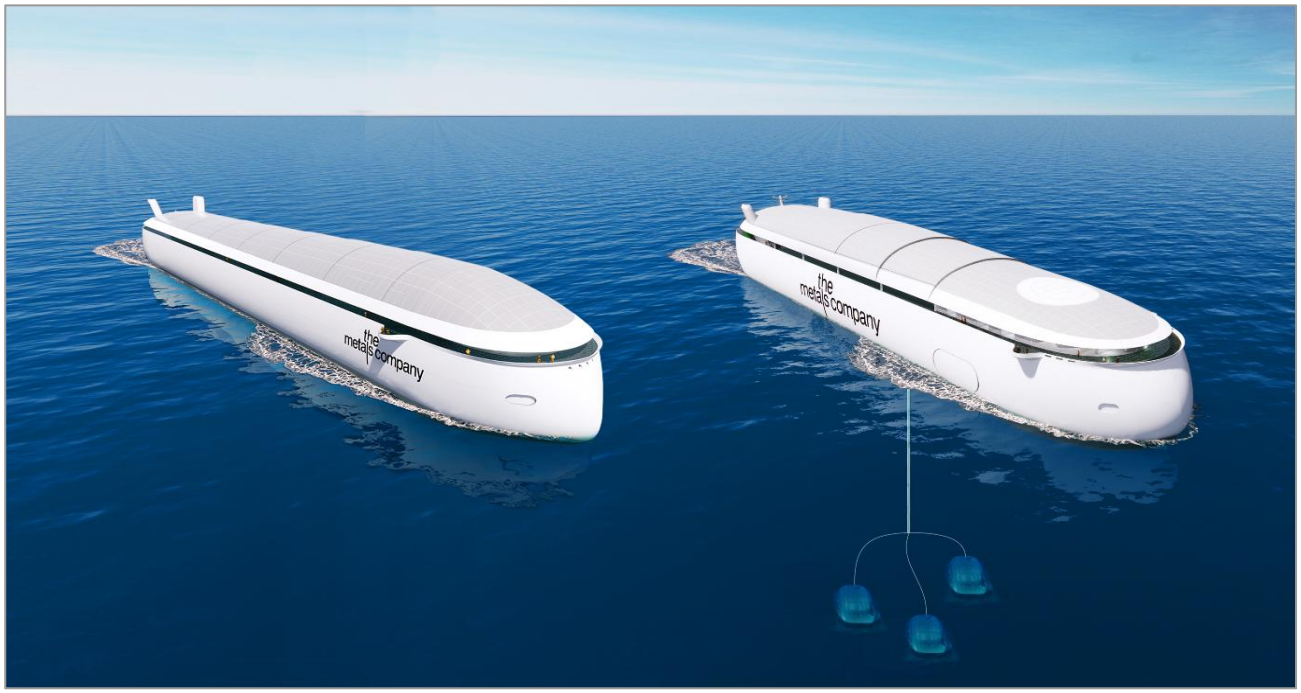
An additional three converted drill ships similar to the Hidden Gem are brought online within the NORI Area D, increasing total production to 12 Mwmtpa. Each PV is expected to have a dedicated TV and fleet of bulk carriers. For further details of NORI Area D operations and the 1st Gen system, see AMC 2025.

13.3.3 Second generation production system (2nd Gen)

Purpose built and identical production systems are expected to conduct mining operations within the Property. Each system will consist of a PV, TV and SVs, with each of the eight systems capable of operating independently of one another. The transfer vessel concept used in 1st Gen systems is assumed to be rendered obsolete by the new bespoke PV and TV in the 2nd Gen system.

The 2nd Gen follows the working principles of the previous systems including multiple tracked seafloor CVs outfitted with nodule collecting Coandă nozzles (collection heads), VTS powered by airlift or hydraulic pumps, PV with DP capabilities and dry bulk offloading technologies. The 2nd Gen system is scheduled to commence mining operations some 15 years after Test Mining and 10 years after the scheduled date of commissioning and first operation of the 1st Gen system and therefore is expected to benefit from approximately a decade of deep sea mining operations and associated lessons and optimizations.

Figure 13.4 Artist impression of a second-generation PV with three seafloor CVs and TV alongside



Source: TMC

13.3.3.1 Mining concept

CVs remove nodules from the seafloor by following a predetermined path designed to avoid obstacles. As nodules are collected, they are separated from entrained seafloor sediment within the CV before being transferred to the VTS for transport to the surface. Residual sediment and the carrier water used during collection are discharged via diffusers located at the rear of each CV.

The VTS consists of a flexible jumper hose that links the CV to the base of a vertical riser that runs from near the seafloor to the PV on the surface. Air is injected to the vertical riser at around 1,500 m below the PV inducing a flow in the riser bringing nodules from the seafloor to the riser head installed on the PV.

Nodules and seawater received from the riser pass through an onboard dewatering system, where nodules are extracted from the flow and deposited into the PV storage holds. Seawater, residual

sediment and fine nodule particles that pass the dewatering system are returned to the midwater at 2,000 m below the vessel via the return water line.

The nodules are offloaded from the PV to a TV via an offloading boom. The TV, once loaded to capacity, departs the mining area and begins transit to port in Indonesia for nodule offloading operation.

The main components and operating details of the 2nd Gen systems are described in further detail in the following sections.

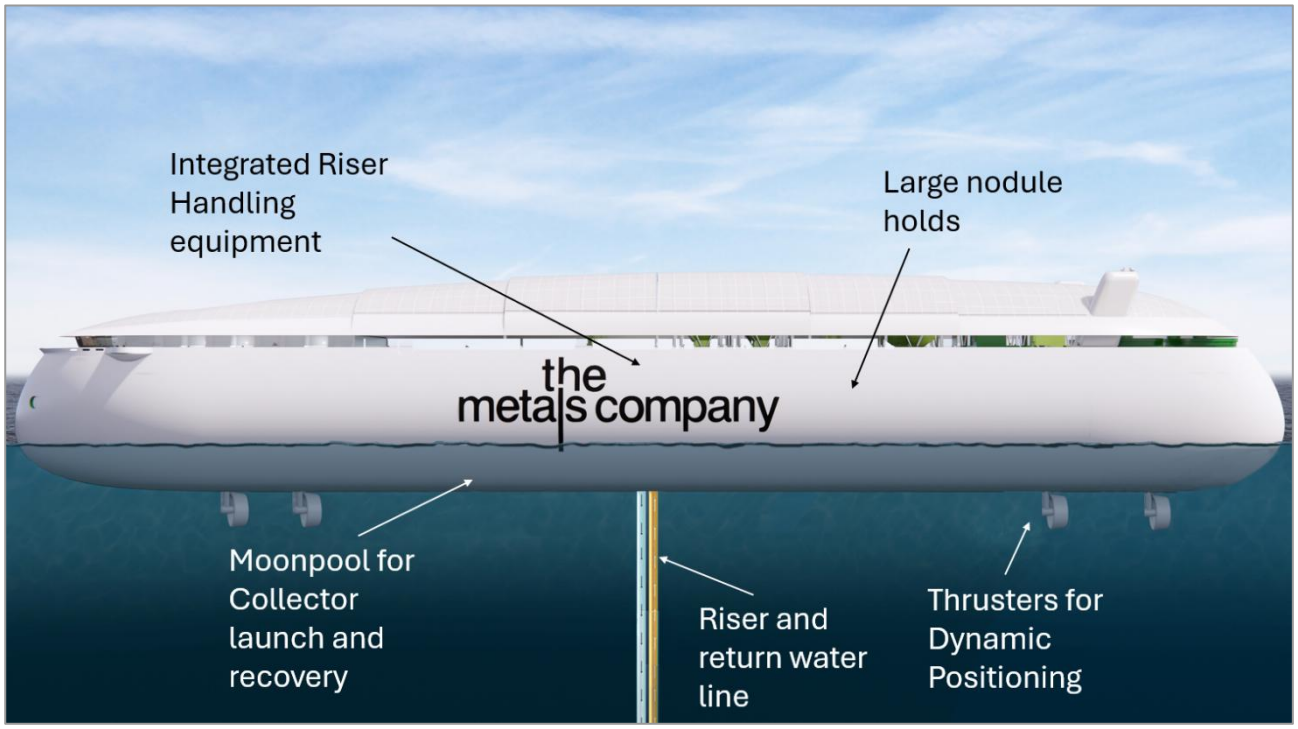
13.3.3.2 PV

The PV houses key mining equipment including the CV, power generation infrastructure, riser and collector umbilical launch, recovery and management systems, nodule dewatering, storage and offloading equipment, in addition to crew accommodation and operation management centers. An overview of the PV key components is provided in Figure 13.5 and key vessel specifications are provided in Table13.1.

The PVs power plants generate electricity to power all the PV equipment, including powering the CVs deployed to the seafloor.

While the current cost model for the power plant is based on conventional diesel generator sets, it is anticipated by TMC that by the projected commissioning date—approximately 15 years from now—significant advancements in low and zero-emission marine energy systems will have reached commercial maturity. In alignment with the International Maritime Organization (IMO) 2050 net-zero emissions goal and the anticipated rise in emissions-related compliance costs under global greenhouse gas pricing schemes, future configurations are expected by the QP to incorporate state-of-the-art solutions such as dual-fuel or ammonia-compatible generator sets. Although current CAPEX for alternative-fuel systems—particularly those based on green ammonia or hydrogen—is higher than for conventional diesel, OPEX is expected to decline over time due to improved fuel efficiency, reduced maintenance requirements, and the scaling of renewable fuel production. TMC has stated that it is committed to proactively adopting these emerging technologies to minimize environmental impact and position the operation as a frontrunner in responsible, climate-aligned offshore industrial development.

Figure 13.5 Artist impression of the PV showing key components



Source: TMC

Table13.1 2nd Gen PV key specifications

Parameter	Value	Unit
Length	265	m
Beam	50	m
Displacement	150,000	tonnes
Installed power	80	MW
Accommodation	100	Beds
Nodule storage capacity	100,000	Wet metric tonnes
Nodule offload rate	5,000	Wet metric tonnes per hour

Electrically driven azimuth thrusters powered by the PV's generators provide the vessel with DP capabilities in order to maintain heading and position during mining operations.

Large nodule storage tanks provide buffer capacity to the mining system, eliminating the need to halt operations when a TV is not available to offload the collected and dewatered nodules.

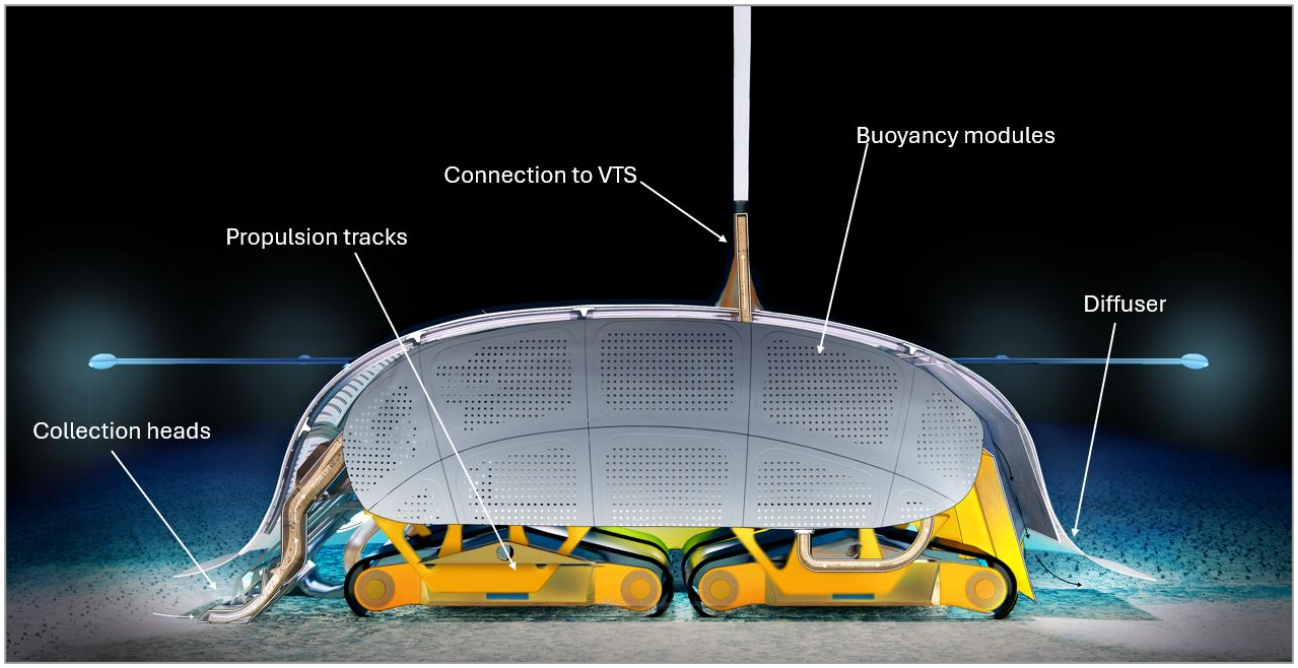
13.3.3.3 Collector Vehicle (CV)

Each PV is equipped with three identical CVs that are launched and recovered through a moonpool. Permanently connected umbilicals supply the CVs with power and control signals during seafloor operations. The self-propelled vehicles are fitted with buoyancy modules to reduce their effective weight on the seafloor, optimizing traction and maneuverability. Nodules are collected using a Coandă nozzle system mounted at the front of each vehicle, which generates a controlled suction flow to lift nodules from the seafloor surface. Once collected, the CVs separate nodules from seafloor sediment and direct the nodules to the VTS.

The CV's main functions are as follows:

- Nodule pick-up.
- Nodule-sediment separation.
- Nodule transfer to VTS.
- Propulsion and navigation of vehicle along the seabed.
- Heading and position control of vehicle during descent/ascent through the water column.
- Environmental monitoring.

Figure 13.6 Artist impression of a single seafloor collector. Note: Umbilical not shown

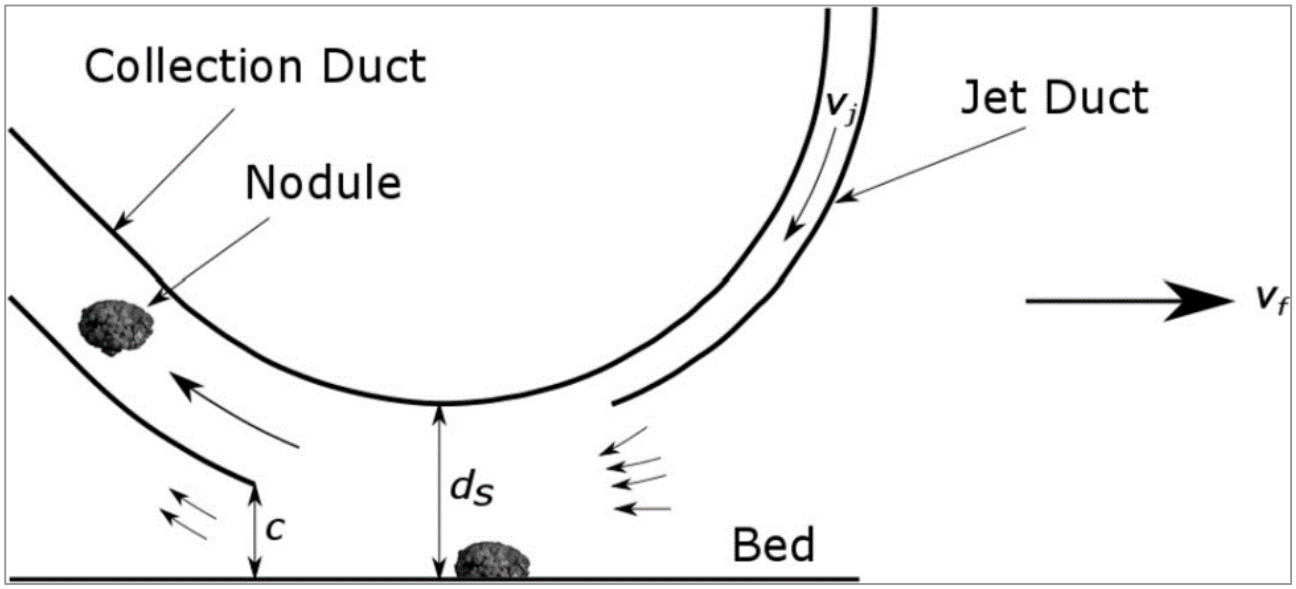


Source: TMC

Nodule pick-up and internal separation

The nodule collection mechanism is based on the working principles validated during the Test Mining campaign and proposed for the 1st Gen system. The collector heads use water jets to pick-up nodules from the seabed. These jets flow over a curved plate, creating a low-pressure zone beneath the nozzles—an effect known as the Coandă principle (Figure 13.7). This mechanism enables the gentle lifting of nodules from the seafloor with minimal erosion and limited disturbance to the surrounding seabed sediment, therefore minimizing the intake of sediment.

Figure 13.7 Schematic representation of the collector head.



Source: TMC
Note: vj is the jet velocity, vf is the forward velocity of the collector and c is clearance. The smallest arrows depict the direction of water entrainment. (Alhaddad et al, 2023

The resulting nodule-laden slurry is drawn upward through a duct into the CV hopper, where the flow velocity decreases. As the flow slows, the heavier particles (nodules) settle at the bottom of the hopper, while lighter particles (seafloor sediment) remain suspended and follow the main flow path toward the aft of the CV and to the diffuser. Washing off the sediment during decanting is further enhanced by introducing clean water from the bottom of the hopper acting as a counter current.

Forward looking sensors installed on the CV monitor variations in seabed height with the collection heads being raised and lowered by the control system to maintain a constant clearance between the seabed and the collection heads, in turn maximizing nodule collection efficiency and minimizing entrainment of seafloor sediment.

The diffuser discharges the sediment laden water at the rear of the CV. The velocity of this discharge is controlled to promote a rapidly settling plume that follows a quickly settling density driven flow regime, rather than suspending upwards into the water column.

Seafloor propulsion

Propulsion is delivered through a system of four individually controlled tracks, enabling precise maneuverability and effective navigation across challenging seafloor terrain. Each CV is equipped with integrated buoyancy modules that reduce its effective weight in water, enhancing traction and mobility on soft or uneven substrates. These modules are specifically sized to limit sinkage while still providing sufficient downward force to minimize track slippage. As a result, it is expected that the CVs can maintain nominal collection performance on slopes of up to 6 degrees from horizontal and can traverse inclines of up to an expected 10 degrees at reduced speeds.

Umbilical - Power and communications

The CV is connected to the PV by an umbilical at all times during operations. The umbilical provides power to the CV electrical consumers and signals to control all the CV mining, navigational and monitoring functions. The umbilical is not used for lifting the collector during launch or recovery from the PV to the seabed.

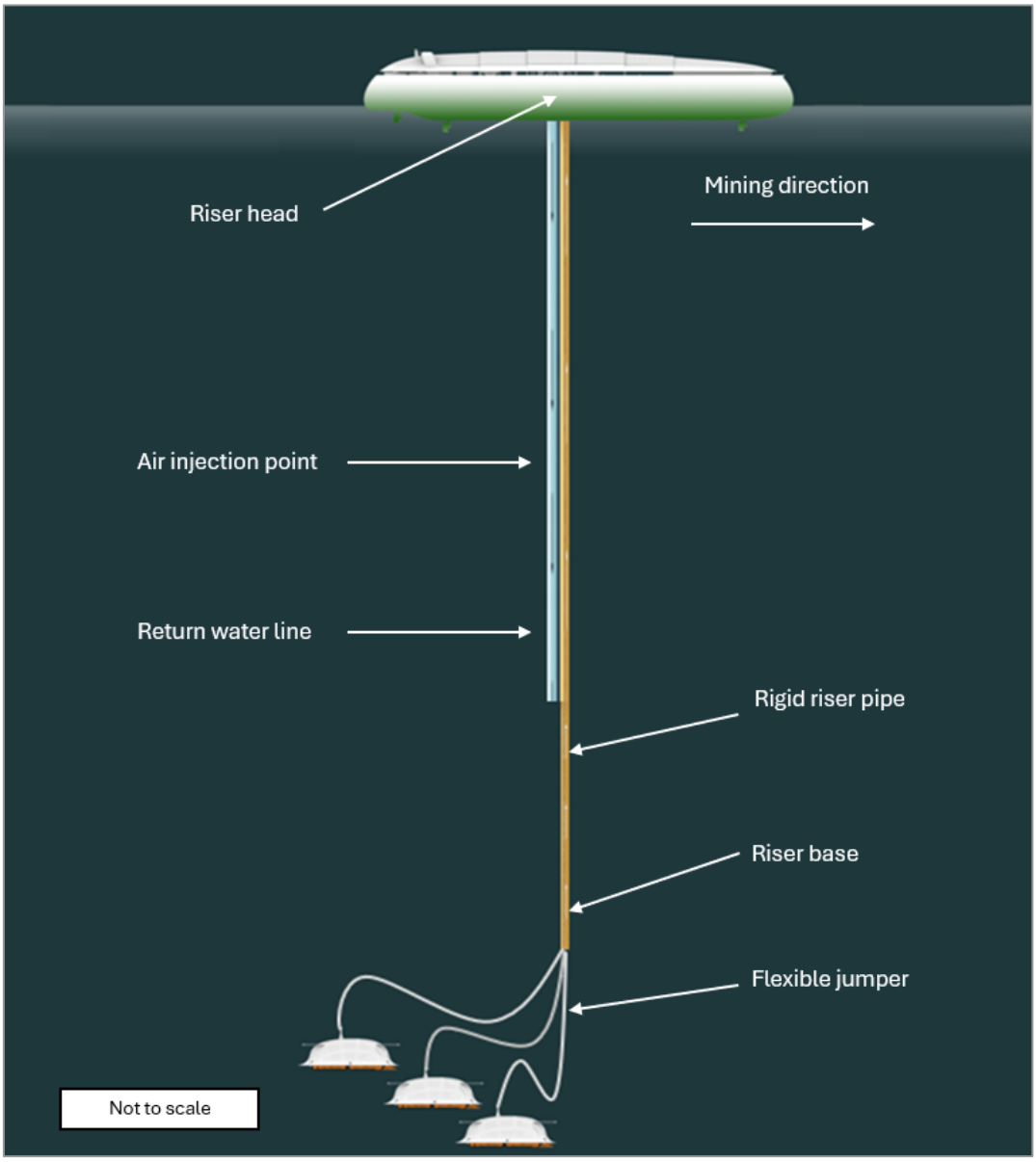
Launch and Recovery System (LARS)

A dedicated winch with heave compensation capabilities and spooled with high tensile fiber rope controls the launch of the CV from the PV internal CV maintenance and storage hangar, through a dedicated CV deployment moonpool to the seafloor. A snubber controls any movement of the CV as it is suspended and lowered through the moonpool and splash zone, releasing the CV below the waterline. Once on the seafloor, the fiber rope is disconnected from the CV, leaving the umbilical to provide power and communications to the CV during mining operations.

13.3.3.4 Vertical Transport System (VTS)

The VTS for the 2nd Gen follows the same working principles as the Test Mining and as proposed for the 1st Gen, with a flexible jumper hose connection to the seafloor CVs and rigid vertical riser with an air injection point to induce a vertical flow bringing nodules from the CV on the seafloor to the PV on the surface. The return water line hangs off the rigid section of the rigid vertical riser.

Figure 13.8 Artist impression of the VTS connecting the PV on the surface to the CV on the seafloor



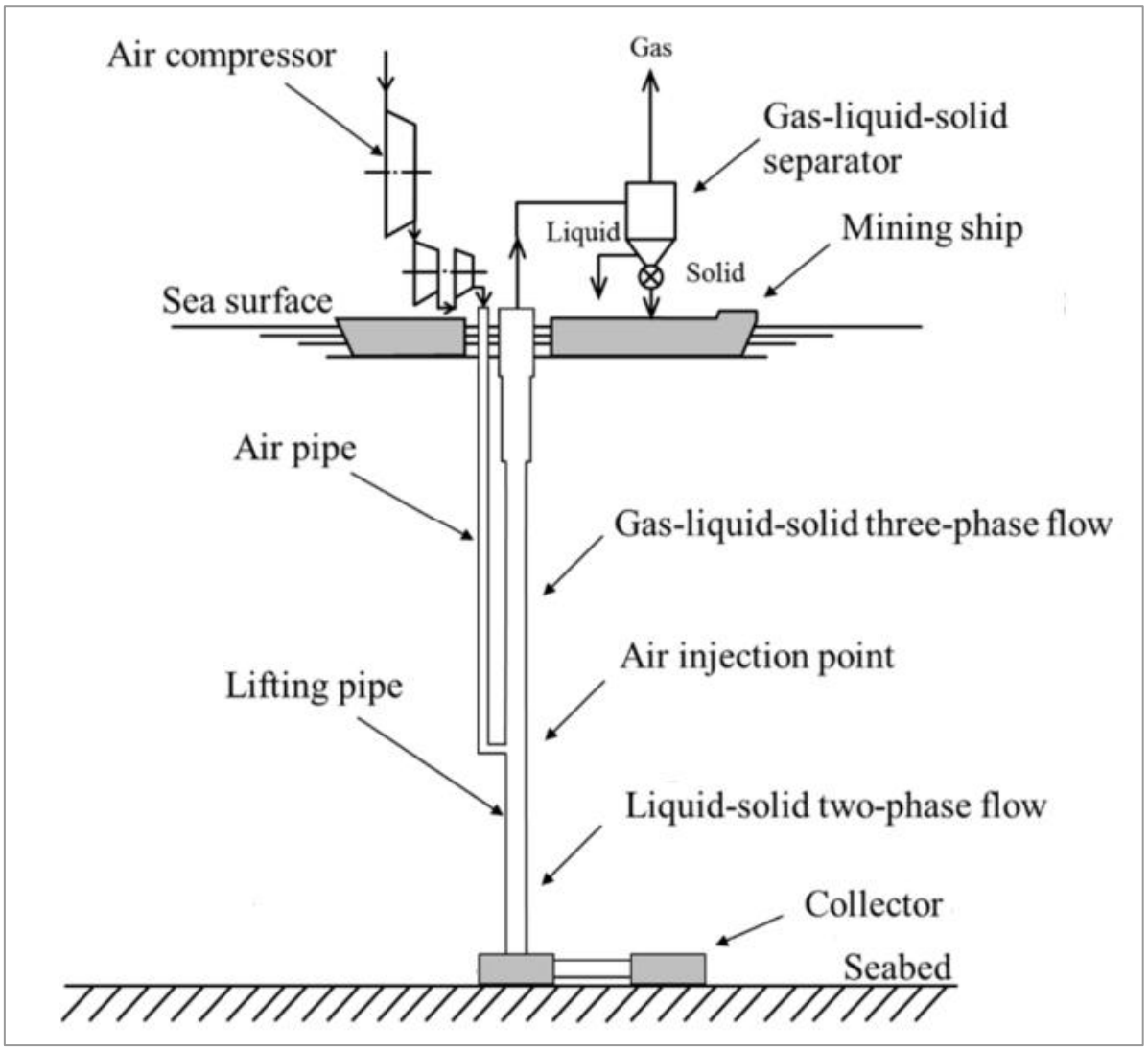
Source: TMC

A flexible jumper hose with approximate length of 500 m connects each CV to the base of the VTS rigid riser pipe sections allowing the CVs to vary their horizontal distance from the riser base when avoiding seabed obstacles and to assist in umbilical and VTS management during turning. The jumper maintains an S shape through installation of buoyancy and ballast along the jumper hose length.

Rigid riser sections make up the majority of the VTS and connect the surface PV to the jumper hose and CVs on the seafloor. The length of this rigid section can be altered from the PV VTS hang off point in varying water depths to keep the riser base close to the seabed but above any seamounts identified within the mine plan.

Air compressors installed on the PV feed compressed air down an airline that is injected into the rigid riser at approximately 1,500 m below sea level. This air injection at depth induces an upwards flow bringing seawater and nodules introduced by the CV at the seafloor to the riser head integrated into the PV. Figure 13.9 provides a schematic overview of the main components included in the airlift configuration.

Figure 13.9 Basic airlift configuration



Source: (Shimizu Y, 2024)

The jumper and rigid riser is deployed from the PV through a dedicated moonpool. The rigid sections are pieced together onboard the PV and built up, as is done in conventional offshore drilling operations.

13.3.3.5 Dewatering

At the riser head, deaeration occurs and the air injected at depth returns to atmospheric pressure. The nodules, water and residual sediment, termed slurry, is fed to the dewatering system installed on the PV. The slurry passes over mechanical dewatering screens that remove the coarse nodules from the slurry while the water, sediment and any fine nodule fragments pass to a bank of hydrocyclones. Here, nodule fragments are captured leaving seawater and sediment remaining in the slurry that is then fed to a return water tank. Return water pumps pass the slurry from this tank, through the return water line to 2,000 m depth where it is discharged.

13.3.3.6 Nodule handling, storage and offload

Nodules that are removed from the slurry by the dewatering system are carried to dedicated nodule storage holds installed on the PV. These holds have a capacity of 100,000t of nodules which reach capacity in three to four days when operating continuously at nominal production. Downtime due to weather and maintenance is expected to extend this average loading time to five days over the year.

Offload operations commence when the PV is approaching maximum hold capacity or as a TV is available to receive the nodule cargo. The nodules within the PV hold are fed through a controllable feed door to a conveyor that runs below the holds and moves the nodules to deck level. An offloading boom extends off the PV and deposits the nodules to a receiving TV.

Handling practices and bulk handling equipment is designed to minimize nodule attrition to maintain a coarse cargo size. The dewatering process removes the majority of free water from the cargo prior to storage and offload to the TV for transport. Test Mining offered valuable insights into the PSD and other physical properties of nodules following collection from the seabed, vertical transport, and dewatering. The nodule product from these trials underwent thorough physical property testing and cargo classification evaluations to assess potential risks related to vessel stability and other hazards during bulk handling and transport. The dewatered nodules in bulk are expected to maintain a particle size and possess free draining characteristics that will not pose a risk to vessel stability due to liquefaction or dynamic separation during storage on the PV and shipping on the TV.

13.3.3.7 TV

A fleet of purpose-built TVs with DP capabilities receive dewatered nodules from the PV via the offloading boom. The PV mining operations continue during the offload that takes approximately 20 hours if the PV holds are at full capacity.

The TV propulsion thrusters and other electrical consumers are powered by the vessel's diesel generator powerplant. The 2nd Gen TV key specifications are detailed in Table 13.2.

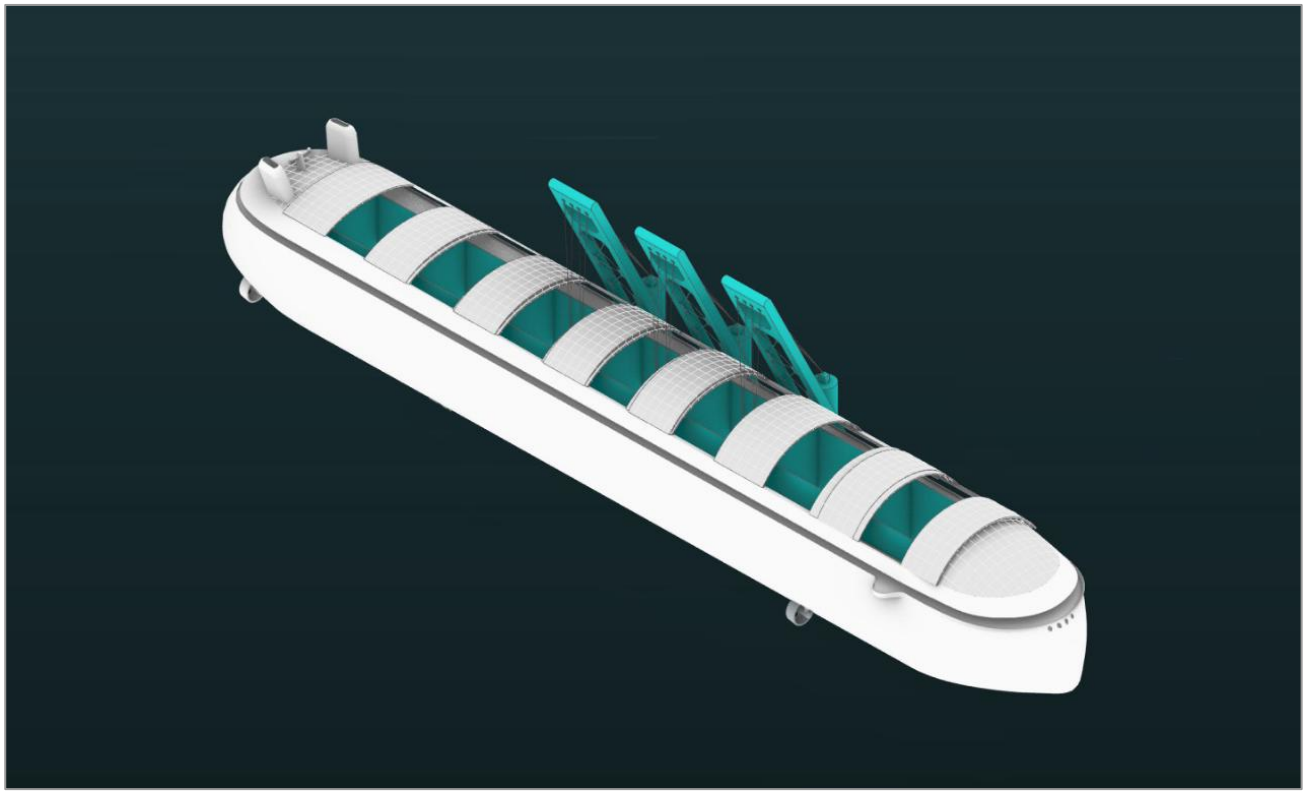
Table 13.2 2nd Gen TV Key Specifications

Parameter	Value	Unit
Length	295	m
Beam	50	m
Displacement	240,000	tonnes
Installed power	30 MW	MW
Accommodation	30	beds
Nodule storage capacity	200,000	Wet metric tonnes

Transit speed	12	knots

The TV is designed to accommodate two full offloads from the PV. Once the vessel reaches its 200,000-tonne nodule hold capacity, it departs the mining area and begins transit to Indonesia for offloading operations. Upon arrival, the TV docks alongside the terminal, where unloading is carried out using shoreside cranes. The vessels multiple hatch covers provide simultaneous access to multiple cargo holds, enabling efficient and timely discharge of the collected nodules (Figure 13.10).

Figure 13.10 Artist impression of TV in port with hatches open during nodule offloading operations



Source: TMC

13.3.3.8 Operating conditions and downtime

The 2nd Gen is designed to allow all nodule collection, dewatering, storage and transfer operations to occur in sea states up to significant wave height (Hs) of 3.5 m and wind speeds up to 25 knots. The PV and TV may be placed into a survival mode in extreme sea states resulting from severe storms or tropical hurricanes. The TV and PV have the option to leave the area if conditions are forecasted that are deemed to put the vessels safety at risk.

Given the extended project timeline and rapid advancements in maritime automation, it is anticipated by the QP that key elements of the transport fleet, particularly the TV, will feature semi- or fully autonomous capabilities by the time of deployment. Developments in autonomous navigation, real-time situational awareness, remote monitoring, and predictive maintenance are expected by the QP to make long-range autonomous cargo operations technically feasible and commercially attractive. The incorporation of these technologies is expected by the QP to enhance operational safety, reduce crew requirements, and optimize routing. As part of its commitment to innovation and sustainability, TMC has stated that it will assess and integrate autonomy-enabling technologies as they mature.

The PV is assumed to undergo survey at sea and at drydock to meet class requirements. In field surveys are planned on an annual basis and include internal inspections and external inspections by divers or ROV. Every 10 years, the PV is expected to return to port for a dry dock survey. The TV is expected to have survey in drydock every 5 years. Due to the proximity of Indonesian unloading ports to potential dry dock locations, the surveys may occur more frequently to clear biofouling from the TV hull and at times that match dips in the PV fleet's production forecasts.

13.4 Offshore support and logistics

Offshore operations in the TMC property are expected to be supported by a fleet of SVs and an operations management and supply base located on the West Coast of the USA. The PVs are expected to be refueled and resupplied at sea, removing the need for the PVs to conduct port calls. The TVs take on bunkers during their offloading operation in Indonesia. Crew changes and resupply for the TVs also occur in Indonesia to avoid at sea personnel, bunker and cargo transfers.

The supply base provides an area for equipment spare storage, area for offshore personnel to prepare for the transit to the TMC property and will be located in proximity to bunkering facilities. All personnel, fuel, equipment, spares and other logistics to support the offshore operations pass through this supply base.

A fleet of SVs provide the connection between offshore operations and the supply base. These vessels are modelled on offshore supply vessels and are capable of carrying personnel, equipment and fuel on the approximate 4 day transit to the field.

Figure 13.11 MV Island Commander, example of offshore supply vessel used in the oil and gas industry



Source: https://www.vard.com/shipbuilding/references/island-centurion

Personnel are transferred from the SV to the PV via man basket or walk to work solution. Bunker fuel is transferred from the SV to the PV via a flexible fueling hose, while other cargo is craned from the deck of the SV by the PV deck cranes.

13.5 Mining philosophy

Eight identical PVs are brought online over the LOM, each supported by a fleet of TVs and SVs, with synergies expected when multiple PVs are operating in the same area concurrently.

Long term mine planning for the fleet of PVs is based on the limited available bathymetry and resource data, with high abundance and high-grade Contract Areas to be targeted first. Production is expected to be scheduled to match onshore processing capacity. Prior to operations, high resolution acoustic and visual survey of the proposed mining areas is conducted from AUV. This survey identified obstacles or conditions that may impede nodule collection and provides detail on nodule abundance and the short-range variability of abundance within the mine plan.

Long mining paths are planned where possible to reduce turn frequencies which require orchestrated maneuvers of the CV umbilical and VTS and may reduce collection speed and therefore production rates. Long runs without turns provide extended periods for TVs to come alongside the PV for offloading operations.

For each PV, a path planning tool is utilized to plan the optimal paths that the three CVs follow on the seafloor. This path considers the overall mining sequence, seafloor bathymetry and obstacles, nodule type and abundance, in addition to other operational constraints such as surface vessel offloading or resupply operations.

13.6 Offshore operations

13.6.1 PVs

The seafloor collection system, PVs, TVs, and SVs must operate in a coordinated and synchronized manner to ensure efficient system-wide performance. Priority is given to maintaining continuous mining operations with minimal downtime. Table 13.3 outlines the key production parameters of the (PV), which form the basis for all transport and offshore logistics planning. Note that the table reflects operations in the lower abundance areas of NORI A-C and TOML A to E where 5 Mwmtpa is expected, rather than the TOML-F area where 7 Mwmtpa is expected in the production schedule.

Table 13.3 PV key operating parameters

Description	Value	unit
Annual Production	5	Mwmtpa
Annual operating time	5,584	h
Nominal production rate	895	wmt/h
Hold capacity	100,000	t
Time to full capacity	5	days
Offloading rate	5,000	wmt/h

13.6.2 TVs

The TV, once loaded to the 200,000 mt capacity by the PV will sail approximately 7,100 nm west to Indonesia for unloading for processing at an RKEF facility.

Table 13.4 summarizes the primary movements of the TVs for a 2nd Gen producing 5 Mwmtpa between the Property and an unloading port in Indonesia. Key assumptions for the TV operations include:

- Offloading from the PV to the TV occurs during daylight hours (12 hours) at 5,000 mtph.

- Time for the PV to reach 100,000 mt capacity is expected to vary and is influenced by planned and unplanned breakdown and weather events leading to a reduction or stop to nominal production rates, and therefore the PV fill rate. This range is reflected in the 'standby between loads'.
- A loading allowance has been included, this covers time required for the TV to come alongside the PV, hatch opening, repositioning of the TV to allow the PV to load a new hatch.
- Unloading in port only conducted during day light hours and at 2,500 mtph.

Table 13.4 TV average cycle time estimate

Activity	Location	Distance (nm)	Speed (kn)	Duration (days)
Loading 100,000 tmo - PV to TV	CCZ			2
Standby between loads	CCZ			4-7
Loading 100,000 mt - PV to TV	CCZ			2
Loading allowance	CCZ			2
Transit	CCZ to Indonesia	7,100	12	25
Port Access	Indonesia			1
Unloading	Indonesia			7
Transit	Indonesia to CCZ	13,200	12	25
Total cycle time				**68 - 71**

To meet the annual production rates of 7 Mwmtpa and 5 Mwmtpa, 35 trips and 25 trips are conducted by the TVs, respectively. To avoid production halting due to TV availability, an allowance of seven and five TVs has been made for operations in the TOML-F and other areas, respectively.

13.6.3 SVs

SVs are brought online as PV operations ramp up. An allowance is made for three SVs for each PV. This brings a total of 24 SVs supporting the eight PVs across the LOM.

The SVs follow a scheduled cycle where personnel, bunker and supplies are delivered to the operating PVs to meet offshore personnel roster timings and bunker consumption requirements

13.6.4 Onshore control centre and Offshore maintenance

To improve operational efficiency and reduce offshore personnel requirements, TMC has stated that it plans to prioritize development of autonomous systems that will be managed remotely from the Supply Base. This centralized approach will enable real-time oversight and decision-making while minimizing the need for continuous crew presence at sea. Maintenance activities are expected to be conducted by specialized mobile teams who travel between vessels as required, rather than stationing dedicated personnel on each unit. This model will not only enhance safety by limiting offshore exposure but also optimize staffing levels and reduce associated logistical and accommodation costs.

13.6.5 Marine infrastructure

TMC is planning to utilize existing marine and port infrastructure to receive and unload nodule cargo from the TVs in Indonesia. Similar and existing ports are assumed to be used to load matte produced by the Indonesian RKEF facilities onto Handymax size bulk carriers. The matte is planned to be packed and shipped in bulk bags for ease of handling.

The matte will be shipped across the Pacific Ocean and through the Panama Canal for offload at an existing port facility in Texas, USA. Here, the bulk bags of matte are expected to be unloaded by shoreside cranes and transferred to a refinery for further processing to marketable material.

13.7 Update of potential mining domains

TOML and NORI collected MBES data in 2012 and 2013, respectively, using the hull-mounted Kongsberg Simrad EM120 12 kHz, full-ocean depth multibeam system aboard the RV Mt. Mitchell. First pass processing of the MBES data was carried out at the time with the intent of identifying areas of nodule abundance to be further surveyed with higher resolution AUV-based sonar and to selecting priority areas for nodule sampling.

More sophisticated processing to clean the MBES data and achieve the highest possible resolution maps of the bathymetry was not carried out at the time. In particular, the MBES survey data for these areas was not processed with identification of slope angles as a specific objective. Interpretation of domains likely to be unsuitable for mining was based on interpretation of the areas of volcanic rocks or nodule-poor areas, based on backscatter data.

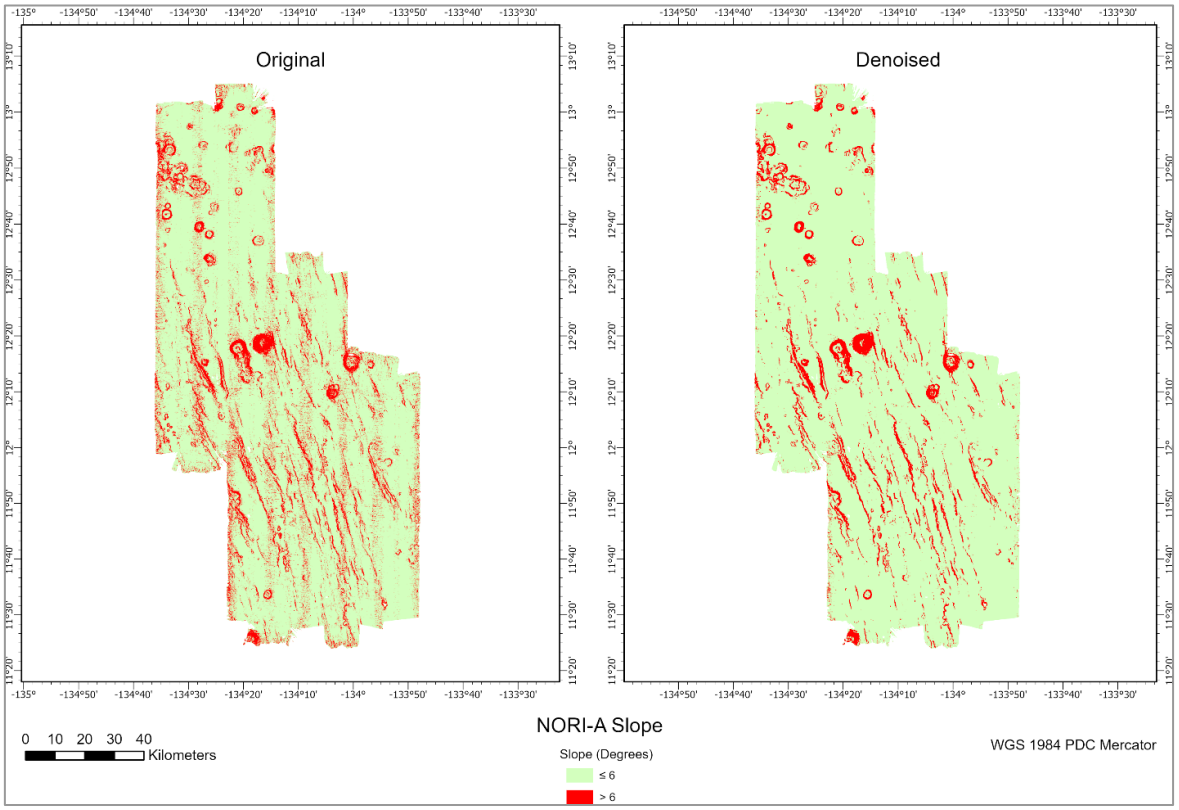
For the conceptual design of a seafloor mining system as part of the IA of TOML Areas A to F and NORI Areas A to C, it is assumed that mining operations are expected to be limited to seafloor slopes less than 6°. To align the domain interpretations with this assumption, the MBES data and domain interpretations were re-examined.

The bathymetry maps produced by the first pass modelling show significant noise in the areas of overlap between the surveyed swaths. The noise included many points with slopes incorrectly modelled as greater than 6°. TMC used the “Mesh Denoise” tool in QGIS software to remove noise from the bathymetric models. The algorithm behind the denoise tool is specifically designed to remove noise that may lower the quality of geomorphometric analyses. The algorithm denoises three-dimensional objects while preserving sharp features. The authors of the algorithm note that “the feature-preserving nature of the algorithm allows significant smoothing to be applied to flat areas of topography while limiting the alterations made in mountainous regions, with clear benefits for geomorphometric analysis in areas of mixed topography (Stevenson et al, 2010).

After applying the mesh denoise tool, the areas with slopes greater than 6° were calculated. The maps of slopes greater than 6° before and after denoising were examined visually and statistically. Figure 13.12 to Source: TMC

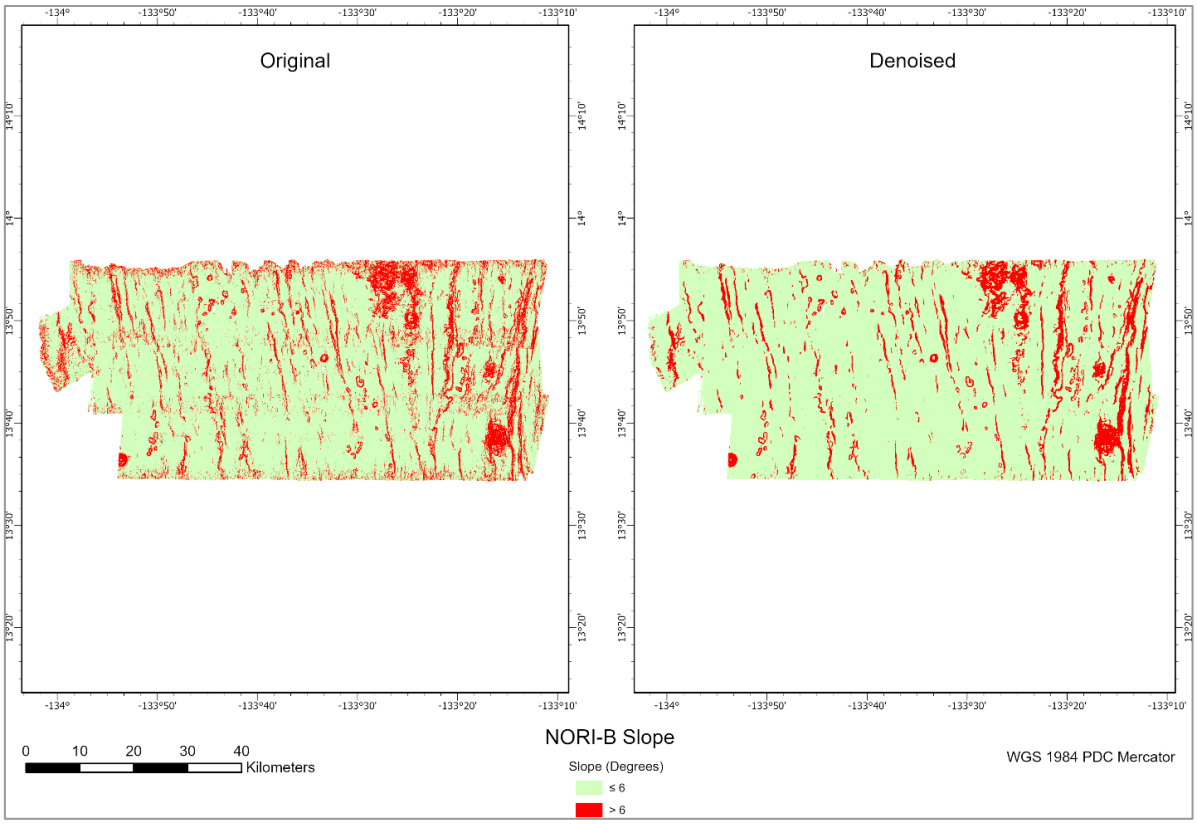
Figure 13.18 compare original and denoised maps for NORI-A to C and TOML-B to F. The maps before denoising (left hand side) show bands of noise in east-west or north-south directions where the MBES swaths overlapped. In the denoised maps on the right-hand side, this noise has been effectively removed. The NNE-trending ridges and volcanic cones do not appear to be significantly affected by the denoising process.

Figure 13.12 Comparison of slopes >6° in original and denoised bathymetry, NORI-A



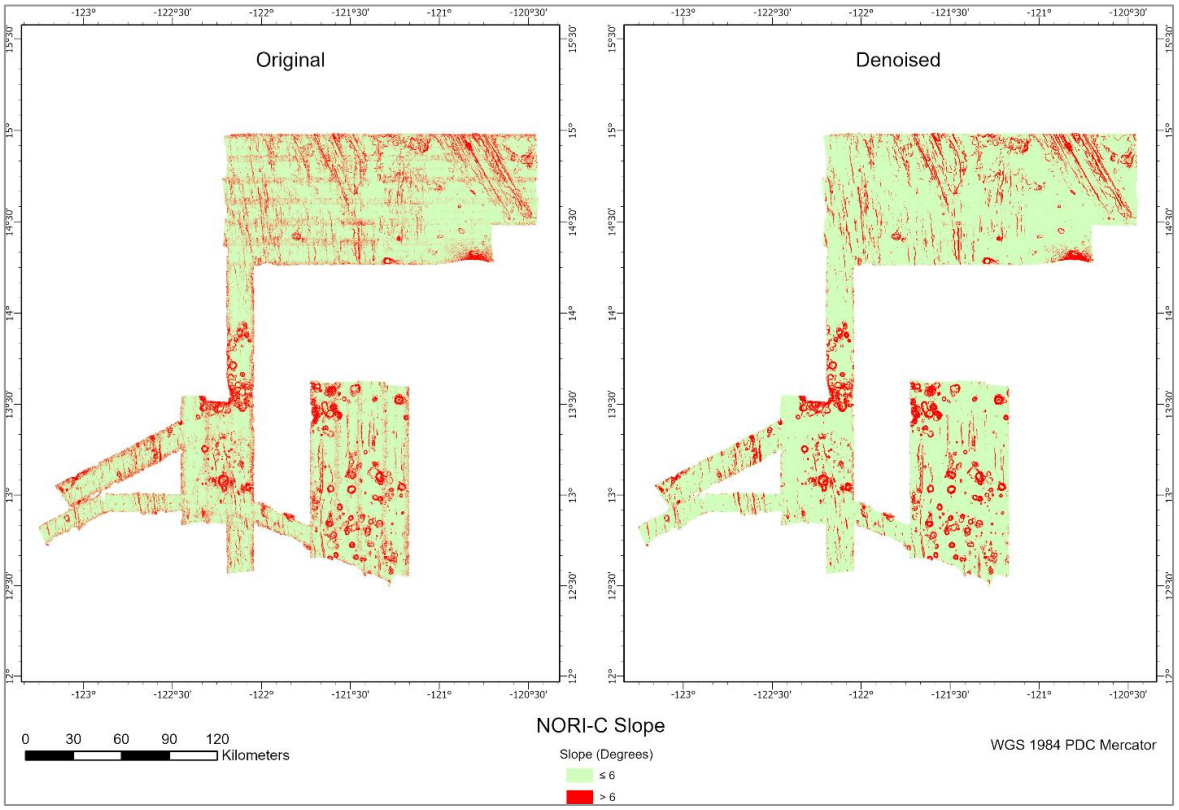
Source: TMC

Figure 13.13 Comparison of slopes >6° in original and denoised bathymetry, NORI-B



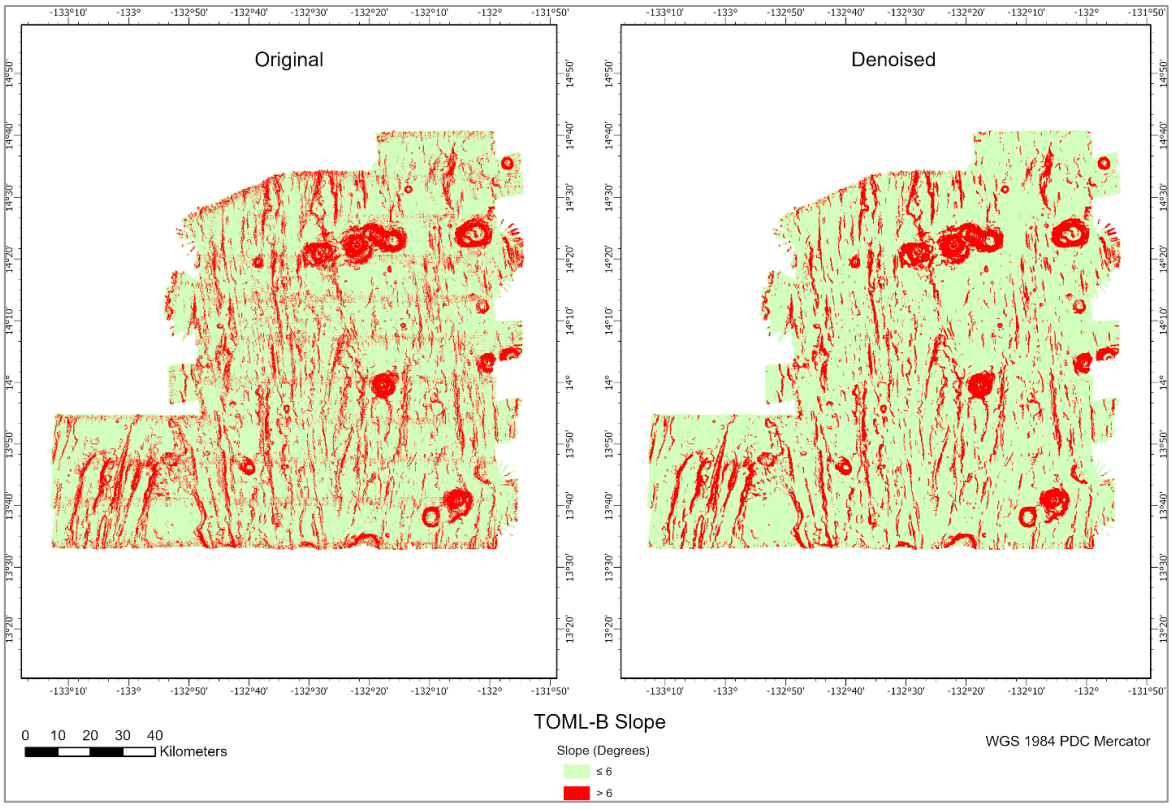
Source: TMC

Figure 13.14 Comparison of slopes >6° in original and denoised bathymetry, NORI-C



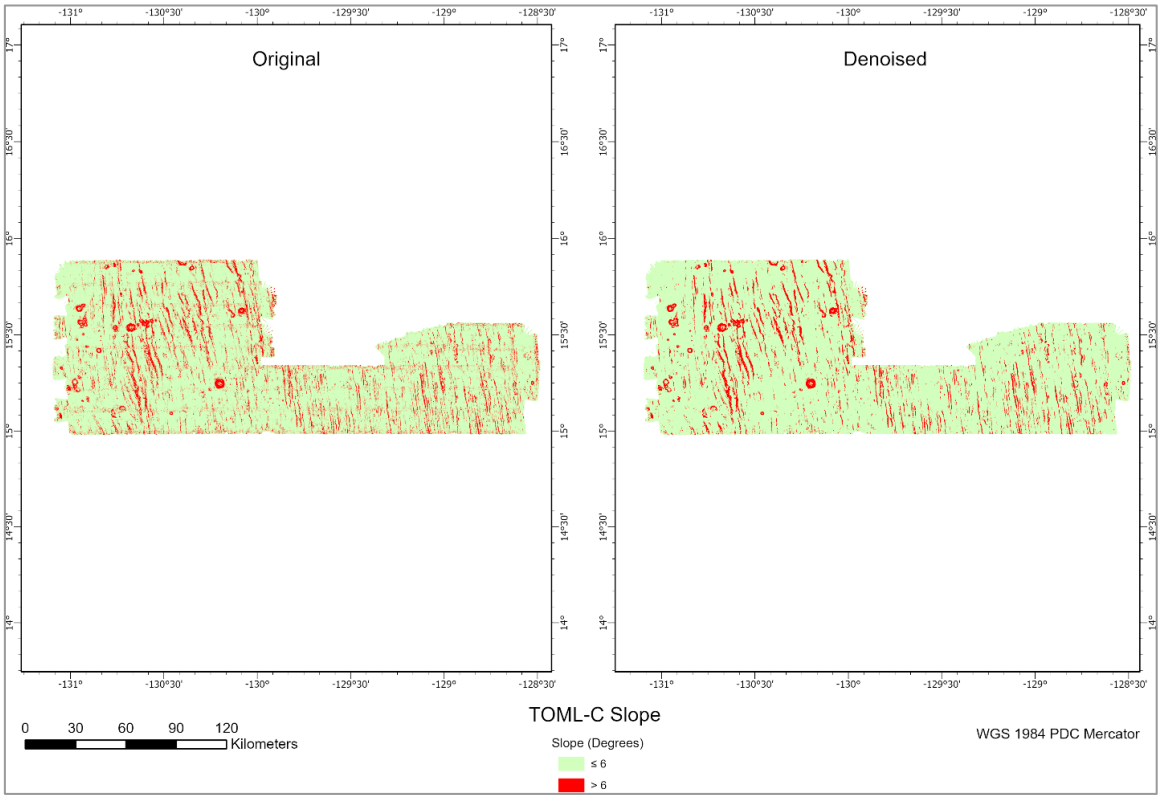
Source: TMC

Figure 13.15 Comparison of slopes >6° in original and denoised bathymetry, TOML-B



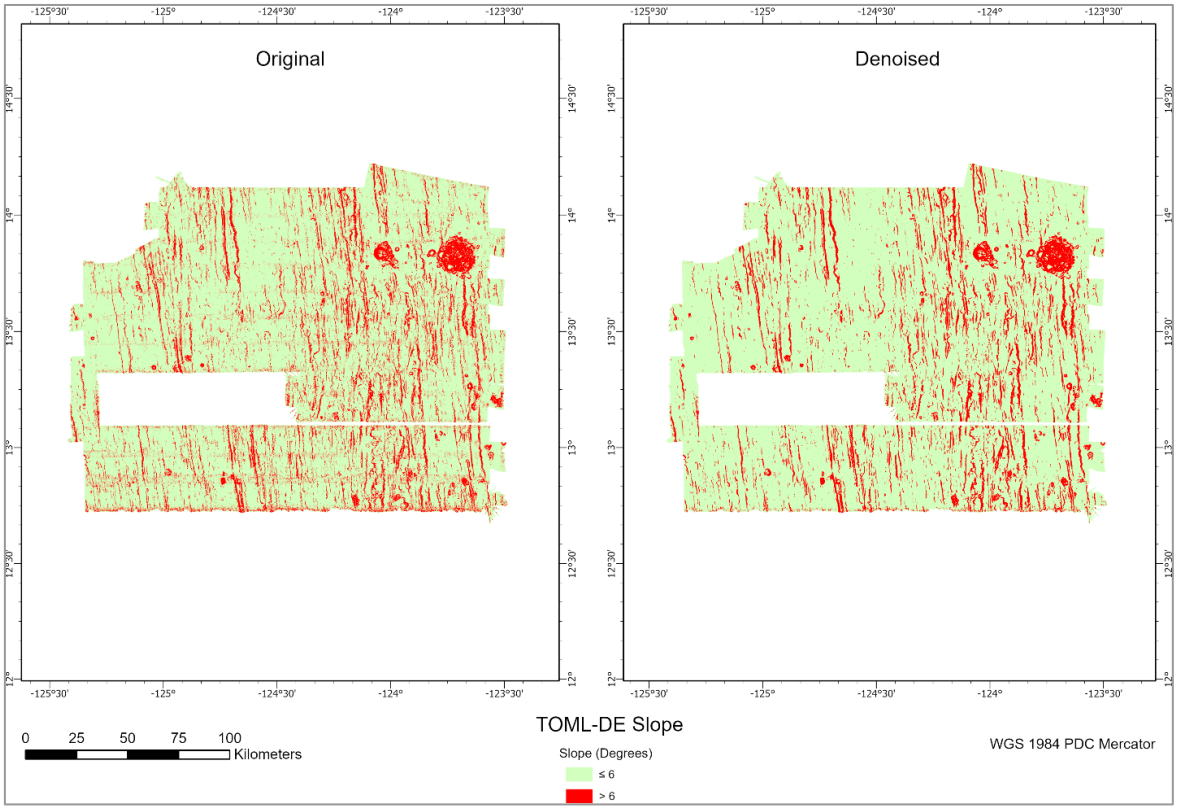
Source: TMC

Figure 13.16 Comparison of slopes >6° in original and denoised bathymetry, TOML-C



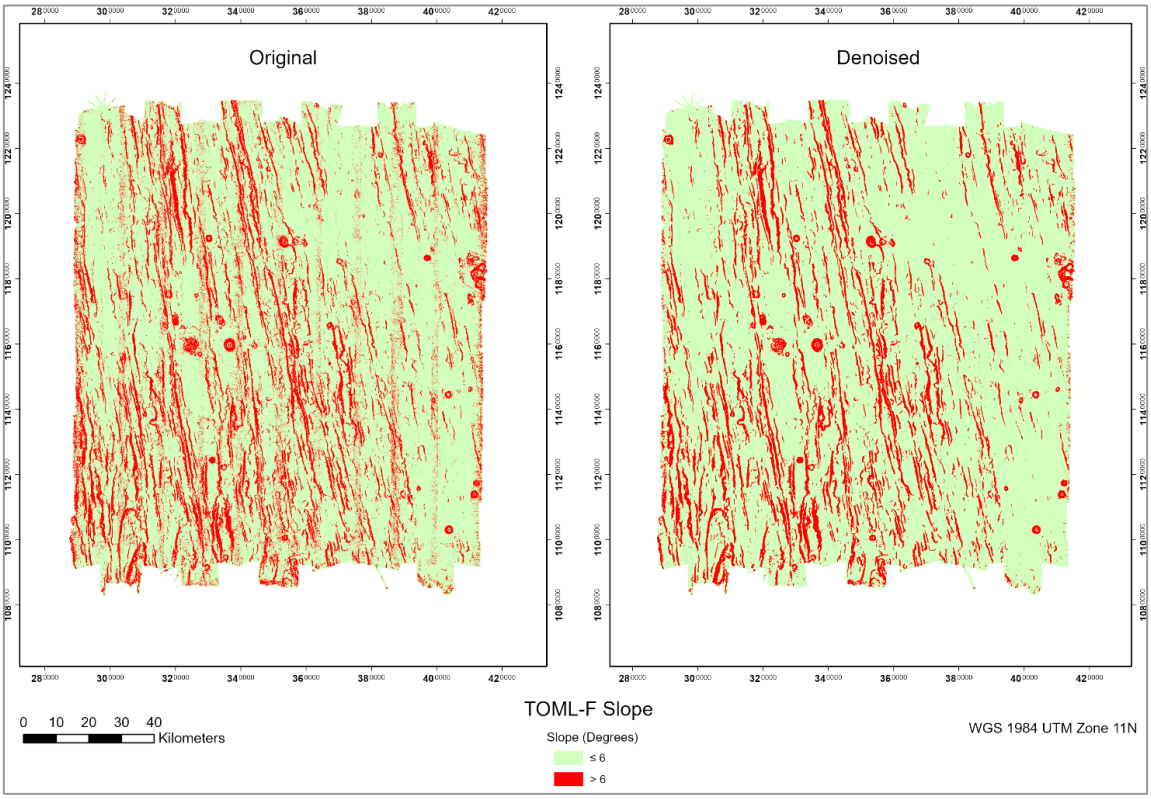
Source: TMC

Figure 13.17 Comparison of slopes >6° in original and denoised bathymetry, TOML-DE



Source: TMC

Figure 13.18 Comparison of slopes >6° in original and denoised bathymetry, TOML-F



Source: TMC

Figure 13.19 compares denoised bathymetric maps of NORI-A, B, C and D, colored by depth below sea level. Source: TMC

Figure 13.20 presents a similar comparison for TOML B, C, DE, and F. Each TOML exhibits elements of the structural features and nine geological domains described in Section 6.2 and Section 6.3. The dominant geological and geomorphological domain in all areas is abyssal plain. Within the plains, abyssal hills with a northerly or north-northeasterly trend and scattered volcanic cones are common but form minor proportions of the areas. Although a bathymetric model of similar resolution is not available for TOML A, its similar regional and geological setting indicates that similar geomorphology can be expected.

These similarities indicate that it can be reasonably assumed that seafloor mining systems designed for NORI Area D may be suitable for mining nodules within the same geomorphological domains in NORI-A, B, C and TOML A, B, C, D, E, and F.

The key geomorphological domains considered in the engineering design and mine planning for NORI Area D are the slopes of the abyssal hills and volcanic cones. In the PFS for NORI Area D, the seafloor mining system was designed to operate on slopes less than 4° and slopes steeper than this limit were excised from the mine plan and production schedule. TMC considers that with the accumulation of operating experience in NORI Area D and further enhancements of engineering design, future mining systems are expected to be able to operate up to 6°, which was the assumption made in the IA of NORI Area D in 2021 (AMC Consultants, 2021a).

Therefore, for the purposes of the 2025 IA of NORI-A, B, C and TOML A, B, C, D, E, and F, it is appropriate to excise areas with slopes greater than 6° from the Mineral Resource that would otherwise be available for mining.

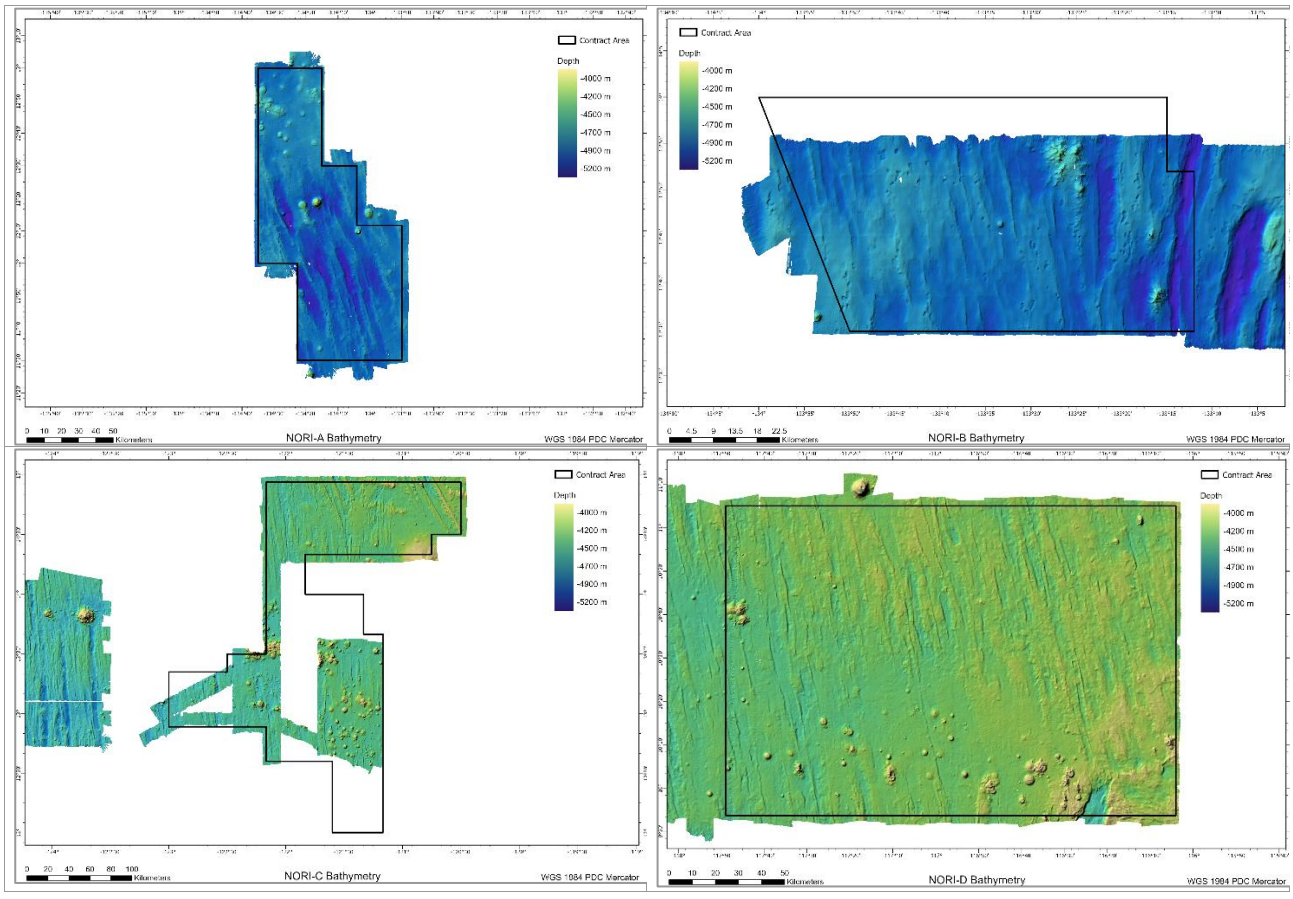
No blocks were excised from the Mineral Resource block models for NORI A, B, and C when the models were generated in 2012 because the areas interpreted from backscatter as nodule-poor were considered to be insignificant in respect to the Inferred Mineral Resources and areas with slopes greater than 6° were not recognized as a potential impediment to mining. Therefore, in these models there are no blocks with zero abundance or zero grades.

The approach taken with the Mineral Resource block models for TOML-A, B, C, D, E and F when they were originally generated in 2013 was different to the NORI models. On average, 16% of blocks were excised from the TOML Mineral Resource block models because they were interpreted as nodule-poor areas of volcanic rocks or sediment cover. Abundance and grades were set to zero in these blocks. Slope angles were not explicitly considered in the interpretation. Therefore, although there is a high degree of overlap between slopes > 6° and volcanic cones, the abyssal ridges > 6° were commonly not excised. Furthermore, the interpreted areas of sediment cover (“no nodule ooze”) were not ground-truthed with BC sampling or photography.

In order to prepare the TOML block models for excision of slopes greater than 6° and volcanic cones, it was first necessary to fill the blocks that had previously been assigned zero abundance and zero grades. This was achieved by estimating the grades of the zero blocks from the grades of the surrounding blocks. IDW with a circular search was used and NN estimates were also generated as a check. The total tonnage and grade of nodules was not materially changed.

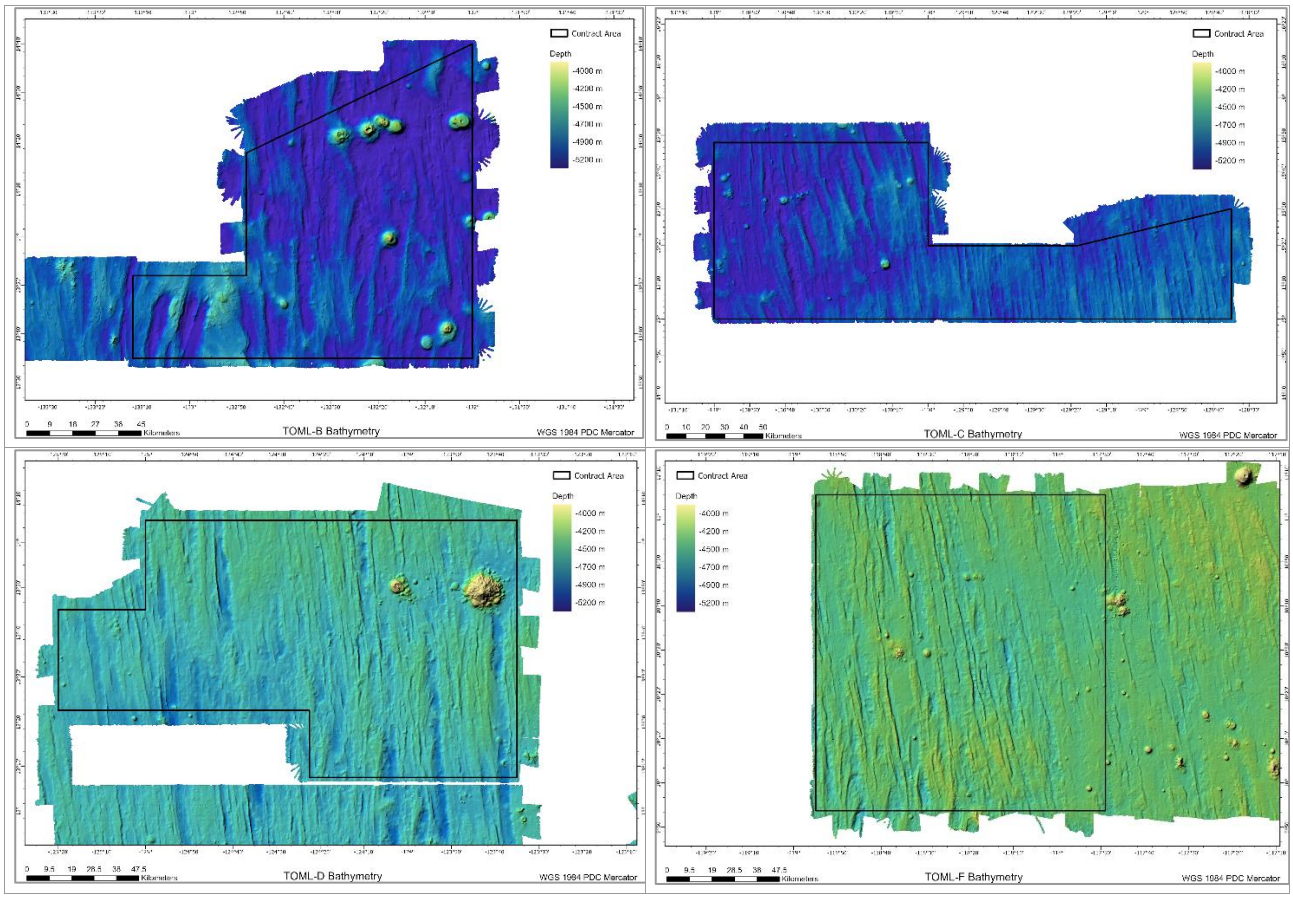
For the 2025 IA, the proportion of seafloor with slopes > 6° within each area were excised from the Mineral Resource models as an average proportion.

Figure 13.19 Bathymetric maps of NORI-A, B, C and D



Source: TMC

Figure 13.20 Bathymetric maps of TOML-B, C, D, E and F



Source: TMC

13.8 LOM basis of design

13.8.1 Mine planning factors overview

Mine planning factors are the assumptions and parameters that are used to quantify the amount of nodules that can be recovered from the seafloor and transported to market. Mine planning factors are broadly separated into three groups:

- Factors used to estimate the quantity of nodules collected.
- Factors used to estimate the rate at which nodules can be collected.
- Factors used to determine the economics of nodules being collected (see Section 19).

To estimate the quantity of nodules collected, the following mine planning factors are taken into consideration:

- Nodules must be located outside sensitive environmental zones (such as seamounts and their associated buffers) and outside the buffer around the lease boundary. Buffer zones of 1 km were applied in both cases to ensure that there is no impact on the sensitive environmental areas or other leases from sediment that is disturbed and mobilized during the nodule collection operation. Buffer zones were not applied to adjoining lease boundaries.
- Nodules must be located in potential mining domains, consisting of areas of less than 6° slopes, which is the maximum slope assumed for safe and productive collector operations. As collector technology matures, this slope may be increased.

- Nodules must be located outside areas of disruption on the seafloor (Geo-obstacles), where depressions, hardgrounds, and minor geological obstacles are expected to prevent collection operations.
- Nodules must be located outside the 1 m gap between collector paths that is left to ensure collectors are not operating over previously collected seafloor.
- Not all nodules traversed by the collector on the seafloor are picked up by the collector, and in addition there are losses caused by some nodules being beneath the collection zone of the collector (top 1-5 cm) or are lost within the collector hopper, VTS, dewatering screens or during transport to market.
- Areas where subsea cables have been installed, including a buffer around the cable.

To estimate the rate at which nodules can be collected, the following mine planning factors are taken into consideration:

- Physical dimensions and capability of the collectors, in particular, width and speed.
- Time the collection system is in operation, accounting for both the impact of the weather and the planned maintenance and repairs of the collector, VTS, and surface SV.
- Field efficiency of collection system, to account for the time the collector may be operating but not collecting nodules, such as when turning around at the end of a collector run, running over previously collected ground in avoiding Geo-obstacles, and general operating issues/delays.

To estimate the economics of nodules being collected, the following mine planning factors are taken into consideration:

- Nodule grades, abundance, moisture content, metal prices, metallurgical recoveries, and payabilities.
- Operating costs of the collection system, transport costs, processing costs and selling costs.
- Capital costs of the collection system and on-shore and off-shore infrastructure.
- Royalties.

13.8.2 Quantity of nodules recovered by the collector vehicle

13.8.2.1 Potential mining domains

Mining domains were delineated through the following process to estimate the quantity of nodules in areas of slope of less than 6° and outside sensitive environmental areas that are available to include in the mine plan. Refer to section 13.7 for a summary of the work to update potential mining domains.

The adjustment factors to account for nodules contained in areas of slope greater than 6° and in seamounts and associated 1 km buffers are shown by lease in Table 13.5.

Table 13.5 Slope and seamount adjustments

Lease	Slope > 6° and Seamount + 1 km Buffer
NORI-A	14.0%
NORI-B	13.7%
NORI-C	21.9%
TOML-A	16.4%
TOML-B	20.7%
TOML-C	13.1%
TOML-D	16.1%

TOML-E	16.3%
TOML-F	16.9%

13.8.2.2 Buffer Zones

Buffer zones of 1 km were used around sensitive environmental areas and the lease boundary to ensure that there is no impact on the sensitive environmental areas or other leases from sediment that is disturbed and mobilized during the nodule collection operation. Although TMC seafloor current modelling and sediment modelling indicate that the zone of disturbance will be significantly less than 1 km, a buffer zone of 1 km was selected to align with assumptions in the NORI Area D PFS TRS (AMC Consultants, 2025).

13.8.2.3 Geo-obstacles

Analysis of the short-scale geological features probability models developed for the NORI Area D was used to estimate nodule losses during collection in the NORI Area D as part of the PFS for NORI Area D (AMC Consultants, 2025). Visual assessment of these areas showed that, in addition to the area covered by the Geo-obstacles themselves, the Collector may not be able to access the areas between adjacent Geo-obstacles, isolating the nodules in these areas from collection.

The sterilization factors from the NORI Area D were used as a basis and were extrapolated over the property considered in this 2025 IA, in addition to assumptions related to the increased size of the 20 m wide CV and its ability to traverse obstacles of larger size than the 15 m wide CV considered under the PFS for NORI Area D (AMC, 2025).

For the IA of mining in NORI-A to C and TOML-A to F, it was assumed that a 20 m CV that was able to operate on slopes up to 6° would be less affected by the Geo-obstacles than the 15 m collector operating on slopes up to 4°. Conceptual-level estimates of the reduction in impacts with the larger collector were applied to the NORI Area D PFS estimates (AMC, 2025) for the smaller collector; firstly to the different types of geo-obstacle in the Initial Mining Area of NORI Area D (see Table 13.6).

A 20 m wide CV able to operate on slopes up to 6º would be able to straddle and therefore mine through larger Geo-obstacles than the 15 m wide CV operating on slopes up to 4º assessed as part of NORI Area D. While design specifications of the 20 m wide CV are unknown at this stage, an allowance for a 20% reduction in losses from depressions was assumed for this 2025 IA. In a similar way, an allowance for a 50% reduction loss in losses was made for the impact of the 2nd Gen CV being able to operate on slopes up to 6º compared to the 1st Gen CV which could only operate on slopes up to 4º. It was assumed that losses due to hardgrounds and volcanic features would not be impacted by the increased width of the CV and its ability to operate on steeper slopes. This resulted in an overall reduction of 26% in losses due to Geo-obstacles (7.7% instead of 10.4%) for the Initial Mining Area of NORI Area D. This was then applied to the areas of the total NORI Area D lease covered by each Geo-obstacle probability class to determine a net loss of nodules due to Geo-obstacles (see Table 13.7). This same percentage (15%) was then applied to NORI-A to C and TOML-A to F.

Table 13.6 Geo-obstacle assumptions

Geo-obstacle	Initial Mining Area, 15 m CV up to 4° Slope	Impact of 20 m CV, 6° Slope	Initial Mining Area, 20 m CV up to 6° Slope
Depression	5.0%	-20%	4.0%
Slope	3.4%	-50%	1.7%
Hardground	1.8%	-	1.8%
Volcanic	0.1%	-	0.1%

Total	**10.4%**	**-26%**	**7.7%**

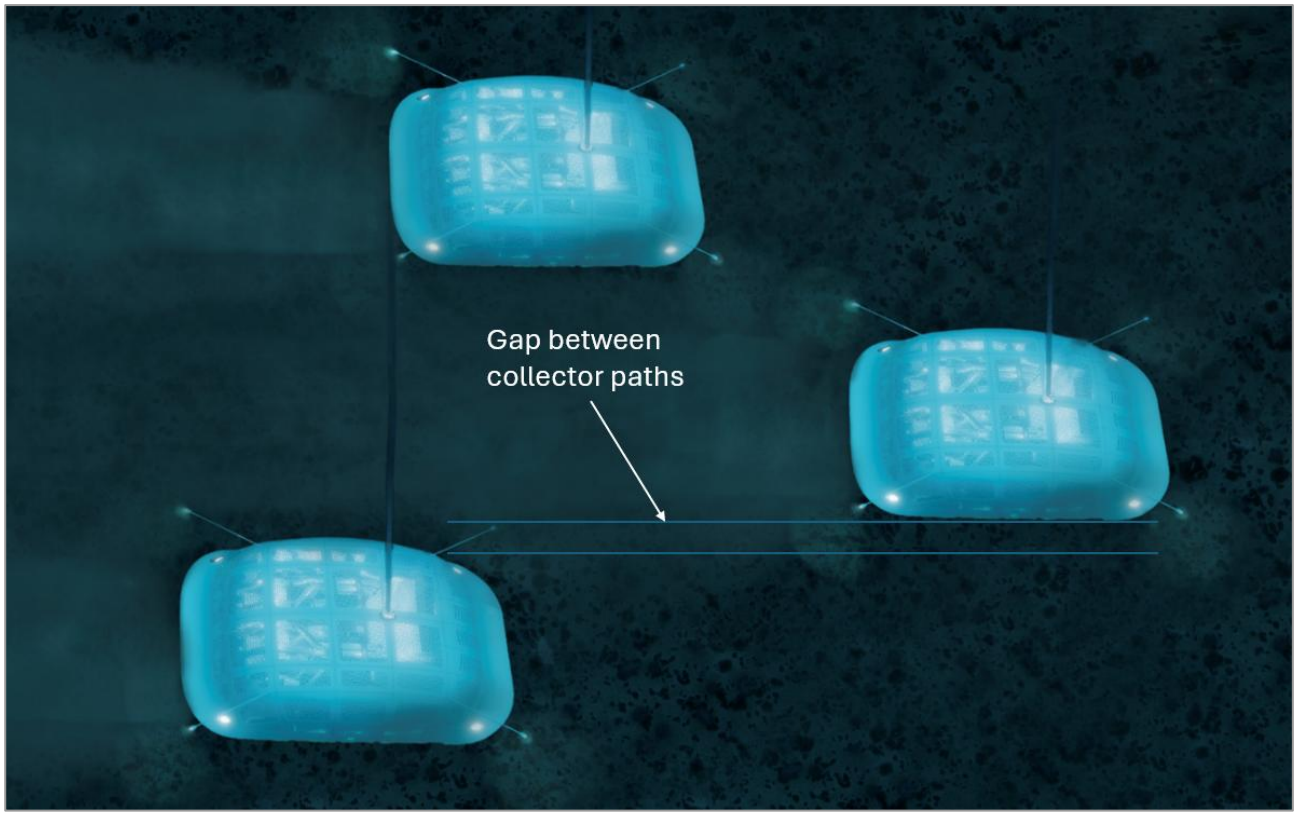
Table 13.7 Geo-obstacle mine planning factors

Probability Class	Total NORI Area D Lease 15 m CV/up to 4° Slope	Impact of 20 m CV, 6° Slope	Total NORI Area D Lease 20 m CV/up to 6° Slope
1	5.1%	-26%	3.8%
2	11.4%	-26%	8.4%
3	3.5%	-26%	2.6%
4	0.5%	-26%	0.3%
Total	20.4%	-26%	15.1%

13.8.2.4 Gap between collector paths

CVs on the seafloor will rely on acoustic systems for relative and absolute positioning. Optical and supplementary acoustic instrumentation installed on the CV will also assist in detecting previous collection paths and unexpected obstacles in the planned path of the vehicle. Inaccuracies resulting from these relative positioning systems are accounted for by the assumption that a 1 m gap will exist between each collection path during nominal operations. This allowance covers the scenario where a CV is operating on ground already mined by a leading CV, or the CV drifts off the collector path leaving a strip of nodules (Figure 13.21). The net size of the gap left by the CVs is 5% of the total collection width.

Figure 13.21 Artistic impression of CV operations showing a gap between collection paths



Source: TMC

13.8.2.5 Nodule collection recovery

The nodule recovery is defined as the mass of nodules removed from the seafloor and delivered to port, divided by the mass of nodules that the CV passes over.

Geological investigations indicate that 96% of nodules are within the collection layer of the top 5 cm of the seafloor, and therefore an allowance is made to account for nodule losses due to the collection heads not being able to access the nodules more than 5 cm below the seafloor.

The collection head efficiency, subsea separation that occurs in the CV hopper, dewatering system efficiency and losses during transfer at sea and from the TV to quayside is derived from results of Test Mining and first-generation collection vessel engineering works (refer to AMC 2025).

Recovery of nodules from the seafloor is itemized in Table 13.8.

Table 13.8 Nodule recovery components

Component	Recovery
Nodules accessed in the collection layer (vertical distribution)	96%
Collection system	85%
Sub-sea separation losses (CV to PV)	98%
Dewatering efficiency (PV)	98%
Transfer efficiency (transport from PV to market)	99%
Overall system recovery	78%

13.8.2.6 Overall recoverable inventory

The quantity of nodules estimated by area is shown in Table 13.9.

Table 13.9 Overall nodule inventory by area, outside of areas >6º and seamount and lease buffers with <4 kg/m^2 abundance cut off.

Recoverable Inventory	Area (km^2)	Mt (wet)	Abundance (kg/m^2)	Ni (%)	Cu (%)	Co (%)	Mn (%)
NORI-A	6,200	58	9.3	1.35	1.06	0.22	28.0
NORI-B	2,686	30	11.0	1.43	1.13	0.25	28.9
NORI-C	27,586	304	11.0	1.26	1.03	0.21	28.3
TOML-A	8,255	91	11.1	1.11	0.96	0.23	25.0
TOML-B	7,370	70	9.5	1.20	0.97	0.25	26.4
TOML-C	13,045	116	8.9	1.28	1.16	0.25	28.5
TOML-D	12,787	124	9.7	1.33	1.16	0.22	29.1
TOML-E	5,482	59	10.7	1.29	1.15	0.21	28.7
TOML-F	12,809	215	16.8	1.40	1.25	0.13	32.2
Total	**96,219**	**1,066**	**11.1**	**1.29**	**1.10**	**0.21**	**28.8**

Note: 1. Losses due to Geo-obstacles included in table below

The additional losses that are considered part of the collection system are shown in Table 13.10.

Table 13.10 Additional losses and recoverable inventory summary

Additional Adjustments	Recovery	Recovered (Mt wet)	Losses (Mt Wet)
Gap between collector paths (1 m per 21 m)	95.2%	1,015	50.8
Geo-obstacles	85%	863	152.3
Nodules accessed (vertical distribution)	96%	829	34.5
Nodule collection efficiency	85%	704	124.3
Collector separation efficiency	98%	690	14.1
Dewatering efficiency	98%	676	13.8
Losses during handling and transport	99%	670	6.8

13.8.3 Quantity of nodules recovered to market

13.8.3.1 Physical capacity of the CVs

The CV are 20 m wide and will travel along the seafloor and vary the forward speed to match the local nodule abundance. In areas of low abundance, the forward speed will be increased to maintain the nominal production rate, while in areas of high abundance, the forward speed will be reduced to control the quantity of nodules collected and avoid overfeeding the VTS with nodules that may cause blockage or overwhelming the vertical transport and dewatering functions. At a nominal forward speed of 0.55 m/s, each PV is expected to produce in excess of 8 Mwmtpa in the TOML-F area and in excess of 5 Mwmtpa in the other (lower abundance) areas. For the purposes of mine planning, the production rates are capped at 7 Mwmtpa and 5 Mwmtpa in the TOML-F and other areas, respectively. This production cap is introduced to account for anticipated constraints derived from limitation in the capacity and size of the VTS.

The CVs are assumed to be capable of maintaining nominal nodule collection rates on seafloor slopes up to 6°.

13.8.3.2 Weather

The production and LOM schedule include an allowance for operational downtime resulting from wave height and strong winds that halt operations. Sea surface conditions exceeding the operational limits of 3.5 m Hs and 25 knot wind speeds, in combination with an allowance for hurricanes, leads to an allowance of annual downtime due to weather of 5% or 18 days.

These weather exceedance events are typically expected to be brief, lasting less than two days. However, large hurricanes in close proximity to the PV may necessitate the recovery of VTS and the relocation of the PV. In such cases, the riser would need to be redeployed once the PV returns to the mining area, resulting in additional downtime. This contributes to the assumption of a 5% allowance, despite the weather condition operational limit exceedance for the area being less than 1% (Table 13.11).

Table 13.11 Metocean statistics for the Property

Significant Wave Height (m)					
Month	**Hs < 1.5**	**1.5 ≤ Hs < 2.0**	**2.0 ≤ Hs < 2.5**	**2.5 ≤ Hs < 3.5**	**Hs ≥ 3.5**
January	3%	26%	43%	27%	1.3%
February	2%	28%	46%	23%	1.3%
March	2%	29%	44%	24%	0.6%
April	4%	36%	44%	16%	0.2%
May	11%	49%	35%	5%	0.0%
June	15%	60%	22%	3%	0.0%
July	17%	54%	26%	3%	0.1%
August	12%	49%	31%	7%	0.2%
September	11%	51%	29%	9%	0.2%
October	12%	49%	31%	7%	0.2%
November	7%	44%	38%	11%	0.2%
December	4%	27%	42%	25%	1.1%
All year	**8%**	**42%**	**36%**	**13%**	**0.4%**

Wind Speed (kn)						
Month	**Wsp < 5**	**5 ≤ Wsp < 10**	**10 ≤ Wsp < 15**	**15 ≤ Wsp < 20**	**20 ≤ Wsp < 25**	**Wsp ≥ 25**
January	1%	10%	47%	40%	1.9%	0.02%
February	0%	8%	52%	39%	1.2%	0.00%
March	0%	7%	51%	41%	0.6%	0.00%
April	1%	9%	61%	29%	0.2%	0.00%
May	5%	31%	55%	9%	0.0%	0.00%
June	3%	50%	42%	5%	0.0%	0.00%
July	5%	44%	29%	6%	0.4%	0.09%
August	3%	37%	52%	5%	0.2%	0.02%
September	1%	14%	35%	35%	1.2%	0.00%
October	2%	33%	45%	17%	0.6%	0.14%
November	1%	16%	42%	39%	1.0%	0.00%
December	4%	18%	49%	28%	1.1%	0.02%
All year	**1%**	**27%**	**42%**	**20%**	**0.7%**	**0.02%**

Source: MetOffice WAVEWATCH III (115168 data points from 24 Jan 1980 to 31 May 2019.

13.8.3.3 Planned maintenance and unplanned repairs

Routine planned maintenance programs covering all critical equipment is assumed to be implemented to minimize unplanned breakdowns. Critical spares are expected to be held onboard the PV with additional parts available for rapid mobilization to field from the supply base onboard a SV.

An unplanned breakdown allowance covers instances where production is halted or reduced due to collector malfunction, VTS issues or other breakdowns of critical nodule production, storage, offloading or transport equipment.

An annual allowance of 20% or 73 days has been included in the production and LOM schedule for planned maintenance and unplanned repairs.

13.8.3.4 Field efficiency

A field efficiency factor was applied to account for loss of production to various operational challenges. These include turning CVs at the end of a collection path, navigating around seafloor obstacles, passing over previously mined areas due to overlapping tracks and the potential impacts of offloading or resupply activities on production. To reflect the field efficiency of operations, a 15% reduction in production rate is added to the production figures.

13.8.3.5 Production rate summary

The above mine planning factors result in a production rate estimate as summarized in Table 13.12. Note that annual production rates for the 2nd Gen are capped at 7 Mwmtpa and 5 Mwmtpa for TOML-F and other areas, respectively. This cap has been introduced to reflect the potential limitations of the VTS to increase production rates due to the diameter of the flexible jumper and rigid section and limits on the concentration of nodules that may be transported through the VTS without causing increased risk of blockages.

Table 13.12 Production rate summary

Parameter	2nd Gen	Unit
CV Width	20	m
CV type	Tracked, Coanda nozzle	
No. CV	3	m
CV Speed	0.55	m/s
Nodule Collection Efficiency - Type 1	85%	%
Nodule Collection Efficiency - Type 2/3	85%	%
CV separation efficiency	98%	%
Dewatering Efficiency	98%	%
Losses during handling and transport	99%	%
Nodules accessed (vertical distribution)	96%	%
Seabed slope constraint	<6	Deg to Horizontal
Gap between runs	1	m
Non-productive time (downtime)	25%	%
Planned maintenance		
Unplanned maintenance/ breakdown		
Waiting on Weather		
Field Efficiency	15%	%
Slopes		
Turning time		
Obstructions		
Total hours	8760	h
Non-productive time (downtime)	25%	%
Collecting hours	5584.5	h
Field efficiency loss in production rate	15%	%
Avg abundance (TOML-F)	16.8	kg/m^2
Avg abundance (Other)	10.3	kg/m^2
Production per annum per PV (TOML-F)	8.65 (capped at 7)	Mwmtpa
Production per annum per PV (Other)	5.29 (capped at 5)	Mwmtpa

13.9 LOM plan

13.9.1 LOM plan assumptions

Production assumptions are discussed in Section 13.4.

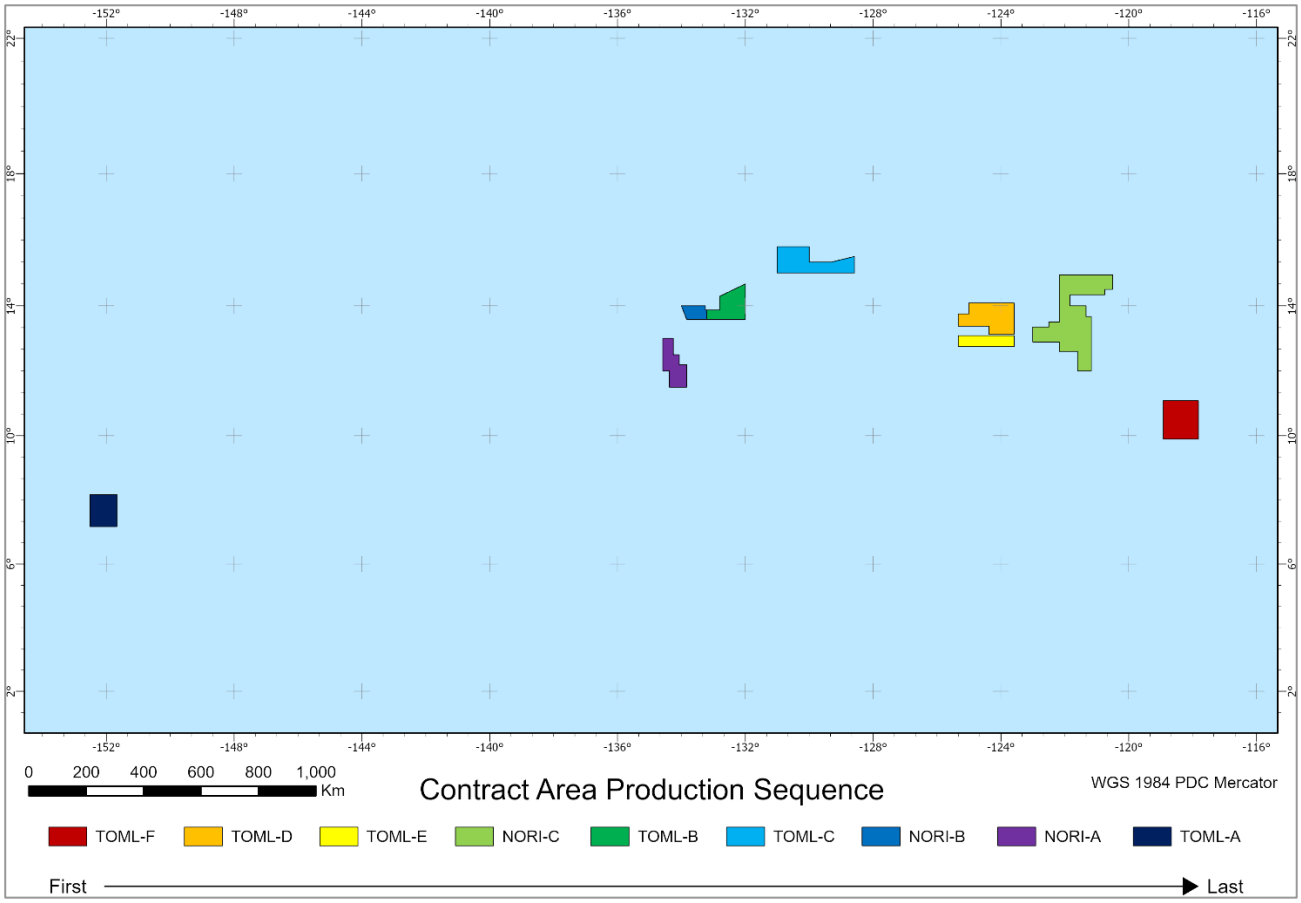
Sequencing of the NORI-TOML area for this IA was assumed in the following order:

- TOML-F – highest abundance, high grade and closest to NORI Area D
- TOML-D – next highest grade close to TOML-F
- TOML-E – mined in conjunction with TOML-D and immediately to the south

- NORI-C – largest lease, close to TOML-D and TOML-E
- TOML-B – close to NORI-C
- TOML-C – close to TOML-B
- NORI-B – next closest
- NORI-A – next closest
- TOML-A – lowest grade, furthest away

This predominantly east to west progression sequence is shown graphically in Figure 13.22.

Figure 13.22 NORI-TOML mining progression by lease



Source: AMC

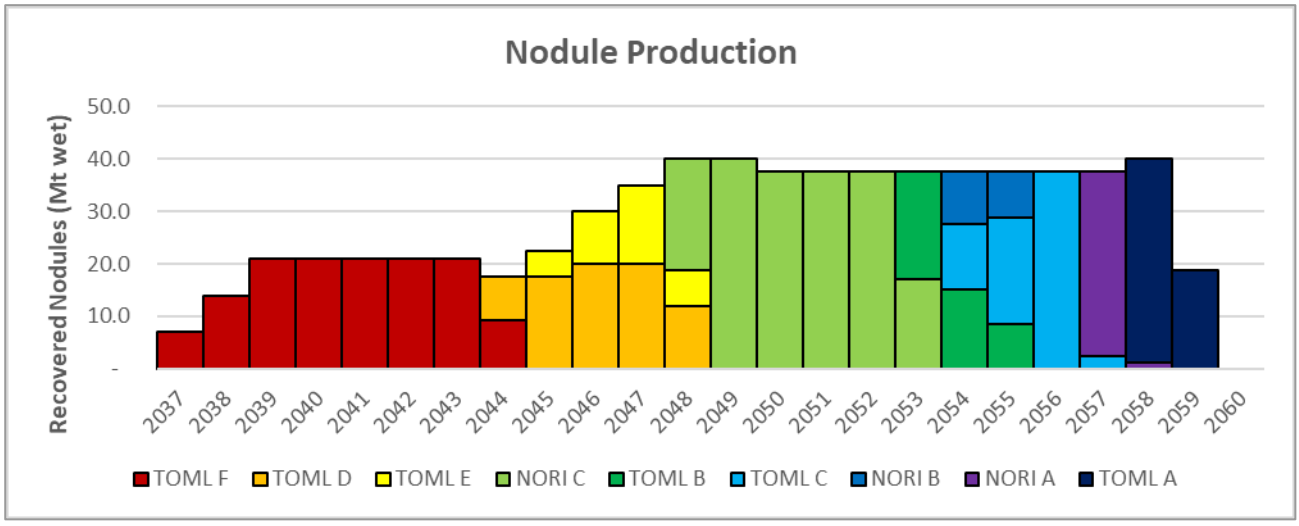
13.9.2 LOM plan result

The annual tonnage profile by lease is shown in Table 13.13 and graphically in Figure 13.25 (annual production by area) and Figure 13.26 (annual nodule abundance and grade).

Table 13.13 LOM plan production summary

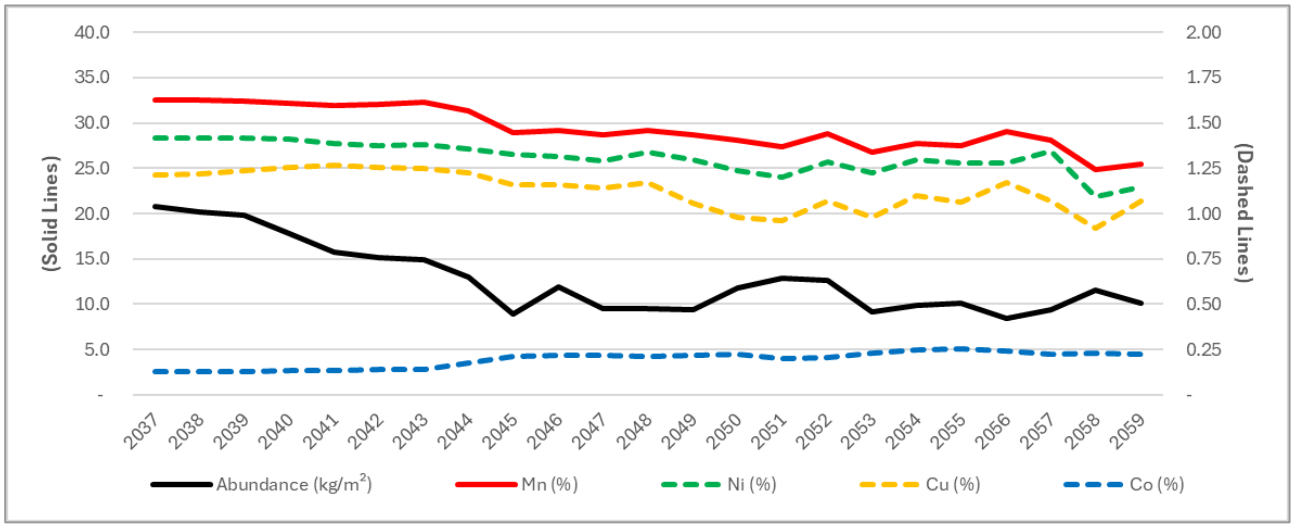
Year	TOML-F	TOML-D	TOML-E	NORI-C	TOML-B	TOML-C	NORI-B	NORI-A	TOML-A	Total
2037	7	0	0	0	0	0	0	0	0	7
2038	14	0	0	0	0	0	0	0	0	14
2039	21	0	0	0	0	0	0	0	0	21
2040	21	0	0	0	0	0	0	0	0	21
2041	21	0	0	0	0	0	0	0	0	21
2042	21	0	0	0	0	0	0	0	0	21
2043	21	0	0	0	0	0	0	0	0	21
2044	9.3	8.2	0	0	0	0	0	0	0	17.5
2045	0	17.5	5	0	0	0	0	0	0	22.5
2046	0	20	10	0	0	0	0	0	0	30
2047	0	20	15	0	0	0	0	0	0	35
2048	0	11.9	6.8	21.3	0	0	0	0	0	40
2049	0	0	0	40	0	0	0	0	0	40
2050	0	0	0	37.5	0	0	0	0	0	37.5
2051	0	0	0	37.5	0	0	0	0	0	37.5
2052	0	0	0	37.5	0	0	0	0	0	37.5
2053	0	0	0	17	20.5	0	0	0	0	37.5
2054	0	0	0	0	15	12.5	10	0	0	37.5
2055	0	0	0	0	8.6	20.3	8.6	0	0	37.5
2056	0	0	0	0	0	37.5	0	0	0	37.5
2057	0	0	0	0	0	2	0	35.2	0	37.5
2058	0	0	0	0	0	0	0	1.2	38.8	40
2059	0	0	0	0	0	0	0	0	18.7	18.7
Total	**135.3**	**77.6**	**36.8**	**190.8**	**44.1**	**72.7**	**18.6**	**36.4**	**57.5**	**669.7**

Figure 13.23 LOM plan annual production by lease



Source: AMC

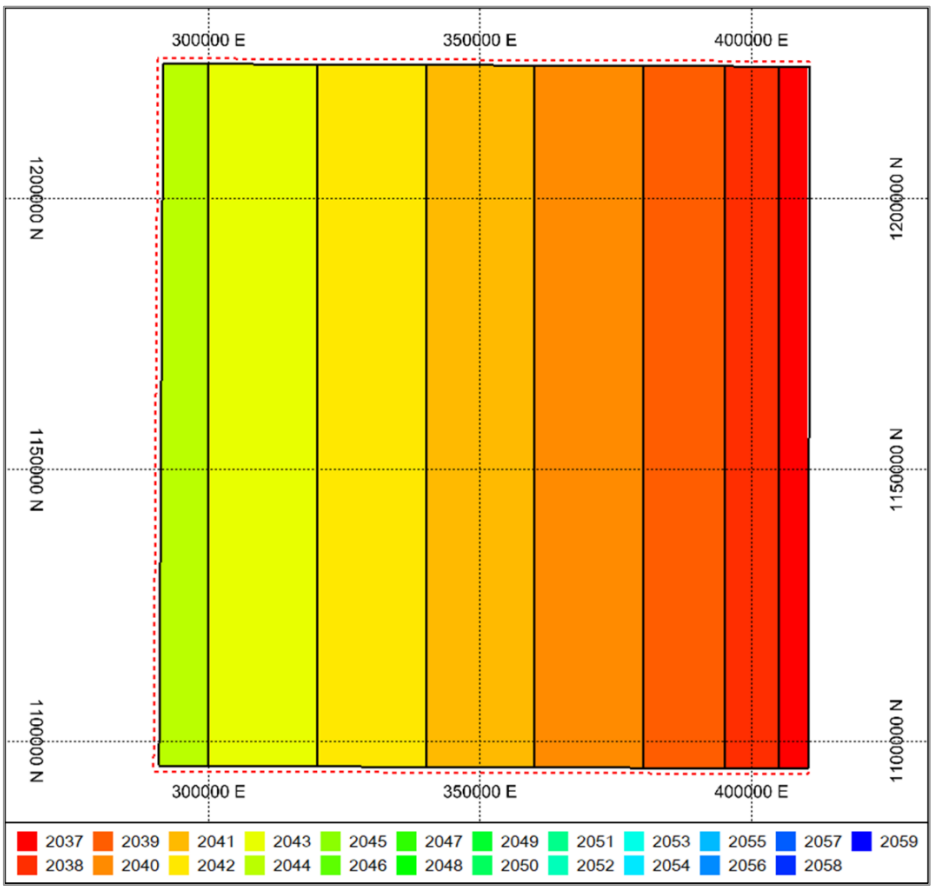
Figure 13.24 LOM plan annual nodule abundance and grades



Source: AMC

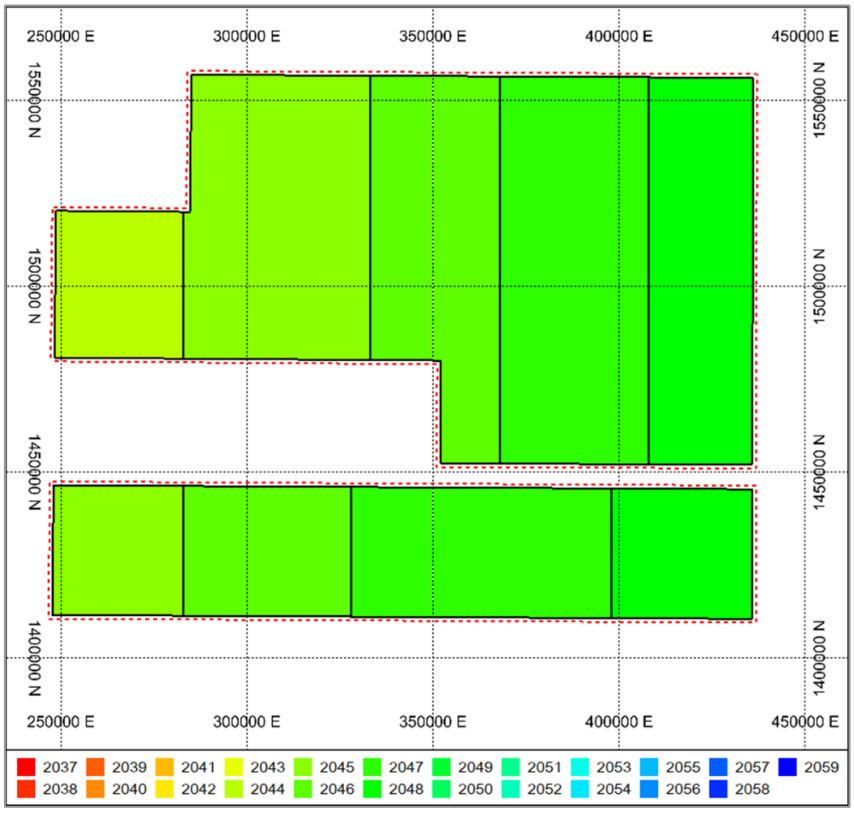
Lease by lease progression plans are shown in Figure 13.25 to Figure 13.32.

Figure 13.25 TOML-F collection sequence by year



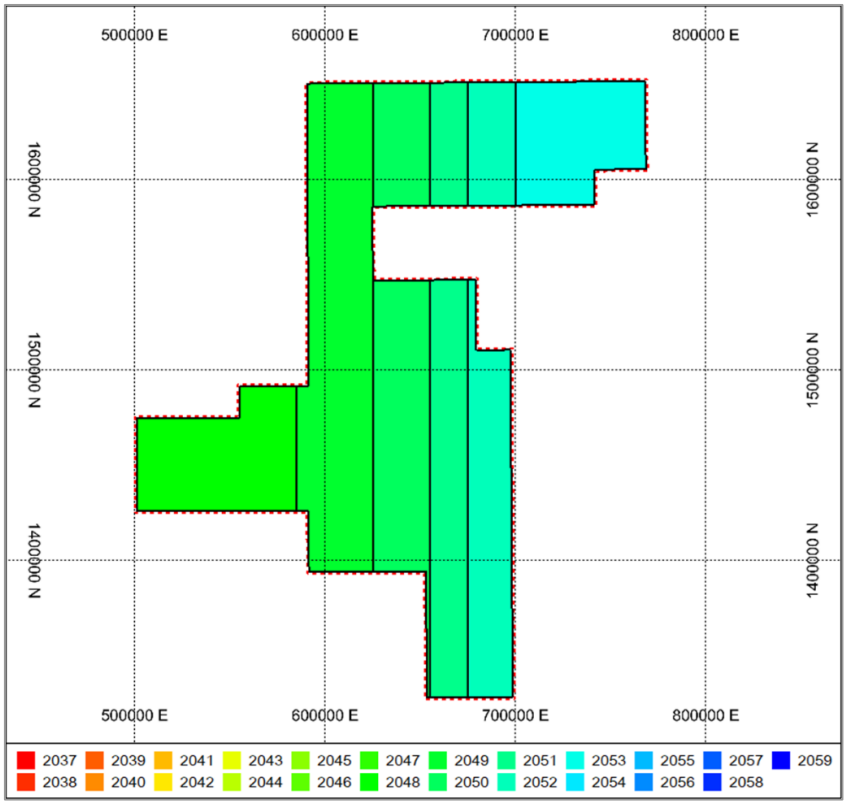
Source: AMC

Figure 13.26 TOML-D/TOML-E collection sequence by year



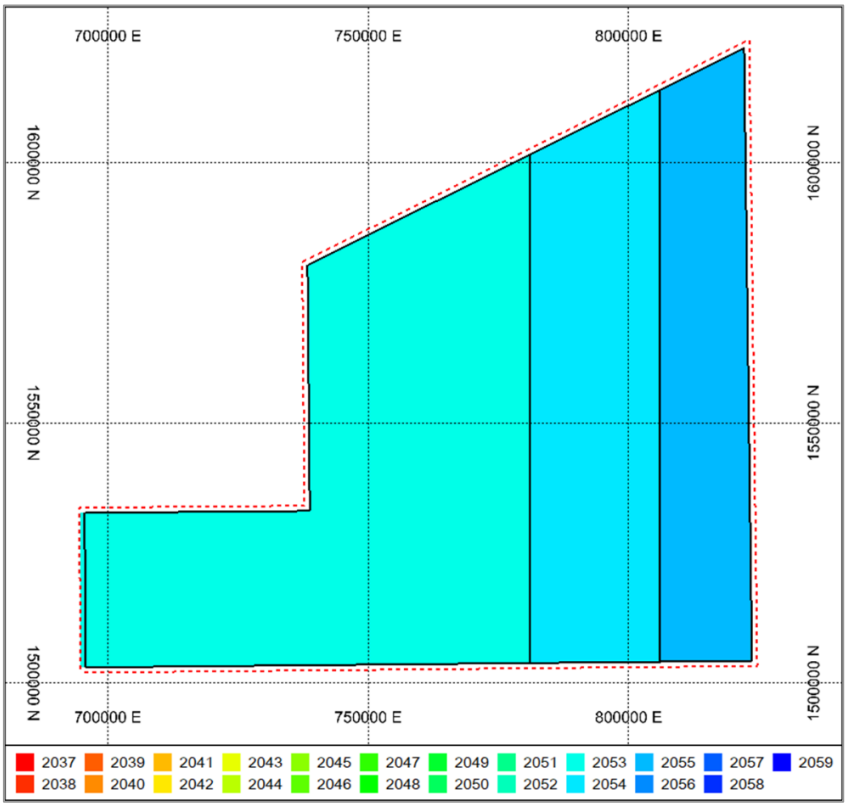
Source: AMC

Figure 13.27 NORI-C collection sequence by year



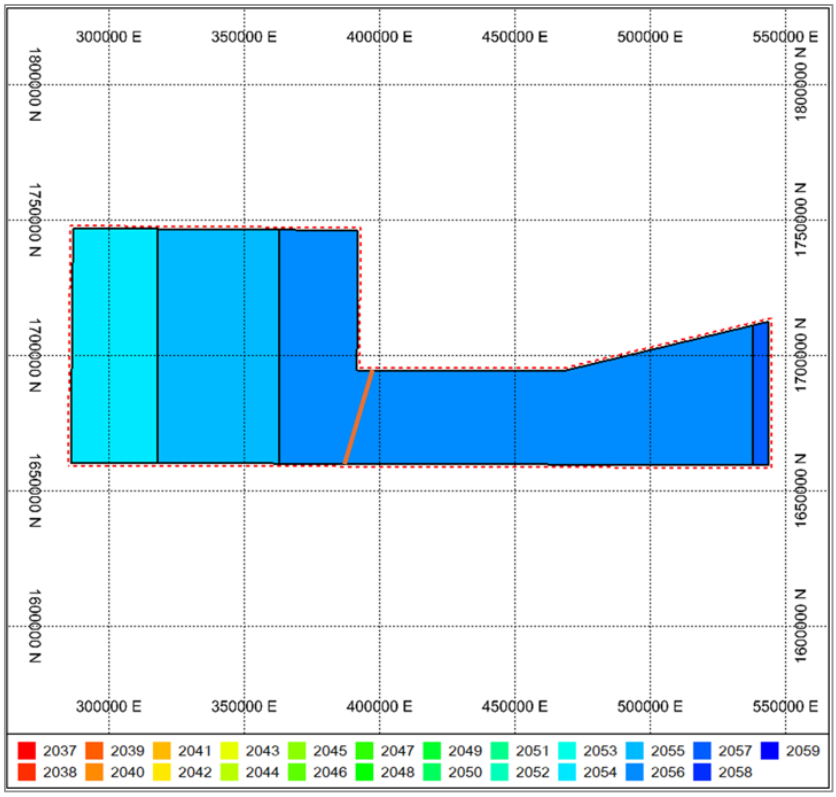
Source: AMC

Figure 13.28 TOML-B collection sequence by year



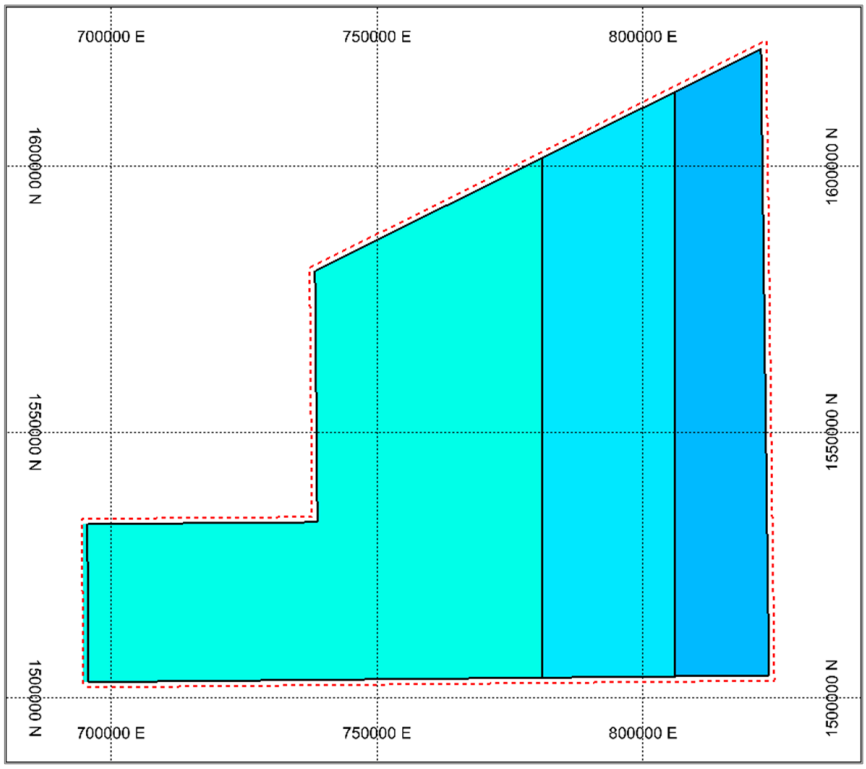
Source: AMC

Figure 13.29 TOML-C collection sequence by year



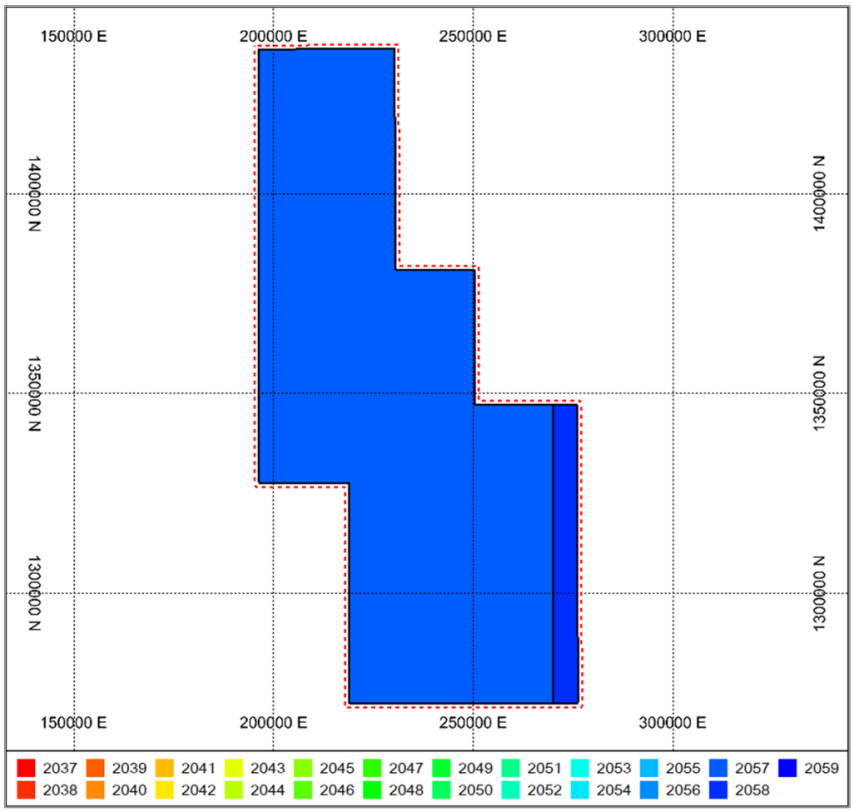
Source: AMC. Note a cable has been identified within the TOML-D area. The cable will be considered within the mine plan when developed with any exclusion zones to be confirmed.

Figure 13.30 NORI-B collection sequence by year



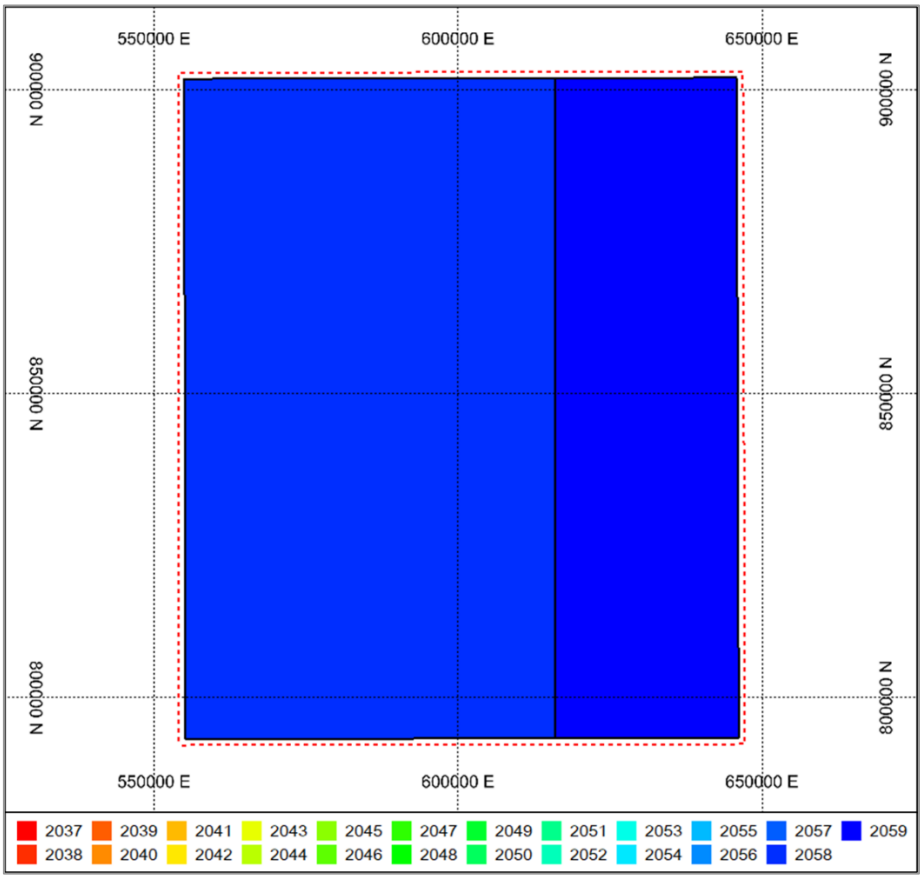
Source: AMC

Figure 13.31 NORI-A collection sequence by year



Source: AMC

Figure 13.32 TOML-A collection sequence by year



Source: AMC

14 Processing and recovery methods

14.1 Overview

Processing of nodules collected from the Property is required to recover the metals contained and realize the economic viability of the project. This section outlines the flowsheet selection process that was undertaken and explains how the selected process works to recover these metals for sale. The flowsheet development process for the selected flowsheet is discussed, though some specific outcomes and learnings from test work can be found in Section 10.

The flowsheet selection process involved ideation of plausible flowsheet configurations and creation of a shortlist. The shortlist of flowsheet options then underwent a screening process, where each was assessed against a range of criteria and objectives as developed by TMC. Eventually, the flowsheet selected for further development was RKEF/Refining, which combines pyrometallurgical unit operations on the front end and hydrometallurgical refining to generate final products. The pyrometallurgical section of the flowsheet combines three existing processes: RKEF technology, sulfidation and converting to generate a matte material. The matte is then fed downstream into conventional hydrometallurgical refinery unit operations to generate final products.

TMC's long term scenario for NORI and TOML involves processing the nodules initially through multiple lines in one or more existing RKEF facilities in Indonesia. The intended commercial agreement would be to process the nodules through a tolling arrangement, where TMC retains ownership of the nodules, any intermediates and final products from the process. The assumption is that each Indonesian operation will process the nodules through a RKEF and Peirce-Smith converter aisle to generate a matte product. The matte is expected to be shipped to the US for further refinement. The refinement facility is expected to be a hydrometallurgical refinery using an existing flowsheet to produce nickel sulfate, cobalt sulfate and copper cathode as the primary final products that may be sold as feedstocks for battery production and energy storage.

This section provides an overview of flowsheet development to date. There is a particular focus on the front-end pyrometallurgical process due to further advancement of the flowsheet development process in preparation for negotiations with existing Indonesian operations, though progress completed to date on downstream refinery testing is also included. Specific outcomes and learnings from all test work can be found in Section 10.

The front-end of this process involves first drying, dehydrating, initiating the reduction and pre-heating the nodules through a rotary kiln, with the resulting calcine discharged at high temperature. The resultant calcined nodules are then transferred from the kiln to feed bins above an electric smelting furnace, where electric power is employed to smelt the material into two immiscible (distinct) layers that are removed from the furnace through tapping at separate height levels. The nickel, copper and cobalt deport to the higher density, and thus bottom alloy phase, while the manganese deports to the lower density, top layer oxide phase, called manganese silicate. The manganese silicate represents a final product from this process and is crushed, screened and sold as feedstock for production of manganese alloys for use in steel production.

The alloy phase is transferred into a two-step process employing Peirce-Smith converters. In this configuration, sulfur, silica flux and air/oxygen as a carrier gas are added in the first (sulfidation) vessel to "convert" the metal to a sulfide phase called "matte" while simultaneously deporting some of the iron to an oxide "slag" phase that floats on the surface of the matte. In the second (finishing) vessel, more air/oxygen and silica flux are added to deport even more iron to the slag phase, which is recycled back into the sulfidation vessel to maximize metal recovery. The matte from the second vessel containing 5% iron is planned to be shipped for refining in the US.

In the refinery, the matte is assumed to undergo a two stage leach process to remove the copper from the nickel and cobalt. The copper will be subject to electrowinning to produce copper cathode, an important product that is most commonly used to make copper wiring. The nickel and cobalt bearing liquor will proceed into a cobalt SX to separate the two components. The resultant cobalt stream will be subject to an IX and manganese removal before being crystallized into pure cobalt sulfate. The nickel phase will undergo its own SX and subsequent crystallization to nickel sulfate. The cobalt and nickel sulfate are final products that will be sold as feedstocks for battery production and energy storage. Ammonium sulfate is also generated during the nickel SX, and this is intended to be sold as a fertilizer material.

14.2 Flowsheet options screening and selection

The foundational objective of the flowsheet development was to create a configuration that can maximize recoveries of battery grade metals and steel-making feedstocks while minimizing solid waste. To achieve the near zero solid waste objective, every product or resultant stream from the eventual process will need to be a useful material with an identifiable, existing market or an identified destination to recycle the stream.

Project objectives were developed for the screening of the plausible flowsheet options. Multiple process types and flowsheet configurations were identified and assessed against these objectives. Technical, financial market, and strategic considerations were all assessed as part of the screening process. Table 14.1 below, shows a simplified description of the screening of the different process options that were assessed, and the project objectives against which they were judged. A green cell indicates that the flowsheet meets requirements for that objective. Orange means the flowsheet partially meets objectives or there is significant uncertainty, while red means the flowsheet does not or is unlikely to meet the objective.

Table 14.1 Simple Screening Process for Various Nodule Processing Flowsheet Options

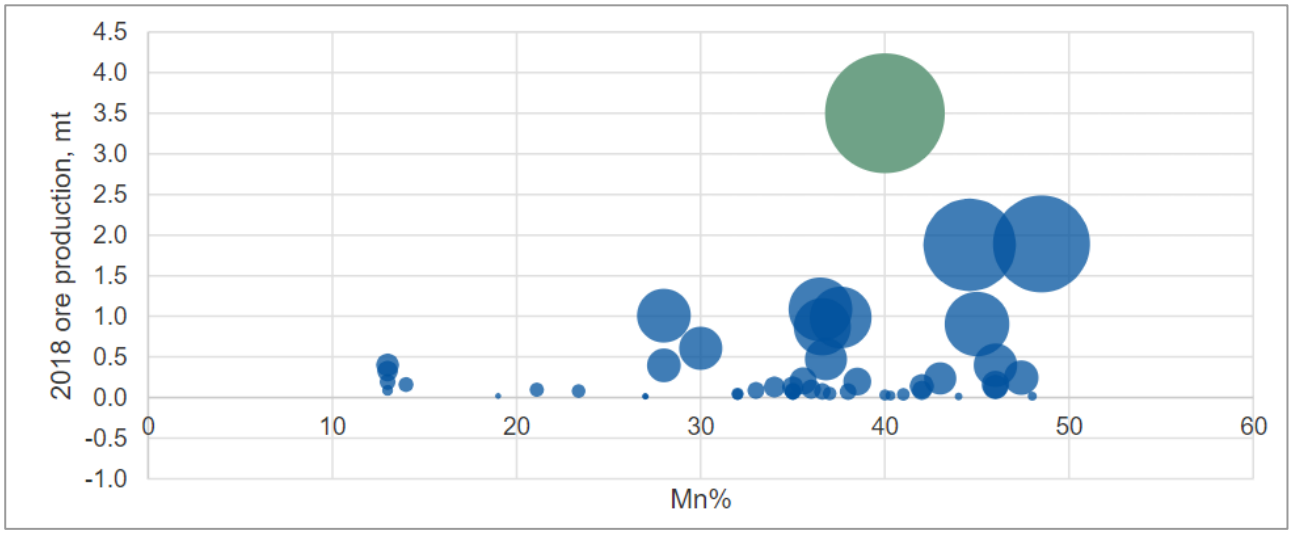
Flowsheet Option	Recoveries	Battery Grade Products	Mn Product Fits Existing Markets	Zero Solid Waste	Q1 Cash Costs	Cost/Time for Development	Risk/Reward
RKEF/Refining							
Thermal Upgrading							
Nitric Leach							
Cuprion Process							
Sulfuric Leach							
Chloride Leach							

The primary differentiating factors for selecting the flowsheet were generation of a manganese product that fits within an existing market and a flowsheet that yields near zero solid waste.

14.2.1 Manganese product and associated market

The development of nodule projects is expected to have a significant impact on the global manganese markets. Figure 14.1 presents the world's existing manganese mines, with a 60 ktpa nickel equivalent mine overlaid in green. A mine of this scale is equivalent to a 6.4 Mwmtpa nodule project, approximately 15% of the peak production reached in year 11 as proposed in this IA.

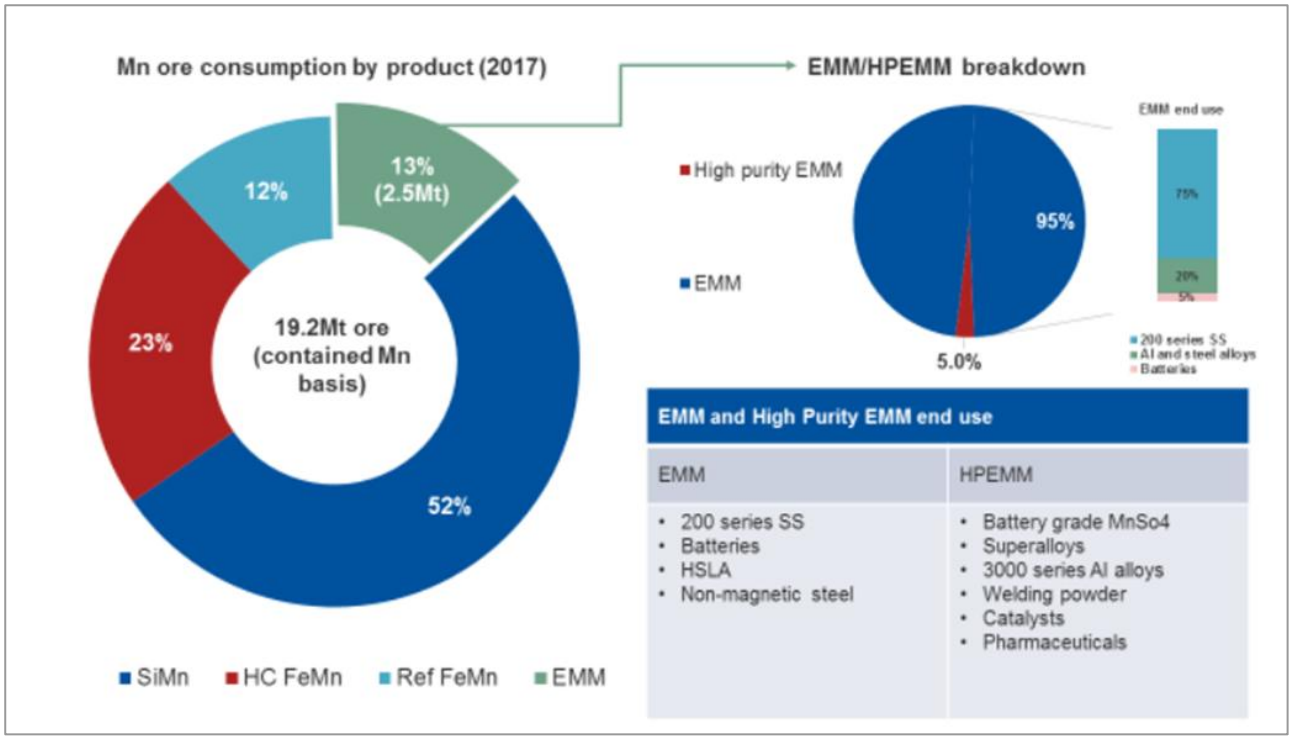
Figure 14.1 2018 production of manganese ore (blue) compared to 60 ktpa nickel equivalent project (green)



Source: CRU 2019. The bubble size indicates the total contained manganese in ore production

The primary uses of manganese are in the steel industry, which consumes upwards of 90% of all production. The manganese reacts with dissolved oxygen in the liquid steel melt and creates an oxide layer that can be removed. Dissolved oxygen in the steel melt creates a porous structure when the melt eventually solidifies. The removal of this dissolved oxygen with manganese creates a stronger and more durable final solid steel product (Kim 2018). Portable batteries and aluminum beverage cans are primary non-steel uses. In each case, manganese plays a vital role in improving the properties of the alloys and compounds. The chart in Figure 14.2 shows an estimate of how much manganese is consumed in each of its end-use applications.

Figure 14.2 2017 Manganese ore consumption by end-use project



Source: CRU 2019.

Processing of the nodules by pyrometallurgy (RKEF) produces a manganese silicate product that can be further processed to manganese alloys (Kim, 2018), (Sridhar et al,1976), (Sridhar et al, 1975). The high grade of manganese in this product rivals conventional high-grade manganese ores. Additionally, the product has a dry, pre-reduced nature, a favorable impurity profile, and the physical attributes of a slag material (strong, dense). The manganese silicate also contains the stable oxides from the nodules, notably silica and a portion of the iron, that are required in the downstream manganese alloying process. All these characteristics make this a potentially disruptive product in the production of manganese alloys, as it conceptually compares favorably in relation to both manganese ore and manganese-rich slags as feed in the production of silico-manganese alloy.

The manganese silicate slag product from the smelting unit operation represents about 90% of the mass of the solids from the operation. Although there is significant growth in manganese sulfate for battery uses and a sizeable market for Electrolytic Manganese Metal (EMM) and other specialized manganese products, the production volumes from nodules overwhelms the manganese demand in these markets. In an effort to achieve TMC's near zero solid waste objective, the selected manganese product had to have a market that could consume the large volumes of manganese being generated. The RKEF flowsheet was the only one from Table 14.1 that was able to fulfill this objective.

14.2.2 Near zero solid waste generation

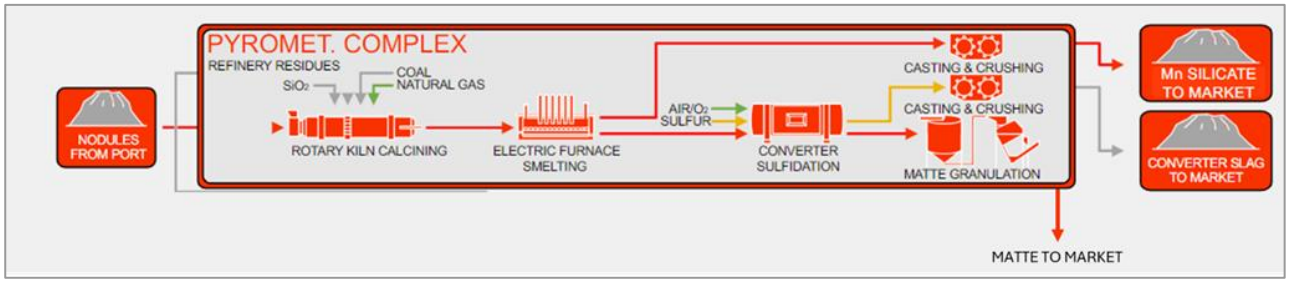
The RKEF and refining flowsheet was the only option to offer near zero waste. This is because of the production of a fayalite slag that is a saleable product, instead of residues that require disposal to residue storage facilities. Slags are commonly employed as construction aggregate, rail ballast, and sand blasting, while there is very little commercial precedence for large scale uses of residues produced in other hydrometallurgical processes used to generate alternative products, such as those described above.

Combined with good performance across other selection criteria and a comparatively straight-forward development pathway given RKEF's extensive global operating experience, this flowsheet was selected for further development.

14.3 Process description

The selected processing route for the nodules originally envisaged a greenfield plant comprising both pyrometallurgical and hydrometallurgical plants, producing nickel and cobalt sulfates (battery grade) as well as copper cathode and a manganese silicate slag product. The converting process also produces a slag by-product, which is intended for sale as a construction aggregate, and therefore should not require disposal as waste. The process to produce matte is depicted in Figure 14.3.

Figure 14.3 Major Equipment and Associated Streams from Pyrometallurgical Process



Source: Hatch

14.3.1 Alloy production

Nodules are reclaimed from stockpiles and fed directly to rotary calcining kilns, together with coal to act as a reductant and silica to regulate slag chemistry. In the rotary kilns, the nodules are heated to high temperatures. Free moisture in the nodules is removed, as is the crystalline moisture (de-hydrated). Higher oxides of manganese first decompose thermally and then are further partially reduced carbothermically together with selected other oxides.

The calcined nodules are transferred hot in refractory-lined containers to the EF. Here, residual carbon left after calcining completes the desired degree of reduction. It is important to control reduction such that most of the manganese remains in the slag phase, while ensuring nickel, copper and cobalt reports to alloy.

The alloy and manganese silicate are tapped periodically at different heights from the furnace. The alloy is transferred to the sulfidation and converting steps (matte production), while the manganese silicate is cast into a pit, allowed to freeze, and then recovered and crushed to a suitable size distribution (based on customer requirements) for sale to the silico-manganese alloy industry.

14.3.2 Matte production

Most ferronickel RKEF plants have refined ferronickel as their final product. At least two plants (Société le Niquel (SLN)'s Doniambo smelter in New Caledonia and PT Vale Indonesia) have produced or currently produce matte by adding sulfur to the process. The Doniambo process is far more efficient in terms of sulfur utilization and has lower SO_2 emissions to the environment, so has been chosen for the matte process.

The production of matte is achieved using a two-step process in a Peirce-Smith converter aisle. The first step is in dedicated sulfidation vessels. Alloy is added to the partially filled vessel and air is blown through most of the vessel tuyères to partially and selectively oxidize some of the iron which deports to slag and combines with silica flux to achieve a manageable fluidity. At the same time, liquid sulfur at 140°C (maintained by steam heated lines) is pumped intermittently through a limited number of dedicated tuyères to transform the alloy to matte. When sulfur is not being injected, steam is used to keep the tuyères open. The sulfidation vessels operate with a large matte heel in a semi-continuous mode (i.e., relatively small amounts of product matte are removed at a time). Slag from the sulfidation vessels represents the converter slag and is sold.

The intermediate matte from the sulfidation vessels is taken to a FV, where blowing commences and more silica flux is added to form slag with the iron that is being oxidized. Blowing continues until the iron in the matte decreases to 5%. The 5% iron matte is sent to a facility in the US for refining into final products. Slag from the FV is rich in pay-metals so it is therefore recycled back to the sulfidation vessels to improve recovery.

14.3.3 Matte refining

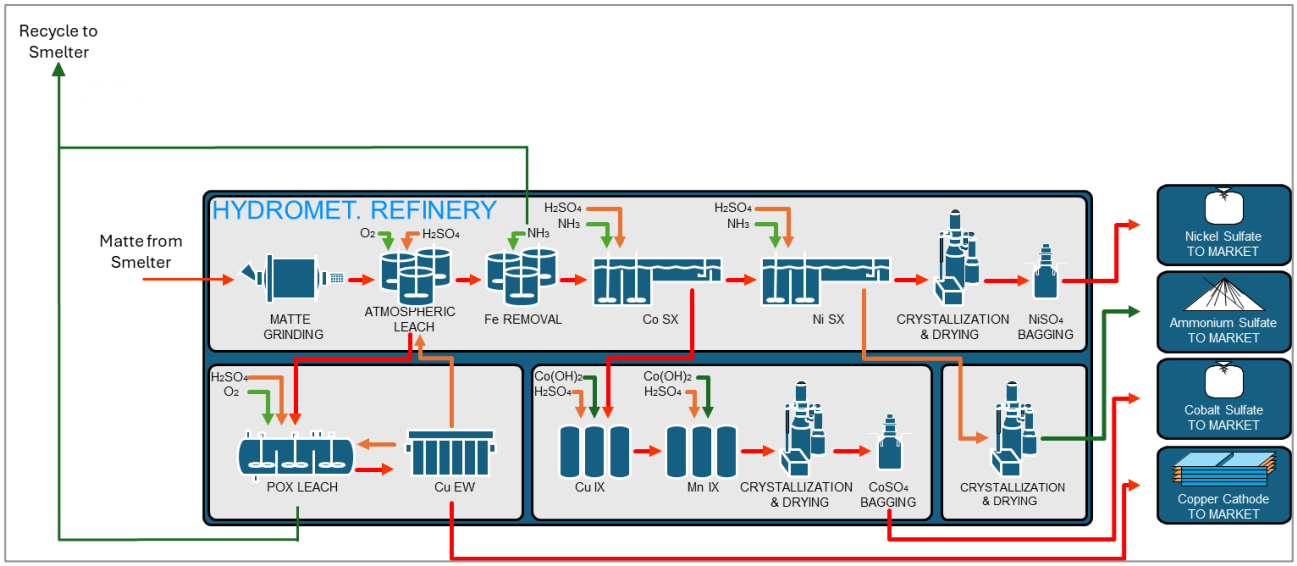
Matte produced at the Indonesian RKEF plants are assumed to be shipped to a dedicated hydrometallurgical refinery in the USA to generate refined products. As with the pyrometallurgical section of the flowsheet, the matte refining process uses existing technologies that are already in use commercially.

The downstream refining program begins by putting the granulated matte through a mill before subjecting it to a two-stage leach process – an initial agitated atmospheric leach (AL) and subsequent pressure oxidation (POX) leach. The leaching process is designed to separate the copper from the nickel and cobalt. Small amounts of nickel and cobalt that remain in the AL residue are removed during the

POX and recycled back to the smelter to maximize recoveries. The copper stream from the POX undergoes electrowinning, resulting in copper cathode which represents a final product from the process.

The nickel and cobalt that is separated during the leaching process is then fed into a cobalt SX, which separates the nickel and cobalt into their individual components. Copper that was not removed during the leaching phase is extracted after the cobalt SX and recycled to the POX. The cobalt phase also undergoes a manganese removal step, with the residual manganese recycled back into the smelter to maximize its recovery to the manganese silicate. The nickel phase resulting from the cobalt SX then proceeds to a nickel SX where it is separated from the ammonium that has been added throughout the process. All three phases – cobalt, nickel and ammonium – proceed to individual crystallization processes to create sulfates, all of which represent final productions from the refinery. Nickel and cobalt sulfate can be sold as feedstocks for battery production and energy storage, while the ammonium sulfate is sold for use as a fertilizer. The process to generate final products from the matte is depicted below in Figure 14.4.

Figure 14.4 Major Equipment and Associated Stream from the Hydrometallurgical Refinery



Source: Hatch

14.4 Flowsheet development

14.4.1 Literature review

Pyrometallurgical processing of nodules has been extensively studied from the early 1970s until the present day and appears to be the preferred process for most of the other currently active nodule processing research groups. Many groups including Kennecott Utah Copper LLC[2] ; Inco Limited[3]; Cuban / Bulgarian; German; Indian; Japanese; and Korean entities have studied pyrometallurgical processing of nodules at a laboratory scale. The nodule samples for these tests were collected from their respective license areas in the CCZ.

[2] Kennecott Utah Copper LLC is a division of Rio Tinto Group. It is a mining, smelting and refining company and has its corporate headquarters in South Jordan Utah.

[3] Inco Limited (Inco) was a Canadian mining company and the world's leading producer of nickel for much of the 20th century. In October 2006, Inco was purchased by the Brazilian mining company Vale.

A detailed review of specific process, modelling and available bench-scale testing data from the following parties was reviewed to inform the design process for TMC's preliminary flowsheet:

- Inco (Canada)
- Sumitomo (Japan)
- German Federal Institute for Geosciences and Natural Resources (Germany)
- US Bureau of Mines (USA)
- Indian National Metallurgical Laboratory (India)

The literature review focused on specific content provided by each of the above groups. Testwork at both bench and pilot scale (if available) involving calcining, smelting and matte production were all assessed. Key results that were analyzed included composition of intermediate materials (calcine, alloy, manganese silicate and matte) as well as energy usage, consumables used and quantity requirements, and operating conditions that were tested by each of the groups. References from the literature review are provided at the end of the chapter. Based on review of the data, it was concluded that the best data for designing a preliminary pyrometallurgical flowsheet for treating nodules was provided by Inco, Japanese and German references.

14.4.2 Bench-scale test work

NORI has commissioned numerous small-scale investigations in support of the project, prior to, during and after the larger scale pilot work described in Section 14.4.4.

The work was carried out at:

- Kingston Process Metallurgy, Ontario (KPM)
- FLS, Pennsylvania
- Expert Process Solutions (Glencore), Ontario (XPS)
- SINTEF, Norway.
- SGS Lakefield, Ontario (SGS)

The test work is summarized in Table 14.2.

Table 14.2 Summary of Bench-scale Test Work

Final Report Date	Facility	Description	Reason
29-May-2019	KPM	Evaluation of alternate manganese products	Exploring potential opportunities for added value for project
19-Nov-2019	FLS	Calcination and carbothermic reduction of nodules in a lab tube furnace and direct-fired batch kiln	Investigation of reduction process prior to pilot-scale work. Preliminary assessment of sintering and dusting behavior.
22-Apr-2020	XPS	Oxidation of artificial matte to final product matte	Investigation of converting prior to pilot-scale work. Measuring elemental partition coefficients as a function of %Fe in matte.
28-Aug-2020	XPS	Chemical analyses of calcine, slag and metal samples as part of a 'Round Robin' campaign	To help establish reliable assaying methods
9-Oct-2020	XPS	Oxidation of Mn in alloy and sulfidation using pyrite and pyrrhotite	Investigation of pre-converting steps ahead of pilot-scale work
11-Dec-2020	KPM	Smelting of calcine produced at FLS part way through piloting	To resolve issues with determining correct reductant coal addition at FLS
7-May-2021	KPM	Small scale calcination of nodules in batch rotary-kilns followed by induction furnace smelting	Inputs to process modelling and for planning pilot-scale work
14-Sep-2021	KPM	Determination of residual moisture in nodules after draining excess water	Provide basis for moisture content of nodules entering process plant
24-Jan-2022	SINTEF	Production of silico-manganese alloy from smelting slag samples	Preliminary investigation of suitability of smelting slag product as feed to silico-manganese industry
16-Mar-2022	KPM	Quantitative SEM investigation of slag samples from smelting and converting tests	Determination of elemental distribution amongst different phases
23-Jun-2022	KPM	Assaying material from FLS and XPS pilot campaigns	Assay cross-checks
10-Oct-2024	SGS	Refining of TMC's pilot matte into nickel and cobalt sulfates	Proof of concept and preliminary data collection for the hydrometallurgical refinery aspect of the flowsheet

14.4.3 Concept engineering

The NORI IA (AMC Consultants, 2021a) study assessed the entire flowsheet as it was then envisaged, with large scale processing of nodules from recovery from the ocean bottom through pyrometallurgical and hydrometallurgical processing plants to final products. The pyrometallurgical component of the IA was based on the process outlined in Section 14.3.

14.4.4 Piloting

14.4.4.1 Piloting overview

A set of pilot-scale pyrometallurgical processing campaigns using a large sample (75 t) of nodules harvested from NORI Area D of the CCZ. The work comprised calcining, smelting, sulfidation and converting steps in accordance with the chosen process for the project.

The main objectives of the pilot scale work were to:

- Demonstrate the chosen pyrometallurgical process.
- Produce on-spec matte for subsequent hydrometallurgical test work and on-spec manganese silicate slag for product development activities.

- Update process design criteria in support of project development and engineering design. The work was carried out in two separate locations:
  - FLS testing facility in Bethlehem, Pennsylvania calcined the nodules, and
  - The XPS technology centre in Falconbridge, Ontario smelted the calcine from FLS, sulfidized the resultant alloy, which was then converted to product matte.

The nodules were calcined at the FLS pilot kiln facility in Pennsylvania and the calcine was shipped to Falconbridge, Ontario, where the remainder of the pyrometallurgical work was performed in the XPS pilot-scale DC arc furnace. The pilot-scale testwork conducted is summarized in Table 14.3. Selected results from the piloting are available in Section 10.

Table 14.3 Summary of pilot scale test work

Final Report Date	Facility	Description
December 2020	FLS	Polymetallic nodule calcining using a pilot rotary kiln system
10-Feb-2022	XPS	Pilot smelting of calcined sea nodules
23-Dec-2021	XPS	Sulfidation and converting of alloy

The pyrometallurgical pilot phase of work is considered complete and was able to demonstrate that:

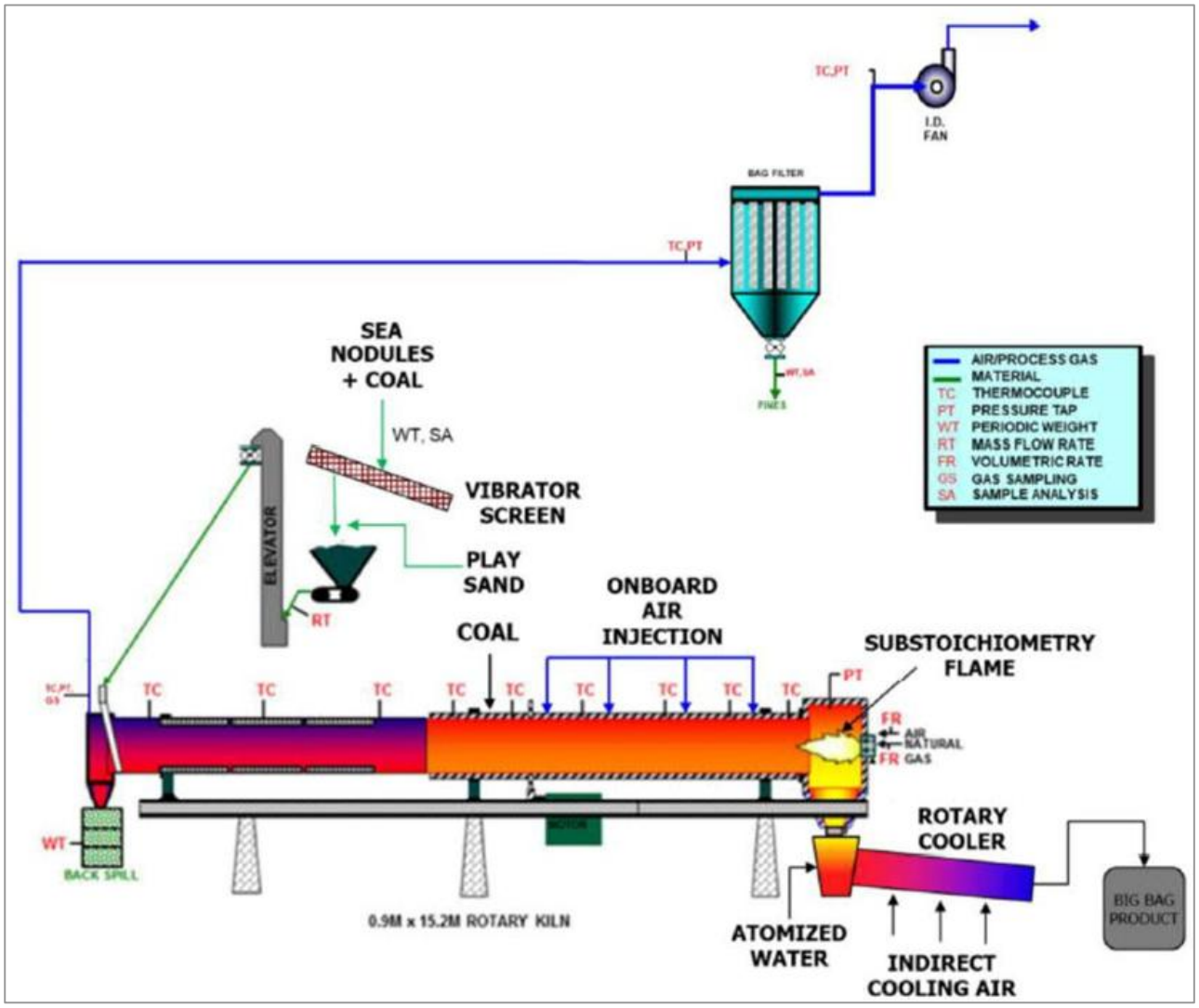
- The nodules can be smelted to an alloy with excellent recoveries of nickel, copper and cobalt.
- A manganese silicate slag product can be made that conforms to TMC's preliminary specification under suitably reducing conditions consistent with the current plan for the process.
- A final matte can be made that is suitable for hydrometallurgical processing (albeit with an iron level that is a little higher than planned for the project).

14.4.4.2 Calcining at FLSmidth

Nodules retrieved during the 2020 campaign were shipped to FLS for calcining, which took place between 12 October and 14 November 2020.

Calcining was performed in the facility's large pilot kiln, which is 15 m long and 0.9 m in diameter. This kiln has been in use for several years, including for test work with which TMC's technical consultant had been involved in and has witnessed in the past. The equipment is depicted in Figure 14.5 and Figure 14.6. Note that feeding and cooling underwent some changes during the work as no-processing had been planned since the currently proposed commercial plant is expected to feed as-received nodules directly to the kilns.

Figure 14.5 Schematic of kiln and ancillary equipment as originally configured



Source: FLSmidth

Figure 14.6 Pilot Plant Rotary Kiln, Feed-End to Right.



Source: FLSmidth

14.4.4.3 Smelting, sulfidation and converting at XPS

Pilot operations vs commercial

The proposed commercial operation for the project closely follows matte production as practiced by SLN at their Doniambo nickel laterite processing facility in New Caledonia until 2016, where calcine is smelted conventionally in an alternating current (AC) furnace to produce a ferronickel alloy, similar to many plants worldwide. Uniquely at SLN, some of this ferronickel was taken to a Peirce-Smith converter aisle where liquid sulfur was added through one of the tuyères, while air was used simultaneously in the other tuyères to oxidize out some of the iron. This first vessel operated under more or less steady chemistry conditions (at the point of an intermediate matte containing around 30% iron). Once the vessel was full of matte, roughly half of the matte was then transferred to a second converter to remove most of the remaining iron to produce a Bessemer matte for downstream hydrometallurgical refining.

There are only a limited number of facilities worldwide that offer pilot-scale EF smelting facilities at a scale suitable for the project needs. Pilot-scale Peirce-Smith converters are not available, and representative liquid sulfur injection would be challenging in other pilot equipment. Under these circumstances, it is not possible to closely replicate the proposed commercial operation. Some degree of compromise is necessary to devise test work that adequately reproduces the key process steps from a metallurgical perspective. Thus, it was decided to proceed with both the smelting and sulfidation/converting work using the same furnace, namely the direct current DC furnace at

Glencore's XPS facility in Falconbridge, Ontario, as it is at least partially analogous of the anticipated industrial process.

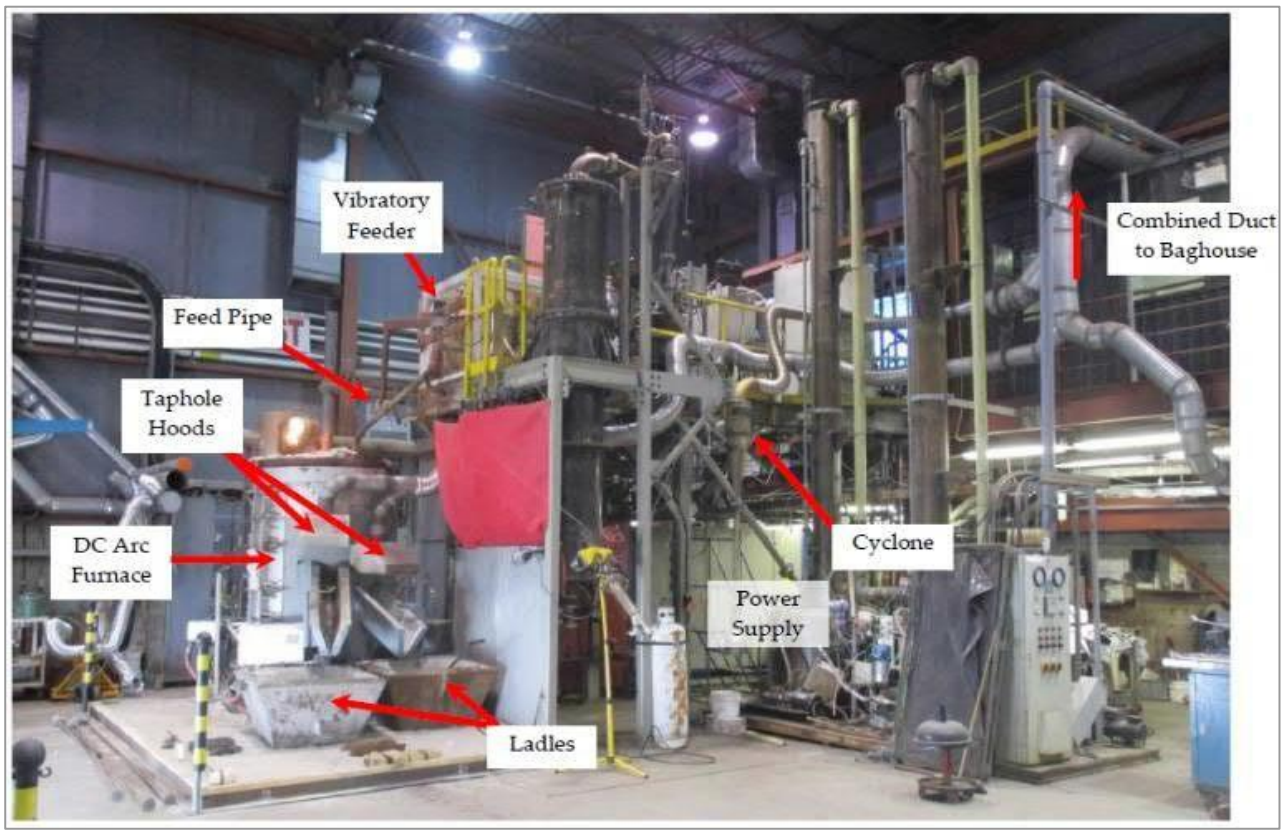
Equipment description

The XPS DC furnace is a 250 kW cylindrical furnace with a diameter inside the refractory lining of 762 mm and a total height of nearly 3 m above the floor. It is equipped with metal and slag tapholes for intermittent removal of molten material. It has an off-gas system for particulate capture. See Figure 14.7 and Figure 14.8 for layout and for dimensions.

A heel of material is needed upon which to strike an arc for the furnace to power up. Feed can then be added semi-continuously through a vibratory feed system connected to a feed pipe through the furnace roof, or to a pneumatic conveying system and injection lances. Lumps can also be added by hand through the roof port. A viewing port can be used to measure melt temperature via optical pyrometer, although that is dependent on not having any solids/partially melted material on top of the slag layer.

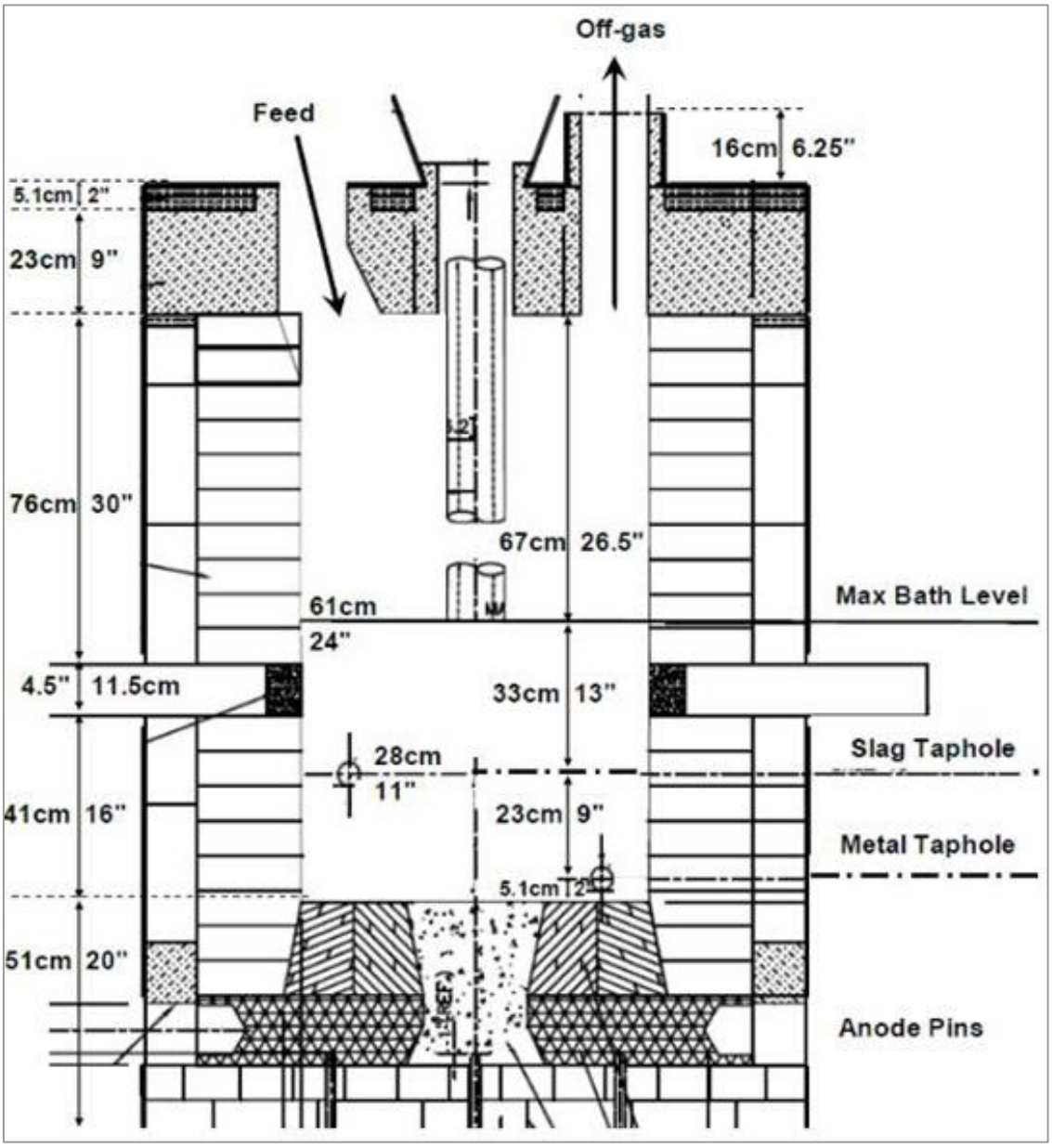
An operator control station has a computer and screen interface that can totalize power input and calculate bath temperature from known heat losses and smelting energy requirements. This is cross-checked against temperatures taken from molten streams when the furnace is tapped for slag and matte.

Figure 14.7 Pilot Plant DC Furnace and Ancillary Equipment



Source: XPS

Figure 14.8 DC Furnace Dimensions



Source: XPS

14.4.5 Demonstration scale calcining and smelting trials

Following the successful pilot mining trial completed in Q4 of 2022, TMC identified an opportunity to process 2,000 tonnes of collected nodules in a demonstration-scale metallurgical test at an existing RKEF facility in Hachinohe, Japan. The nodules were delivered to Japan in April of 2024, and testing was completed in April of 2025.

The trial involved first processing the nodules in one of the commercial kilns over six campaigns. Multiple campaigns were required as the nodules could not be calcined all at once due to limited hot calcine storage, and the calcine had to be cooled prior to transfer to the smelting facility. The calcine generated was stored and cooled over several weeks before transfer to an adjacent smelting facility containing a 4,000 kVA furnace that was used for smelting. The smelting took place over four campaigns.

The overall goals of the trial were to confirm the metallurgy (confirm operating parameters, process control approaches and gather data), gain operations experience with nodules and their derived intermediates, generate samples for product marketing and downstream metallurgical testing and to assess the slag behavior during smelting and associated refractory wear.

The tests were able to achieve all objectives and confirm that stable operations can be achieved at commercial scale. Commentary on technical outcomes from the trials can be found in Section 10.

14.4.6 Manganese silicate slag quality

The slag from the EF smelting process is intended to be sold as a feed to the silico-manganese industry and constitutes a significant portion of the project's revenue stream. The potential customers have certain parameters in mind that may make the slag more or less desirable. This imposes some additional constraints on running the smelting operation for optimal products.

A slag high in manganese and low in phosphorus is desirable. Low phosphorus is achieved by using high degrees of reduction to bring the phosphorus into the alloy. On the other hand, this also tends to bring more manganese into the alloy, depleting the slag to some extent. The mass ratio of slag to metal is quite high however, which helps to mitigate this. High degrees of reduction are, of course, beneficial to pay-metal recovery, but they also lead to more blowing requirements to remove iron, manganese, silicon, carbon, and phosphorus in the downstream converting/sulfidation process.

The XPS pilot campaigns indicate that a preliminary specification for slag can be met by reducing to the point where iron in slag is below 2% without raising manganese in alloy to high levels or significantly depleting manganese in slag. Outcomes from the commercial scale trial indicate that a target iron in slag is about 1.1%, and the associated manganese to phosphorus ratio would exceed 1000, which is desirable for most potential customers of the product.

15 Project infrastructure

15.1 Onshore engineering

15.1.1 Overview

TMC intends to begin operations onshore by using existing facilities in Indonesia that are already operating RKEF equipment, presently processing nickel laterite ores.

TMC has assumed that its onshore capacity through third party processing facilities is expected be able to handle up to 40 Mwmtpa of nodules, all of which are processed at existing RKEF facilities in Indonesia. The Indonesian operations are assumed to produce a nickel-copper-cobalt matte, a manganese silicate and a converter slag. The matte is assumed to be shipped to a dedicated US-based refinery that is owned and operated by TMC and further refined in nickel and cobalt sulfates and copper cathode.

The manganese silicate represents a final product from the process and is planned to be sold as a feedstock to silico-manganese alloy producers supplying the steel industry with this important consumable. The proximity of Indonesia to the Asian target market countries for manganese silicate, considering this product can constitute up to 90% of product production by mass, is an advantage to processing the nodules through these locations.

The converter slag is a product of the Peirce-Smith converting process and is assumed be sold for use as a construction aggregate. All capital scope required by the Indonesian operations to prepare plants to accept nodules is assumed by TMC to be the responsibility of that operator, with the cost being considered in the commercial arrangement between TMC and the third party.

15.1.2 Front-end nodule processing to matte in Indonesia

TMC has developed a strategy to de-risk and reduce capital required to perform preliminary processing on nodules. The front-end pyrometallurgical section of the selected flowsheet uses conventional RKEF technology that is employed in many existing processing facilities worldwide. This has informed the TMC approach to process the nodules at existing facilities under a tolling arrangement. In this setup, the nodules are assumed to be processed through an RKEF configuration followed by a Peirce-Smith converter aisle, ultimately producing a nickel-copper-cobalt matte, which is brought to a dedicated TMC-owned facility in the US for refining to final products. This strategy allows TMC USA to retain sole ownership of the nodules, and all intermediate and final products generated at all stages of the processing operations. TMC has assumed that the operators of the existing RKEF facilities are responsible for any capital modifications to prepare the plant to operate and compensated under an appropriate commercial arrangement.

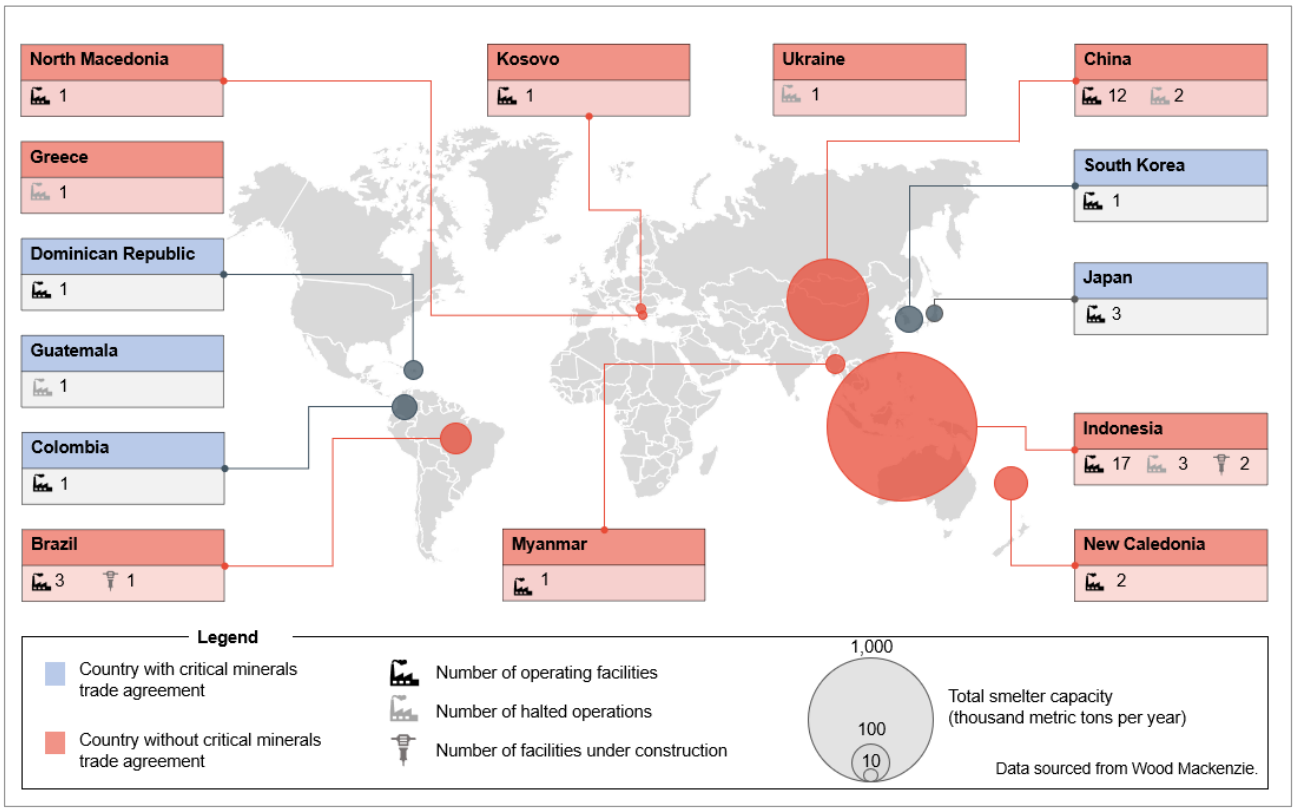
Several factors contributed to the pursuit of this strategy for Indonesian processing to matte, of which some are highlighted below.

- The construction of a new processing plant is extremely capital intensive.
- No construction or long lead item procurement issues will arise.
- There will be no requirement to hire and train operators or plant staff, as experienced personnel are already on-site.
- Recently and/or currently operating equipment does not require (re)commissioning.

This strategy is low risk, eliminates almost all capital expenses required to get into operation, and allows for the onshore timeline to align with anticipated commercial recovery permitting and offshore commercial recovery capabilities.

TMC actively investigated options for potential facilities to perform this front-end processing. Figure 15.1 shows a map of RKEF facility distribution worldwide, compiled by Hatch using data supplied by Wood Mackenzie (Jabber et al, 2024).

Figure 15.1 Total 2023 production capacity for ferronickel and nickel pig iron smelting, and number of existing smelting facilities by country



Source:

As shown in the figure, the biggest opportunity is clearly in Indonesia.

15.1.2.1 Recent build-out of RKEF processing capacity in Indonesia

In the past seven years, Indonesia has experienced a dramatic expansion in RKEF processing capacity, emerging as the world's leading nickel producer and processor. Following the 2014 ban on raw ore exports which was finalized in 2020, the nation initiated an aggressive downstream policy, prompting a surge in investments – primarily from Chinese firms – in onshore smelters and associated infrastructure. The number of operational nickel smelters rose from 13 in 2019 to over 100 lines by 2025, with total installed RKEF capacity exceeding 260 Mwmtpa with additional projects under construction. This rapid growth has made Indonesia responsible for over 60% of global nickel production, solidifying its strategic importance within the steel, EV battery, and stainless-steel industries.

15.1.2.2 Increasing difficulty sourcing high-grade saprolite ores

The proliferation of RKEF smelters has considerably increased demand for high-grade saprolite ore (typically >1.5% nickel grade). However, ore supply growth has not matched the pace of smelter build-out. High rainfall – particularly on Sulawesi and Halmahera – has hampered mine operations, and new Indonesian Government regulatory nickel ore quota (RKAB) requirements have further constrained availability, encouraging increasing ore imports from the Philippines, as shown in Figure 15.2

(Benchmark Mineral Intelligence, 2025b). Premiums for high-grade saprolite have persisted amid supply tightness, with market participants reporting record tender prices for 1.6% nickel ore in 2025 (SMM, 2025).

Figure 15.2 Rapid increase in Indonesian ore demand, decreasing saprolite ore grades and increase ore imports from the Philippines



Source: Benchmark Mineral Intelligence.

The push to maximize throughput has led to declining average nickel grades in the ore feed for many RKEF facilities, as shown in Figure 15.2. Ore blending and longer haulages from more remote or lower-quality deposits are increasingly necessary to maintain plant utilization, further deteriorating grade profiles. These lower grades directly impact smelter economics via increased energy consumption and reduced nickel output per tonne processed, exacerbating operational cost pressures. The Indonesian Mining Ministry estimates that laterite reserves total around 5.3 billion tonnes and the Indonesia Nickel Miners Association projected that the country's high-grade ore reserves may be depleted in the next six years (Reuters, 2024 and Subarna, 2024).

15.1.2.3 Economic performance: Increasing losses

The supply-demand imbalance, combined with global oversupply and weak stainless steel and EV demand, has resulted in a sustained decline in nickel prices since 2023. As prices have approached multi-year lows, a significant portion of Indonesia's RKEF operations – especially those with outdated technology or high reliance on market-bought high-grade saprolite – have become loss-making. (The Star, 2025). Industry insiders report delayed payments to suppliers and plant curtailments, with risks of further closures unless prices or input costs recover. The margin squeeze is compounded by persistent operational challenges, such as rising fuel costs and environmental compliance expenses.

15.1.2.4 Prospects for polymetallic nodule processing

Based on the above struggles in Indonesia, the country's established RKEF infrastructure is well-suited for adapting to alternative feedstocks, notably polymetallic nodules from deep-sea sources. Recent developments, such as the TMC-PAMCO arrangement in Japan, have demonstrated the technical viability of processing nodules containing nickel, copper, cobalt, and manganese in RKEF lines with minimal plant modifications. The partnership's success in pilot and feasibility phases – producing high-grade nickel-copper-cobalt alloy and manganese silicate – offers a model Indonesia could readily emulate, leveraging its processing capacity to diversify beyond terrestrial ores and access new revenue streams from the growing battery metals market.

TMC has engaged in discussions with key Indonesian processing counter-parties and entered into a non-binding MOU with a major processor who has indicated the potential to process 80 Mwmtpa of polymetallic nodules.

PT Gunbuster Nickel Industries provides an example of potential assets that could become available for toll treatment. Established in 2021, with a nameplate capacity of 1.8 Mwmtpa of nickel pig iron (NPI) per year with the capacity to process 21 Mwmtpa of laterite ore and representing about 9% of Indonesian refined nickel capacity. The facility owner Jiangsu Delong Nickel Industry has entered bankruptcy, caused by weak nickel prices and ore supply constraints and is currently only operating at 30% of capacity. (Bloomberg News, 2025). Experts suggest that a government-backed or national consortium acquisition could ensure operational continuity, advance environmental and labor standards, and further Indonesia's ambitions in nickel value addition and battery manufacturing, especially if aligned with domestic partners such as MIND ID or Indonesia Battery Corporation (Rakhmat et al, 2025)

15.1.2.5 Indonesian processing cost benchmarking

To establish a cost basis for the future cost of processing through existing capacity in Indonesia, TMC USA engaged Shanghai Metal Markets (SMM) to benchmark costs of these operations and opine on tolling rates required to incentivize nodules processing on this basis. The benchmarking exercise was done on a laterite ore basis with the assumption that the processing costs of nodules are the same on a dry basis (nodules have lower water content). PAMCO work to date has concluded that nodule processing consumes less power than laterite ores and has similar or potentially less cost in comparison to laterite ore processing.

SMM is a credible and well-established source for benchmarking RKEFprocessing costs in Indonesia. They provide detailed cost analysis comparing Indonesian and Chinese RKEF operations, publish an Indonesia NPI FOB price index, and offer real-time tracking of nickel ore quotas (RKAB) that affect feedstock availability and smelter economics. SMM also delivers in-depth consulting and strategic procurement reports, backed by direct project-level intelligence and extensive market data, making them a reliable authority on cost structures and operational dynamics in the Indonesian nickel smelting sector. SMM teams are based in Indonesia and frequently visit the relevant operations.

The benchmarking of the NPI processing costs was conducted through direct interviews, data and information processing, analysis as well as employing information already in SMM's extensive in-house database and is summarized below in Table 15.1.

Table 15.1 Summary of the benchmarked costs derived from SMM source data

	Total Processing Cost				
	Large RKEF 1	**Large RKEF 2**	**Large RKEF 3**	**Average**	**Ore Equivalent**
	$/t Ni			**$/wt ore**	
Power	1,700	1,722	1,946	1,789	16.85
Coke	689	668	1021	793	7.47
Coal	931	917	1,135	995	9.37
Other Materials	372	367	443	394	3.71
Labour & Management	1,203	1,203	1,253	1,220	11.49
Environmental	100	119	104	108	1.01
Depreciation	671	602	817	697	6.56
Others	300	269	323	297	2.80
Alloy to Matte				685	6.45
Capital Modification Recovery					3.85
Toll Profit (10%)					**6.57**
Contingency (5%)					3.81
Total	**5,966**	**5,866**	**7,043**	**6,977**	**79.95**

The key cost components are the cost of power at $0.06 per kWh and coal at $176 per mt. The capital modification recovery cost assumed $50M, depreciated over 10 years at a production rate of 1.3 Mwmtpa.

On this basis, a tolling rate of $80/wet tonne has been used as a cost basis for nodule processing in Indonesia.

15.1.2.6 Product quality specifications

The commercial arrangement between TMC and any Indonesian RKEF operators are expected to have agreed upon targets for specific pay metals in matte and manganese silicate which are required to be met to achieve intermediate/final product quality specifications. Table 15.2 below shows a sample of these grades for matte and manganese silicate, though the exact specifications will be part of commercial arrangement negotiations between TMC and the party and may vary depending on the plant based on a variety of factors.

Table 15.2 Sample grades of key pay metals for the matte being generated in Indonesia

Component	Grade (wt %)
Nickel (Ni)	43.4
Copper (Cu)	29.3
Cobalt (Co)	3.48
Iron (Fe)	5.00
Sulfur (S)	18.5

A sample of target parameters for the manganese silicate product are shown below in Table 15.3, though exact specifications will be subject to negotiation with each individual party.

Table 15.3 Sample specification for the manganese silicate product generated in Indonesia

Parameter	Units	Specification
Mn Composition	wt %	> 40
Fe Composition	wt %	1 to 2
Cr Composition	wt %	< 0.1
S Composition	wt %	< 0.3
MnO:SiO_2 Ratio		2.25 to 2.6
Mn:P Ratio		> 670

The above tables represent a sample of select components that will be considered in the target specifications. In addition to pay metal grades, all commercial arrangements with Indonesian operators will reference other elements that will be of material interest by TMC's potential customers.

There is a target of 5% iron in the final matte. This value was determined as it allowed for manageable levels of iron being introduced into the refinery while not sacrificing recoveries of key pay metals. The iron in matte is subject to change dependent on customer negotiations.

The sample process to determine product quality for this purpose is:

- Definitive sampling is supervised by a third party and samples are to be delivered to both parties.
- Subject to finalization of agreed upon sampling protocol, final weights, moisture determination and assays completed at an Indonesian location.

- Both parties develop an effective metallurgical accounting sampling protocol for each monthly throughput for the final determination of nickel, copper, cobalt and manganese recoveries to determine the Recovery Incentive Bonus Payment and Recovery Non-Performance Penalty Payment.
- Multiple assays of a single sample is conducted by both the operator and TMC USA, with the mean of the respective assays being used to govern activities.
- The difference between the TMC USA and Indonesian assays (mean assays per above) cannot exceed:
  - ± 0.05% for Ni,
  - ± 0.05% for Cu,
  - ± 0.01% for Co, and
  - TBD for Mn.
- Should the difference be outside of these splitting limits, a third party that is mutually agreed upon by the parties will perform umpire analysis using a sample taken by the operator.
- If the analysis done by the umpire is between the results of the TMC USA and the operator analyses, or is consistent with the result of either party, that result shall be the conclusive result.
- If the umpire's analysis is not between the results of the TMC USA and operator analyses, or is not consistent with either, then the exact mean of the umpire result and the nearest assay result that is conducted by either TMC USA or the operator is deemed to be the conclusive result.

15.1.3 Matte refining in the US

15.1.3.1 Further processing of nodules in the US

Existing capacity to process and refine nodules does not currently exist in the US with onshore processing capabilities between now and Project Commencement uncertain. In the USA, TMC propose to convert the matte delivered from Indonesia into saleable products including nickel sulfate, cobalt sulfate and copper cathode. TMC is also evaluating the possibility of this facility being an integrated plant that can further process the nickel and cobalt sulfate into downstream products such battery pre-cursor materials Processing capacity of this type is proposed to be online by the time the Project commenced, largely driven by the need for USA processing capacity derived from nodule matte from the NORI Area D.

TMC recently completed a study evaluating possible refinery site locations in the U.S. The study also included a preliminary refinery design, plant layout, permitting and construction execution schedule schedules and 2025 basis capital and operating costs. The site options focused on the Gulf region with a final recommendation for locations in Texas near existing ports.

15.1.4 Production plan

The production plan is structured to align and balance the offshore collection capabilities with availability of onshore processing capacity in Indonesia and the US. Table 15.4 below shows the updated production plan through 2067, and this also serves as a basis for the Marketing and Economics sections of this IA.

Table 15.4 TMC USA IA production plan

Macro Assumptions	Units	LOM Total	Year 1 2037	Year 2 2038	Year 3 2039	Year 4 2040	Year 5 2041
Total Wet Ore Collected	Mwmt	670.0	7.0	14.0	21.0	21.0	21.0
Total Dry Ore Collected	Mwmt	492.2	5.0	10.1	15.1	15.1	15.1
Matte							
Nickel (Ni) (Recovered Metal)	kmt	302.9	-	4.8	14.3	14.3	28.6
Cobalt (Co) (Recovered Metal)	kmt	37.9	-	0.4	1.1	1.1	2.2
Copper (Cu) (Recovered Metal)	kmt	237.3	-	3.9	11.6	11.6	23.3
Manganese Silicate							
Manganese (Mn) (Recovered Metal)	kmt	140,229.0	1,605.6	3,211.1	4,816.7	4,816.7	4,816.7
Refined Product							
Nickel Sulfate (NiSO4) (Recovered Metal)	kmt	5,708.2	66.6	128.3	185.4	185.4	171.1
Cobalt Sulfate (CoSO4) (Recovered Metal)	kmt	745.8	5.2	10.0	14.4	14.4	13.3
Copper (Cu) (Recovered Metal)	kmt	4,444.8	54.1	104.4	150.7	150.7	139.1

Macro Assumptions	Units	Year 6 2042	Year 7 2043	Year 8 2044	Year 9 2045	Year 10 2046	Year 11 2047
Total Wet Ore Collected	Mwmt	21	21	17.6	22.5	30	35
Total Dry Ore Collected	Mwmt	15.1	15.1	12.8	16.6	22.2	25.8
Matte							
Nickel (Ni) (Recovered Metal)	kmt	14.3	14.3	-	-	-	-
Cobalt (Co) (Recovered Metal)	kmt	1.1	1.1	-	-	-	-
Copper (Cu) (Recovered Metal)	kmt	11.6	11.6	-	-	-	-
Manganese Silicate							
Manganese (Mn) (Recovered Metal)	kmt	4,816.7	4,816.7	3,815.0	4,595.5	6,127.3	7,148.5
Refined Product							
Nickel Sulfate (NiSO4) (Recovered Metal)	kmt	185.4	185.4	161.3	198.8	265.1	309.3
Cobalt Sulfate (CoSO4) (Recovered Metal)	kmt	14.4	14.4	17.6	28.8	38.3	44.7
Copper (Cu) (Recovered Metal)	kmt	150.7	150.7	127.9	153	204	230

Macro Assumptions	Units	Year 12 2048	Year 13 2049	Year 14 2050	Year 15 2051	Year 16 2052	Year 17 2053
Total Wet Ore Collected	Mwmt	40	40	37.5	37.5	37.5	37.5
Total Dry Ore Collected	Mwmt	29.5	29.5	27.7	27.7	27.7	27.7
Matte							
Nickel (Ni) (Recovered Metal)	kmt	35.4	35.4	13.3	13.3	13.3	13.3
Cobalt (Co) (Recovered Metal)	kmt	5.1	5.1	1.9	1.9	1.9	1.9
Copper (Cu) (Recovered Metal)	kmt	27.3	27.3	10.2	10.2	10.2	10.2
Manganese Silicate							
Manganese (Mn) (Recovered Metal)	kmt	8,169.8	8,169.8	7,659.2	7,659.2	7,659.2	7,659.2
Refined Product							
Nickel Sulfate (NiSO4) (Recovered Metal)	kt	318.1	318.1	318.1	318.1	318.1	318.1
Cobalt Sulfate (CoSO4) (Recovered Metal)	kt	46	46	46	46	46	46
Copper (Cu) (Recovered Metal)	kt	244.8	244.8	244.8	244.8	244.8	244.8

Macro Assumptions	Units	Year 18 2054	Year 19 2055	Year 20 2056	Year 21 2057	Year 22 2058	Year 23 2059
Total Wet Ore Collected	Mwmt	37.5	37.5	37.5	37.5	40	18.9
Total Dry Ore Collected	Mwmt	27.7	27.7	27.7	27.7	29.5	14
Matte							
Nickel (Ni) (Recovered Metal)	kt	13.3	13.3	13.3	13.3	35.4	-
Cobalt (Co) (Recovered Metal)	kt	1.9	1.9	1.9	1.9	5.1	-
Copper (Cu) (Recovered Metal)	kt	10.2	10.2	10.2	10.2	27.3	-
Manganese Silicate							
Manganese (Mn) (Recovered Metal)	kt	7,659.2	7,659.2	7,659.2	7,659.2	8,169.8	3,860.2
Refined Product							
Nickel Sulfate (NiSO4) (Recovered Metal)	kt	318.1	318.1	318.1	318.1	318.1	167
Cobalt Sulfate (CoSO4) (Recovered Metal)	kt	46	46	46	46	46	24.2
Copper (Cu) (Recovered Metal)	kt	244.8	244.8	244.8	244.8	244.8	128.5

Scheduled maintenance and shutdowns of both offshore technology and onshore facilities are considered in the production plan, as nodule delivery volumes can be affected by these periods.

15.2 Offshore infrastructure

All details of offshore and marine infrastructure, including ports and quayside bulk cargo facilities are described in Section 13.6.5.

16 Market studies

16.1 TMC offtake agreement

On 25 May 2012, DeepGreen Engineering Pte. Ltd. (DGE) (a wholly owned subsidiary of TMC) and Glencore International AG (Glencore) entered into a copper off-take agreement and a nickel off-take agreement whereby DGE agreed to deliver to Glencore 50% of the annual quantity of copper material and 50% of the annual quantity of nickel material produced by DGE owned and operated facilities fed by ore from the NORI project area.

The pricing mechanism was agreed as follows:

- For London Metals Exchange (LME) Registered Grade "A" Copper Cathodes, the delivered price is the official LME Copper Grade "A" Cash Settlement quotation as published in the Metal Bulletin averaged over the month of shipping or the following month at Glencore's choice, plus the official long-term contract premium as announced annually by Codelco, basis cost, insurance and freight (CIF) Main European Ports.
- For LME Registered Primary Nickel, the delivered price is the official LME Primary Nickel Cash Settlement averaged over the month of shipping or the following month at Glencore's choice. For other copper-bearing material and other nickel-bearing material, the parties shall agree a price annually for the forthcoming calendar year on the basis of prevailing market prices for such copper products and such nickel products.

Both the nickel and copper off-take agreements are for the life of the NORI Areas, and either party may terminate the agreement upon a material breach or insolvency of the other party. Glencore may also terminate the agreement by giving 12 months' notice.

16.2 Marketing analysis

BMI was contracted by TMC to provide market overviews for three commodities from NORI and TOML areas: nickel, cobalt, and copper (BMI, 2025a) and to provide forecasts for the premia/discounts that nickel and cobalt sulfate over nickel metal price forecasts (BMI, 2025a).

CRU was commissioned by NORI to examine the marketability and pricing for the three intermediate products that are expected to be produced by TMC from the NORI and TOML areas (CRU, 2024):

- Nickel-cobalt-copper alloy.
- Nickel-cobalt-copper matte.
- Manganese silicate.

Additionally, CRU was retained to provide manganese ore market forecasts.

Over a five-year horizon, BMI and CRU’s price forecasts are based primarily on supply and demand fundamentals. These are established from detailed bottom-up analysis of supply by individual mine and intermediate product or refined metal producer, and in-depth analysis of demand from individual applications. Both BMI and CRU also consider operating costs and inventories in its forecasts, as well as various other factors where relevant.

For the forecast beyond a five-year horizon, cyclical supply-demand balances become hard to predict. Therefore, the longer term price forecasts are based on the Long Run Marginal Cost (LRMC) concept. That is, that prices in the long term will trend towards, and fluctuate around, the full economic costs (i.e., operating costs including an allowance for a return on capital) of the marginal tonne required to meet long term demand. For example, when prices are above the LRMC, it would be assumed that

supply will be added, and prices will subside. Assets selected for the LRMC analysis are a representative sample that are likely to be in production to satisfy future demand. They use the Project Gateway classification system to select projects. It is important to consider where these new assets are expected to be located, how large they will be and what processing technology they will adapt. The composition of future capacity and accompanying demand levels will have a significant impact not just on the LRMC assessment, but also the upside and downside risk associated with that assessment.

Two exceptions to this long-term price forecasting methodology are the cobalt market and copper forecast. Since the majority of cobalt is produced as a by-product of copper or nickel mining, supply is inelastic to the cobalt price, with supply decisions instead more likely to be driven by the market environment for the operations' main copper or nickel product. This means that the LRMC concept cannot readily be applied. Instead, estimates refer to historic pricing trends to establish a long-term equilibrium price, taking into account longer term factors, such as the increasing importance of batteries as a cobalt end use, that might result in cobalt prices and product premia differing with historical trends. BMI have completed price forecast out to 2030 based on fundamental supply demand balance. The 2030 price has been projected forward long-term. Copper represents about 18% of total revenue.

16.3 Market outlook

16.3.1 Nickel

16.3.1.1 Nickel market overview

Nickel is a high-melting-point, silvery-white metal valued for its hardness and resistance to oxidation. Traditionally found with copper, iron, and cobalt, nickel is extracted from two main ore types: sulfide and laterite. Historically, sulfide ores dominated production, but laterite ores, particularly saprolite and limonite types, now predominate due to scarce new sulfide deposits. Laterite ores are commonly processed via RKEF to produce ferronickel or NPI or high-pressure acid leaching (HPAL) to produce intermediates like mixed hydroxide precipitate (MHP) and mixed sulfide precipitate (MSP). Nickel products are typically classified as Class 1 (high-purity, such as nickel sulfate) and Class 2 (nickel alloy products, such as ferronickel). Nickel is primarily used in stainless steel (65% market share) and increasingly in batteries for EVs. BMI predict total nickel market CAGR of 5.4% and 11.3% growth in nickel demand in lithium ion batteries to 2040 (BMI, 2025b).

16.3.1.2 Nickel supply

Global refined nickel production is forecast to grow from 3.6 Mt nickel in 2025 to 4.9 Mt by 2035 (CAGR of 2.95%). Indonesia is projected to drive this growth, increasing from 2.3 Mt nickel in 2025 to 3.3 Mt nickel by 2035 representing about 70% of global production. However, production in other parts of Asia, such as the Philippines, is expected to decline as reserves dwindle. The majority of Indonesian refined nickel output is expected to be in NPI, while China is adding capacity for nickel sulfate production, led by major companies like Huayou Cobalt and CNGR. Indonesian MHP production is expected to more than double from 493 Kt in 2025 to 989 Kt 2029 in with the rapid construction HPAL plants largely driven by Chinese interests.

16.3.1.3 Nickel demand

Global nickel consumption is projected to grow significantly at a CAGR of 5.4% from 2025-2035, largely due to rising demand for 300-series stainless steel and high-nickel NMC (nickel-manganese-cobalt) cathodes in lithium-ion batteries for the EV sector. Currently, stainless steel represents 65% of total nickel demand, while batteries are expected to constitute 28% of demand by 2035, driven by a 2.4 Mt nickel increase. China, already accounting for over half of global nickel consumption, is anticipated to remain the primary demand driver with a forecasted CAGR of 5.5% from 2022-2035. Indonesia is also

emerging as a major consumer, developing domestic industries due to its export ban on laterite ore, leading to significant growth in NPI and stainless-steel production.

16.3.1.4 Nickel supply gap and prices

Nickel supply is expected to slightly exceed demand until 2030, after which production must increase by 0.8 Mt to meet projected 2035 demand. Tight supply pushed prices up in 2020-2022, with the Russia-Ukraine conflict further spiking prices to $100,000/t, prompting market intervention. Rapid expansion of nickel supply from Indonesia has depressed prices to around the current value of $US15,000-15,500 tonne. BMI estimates that 20% of the nickel industry is currently loss making including non-integrated Indonesian and Chinese NPI and FeNi producers. Increasingly challenged access to, lower quality of and increased price of Indonesian laterite ores are expected to apply increased cost pressure on Indonesian RK-EF operations and provide upward nickel price pressure. BMI predict that long-term demand will likely drive prices above $21,000 (2025 US$) by 2032 to provide the inducement price to bring on required additional production to expected supply shortfall at this time.

16.3.2 Cobalt

16.3.2.1 Cobalt market overview

Global cobalt reserves, currently at 7.65 Mt, are concentrated in the African copper belt, particularly in the DRC, which provides cobalt as a by-product of copper-cobalt mining. Secondary reserves are found in nickel laterites in countries like Australia, Indonesia, Cuba, and the Philippines, as well as in nickel sulfide deposits in Canada, Russia, and Western Australia. The cobalt value chain involves diverse ore types, processing methods, intermediates, and final products, mainly split between hydrometallurgical and pyrometallurgical routes, ultimately yielding cobalt in forms like metal, chemicals, and other compounds.

16.3.2.2 Cobalt supply

The DRC dominates global cobalt production, supplying nearly 75% of mined cobalt, of which 50% is processed in China. Chinese ownership of DRC mines and significant imports make China the main producer of refined cobalt, accounting for 80% of total supply and nearly 90% in cobalt chemicals. Indonesia is an emerging supplier, producing cobalt as a by-product from its growing laterite ore mining sector. By 2030, Indonesia's share of global cobalt supply is projected to reach 24%. However, the DRC and Indonesia alone are expected to drive 93% of supply growth from 2025 to 2030. BMI forecast that primary cobalt supply will reach 324 kt in 2030, up by 32% compared with projected 2025 levels of 245 kt. But as mines begin to run through reserves and the visibility for new assets into the 2030s is limited, BMI expectation for mine supply is a slight decline into the 2030s, although secondary supply will continue to increase: by 2040, recycled material will account for 36% of total supply, up from 8% in 2024.

16.3.2.3 Cobalt demand

Battery production has become the primary end use of cobalt, driven by the rapid expansion of the EV market. In 2035, battery demand is expected to account for 84% of overall cobalt demand, up from less than half in 2017. Cobalt demand from the battery sector is anticipated to grow more than 100% between 2024 to 2034, despite decreasing cobalt intensities in batteries. China and Europe currently lead demand growth due to transportation electrification, but North America's demand is expected to increase substantially, from 17 kt in 2020 to 50 kt in 2035.

16.3.2.4 Cobalt supply gap and prices

BMI expects the cobalt market to remain oversupplied throughout the 2020s, with the market rebalancing in 2032 and shifting to deficit from 2033 onwards. Refined cobalt supply will see strong

growth in the short term, driven largely by output from China. However, by 2033, supply is forecast to struggle to keep pace with demand, leading to a projected 46 kt supply gap by 2035. Additional production beyond current forecasts will be required to meet future demand.

Cobalt prices are historically volatile, given that much of the production is a by-product of copper and nickel mining, making supply less responsive to demand. Long-term price estimates from BMI suggest that European cobalt prices will average around $62,500/tonne in $2025 real terms. Cobalt's price inelasticity is due to its low proportion of costs in most applications, where alternatives are limited or costs are passed downstream (such as batteries and pharmaceuticals).

16.3.3 Manganese

16.3.3.1 Manganese market overview

Manganese is a critical metal with high chemical reactivity and melting point, essential in steelmaking for its deoxidizing and alloying properties. About 85-90% of current manganese demand is for steel production, including in high-strength low alloy, stainless, and engineered steels. Additionally, manganese is used in aluminum alloys and in chemicals, particularly manganese sulfate for agriculture and battery applications.

16.3.3.2 Manganese supply

Manganese ore production is concentrated in Africa, especially South Africa, Gabon, and Ghana, along with Australia, representing over 75% of global supply. Africa's production is forecast to grow by 722 kt of contained manganese from 2023 to 2028, with significant expansions in Gabon and Ghana. In contrast, China’s production is declining at a 1.7% CAGR due to high costs and declining ore quality. While China leads in global manganese ferroalloy production, declining domestic steel demand is expected to reduce production by 3% CAGR from 2024 to 2028. Other regions, including Asia, CIS, and Europe, will compensate partially, keeping global ferroalloy supply stable.

16.3.3.3 Manganese demand

China, consuming 60% of global manganese ore, is set to reduce its demand by 600 kt through 2028, driven by lower ferroalloy demand. However, demand from other regions is expected to offset this, with a global increase of over 4 Mt of contained manganese forecast by CRU by 2035. Silicomanganese alloy will maintain the largest share of demand (52%), but growth will be highest for Electrolytic Manganese Metal[4](EMM) and battery applications, with projected CAGRs of 10% and 22%, respectively. These segments will constitute 21% of demand by 2035, up from 9% today.

16.3.3.4 Manganese supply gap and prices

A supply deficit of 3.3 Mt over and above existing mines and committed projects is anticipated by 2035 due to rising demand, particularly for EMM and battery uses. Prices are expected to grow in real terms by 2035, with 44% Mn lump prices reaching $5.50/dmtu5 and 36-39% Mn lump at $4.90/dmtu (both real 2025 US$).

---

[4] Electrolytic Manganese Metal (EMM) is a significant alloy component in the production of stainless steel, high-strength low-alloy steel, aluminium-manganese alloy, and copper-manganese alloy. It is also used as a primary ingredient for producing Manganese tetraoxide (Mn_3O_4) and sulfate ($MnSO_4$).

[5] dtmu means dry metric tonne unit. A ‘unit’ is 10 kg, or 1 tonne divided into 100 units. For example, $8/dmtu is equal to $800/tonne of pure manganese metal. This pricing structure is commonly used for manganese ore sales (as opposed to pure manganese metal). A typical manganese ore will grade 45% Manganese so a price per tonne of this ‘impure’ ore will be 45% of $800/tonne = $360/tonne.

16.3.3.5 EMM and MnSO4

While it is expected that most of the manganese silicate product will be sold as feedstock for silico-manganese alloy production, it is also suitable as feedstock for EMM and MnSO4 production. Approximately 10% of manganese is processed into EMM and $MnSO_4$, the latter being vital for fertilizers and lithium-ion battery production. Demand for high-purity $MnSO_4$ monohydrate (HPMSM) is surging due to EV demand, with prices expected to grow alongside EMM costs. By 2035, EMM prices are forecast at $2,110/t and HPMSM at over $2,200/t (both real 2023 US$).

16.3.4 Copper

16.3.4.1 Copper market overview

Copper is primarily mined as sulfide or oxide ore, with sulfide ores containing 0.3-1.5% copper and oxide ores reaching 4% or higher. Around 80% of copper mining is done via open-pit operations. Oxide ores are processed through SX-electrowinning (SXEW) to produce high-purity copper cathodes. Sulfide ores undergo flotation, yielding copper concentrate (20-40% copper) for smelting and refining.

16.3.4.2 Copper supply

BMI forecast global copper mine production is forecast to grow from 22.9 Mt in 2025 to 25.6 Mt by 2028, driven by African output, particularly in the DRC (+436 kt) and Zambia (+306 kt). Chile is expected to remain the largest producer with modest 0.4% CAGR from 2025 to 2030 producing around 5.8 Mt in 2030. The DRC, the world's second largest producer is expected to increase 436 kt to 3.5 Mt, with Peru (third largest producer) increasing 330 kt at a CAGR of 2.4% to 2.9 Mt over the same period. US domestic policy favoring reshoring of industrial production is expected to drive copper production growth by a CAGR of 4.4% to 1.4 Mt for an increase of 275 kt from 2025 to 2030.

16.3.4.3 Copper demand

Copper demand is projected to rise from 34 Mt in 2025 to 42 Mt by 2035, driven by the transportation, electrical infrastructure and consumer goods sectors. By 2035, green-energy applications like EVs, renewable energy, and storage are forecast to account for ~20% of copper demand, up from 4% in 2020. Significant consumption growth is expected in North America, Europe, India, and Southeast Asia, with each region adding 1.1-1.7 Mt of demand.

16.3.4.4 Copper supply gap and prices

A 7.9 Mt supply gap is anticipated by 2035, as demand for primary copper surpasses production from current and committed projects. To bridge this gap, the industry needs to advance a significant portion of "Probable" and "Possible" projects over the next decade.

The copper price averaged $9,147/t in 2024, and is currently above $9,800/t. With the expected supply gap widening towards the late 2020s, prices are expected to reach $11,126/t by 2029. The long-term price for is estimated at $11,456/t (real 2025 US$).

16.4 TMC manganese silicate

The manganese silicate presents a unique profile as a feedstock for silico-manganese alloy production, offering high manganese content (42-43%), comparable to high-grade manganese ore or slag, with controlled SiO_2, Al_2O_3, CaO, and MgO levels and manganese in a reduced 2+ valence state. This offers value in use advantages to customers using the manganese silicate product to produce silico-manganese alloy – the largest sector of the manganese market. These attributes position TMC manganese silicate as a competitive material against traditional high-grade slags and ores. However,

phosphorus levels from pilot testwork showed variability which is likely to be well controlled in the industrial process at PAMCO and other future processors. The optimized Mn/Fe ratio of 22:1 and Mn/P ratio above 500:1 are positive market indicators. Additional testing just completed by PAMCO demonstrated the ability to produce manganese silicate with Mn/P ratio greater than 1,000:1 confirming, effective phosphorus control which is critical for broader market acceptance.

Nodule-sourced manganese silicate could also serve as feedstock for EMM, Electrolytic Manganese Dioxide (EMD)[6], and HPMSM production due to its MnO form, which simplifies acid solubility without needing roasting. Although current consumption of manganese ore in these chemical sectors is lower than silico-manganese alloy, forecasts suggest growth from 2 Mt in 2023 to 4.8 Mt by 2035, potentially increasing demand for nodule-sourced manganese silicate over time. TMC currently has test work ongoing with KPM in Canada to demonstrate production of battery grade HPMSM from the manganese silicate.

From a value perspective, nodule-sourced manganese silicate is expected to be competitive, aligning closely with the 44% Mn ore benchmark price, provided it is integrated into optimized ore blends. Depending on blend composition, its implied value ranges from $5.18 to $5.406 per dmtu ($US 2023 basis). Key blends with high grade South African ore (Wessels ore) and iron ore are expected to perform comparably to the benchmark, although the value could vary depending on market conditions and processing costs for other feedstocks.

The marketing strategy for nodule-sourced manganese silicate must carefully manage blending practices to ensure its characteristics maximize value.

The proposed production profile would see TMC producing 2.4 to 2.8 Mt of manganese contained in silicate from 2031 to 2036 from the NORI Area D (AMC, 2025), however a significant increase in production to 7.5 Mt of manganese contained in silicate to 2039 is proposed, which would represent about 29% of the total manganese market. This would represent 40% of the silico-manganese and EMM and HPMSM markets which is about 73% of the total manganese market and is effectively the total available market for the manganese silicate product. Review of manganese ore industry producer cost curves prepared by CRU indicates that 7.5 Mt of manganese ore production has a cost of $US 4.70/dmtu or greater providing an indication of the pricing that would be required to displace this production. Manganese pricing after 2036 has assumed a linear decreasing price from $US 5.50 per dmtu (2025 real CRU forecast) in 2036 to $US 4.70/dmtu in 2039 and remaining flat after this.

16.5 TMC matte

TMC matte, with composition and characteristics resembling Anglo Converter Matte and Jinchuan Converter Matte, is projected to have high compatibility in refining processes. Key refineries, including Vale Canada, Glencore Nikkelverk, and Jinchuan, collectively account for approximately 85% of spare global refining capacity and are primary candidates for NORI matte processing. CRU expects NORI matte's net value to reach 75% of its gross metal value, contingent on forming long-term partnerships with these facilities.

However, the matte market could become buyer-dominant with growing feedstock supply, possibly pushing payables down to 80% for nickel, 70% for copper, and 60% for cobalt. Establishing stable refinery relationships will enhance payables over time, securing a consistent outlet for NORI matte substantial volumes.

[6] Electrolytic Manganese Dioxide (EMD) is a critical component of the cathode material in modern alkaline, lithium and sodium batteries.

CRU estimates a total available refining capacity for TMC matte of about 200 Kt contained nickel per annum. TMC nickel refining in the US mitigates the risk of increasing matte production exceeding the global matte refining capability.

16.6 Refinery products

It is intended TMC US subsidiary TMC USA will construct refining facilities in Texas to produce battery-grade nickel and cobalt sulfate crystal, copper cathode and fertilizer grade ammonium sulfate. Forecasts for cathode and sulfate prices are included in Table 6.1 based on the forecasts from BMI.

16.7 Revenue forecasts

Revenue assumptions are outlined in this section using the forecast data provided by CRU and BMI.

Table 16.1 outlines the metal price forecast in 2025 real $US dollars based on the CRU and BMI forecasts outlined above. Table 16.2 shows the metallurgical recoveries used in the revenue estimate as outlined in Section 14. Table 16.3 outlines the payable factors provided by CRU and outlined above for nickel-copper-cobalt matte. Table 16.4 to Table 16.6 provide forecasts of payable metal production in matte, refinery products and manganese silicate respectively. Table 16.7 provides the revenue forecast by metal.

Table 16.1 Metal and metal sulfate price forecasts (real US$ 2025)

Commodity Pricing - Real	LOM Average	2037-2041	2042-2046	2047-2059
Price - Nickel Class 1 LME (US$/t)	20,360	20,360	20,360	20,360
Price - Cobalt LME (US$/t)	62,530	62,530	62,530	62,530
Price - Copper Class 1 LME(US$/t)	11,456	11,456	11,456	11,456
Price - Manganese (US$/dmtu)	4.71	4.79	4.70	4.70
Price – Ni Sulfate (Contained Ni basis)	21,835	21,835	21,835	21,835
Price – Co Sulfate (Contained Co basis)	62,530	62,530	62,530	62,530

Source: CRU, BMI

Table 16.2 Metallurgical recoveries

Product	Recovery (%)
Matte – nickel recovery – nodule to matte	94.76
Matte – cobalt recovery – nodule to matte	77.54
Matte – copper recovery – nodule to matte	86.43
Sulfate – nickel recovery – nodule to sulfate	94.60
Sulfate – cobalt recovery – nodule to sulfate	77.20
Cathode – copper recovery – nodule to cathode	86.20
Manganese recovery – nodule to Manganese Silicate	98.9

Source: TMC

Table 16.3 Ni-Co-Cu matte payable terms percentage of LME benchmark prices

Payable Terms	Terms
Matte - Payable Terms – Ni	80.0%
Matte - Payable Terms – Co	60.0%
Matte - Payable Terms – Cu	70.0%

Source: CRU

Table 16.4 Forecast payable metal production - metal in matte

Metal	LOM Total Kt	Year 1 2037	Year 2 2038	Year 3 2039	Year 4 2040	Year 5 2041
Payable Nickel	242.3	--	3.8	11.4	11.4	22.9
Payable Cobalt	22.7	--	0.2	0.7	0.7	1.3
Payable Copper	166.1	--	2.7	8.1	8.1	16.3
Metal	**Year 6 2042**	**Year 7 2043**	**Year 8 2044**	**Year 9 2045**	**Year 10 2046**	**Year 10+ 2047+**
Payable Nickel	11.4	11.4	--	--	--	170.0
Payable Cobalt	0.7	0.7	--	--	--	18.5
Payable Copper	8.1	8.1	--	--	--	114.6

Source: TMC, Note: All matte is used in the US refineries for years 2038, 2039 and 2040

Table 16.5 Forecast payable refined metal production - metal in sulfate and cathode

Metal	LOM Total Kt	Year 1 2037	Year 22038	Year 3 2039	Year 4 2040	Year 5 2041
Payable Nickel in Sulfate	5,759.8	71.6	128.3	185.4	185.4	171.1
Payable Cobalt in Sulfate	752.3	5.6	10.0	14.4	14.4	13.3
Payable Copper in Cathode	4,485.2	58.2	104.4	150.7	150.7	139.1
Metal	**Year 6 2042**	**Year 7 2043**	**Year 82044**	**Year 9 2045**	**Year 10 2046**	**Year 10+ 2047+**
Payable Nickel in Sulfate	185.4	185.4	179.8	217.8	265.1	3,984.5
Payable Cobalt in Sulfate	14.4	14.4	19.6	31.5	38.3	576.2
Payable Copper in Cathode	150.7	150.7	142.5	167.7	204.0	3,066.3

Source: TMC

Table 16.6 Forecast production – manganese in manganese silicate

Product	LOM Total Kt	Year 10 2037	Year 11 2038	Year 12 2039	Year 13 2040	Year 14 2041
Mn in manganese silicate	140,229.0	1,605.6	3,211.1	4,816.7	4,816.7	4,816.7
Product	**Year 15 2042**	**Year 16 2043**	**Year 17 2044**	**Year 18 2045**	**Year 19 2046**	**Year 20+ 2047+**
Mn in manganese silicate	4,816.7	4,816.7	3,815.0	4,595.5	6,127.3	96,791.3

Source: TMC

Table 16.7 Revenue Forecast US$ 2025 Real

Metal	LOM Total	Year 10 2037	Year 11 2038	Year 12 2039	Year 13 2040	Year 14 2041
Nickel Revenue	130,670.3	1,557.0	2,880.2	4,280.9	4,280.9	4,202.2
Cobalt Revenue	48,456.4	347.2	638.9	944.6	944.6	917.0
Copper Revenue	53,278.3	664.4	1,226.9	1,820.6	1,820.6	1,781.0
Manganese Revenue	66,078.1	839.9	1,594.5	2,263.8	2,263.8	2,263.8
Metal	Year 15 2042	Year 16 2043	Year 17 2044	Year 18 2045	Year 19 2046	Year 20+ 2047+
Nickel Revenue	4,280.9	4,280.9	3,908.9	4,744.9	5,788.7	90,464.7
Cobalt Revenue	944.6	944.6	1,222.6	1,965.1	2,397.5	37,189.6
Copper Revenue	1,820.6	1,820.6	1,625.9	1,916.0	2,337.5	36,444.5
Manganese Revenue	2,263.8	2,263.8	1,793.0	2,159.9	2,879.8	45,491.9

Source: CRU

17 Environmental studies, permitting and social or community impact

TMC, through their wholly owned subsidiaries NORI and TOML, hold exploration rights under the ISA regulatory framework to the NORI and TOML areas. TMC, through its affiliate TMC USA is in the process of applying for exploration rights for these areas under the existing DSHMRA regulatory regime administered by NOAA. TMC USA has submitted a commercial recovery permit application to NOAA for the NORI Area D (identified as TMC USA A-A under the DSHMRA application process), see Section 3.1 for more information on existing exploration areas and the current commercial recovery application.

TMC, through its subsidiaries, has completed extensive offshore environmental baseline and impact assessment studies with efforts focused on the NORI Area D and TOML-F areas. Section 17.2 describes the information collected during these studies that is transferable to the other TMC USA application areas.

The development and status of the environmental and social program for the NORI and TOML Contract Areas is described below. Note that details pertaining to NORI Area D can be found in the Technical Report Summary for NORI-D (AMC Consultants, 2025), with this report focusing specifically on the areas outside of NORI Area D under exploration.

17.1 Permitting process

17.1.1 ISA

The ISA is mandated through UNCLOS to organize, regulate, and control all mineral-related activities in Areas Beyond National Jurisdiction (ABNJ) whilst preserving and protecting the marine environment. As NORI and TOML are in the ABNJ, the ISA is responsible for assessing any ESIA prepared by Contractors and for granting the relevant contracts. TMC, through affiliates NORI and TOML are currently one of 16 contractors with a license to explore for polymetallic nodules in the CCZ (refer ISBA/23/C/7, 5 June 2017).

Between 1998 and 2014, the ISA conducted workshops and developed several documents to guide contractors on expectations for responsible environmental management during the exploration and exploitation phases of mineral development. The ISA held a workshop “Towards an ISA environmental management strategy for the Area” over 20-24 March 2017 in Berlin Germany. The results of the workshop were published as ISA Technical Study 17 (ISA 2017).

The ISA has issued Regulations on Prospecting and Exploration for Polymetallic Nodules (adopted on 13 July 2000, updated on 25 July 2013). The regulations were complemented by the Legal and Technical Commission (LTC) recommendations for the guidance of contractors on assessing the environmental impacts of exploration (ISBA/25/LTC/6/Rev.1) which was updated on 30 March 2020. The draft exploitation regulations on deep-seabed mining were discussed at the 25th Session of the ISA (25 February to 1 March 2019 in Kingston, Jamaica). The ISA had declared a target of 2020 to have the regulations approved, but the COVID-19 pandemic disrupted the ISA program.

Although the environmental impact review process has not yet been finalized, the draft regulations outline the application process and the conditions that contractors would need to implement during operations. All contractors have been made aware that the ISA requires the completion of the ESIA studies, culminating in an EIS, in support of an applications for an exploitation license. Guidance for contractors in terms of what is expected in the EIS has been provided in ISA Technical Study No. 10 (ISA 2012). Further guidance will be provided with the completion of Standards and Guidelines for exploitation activities. The EIS, along with an Environmental Management System (EMS) with subordinate Environmental Management and Monitoring Plans (EMMP), are stated as requirements as part of the application for an exploitation license within the Area.

The environmental permitting process for the Area has been developed through a consultation program initiated by the ISA in 2013 and includes feedback obtained from multiple stakeholder groups. It is expected to involve a series of checks and balances, with reviews being conducted by the LTC with input from independent experts, as required. The recommendations of the LTC are expected to then go before the ISA Council, which review the information provided and decide whether to approve the license application and, if so, what conditions should be applied.

TMC conducted ESIA studies under the draft ISA guidelines "Recommendations for the guidance of contractors for the assessment of the possible environmental impacts arising from exploration for marine minerals in the Area issued by the Legal and Technical Commission".

17.1.1.1 NORI

As a sponsoring state, Nauru has a responsibility to ensure that NORI's activities in the international seabed area are carried out in conformity with Part XI of UNCLOS.

NORI is regulated by Nauru's International Seabed Minerals Act 2015 ("Nauru Act"), which requires NORI to, amongst other things, "*apply the Precautionary Principle, and employ best environmental practice in accordance with prevailing international standards in order to avoid, mitigate or remedy adverse effects of Seabed Mineral Activities on the Marine Environment*".

The Nauru Seabed Minerals Authority, established under the Nauru Act, has several functions, including , *inter alia*:

- Develop policies and institutional arrangements for the purpose of regulating and monitoring the development of seabed minerals in the international seabed area.
- Develop standards and guidelines for Seabed Mineral Activities.
- Conduct due diligence enquiries into Sponsorship Applicants or Sponsored Parties.
- Assist the ISA in its work to establish, monitor, implement and secure compliance with the Rules of the ISA.
- Undertake any advisory, supervisory or enforcement activities in relation to Seabed Mineral Activities or the protection of the Marine Environment, insofar as this is required in addition to the ISA's work in order for Nauru to meet its obligations under the UNCLOS as a Sponsoring State.

17.1.1.2 TOML

As the sponsoring state, Tonga has a responsibility to ensure that TOML's activities in the international seabed area are carried out in conformity with Part XI of UNCLOS. Similar to NORI's obligations under the exploration regulations, TOML is to submit annual reports summarizing exploration progress activities and 5-year plans detailing future exploration activities.

17.1.1.3 Compliance status

At the effective date of this report, NORI and TOML are in compliance with their exploration contracts. NORI and TOML are required to submit 5-year work plans which they report on annually to the ISA. Every 5 years the ISA reviews the work completed in the past 5 years and then NORI and TOML develop and submit new 5-year work plans.

It is planned for the following tasks to be undertaken:

- Characterizing nodule mineralization.
- Characterizing the nature of the seabed, water column and biology.
- Conducting environmental baseline studies and impact assessments.

- Characterizing the nature of any materials returned to the environment.
- Developing oceanographic and physical information to inform models (e.g., sediment plume models).
- Developing other plans, including the master environmental management plan (EMP) and the various subordinate plans.

TOML is in the process of conducting a scoping study from which a plan of work for the studies required to inform the EIA are expected to be developed.

17.1.2 Deep Seabed Hard Mineral Resources Act

TMC USA is currently exploring a parallel regulatory route through the DSHMRA. DSHMRA is an established framework authorizing U.S. citizens (e.g., individuals, corporations) to explore for and recover minerals from the seabed in ABNJ. DSHMRA defines exploration as the at-sea observation and evaluation of seabed Mineral Resources and the taking of the resource as needed to design and test mining equipment, and commercial recovery (or exploitation) as the actual at-sea mining and processing of seabed minerals for the primary purpose of commercial use.

While DSHMRA has long been in force, no commercial recovery permit has ever been issued under this regime. In 2025, NOAA published proposed revisions to its implementing regulations under 15 C.F.R. Parts 970 and 971, which introduce new procedures for consolidated applications, environmental reviews, and information disclosure. As of the date of this report, the rulemaking process remains ongoing, and the practical application of the commercial recovery permit process is untested. TMC USA is actively evaluating its eligibility under DSHMRA and has engaged with NOAA and other U.S. federal agencies; however, the permitting pathway under DSHMRA involves material legal and procedural uncertainty.

Major Federal actions covered by the Act include:

- Designation of Reciprocating States.
- Regulatory Framework.
- Possibilities for Retaining Manganese Tailings.
- NPDES Findings by EPA.

17.1.2.1 Compliance status

Executive Order (EO) 14258 directed NOAA, in consultation with the Department of State and BOEM, to expedite the process for reviewing and issuing exploration licenses and commercial recovery permits under DSHMRA, among other actions. On April 29, 2025, TMC's U.S. subsidiary TMC USA, submitted applications to NOAA for two exploration licenses and one commercial recovery permit under DSHMRA for areas in the CCZ. According to the Code of Federal Regulations, NOAA is to make an initial determination within 30 days of receipt for exploration license applications (15 C.F.R. §970.209) and within 60 days of receipt for commercial recovery permit applications (15 C.F.R. §971.210).

17.1.2.2 Alternate permitting pathways

The exploration of permitting opportunities through both ISA and DSHMRA increases the project's potential for permitting success. By progressing through both systems, the company mitigates geopolitical, legal, and regulatory risk by demonstrating flexibility in adapting to global political or regulatory shifts in seabed governance. If one pathway is delayed or faces legal challenges, a contingency is in place.

17.2 Transferable information from NORI Area D and TOML-F

TMC has conducted 22 research cruises to the CCZ over the past 12 years, primarily focusing on the NORI Area D, with some data also collected from TOML-F. During this time, TMC has built a substantial database of information on the physical and environmental baselines of both areas, some of which can be applied to other parts of the CCZ. This transferable information provides a foundation for developing the scope of offshore studies in other areas covered under the exploration applications. An overview of the transferable information is provided below.

Details of the environmental baseline studies conducted by TMC can be found in Section 17 of the Technical Report Summary for NORI-D (AMC Consultants, 2025) The following summary integrates geological, oceanographic, biogeochemical, benthic ecological, and trace metal baseline data from multiple campaigns and scientific investigations that may be of relevance to areas outside of NORI Area D and TOML-F.

17.2.1 Baseline studies

17.2.1.1 Regional geological setting

The NORI Area D lies within the eastern equatorial Pacific Ocean, approximately 1,500 km southwest of Mexico's coast, situated towards the far east of the CCZ (Menard, 1955, 1966; Seton et al., 2020). This region is characterized by young oceanic crust formed at the East Pacific Rise about 18 to 20 million years ago, bounded by major fracture zones—the Clipperton Fracture Zone to the south and the Clarion Fracture Zone to the north (Menard & Fisher, 1958). The basement rock is overlain by a thin sediment veneer composed variably of carbonaceous and siliceous materials, which has allowed the formation of polymetallic nodules rich in manganese, cobalt, nickel, copper, and trace metals at the sediment-water interface (ISA, 2010b; Parianos, 2021).

The geological units in NORI Area D reflect a restricted stratigraphy from the lower Miocene onwards, with sediment thickness reaching up to 90 m, comprising siliceous ooze overlying carbonate sediments (Parianos et al., 2022). Sediment distribution varies spatially, with thicker deposits in flatter central areas and thinner sequences over ridges and abyssal hills, likely influenced by bottom currents and sediment remobilization processes (Parianos, 2021). These features are broadly representative of the eastern CCZ, where sedimentation rates are low (~0.3 cm/1,000 years), and sediment remobilization plays a significant role in shaping benthic habitats.

17.2.1.2 Substrate composition and geotechnical characteristics

NORI Area D sediments can be visually divided into four layers, with the uppermost layer being a dark brown, poorly consolidated silty clay with high water content, transitioning downward into more consolidated beige matrices with bioturbation traces (O'Malley et al., 2023). The flat seafloor areas predominantly consist of silty clay or clayey silt, though variations occur near topographic highs such as ridges and abyssal hills, where soils exhibit greater stiffness (APYS, 2024). In situ cone penetration tests (CPT) reveal undrained shear strength increasing steadily with depth, indicating geotechnical properties important for mining equipment design and environmental impact assessments.

These substrate characteristics align with observations from other CCZ Contract Areas, suggesting that similar sedimentary and mechanical properties may be expected regionally, particularly in areas with comparable bathymetry and sediment thickness (Volz et al., 2018; Kuhn & Rühlemann, 2021a).

17.2.1.3 Polymetallic nodules: Abundance, chemistry, and variability

Nodule abundance in NORI Area D varies considerably over scales of ~10 km, ranging between 8 kg/m^2 and 30 kg/m^2, consistent with patterns observed throughout the CCZ.

Chemical analyses indicate relatively uniform grades of cobalt, nickel, copper, manganese, and iron across NORI Area D, with cobalt concentrations higher in the northern part of the lease area and slightly lower in the south (ISA, 2010b). These grade distributions demonstrate spatial continuity, supported by multiple sampling campaigns and equiprobable simulations.

Solid-phase metal contents in sediments beneath nodules also reflect elevated manganese and cobalt levels compared to deeper sediment layers, with surface enrichments attributed to micronodules and nodule fragments (Volz et al., 2020). Porewater dissolved metal concentrations, including manganese and cobalt, exhibit peaks near the sediment-water interface, indicating active diagenetic cycling and metal mobilization processes common to the southeastern CCZ (Paul et al., 2024).

17.2.1.4 Water mass distribution and circulation dynamics

The northeastern tropical Pacific, encompassing the CCZ and NORI Area D, exhibits complex hydrographic structures shaped by both locally formed and advected water masses (Fiedler & Talley, 2006). Deep-sea circulation in NORI Area D is influenced by abyssal flows varying in intensity and direction, modulated by mesoscale eddies, deep recirculation, and topographically steered currents (Pegliasco et al., 2022).

Mooring arrays deployed from 2019 to 2023 recorded zonal and meridional currents, revealing high-frequency tidal components dominated by semidiurnal M_2 tides and near-inertial oscillations, especially in the upper 500 m of the water column. Internal wave dynamics include semidiurnal internal tides propagating westward and near-inertial waves exhibiting complex vertical energy redistribution, with enhanced mixing near seamounts and abyssal hills (Xie et al., 2023).

Mesoscale eddy activity is prominent, with local cyclonic (CC) and anticyclonic (AC) eddies frequently crossing NORI Area D. AC eddies originate both locally and remotely (e.g., Gulf of Tehuantepec), whereas CC eddies appear primarily local. Eddy lifecycles feature growth, maturity, and decay phases, influencing regional heat, salt, and tracer transport critical for nutrient and oxygen distributions (Pegliasco et al., 2022). These circulation patterns and eddy dynamics are characteristic of the broader CCZ and inform understanding of physical drivers affecting benthic ecosystems.

17.2.1.5 Biogeochemical baselines: Nutrients, organic carbon, and carbonate chemistry

Baseline measurements in NORI Area D demonstrate that bottom water nitrate concentrations range narrowly around 36.9 to 39.3 µmol L^{-1}, consistent with values reported for the wider southeastern CCZ (Shulse et al., 2017; Washburn et al., 2021). Phosphate, silicate, ammonia, and nitrite concentrations align similarly with regional datasets, reflecting the homogeneity in deep-water nutrient profiles across the CCZ.

Particulate organic carbon (POC) fluxes measured at depths near 2,000 m and 500 m above the seafloor correspond closely with satellite-derived net primary productivity (NPP) estimates, showing seasonal and interannual variability linked to climatic events such as La Niña (Dunne et al., 2005; Henson et al., 2012; Li & Cassar, 2016). Approximately 1.2% of surface NPP reaches 1,000 m depth, with only 0.4% reaching the seafloor, equating to about 0.63 g C m^{-2} yr^{-1}, slightly lower than some modelled estimates for the CCZ (Lutz et al., 2007; McQuaid et al., 2020).

Sediment inorganic carbon (IC) content in NORI Area D ranges from 0.04% to 1.69%, generally below global averages but higher than neighboring BGR-E Contract Area sediments due to proximity to calcareous ooze zones (Kuhn & Rühlemann, 2021b). IC depth profiles typically increase with burial depth, reflecting depositional regimes common to equatorial Pacific sediments (Archer, 1996; Jahnke et al., 1982). Total organic carbon (TOC) content at the sediment surface averages around 0.56%,

comparable to BGR-E but higher than UK-1 Contract Area sediments, highlighting regional consistency in organic matter deposition (Macheriotou et al., 2022; Hollingsworth et al., 2021).

Carbon-to-nitrogen (C:N) ratios in surface sediments hover around 5, indicating mixed marine organic matter inputs consistent with mid-range values for unaltered phytoplanktonic material (Prahl et al., 1980; Redfield et al., 1963). Temporal stability in these ratios suggests consistent organic matter quality across seasons and years.

Seafloor pH and total alkalinity (TA) measurements in NORI Area D align with regional patterns observed in the eastern tropical Pacific, providing essential baselines for assessing potential acidification impacts related to mining activities (Jahnke et al., 1982; Fitzsimmons et al., 2024).

17.2.1.6 Benthic biological communities: Diversity, connectivity, and temporal variability

The benthic baseline studies conducted in NORI Area D represent one of the most comprehensive efforts in the CCZ, employing multidisciplinary approaches to characterize sediment microbial communities, meiofauna, macrofauna, megafauna, and nodule-associated fauna (Gooday et al., 2021; Lejzerowicz et al., 2021; Rabone et al., 2023).

Sediment microbial assemblages sampled via multicorer deployments during campaigns 5A, 5D, and 7A revealed diverse communities structured by sediment depth and substrate type. Foraminiferal studies identified over 900 species dominated by monothalamids, with diversity exceeding that reported in other CCZ Contract Areas, although densities were comparatively lower (Nozawa et al., 2006). Nematode genera richness was substantial, with 167 genera documented, showing spatial structuring and significant temporal variability exceeding spatial differences (Ingels, 2024).

Macrofaunal community composition exhibited complex spatial and temporal patterns, with significant temporal shifts between campaigns surpassing spatial heterogeneity among management zones (TF, EMS, PRZ). Species richness and community similarity analyses indicated high connectivity across NORI Area D, with many species shared between zones, underscoring ecological linkages within the lease area and potentially extending to adjacent CCZ regions (Glover et al., 2024).

Megafauna surveys using ROVs collected tens of thousands of images across multiple sites, documenting standing stocks, diversity, and community structure. Xenophyophores and other large benthic organisms showed spatial variation linked to substrate type and nodule coverage, with temporal monitoring revealing natural fluctuations critical for impact assessment baselines (O'Malley et al., 2023).

Nodule-dwelling fauna, examined through BC samples, yielded 259 species from 1,441 specimens, representing the largest quantitative dataset for this habitat in the CCZ.

Genetic connectivity analyses demonstrated significant gene flow among eastern CCZ Contract Areas, including NORI Area D, UK-1, and BGR, supporting the concept of a connected metapopulation across the region. However, genetic differentiation increased with geographic distance, notably between eastern CCZ sites and more remote locations such as IFREMER and Cape & Guinea Basin sites (Glover et al., 2024).

Megafauna surveys were also conducted in TOML B, C and D (Simon-Lledó et al, 2020). In this study, seabed image surveys were used to assess distribution patterns in invertebrate and fish megafauna (>1 cm) at multiple scales in relation to key environmental factors: food supply to the seabed varying at the regional scale (hundreds of km), seabed geomorphological variations varying at the broad local scale (tens of km), and seabed nodule cover varying at the fine local scale (tens of meters). Significant

differences in megafaunal density and community composition were found between all study areas. Geomorphology and nodule cover appeared to exert strong control on local faunal abundance and community composition, but not in species richness. Local variations in faunal density and beta-diversity, particularly those driven by nodule presence (within study areas), were of comparable magnitude to those observed at a regional level (between study areas). However, regional comparisons of megabenthic assemblages showed clear shifts in dominance between taxonomic groups (perceivable even at Phylum levels) across the mid-eastern CCZ seabed.

17.2.1.7 Trace metals in sediments and porewaters

Trace metal analyses in NORI Area D sediments confirm elevated manganese and cobalt concentrations in surface layers, consistent with nodule presence and fragmentation. Solid-phase metal contents decrease with depth, converging toward regional background levels beyond 10 cm below seafloor (bsf) (Volz et al., 2018; Paul et al., 2024). Iron content remains relatively stable with depth, mostly present as reducible iron oxyhydroxides.

Porewater dissolved metal concentrations peak near the sediment-water interface, reflecting active redox cycling and metal mobilization. Although filter size differences complicate direct comparisons, trends in NORI Area D mirror those observed in the southeastern CCZ, with localized variability likely driven by microhabitat conditions and sediment handling artifacts (Paul et al., 2024).

Temporal and spatial variability in metal concentrations appears limited within NORI Area D, suggesting stable geochemical conditions over the study period. These findings provide a valuable regional benchmark for evaluating potential mining-induced perturbations.

17.2.2 Test mining

NORI conducted a comprehensive engineering and environmental Test Mining trial between September and November 2022 in the NORI area D. The test successfully collected over 4,200 tonnes of polymetallic nodules from depths ranging between 3,800 m and 4,200 m, with the test collector driving 84 km on the seabed and achieving a maximum sustained production rate of 24 kg/s and nominal rate of 18 kg/s. The test collector demonstrated good stability, maneuverability, and an average collection efficiency estimated above 80%, confirming the feasibility of the mining technology at scale (NORI, 2025a).

Environmental monitoring was extensive and multi-phased, covering pre-test baseline, active mining, and post-mining periods. Pre-test baseline activities included 33 BC deployments for nodule abundance and geotechnical data, 35 multicore deployments for biological communities and geochemistry, deployment of respirometer and baited trap landers, time-lapse camera landers, ROV cone penetration tests, acoustic and plume-monitoring assets, and high-resolution seafloor mapping via AUVs capturing over 650,000 images (NORI, 2025a). During mining, ten AUV transects monitored benthic plumes, multiple CTD deployments sampled dissolved oxygen, pH, trace metals, and particulate matter, while far-field and near-field ROV dives collected hundreds of water samples. Post-mining monitoring replicated many of these efforts to assess recovery and impacts, including additional box cores, multicore deployments, and extensive imaging campaigns totaling over 2.5 million images (NORI, 2025).

Key lessons learned from the Test Mining trial informed design improvements aimed at reducing environmental impacts. For example, modifications to the Coandă nozzle geometry and hopper design are expected to improve nodule pick-up efficiency and reduce sediment disturbance. The diffuser's conical design was found effective in generating a turbidity current that promotes local settling of the benthic plume, thereby limiting sediment dispersion (NORI, 2025b) (Allseas, 2024). The return-water discharge depth was increased from 1,200 m during the test to 2,000 m for commercial operations,

based on preliminary baseline studies and emerging evidence indicating that deeper discharge reduces the risk of ecological impacts.

Sediment plume modeling and monitoring during test mining supported establishing an exclusion buffer zone around sensitive environmental areas and project boundaries to contain secondary impacts such as sedimentation (DHI, 2025). Seafloor current assessments indicated highly variable directions without seasonal trends, suggesting no need for seasonally adjusted collector paths to manage sediment dispersal. Geotechnical analyses confirmed the seafloor substrate can support the 1st Gen Collector on slopes up to 4°, with no trafficability issues observed during the test (APYS, 2024 (Allseas, 2024b).

Overall, the test mining program provided critical empirical data validating the technological approach and enabling refinement of operational parameters to mitigate environmental risks. The integration of detailed environmental monitoring with engineering feedback loops ensures that the commercial-scale system is expected to operate within defined environmental safeguards, minimizing benthic disturbance and sediment plume spread while maintaining efficient resource recovery (NORI, 2025a) (DHI, 2025).

17.2.3 Summary and implications for the wider CCZ

The results of test mining and comprehensive environmental baseline studies in NORI Area D offer vital insights applicable throughout the wider CCZ. The geological, geotechnical, and sedimentological features observed here reflect broader regional patterns, enabling informed extrapolation to nearby Contract Areas. Hydrodynamic and circulation processes, such as mesoscale eddies and internal waves, impact benthic habitats and biogeochemical cycles across the CCZ.

Biological communities in NORI Area D are highly diverse, connected, and vary over time, underscoring the importance of long-term monitoring to distinguish human impacts from natural variations. Trace metal levels in sediments and porewaters help clarify the chemical environment supporting benthic life. Insights from test mining is expected to inform the design of mining equipment for other areas, reducing environmental impacts. Overall, these findings provide a solid foundation for developing EIA scopes for other CCZ Contract Areas.

17.3 Scope of baseline studies

TMC, through its NORI subsidiary, has conducted extensive baseline studies in the NORI Area D lease of the CCZ. These studies re planned to be expanded to include the areas covered in the TMC USA applications. A comprehensive Scoping Study is planned to identify gaps in the existing knowledge base. An outline of the baseline studies that are planned is provided below.

Physicochemical environmental baseline:

- Meteorology and air quality.
- Geological regional and site-specific setting.
- Seabed substrate characteristics:
  - Sediment physical properties .
  - Sediment mechanics.
  - Porewater properties.

Physical oceanographic regional and site-specific setting:

- Water masses.

- Currents.
- Tides and surface waves.
- Internal waves .
- Stratification and mixing.
- Mesoscale eddies.
- Bottom mixed layer.

Chemical oceanographic regional and site-specific setting:

- Nutrients water column.
- Oxygen water column.
- Carbonate system water column.
- Trace metals water column .
- Organic and inorganic matter water column.
- Nutrients seafloor.
- Oxygen seafloor.
- Carbonate system seafloor .
- Trace metals seafloor.
- Organic matter seafloor.
- Inorganic matter seafloor.
- Natural hazards.
- Noise and light.

Biological environment baseline:

- Biological site-specific setting:
  - Surface (from the surface to a depth of approximately 200 m):
    - Phytoplankton.
    - Zooplankton.
    - Surface fish.
    - Near-surface fish.
    - Seabirds.
    - Turtles and marine mammals.
  - Midwater (from a depth of approximately 200 m to approximately 50 m above the sea floor).
  - Zooplankton.
  - Nekton .
  - Mesopelagic and bathypelagic fish.
  - Deep-diving mammals.
- Benthic (from approximately 50 m above the sea floor to the sea floor's surface):
  - Benthic invertebrates (mega, macro, meio, forams, and microfauna).
  - Fish communities .
- Ecosystem models and trophic interactions between depths.
- Socioeconomic Baseline:

- Social impacts on people, including:
  - Way of life (lifestyles, work, interactions, recreation, etc.).
  - Culture (customs, values and beliefs) .
  - Community (cohesion, stability, character and services).
  - Political and governance systems.
  - Environment (quality, food security and safety) .
  - Health and well-being (physical, mental, social and spiritual).
  - Personal and property rights (economic effects and customary rights).
  - Potential impacts on ecosystem services, including fisheries.
- Marine traffic.
- Tourism.
- Marine scientific research.
- Other uses of the area in and around the proposed Contract Area.
- Sites of archaeological or historical significance.
- Relevant area-based management classifications or tools established under subregional, regional or global processes.
- Workforce characteristics.

17.4 Post mining land uses

The NORI and TOML areas are located in the CCZ, a 4.5-million-km^2 region in the northern part of the Central Pacific Ocean, approximately 1,700 km to the northwest of Mexico. The western end of the CCZ is approximately 1,000 km south of the Hawaiian island group. From here, the CCZ extends over 4,500 km east-northeast, in an approximately 750 km wide trend, with the eastern limits approximately 2,000 km west of southern Mexico.

The mine site is located on the seabed at a depth of approximately 4,000+ m.

No post-mining land uses are anticipated.

17.5 Remediation

No remediation is anticipated for the mined site due to its inaccessibility and absence of potentially impacting post-mining land uses. The site are expected to remain undisturbed post-closure to allow for natural recolonization.

17.6 Tailings

Nodule collection does not produce tailings in the traditional sense. Tailings are typically the materials left over after the process of separating the valuable fraction from the uneconomic fraction of an ore. In the case of nodule collection, the process is designed to eliminate tailings by not chemically processing the material at sea. Instead, small amounts of residual sediment and abraded nodules found in the seawater used for nodule transport are more analogous to the removal and redeposition of overburden during a terrestrial mining operation. The sediment-seawater mixture returned into the midwater column is often mistakenly referred to as "tailings," but it should not be confused with the traditional definition of tailings, which are a by-product of processing.

17.7 Mitigation plans

Mitigation measures and implementation plans are planned to be developed based on the findings of the EIA. Based on the results of test mining conducted on NORI Area D in 2022 the key mitigation measures are expected to involve modifications and improvements to the mining system and operational plan to minimize the environmental impact of nodule collection.

18 Capital and operating costs

18.1 Introduction

The Project capital and operating costs were prepared based on the following execution strategy as described in the previous sections:

Nodule Collection and Shipping:

- Contract Mining basis (OPEX) with contractor capital recovered by the contractor over the first 10 years of operation.
- Specific sustaining capital related to the collection equipment is included for PV class surveys to de-risk initial Contract Mining assumptions and facilitate lowest cost incorporation of technology advancements and improvements identified during initial collection equipment operation and maintenance.

Processing (RKEF):

- Based on tolling through existing RKEF facilities with all capital modifications to those facilities captured in the tolling charge.

US Refining:

- All capital costs and operating costs included based on traditional owner build/own/operate model with assistance from strategic partners as required.

The Project capital expenditure (CAPEX) and operating expenditure (OPEX) estimates were prepared by specialists in the following areas:

- Collection CAPEX and OPEX were estimated by Allseas and TMC.
- Shipping CAPEX and OPEX were estimated by Allseas and TMC.
- Contractor (offshore) OPEX was estimated by Allseas and TMC.
- Consumables (offshore fuel) was estimated by Allseas and TMC.
- Processing facility OPEX was estimated by TMC.
- Refining facility CAPEX and OPEX were estimated by a global leading consulting engineering firm.
- Corporate OPEX was estimated by TMC.

All costs in this section are presented in US dollars (US$). The number of significant figures presented in this report is not necessarily indicative of the accuracy or precision of the underlying data or calculations. Significant figures have been used for clarity and convenience in reporting but do not imply a specific confidence level or measurement uncertainty.

18.2 Operating strategy

The execution strategy is based on the collection of nodules from high abundance and high metal grade areas first with bespoke 2nd Gen systems. Nodules are expected to be transported to Indonesia for processing to a matte product and manganese silicate through a tolling arrangement utilising existing processing infrastructure. Matte product is expected to be shipped to Texas, USA on market bulk carriers for refining through a new refining facility developed by TMC with support from strategic partners.

Operations are expected to commence in TOML-F with one PV producing 7 Mwmtpa coming online in 2037. An additional two PVs are planned to come online in 2038 and 2039 bringing total production from TOML-F to 21 Mwmtpa. TOML-F is scheduled to be mined before the PVs relocate to the west for

collection in TOML-D and TOML-E areas. Areas outside of TOML-F have lower abundance and hence annual production per PV of 5 Mwmtpa was modelled. Another 5 PVs are expected to come online between 2044 and 2048 to increase total production to 40 Mwmtpa.

On arrival to Indonesia, nodules will be offloaded from the TVs for transfer to existing RKEF facilities for processing the nodules to a nickel-copper-cobalt matte and manganese silicate product. Using existing RKEF facilities through tolling arrangement reduces upfront capital and aligns processing capabilities with offshore production ramp-up.

The processed matte is loaded to bulk carriers and shipped to Texas. Manganese silicate is planned to be sold to market. The long-term refining strategy involves construction of two refining facilities (12 Mwmtpa nodule equivalent capacity each) in US which refine the matte and produce copper cathode, nickel sulfate, and cobalt sulfate. Processing is assumed to be on a tolling arrangement with TMC entering agreements with third parties that will operate the new refineries on behalf of TMC.

Environmental management is planned to be embedded throughout the operations. A robust EMMP will support adaptive management practices, allowing staged expansion contingent on meeting environmental thresholds and minimizing ecological impacts.

CAPEX on offshore operations and RKEF facilities are expected to be managed as capital-light, by TMC entering operating agreements with contract miners and transport providers who manage the collection and delivery of nodules to shore. Bulk carriers running between Indonesia and the USA are owned and operated by third parties, with TMC paying through standard shipping charges agreed between the parties. All processing facilities in Indonesia are assumed to be owned and operated by third parties, with TMC paying for toll treatment per tonne of nodules. All refining facilities in the US will be a TMC asset.

18.2.1 Baseline operating assumptions

The following scope and execution assumptions underpin the CAPEX/OPEX estimates detailed in Section 18.3 and Section 18.4.

Offshore Operations vessel numbers:

- Ramp up to 3 x PVs, each with 3 x20 m collectors and associated equipment to achieve 7 Mwmtpa mining production each in the TOML-F area.
- Addition of 5 x PVs to the other NORI and TOML areas, each producing 5 Mwmtpa. The 3 x PVs also move from TOML-F to the NORI and TOML areas resulting in a total capacity of 40 Mwmtpa from year 12.
- Each PV serviced by 7 TVs in the high abundance TOML-F area and 5 TVs in the other lower abundance TOML and NORI areas.
- Ramp-up to 24 x SVs for personnel, supplies and equipment change out.

Production Schedule and capital cost :

- All PVs– Contractor Miner strategy; 100% capital cost recovered in operations over 10 years from PVs commencement dates.
- Total production 670 Mwmt.
- Life-of-mine of 23 years.

Nodule Processing:

- Indonesia
  - Existing Indonesian RKEF plants process all nodule production.
- Texas, USA
  - Matte is converted to nickel sulfates, cobalt sulfates, and copper cathode.

18.3 CAPEX

The CAPEX estimate (Table 18.1) is reported in Q2 2025 US$. CAPEX estimates are at an IA level of confidence and are prepared using the AACE International Class 5 estimate standards, with a contingency of 25%.

The estimate includes the cost to complete the design, procurement, fabrication, assembly, installation and commissioning associated with mining, transporting and processing nodules as per the Mine Plan. The estimate was based on a contractor, Allseas or equivalent, overseeing and delivering the engineering, procurement, fabrication, assembly and installation for the associated offshore infrastructure and equipment.

The estimate was derived from a combination of budgetary pricing, historical data and allowances. The estimates were based on a number of fundamental assumptions, such as indicated in process flow diagrams, general arrangements, scope definition and work breakdown structures.

Table 18.1 Total CAPEX summary

		Development	Sustaining	Closure
Item	**Total**	**PP5-Year 3**	**Year 17-30**	**Year 33-42**
Project CAPEX	8,852	8,852		
Sustaining CAPEX	5,318		5,318	
Closure CAPEX	805			805.3
Total CAPEX	**14,975**	**8,852**	**5,318**	**805.3**

Note: PP = Pre-Production

18.3.1 Production vessel #5-12

Total estimate for each PV is utilized to determine the payback costs under contractor mining strategy to be recovered over the first ten years of operating.

The PV CAPEX estimate of US$1,568M, is summarized in Table 18.2.

Table 18.2 PV recovered CAPEX summary

Description	**US$ M**
Production Vessel	915
Transport Vessel	180
Direct Subtotal	1,095
Indirect	159
Contingency	314
Production Vessel Recovered CAPEX	1,568

18.3.2 Refining facility

The refining facility CAPEX estimate of US$8,852M, is summarized in Table 18.3 .

Table 18.3 Refining facility recovered CAPEX summary

Description	US$ M
General/Infrastructure	234
Port Facilities	455
Hydrometallurgy	1,663
Direct Subtotal	2,352
Indirect Costs	930
Contingency	1,144
Refining Facility CAPEX per 12 Mwmtpa nodule equivalent	4,426
Number of 12 Mwmtpa refining facility	2
Total Project Capital	**8,852**

18.3.3 Sustaining CAPEX

The sustaining capital costs (dry dock) for the 2nd Gen PV is US$483M per occurrence totaling US$5,318M (Table 18.4). The sustaining capital includes replacement of collectors and risers during each 10-year dry docking cycle, as well as statutory maintenance required to maintain the vessels in class.

Table 18.4 Sustaining CAPEX

Sustaining Capital	UOM	Qty	US$ M
Collector Design life	Years	10	
Collector x 3 CAPEX	Lot	1	193
Umbilical Design life	Years	10	
Umbilical x 3 CAPEX	Lot	1	35
Compressor Design life	Years	10	
Compressor CAPEX	Lot	1	87
Riser System Design life (riser considered consumable)	Years	10	
Riser System CAPEX	Lot	1	106
Vessel compounds incl LARs/Derrick Design life	Years	30	
Vessel compounds incl LARs/Derrick service period	Years	10	
Vessel compounds incl LARs/Derrick CAPEX	Lot	1	63
Class Survey Intervals	Years	10	
Class Survey Duration	Months	6	
Estimated Total Sustaining Capital every 10 years per vessel (Class survey)	Lot	1	483
Total Class surveys across all PVs LoM	Units	11	5,318

18.3.4 Closure CAPEX

A closure cost of US$690M has been allowed between 2060 and 2064 for remediation of the onshore refining facilities. While US$115M has been allowed for post-closure offshore monitoring

The Closure CAPEX estimate of US$805M, is summarized in Table 18.5

Table 18.5 Closure CAPEX

Closure Capital	US$ M
Vessel Supply	6.8
Mobilisation	1.2
Other Cost	0.4
Fuel	0.9
Onboard personnel/Equipment	0.9
Other Cost	0.2
Third Party Cost	1.1
Total Closure Offshore Capital per year	11.5
Total Closure Offshore Capital 10-year post mining operations	115
Onshore Refining plant	138
Total Closure Onshore Capital per year	138
Total Closure Onshore Capital 5-year post mining operations	690
Total Closure Capital	**805**

18.4 OPEX

The OPEX estimate is reported in Q2 2025 US$. OPEX estimates are at an IA level of confidence and are prepared using the AACE Class 5 estimate standards. OPEX for the project are summarized in Table 18.6 and Table 18.7.

OPEX is summarized below for the LOM and average unit costs per wmt of nodules collected over the LOM:

- LOM collection costs are estimated at US$31,139M and average US$46.5/wmt of nodules.
- LOM shipping costs are estimated at US$6,066M and average US$9.1/wmt of nodules.
- LOM contractor (offshore) costs are estimated at US$3,584M and average US$5.3/wmt of nodules.
- LOM consumables (offshore fuel) costs are estimated at US$11,884M and average US$17.7/wmt of nodules.
- LOM processing costs are estimated at US$53,598M and average US$80.0/wmt of nodules.
- LOM refining costs are estimated at US$15,978M and average US$23.8/wmt of nodules.
- LOM G&A costs are estimated at US$3,926M and average US$5.9/wmt of nodules.

Table 18.6 OPEX summary

OPEX component	Total LOM (US$M)	LOM %
Collection Costs	31,139	25%
Shipping Costs	6,066	5%
Contractor (offshore) Costs	3,584	3%
Consumables (offshore fuel) Costs	11,884	9%
Processing Cost	53,598	42%
Refining Cost	15,978	13%
Corporate Cost	3,926	3%
Total OPEX	**126,175**	**100%**

Table 18.7 OPEX unit cost US$/wmt summary

OPEX component	Average LOM US$/wmt
Collection Costs	46.5
Shipping Costs	9.1
Contractor (offshore) Costs	5.3
Consumables (offshore fuel) Costs	17.7
Processing Cost	80.0
Refining Cost	23.8
Corporate Cost	5.9
Total OPEX	**188.3**

18.4.1 Collection costs

The Collection Cost OPEX totals US$31,139M or US$46.5/wmt. The Collection Cost OPEX is summarized in Table 18.8, and considers the operation of the offshore mining system and SVs, as detailed in Section 13.6.1 and 13.6.3.

Table 18.8 Collection costs summary

OPEX component	Total LOM (US$M)	Average LOM US$/wmt
Supply vessel	3,753	5.6
Production Vessel	12,391	18.5
Corporate - Production Support	1,199	1.8
PV5-12 CAPEX Recovery	13,796	20.6
Collection Costs Total	31,139	46.5

Key inputs and assumptions used in the cost estimate were:

- Contractor operator.
- PV cost was provided by Allseas and includes:
  - PV day rate provided by Allseas.
  - Labor rates for expatriate and nationals including base salaries, benefits, bonuses; and overhead burdens were provided by Allseas.
  - Travel costs are estimated as an allowance.
  - Other support costs including, ROVs and maintenance allowances.
- Production support – Allseas onshore salaries for expatriate and nationals including base salaries, benefits, bonuses; and overhead burdens were provided by Allseas.
- SV cost was provided by Allseas:
  - Labor rates for expatriate and nationals including base salaries, benefits, bonuses; and overhead burdens were provided by Allseas.
  - Travel costs are estimated as an allowance.
  - Other support costs including maintenance allowances etc.
- System #5-12 – contractor mining capital recovery as per Table 18.8 and cost of working capital (10%) for first 10 years of production of each PV.

18.4.2 Shipping costs

The Shipping Cost OPEX, covering operation of the TVs(see Section 13.6.2) and Handymax bulk carrier totals US$6,066M or US$9.1/wmt. The Shipping Cost OPEX is summarized in Table 18.9.

Table 18.9 Shipping Costs Summary

OPEX component	Total LOM (US$M)	Average LOM US$/wmt
Transport Vessel CCZ to Indonesia - Capesize	5,162	7.7
Transport Vessel Indonesia to Texas - Handymax	905	1.4
Shipping Costs Total	6,066	9.1

Key inputs and assumptions used in the cost estimate were:

- Contractor operator.
- TV CCZ to Indonesia :
  - Market pricing used for all in day rate.
  - Fleet sizing based on logistics cycle times calculated by TMC.
- Bulk Carrier Indonesia to Texas – Handymax:
  - Market pricing used for all in day rate.
  - based on logistics cycle times calculated by TMC.
  - Loading/unloading of matte product.
  - Panama Canal fees.
  - MGO fuel price of US$700/t, this is based on end of Q1 2025 data obtained from Ship and bunker spot pricing.
  - Fuel consumption was calculated by industry norms.

18.4.3 Contractor (offshore) costs

The contractor (offshore) costs OPEX totals US$3,584M or US$5.3/wmt. The contractor (offshore) costs OPEX is summarized in Table 18.10.

Table 18.10 Offshore contractor costs summary

OPEX component	Total LOM (US$M)	Average LOM US$/wmt
Performance Incentive Payment	3,584	5.3
Contractor (offshore) Costs Total	3,584	5.3

Key inputs and assumptions used in the cost estimate were:

- An assumed Contract Miner Performance Incentive

18.4.4 Consumables (offshore fuel) costs

The consumables (offshore fuel) costs OPEX totals US$11,884M or US$17.7/wmt. The consumables (offshore fuel) costs OPEX is summarized in Table 18.11.

Table 18.11 Offshore fuel costs summary

OPEX component	Total LOM (US$M)	Average LOM US$/wmt
Fuel - SV	581	0.9
Fuel - PV	1,452	2.2
Fuel - CVs	4,517	6.7
Fuel – TV CCZ to Indonesia - Capesize	5,334	8.0
Consumables (offshore fuel) Costs Total	11,884	17.7

Key inputs and assumptions used in the cost estimate were:

- Fuel – SV:
  - MGO fuel price of US$700/t, this is based on end of Q1 2025 data obtained from ship and bunker spot pricing.
  - Fleet sizing based on logistics cycle times calculated by TMC.
  - Fuel consumption was calculated by industry norms.
- Fuel - PV (DP, auxiliary power consumers and accommodation):
  - MGO fuel price of US$700/t, this is based on end of Q1 2025 data obtained from ship and bunker spot pricing.
  - Fuel consumption was calculated by Allseas.
- Fuel - CVs (compressor spread for the VTS):
  - MGO fuel price of US$700/t, this is based on end of Q1 2025 data obtained from ship and bunker spot pricing.
  - Fuel consumption was calculated by Allseas.
- Fuel – TV CCZ to Indonesia – Capesize:
  - MGO fuel price of US$700/t, this is based on end of Q1 2025 data obtained from ship and bunker spot pricing.
  - Fleet sizing based on logistics cycle times calculated by TMC.
  - Fuel consumption was calculated by industry norms.

18.4.5 Processing cost

The Processing Costs OPEX totals US$53,598M or US$80.0/wmt. The Processing Costs OPEX is summarized in Table 18.12.

Table 18.12 Processing costs summary

OPEX component	Total LOM (US$M)	Average LOM US$/wmt
Indonesia Matte Toll Charge	53,598	80.0
Processing Cost Total	53,598	80.0

Key inputs and assumptions used in the cost estimate were:

- Indonesia Matte Tolling Charge – All in tolling charge estimated by SMM Information & Technology Co., Ltd processing cost study. Benchmarked against known/published NPI processing cost in Indonesia. NPI processing is closely related to nodule processing for TMC's product. Refer to Section 15.1.2.5.

18.4.6 Refining cost

The refining costs OPEX totals US$15,978.4M or US$23.8/wmt. The refining costs OPEX is based on a global leading consulting engineering firm, which are summarized in Table 18.13.

Table 18.13 Refining summary

OPEX component	Total LOM (US$M)	Average LOM US$/wmt
US Refining Toll Opex	14,704	21.9
Purchase of 3rd party Matte Feed	1,275	1.9
Refining Cost Total	15,978	23.8

Key inputs and assumptions used in the cost estimate were:

- US Refining OPEX provided by a global leading consulting engineering firm cost study and includes:
  - Plant Labor including supervisors, engineers, laboratory, site workers and operators.
  - Plant equipment, materials, supplies, first fills.
  - Maintenance materials.
  - Plant management.
  - Reagents including sulfuric acid, sodium hydroxide, anhydrous liquid ammonia, sulfur dioxide, oxygen, nickel and cobalt extractants, SX diluent, copper IX resin, granular activated carbon and flocculant & coagulant.
  - Energy including electricity, natural gas, diesel.
  - Water including makeup water acquisition, pretreated water, demineralized water.
  - Other consumables including effluent treatment, manganese oxidation scrubber consumables, filtration consumables and additives, product packaging.
- Purchase of 3rd party matte feed:
  - Based on payable terms from CRU.

18.4.7 Corporate cost

The Corporate Costs OPEX totals US$3,926M or US$5.9/wmt. The Corporate Costs OPEX is summarized in Table 18.14.

Table 18.14 Corporate costs summary

OPEX component	Total LOM (US$M)	Average LOM US$/wmt
Overhead - Corporate	575	0.9
Campaign/EMMP	829	1.2
Offshore operations support	256	0.4
OPEX Contingency	2,267	3.4
Corporate Cost Total	3,926	5.9

Key inputs and assumptions used in the cost estimate were:

- Overhead – Corporate cost estimated by TMC based on actual and projected overhead cost.
- Campaign/EMMP cost estimated by TMC based on actual campaign and EMMP costs.
- Offshore operations support facilities cost estimated by TMC based on historical knowledge and actual costs of operations support facilities including:
  - Contractor personal – office and site.
  - TMC personal.
  - Service contracts - waste, security etc.
  - Office/laydown/warehouse lease costs.
  - Office / laydown / warehouse material, equipment, supplies.
- OPEX Contingency.

19 Economic analysis

19.1 Cautionary statement regarding forward-looking information

The results of the economic analysis discussed in this section includes forward looking information and statements. TMC as the author of this Section, provides the following cautionary statement regarding forward looking information.

TMC is subject to the reporting requirements of the Exchange Act. The results of the financial and economic analyses discussed in this section represent forward-looking statements within the meaning of applicable securities laws relating to TMC. These statements by their nature involve substantial risks and uncertainties. Statements involving the foregoing results of financial and economic analyses are forward-looking statements. Without limiting the generality of the foregoing, words such as “may”, “anticipate”, “intend”, “could”, “estimate”, or “continue” or the negative or other comparable terminology are intended to identify forward-looking statements. Should one or more of these risks or uncertainties materialize or should the underlying assumptions prove incorrect, actual outcomes and results could differ materially from those indicated in the forward-looking statements.

This economic analysis is based on Measured, Indicated and Inferred Mineral Resources and does not support a determination of Mineral Reserves. The outcomes presented are preliminary in nature, and no pre-feasibility or feasibility study has been completed. These forward-looking statements are subject to change based on additional technical work, permitting outcomes, financing availability, or market conditions.

Information that is forward-looking includes, but is not limited to, the following:

- Assumed commodity prices and exchange rates.
- Proposed mine production plan.
- Projected mining and process recovery rates.
- Assumptions as to mining dilution.
- Assumptions as to geotechnical requirements for collector on the seabed.
- Proposed sustaining costs and operating costs.
- TMC’s intentions on payback of LCR royalty.
- Assumptions as to closure costs and closure requirements.
- Assumptions as to environmental, permitting, and social risks.
- Assumptions regarding permitting timelines, including under both the ISA and the U.S. Deep Seabed Hard Mineral Resources Act (DSHMRA).

Additional risks to the forward-looking information include:

- Changes to the costs of production from what is assumed.
- Unexpected variations in quantity of mineralized material, grade or recovery rates.
- Geotechnical considerations during mining being different from what was assumed.
- Failure of mining methods to operate as anticipated.
- Failure of plant, equipment or processes to operate as anticipated.
- Changes to assumptions as to the availability of electrical power, and the power rates used in the operating cost estimates and financial analysis.
- Unrecognized environmental risks.
- Unanticipated closure expenses.

- Ability to maintain social license to operate.
- Accidents, labour disputes and other risks of the mining industry.
- Changes to interest rates.
- Changes to tax rates.
- Uncertainty in the legal, regulatory, or geopolitical frameworks that may govern deep seabed mineral production.

Other key considerations when reviewing the content within this Section:

- Calendar years used in the financial analysis are provided for conceptual purposes only.
- Notional model start date of 1 July 2025 and annual discounting combined with the assumption of mid-period cash flows results in effective model years commencing 1 July and ending 30 June.
- Totals may not reflect the sum of table contents due to the effects of rounding.
- Environmental approval must still be obtained in support of operations.
- The results do not demonstrate economic viability and should not be construed as such.

19.2 Methodology used

An economic model was developed to estimate annual pre-tax and post-tax cash flows and sensitivities of the Project based on an 8% discount rate. Tax estimates involve complex variables that can only be accurately calculated during operations and, as such, the after-tax results are approximations. The economic analysis was run in real, ungeared, post-tax terms.

19.3 Economic model parameters

The economic analysis was performed using the following key assumptions:

- Cost estimates with no inflation of escalation attributed.
- Valuation date of 1 July 2025.
- Commercial production starting 2037.
- LOM of 23 years.
- All cash flows discounted at an 8% discount rate representing the Registrant's assumption of the Project weighted average cost of capital (WACC).

19.4 Total development costs

The Project Cost estimate of US$8,852M detailed in Chapter 18 of this document.

19.5 Total sustaining costs

The Sustaining Cost estimate of US$5,318M during operations as detailed in Chapter 18 of this document.

19.6 Total closure costs

The Sustaining Cost estimate of US$805M as detailed in Chapter 18 of this document.

19.7 Total operating costs

The Project OPEX estimate of US$126,175M, is summarized in Table 19.1.

Table 19.1 Total operating costs

OPEX component	Total LOM (US$M)	Average LOM US$/wmt
Collection Costs	31,139	46.5
Shipping Costs	6,066	9.1
Contractor (offshore) Costs	3,584	5.3
Consumables (offshore fuel) Costs	11,884	17.7
Processing Cost	53,598	80.0
Refining Cost	15,978	23.8
Corporate Cost	3,926	5.9
Total OPEX	126,175	188.3

19.8 Commodity prices

Metal and sulfate price assumptions for nickel, cobalt and copper were provided BMI as of 30 June 2025. Manganese metal price assumption detailed in Table 16.1. Both sources provided long-term price forecasts based on a market analysis of supply and demand at the time of this report.

The average LOM commodity prices are summarized in Table 19.2.

Table 19.2 Average LOM commodity prices

Commodity	UOM	Price per UOM
Nickel Price (C1 LME)	US$/t	20,360
Cobalt Price (C1 LME)	US$/t	62,530
Copper Cathode Price (C1 LME)	US$/t	11,456
Manganese ore Price	US$/dmtu	4.7
Nickel Sulfate Price (100% contained Ni basis)	US$/t	21,835
Cobalt Sulfate Price (100% contained Co basis)	US$/t	62,530

19.9 Recovery rates

Recovery assumptions were provided by HATCH, which performed a series of mass energy balance recoveries calculation. The recovery rates are summarized in Table 19.3.

Table 19.3 Recovery rates

Recovery	Value
Nickel Recovery Nodule to Matte	94.8%
Cobalt Recovery Nodule to Matte	77.5%
Copper Recovery Nodule to Matte	86.4%
Manganese Recovery to Manganese Silicate	98.9%
Nickel Recovery - Nodule to Sulfate	94.6%
Cobalt Recovery - Nodule to Sulfate	77.2%
Copper Recovery - Nodule to Cathode	86.2%

19.10 Payable terms

Metal payable term assumptions were provided by CRU Consulting. This provides long-term payable terms forecasts based on the market analysis of supply and demand. The average LOM payable terms are summarized in Table 19.4.

Table 19.4 LOM average payable terms

Recovery	Value
Nickel Payable Factor for Matte	80%
Cobalt Payable Factor for Matte	60%
Copper Payable Factor for Matte	70%

19.11 Royalty / Payments

The economic model assumes that the TMC will be subject to three royalty/payment structures, as per below.

19.11.1 Nauru continuity benefits

The structure for the Nauru Continuity Benefits payment is based on the NORI Sponsorship Agreement. The Nauru Continuity Benefits is based on the payment schedule in Table 19.5. An annual US$0.5M administrative fee is allowed. The Nauru Continuity Benefits are only applicable to NORI Area A, B, C. In the first nine years of the project, all mining is expected to be in TOML-F, therefore no Nauru benefits would be payable in this period.

The total benefit payment has been capped at US$109.5M.

Table 19.5 Nauru continuity benefits payment schedule

Item	US$ M
Year 19-28	10.5
Year 29	4.5

Total undiscounted royalty payments to Nauru are approximately US$137M (inclusive of gross up withholding tax) over the LOM.

19.11.2 Tonga continuity benefits

The structure for the Tonga Continuity Benefits payment is based on the draft Tonga Sponsorship Agreement. The Tonga Continuity Benefits is based on the payment schedule in Table 19.6. An annual US$90K administrative fee is allowed. The Tonga Continuity Benefits are only applicable to TOML Area A, B, C D, E, and F. The total benefit payment has been capped at US$75M.

Table 19.6 Tonga continuity benefits payment schedule

Item	US$ M
Year 1	1.0
Year 2	2.0
Year 3	4.0
Year 4	8.0
Year 5+	10.0

Total undiscounted continuity benefit payments to Tonga are approximately US$75M over the LOM.

19.11.3 Low Carbon Royalty (LCR)

TMC entered a strategic partnership with LCR, a private royalty financing company, in 2023. Terms of the agreement include TMC paying a royalty to LCR[7]. The LCR royalty is only applicable to NORI Areas and based on 0.5% of total revenue.

Total undiscounted royalty payments to LCR are approximately US$684M over the LOM.

19.12 Taxes

It has been assumed that Project will be subject to a single taxation structure. The USA Federal taxation rate and structure assumed in the economic model is as follows:

- Federal taxation rate at 21%.
- Depreciation based on straight-line basis, based on the assumed system design life.
- Total undiscounted taxation is approximately US$33,753M over the LOM.

19.13 Economic analysis

The economic analysis was performed assuming an 8% discount rate, representing the Registrant's assumption of the Project weighted average cost of capital (WACC). Compared to the 9% discount rate used in the 2021 IA for NORI Area D, the discount rate of 8% reflects the Registrant's view that the achievement of de-risking milestones on the project in the last several years has lowered the WACC for the Project. De-risking milestones include:

- Successful pilot collection system trial (Test Mining) in 2022 in which over 3,000 wet tonnes of nodules were lifted to the surface.
- Improved confidence in the permitting pathway through the existing U.S. regulatory regime.

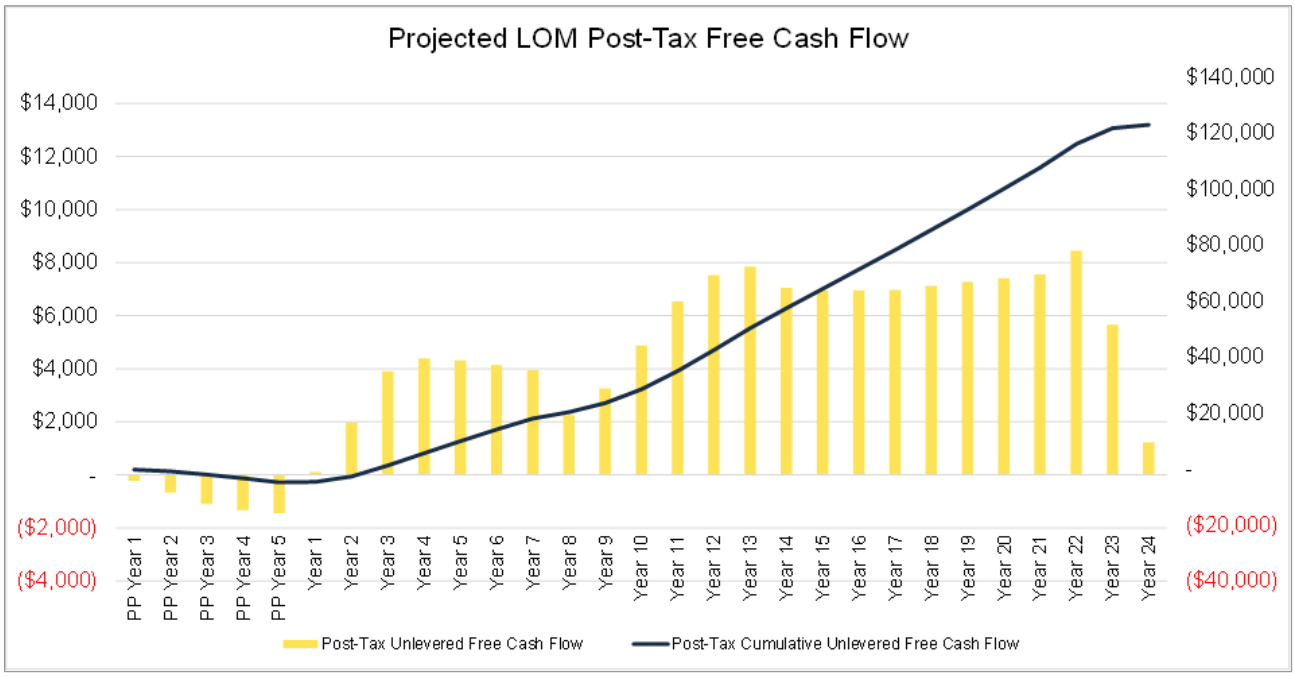
The post-tax NPV discounted at 8% is approximately US$18,100M.

The economic projections presented in this section are based on Measured, Indicated, and Inferred Mineral Resources and do not support a determination of Mineral Reserves or demonstrate economic viability.

A summary of forecast Project economics is shown graphically in Figure 19.1 and listed in Table 19.7.

[7] https://investors.metals.co/news-releases/news-release-details/metals-company-and-low-carbon-royalties-form-strategic

Figure 19.1 Forecast project post-tax free cash flow (US$ M)



Source: TMC
Note: PP = pre-production

Table 19.7 Summary of forecast project economics

Area	Item	Units	LOM Total/Avg.
General	Nickel Price (C1 LME)	Avg. US$/t	20,360.0
	Cobalt Price (C1 LME)	Avg. US$/t	62,529.6
	Copper Cathode Price (C1 LME)	Avg. US$/t	11,456.4
	Manganese Price	Avg. US$/dmtu	4.7
	Nickel Sulfate Price (100% contained Ni basis)	Avg. US$/t	21,835.0
	Cobalt Sulfate Price (100% contained Co basis)	Avg. US$/t	62,529.6
	Mine Life	Years	23.0
	Total Ore Collected (wet)	Mmt	670.0
Production (Nickel)	Resource Grade TOML F	%	1.40%
	Resource Grade TOML A-E & NORI A-C	%	1.27%
	Contained Metal in Recovered Nodules	Kt	6,354.2
	Recovery Nodule to Matte	%	94.76%
	Recovery Nodule to Sulfate	%	94.60%
	Recovered Metal in Matte	Kt	302.9
	Recovered Metal in Sulfate	Kt	5,759.8
	Payable Factor for Matte	%	80.00%
	Payable Factor for Sulfate	%	100.00%
	Payable Metal in Matte	Kt	242.3
	Payable Metal in Sulfate	Kt	5,759.8
	Nickel Products Total Revenue	US$ M	130,670
Production (Cobalt)	Resource Grade TOML F	%	0.13%
	Resource Grade TOML A-E & NORI A-C	%	0.22%
	Contained Metal in Recovered Nodules	Kt	1,015.1
	Recovery Nodule to Matte	%	77.54%
	Recovery Nodule to Sulfate	%	77.20%

Area	Item	Units	LOM Total/Avg.
	Recovered Metal in Matte	Kt	37.9
	Recovered Metal in Sulfate	Kt	752.3
	Payable Factor for Matte	%	60.00%
	Payable Factor for Sulfate	%	100.00%
	Payable Metal in Matte	Kt	22.7
	Payable Metal in Sulfate	Kt	752.3
	Cobalt Products Total Revenue	US$ M	48,456
Production (Copper)	Resource Grade TOML F	%	1.25%
	Resource Grade TOML A-E & NORI A-C	%	1.07%
	Contained Metal in Recovered Nodules	Kt	5,431.7
	Recovery Nodule to Matte	%	86.43%
	Recovery Nodule to Sulfate	%	86.20%
	Recovered Metal in Matte	Kt	237.3
	Recovered Metal in Sulfate	Kt	4,485.2
	Payable Factor for Matte	%	70.00%
	Payable Factor for Sulfate	%	100.00%
	Payable Metal in Matte	Kt	166.1
	Payable Metal in Sulfate	Kt	4,485.2
	Copper Products Total Revenue	US$ M	53,278
Production (Manganese)	Resource Grade TOML F	%	32.21%
	Resource Grade TOML A-E & NORI A-C	%	27.97%
	Contained Metal in Recovered Nodules	Kt	141,788.7
	Recovery Nodule to Manganese	%	98.90%
	Recovered Metal in Manganese	Kt	140,229.0
	Payable Factor for Manganese	%	100.00%
	Payable Metal in Manganese	Kt	140,229.0
	Manganese Products Total Revenue	US$ M	66,078.1
Operating Cost	Collection Costs	US$/wmt	46.5
	Shipping Costs	US$/wmt	9.1
	Contractor (offshore) Costs	US$/wmt	5.3
	Consumables (offshore fuel) Costs	US$/wmt	17.7
	Processing Cost	US$/wmt	80.0
	Refining Cost	US$/wmt	23.8
	Corporate Cost	US$/wmt	5.9
Royalty Cost	Nauru Continuity Payment	US$/wmt	0.2
	Tonga Continuity Payment	US$/wmt	0.1
	LCR Royalty	US$/wmt	1.0
Capital Cost	Project Capital	US$ M	8,852.1
	Sustaining Capital	US$ M	5,318.0
	Closure Cost	US$ M	805.3
Financials	Total Revenue	US$ M	298,923
	Post-Tax NPV8	US$ M	18,081
	Post-Tax NPV0	US$ M	122,364
	Project IRR (Real Terms)	%	35.6%
	Project Payback – Production	Years	2
	EBITDA	US$ M	171,852
	EBITDA per tonne (dry nodules)	US$/wmt	349
	Project Capital	US$ M	8,852

A cashflow on an annualized basis is provided in Table 19.8.

Table 19.8 Project cash flow on an annualized basis

Macro Assumptions	Units	LOM Total/Avg.	PP Year 1 2032	PP Year 2 2033	PP Year 3 2034	PP Year 4 2035	PP Year 5 2036
Nickel Price (C1 LME)	US$/t	20,360.0	--	--	--	--	--
Cobalt Price (C1 LME)	US$/t	62,529.6	--	--	--	--	--
Copper Cathode Price (C1 LME)	US$/t	11,456.4	--	--	--	--	--
Manganese Price	US$/t	471.1	--	--	--	--	--
Manganese Price	US$/dmtu	4.7	--	--	--	--	--
Nickel Sulfate Price (100% contained Ni basis)	US$/t	21,835.0	--	--	--	--	--
Cobalt Sulfate Price (100% contained Co basis)	US$/t	62,529.6	--	--	--	--	--
Revenue	US$ M	298,923.1	--	--	--	--	--
Total Operating Costs	US$ M	(126,175.2)	--	--	--	--	--
Total Royalties	US$ M	(896.3)	--	--	--	--	--
EBITDA (non-GAAP[1])	US$ M	171,851.7	--	--	--	--	--
Depreciation	US$ M	(12,029.2)	--	(8.7)	(34.5)	(77.3)	(127.8)
EBIT	US$ M	159,822.5	--	(8.7)	(34.5)	(77.3)	(127.8)
Taxation	US$ M	(33,752.7)	--	--	--	--	--
Net Profit After Tax	US$ M	126,069.8	--	(8.7)	(34.5)	(77.3)	(127.8)
Free Cash Flow	US$ M	122,363.6	(221.3)	(663.9)	(1,106.5)	(1,327.8)	(1,438.5)
Project Capital	US$ M	(8,852.1)	(221.3)	(663.9)	(1,106.5)	(1,327.8)	(1,438.5)
Sustaining Capital	US$ M	(5,318.0)	--	--	--	--	--
Closure Capital	US$ M	(805.3)	--	--	--	--	--
Total Capital	US$ M	(14,975.3)	(221.3)	(663.9)	(1,106.5)	(1,327.8)	(1,438.5)
Production Summary							
Total Wet Ore Collected	Mwmtpa	670.0	--	--	--	--	--
TOML F wet Ore Collected	Mwmtpa	135.0	--	--	--	--	--
TOML A-E & NORI A-C wet Ore Collected	Mwmtpa	535.0	--	--	--	--	--
Life of Mine	Years	23.0	--	--	--	--	--
Physicals Nickel Products							
Resource Grade TOML F	%	1.4%	--	--	--	--	--
Resource Grade TOML A-E & NORI A-C	%	1.3%	--	--	--	--	--
Contained Metal in Recovered Nodules	Kt	6,354.2	--	--	--	--	--
Recovery Nodule to Matte	%	94.8%	--	--	--	--	--
Recovery Nodule to Sulfate	%	94.6%	--	--	--	--	--
Recovered Metal in Matte	Kt	302.9	--	--	--	--	--
Recovered Metal in Sulfate	Kt	5,759.8	--	--	--	--	--
Payable Factor for Matte	%	80.0%	--	--	--	--	--
Payable Factor for Sulfate	%	100.0%	--	--	--	--	--
Payable Metal in Matte	Kt	242.3	--	--	--	--	--

Macro Assumptions	Units	LOM Total/Avg.	PP Year 1 2032	PP Year 2 2033	PP Year 3 2034	PP Year 4 2035	PP Year 5 2036
Payable Metal in Sulfate	Kt	5,759.8	--	--	--	--	--
Nickel Products Total Revenue	US$ M	130,670.3	--	--	--	--	--
Physicals Cobalt							
Resource Grade TOML F	%	0.13%	--	--	--	--	--
Resource Grade TOML A-E & NORI A-C	%	0.22%	--	--	--	--	--
Contained Metal in Recovered Nodules	Kt	1,015.1	--	--	--	--	--
Recovery Nodule to Matte	%	77.5%	--	--	--	--	--
Recovery Nodule to Sulfate	%	77.2%	--	--	--	--	--
Recovered Metal in Matte	Kt	37.9	--	--	--	--	--
Recovered Metal in Sulfate	Kt	752.3	--	--	--	--	--
Payable Factor for Matte	%	60.0%	--	--	--	--	--
Payable Factor for Sulfate	%	100.0%	--	--	--	--	--
Payable Metal in Matte	Kt	22.7	--	--	--	--	--
Payable Metal in Sulfate	Kt	752.3	--	--	--	--	--
Cobalt Products Total Revenue	US$ M	48,456.4	--	--	--	--	--
Physicals Copper							
Resource Grade TOML F	%	1.25%	--	--	--	--	--
Resource Grade TOML A-E & NORI A-C	%	1.07%	--	--	--	--	--
Contained Metal in Recovered Nodules	Kt	5,431.7	--	--	--	--	--
Recovery Nodule to Matte	%	86.4%	--	--	--	--	--
Recovery Nodule to Sulfate	%	86.2%	--	--	--	--	--
Recovered Metal in Matte	Kt	237.3	--	--	--	--	--
Recovered Metal in Sulfate	Kt	4,485.2	--	--	--	--	--
Payable Factor for Matte	%	70.0%	--	--	--	--	--
Payable Factor for Sulfate	%	100.0%	--	--	--	--	--
Payable Metal in Matte	Kt	166.1	--	--	--	--	--
Payable Metal in Sulfate	Kt	4,485.2	--	--	--	--	--
Copper Products Total Revenue	US$ M	53,278.3	--	--	--	--	--
Physicals Manganese							
Resource Grade TOML F	%	32.2%	--	--	--	--	--
Resource Grade TOML A-E & NORI A-C	%	28.0%	--	--	--	--	--
Contained Metal in Recovered Nodules	Kt	141,788.7	--	--	--	--	--
Recovery Nodule to Manganese	%	98.9%	--	--	--	--	--
Recovered Metal in Manganese	Kt	140,229.0	--	--	--	--	--
Payable Factor for Manganese	%	100.0%	--	--	--	--	--
Payable Metal in Manganese	Kt	140,229.0	--	--	--	--	--
Manganese Products Total Revenue	US$ M	66,078.1	--	--	--	--	--

Macro Assumptions	Units	LOM Total/Avg.	PP Year 1 2032	PP Year 2 2033	PP Year 3 2034	PP Year 4 2035	PP Year 5 2036
Operating Costs							
Collection Costs	US$ M	(31,138.8)	--	--	--	--	--
Shipping Costs	US$ M	(6,066.3)	--	--	--	--	--
Contractor (offshore) Costs	US$ M	(3,583.9)	--	--	--	--	--
Consumables (offshore fuel) Costs	US$ M	(11,883.7)	--	--	--	--	--
Processing Cost	US$ M	(53,597.7)	--	--	--	--	--
Refining Cost	US$ M	(15,978.4)	--	--	--	--	--
Corporate Cost	US$ M	(3,926.4)	--	--	--	--	--
Royalty Costs							
Nauru Payment	US$ M	(136.9)	--	--	--	--	--
Tonga Payment	US$ M	(75.0)	--	--	--	--	--
LCR Royalty	US$ M	(684.4)	--	--	--	--	--

Notes: 1. Generally Accepted Accounting Principles

Macro Assumptions	Units	Year 1 2037	Year 2 2038	Year 3 2039	Year 4 2040	Year 5 2041
Nickel Price (C1 LME)	US$/t	20,360.0	20,360.0	20,360.0	20,360.0	20,360.0
Cobalt Price (C1 LME)	US$/t	62,529.6	62,529.6	62,529.6	62,529.6	62,529.6
Copper Cathode Price (C1 LME)	US$/t	11,456.4	11,456.4	11,456.4	11,456.4	11,456.4
Manganese Price	US$/t	523.1	496.5	470.0	470.0	470.0
Manganese Price	US$/dmtu	5.2	5.0	4.7	4.7	4.7
Nickel Sulfate Price (100% contained Ni basis)	US$/t	21,835.0	21,835.0	21,835.0	21,835.0	21,835.0
Cobalt Sulfate Price (100% contained Co basis)	US$/t	62,529.6	62,529.6	62,529.6	62,529.6	62,529.6
Revenue	US$ M	3,408.4	6,340.5	9,309.9	9,309.9	9,164.0
Total Operating Costs	US$ M	(1,426.8)	(2,544.8)	(3,778.3)	(3,778.3)	(3,753.8)
Total Royalties	US$ M	(0.1)	(1.1)	(2.1)	(4.1)	(8.1)
EBITDA (non-GAAP[1])	US$ M	1,981.6	3,794.6	5,529.5	5,527.5	5,402.1
Depreciation	US$ M	(181.7)	(221.5)	(243.2)	(242.8)	(238.0)
EBIT	US$ M	1,799.9	3,573.1	5,286.3	5,284.7	5,164.1
Taxation	US$ M	(327.6)	(750.6)	(1,110.6)	(1,110.7)	(1,086.2)
Net Profit After Tax	US$ M	1,472.3	2,822.5	4,175.7	4,174.1	4,077.9
Free Cash Flow	US$ M	104.5	1,981.4	3,905.3	4,393.0	4,314.0
Project Capital	US$ M	(1,106.5)	(663.9)	(110.7)	--	--
Sustaining Capital	US$ M	--	--	--	--	--
Closure Capital	US$ M	--	--	--	--	--
Total Capital	US$ M	(1,106.5)	(663.9)	(110.7)	--	--
Production Summary						
Total Wet Ore Collected	Mwmtpa	7.0	14.0	21.0	21.0	21.0
TOML F wet Ore Collected	Mwmtpa	7.0	14.0	21.0	21.0	21.0
TOML A-E & NORI A-C wet Ore Collected	Mwmtpa	--	--	--	--	--

Macro Assumptions	Units	Year 1 2037	Year 2 2038	Year 3 2039	Year 4 2040	Year 5 2041
Life of Mine	Years	1.0	1.0	1.0	1.0	1.0
Physicals Nickel Products						
Resource Grade TOML F	%	1.40%	1.40%	1.40%	1.40%	1.40%
Resource Grade TOML A-E & NORI A-C	%	--	--	--	--	--
Contained Metal in Recovered Nodules	Kt	70.4	140.7	211.1	211.1	211.1
Recovery Nodule to Matte	%	94.76%	94.76%	94.76%	94.76%	94.76%
Recovery Nodule to Sulfate	%	94.60%	94.60%	94.60%	94.60%	94.60%
Recovered Metal in Matte	Kt	--	4.8	14.3	14.3	28.6
Recovered Metal in Sulfate	Kt	71.6	128.3	185.4	185.4	171.1
Payable Factor for Matte	%	80.00%	80.00%	80.00%	80.00%	80.00%
Payable Factor for Sulfate	%	100.00%	100.00%	100.00%	100.00%	100.00%
Payable Metal in Matte	Kt	--	3.8	11.4	11.4	22.9
Payable Metal in Sulfate	Kt	71.6	128.3	185.4	185.4	171.1
Nickel Products Total Revenue	US$ M	1,557.0	2,880.2	4,280.9	4,280.9	4,202.2
Physicals Cobalt						
Resource Grade TOML F	%	0.13%	0.13%	0.13%	0.13%	0.13%
Resource Grade TOML A-E & NORI A-C	%	--	--	--	--	--
Contained Metal in Recovered Nodules	Kt	6.7	13.4	20.1	20.1	20.1
Recovery Nodule to Matte	%	77.54%	77.54%	77.54%	77.54%	77.54%
Recovery Nodule to Sulfate	%	77.20%	77.20%	77.20%	77.20%	77.20%
Recovered Metal in Matte	Kt	--	0.4	1.1	1.1	2.2
Recovered Metal in Sulfate	Kt	5.6	10.0	14.4	14.4	13.3
Payable Factor for Matte	%	60.00%	60.00%	60.00%	60.00%	60.00%
Payable Factor for Sulfate	%	100.00%	100.00%	100.00%	100.00%	100.00%
Payable Metal in Matte	Kt	--	0.2	0.7	0.7	1.3
Payable Metal in Sulfate	Kt	5.6	10.0	14.4	14.4	13.3
Cobalt Products Total Revenue	US$ M	347.2	638.9	944.6	944.6	917.0
Physicals Copper						
Resource Grade TOML F	%	1.25%	1.25%	1.25%	1.25%	1.25%
Resource Grade TOML A-E & NORI A-C	%	--	--	--	--	--
Contained Metal in Recovered Nodules	Kt	62.8	125.6	188.4	188.4	188.4
Recovery Nodule to Matte	%	86.43%	86.43%	86.43%	86.43%	86.43%
Recovery Nodule to Sulfate	%	86.20%	86.20%	86.20%	86.20%	86.20%
Recovered Metal in Matte	Kt	--	3.9	11.6	11.6	23.3
Recovered Metal in Sulfate	Kt	58.2	104.4	150.7	150.7	139.1
Payable Factor for Matte	%	70.00%	70.00%	70.00%	70.00%	70.00%
Payable Factor for Sulfate	%	100.00%	100.00%	100.00%	100.00%	100.00%
Payable Metal in Matte	Kt	--	2.7	8.1	8.1	16.3
Payable Metal in Sulfate	Kt	58.2	104.4	150.7	150.7	139.1

Macro Assumptions	Units	Year 1 2037	Year 2 2038	Year 3 2039	Year 4 2040	Year 5 2041
Copper Products Total Revenue	US$ M	664.4	1,226.9	1,820.6	1,820.6	1,781.0
Physicals Manganese						
Resource Grade TOML F	%	32.21%	32.21%	32.21%	32.21%	32.21%
Resource Grade TOML A-E & NORI A-C	%	--	--	--	--	--
Contained Metal in Recovered Nodules	Kt	1,623.4	3,246.8	4,870.2	4,870.2	4,870.2
Recovery Nodule to Manganese	%	98.90%	98.90%	98.90%	98.90%	98.90%
Recovered Metal in Manganese	Kt	1,605.6	3,211.1	4,816.7	4,816.7	4,816.7
Payable Factor for Manganese	%	100.00%	100.00%	100.00%	100.00%	100.00%
Payable Metal in Manganese	Kt	1,605.6	3,211.1	4,816.7	4,816.7	4,816.7
Manganese Products Total Revenue	US$ M	839.9	1,594.5	2,263.8	2,263.8	2,263.8
Operating Costs						
Collection Costs	US$ M	(309.8)	(619.6)	(929.4)	(929.4)	(929.4)
Shipping Costs	US$ M	(64.2)	(126.3)	(188.4)	(188.4)	(186.3)
Contractor (offshore) Costs	US$ M	(28.4)	(56.8)	(85.1)	(85.1)	(85.1)
Consumables (offshore fuel) Costs	US$ M	(107.3)	(214.6)	(321.9)	(321.9)	(321.9)
Processing Cost	US$ M	(560.0)	(1,120.0)	(1,680.0)	(1,680.0)	(1,680.0)
Refining Cost	US$ M	(276.7)	(300.0)	(438.8)	(438.8)	(416.4)
Corporate Cost	US$ M	(80.4)	(107.5)	(134.6)	(134.6)	(134.6)
Royalty Costs						
Nauru Payment	US$ M	--	--	--	--	--
Tonga Payment	US$ M	(0.1)	(1.1)	(2.1)	(4.1)	(8.1)
LCR Royalty	US$ M	--	--	--	--	--

Notes: 1. Generally Accepted Accounting Principles

Macro Assumptions	Units	Year 6 2042	Year 7 2043	Year 8 2044	Year 9 2045	Year 10 2046	Year 11 2047
Nickel Price (C1 LME)	US$/t	20,360.0	20,360.0	20,360.0	20,360.0	20,360.0	20,360.0
Cobalt Price (C1 LME)	US$/t	62,529.6	62,529.6	62,529.6	62,529.6	62,529.6	62,529.6
Copper Cathode Price (C1 LME)	US$/t	11,456.4	11,456.4	11,456.4	11,456.4	11,456.4	11,456.4
Manganese Price	US$/t	470.0	470.0	470.0	470.0	470.0	470.0
Manganese Price	US$/dmtu	4.7	4.7	4.7	4.7	4.7	4.7
Nickel Sulfate Price (100% contained Ni basis)	US$/t	21,835.0	21,835.0	21,835.0	21,835.0	21,835.0	21,835.0
Cobalt Sulfate Price (100% contained Co basis)	US$/t	62,529.6	62,529.6	62,529.6	62,529.6	62,529.6	62,529.6
Revenue	US$ M	9,309.9	9,309.9	8,550.4	10,785.8	13,403.5	15,988.2
Total Operating Costs	US$ M	(3,778.3)	(3,778.3)	(4,110.4)	(5,169.2)	(6,119.5)	(7,164.4)
Total Royalties	US$ M	(10.1)	(10.1)	(22.4)	(41.1)	(61.7)	(68.2)
EBITDA (non-GAAP[1])	US$ M	5,521.5	5,521.5	4,417.6	5,575.5	7,222.3	8,755.6
Depreciation	US$ M	(233.4)	(237.5)	(250.2)	(452.2)	(555.5)	(566.3)
EBIT	US$ M	5,288.2	5,284.1	4,167.5	5,123.3	6,666.8	8,189.3
Taxation	US$ M	(1,112.6)	(1,111.8)	(879.9)	(1,084.5)	(1,413.0)	(1,734.1)

Macro Assumptions	Units	Year 6 2042	Year 7 2043	Year 8 2044	Year 9 2045	Year 10 2046	Year 11 2047
Net Profit After Tax	US$ M	4,175.5	4,172.3	3,287.6	4,038.8	5,253.8	6,455.2
Free Cash Flow	US$ M	4,142.2	3,943.3	2,256.5	3,263.6	4,877.4	6,538.5
Project Capital	US$ M	(221.3)	(442.6)	(442.6)	(442.6)	(553.3)	(110.7)
Sustaining Capital	US$ M	--	--	(966.9)	(483.5)	--	--
Closure Capital	US$ M	--	--	--	--	--	--
Total Capital	US$ M	(221.3)	(442.6)	(1,409.5)	(926.1)	(553.3)	(110.7)
Production Summary-							
Total Wet Ore Collected	Mwmtpa	21.0	21.0	17.6	22.5	30.0	35.0
TOML F wet Ore Collected	Mwmtpa	21.0	21.0	9.0	--	--	--
TOML A-E & NORI A-C wet Ore Collected	Mwmtpa	--	--	8.6	22.5	30.0	35.0
Life of Mine	Years	1.0	1.0	1.0	1.0	1.0	1.0
Physicals Nickel Products							
Resource Grade TOML F	%	1.40%	1.40%	1.40%	--	--	--
Resource Grade TOML A-E & NORI A-C	%	--	--	1.27%	1.27%	1.27%	1.27%
Contained Metal in Recovered Nodules	Kt	211.1	211.1	170.5	210.2	280.2	327.0
Recovery Nodule to Matte	%	94.76%	94.76%	94.76%	94.76%	94.76%	94.76%
Recovery Nodule to Sulfate	%	94.60%	94.60%	94.60%	94.60%	94.60%	94.60%
Recovered Metal in Matte	Kt	14.3	14.3	--	--	--	--
Recovered Metal in Sulfate	Kt	185.4	185.4	179.8	217.8	265.1	318.4
Payable Factor for Matte	%	80.00%	80.00%	80.00%	80.00%	80.00%	80.00%
Payable Factor for Sulfate	%	100.00%	100.00%	100.00%	100.00%	100.00%	100.00%
Payable Metal in Matte	Kt	11.4	11.4	--	--	--	--
Payable Metal in Sulfate	Kt	185.4	185.4	179.8	217.8	265.1	318.4
Nickel Products Total Revenue	US$ M	4,280.9	4,280.9	3,908.9	4,744.9	5,788.7	6,946.5
Physicals Cobalt							
Resource Grade TOML F	%	0.13%	0.13%	0.13%	--	--	--
Resource Grade TOML A-E & NORI A-C	%	--	--	0.22%	0.22%	0.22%	0.22%
Contained Metal in Recovered Nodules	Kt	20.1	20.1	22.8	37.2	49.7	57.9
Recovery Nodule to Matte	%	77.54%	77.54%	77.54%	77.54%	77.54%	77.54%
Recovery Nodule to Sulfate	%	77.20%	77.20%	77.20%	77.20%	77.20%	77.20%
Recovered Metal in Matte	Kt	1.1	1.1	--	--	--	--
Recovered Metal in Sulfate	Kt	14.4	14.4	19.6	31.5	38.3	46.0
Payable Factor for Matte	%	60.00%	60.00%	60.00%	60.00%	60.00%	60.00%
Payable Factor for Sulfate	%	100.00%	100.00%	100.00%	100.00%	100.00%	100.00%
Payable Metal in Matte	Kt	0.7	0.7	--	--	--	--
Payable Metal in Sulfate	Kt	14.4	14.4	19.6	31.5	38.3	46.0
Cobalt Products Total Revenue	US$ M	944.6	944.6	1,222.6	1,965.1	2,397.5	2,877.0

Macro Assumptions	Units	Year 6 2042	Year 7 2043	Year 8 2044	Year 9 2045	Year 10 2046	Year 11 2047
Physicals Copper							
Resource Grade TOML F	%	1.25%	1.25%	1.25%	--	--	--
Resource Grade TOML A-E & NORI A-C	%	--	--	1.07%	1.07%	1.07%	1.07%
Contained Metal in Recovered Nodules	Kt	188.4	188.4	148.4	177.5	236.7	276.1
Recovery Nodule to Matte	%	86.43%	86.43%	86.43%	86.43%	86.43%	86.43%
Recovery Nodule to Sulfate	%	86.20%	86.20%	86.20%	86.20%	86.20%	86.20%
Recovered Metal in Matte	Kt	11.6	11.6	--	--	--	--
Recovered Metal in Sulfate	Kt	150.7	150.7	142.5	167.7	204.0	245.0
Payable Factor for Matte	%	70.00%	70.00%	70.00%	70.00%	70.00%	70.00%
Payable Factor for Sulfate	%	100.00%	100.00%	100.00%	100.00%	100.00%	100.00%
Payable Metal in Matte	Kt	8.1	8.1	--	--	--	--
Payable Metal in Sulfate	Kt	150.7	150.7	142.5	167.7	204.0	245.0
Copper Products Total Revenue	US$ M	1,820.6	1,820.6	1,625.9	1,916.0	2,337.5	2,805.0
Physicals Manganese							
Resource Grade TOML F	%	32.21%	32.21%	32.21%	--	--	--
Resource Grade TOML A-E & NORI A-C	%	--	--	27.97%	27.97%	27.97%	27.97%
Contained Metal in Recovered Nodules	Kt	4,870.2	4,870.2	3,857.4	4,646.6	6,195.5	7,228.0
Recovery Nodule to Manganese	%	98.90%	98.90%	98.90%	98.90%	98.90%	98.90%
Recovered Metal in Manganese	Kt	4,816.7	4,816.7	3,815.0	4,595.5	6,127.3	7,148.5
Payable Factor for Manganese	%	100.00%	100.00%	100.00%	100.00%	100.00%	100.00%
Payable Metal in Manganese	Kt	4,816.7	4,816.7	3,815.0	4,595.5	6,127.3	7,148.5
Manganese Products Total Revenue	US$ M	2,263.8	2,263.8	1,793.0	2,159.9	2,879.8	3,359.8
Operating Costs							
Collection Costs	US$ M	(929.4)	(929.4)	(1,101.8)	(1,480.3)	(1,858.7)	(1,996.1)
Shipping Costs	US$ M	(188.4)	(188.4)	(188.4)	(207.1)	(272.2)	(319.0)
Contractor (offshore) Costs	US$ M	(85.1)	(85.1)	(85.1)	(127.7)	(170.3)	(198.7)
Consumables (offshore fuel) Costs	US$ M	(321.9)	(321.9)	(321.9)	(411.6)	(548.8)	(640.3)
Processing Cost	US$ M	(1,680.0)	(1,680.0)	(1,405.7)	(1,800.0)	(2,400.0)	(2,800.0)
Refining Cost	US$ M	(438.8)	(438.8)	(884.3)	(997.6)	(694.0)	(1,014.6)
Corporate Cost	US$ M	(134.6)	(134.6)	(123.0)	(144.9)	(175.4)	(195.8)
Royalty Costs							
Nauru Payment	US$ M	--	--	--	--	(13.1)	(13.1)
Tonga Payment	US$ M	(10.1)	(10.1)	(10.1)	(10.1)	(10.1)	(9.1)
LCR Royalty	US$ M	--	--	(12.3)	(31.0)	(38.5)	(46.0)

Notes: 1. Generally Accepted Accounting Principles

Macro Assumptions	Units	Year 12 2048	Year 13 2049	Year 14 2050	Year 15 2051	Year 16 2052	Year 17 2053
Nickel Price (C1 LME)	US$/t	20,360.0	20,360.0	20,360.0	20,360.0	20,360.0	20,360.0
Cobalt Price (C1 LME)	US$/t	62,529.6	62,529.6	62,529.6	62,529.6	62,529.6	62,529.6
Copper Cathode Price (C1 LME)	US$/t	11,456.4	11,456.4	11,456.4	11,456.4	11,456.4	11,456.4
Manganese Price	US$/t	470.0	470.0	470.0	470.0	470.0	470.0
Manganese Price	US$/dmtu	4.7	4.7	4.7	4.7	4.7	4.7
Nickel Sulfate Price (100% contained Ni basis)	US$/t	21,835.0	21,835.0	21,835.0	21,835.0	21,835.0	21,835.0
Cobalt Sulfate Price (100% contained Co basis)	US$/t	62,529.6	62,529.6	62,529.6	62,529.6	62,529.6	62,529.6
Revenue	US$ M	17,456.2	17,456.2	16,598.7	16,598.7	16,598.7	16,598.7
Total Operating Costs	US$ M	(7,698.5)	(7,526.0)	(7,168.1)	(7,168.1)	(7,168.1)	(7,168.1)
Total Royalties	US$ M	(63.3)	(63.3)	(60.8)	(60.8)	(60.8)	(60.8)
EBITDA (non-GAAP[1])	US$ M	9,694.5	9,866.9	9,369.8	9,369.8	9,369.8	9,369.8
Depreciation	US$ M	(559.5)	(548.6)	(366.1)	(367.9)	(455.4)	(541.3)
EBIT	US$ M	9,134.9	9,318.4	9,003.7	9,001.9	8,914.3	8,828.5
Taxation	US$ M	(1,931.6)	(1,970.1)	(1,903.6)	(1,903.2)	(1,884.8)	(1,866.8)
Net Profit After Tax	US$ M	7,203.3	7,348.2	7,100.1	7,098.7	7,029.6	6,961.7
Free Cash Flow	US$ M	7,525.4	7,838.7	7,050.2	6,941.2	6,959.6	6,977.6
Project Capital	US$ M	--	--	--	--	--	--
Sustaining Capital	US$ M	--	--	(483.5)	(483.5)	(483.5)	(483.5)
Closure Capital	US$ M	--	--	--	--	--	--
Total Capital	US$ M	--	--	(483.5)	(483.5)	(483.5)	(483.5)
Production Summary							
Total Wet Ore Collected	Mwmtpa	40.0	40.0	37.5	37.5	37.5	37.5
TOML F wet Ore Collected	Mwmtpa	--	--	--	--	--	--
TOML A-E & NORI A-C wet Ore Collected	Mwmtpa	40.0	40.0	37.5	37.5	37.5	37.5
Life of Mine	Years	1.0	1.0	1.0	1.0	1.0	1.0
Physicals Nickel Products							
Resource Grade TOML F	%	--	--	--	--	--	--
Resource Grade TOML A-E & NORI A-C	%	1.27%	1.27%	1.27%	1.27%	1.27%	1.27%
Contained Metal in Recovered Nodules	Kt	373.7	373.7	350.3	350.3	350.3	350.3
Recovery Nodule to Matte	%	94.76%	94.76%	94.76%	94.76%	94.76%	94.76%
Recovery Nodule to Sulfate	%	94.60%	94.60%	94.60%	94.60%	94.60%	94.60%
Recovered Metal in Matte	Kt	35.4	35.4	13.3	13.3	13.3	13.3
Recovered Metal in Sulfate	Kt	318.1	318.1	318.1	318.1	318.1	318.1
Payable Factor for Matte	%	80.00%	80.00%	80.00%	80.00%	80.00%	80.00%
Payable Factor for Sulfate	%	100.00%	100.00%	100.00%	100.00%	100.00%	100.00%
Payable Metal in Matte	Kt	28.3	28.3	10.6	10.6	10.6	10.6
Payable Metal in Sulfate	Kt	318.1	318.1	318.1	318.1	318.1	318.1
Nickel Products Total Revenue	US$ M	7,523.2	7,523.2	7,162.7	7,162.7	7,162.7	7,162.7

Macro Assumptions	Units	Year 12 2048	Year 13 2049	Year 14 2050	Year 15 2051	Year 16 2052	Year 17 2053
Physicals Cobalt							
Resource Grade TOML F	%	--	--	--	--	--	--
Resource Grade TOML A-E & NORI A-C	%	0.22%	0.22%	0.22%	0.22%	0.22%	0.22%
Contained Metal in Recovered Nodules	Kt	66.2	66.2	62.1	62.1	62.1	62.1
Recovery Nodule to Matte	%	77.54%	77.54%	77.54%	77.54%	77.54%	77.54%
Recovery Nodule to Sulfate	%	77.20%	77.20%	77.20%	77.20%	77.20%	77.20%
Recovered Metal in Matte	Kt	5.1	5.1	1.9	1.9	1.9	1.9
Recovered Metal in Sulfate	Kt	46.0	46.0	46.0	46.0	46.0	46.0
Payable Factor for Matte	%	60.00%	60.00%	60.00%	60.00%	60.00%	60.00%
Payable Factor for Sulfate	%	100.00%	100.00%	100.00%	100.00%	100.00%	100.00%
Payable Metal in Matte	Kt	3.1	3.1	1.2	1.2	1.2	1.2
Payable Metal in Sulfate	Kt	46.0	46.0	46.0	46.0	46.0	46.0
Cobalt Products Total Revenue	US$ M	3,069.6	3,069.6	2,949.2	2,949.2	2,949.2	2,949.2
Physicals Copper							
Resource Grade TOML F	%	--	--	--	--	--	--
Resource Grade TOML A-E & NORI A-C	%	1.07%	1.07%	1.07%	1.07%	1.07%	1.07%
Contained Metal in Recovered Nodules	Kt	315.6	315.6	295.9	295.9	295.9	295.9
Recovery Nodule to Matte	%	86.43%	86.43%	86.43%	86.43%	86.43%	86.43%
Recovery Nodule to Sulfate	%	86.20%	86.20%	86.20%	86.20%	86.20%	86.20%
Recovered Metal in Matte	Kt	27.3	27.3	10.2	10.2	10.2	10.2
Recovered Metal in Sulfate	Kt	244.8	244.8	244.8	244.8	244.8	244.8
Payable Factor for Matte	%	70.00%	70.00%	70.00%	70.00%	70.00%	70.00%
Payable Factor for Sulfate	%	100.00%	100.00%	100.00%	100.00%	100.00%	100.00%
Payable Metal in Matte	Kt	19.1	19.1	7.2	7.2	7.2	7.2
Payable Metal in Sulfate	Kt	244.8	244.8	244.8	244.8	244.8	244.8
Copper Products Total Revenue	US$ M	3,023.7	3,023.7	2,887.0	2,887.0	2,887.0	2,887.0
Physicals Manganese							
Resource Grade TOML F	%	--	--	--	--	--	--
Resource Grade TOML A-E & NORI A-C	%	27.97%	27.97%	27.97%	27.97%	27.97%	27.97%
Contained Metal in Recovered Nodules	Kt	8,260.6	8,260.6	7,744.3	7,744.3	7,744.3	7,744.3
Recovery Nodule to Manganese	%	98.90%	98.90%	98.90%	98.90%	98.90%	98.90%
Recovered Metal in Manganese	Kt	8,169.8	8,169.8	7,659.2	7,659.2	7,659.2	7,659.2
Payable Factor for Manganese	%	100.00%	100.00%	100.00%	100.00%	100.00%	100.00%
Payable Metal in Manganese	Kt	8,169.8	8,169.8	7,659.2	7,659.2	7,659.2	7,659.2
Manganese Products Total Revenue	US$ M	3,839.8	3,839.8	3,599.8	3,599.8	3,599.8	3,599.8
Operating Cost							
Collection Costs	US$ M	(2,133.4)	(1,960.9)	(1,892.3)	(1,892.3)	(1,892.3)	(1,892.3)
Shipping Costs	US$ M	(357.3)	(357.3)	(338.2)	(338.2)	(338.2)	(338.2)

Macro Assumptions	Units	Year 12 2048	Year 13 2049	Year 14 2050	Year 15 2051	Year 16 2052	Year 17 2053
Contractor (offshore) Costs	US$ M	(227.0)	(227.0)	(212.9)	(212.9)	(212.9)	(212.9)
Consumables (offshore fuel) Costs	US$ M	(731.8)	(731.8)	(686.0)	(686.0)	(686.0)	(686.0)
Processing Cost	US$ M	(3,200.0)	(3,200.0)	(3,000.0)	(3,000.0)	(3,000.0)	(3,000.0)
Refining Cost	US$ M	(832.8)	(832.8)	(832.8)	(832.8)	(832.8)	(832.8)
Corporate Cost	US$ M	(216.1)	(216.1)	(206.0)	(206.0)	(206.0)	(206.0)
Royalty Costs							
Nauru Payment	US$ M	(13.1)	(13.1)	(13.1)	(13.1)	(13.1)	(13.1)
Tonga Payment	US$ M	--	--	--	--	--	--
LCR Royalty	US$ M	(50.2)	(50.2)	(47.7)	(47.7)	(47.7)	(47.7)

Notes: 1. Generally Accepted Accounting Principles

Macro Assumptions	Units	Year 18 2054	Year 19 2055	Year 20 2056	Year 21 2057	Year 22 2058	Year 23 2059
Nickel Price (C1 LME)	US$/t	20,360.0	20,360.0	20,360.0	20,360.0	20,360.0	20,360.0
Cobalt Price (C1 LME)	US$/t	62,529.6	62,529.6	62,529.6	62,529.6	62,529.6	62,529.6
Copper Cathode Price (C1 LME)	US$/t	11,456.4	11,456.4	11,456.4	11,456.4	11,456.4	11,456.4
Manganese Price	US$/t	470.0	470.0	470.0	470.0	470.0	470.0
Manganese Price	US$/dmtu	4.7	4.7	4.7	4.7	4.7	4.7
Nickel Sulfate Price (100% contained Ni basis)	US$/t	21,835.0	21,835.0	21,835.0	21,835.0	21,835.0	21,835.0
Cobalt Sulfate Price (100% contained Co basis)	US$/t	62,529.6	62,529.6	62,529.6	62,529.6	62,529.6	62,529.6
Revenue	US$ M	16,598.7	16,598.7	16,598.7	16,598.7	17,456.2	8,444.2
Total Operating Costs	US$ M	(6,995.6)	(6,823.2)	(6,650.7)	(6,478.3)	(6,663.8)	(3,264.9)
Total Royalties	US$ M	(60.8)	(60.8)	(53.3)	(47.7)	(50.2)	(24.3)
EBITDA (non-GAAP[1])	US$ M	9,542.2	9,714.7	9,894.6	10,072.7	10,742.3	5,155.0
Depreciation	US$ M	(625.5)	(708.0)	(703.1)	(698.2)	(688.2)	(2,096.6)
EBIT	US$ M	8,916.7	9,006.7	9,191.6	9,374.5	10,054.1	3,058.4
Taxation	US$ M	(1,885.3)	(1,904.2)	(1,941.4)	(1,978.7)	(2,121.9)	(647.4)
Net Profit After Tax	US$ M	7,031.5	7,102.5	7,250.1	7,395.8	7,932.2	2,411.0
Free Cash Flow	US$ M	7,117.4	7,270.7	7,413.1	7,553.6	8,451.6	5,664.2
Project Capital							
Sustaining Capital	US$ M	(483.5)	(483.5)	(483.5)	(483.5)	--	--
Closure Capital	US$ M	--	--	--	--	--	--
Total Capital	US$ M	(483.5)	(483.5)	(483.5)	(483.5)	--	--
Production Summary		--	--	--	--	--	--
Total Wet Ore Collected	Mwmtpa	37.5	37.5	37.5	37.5	40.0	18.9
TOML F wet Ore Collected	Mwmtpa	--	--	--	--	--	--
TOML A-E & NORI A-C wet Ore Collected	Mwmtpa	37.5	37.5	37.5	37.5	40.0	18.9
Life of Mine	Years	1.0	1.0	1.0	1.0	1.0	1.0
Physicals Nickel Products							
Resource Grade TOML F	%	--	--	--	--	--	--

Macro Assumptions	Units	Year 18 2054	Year 19 2055	Year 20 2056	Year 21 2057	Year 22 2058	Year 23 2059
Resource Grade TOML A-E & NORI A-C	%	1.27%	1.27%	1.27%	1.27%	1.27%	1.27%
Contained Metal in Recovered Nodules	Kt	350.3	350.3	350.3	350.3	373.7	176.6
Recovery Nodule to Matte	%	94.76%	94.76%	94.76%	94.76%	94.76%	94.76%
Recovery Nodule to Sulfate	%	94.60%	94.60%	94.60%	94.60%	94.60%	94.60%
Recovered Metal in Matte	Kt	13.3	13.3	13.3	13.3	35.4	--
Recovered Metal in Sulfate	Kt	318.1	318.1	318.1	318.1	318.1	167.0
Payable Factor for Matte	%	80.00%	80.00%	80.00%	80.00%	80.00%	80.00%
Payable Factor for Sulfate	%	100.00%	100.00%	100.00%	100.00%	100.00%	100.00%
Payable Metal in Matte	Kt	10.6	10.6	10.6	10.6	28.3	--
Payable Metal in Sulfate	Kt	318.1	318.1	318.1	318.1	318.1	167.0
Nickel Products Total Revenue	US$ M	7,162.7	7,162.7	7,162.7	7,162.7	7,523.2	3,646.9
Physicals Cobalt							
Resource Grade TOML F	%	--	--	--	--	--	--
Resource Grade TOML A-E & NORI A-C	%	0.22%	0.22%	0.22%	0.22%	0.22%	0.22%
Contained Metal in Recovered Nodules	Kt	62.1	62.1	62.1	62.1	66.2	31.3
Recovery Nodule to Matte	%	77.54%	77.54%	77.54%	77.54%	77.54%	77.54%
Recovery Nodule to Sulfate	%	77.20%	77.20%	77.20%	77.20%	77.20%	77.20%
Recovered Metal in Matte	Kt	1.9	1.9	1.9	1.9	5.1	--
Recovered Metal in Sulfate	Kt	46.0	46.0	46.0	46.0	46.0	24.2
Payable Factor for Matte	%	60.00%	60.00%	60.00%	60.00%	60.00%	60.00%
Payable Factor for Sulfate	%	100.00%	100.00%	100.00%	100.00%	100.00%	100.00%
Payable Metal in Matte	Kt	1.2	1.2	1.2	1.2	3.1	--
Payable Metal in Sulfate	Kt	46.0	46.0	46.0	46.0	46.0	24.2
Cobalt Products Total Revenue	US$ M	2,949.2	2,949.2	2,949.2	2,949.2	3,069.6	1,510.4
Physicals Copper							
Resource Grade TOML F	%	--	--	--	--	--	--
Resource Grade TOML A-E & NORI A-C	%	1.07%	1.07%	1.07%	1.07%	1.07%	1.07%
Contained Metal in Recovered Nodules	Kt	295.9	295.9	295.9	295.9	315.6	149.1
Recovery Nodule to Matte	%	86.43%	86.43%	86.43%	86.43%	86.43%	86.43%
Recovery Nodule to Sulfate	%	86.20%	86.20%	86.20%	86.20%	86.20%	86.20%
Recovered Metal in Matte	Kt	10.2	10.2	10.2	10.2	27.3	--
Recovered Metal in Sulfate	Kt	244.8	244.8	244.8	244.8	244.8	128.5
Payable Factor for Matte	%	70.00%	70.00%	70.00%	70.00%	70.00%	70.00%
Payable Factor for Sulfate	%	100.00%	100.00%	100.00%	100.00%	100.00%	100.00%
Payable Metal in Matte	Kt	7.2	7.2	7.2	7.2	19.1	--
Payable Metal in Sulfate	Kt	244.8	244.8	244.8	244.8	244.8	128.5
Copper Products Total Revenue	US$ M	2,887.0	2,887.0	2,887.0	2,887.0	3,023.7	1,472.6
Physicals Manganese							
Resource Grade TOML F	%	--	--	--	--	--	--

Macro Assumptions	Units	Year 18 2054	Year 19 2055	Year 20 2056	Year 21 2057	Year 22 2058	Year 23 2059
Resource Grade TOML A-E & NORI A-C	%	27.97%	27.97%	27.97%	27.97%	27.97%	27.97%
Contained Metal in Recovered Nodules	Kt	7,744.3	7,744.3	7,744.3	7,744.3	8,260.6	3,903.1
Recovery Nodule to Manganese	%	98.90%	98.90%	98.90%	98.90%	98.90%	98.90%
Recovered Metal in Manganese	Kt	7,659.2	7,659.2	7,659.2	7,659.2	8,169.8	3,860.2
Payable Factor for Manganese	%	100.00%	100.00%	100.00%	100.00%	100.00%	100.00%
Payable Metal in Manganese	Kt	7,659.2	7,659.2	7,659.2	7,659.2	8,169.8	3,860.2
Manganese Products Total Revenue	US$ M	3,599.8	3,599.8	3,599.8	3,599.8	3,839.8	1,814.3
Operating Costs							
Collection Costs	US$ M	(1,719.8)	(1,547.4)	(1,374.9)	(1,202.5)	(1,098.7)	(519.1)
Shipping Costs	US$ M	(338.2)	(338.2)	(338.2)	(338.2)	(357.3)	(171.5)
Contractor (offshore) Costs	US$ M	(212.9)	(212.9)	(212.9)	(212.9)	(227.0)	(107.3)
Consumables (offshore fuel) Costs	US$ M	(686.0)	(686.0)	(686.0)	(686.0)	(731.8)	(345.8)
Processing Cost	US$ M	(3,000.0)	(3,000.0)	(3,000.0)	(3,000.0)	(3,200.0)	(1,512.0)
Refining Cost	US$ M	(832.8)	(832.8)	(832.8)	(832.8)	(832.8)	(479.0)
Corporate Cost	US$ M	(206.0)	(206.0)	(206.0)	(206.0)	(216.1)	(130.2)
Royalty Costs							
Nauru Payment	US$ M	(13.1)	(13.1)	(5.6)	--	--	--
Tonga Payment	US$ M	--	--	--	--	--	--
LCR Royalty	US$ M	(47.7)	(47.7)	(47.7)	(47.7)	(50.2)	(24.3)

Notes: 1. Generally Accepted Accounting Principles

Macro Assumptions	Units	Year 24 2060	Year 25 2061	Year 26 2062	Year 27 2063	Year 28 2064	Year 29 2065
Nickel Price (C1 LME)	US$/t	--	--	--	--	--	--
Cobalt Price (C1 LME)	US$/t	--	--	--	--	--	--
Copper Cathode Price (C1 LME)	US$/t	--	--	--	--	--	--
Manganese Price	US$/t	--	--	--	--	--	--
Manganese Price	US$/dmtu	--	--	--	--	--	--
Nickel Sulfate Price (100% contained Ni basis)	US$/t	--	--	--	--	--	--
Cobalt Sulfate Price (100% contained Co basis)	US$/t	--	--	--	--	--	--
Revenue	US$ M	440.0	--	--	--	--	--
Total Operating Costs	US$ M	--	--	--	--	--	--
Total Royalties	US$ M	--	--	--	--	--	--
EBITDA (non-GAAP[1])	US$ M	440.0	--	--	--	--	--
Depreciation	US$ M	--	--	--	--	--	--
EBIT	US$ M	440.0	--	--	--	--	--
Taxation	US$ M	(92.4)	--	--	--	--	--
Net Profit After Tax	US$ M	347.6	--	--	--	--	--
Free Cash Flow	US$ M	1,223.5	(78.6)	(149.5)	(149.5)	(149.5)	(11.5)

Macro Assumptions	Units	Year 24 2060	Year 25 2061	Year 26 2062	Year 27 2063	Year 28 2064	Year 29 2065
Project Capital							
Sustaining Capital	US$ M	--	--	--	--	--	--
Closure Capital	US$ M	(149.5)	(149.5)	(149.5)	(149.5)	(149.5)	(11.5)
Total Capital	US$ M	(149.5)	(149.5)	(149.5)	(149.5)	(149.5)	(11.5)
Production Summary		--	--	--	--	--	--
Total Wet Ore Collected	Mwmtpa	--	--	--	--	--	--
TOML F wet Ore Collected	Mwmtpa	--	--	--	--	--	--
TOML A-E & NORI A-C wet Ore Collected	Mwmtpa	--	--	--	--	--	--
Life of Mine	Years	--	--	--	--	--	--
Physicals Nickel Products							
Resource Grade TOML F	%	--	--	--	--	--	--
Resource Grade TOML A-E & NORI A-C	%	--	--	--	--	--	--
Contained Metal in Recovered Nodules	Kt	--	--	--	--	--	--
Recovery Nodule to Matte	%	--	--	--	--	--	--
Recovery Nodule to Sulfate	%	--	--	--	--	--	--
Recovered Metal in Matte	Kt	--	--	--	--	--	--
Recovered Metal in Sulfate	Kt	--	--	--	--	--	--
Payable Factor for Matte	%	--	--	--	--	--	--
Payable Factor for Sulfate	%	--	--	--	--	--	--
Payable Metal in Matte	Kt	--	--	--	--	--	--
Payable Metal in Sulfate	Kt	--	--	--	--	--	--
Nickel Products Total Revenue	US$ M	--	--	--	--	--	--
Physicals Cobalt							
Resource Grade TOML F	%	--	--	--	--	--	--
Resource Grade TOML A-E & NORI A-C	%	--	--	--	--	--	--
Contained Metal in Recovered Nodules	Kt	--	--	--	--	--	--
Recovery Nodule to Matte	%	--	--	--	--	--	--
Recovery Nodule to Sulfate	%	--	--	--	--	--	--
Recovered Metal in Matte	Kt	--	--	--	--	--	--
Recovered Metal in Sulfate	Kt	--	--	--	--	--	--
Payable Factor for Matte	%	--	--	--	--	--	--
Payable Factor for Sulfate	%	--	--	--	--	--	--
Payable Metal in Matte	Kt	--	--	--	--	--	--
Payable Metal in Sulfate	Kt	--	--	--	--	--	--
Cobalt Products Total Revenue	US$ M	--	--	--	--	--	--
Physicals Copper							
Resource Grade TOML F	%	--	--	--	--	--	--
Resource Grade TOML A-E & NORI A-C	%	--	--	--	--	--	--

Macro Assumptions	Units	Year 24 2060	Year 25 2061	Year 26 2062	Year 27 2063	Year 28 2064	Year 29 2065
Contained Metal in Recovered Nodules	Kt	--	--	--	--	--	--
Recovery Nodule to Matte	%	--	--	--	--	--	--
Recovery Nodule to Sulfate	%	--	--	--	--	--	--
Recovered Metal in Matte	Kt	--	--	--	--	--	--
Recovered Metal in Sulfate	Kt	--	--	--	--	--	--
Payable Factor for Matte	%	--	--	--	--	--	--
Payable Factor for Sulfate	%	--	--	--	--	--	--
Payable Metal in Matte	Kt	--	--	--	--	--	--
Payable Metal in Sulfate	Kt	--	--	--	--	--	--
Copper Products Total Revenue	US$ M	--	--	--	--	--	--
Physicals Manganese							
Resource Grade TOML F	%	--	--	--	--	--	--
Resource Grade TOML A-E & NORI A-C	%	--	--	--	--	--	--
Contained Metal in Recovered Nodules	Kt	--	--	--	--	--	--
Recovery Nodule to Manganese	%	--	--	--	--	--	--
Recovered Metal in Manganese	Kt	--	--	--	--	--	--
Payable Factor for Manganese	%	--	--	--	--	--	--
Payable Metal in Manganese	Kt	--	--	--	--	--	--
Manganese Products Total Revenue	US$ M	--	--	--	--	--	--
Operating Costs							
Collection Costs	US$ M	--	--	--	--	--	--
Shipping Costs	US$ M	--	--	--	--	--	--
Contractor (offshore) Costs	US$ M	--	--	--	--	--	--
Consumables (offshore fuel) Costs	US$ M	--	--	--	--	--	--
Processing Cost	US$ M	--	--	--	--	--	--
Refining Cost	US$ M	--	--	--	--	--	--
Corporate Cost	US$ M	--	--	--	--	--	--
Royalty Costs							
Nauru Payment	US$ M	--	--	--	--	--	--
Tonga Payment	US$ M	--	--	--	--	--	--
LCR Royalty	US$ M	--	--	--	--	--	--

Notes: 1. Generally Accepted Accounting Principles

Macro Assumptions	Units	Year 30 2066	Year 31 2067	Year 32 2068	Year 33 2069
Nickel Price (C1 LME)	US$/t	--	--	--	--
Cobalt Price (C1 LME)	US$/t	--	--	--	--
Copper Cathode Price (C1 LME)	US$/t	--	--	--	--
Manganese Price	US$/t	--	--	--	--
Manganese Price	US$/dmtu	--	--	--	--

Macro Assumptions	Units	Year 30 2066	Year 31 2067	Year 32 2068	Year 33 2069
Nickel Sulfate Price (100% contained Ni basis)	US$/t	--	--	--	--
Cobalt Sulfate Price (100% contained Co basis)	US$/t	--	--	--	--
Revenue	US$ M	--	--	--	--
Total Operating Costs	US$ M	--	--	--	--
Total Royalties	US$ M	--	--	--	--
EBITDA (non-GAAP[1])	US$ M	--	--	--	--
Depreciation	US$ M	--	--	--	--
EBIT	US$ M	--	--	--	--
Taxation	US$ M	--	--	--	--
Net Profit After Tax	US$ M	--	--	--	--
Free Cash Flow	US$ M	(11.5)	(11.5)	(11.5)	(11.5)
Project Capital	US$ M	--	--	--	--
Sustaining Capital	US$ M	--	--	--	--
Closure Capital	US$ M	(11.5)	(11.5)	(11.5)	(11.5)
Total Capital	US$ M	(11.5)	(11.5)	(11.5)	(11.5)
Production Summary					
Total Wet Ore Collected	Mwmtpa	--	--	--	--
TOML F wet Ore Collected	Mwmtpa	--	--	--	--
TOML A-E & NORI A-C wet Ore Collected	Mwmtpa	--	--	--	--
Life of Mine	Years	--	--	--	--
Physicals Nickel Products					
Resource Grade TOML F	%	--	--	--	--
Resource Grade TOML A-E & NORI A-C	%	--	--	--	--
Contained Metal in Recovered Nodules	Kt	--	--	--	--
Recovery Nodule to Matte	%	--	--	--	--
Recovery Nodule to Sulfate	%	--	--	--	--
Recovered Metal in Matte	Kt	--	--	--	--
Recovered Metal in Sulfate	Kt	--	--	--	--
Payable Factor for Matte	%	--	--	--	--
Payable Factor for Sulfate	%	--	--	--	--
Payable Metal in Matte	Kt	--	--	--	--
Payable Metal in Sulfate	Kt	--	--	--	--
Nickel Products Total Revenue	US$ M	--	--	--	--
Physicals Cobalt					
Resource Grade TOML F	%	--	--	--	--
Resource Grade TOML A-E & NORI A-C	%	--	--	--	--
Contained Metal in Recovered Nodules	Kt	--	--	--	--
Recovery Nodule to Matte	%	--	--	--	--
Recovery Nodule to Sulfate	%	--	--	--	--
Recovered Metal in Matte	Kt	--	--	--	--
Recovered Metal in Sulfate	Kt	--	--	--	--

Macro Assumptions	Units	Year 30 2066	Year 31 2067	Year 32 2068	Year 33 2069
Payable Factor for Matte	%	--	--	--	--
Payable Factor for Sulfate	%	--	--	--	--
Payable Metal in Matte	Kt	--	--	--	--
Payable Metal in Sulfate	Kt	--	--	--	--
Cobalt Products Total Revenue	US$ M	--	--	--	--
Physicals Copper					
Resource Grade TOML F	%	--	--	--	--
Resource Grade TOML A-E & NORI A-C	%	--	--	--	--
Contained Metal in Recovered Nodules	Kt	--	--	--	--
Recovery Nodule to Matte	%	--	--	--	--
Recovery Nodule to Sulfate	%	--	--	--	--
Recovered Metal in Matte	Kt	--	--	--	--
Recovered Metal in Sulfate	Kt	--	--	--	--
Payable Factor for Matte	%	--	--	--	--
Payable Factor for Sulfate	%	--	--	--	--
Payable Metal in Matte	Kt	--	--	--	--
Payable Metal in Sulfate	Kt	--	--	--	--
Copper Products Total Revenue	US$ M	--	--	--	--
Physicals Manganese					
Resource Grade TOML F	%	--	--	--	--
Resource Grade TOML A-E & NORI A-C	%	--	--	--	--
Contained Metal in Recovered Nodules	Kt	--	--	--	--
Recovery Nodule to Manganese	%	--	--	--	--
Recovered Metal in Manganese	Kt	--	--	--	--
Payable Factor for Manganese	%	--	--	--	--
Payable Metal in Manganese	Kt	--	--	--	--
Manganese Products Total Revenue	US$ M	--	--	--	--
Operating Costs					
Collection Costs	US$ M	--	--	--	--
Shipping Costs	US$ M	--	--	--	--
Contractor (offshore) Costs	US$ M	--	--	--	--
Consumables (offshore fuel) Costs	US$ M	--	--	--	--
Processing Cost	US$ M	--	--	--	--
Refining Cost	US$ M	--	--	--	--
Corporate Cost	US$ M	--	--	--	--
Royalty Costs					
Nauru Payment	US$ M	--	--	--	--
Tonga Payment	US$ M	--	--	--	--
LCR Royalty	US$ M	--	--	--	--

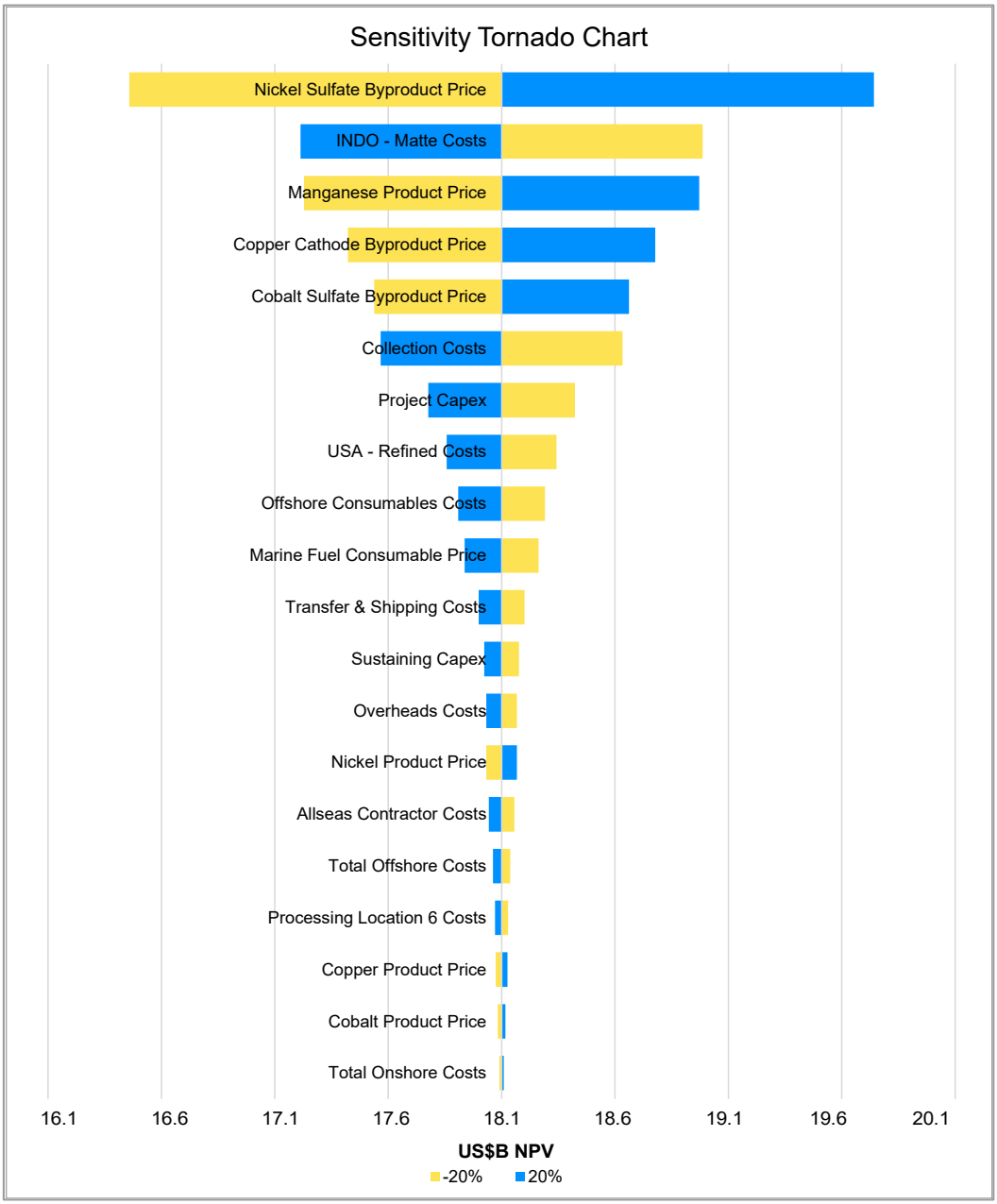
Notes: 1. Generally Accepted Accounting Principles

19.14 Sensitivity analysis

To examine the impact of changes in base case assumptions, sensitivity analysis has been performed. The analysis performed allows identification of the critical components of the economic model, to determine which variables have little impact on outcomes and which have significant. To graphically display the relative impact and ranking of each variable on the post-tax NPV (base case NPV); the results have been displayed as a Tornado chart

Figure 19.2 presents a tornado chart which compares the range of each variable and calculates the NPV at each point. For each line item flexed between -20 percent and +20 percent, the length of the bar indicates the change to the NPV with the color of the bar indicating the direction of the relationship between the variable and the NPV movement. Upper variables (and longest bar) have the most effect and the lower the least effect to NPV.

Figure 19.2 Tornado Graph



Source: TMC

19.15 Cash cost analysis

TMC has selected nickel as the primary commodity for the Project and so unit costs are presented in terms of C1 Nickel Cash Cost. C1 Cash Costs are calculated as the total direct costs associated with mining, processing, G&A, and marketing costs. C1 Cash Cost is not a measure recognized by GAAP but is a standard measure used in mining as a reference point to denote the basic cash costs of running a mining operation to allow a comparison across the industry which may then be plotted on a global cost curve.

The cost curve is divided into four quartiles, with the lowest operating cost mines falling within the first quartile. In general, achieving a first quartile C1 cash cost means that the operation is expected to be resilient to all stages of the price cycles and remain profitable during these price cycles. The cost is typically expressed as US$/t nickel or US cents/lb nickel and is presented both exclusive and inclusive of by-product credits for other elements contained within the nodules (copper, cobalt, manganese). Table 19.9 presents the C1 Nickel Cash Cost (US$/t Ni) through the life of mine.

The NORI and TOML areas Cash Cost including by-product credits equals US$(6,939)/t nickel.

Table 19.9 C1 Nickel cash cost

Item	Units	Value
Collection Costs	US$'M	31,139
Shipping Costs	US$'M	6,066
Contractor (offshore) Costs	US$'M	3,584
Consumables (offshore fuel) Costs	US$'M	11,884
Processing Cost	US$'M	53,598
Refining Cost	US$'M	15,978
Corporate Cost	US$'M	3,926
Total Operating Costs	US$'M	126,175
Total Nickel Production	kt	6,001
C1 Cash Cost excl. Byproducts credits	US$/mt Ni	21,026
Byproduct credits	US$/mt Ni	(27,965)
Period C1 Cash Cost incl. Byproducts credits	US$/mt Ni	(6,939)

Table 19.10 presents the all-in sustaining cost (AISC) in US$/t Ni through the LOM. The AISC is calculated using the same costs as the C1 Cash Cost, plus royalties and sustaining capital. This figure represents the realistic minimum revenue per unit of production that is required to continue operating the business and as such is a proxy for the operational break-even nickel price, subject to the pricing of by-products.

The NORI and TOML area all-in sustaining cost (AISC) including by-product credits equals US$(5,903)/t nickel.

Table 19.10 All-in Sustaining Cost

Item	Units	Value
Collection Costs	US$'M	31,139
Shipping Costs	US$'M	6,066
Contractor (offshore) Costs	US$'M	3,584
Consumables (offshore fuel) Costs	US$'M	11,884
Processing Cost	US$'M	53,598
Refining Cost	US$'M	15,978
Corporate Cost	US$'M	3,926
Total Operating Costs	US$'M	126,175
Total Royalties	US$'M	896
Sustaining Capital	US$'M	5,318
Total All-in Sustaining Cost	US$'M	132,389
Total Nickel Production	kt	6,001
AISC excl. Byproducts credits	US$/t Ni	22,062
Byproduct credits	US$/t Ni	(27,965)
AISC incl. Byproducts credits	US$/t Ni	(5,903)

19.16 Conclusion economic analysis

Based on the assumptions and parameters presented, the economic analysis shows positive economics supported by a post-tax NPV (8%) of approximately US$18,100M.

The project undiscounted LOM revenue of approximately US$300,000M, project capital of approximately US$8,900M sustaining capital of approximately US$5,300M, all-in operating cost of approximately US$126,000M, all-in royalty cost of approximately US$900 M, and closure costs of approximately US$800M.

20 Adjacent properties

From the perspective of exploration licensing, the seafloor in the CCZ can be considered in terms of five categories:

- Areas held by other parties under exploration contracts issued by the ISA under UNCLOS.
- Areas classified by the ISA as Reserved Areas. Under UNCLOS, the Reserved Areas are reserved for access by developing countries or the Enterprise (UNCLOS, Article 170, Annex IV and 1994 Agreement, Annex, Section 2).
- Areas of Particular Environmental Interest (APEIs) declared under UNCLOS and considered by the ISA to be excluded from mineral exploration.
- Areas within the central portion of the CCZ that are not classified by the ISA because there are exploration claims in place that pre-date the ISA. These include areas known as USA-1 and USA-4, for which exploration permits were granted by NOAA, under the DSHMRA of the USA.
- Other areas, generally peripheral to the CCZ, that are not reserved or contracted under the ISA or NOAA systems.

The ISA publishes a map of the CCZ Exploration and Reserved Areas for Polymetallic Nodules (Figure 3.1). NOAA does not publish a map of exploration permits or applications therefore the QP was unable to confirm the status of areas of the CCZ under the NOAA system.

The NORI and TOML areas that are the subject of this IA are spread across the CCZ. The adjacent properties are briefly described, from east to west, based on Figure 3.1 and historical information about the USA-1 and USA-4 areas. The descriptions of current status may not be up to date or accurate and should not be relied upon.

20.1 TOML-F

The eastern boundary of TOML-F is adjacent to the eastern boundary of NORI Area-D, held under an ISA exploration contract by NORI. Polymetallic nodule mineralization is well-developed in NORI Area-D and is the subject of a pre-feasibility study completed in 2025 (AMC Consultants, 2025). The NORI Area D Mineral Resource is reported at 30 June 2025 in Table 20.1 at an abundance cut-off of 4 wet kg/m^2. The average abundance and grades in TOML-F are similar to those in NORI Area-D.

Table 20.1 Mineral Resource for NORI Area D, at 30 June 2025, at 4 wet kg/m^2 abundance cut-off

Category	Tonnes (Mwmt)	Abundance (wet kg/m^2)	Ni (%)	Cu (%)	Co (%)	Mn (%)	Si (%)	Fe (%)	P (%)
Inferred	11	15.4	1.38	1.14	0.12	30.96	5.46	6.92	0.16
Indicated	347	17.4	1.40	1.14	0.14	31.15	5.45	6.84	0.16
Measured	5	20.6	1.41	1.15	0.13	31.91	5.16	6.59	0.15
All	363	17.4	1.40	1.14	0.14	31.15	5.44	6.83	0.16

Notes:
1. Effective date of the Mineral Resource is 31 December 2024.
2. Moisture content assumed to be 28% (mass of solid/(mass of solid + mass of water).
3. The volcanic outcrop, volcanic high, volcanic cones, sediment drift, and high-slope (>6°) domains were excluded from the estimate.
4. Samples collected by the Pioneer Contractors were excluded due to the lower level of confidence associated with this data and their replacement by box core data collected by TMC.
5. Abundance cut-off and assumption of reasonable prospects for economic extraction are based on the engineering, metallurgical, environmental, scientific and other studies presented in this report.
6. Rounding estimates to two significant figures may result in computational discrepancies

The northern boundary of TOML-F is adjacent to the southern boundary of the area held under an ISA exploration contract by the Federal Institute for Geosciences and Natural Resources of Federal Republic of Germany (BGR). BGR completed multibeam bathymetry and backscatter mapping, BC sampling and geochemical analysis of nodules and used this data as the basis for an estimate of Mineral Resources in the eastern part of their Contract Area (~60,000 km^2) (Kuhn and Rühlemann 2021b). The Mineral Resources reported by Kuhn and Rühlemann are summarized in Table 20.2. The QP has been unable to verify the information. The average abundance and grades reported in the BGR area are similar to those in TOML-F.

Table 20.2 Summary of Mineral Resource reported for BGR exploration Contract Area

Mineral Resource Classification	M dry mt	Abundance (kg/m^2)	Ni (%)	Cu (%)	Co (%)	Mn (%)
Measured	7.14	14.6	1.43	1.19	0.17	31.5
Indicated	11.21	14.2	1.32	1.18	0.13	30.8
Inferred	35.53	13.4	1.39	1.17	0.17	31.1
Inferred	486.2	10.1	1.39	1.17	0.17	31.1

Source: Kuhn and Rühlemann 2021b

Global Sea Resources (GSR, a Belgian consortium) carried out a mining trial in the BGR area with a pre-prototype, crawler-mounted collector in 2021. The trial demonstrated that the collector could be successfully maneuvered and nodules could be collected and stockpiled on the seafloor.

The western and southern boundaries of TOML-F are adjacent to Reserved Areas declared by the ISA.

20.2 NORI-C

NORI-C is an irregular-shaped area that abuts ISA exploration areas held by IOM and Global Sea Resources (GSR, a Belgian consortium). It is also, in part, adjacent to ISA Reserved Areas and areas that are not reserved or contracted under the ISA or NOAA systems.

GSR carried out a successful mining trial in the GSR area, as it had done in the BGR area, with a pre-prototype, crawler-mounted collector in 2021.

20.3 TOML-D and TOML-E

TOML-D and TOML-E are located about 100 km to the west of NORI-C. The southern boundary of TOML-D is separated from the northern boundary of TOML-E by a narrow strip of ISA Reserved Area. TOML -D and TOML-E adjoin the eastern boundary of the USA-4 area, licensed under the DSHMRA. Exploration rights to USA-4 have been held by forerunners and subsidiaries of Lockheed Martin since the 1970s.

The southern boundary of TOML-E abuts ISA exploration areas held by Marawa Research and Exploration Ltd, and the northern boundary of TOML-D abuts ISA exploration areas held by GSR and the Cook Islands Investment Corporation (CIIC).

20.4 TOML-C

TOML-C adjoins ISA exploration areas held by IFREMER and DORD. The area to the northeast is ISA Reserved Area.

20.5 TOML-B and NORI-B

The eastern boundary of NORI-B abuts the western boundary of TOML-B. The combined areas adjoin ISA exploration areas held by DORD and Yuzhmorgeologya. The area to the northeast is an ISA Reserved Area.

20.6 NORI-A

To the north and west, NORI-A adjoins ISA exploration areas held by Yuzhmorgeologya. To the east, NORI-A adjoins the western portion of USA-1. Exploration rights to USA-1 have been held by forerunners and subsidiaries of Lockheed Martin since the 1970s. The southern boundary of NORI-A is adjacent to Reserved Areas declared by the ISA.

20.7 TOML-A

TOML-A is located at the western end of the CCZ. Its northern and western boundaries are adjacent to Reserved Areas declared by the ISA. The eastern and southern boundaries are unallocated.

21 Other relevant data and information

No additional information or explanation is necessary to make this IA Technical Report understandable and not misleading.

22 Interpretation and conclusions

22.1 Mineral tenure

The mineral tenure for the Project is backed by exploration contracts granted by the ISA that provides exclusive rights to explore and a priority right to apply for an exploitation contract. NORI and TOML have complied with all contractual obligations to date with respect to the ISA requirements. To the extent known to the QP, there are no other significant factors and risks that may affect access, title, or the right to perform work on the Project that are not discussed in this Technical Report.

The ISA is currently working on the development of the legal framework to regulate the exploitation of nodules in the Area and at the time of this report the ISA has not finalized the regulations for Nodule Exploitation. TMC has submitted an application to NOAA under DSHMRA for an exploration license that covers the TOML and NORI areas described in this IA. At the time of this report, this application is still under review and not yet approved. As part of estimating the recovered resource in this IA, an allowance for appropriate buffer zones to prevent impact to areas outside the NORI and TOML areas and sensitive environmental areas within the areas is included. Other than those allowances, the QPs have not included any measures to comply with the yet to be approved commercial recovery permit conditions, and the impact of those conditions on the recovered resource and associated economic evaluation is to be confirmed.

22.2 Exploration and data verification

The exploration program for the NORI and TOML properties has been extensive, spanning multiple offshore campaigns conducted between 2012 and 2023, including significant efforts in 2012, 2013, 2018, 2019, and a collector system test in 2022. This is in addition to exploration data from Pioneer Contractors and explorers. The campaigns involved a combination of sampling methods such as free fall grab (FFG) samplers, box coring, bulk nodule dredging, and geophysical surveys including multibeam echosounder (MBES), side scan sonar (SSS), sub-bottom profiling (SBP), autonomous underwater vehicle (AUV) deployments, and photographic seabed imaging. The collected data provided geological, geotechnical, and environmental baselines critical to resource estimation and mine planning.

Data verification processes confirmed the reliability and consistency of the datasets. Assay results from recent campaigns by NORI and TOML validated historical Pioneer Contractor data, which underpin much of the Inferred Mineral Resource estimates for NORI Areas A, B, C, and TOML Areas A through F. QA/QC measures included the use of CRMs, duplicate samples, secure chain-of-custody protocols, and cross-comparisons between different sampling techniques and laboratories. Although original assay sheets from Pioneer Contractors were unavailable, the consistency across independent datasets and acceptance by the ISA support their adequacy for resource modeling at an Inferred confidence level.

Moisture content measurements, essential for converting wet abundance to dry metal grades, were assessed, with current estimates of 24% moisture for NORI-A, B, and C, and 28% for NORI Area D and TOML areas, based on BC sampling of nodules recovered during 2022 Test Mining. No significant correlations were found between moisture content and other variables such as nodule size or grade.

Geotechnical data, including vane shear strength classifications derived from box core locations, indicate variable sediment stiffness across the TOML areas but suggest that mining systems designed for NORI Area D can be assumed to be broadly applicable throughout the Property. Photo-profile analyses and long-axis estimation (LAE) methods further enhanced confidence in spatial continuity and representativeness of nodule abundance and grade distributions.

Overall, the integration of multi-method sampling, rigorous QA/QC, and detailed geospatial analysis provides a solid foundation for the Mineral Resource estimates presented in this report. The QPs consider the data sufficient to support ongoing project development and future refinement of resource classification as additional operational data becomes available.

22.3 Mineral processing testwork

TMC has completed an extensive program of metallurgical testing involving nodule characterization, process flowsheet selection, bench-scale and pilot-scale confirmation on a 75 t sample of nodules collected from NORI Area D. The selected RKEF flow sheet involves calcining and smelting nodules to produce a nickel-copper-cobalt alloy and a silico-manganese product. The alloy is subsequently converted into a nickel-copper-cobalt matte. The selected process involve near zero solid waste generation. TMC polymetallic nodules have very little variation in chemical and mineralogical composition and accordingly, samples selected for testing were representative of the mineralization and sufficient samples were taken so that tests were performed on sufficient sample mass.

Estimated recovery factors estimated are based on appropriate metallurgical testwork and are appropriate to the mineralization and the selected process route.

The metallurgical recoveries to matte are estimated at 94.8% for nickel, 77.5% for cobalt, 86.4% for copper, and 98.9% for manganese, with manganese being recovered as manganese silicate and nickel-copper-cobalt recovered as a matte.

22.4 Mineral Resource

Data collected by NORI and TOML is well-documented and was subject to satisfactory QA/QC processes. Documentation verified by the QP includes photographs, daily exploration reports, digital logging sheets and original assay reports. In the opinion of the QP the NORI and TOML Area data is of good quality and suitable for estimating Mineral Resources. These estimates rely on sample data obtained by Pioneer Contractors using FFG samplers and BCs, supplemented by more recent exploration efforts including multibeam bathymetry surveys, photographic seabed imaging, and geotechnical sampling.

For NORI Areas A, B, and C, the Mineral Resource estimate remains unchanged since 2012, reflecting a stable dataset with no new exploratory work warranting an update. The estimation process involved geological domain interpretation, declustering of sample data, and spatial continuity analysis using variogram modeling to support Mineral resource classification at the Inferred level. A nodule abundance cut-off was applied at 4 kg/m^2 to define Mineral Resources with realistic prospects of economic extraction.

Similarly, the TOML Contract Areas have been modeled using integrated datasets combining historical samples and recent BC and photo-profile data. Geological domains were delineated into polymetallic nodule-bearing zones and non-nodule zones based on MBES bathymetry and backscatter data, with zero abundance assigned to non-nodule domains. Spatial continuity was assessed through variogram analysis, enabling block model construction with sub-block resolution sufficient to capture grade variability and boundary definitions. A nodule abundance cut-off was applied at 4 kg/m^2 to define Mineral Resources with realistic prospects of economic extraction.

Moisture content assumptions of approximately 24% for NORI-A, B, and C, and 28% for TOML areas were applied to convert wet tonnage to dry basis metal grades, consistent with measured values from sampling programs. The homogeneity of nodule chemistry across the TOML areas supports the use of uniform metallurgical recovery factors in economic assessments.

Geotechnical data from TOML areas indicate sediment characteristics compatible with mining systems designed for similar seafloor conditions, supporting operational feasibility.

Overall, the Mineral Resource estimates reported for NORI Areas A, B, C, and TOML Areas A-F are of suitable confidence for this IA.

22.5 Mining methods

The mining methods developed for the NORI and TOML properties represent a comprehensive and technically advanced approach to polymetallic nodule extraction from the deep seafloor. The phased development strategy, beginning with prototype test mining and progressing to a second-generation production system provides confidence from validating operational concepts through practical experience and iterative design improvements.

The proposed offshore mining system, featuring a 20-meter-wide tracked CV equipped with Coandă nozzles, is capable of effectively recovering nodules across varied seafloor terrains, and assuming slopes up to 6°. Bathymetric surveys have been integrated into mine planning to identify and mitigate challenges posed by geo-obstacles such as lava flows and sediment drifts, ensuring collector path design includes maximizing resource recovery while minimizing unmined areas.

Operational planning incorporates realistic allowances for weather-related downtime, maintenance activities, and logistical support, resulting in productive operating time of 273 days per year, or 75% of the year. The coordinated use of PVs, TVs, and SVs, managed via a centralized offshore communication centre located at the Supply Base, supports safe and efficient operations with reduced offshore personnel exposure.

22.6 LOM planning

Buffer zones of 1 km around lease boundaries and environmentally sensitive areas have been incorporated into mine planning to mitigate potential environmental impacts.

Key risks identified include potential delays or interruptions due to adverse metocean conditions, equipment reliability challenges inherent in deep-sea mining environments, and uncertainties related to seafloor variability beyond currently surveyed areas. These risks will be addressed through robust contingency planning, adaptive mine scheduling, and ongoing environmental monitoring to inform operational adjustments.

Recommendations emphasize continued refinement of mining system designs, to improve reliability, maximize operability, reduce maintenance and increase durations between maintenance periods, reduce energy consumption and improve production efficiency, simplify operational procedures, transient to (semi-)autonomous operation. Geotechnical investigations are advised to validate assumptions extrapolated from initial survey areas to the broader NORI and TOML Contract Areas. Additionally, progressive reconciliation of production data against Mineral Resource models will be critical to confirming resource estimates and optimizing future mine plans.

In summary, the IA shows that the proposed mining methods are potentially technically feasible and with continued engineering development might provide that the basis for commercial-scale polymetallic nodule mining within the NORI and TOML Contract Areas. There are no Mineral Reserve estimates for the TMC Property outside of the NORI Area D, and the potential viability of the Mineral Resources has not yet been supported by detailed mine design or optimization processes nor a PFS or a feasibility study.

22.7 Processing

The results of TMC's bench-scale testing, piloting and commercial-scale demonstration have shown that RKEF facilities are well suited to process nodules. Calcining and smelting temperatures, throughputs, material handling capabilities and other key operating parameters are very similar to those for nickel laterites, which the RKEF plants in Indonesia were designed and built to process.

The outcomes from the bench scale processing at SGS indicate that sulfate products derived exclusively from polymetallic nodules are suitable for use in battery applications. The work at SINTEF not only shows that TMC's manganese silicate product is capable of rivaling conventional manganese ores as feed for silico manganese production but also offers inherent value due to its pre-reduced nature.

Outcomes from the commercial-scale trials are expected to inform any plant modifications that may be required in preparation for nodule processing. The modifications required will depend on the specific plant, but experience with plant preparation is assumed given the capacity required to process nodules from the NORI Area D.

22.8 Infrastructure

All nodules are assumed to undergo initial pyrometallurgical processing under a tolling arrangement in Indonesia. The Indonesian operations are assumed to require minimal plant modifications in preparation to process nodules. All pyrometallurgical unit operations, port facilities and drayage/materials handling equipment are assumed to exist. The nodules are assumed to be refined at a US-based facility, which have been previously constructed as part of the need for USA refinery capacity derived from matte processing from the NORI Area D.

22.9 Market studies

The market studies for the NORI and TOML projects provide a comprehensive analysis of the demand, supply, and pricing outlooks for key metals contained in polymetallic nodules, including nickel, cobalt, manganese, and copper. These studies are based on forecasts from reputable industry sources such as CRU and BMI, incorporating both short- and long-term perspectives to inform project revenue assumptions, and consider the marketability of the suit of products that TMC are expected to produce over the project life; manganese silicate, nickel-copper-cobalt matte, nickel sulfate, cobalt sulfate, and copper cathode.

Nickel remains the primary commodity driving the project economics, with detailed assessments of its market dynamics highlighting supply constraints and growing demand driven by EV battery production and stainless steel manufacturing. The forecast anticipates a sustained supply gap after 2032 that supports favourable price levels over the life of the project.

Cobalt's market outlook reflects its critical role in battery chemistries, with supply-demand balances influenced by geopolitical factors and increasing recycling efforts. Manganese silicate is evaluated both as a feedstock for silico-manganese alloy and as a feedstock for value-added forms such as EMM and manganese sulfate ($MnSO_4$), which have expanding markets linked to battery applications and steelmaking.

Copper demand projections emphasize its essential function in electrification and infrastructure development globally. Supply-side analyses consider potential disruptions and the need for new sources to meet rising demand.

TMC's manganese silicate offers high-grade manganese content and favorable chemical properties, making it a strong contender for use in silico-manganese alloy production, as well as growing battery-related markets such as EMD and HPMSM. Its competitive pricing, manageable impurity levels, and strategic blending potential position it well to displace costlier manganese sources.

TMC's matte is compositionally similar to established converter mattes and is well-suited for refining at major facilities like Vale, Glencore, and Jinchuan, which together hold about 85% of spare global refining capacity. While growing supply may pressure payables, securing long-term refinery partnerships are assumed to help maintain value and ensure stable processing capacity for up to 200 Kt of contained nickel annually.

It is intended TMC US subsidiary TMC USA will construct refining facilities in Texas to produce battery-grade Ni and Co sulfate crystal, copper cathode and fertilizer grade ammonium sulfate. Forecasts for cathode and sulfate prices are based on forecasts from BMI.

Metallurgical recoveries and payable factors derived from these studies underpin revenue estimates used in economic modelling.

Overall, the market studies confirm robust demand fundamentals and supportive pricing environments for the suite of metals targeted by the project. This provides confidence in the commercial viability of the NORI and TOML resources and informs ongoing investment and operational planning.

22.10 Environmental studies

The environmental management framework for the NORI and TOML projects is grounded in extensive baseline studies, regulatory compliance, and proactive stakeholder engagement to ensure responsible development within the CCZ. The ISA serves as a regulatory body overseeing mineral exploration activities in these international seabed areas, mandating rigorous ESIA and EIS as prerequisites for exploitation licensing.

TMC, through its subsidiaries NORI and TOML, has conducted multiple offshore campaigns since 2012 to collect comprehensive geological, biological, and oceanographic data. These efforts include benthic and water column biological monitoring using ROVs, AUVs, and other advanced instruments, alongside geotechnical and sediment plume modeling to understand potential mining impacts.

Permitting processes under the ISA require submission of detailed five-year work plans and annual reports demonstrating adherence to environmental standards and contract obligations. Both NORI and TOML are currently compliant with their exploration contracts and actively preparing for the transition to commercial recovery permits, which necessitate further environmental documentation and adaptive management strategies.

Parallel permitting pathways exist under the U.S. Deep Seabed Hard Mineral Resources Act (DSHMRA), where TMC USA has submitted applications for exploration licenses and commercial recovery permits.

Ongoing environmental monitoring programs aim to detect and manage any adverse effects on marine ecosystems, with adaptive management plans designed to respond to changing conditions throughout the project lifecycle.

In summary, the environmental and social program supporting the NORI and TOML projects reflects a robust commitment to sustainable seabed mineral development, integrating scientific research, regulatory compliance, and stakeholder collaboration to minimize ecological disturbance and support long-term ocean health

22.11 Capital and operating costs

The capital expenditure (CAPEX) for the NORI and TOML projects is estimated at approximately US$14.975 billion, encompassing Project development capital of $8.8 billion, sustaining capital over the life of mine (LOM) is projected at US$5.3 billion, with closure costs estimated at US$805 million.

Operating cost estimates are reported in Q2, 2025 US$. The operating costs are at an IA level of confidence. LOM and average unit operating costs per wet metric tonne (wmt) of nodules collected are estimated as follows:

- LOM collection costs are estimated at US$31,139M and average US$46.5/wmt of nodules.
- LOM shipping costs are estimated at US$6,066M and average US$9.1/wmt of nodules.
- LOM contractor (offshore) costs are estimated at US$3,584M and average US$5.3/wmt of nodules.
- LOM consumables (offshore fuel) costs are estimated at US$11,884M and average US$17.7/wmt of nodules.
- LOM processing costs are estimated at US$53,598M and average US$80.0/wmt of nodules.
- LOM refining costs are estimated at US$15,978M and average US$23.8/wmt of nodules.
- LOM G&A costs are estimated at US$3,926M and average US$5.9/wmt of nodules.

22.12 Economic evaluation

The economic analysis employs a real, ungeared, post-tax discounted cash flow model using an 8% discount rate over a 23-year LOM, commencing commercial production in 2037. Key assumptions include stable metal prices based on CRU and BMI forecasts, metallurgical recoveries, payabilities, and cost structures without inflation or escalation. The model integrates royalty payments under agreements with Nauru and Tonga, as well as a Low Carbon Royalty (LCR).

Results indicate a strong project economics profile, with a post-tax net present value (NPV8) of approximately US$18.1 billion and an EBITDA of US$172 billion over the LOM. Sensitivity analyses highlight the project's resilience to fluctuations in metal prices, operating costs, and capital expenditures, underscoring its economic robustness.

In conclusion, the capital and operating cost frameworks combined with detailed economic modeling provide confidence in the technical and financial viability of the NORI and TOML projects. Continued refinement of cost estimates and economic parameters are assumed to be essential as the project advances toward development and commercial production.

This IA indicates that development of the resource within the NORI and TOML Areas, termed the TMC Property, is potentially technically and economically viable and indicates a positive economic outcome.

Due to the low level of confidence in much of the Mineral Resource base, the need for more exploration, and the need for more detailed evaluation of aspects of the Project, such as seafloor bathymetry, environmental characterization, and mine planning, the technical and economic viability has not yet been demonstrated.

23 Recommendations

The QPs consider that the evaluation work to date on the TOML and NORI area including offshore exploration and data management, off-shore Production System concepts, Onshore Processing strategy, marketing, and environmental framework and scoping assessments has demonstrated the potential technical and economic viability of the Project.

The buildup of experience expected through development and operation of the 1st Gen systems in NORI Area D are expected to be important for derisking the Project.

The QPs recommend advancing the NORI and TOML projects through continued engineering development, environmental assessment, and operational planning to support a pre-feasibility study.

Key priorities include:

- More detailed bathymetric surveys.
- Detailed definition and increase in confidence in the Mineral Resources.
- Developing mine plans with more detailed data, aligned with expected Commercial Recovery Permit conditions.
- Design and testing of 2nd Gen CVs, VTSs, PVs, and associated infrastructure, informed, where possible, from learnings from 1st Gen systems.
- Refinement of CAPEX and OPEX estimates.
- Continue to expand and finalize onshore tolling capacity in Indonesia in order to match offshore collection volumes.
- Expanding engineering studies and design efforts for the hydrometallurgical plant capabilities to meet required plant availability to manage proposed production volumes.
- Refine product to meet market placement in the US at a pre-built hydrometallurgical facility.
- Explore opportunities for onshore RKEF optimisations (power, cost, emissions).
- Progress engagement and commercial arrangements with existing or emerging industry partners to validate the operating strategy.
- Environmental monitoring and adaptive management frameworks should be refined and aligned with expected Commercial Recovery Permit conditions.

These recommendations collectively aim to mitigate risks, improve technical and economic outcomes, and support responsible advancement of the TMC Property.

24 References

Agarwal JC, Barner HEM, Beecher N., 1979. The cuprion process for ocean nodules, Chem. Eng. Prog 75(1):59-63.

Alhaddad S., Mehta D., Helmons R., 2023. Mining of deep-seabed nodules using a coanda-effect-based collector, Results in Engineering 17

Allseas Base Specification 2024. Engineering specifications for the CV and associated systems. Confidential report.

Allseas Propulsion and Maneuverability Analysis 2024b. Assessment of Collector Vehicle operational capabilities on slopes and terrain Confidential report.

AMC Consultants, 2016. TOML Clarion Clipperton Zone Project, Pacific Ocean. Technical Report compiled under NI-43-101 by AMC Consultants Pty Ltd for Nautilus Minerals, March 2016.

AMC Consultants, 2019. NORI Area D, Clarion Clipperton Zone Mineral Resource Estimate, April 2019 Technical Report compiled under NI-43-101 for DeepGreen Metals Inc.

AMC Consultants, 2021a. Technical Report Summary--Initial Assessment of the NORI Property, Clarion-Clipperton Zone, for DeepGreen Metals Inc.

AMC Consultants, 2021b. Technical Report Summary-- TOML Mineral Resource, Clarion-Clipperton Zone, Pacific Ocean, for DeepGreen Metals Inc.

AMC Consultants, 2025. Technical Report Summary of Prefeasibility Study for NORI Area D, for TMC the metals company Inc..

American Society of International Law. 1975. DeepSea Ventures Inc: notice of discovery and claim of exclusive mining rights, and request for diplomatic protection and protection of investment. International Legal Materials 14(1) (January 1975): 51-68.

APYS Subsea Ltd, 2024. Geotechnical analysis report supporting seafloor substrate strength and vehicle trafficability. Confidential report.

Archer, D., 1996. Global-scale dissolution of calcium carbonate in deep-sea sediments. Global Biogeochemical Cycles, 10(1), 103-116.

Baláž, P., 2022. Results of the second phase of deep-sea polymetallic nodules geological survey in Interoceanmetal Joint Organization licence area (2016–2021). Mineralia Slovaca, 54, 2 (2022), 95 – 118. Web ISSN 1338-3523, ISSN 0369-2086, https://doi.org/10.56623/ms.2022.54.2.1.

Benchmark Mineral Intelligence, 2025a. Forecast Reports June, 2025 for copper, nickel and cobalt Confidential report.

Benchmark Mineral Intelligence, 2025b. Q2 2025 Nickel Forecast Report, Technical report. Confidential report.

Bloomberg News, 2025. China-back $3 billion Indonesia nickel smelter risks shutdown. Available online at https://www.mining.com/web/china-backed-3-billion-indonesia-nickel-smelter-risks-shutdown/

CRU Group, 2019. Manganese market strategy. Technical report. Confidential report.

CRU Group, 2024. NORI Area D project: Preliminary market research report. Technical report. Confidential report.

DHI, 2025. Sediment plume modeling and environmental impact assessment. Confidential report.

Dunne, J. P., Armstrong R. A., Gnanadesikan A., and Sarmiento J. L., 2005. Empirical and mechanistic models for the particle export ratio, Global Biogeochem. Cycles, 19, GB4026, doi:10.1029/2004GB002390

Earney FCF. 1990. Marine Mineral Resources. Routledge, p 387. Cited in: ISA. 2010. A geological model of polymetallic nodule deposits in the Clarion-Clipperton Fracture Zone and prospector's guide for polymetallic nodule deposits in the Clarion-Clipperton Fracture Zone. International Seabed Authority Technical Study: No. 6.

Felix, D. 1980. Some problems in making nodule abundance estimates from seafloor photographs. Marine Mining, Volume 2 Number 3, 293-302.

Fiedler, P.C., & Talley, L.D., 2006. Hydrography of the eastern tropical Pacific: A review. Progress in Oceanography, 69(2-4), 143-180.

Fitzsimmons, J.N., et al., 2024. Dissolved and particulate seawater metal concentrations within NORI Area D. Texas A&M University Report. Confidential report.

Flanagan F.J. and Gottfried D., 1980. USGS Rock Standards, III. Manganese-Nodule Reference Samples USGS-Nod-A-1 and USGS-Nod-P-1. Geological Survey Professional Paper 1155.

Glover, A.G., et al., 2024. Genetic connectivity and population structure of benthic macrofauna in the CCZ. Deep Sea Research Part I.

Golder 2015. Preliminary economic assessment, NORI Clarion-Clipperton Zone Area D Project, Pacific Ocean. Report prepared by Golder Associates for Deep Green Resources Inc.

Gooday, A.J., et al., 2021. Abyssal benthos in the CCZ: Synthesis and perspectives. Marine Ecology Progress Series, 678, 1-25.

GSR 2018. Global Sea Mineral Resources NV 2018. Environmental Impact Statement. Small-scale testing of nodule collector components on the seafloor of the Clarion-Clipperton Fracture Zone and its environmental impact (ISA_EIA_2018_GSRNOD2019)

Henson, S. A., Sanders, R., & Madsen, E., 2012. Global patterns in efficiency of particulate organic carbon export and transfer to the deep ocean. *Global Biogeochemical Cycles*, *26*(1)

Hessler R.R., Jumars P.A., 1974. Abyssal community analysis from replicate box cores in the central north pacific. Deep Sea Research, 21, 185 209.

Hollingsworth, A. L., Jones, D. O. B., & Young, C. R., 2021. *Spatial Variability of Abyssal Nitrifying Microbes in the North-Eastern Clarion-Clipperton Zone. Frontiers in Marine Science, 8*.

Ingels, J., 2024. Nematode community structure and diversity in NORI Area D. Journal of Marine Biology.

ISA, 2001. Proposed technologies for mining deep-seabed polymetallic nodules. International Seabed Authority. https://www.isa.org.jm/ publications/proposed-technologies-for-mining-deep-seabed-polymetallic-nodules.

ISA. 2003. Establishment of a geological model of the polymetallic nodule resources in the Clarion-Clipperton Fracture Zone of the Equatorial North Pacific Ocean. Proceedings of the May 13-20, 2003, International Seabed Authority workshop held in Nadi, Fiji.

ISA. 2004. Marine Mineral Resources - scientific advances and economic perspectives. United Nations Division for Ocean Affairs and the Law of the Sea, Office of Legal Affairs.

ISA, 2010a. A Geological Model of Polymetallic Nodule Deposits in the Clarion-Clipperton Fracture Zone and Prospector's Guide for Polymetallic Nodule Deposits in the Clarion-Clipperton Fracture Zone. International Seabed Authority Technical Study: No. 6 ISBN: 978-976-95268-2-2.

ISA, 2010b. Environmental Management Plan for the Clarion-Clipperton Zone.

ISA, 2012. Report on the International Workshop on Environmental Management Needs for Exploration and Exploitation of Deep Sea Minerals. International Seabed Authority Technical Study: No.10.

ISA, 2017. Workshop on the Development of a Regional Environmental Management Plan for the Clarion-Clipperton Fracture Zone. 2017. https://dredging.org/media/ceda/org/documents /projects/deep_sea_mining/05_isa_workshop_on_environmental_management_strategy_2017.pdf. Accessed July 26, 2025.

Jabber. R., et al., 2024. Polymetallic Nodules and the Critical Minerals Supply Chain: A North American Approach. Report produced for Wilson Center.

Jahnke, R.A., et al., 1982. Bottom water chemistry in the central equatorial Pacific. Deep-Sea Research, 29 (12), 1231-1245.

Kaluza P., Kolzsch A., Gastner M.T., and Blasius B., 2010. The Complex Network of Global Cargo Ship Movements. Journal of the Royal Society Interface, v7, pp.1093-1094. https://doi.org/10.1098/rsif.2009.0495 Kotlinski, R. and Stoyanova, V., 2006 Buried and surface polymetallic nodule distribution in the eastern Clarion–Clipperton Zone: main distinctions and similarities. Advances in Geosciences Vol. 9: Solid Earth, Ocean Science & Atmospheric Science (2006) Eds. Yun-Tai Chen et al. World Scientific Publishing Company, pp 67-74.

Kim, P.P., 2018. Reduction rates of SiMn slags from various raw materials. Paper, Norwegian University of Science and Technology

Kuhn, T., & Rühlemann, C., 2021a. Sedimentology and geochemistry of the southeastern CCZ. Geochimica et Cosmochimica Acta, 295, 45-60.

Kuhn, T., Rühlemann, C., 2021b. Exploration of Polymetallic Nodules and Resource Assessment: A Case Study from the German Contract Area in the Clarion-Clipperton Zone of the Tropical Northeast Pacific. Minerals 2021, 11, 618. https:// doi.org/10.3390/min11060618.

Lee, G.C, Kim, J., Chi, S.B., Ko, Y.T and Ham, D.J., 2008. Examination for correction factor for manganese nodule abundance using the free fall grab and box corer. The Sea: Journal of the Korean Society of Oceanography, Vol 13, No. 3 pp 280-285.

Li, W.K.W., & Cassar, N., 2016. Satellite-based estimates of export production in the Pacific Ocean. Global Biogeochemical Cycles, 30(11), 1500-1515.

Lutz, M.A., et al., 2007. Particle fluxes in the CCZ. Deep Sea Research Part II, 54(23-26), 2243-2259.

Macheriotou, L., et al., 2022. Organic carbon content in CCZ sediments. Marine Geology, 450, 106-118.

McQuaid, K. A., Attrill, M. J., Clark, M. R., Cobley, A., Glover, A. G., Smith, C. R., & Howell, K. L. (2020). Using habitat classification to assess representativity of a protected area network in a large, data-poor area targeted for deep-sea mining. *Frontiers in Marine Science*, *7*, 558860.

Menard, H. W., & Fisher, R. L., 1958. Clipperton fracture zone in the northeastern equatorial Pacific. The Journal of Geology, 66(3), 239-253

Menard, H.W. (1955, 1966). Geological studies of the Pacific Plate and fracture zones. Journal of Geophysical Research.

Mero J, 1965. The Mineral Resources of the Sea. Volume 1 (Elsevier Oceanography Series).

NORI, 2025a. Area D-THEME-0200-MUL-RPT-00001 — Test Mining Report documenting the 2022 mining test and associated environmental monitoring. Confidential report.

NORI, 2025b. Technical Memorandum—CV Depth of Penetration — Document detailing design improvements related to the Coandă nozzle and sediment disturbance. Confidential report.

Novikov G.V. and Bogdanova O. Y., 2007, Transformations of Ore Minerals in Genetically Different Oceanic Ferromanganese Rocks, ISSN 0024-4902, Lithology and Mineral Resources, 2007, Vol. 42, No. 4, pp. 303–317.

Nozawa, Y., et al., 2006. Foraminifera diversity in the Kaplan East area. Marine Micropaleontology, 59(1-2), 1-15.

O'Malley, J., et al., 2023. Substrate composition and geotechnical soil classification in NORI Area D. Fugro USA Marine Inc. Report. Confidential report.

Olive JA, Behn MD, Ito G, Buck WR, Escartìn J, and Howell S, 2015. Sensitivity of seafloor bathymetry to climate-driven fluctuations in mid-ocean ridge magma supply, Sciencemag.org., Vol 350, Issue 6258.

Parianos, J., Lipton, I., & Nimmo, M., 2021. Aspects of estimation and reporting of Mineral Resources of seabed polymetallic nodules: A contemporaneous case study. Minerals, 11(2), 200.

Parianos, J., O'Sullivan, A., & Madureira, P., 2022. Geology of parts of the central and eastern Clarion Clipperton Zone. Journal of Maps, 18(2), 232-245.

Paul, S., et al., 2024. Porewater trace metal concentrations in the southeastern CCZ. Environmental Science & Technology.

Pegliasco, C., et al., 2022. Mesoscale eddy trajectories in the CCZ. Journal of Physical Oceanography, 52(3), 789-810.

Prahl, F.G., et al., 1980. C:N ratios in marine organic matter. Limnology and Oceanography, 25(4), 620-627.

Rabone, M., et al., 2023. Benthic biodiversity in the CCZ. Frontiers in Marine Science.

Rakhmat, M.Z., et al., 2025. The Fallout of PT Gunbuster Nickel Industry Closure: How Danantara Can Save Indonesia's Critical Minerals. Center of Economic and Law Studies. Available online at https://celios.co.id/the-fallout-of-pt-gunbuster-nickel-industry-closure-how-danantara-can-save-indonesias-critical-minerals/

Redfield, A.C., et al., 1963. The influence of organisms on the composition of seawater. In The Sea, Vol. 2.

Reuters, 2024. Indonesia says nickel reserves enough for expansion, despite moratorium call. Available online at https://www.mining.com/web/indonesia-nickel-reserves-enough-for-further-expansions-official-says/

Seton, M., et al., 2020. Age and spreading history of the Pacific Plate. Earth-Science Reviews, 203, 103-120.

Shanghai Metal Market, 2025. Both Indonesia's saprolite ore and limonite ore prices strengthen. SMM Weekly Review of Nickel Ore Market. https://www.metal.com/en/newscontent/103364124.

Shulse, C.N., et al., 2017. Nutrient distributions in the CCZ. Deep Sea Research Part I, 121, 1-14.

Simon-Lledó, E., Pomee, C., Ahokava, A., Drazen, J. C., Leitner, A. B., Flynn, A., and Jones, D. O., 2020. Multi-scale variations in invertebrate and fish megafauna in the mid-eastern Clarion Clipperton Zone. *Progress in Oceanography*, *187*, 102405

Skowronek, A., Macia ̨g, Ł., Zawadzki, D., Strzelecka, A., Baláž, P., Mianowicz, K., Abramowski, T., Kone ̌cný, P., Krawcewicz, A., 2021. Chemostratigraphic and Textural Indicators of Nucleation and Growth of Polymetallic Nodules from the Clarion-Clipperton Fracture Zone (IOM Claim Area). Minerals 2021, 11, 868. https://doi.org/10.3390/ min11080868

Spickermann R, 2012. Rare earth content of manganese nodules in the Lockheed Martin Clarion-Clipperton Zone exploration areas. Proceedings Off-shore Technology Conference, Houston Texas.

Sridhar, R., et al., 1975. US Patent #4,049,438, Filed February 14, 1975.

Sridhar, R., et al., 1976. Extraction of copper, nickel and cobalt from sea nodules. Journal of Mines. 1976;28:32–7.

Subarna, R.A., 2024. Smelter squeeze Indonesia's nickel ore supply. Article for East Asia Forum. Available online at https://eastasiaforum.org/2024/09/14/smelters-squeeze-indonesias-nickel-ore-supply/

The Star, 2025. Indonesia nickel boom is forcing its own smelters to shut down. Available online at https://www.thestar.com.my/aseanplus/aseanplus-news/2025/03/04/indonesia-nickel-boom-is-forcing-its-own-smelters-to-shut-down

Tilot V,, 2006. Biodiversity and distribution of megafauna. Vol. 1: The polymetallic nodule ecosystem of the Eastern Equatorial Pacific Ocean; Vol. 2: Annotated photographic atlas of the echinoderms of the Clarion-Clipperton fracture zone. Paris, UNESCO/IOC, 2006 (IOC Technical Series, 69).

Volz, C., et al., 2018. Metal cycling in CCZ sediments. Geochimica et Cosmochimica Acta, 237, 1-17.

Volz, J. B., Haffert, L., Haeckel, M., Koschinsky, A., and Kasten, S., 2020. Impact of small-scale disturbances on geochemical conditions, biogeochemical processes and element fluxes in surface sediments of the eastern Clarion–Clipperton Zone, Pacific Ocean, Biogeosciences, 17, 1113–1131, https://doi.org/10.5194/bg-17-1113-2020, 2020.

von Stackelberg U. and Beiersdorf H., 1991. The formation of manganese nodules between the Clarion and Clipperton fracture zones southeast of Hawaii. Marine Geology v.98, pp 411 – 423.

Washburn, T., et al., 2021. Organic matter and biogeochemistry in the CCZ. Marine Chemistry, 234, 104-115.

Xie, Z., et al., 2023. Near-inertial wave generation over seamounts in the CCZ. Journal of Geophysical Research: Oceans, 128(4).

XPS, 2020. Sea Nodules Converting Testwork XPS project 3019815.00, 22-Apr-2020. Confidential report.

25 Reliance on information provided by the registrant

In preparing inputs for this IA and the economic evaluation of the project, QPs have relied on information provided by the registrant, TMC, regarding the following aspects:

- Macroeconomic trends, data, and assumptions, (see Section 19).
- Legal matters outside the expertise of the QPs, such as statutory and regulatory interpretations affecting the mine plan (see parts of Section 3).
- Governmental factors outside the expertise of the QPs (see parts of Section 3 and Section 19).

The QPs consider it is reasonable to rely upon the information provided by the registrant in respect of the above factors as the registrant employs specialist personnel in these areas who have access to information to which the QPs do not.

Our offices

Australia

Adelaide

Level 1, 12 Pirie Street
Adelaide SA 5000 Australia

T +61 8 8201 1800
E adelaide@amcconsultants.com

Brisbane

Level 15, 100 Creek Street
Brisbane Qld 4000 Australia

T +61 7 3230 9000
E brisbane@amcconsultants.com

Melbourne

Level 12, 477 Collins Street
Melbourne Vic 3000 Australia

T +61 3 8601 3300
E melbourne@amcconsultants.com

Perth

Level 3, 1100 Hay Street
West Perth WA 6005 Australia

T +61 8 6330 1100
E perth@amcconsultants.com

Canada

Toronto

140 Yonge Street, Suite 200
Toronto ON M5C 1X6 Canada

T +1 647 953 9730
E toronto@amcconsultants.com

Vancouver

200 Granville Street, Suite 202
Vancouver BC V6C 1S4 Canada

T +1 604 669 0044
E vancouver@amcconsultants.com

South Africa

Cape Town

First Floor, Willowbridge Centre
Carl Cronje Drive
Cape Town 7530 South Africa

T +27 720 833 231
E capetown@amcconsultants.com

Centurion

Ground Floor (G05), Building 14, Block B
Byls Bridge Office Park
Corner of Olievenhoutbosch and Jean Ave
Centurion 0157 South Africa

T +27 720 833 231
E capetown@amcconsultants.com

United Kingdom

Reading

Registered in England and Wales
Company No. 3688365

Office 336a, Davidson House
Forbury Square
Reading, Berkshire RG1 3EU United Kingdom

T +44 1628 778 256
E unitedkingdom@amcconsultants.com

Registered Office:
Kinetic Centre
Theobald Street
Elstree
Hertfordshire WD6 4PG United Kingdom